ISSN 2307-8960 (online)

World Journal of *Clinical Cases*

World J Clin Cases 2023 March 26; 11(9): 1888-2122

Published by Baishideng Publishing Group Inc

World Journal of Clinical Cases

Contents

Thrice Monthly Volume 11 Number 9 March 26, 2023

REVIEW

MINIREVIEWS

ORIGINAL ARTICLE

Observational Study

Randomized Controlled Trial

CASE REPORT

World Journal of Clinical Cases

Thrice Monthly Volume 11 Number 9 March 26, 2023

Contents

World Journal of Clinical Cases

Thrice Monthly Volume 11 Number 9 March 26, 2023

Contents

ABOUT COVER

Editorial Board Member of *World Journal of Clinical Cases*, Marilia Carabotti, MD, PhD, Academic Research, Medical-Surgical Department of Clinical Sciences and Translational Medicine, University Sapienza Rome, Rome 00189, Italy. mariliacarabotti@gmail.com

AIMS AND SCOPE

The primary aim of *World Journal of Clinical Cases* (*WJCC*, *World J Clin Cases*) is to provide scholars and readers from various fields of clinical medicine with a platform to publish high-quality clinical research articles and communicate their research findings online.

WJCC mainly publishes articles reporting research results and findings obtained in the field of clinical medicine and covering a wide range of topics, including case control studies, retrospective cohort studies, retrospective studies, clinical trials studies, observational studies, prospective studies, randomized controlled trials, randomized clinical trials, systematic reviews, meta-analysis, and case reports.

INDEXING/ABSTRACTING

The *WJCC* is now abstracted and indexed in Science Citation Index Expanded (SCIE, also known as SciSearch®), Journal Citation Reports/Science Edition, Current Contents®/Clinical Medicine, PubMed, PubMed Central, Scopus, Reference Citation Analysis, China National Knowledge Infrastructure, China Science and Technology Journal Database, and Superstar Journals Database. The 2022 Edition of Journal Citation Reports® cites the 2021 impact factor (IF) for *WJCC* as 1.534; IF without journal self cites: 1.491; 5-year IF: 1.599; Journal Citation Indicator: 0.28; Ranking: 135 among 172 journals in medicine, general and internal; and Quartile category: Q4. The *WJCC*'s CiteScore for 2021 is 1.2 and Scopus CiteScore rank 2021: General Medicine is 443/826.

RESPONSIBLE EDITORS FOR THIS ISSUE

Production Editor: *Ying-Yi Yuan*; **Production Department Director:** *Xiang Li*; **Editorial Office Director:** *Jin-Lei Wang*.

NAME OF JOURNAL
World Journal of Clinical Cases

ISSN
ISSN 2307-8960 (online)

LAUNCH DATE
April 16, 2013

FREQUENCY
Thrice Monthly

PUBLICATION DATE
March 26, 2023

INSTRUCTIONS TO AUTHORS
https://www.wjgnet.com/bpg/gerinfo/204

GUIDELINES FOR ETHICS DOCUMENTS
https://www.wjgnet.com/bpg/GerInfo/287

GUIDELINES FOR NON-NATIVE SPEAKERS OF ENGLISH
https://www.wjgnet.com/bpg/gerinfo/240

PUBLICATION ETHICS
https://www.wjgnet.com/bpg/GerInfo/288

PUBLICATION MISCONDUCT
https://www.wjgnet.com/bpg/gerinfo/208

ARTICLE PROCESSING CHARGE
https://www.wjgnet.com/bpg/gerinfo/242

STEPS FOR SUBMITTING MANUSCRIPTS
https://www.wjgnet.com/bpg/GerInfo/239

ONLINE SUBMISSION
https://www.f6publishing.com

World Journal of Clinical Cases

Submit a Manuscript: https://www.f6publishing.com

World J Clin Cases 2023 March 26; 11(9): 1888-1902

DOI: 10.12998/wjcc.v11.i9.1888

ISSN 2307-8960 (online)

REVIEW

Endoscopic transluminal drainage and necrosectomy for infected necrotizing pancreatitis: Progress and challenges

Yan Zeng, Jian Yang, Jun-Wen Zhang

Specialty type: Medicine, research and experimental

Provenance and peer review: Invited article; Externally peer reviewed.

Peer-review model: Single blind

Peer-review report's scientific quality classification

Grade A (Excellent): 0
Grade B (Very good): 0
Grade C (Good): C, C
Grade D (Fair): 0
Grade E (Poor): 0

P-Reviewer: Anandan H, India; Ban T, Japan

Received: December 9, 2022
Peer-review started: December 9, 2022
First decision: February 1, 2023
Revised: February 6, 2023
Accepted: March 1, 2023
Article in press: March 1, 2023
Published online: March 26, 2023

Yan Zeng, Department of Psychology, The Second Affiliated Hospital of Chongqing Medical University, Chongqing 400010, China

Jian Yang, Jun-Wen Zhang, Department of Gastroenterology, The First Affiliated Hospital of Chongqing Medical University, Chongqing 400016, China

Corresponding author: Jian Yang, MD, PhD, Associate Chief Physician, Lecturer, Department of Gastroenterology, The First Affiliated Hospital of Chongqing Medical University, No. 1 Youyi Road, Yuzhong District, Chongqing 400016, China. yangjian@hospital.cqmu.edu.cn

Abstract

Infected necrotizing pancreatitis (INP) represents a severe condition in patients with acute pancreatitis. Invasive interventions are recommended in symptomatic INP. Growing evidence has suggested interventional strategies of INP evolving from traditional surgery to minimally invasive step-up endoscopic procedures. However, there is still no standardized protocol for endoscopic interventions. Recently, various studies have been published about the endoscopic management of INP. This article reviews published articles and guidelines to present the progress and challenges of endoscopic transluminal drainage and necrosectomy in INP.

Key Words: Endoscopic; Drainage; Necrosectomy; Infected necrotizing pancreatitis; Progress; Challenge

Core Tip: Infected necrotizing pancreatitis (INP) is a severe condition in patients with acute pancreatitis. Endoscopic transluminal drainage and necrosectomy, especially endoscopic ultrasound-guided treatments, have become the mainstream minimally-invasive treatment for symptomatic INP. Growing evidence has proven progress in endoscopic transluminal interventions, while challenges and unsolved problems still need further investigation. Endoscopic transluminal interventions are neither omnipotent nor perfect. The predominant role of endoscopic treatment will be further developed with the advancements, standardization, and popularization of endoscopic techniques and devices in the near future.

Citation: Zeng Y, Yang J, Zhang JW. Endoscopic transluminal drainage and necrosectomy for infected necrotizing pancreatitis: Progress and challenges. *World J Clin Cases* 2023; 11(9): 1888-1902
URL: https://www.wjgnet.com/2307-8960/full/v11/i9/1888.htm
DOI: https://dx.doi.org/10.12998/wjcc.v11.i9.1888

INTRODUCTION

Acute pancreatitis (AP) is one of the most common gastrointestinal (GI) discharge diagnoses and accounts for high medical costs, and its hospitalization rate has recently increased[1,2]. AP can be pathologically classified as interstitial edematous and necrotizing pancreatitis (NP)[3]. Infected NP (INP) is usually a result of fungal or bacterial infection of necrosis that occurs in approximately a third of patients with NP[3]. Infected necrosis leads to increased mortality in NP. In a systematic review and meta-analysis of 6970 patients, the mortality rates of infected necrosis with organ failure and sterile necrosis with organ failure have been reported to be 35.2% and 19.8%, respectively[4]. Therefore, effective interventions are needed in INP patients. Current treatment strategies consist of conservative therapy, endoscopic transluminal drainage and necrosectomy, percutaneous drainage and necrosectomy, minimally invasive surgery, and open necrosectomy[3,5-7]. Endoscopic transluminal drainage and necrosectomy are recommended as first-line therapy for patients with INP due to significantly reduced proinflammatory response, complications, hospitalization time and costs, new-onset multiple organ failure (MOF), and increased life quality of these patients[6,8,9]. Despite that growing evidence suggests interventional strategies of INP evolving from minimally invasive surgery to endoscopic therapy, a single treatment option may not suit all INP patients[10]. Meanwhile, other issues are still to be further investigated, such as standardizing endoscopic therapy[11], predicting and managing complications, and optimizing endoscopic drainage and debridement[12]. By comprehensively performing an electronic literature search of Medline/PubMed, Embase, *Reference Citation Analysis* (RCA, https://www.referencecitationanalysis.com/) databases, and Web of Science databases from inception to November 30, 2022, we have reviewed published articles and guidelines to present the progress and challenges of endoscopic transluminal drainage and necrosectomy for patients with INP.

CLASSIFICATION

Pancreatic parenchyma and peripancreatic tissue are most commonly involved in NP. Therefore, NP is classified into three types: Pancreatic parenchymal alone, peripancreatic necrosis alone, and a combination of the former two types[13]. NP may also be categorized as an acute necrotic collection (ANC) or walled-off necrosis (WON) based on the duration of the collection (≤ 4 wk or > 4 wk) and a well-defined encapsulation[14]. Four kinds of local complications caused by AP are classified by the revised Atlanta Classification, and acute peripancreatic fluid collection, ANC, pancreatic pseudocyst (PPC), and WON are included[15]. Sterile and infected types exist in PPC and WON[15]. Although a well-defined wall could be identified in PPC and WON by endoscopic ultrasound (EUS) or imaging examinations, their drainage effects are quite different[16].

ENDOSCOPIC TRANSLUMINAL DRAINAGE

Drainage and debridement of pancreatic necrosis are recommended for INP patients by multiple guidelines and consensus[5,17,18]. Endoscopic drainage, especially EUS-guided drainage, is a minimally invasive treatment for the drainage of pancreatic fluid collection (PFC)[19-21]. Compared with surgical cystogastrostomy, EUS-guided procedures demonstrates shorter hospital stay and lower mortality[19]. Although percutaneous drainage has proven efficient in INP[22,23], endoscopic drainage presents lower reintervention rates, shorter length of hospital stay, and decreased number of follow-up abdominal imaging than percutaneous drainage[24,25]. Thus, EUS-guided drainage has been recommended as the optimal drainage method for lesions near the stomach or duodenum (Table 1)[18].

Progress

Since the initially reported successful application of EUS-guided drainage in a patient with PPC[26], endoscopic transluminal drainage has proved effective and minimally invasive in treating INP. Moreover, indications for drainage have already evolved from a specific cystic diameter (> 6 cm) to the presence of INP-associated symptoms (abdominal pain, early satiety), lesion enlargement, and complications which include infection, hemorrhage, rupture, and obstruction[27,28]. Drainage options depend on various factors, including the patient's general condition; the size, number, and location of PFC; communication with the main pancreatic duct (PD); infection or other symptoms; and the expertise of

Table 1 Characteristics of endoscopic transluminal drainage and stents

	Recommendations and benefits	Areas of concern	Ref.
Recommending EUS guidance	Effective and minimally invasive; lower morbidity; reduced reinterventions; decreased follow-up imaging; shorter hospital stay	-	[18-21,24,25,66]
Indications for drainage	INP-associated symptoms and complications	Patients' general conditions and symptoms; PFC characteristics; endoscopic experience	[27-28]
Timing of intervention			
Early intervention (< 2 wk)	Not recommended; no superiority in complications	Increased mortality and invasive interventions	[5,45]
Early intervention (3–4 wk)	Safe and effective when identifying a partial collection	Increased mortality, endoscopic necrosectomy, and rescue surgery	[14,50,51]
Delayed intervention (> 4 wk)	Generally recommended; after INP encapsulation; excellent clinical success; reduced reinterventions and mortality	-	[17,45-49]
Stents			
DPPS	Affordable, safe, and easily accessible; recommended for little debris (≤ 10 %) or pure PPC	Stent occlusion; possible leakage; limited endoscopic access to the necrotic cavity	[18,28-30,54,57]
SEMS	Feasible; deployed when LAMS is unavailable	-	[32]
LAMS	Simpler procedure; higher technical and long-term success rates; less AD than DPPS; recommended for significant debris (≥ 30 %)	Higher cost; increased risks of pseudoaneurysm bleeding, delayed bleeding, perforation, and buried stent syndrome	[12,29,33,34,52-55,60-63]
Negative predictors for drainage effect	Male; MOF; extensive necrosis (≥ 150 mm); heterogeneity (necrosis ≥ 50%)	-	[35-37]
Improving drainage	Additional nasocystic drainage; multiple transluminal gateway technique; hybrid techniques	-	[28,31,38,39,42,43]
Technical aspects	Not always requiring fluoroscopy and LAMS dilation; novel techniques for complicated deployments; timely stent removal; endoscopic closure for patients with a poor situation or early needs for transoral feeding	Lack of standardized protocol	[11,12,17,61,62,68,69]

EUS: Endoscopic ultrasound; INP: Infected necrotizing pancreatitis; PPC: Pancreatic pseudocyst; PFC: Pancreatic fluid collection; DPPS: Double-pigtail plastic stents; SEMS: Self-expanding metal stents; LAMS: Lumen-apposing metal stents; AD: Adverse events; MOF: Multiple organ failure.

the endoscopists[27].

Stents commonly used in endoscopic transluminal drainage include double-pigtail plastic stents (DPPS), fully-covered self-expanding metal stents (SEMS), and fully-covered self-expanding lumen-apposing metal stents (LAMS)[29]. The initial application of DPPS in treating PPC was reported in 1989 [30]. DPPS is an affordable, safe, and easily accessible choice for INP drainage with satisfactory technical and clinical success rates (> 90%)[18]. Additional nasocystic drainage helps to reduce adverse events and increase drainage efficiency, thus significantly shortening the length of hospital stay for patients [31]. Therefore, nasocystic catheters are recommended by high evidence levels, especially in large or infected PPCs[18]. In addition, esophageal or biliary SEMS with a large diameter is reportedly feasible in treating large WON[32], and SEMS is usually used when LAMS is unavailable. With increasing applications, LAMS has proven the advantages of simplifying EUS-guided management with high technical and long-term success rates[33,34]. In addition to its safety and efficacy, the deployment of LAMS would facilitate subsequent endoscopic necrosectomy procedures, if necessary[34].

Since ineffective drainage is a significant cause of poor prognosis in INP patients, how could endoscopists predict the success of catheter drainage? Several studies have revealed that male, MOF, extensive pancreatic necrosis (≥ 150 mm), and heterogeneity of the collections (necrosis ≥ 50%) are negative predictors for the success of endoscopic drainage in INP[35-37]. Therefore, novel and effective drainage methods need to be introduced. Firstly, multiple transluminal gateway technique has been reported to improve drainage of sub-cavities and areas distant from the GI lumen in patients with multilocular or huge infected pancreatic collections[38,39]. Moreover, in addition to endoscopic transluminal drainage, percutaneous endoscopic step-up therapy also demonstrates an effective strategy for IPN[40]. The above research has also found that early organ failure and extensive pancreatic necrosis (> 50%) are independent predictors of mortality in this percutaneous procedure[40]. Moreover, although percutaneous drainage may not be suitable for young, active INP patients, it is more convenient for content analysis, flow monitoring, and catheter adjustment[41]. Therefore, for poor drainage, especially in WON patients, several hybrid techniques, including endoscopic drainage combined with percutaneous drainage or laparoscopic drainage, are also essential and practical solutions to complicated INP drainage[28,42,43].

Challenges

Timing of intervention: Although some experts believe that the conservative treatment of IPN with antibiotics could avoid invasive procedures, studies have revealed that an antibiotics-only protocol is a valid option only for hemodynamically stable and carefully selected patients[44]. Thus, invasive interventions are recommended for clinically suspected or proven INP by worldwide guidelines, including those from the American Gastroenterological Association, the European Society of Gastrointestinal Endoscopy (ESGE), and the Asian EUS group[5,17,18]. However, the choice of early or delayed intervention is still controversial for patients preparing for invasive intervention. The generally accepted recommendation for the first invasive interventions is at least 4 wk after pancreatitis until confirmation of INP encapsulation[17,45-47]. These delayed endoscopic interventions in INP demonstrates excellent clinical success, lower reintervention rates, and lower mortality[48,49]. At the same time, early drainage, whose efficacy, safety, and necessity of early drainage still need to be investigated, has received much attention recently. In exploring early drainage, one radical attempt is to perform drainage within 24 h after INP diagnosis. However, the results show no superiority of immediate drainage concerning complications, and these patients received more invasive interventions than those undergoing postponed drainage[45]. Therefore, due to increased morbidity and mortality, it is currently recommended that endoscopic interventions should be avoided in the early, acute period (< 2 wk)[5]. Endoscopic intervention in the third or fourth weeks of INP patients seems safe and effective when identifying a partial collection[14]. In contrast, other studies have revealed that early intervention would lead to increased mortality, more need for endoscopic necrosectomy, and rescue open necrosectomy[50,51]. Diverse studies have reached inconsistent conclusions about whether early intervention increases complications[50,51], which may be related to the patients' heterogeneity and sample sizes.

Endoscopists also have varied or even contrary opinions. Although early interventions do not apply to all INP patients, there must also be patients who need this procedure. Whether early interventions are performed depends on the patient's condition (such as infection and organ failure that need urgent interventions), the location and morphology of INP, the patient's tolerance for possible complications, and the operator's experience[50,51]. This process undoubtedly requires a comprehensive balance of advantages and disadvantages.

LAMS or DPPS: LAMS has received much attention since its application in the drainage of patients with INP[21,52], and research and debate on the merits of LAMS versus DPPs remains one of the hot issues. EUS-guided drainage with LAMS provides superior overall treatment efficacy with reduced numbers of interventional procedures[29]. Moreover, it demonstrates a lower adverse events rate than DPPS drainage for managing PFCs in a recent systematic review and meta-analysis comprising 1584 patients[53]. Thus, LAMS has been recommended by a multi-institutional consensus made by 22 experts as the standard procedure for WON drainage[12]. Most experts believe that metal stents with a large caliber should be considered for WON with significant debris (≥ 30 %), while DPPS may already be enough for WON with little debris (≤ 10 %) or pure PPC[54]. Although a large diameter (d = 15 mm) LAMS has been recommended for drainage in patients with WON[12,55], LAMS with a larger diameter (d = 20 mm) demonstrate comparable clinical outcomes with fewer subsequent endoscopic necrosectomy[56]. Meanwhile, previous studies have revealed that DPPS is cheap and easy to revise, while disadvantages and concerns include stent occlusion, possible leakage, and limited endoscopic access to the necrotic cavity[28,29,57]. Furthermore, there have been reports on novel devices and the double guidewire technique in EUS-guided DPPS drainage[58,59]. However, if multiple DPPS are introduced to maintain a large fistula for effective drainage, it would still lead to prolonged operation time, stent migration, and other complications[28].

Although clinically significant bleeding requiring endoscopic intervention has been less observed in large-caliber metal stents than in DPPS in some studies[55], contradictory conclusions from other studies have indicated more bleeding and endoscopic re-interventions in LAMS than in DPPS[60]. With the increasing applications of LAMS in endoscopic drainage, LAMS-related complications gradually attract general concerns, which include a higher risk of pseudoaneurysm bleeding, delayed bleeding, perforation, buried stent syndrome, and biliary stricture[52,60-63]. Endoscopists attempt to reduce LAMS-related adverse events by additionally placing DPPS through LAMS. However, a recent multicenter retrospective study revealed that deployment of DPS through LAMS had no significant effect on clinical outcomes, adverse events, or the need for re-interventions[64]. Thus, given the relatively higher cost[65], various possible complications, and the lack of significant differences with DPPS in outcomes, the non-clinical-trial application of SEMS and LAMS is not recommended for pancreatic PPC drainage by the Asian EUS group RAND/UCLA expert panel[18].

The results of studies on endoscopic drainage with LAMS are mixed. In some of the above studies, the size of the PFCs for drainage using LAMS tends to be larger[61], which seems to have a relatively higher risk of drainage-related complications. Moreover, the optimal stent for endoscopic drainage is determined by many factors, including the size of the PFCs, the proportion of solid necrosis, the patient's economic conditions, the therapeutic expectations of physicians and patients, and the endoscopic devices and operating experiences of the local medical center. Therefore, there is no best stent, only the most suitable stent for a specific patient. Furthermore, attention should be shifted to early

detection and effective treatment of these complications.

Technical aspects of endoscopic transluminal drainage: Although growing evidence has proven endoscopic transluminal drainage effective and minimally invasive in INP, endoscopic treatment has not been standardized yet[11], which is one of the fundamental reasons for the difference in clinical outcomes. As there are no multicenter randomized controlled trials (RCT) or guidelines for standard procedures of endoscopic interventions, the following hot issues will be emphatically discussed.

Is EUS guidance necessary? Although transmural drainage only *via* conventional endoscopy is technically available, previous studies have revealed its relatively low technical success rate with possible fatal bleeding[66]. Meanwhile, selected INP patients with bulging lesions without prominent portal hypertension may be more suitable for conventional endoscopic drainage without EUS guidance [67]. Therefore, EUS-guided drainage should be considered the first-line endoscopic drainage procedure when available.

Is fluoroscopy necessary? Fluoroscopy is recommended during EUS-guided PPC drainage by the Asian EUS group RAND/UCLA expert panel with low evidence level[18]. However, EUS-guided drainage can be completed without fluoroscopy[68]. Experienced endoscopists may choose to perform endoscopic drainage under EUS guidance alone to shorten the operation and reduce unnecessary radiation exposure for the physician and the patient.

How could endoscopists deal with complicated deployments of LAMS? Several novel techniques have been reported, among which the two-step puncture technique is recommended for IPN patients with massive solid necrosis and little fluid content, and the back-and-forth technique is intended for insufficient expansion of the distal flange[69].

Whether should LAMS be dilated after deployment? Some experts support dilation to increase rapid drainage, while others claim it is unnecessary and may cause increased dislodgment risks[12]. Although no consensus has been reached, dilation mostly depends on the endoscopists' subjective judgment of the intraoperative drainage effect and the content of PFCs[12].

When should the LAMS be removed? Literature on the removal timing of drainage stents is limited [70]. From the perspective of therapeutic purposes, stent removal should be considered when PPCs and WONs are entirely or at least mainly resolved[[68]. However, due to various complications that may occur during long-term placement[61,62], the recommended time of removal is 4 wk[17]. Recent research proposes an early removal of LAMS 3 wk after necrosectomy if WON resolution has been confirmed[71]. In some previous studies, the median indwelling time for LAMS is prolonged[33], but surprisingly, no significant increases in complications have been reported when even prolonged to 7.8 mo[68]. Another concern is that premature stent removal may lead to an increased recurrence of pancreatic collections[72]. Therefore, a long-term indwelling of transluminal DPPS is recommended in INP patients with disconnected PD syndrome by ESGE guidelines[17]. In addition, transpapillary PD stenting has proven improvements in treating IPN patients with PD disruption undergoing endoscopic transluminal drainage[73].

Is endoscopic closure necessary? Several studies have recommended metal clips or the over-the-scope clip for the endoscopic closing of gastroduodenal fistula after completing all endoscopic treatments and removing all stents[74]. Other experts may claim it is not necessary. Our experience is that endoscopic closure may not be essential for patients with satisfactory general conditions and relatively short disease duration. However, endoscopic closure should be performed for patients with the opposite situations or early needs for transoral feeding; otherwise, it may cause further infection, a long-lasting unhealed GI wall, and the recurrence of INP. Several combined techniques for managing other digestive fistulas may also be practical and feasible for a few complicated cases with poor efficiency by standard suture methods[75].

ENDOSCOPIC TRANSLUMINAL NECROSECTOMY

ANC occurs in most NP patients, and WON appears in more than half of them[76]. Previous studies have demonstrated that conservative management without necrosectomy could be a successful approach for 64% of patients with INP[77]. More than half of INP patients could be treated by catheter drainage alone and did not require necrosectomy procedures[20]. Moreover, endoscopic drainage with plastic double pigtail stents has been reported as sufficient in most PPC and WON, with or without infection[19]. However, there are significant differences in the pancreatic collections and drainage effect of varied INP patients. Although the natural resolution has been noted in more than one-half of WONs within 6 mo of onset[78], interventions should be considered when patients develop INP-associated fever, infection, abdominal pain, or GI obstruction[79]. Endoscopic transmural necrosectomy involves endoscopic access to the necrotic area and gradual removal of the necrotic tissue (Table 2)[80]. Endoscopic transmural necrosectomy is a natural orifice transluminal endoscopic surgery (NOTES) that combines endoscopic and surgical techniques[8,81,82].

Table 2 Characteristics of endoscopic transluminal necrosectomy

	Recommendations and benefits	Areas of concern	Ref.
Indications for necrosectomy	Unsolved INP-associated symptoms	Conservative management or endoscopic drainage alone is sufficient in selected patients	[77-80]
Endoscopic transluminal necrosectomy	First-line therapy; recommended endoscopic step-up approach; increased life quality; reduced proinflammatory response, complications, hospitalization time, costs, and new-onset multiple organ failure	One single treatment may not suit all INP patients; no superiority in reducing major complications or mortality when compared with the surgical step-up procedure	[6,8-10, 71,83-85]
Improve necrosectomy efficiency	A solid component is better assessed by EUS than by CT scanning	Lack of unified assessment protocol for necrosis proportion	[54]
Irrigation techniques	A three-step structured approach; saline, streptokinase, antibiotics, and hydrogen peroxide; reduced mortality and debridements	Lack of optimal procedure and concentration; prolonged stent retrieval; perforation caused by forced irrigation	[79,86-97]
Dedicated instruments	OTSG; PED; WAND; safe and effective; reduced interventions and hospital duration	Efficacy and indispensable safety; further research and popularization	[98-100]
Predictors for complications	Small size (≤ 7 cm) and delayed stent removal (≥ 4 w); PD disruption, abnormal vessels, and requirements of percutaneous drainage or hybrid techniques; elevated intracavitary amylase; exocrine insufficiency	Lack of prospective multicenter large-scale RCT	[37,106-109]
Managing complications	A novel algorithm for systematically managing hemorrhage events; LAMS with a larger diameter; mouthwash with chlorhexidine; suspension of PPI; timely follow-up and endoscopic management		[60,62, 63,74,79, 101-104]
MDT strategy	Individualized treatment; reduced mortality; improved clinical outcomes; optimal strategy for patients with high risks of potential complications	Lack of standardized endoscopic protocol; considerable variations among endoscopists	[11,79, 110-112]

EUS: Endoscopic ultrasound; INP: Infected necrotizing pancreatitis; OTSG: Over-the-scope grasper; PED: Powered endoscopic debridement system; WAND: Waterjet necrosectomy device; PD: Pancreatic duct; RCT: Randomized controlled trials; LAMS: Lumen-apposing metal stents; MDT: Multidisciplinary treatment.

Progress

Endoscopic transluminal necrosectomy demonstrates increased life quality of INP patients and significantly reduced proinflammatory response, complications, hospitalization time and costs, and new-onset multiple organ failure[6,71]. Therefore, it has become a first-line option for INP patients who require necrosectomy.

The endoscopic step-up approach refers to EUS-guided transluminal drainage followed by endoscopic necrosectomy if necessary. Although the conclusions of comparative studies on major complications and mortality of endoscopic transluminal and surgical step-up procedures are inconsistent, the rate of pancreatic fistulas and hospitalization time is lower in the endoscopy group in most studies[9,83]. Pancreatic fistula is one of the critical reasons for prolonged hospitalization, increased treatment costs, and reduced treatment experience and life quality in patients with INP. Therefore, endoscopic transluminal necrosectomy should be recommended as a first-line option for patients with debridement needs.

Challenges

Superior to surgical approaches or not: Endoscopic necrosectomy has often been compared with surgical approaches to answer whether it is superior to surgical techniques, but conclusions varied[6,9, 83]. The first-step comparison has been conducted in minimally invasive interventions and surgical open necrosectomy, and the following results are generally accepted. That is, minimally invasive approaches have replaced surgical open necrosectomy due to their advantages in the rate of the composite end point of major complications[7]. Moreover, minimally-invasive surgical and endoscopic necrosectomy demonstrated lower mortality than open necrosectomy in a pooled analysis of 1980 patients[84]. However, Comparing endoscopic step-up procedures to direct surgical necrosectomy may also lead to a bias in favor of endoscopic treatment[85].

Next, the second step compares two minimally invasive interventions, including the endoscopic transluminal and surgical step-up approaches. Reductions in the major complications, hospitalization time, and medical costs have been observed in the endoscopic transluminal step-up group in the TENSION trial, a randomized controlled, parallel-group superiority multicenter trial by the Dutch Pancreatitis Study Group[83]. Moreover, besides reduced major complications and therapeutic costs, increased life quality has also been revealed in the endoscopic transluminal approach when compared with minimally invasive surgery in INP patients[6]. In contrast, other studies have found that although

the rate of pancreatic fistulas and hospitalization time is lower in the endoscopic group, no superiority in reducing major complications or mortality has been noted in the endoscopic step-up approach (EUS-guided transluminal drainage followed by endoscopic necrosectomy if necessary) when comparing with the surgical step-up procedure (percutaneous catheter drainage followed by video-assisted retroperitoneal debridement if required)[9]. The reasons for the differences or even the contradictions of various studies may be related to the differences in the sample size, the INP lesions, the specific endoscopic procedures, and the experience and perioperative management in different medical centers. In general, minimally invasive necrosectomy is currently recommended, among which endoscopic necrosectomy may be a better first-step option. When it comes to a specific patient, it is necessary to consider all INP-related factors and the therapeutic experience of the local medical institution.

How to improve the efficiency: If endoscopic necrosectomy sessions can be effectively decreased, it will reduce the operation-related complications and costs, shorten the treatment process, and improve the overall experience. Therefore, it has always been a hot issue in INP treatment. Since the frequency of endoscopic necrosectomy is affected by the necrotic proportion in INP patients, assessing the necrosis proportion is the first problem. However, there is yet to be a unified assessment protocol[54]. Based on the current literature, the following drugs, devices, and techniques may help reduce endoscopic debridements.

Irrigation of the INP cavity is a commonly used procedure in INP patients undergoing invasive intervention. A three-step structured approach (debridement, necrosis extraction, and irrigation) has been developed and demonstrated fewer interventions[86]. Irrigation can be accomplished by a nasal catheter, a percutaneous catheter, or a combination[79]. Although percutaneous drainage has been considered one primary treatment for INP and helps most patients reduce open debridement in some studies, about one in five patients gets worse and requires open surgical intervention[87]. Furthermore, recent research has revealed that streptokinase irrigation through a percutaneous catheter helps reduce necrosectomy sessions and mortality in a step-up approach. Constant saline instillation *via* nasocystic catheter between each necrosectomy procedure has been reported effective for improving drainage and reducing debridement operations[88,89]. However, it still needs to be determined whether continuous or intermittent lavage is more suitable for the INP cavity[79]. In the meantime, complications have also been noticed, including forced irrigation-caused perforation, subsequent organ failure, and death[88]. Another study has introduced a vigorous irrigation technique to reduce mechanical debridement, and no mortalities or following surgical needs have been reported in these patients[90]. However, the reported mean time of stent retrieval seems prolonged than the recommended[90]. Moreover, aggressive lavage with large-volume warmed antibiotic solution has also been reported as an efficient alternative to saline irrigation, and reduced rates of adverse events and mortality have been noted in previous studies[91]. In addition, cessation of PPIs, local infusion of antibiotics, maximal fragmentation of necrotic tissue, and disruption of internal septate structures during the first necrosectomy can also improve drainage and reduce debridements[91-93].

In several previous studies, hydrogen peroxide has proven effective and safe in reducing debridements, even making external irrigation unnecessary in selected IPN patients[82,94]. Hydrogen peroxide has the advantage of healing INP by stimulating granulation and fibrosis, and foams produced by hydrogen peroxide in contact with organic tissue help remove the attached necrotic debris[95]. However, its operation time and treatment course to achieve equal clinical efficacy with routine debridement seem prolonged[96], and this technique's optimal procedure and concentration remain to be further studied[94]. Another recent single-center randomized pilot study has revealed that streptokinase irrigation in complicated INP cases demonstrates a lesser post-irrigation hospital stay and a reduced trend for mortality and necrosectomy sessions, while H_2O_2 irrigation may cause more bleedings, in contrast[97].

Besides, the optimal interval between each endoscopic necrosectomy remains unsettled. One possible reason may be the lack of data from large-scale multicenter RCTs. The current recommendation is 6.23 ± 4.71 d (range, 3-21 d), which is also based on endoscopists' experience[12]. Suppose the interval can be shortened, or even an endoscopic debridement is performed at the same time as the first drainage; in that case, it seems beneficial in shortening the overall treatment duration. Although studies have reported that simultaneous drainage and debridement in a small number of selected patients does not significantly increase the incidence of serious complications[90], most experts do not recommend such procedures[12].

Furthermore, endoscopic transluminal necrosectomy still lacks dedicated instruments. However, some innovations have emerged in recent years. A new grasping tool, the over-the-scope grasper (OTSG), has been reported to overcome the disadvantages of time-consuming endoscopic removals of necrotic debris[98]. OTSG can be attached to any standard gastroscope. Additionally, a novel powered endoscopic debridement system has been developed to achieve simultaneous resection and removal of solid debris. In recent research of a prospective, multicenter, international device trial, this system has revealed fewer interventions and shorter hospital duration in INP patients[99]. Thus, it seems to be a safe and effective dedicated instrument for WON. Another novel prototype of the waterjet necrosectomy device has also been designed and has already demonstrated effectiveness in fragmenting necrotic debris and avoiding trauma to healthy tissue in animal experiments[100]. The above-mentioned

two new devices are compatible with therapeutic endoscopes with at least a 3.2-mm and a 2.8-mm working channel, respectively[99,100].

Additionally, it seems lacking attractive to compare the advantages and disadvantages of traditional endoscopic necrosectomy devices, and related comparative trials of these devices barely exist. In all cases, any device or technique used in endoscopic procedures must balance necrosectomy's efficacy with safety.

Predicting and managing complications: Despite all the aforementioned advantages and the promising future of endoscopic interventions, various complications should be addressed. Moreover, the prediction and management of potential complications should also be emphasized.

Common complications of endoscopic interventions in INP include bleeding, infection, perforation, pneumoperitoneum, and stent migration[33,62,63,101]. Bleeding is a dangerous complication with serious, even deadly outcomes, and it can be classified into two types: Intraoperative and postoperative bleeding[102]. Intraoperative bleeding may occur near the fistula or inside the pancreatic collection. Common causes of bleeding include mechanical injuries and ruptures of pseudoaneurysm, collateral vessels, or other intracavitary blood vessels[60,102,103]. Timely and effective endoscopic management of these mild bleedings may not require interventional radiology-guided coil embolization or emergency surgery. Still, sometimes severe bleeding leads to the unfortunate outcome of the patient's death[60,62,63]. To date, the occurrence of bleeding has been presumed to be related to the type, size, and location of pancreatic collections; the type, diameter, and length of stents; varied intracavitary components; the time and protocol of endoscopic interventions; the experience of endoscopists; and the general health condition of the patient[62,102]. A novel algorithm has already been proposed for systematically managing hemorrhage events, which needs to be proven and refined in further RCT[102].

Moreover, infection often occurs in patients with poor drainage or a significant amount of solid necrosis. Using LAMS with a larger diameter, improving drainage efficiency, cooperating with antibiotics, and timely endoscopic debridement will help to improve or avoid severe infection in these patients[17,18,31,56,79]. Another human research has also demonstrated reduced intraabdominal infection by mouthwash with chlorhexidine and suspension of PPI before operation[74]. Stent migration needs to be paid enough attention to in patients using LAMS or SEMS. Endoscopic or imaging follow-up and timely removal of the stent will help reduce the occurrence of stent migration[71]. For long-term stent retention events caused by loss of follow-up or other reasons, most can also be solved by endoscopic interventions[104]. In addition, intraoperative perforation, pneumoperitoneum, and postoperative obstructive jaundice caused by stent compression could be reduced or timely treated to avoid fatal consequences in an experienced endoscopic center[16,105].

Furthermore, how to predict high-risk patients with these potential complications? Several predictors have been studied. A relatively small size (≤ 7 cm) and delayed removal of the stent (≥ 4 wk) have both been reported as effective predictors for delayed bleeding and buried stent syndrome[106]. Identifying intracavitary vessels during endoscopic interventions could also predict intraoperative bleeding, and patients with more transfusion requirements before interventions may require earlier radiological interventions[107]. Meanwhile, a predictive model for potential complications after LAMS deployment in INP patients has been reported. Higher risks for adverse events have already been identified in patients with preoperative evidence of PD disruption, abnormal vessels (perigastric varices and pseudoaneurysm), and requirements of percutaneous drainage or hybrid techniques[108]. Another research has also found that a significantly higher level of intracavitary amylase may indicate a higher risk of recurrence in INP patients[37]. In addition, long-term sequelae in patients undergoing endoscopic therapy include pancreatic endocrine insufficiency, exocrine insufficiency, and long-term opiate use. These long-term complications should not be overlooked. Previous research has revealed that patients with exocrine insufficiency may have a significantly poorer health-related quality of life [109]. These above studies help evaluate the potential risks and predict the prognosis before endoscopic interventions in INP patients. Further research will promote the continuous development of endoscopic interventional technology based on patient safety.

A multi-disciplinary treatment strategy: Despite all the progress of endoscopic transluminal interventions, INP remains a challenging and fatal condition. Due to lacking standardized endoscopic treatment protocol and considerable variations in the treatment selections among various endoscopists and medical centers[11], the short-term and long-term results of INP patients are affected by many factors. The optimal strategy varies in patients, especially those with high risks of potential complications. Moreover, not all patients with INP can be completely cured through endoscopic transluminal interventions alone. Thus it needs a multi-disciplinary treatment strategy in the whole clinical management of INP[110]. A multi-disciplinary team (MDT) consists of therapeutic endoscopists, gastroenterologists, anaesthesiologists, intensive care unit physicians, sonographers, interventional radiologists, and surgeons[111]. MDT aims to determine individualized treatment options for every INP patient, reduce mortality, improve clinical outcomes[79], and improve the risk-benefit ratio throughout the clinical treatment process. A staged, multi-disciplinary, minimally invasive "step-up" approach has already been proposed as an optimal treatment strategy for patients with INP, especially those with severe and complicated conditions[110-112].

LIMITATIONS

Increasing evidence has demonstrated promising benefits of endoscopic transluminal drainage and necrosectomy in patients with INP. Numerous experts and guidelines have also recommended endoscopic interventions as a first-line strategy. However, endoscopic transluminal interventions are neither omnipotent nor perfect. Moreover, endoscopic transluminal interventions represent only one invasive option for INP patients. It is also necessary to consider when and how to better connect with surgical treatment and other methods so that patients can obtain better overall therapeutic effects. In addition, there still lacks a standard protocol for endoscopic transluminal interventions, while surgical treatment of INP has already been standardized, in contrast[11].

Endoscopic transluminal drainage and necrosectomy are definitely hot in the field of INP therapy and advanced endoscopic techniques. However, differences and contradictions exist in the conclusions of various studies, which may be related to the sample size, the patients' heterogeneity, especially the varied ratios of patients with organ failure, and different proportions of patients with a significant amount of necrosis (≥ 50%)[113]. Further prospective multicenter large-scale RCTs are still needed for investigating the following contents: The standard protocol of endoscopic interventions, multi-disciplinary support strategies, accurate preoperative assessments (including necrosis proportion), optimal intervention time, predictors for perioperative complications, emergency treatment of severe complications, novel techniques and devices with improved efficiency, non-endoscopic supportive strategies [79], and predictors for short-term and long-term outcomes.

CONCLUSION

Endoscopic transluminal drainage and necrosectomy, especially EUS-guided treatments, have become the mainstream minimally-invasive treatment for symptomatic INP. A staged multi-disciplinary strategy may ensure an individualized treatment in appropriate patients. The optimal risk-benefit ratio of endoscopic transluminal interventions could be achieved by skilled endoscopists at the proper timing. Growing evidence has proven progress in endoscopic transluminal interventions, while challenges and unsolved problems still need further investigation. Furthermore, the predominant role of endoscopic treatment in INP will be further developed with advancements, standardization, and popularization in endoscopic techniques and devices in the near future.

FOOTNOTES

Author contributions: Yang J and Zhang JW conceptualized and designed the research; Zeng Y and Yang J performed the literature search and analyzed the data; Zeng Y wrote the original manuscript; Yang J and Zhang JW reviewed and edited the final manuscript; All authors have read and approved the final manuscript.

Conflict-of-interest statement: All authors declare no conflicts of interest associated with this manuscript.

Country/Territory of origin: China

ORCID number: Yan Zeng 0000-0003-4935-1306; Jian Yang 0000-0001-8170-0727; Jun-Wen Zhang 0000-0003-2911-598X.

Corresponding Author's Membership in Professional Societies: Chinese Society of Gastroenterology.

S-Editor: Fan JR
L-Editor: A
P-Editor: Fan JR

REFERENCES

1 **Peery AF**, Crockett SD, Murphy CC, Lund JL, Dellon ES, Williams JL, Jensen ET, Shaheen NJ, Barritt AS, Lieber SR, Kochar B, Barnes EL, Fan YC, Pate V, Galanko J, Baron TH, Sandler RS. Burden and Cost of Gastrointestinal, Liver, and Pancreatic Diseases in the United States: Update 2018. *Gastroenterology* 2019; **156**: 254-272.e11 [PMID: 30315778 DOI: 10.1053/j.gastro.2018.08.063]

2 **Gapp J**, Hall AG, Walters RW, Jahann D, Kassim T, Reddymasu S. Trends and Outcomes of Hospitalizations Related to Acute Pancreatitis: Epidemiology From 2001 to 2014 in the United States. *Pancreas* 2019; **48**: 548-554 [PMID: 30946239 DOI: 10.1097/MPA.0000000000001275]

3 **Purschke B**, Bolm L, Meyer MN, Sato H. Interventional strategies in infected necrotizing pancreatitis: Indications, timing, and outcomes. *World J Gastroenterol* 2022; **28**: 3383-3397 [PMID: 36158258 DOI: 10.3748/wjg.v28.i27.3383]

4 **Werge M**, Novovic S, Schmidt PN, Gluud LL. Infection increases mortality in necrotizing pancreatitis: A systematic review and meta-analysis. *Pancreatology* 2016; **16**: 698-707 [PMID: 27449605 DOI: 10.1016/j.pan.2016.07.004]

5 **Baron TH**, DiMaio CJ, Wang AY, Morgan KA. American Gastroenterological Association Clinical Practice Update: Management of Pancreatic Necrosis. *Gastroenterology* 2020; **158**: 67-75.e1 [PMID: 31479658 DOI: 10.1053/j.gastro.2019.07.064]

6 **Bang JY**, Arnoletti JP, Holt BA, Sutton B, Hasan MK, Navaneethan U, Feranec N, Wilcox CM, Tharian B, Hawes RH, Varadarajulu S. An Endoscopic Transluminal Approach, Compared With Minimally Invasive Surgery, Reduces Complications and Costs for Patients With Necrotizing Pancreatitis. *Gastroenterology* 2019; **156**: 1027-1040.e3 [PMID: 30452918 DOI: 10.1053/j.gastro.2018.11.031]

7 **van Santvoort HC**, Besselink MG, Bakker OJ, Hofker HS, Boermeester MA, Dejong CH, van Goor H, Schaapherder AF, van Eijck CH, Bollen TL, van Ramshorst B, Nieuwenhuijs VB, Timmer R, Laméris JS, Kruyt PM, Manusama ER, van der Harst E, van der Schelling GP, Karsten T, Hesselink EJ, van Laarhoven CJ, Rosman C, Bosscha K, de Wit RJ, Houdijk AP, van Leeuwen MS, Buskens E, Gooszen HG; Dutch Pancreatitis Study Group. A step-up approach or open necrosectomy for necrotizing pancreatitis. *N Engl J Med* 2010; **362**: 1491-1502 [PMID: 20410514 DOI: 10.1056/NEJMoa0908821]

8 **Bakker OJ**, van Santvoort HC, van Brunschot S, Geskus RB, Besselink MG, Bollen TL, van Eijck CH, Fockens P, Hazebroek EJ, Nijmeijer RM, Poley JW, van Ramshorst B, Vleggaar FP, Boermeester MA, Gooszen HG, Weusten BL, Timmer R; Dutch Pancreatitis Study Group. Endoscopic transgastric vs surgical necrosectomy for infected necrotizing pancreatitis: a randomized trial. *JAMA* 2012; **307**: 1053-1061 [PMID: 22416101 DOI: 10.1001/jama.2012.276]

9 **van Brunschot S**, van Grinsven J, van Santvoort HC, Bakker OJ, Besselink MG, Boermeester MA, Bollen TL, Bosscha K, Bouwense SA, Bruno MJ, Cappendijk VC, Consten EC, Dejong CH, van Eijck CH, Erkelens WG, van Goor H, van Grevenstein WMU, Haveman JW, Hofker SH, Jansen JM, Laméris JS, van Lienden KP, Meijssen MA, Mulder CJ, Nieuwenhuijs VB, Poley JW, Quispel R, de Ridder RJ, Römkens TE, Scheepers JJ, Schepers NJ, Schwartz MP, Seerden T, Spanier BWM, Straathof JWA, Strijker M, Timmer R, Venneman NG, Vleggaar FP, Voermans RP, Witteman BJ, Gooszen HG, Dijkgraaf MG, Fockens P; Dutch Pancreatitis Study Group. Endoscopic or surgical step-up approach for infected necrotising pancreatitis: a multicentre randomised trial. *Lancet* 2018; **391**: 51-58 [PMID: 29108721 DOI: 10.1016/S0140-6736(17)32404-2]

10 **Garg PK**, Zyromski NJ, Freeman ML. Infected Necrotizing Pancreatitis: Evolving Interventional Strategies From Minimally Invasive Surgery to Endoscopic Therapy-Evidence Mounts, But One Size Does Not Fit All. *Gastroenterology* 2019; **156**: 867-871 [PMID: 30776344 DOI: 10.1053/j.gastro.2019.02.015]

11 **Rizzatti G**, Rimbaş M, Larghi A. Endoscopic Ultrasound-Guided Drainage for Infected Necrotizing Pancreatitis: Better Than Surgery But Still Lacking Treatment Protocol Standardization. *Gastroenterology* 2019; **157**: 582-583 [PMID: 31102662 DOI: 10.1053/j.gastro.2019.01.274]

12 **Guo J**, Saftoiu A, Vilmann P, Fusaroli P, Giovannini M, Mishra G, Rana SS, Ho S, Poley JW, Ang TL, Kalaitzakis E, Siddiqui AA, De La Mora-Levy JG, Lakhtakia S, Bhutani MS, Sharma M, Mukai S, Garg PK, Lee LS, Vila JJ, Artifon E, Adler DG, Sun S. A multi-institutional consensus on how to perform endoscopic ultrasound-guided peri-pancreatic fluid collection drainage and endoscopic necrosectomy. *Endosc Ultrasound* 2017; **6**: 285-291 [PMID: 29063871 DOI: 10.4103/eus.eus_85_17]

13 **Sarr MG**, Banks PA, Bollen TL, Dervenis C, Gooszen HG, Johnson CD, Tsiotos GG, Vege SS. The new revised classification of acute pancreatitis 2012. *Surg Clin North Am* 2013; **93**: 549-562 [PMID: 23632143 DOI: 10.1016/j.suc.2013.02.012]

14 **Oblizajek N**, Takahashi N, Agayeva S, Bazerbachi F, Chandrasekhara V, Levy M, Storm A, Baron T, Chari S, Gleeson FC, Pearson R, Petersen BT, Vege SS, Lennon R, Topazian M, Abu Dayyeh BK. Outcomes of early endoscopic intervention for pancreatic necrotic collections: a matched case-control study. *Gastrointest Endosc* 2020; **91**: 1303-1309 [PMID: 31958461 DOI: 10.1016/j.gie.2020.01.017]

15 **Banks PA**, Bollen TL, Dervenis C, Gooszen HG, Johnson CD, Sarr MG, Tsiotos GG, Vege SS; Acute Pancreatitis Classification Working Group. Classification of acute pancreatitis--2012: revision of the Atlanta classification and definitions by international consensus. *Gut* 2013; **62**: 102-111 [PMID: 23100216 DOI: 10.1136/gutjnl-2012-302779]

16 **Baron TH**, Harewood GC, Morgan DE, Yates MR. Outcome differences after endoscopic drainage of pancreatic necrosis, acute pancreatic pseudocysts, and chronic pancreatic pseudocysts. *Gastrointest Endosc* 2002; **56**: 7-17 [PMID: 12085029 DOI: 10.1067/mge.2002.125106]

17 **Arvanitakis M**, Dumonceau JM, Albert J, Badaoui A, Bali MA, Barthet M, Besselink M, Deviere J, Oliveira Ferreira A, Gyökeres T, Hritz I, Hucl T, Milashka M, Papanikolaou IS, Poley JW, Seewald S, Vanbiervliet G, van Lienden K, van Santvoort H, Voermans R, Delhaye M, van Hooft J. Endoscopic management of acute necrotizing pancreatitis: European Society of Gastrointestinal Endoscopy (ESGE) evidence-based multidisciplinary guidelines. *Endoscopy* 2018; **50**: 524-546 [PMID: 29631305 DOI: 10.1055/a-0588-5365]

18 **Teoh AYB**, Dhir V, Kida M, Yasuda I, Jin ZD, Seo DW, Almadi M, Ang TL, Hara K, Hilmi I, Itoi T, Lakhtakia S, Matsuda K, Pausawasdi N, Puri R, Tang RS, Wang HP, Yang AM, Hawes R, Varadarajulu S, Yasuda K, Ho LKY. Consensus guidelines on the optimal management in interventional EUS procedures: results from the Asian EUS group RAND/UCLA expert panel. *Gut* 2018; **67**: 1209-1228 [PMID: 29463614 DOI: 10.1136/gutjnl-2017-314341]

19 **Shekhar C**, Maher B, Forde C, Mahon BS. Endoscopic ultrasound-guided pancreatic fluid collections' transmural drainage outcomes in 100 consecutive cases of pseudocysts and walled off necrosis: a single-centre experience from the United Kingdom. *Scand J Gastroenterol* 2018; **53**: 611-615 [PMID: 29117722 DOI: 10.1080/00365521.2017.1398346]

20 **van Santvoort HC**, Bakker OJ, Bollen TL, Besselink MG, Ahmed Ali U, Schrijver AM, Boermeester MA, van Goor H,

Dejong CH, van Eijck CH, van Ramshorst B, Schaapherder AF, van der Harst E, Hofker S, Nieuwenhuijs VB, Brink MA, Kruyt PM, Manusama ER, van der Schelling GP, Karsten T, Hesselink EJ, van Laarhoven CJ, Rosman C, Bosscha K, de Wit RJ, Houdijk AP, Cuesta MA, Wahab PJ, Gooszen HG; Dutch Pancreatitis Study Group. A conservative and minimally invasive approach to necrotizing pancreatitis improves outcome. *Gastroenterology* 2011; **141**: 1254-1263 [PMID: 21741922 DOI: 10.1053/j.gastro.2011.06.073]

21 **Kumta NA**, Tyberg A, Bhagat VH, Siddiqui AA, Kowalski TE, Loren DE, Desai AP, Sarkisian AM, Brown EG, Karia K, Gaidhane M, Kedia P, Tarnasky PR, Patel U, Adler D, Taylor LJ, Petrone M, Arcidiacono P, Yachimski PS, Weine D, Sundararajan S, Deprez PH, Mouradides C, Ho S, Javed S, Easler JJ, Raijman I, Vazquez-Sequeiros E, Sawhney M, Berzin TM, Kahaleh M. EUS-guided drainage of pancreatic fluid collections using lumen apposing metal stents: An international, multicenter experience. *Dig Liver Dis* 2019; **51**: 1557-1561 [PMID: 31272934 DOI: 10.1016/j.dld.2019.05.033]

22 **Singh S**, Prakash S, Kaushal D, Chahal H, Sood A. Percutaneous Catheter Drainage in Acute Infected Necrotizing Pancreatitis: A Real-World Experience at a Tertiary Care Hospital in North India. *Cureus* 2022; **14**: e27994 [PMID: 36120245 DOI: 10.7759/cureus.27994]

23 **Sugimoto M**, Sonntag DP, Flint GS, Boyce CJ, Kirkham JC, Harris TJ, Carr SM, Nelson BD, Bell DA, Barton JG, Traverso LW. Better Outcomes if Percutaneous Drainage Is Used Early and Proactively in the Course of Necrotizing Pancreatitis. *J Vasc Interv Radiol* 2016; **27**: 418-425 [PMID: 26806694 DOI: 10.1016/j.jvir.2015.11.054]

24 **Keane MG**, Sze SF, Cieplik N, Murray S, Johnson GJ, Webster GJ, Thorburn D, Pereira SP. Endoscopic versus percutaneous drainage of symptomatic pancreatic fluid collections: a 14-year experience from a tertiary hepatobiliary centre. *Surg Endosc* 2016; **30**: 3730-3740 [PMID: 26675934 DOI: 10.1007/s00464-015-4668-x]

25 **Akshintala VS**, Saxena P, Zaheer A, Rana U, Hutfless SM, Lennon AM, Canto MI, Kalloo AN, Khashab MA, Singh VK. A comparative evaluation of outcomes of endoscopic versus percutaneous drainage for symptomatic pancreatic pseudocysts. *Gastrointest Endosc* 2014; **79**: 921-8; quiz 983.e2, 983.e5 [PMID: 24315454 DOI: 10.1016/j.gie.2013.10.032]

26 **Grimm H**, Binmoeller KF, Soehendra N. Endosonography-guided drainage of a pancreatic pseudocyst. *Gastrointest Endosc* 1992; **38**: 170-171 [PMID: 1568613 DOI: 10.1016/s0016-5107(92)70384-8]

27 **Pitchumoni CS**, Agarwal N. Pancreatic pseudocysts. When and how should drainage be performed? *Gastroenterol Clin North Am* 1999; **28**: 615-639 [PMID: 10503140 DOI: 10.1016/s0889-8553(05)70077-7]

28 **Kawakami H**, Itoi T, Sakamoto N. Endoscopic ultrasound-guided transluminal drainage for peripancreatic fluid collections: where are we now? *Gut Liver* 2014; **8**: 341-355 [PMID: 25071899 DOI: 10.5009/gnl.2014.8.4.341]

29 **Siddiqui AA**, Kowalski TE, Loren DE, Khalid A, Soomro A, Mazhar SM, Isby L, Kahaleh M, Karia K, Yoo J, Ofosu A, Ng B, Sharaiha RZ. Fully covered self-expanding metal stents versus lumen-apposing fully covered self-expanding metal stent versus plastic stents for endoscopic drainage of pancreatic walled-off necrosis: clinical outcomes and success. *Gastrointest Endosc* 2017; **85**: 758-765 [PMID: 27566053 DOI: 10.1016/j.gie.2016.08.014]

30 **Cremer M**, Deviere J, Engelholm L. Endoscopic management of cysts and pseudocysts in chronic pancreatitis: long-term follow-up after 7 years of experience. *Gastrointest Endosc* 1989; **35**: 1-9 [PMID: 2920879 DOI: 10.1016/s0016-5107(89)72677-8]

31 **Gurusamy KS**, Pallari E, Hawkins N, Pereira SP, Davidson BR. Management strategies for pancreatic pseudocysts. *Cochrane Database Syst Rev* 2016; **4**: CD011392 [PMID: 27075711 DOI: 10.1002/14651858.CD011392.pub2]

32 **Attam R**, Trikudanathan G, Arain M, Nemoto Y, Glessing B, Mallery S, Freeman ML. Endoscopic transluminal drainage and necrosectomy by using a novel, through-the-scope, fully covered, large-bore esophageal metal stent: preliminary experience in 10 patients. *Gastrointest Endosc* 2014; **80**: 312-318 [PMID: 24721519 DOI: 10.1016/j.gie.2014.02.013]

33 **Siddiqui AA**, Adler DG, Nieto J, Shah JN, Binmoeller KF, Kane S, Yan L, Laique SN, Kowalski T, Loren DE, Taylor LJ, Munigala S, Bhat YM. EUS-guided drainage of peripancreatic fluid collections and necrosis by using a novel lumen-apposing stent: a large retrospective, multicenter U.S. experience (with videos). *Gastrointest Endosc* 2016; **83**: 699-707 [PMID: 26515956 DOI: 10.1016/j.gie.2015.10.020]

34 **Shah RJ**, Shah JN, Waxman I, Kowalski TE, Sanchez-Yague A, Nieto J, Brauer BC, Gaidhane M, Kahaleh M. Safety and efficacy of endoscopic ultrasound-guided drainage of pancreatic fluid collections with lumen-apposing covered self-expanding metal stents. *Clin Gastroenterol Hepatol* 2015; **13**: 747-752 [PMID: 25290534 DOI: 10.1016/j.cgh.2014.09.047]

35 **Hollemans RA**, Bollen TL, van Brunschot S, Bakker OJ, Ahmed Ali U, van Goor H, Boermeester MA, Gooszen HG, Besselink MG, van Santvoort HC; Dutch Pancreatitis Study Group. Predicting Success of Catheter Drainage in Infected Necrotizing Pancreatitis. *Ann Surg* 2016; **263**: 787-792 [PMID: 25775071 DOI: 10.1097/SLA.0000000000001203]

36 **Garret C**, Douillard M, David A, Péré M, Quenehervé L, Legros L, Archambeaud I, Douane F, Lerhun M, Regenet N, Gournay J, Coron E, Frampas E, Reignier J. Infected pancreatic necrosis complicating severe acute pancreatitis in critically ill patients: predicting catheter drainage failure and need for necrosectomy. *Ann Intensive Care* 2022; **12**: 71 [PMID: 35916981 DOI: 10.1186/s13613-022-01039-z]

37 **Watanabe Y**, Mikata R, Yasui S, Ohyama H, Sugiyama H, Sakai Y, Tsuyuguchi T, Kato N. Short- and long-term results of endoscopic ultrasound-guided transmural drainage for pancreatic pseudocysts and walled-off necrosis. *World J Gastroenterol* 2017; **23**: 7110-7118 [PMID: 29093619 DOI: 10.3748/wjg.v23.i39.7110]

38 **Mukai S**, Itoi T, Sofuni A, Itokawa F, Kurihara T, Tsuchiya T, Ishii K, Tsuji S, Ikeuchi N, Tanaka R, Umeda J, Tonozuka R, Honjo M, Moriyasu F. Novel single transluminal gateway transcystic multiple drainages after EUS-guided drainage for complicated multilocular walled-off necrosis (with videos). *Gastrointest Endosc* 2014; **79**: 531-535 [PMID: 24287280 DOI: 10.1016/j.gie.2013.10.004]

39 **Varadarajulu S**, Phadnis MA, Christein JD, Wilcox CM. Multiple transluminal gateway technique for EUS-guided drainage of symptomatic walled-off pancreatic necrosis. *Gastrointest Endosc* 2011; **74**: 74-80 [PMID: 21612778 DOI: 10.1016/j.gie.2011.03.1122]

40 **Jain S**, Padhan R, Bopanna S, Jain SK, Dhingra R, Dash NR, Madhusudan KS, Gamanagatti SR, Sahni P, Garg PK. Percutaneous Endoscopic Step-Up Therapy Is an Effective Minimally Invasive Approach for Infected Necrotizing

Pancreatitis. *Dig Dis Sci* 2020; **65**: 615-622 [PMID: 31187325 DOI: 10.1007/s10620-019-05696-2]
41 **Zerem E**, Hauser G, Loga-Zec S, Kunosić S, Jovanović P, Crnkić D. Minimally invasive treatment of pancreatic pseudocysts. *World J Gastroenterol* 2015; **21**: 6850-6860 [PMID: 26078561 DOI: 10.3748/wjg.v21.i22.6850]
42 **Varadarajulu S**. A hybrid endoscopic technique for the treatment of walled-off pancreatic necrosis. *Am J Gastroenterol* 2013; **108**: 1015-1017 [PMID: 23735926 DOI: 10.1038/ajg.2013.113]
43 **Pérez-Cuadrado Robles E**, Ragot E, Alric H, Di Gaeta A, Benosman H, Cellier C, Rahmi G. Hybrid retroperitoneal necrosectomy using a triple-port approach under endoscopic guidance. *Rev Esp Enferm Dig* 2022; **114**: 694 [PMID: 35815789 DOI: 10.17235/reed.2022.9055/2022]
44 **Al-Sarireh B**, Mowbray NG, Al-Sarira A, Griffith D, Brown TH, Wells T. Can infected pancreatic necrosis really be managed conservatively? *Eur J Gastroenterol Hepatol* 2018; **30**: 1327-1331 [PMID: 30148805 DOI: 10.1097/MEG.0000000000001231]
45 **Boxhoorn L**, van Dijk SM, van Grinsven J, Verdonk RC, Boermeester MA, Bollen TL, Bouwense SAW, Bruno MJ, Cappendijk VC, Dejong CHC, van Duijvendijk P, van Eijck CHJ, Fockens P, Francken MFG, van Goor H, Hadithi M, Hallensleben NDL, Haveman JW, Jacobs MAJM, Jansen JM, Kop MPM, van Lienden KP, Manusama ER, Mieog JSD, Molenaar IQ, Nieuwenhuijs VB, Poen AC, Poley JW, van de Poll M, Quispel R, Römkens TEH, Schwartz MP, Seerden TC, Stommel MWJ, Straathof JWA, Timmerhuis HC, Venneman NG, Voermans RP, van de Vrie W, Witteman BJ, Dijkgraaf MGW, van Santvoort HC, Besselink MG; Dutch Pancreatitis Study Group. Immediate versus Postponed Intervention for Infected Necrotizing Pancreatitis. *N Engl J Med* 2021; **385**: 1372-1381 [PMID: 34614330 DOI: 10.1056/NEJMoa2100826]
46 **Isayama H**, Nakai Y, Rerknimitr R, Khor C, Lau J, Wang HP, Seo DW, Ratanachu-Ek T, Lakhtakia S, Ang TL, Ryozawa S, Hayashi T, Kawakami H, Yamamoto N, Iwashita T, Itokawa F, Kuwatani M, Kitano M, Hanada K, Kogure H, Hamada T, Ponnudurai R, Moon JH, Itoi T, Yasuda I, Irisawa A, Maetani I. Asian consensus statements on endoscopic management of walled-off necrosis. Part 2: Endoscopic management. *J Gastroenterol Hepatol* 2016; **31**: 1555-1565 [PMID: 27042957 DOI: 10.1111/jgh.13398]
47 **Yokoe M**, Takada T, Mayumi T, Yoshida M, Isaji S, Wada K, Itoi T, Sata N, Gabata T, Igarashi H, Kataoka K, Hirota M, Kadoya M, Kitamura N, Kimura Y, Kiriyama S, Shirai K, Hattori T, Takeda K, Takeyama Y, Sekimoto M, Shikata S, Arata S, Hirata K. Japanese guidelines for the management of acute pancreatitis: Japanese Guidelines 2015. *J Hepatobiliary Pancreat Sci* 2015; **22**: 405-432 [PMID: 25973947 DOI: 10.1002/jhbp.259]
48 **Rana SS**. An overview of walled-off pancreatic necrosis for clinicians. *Expert Rev Gastroenterol Hepatol* 2019; **13**: 331-343 [PMID: 30791769 DOI: 10.1080/17474124.2019.1574568]
49 **Xiao NJ**, Cui TT, Liu F, Li W. Invasive intervention timing for infected necrotizing pancreatitis: Late invasive intervention is not late for collection. *World J Clin Cases* 2022; **10**: 8057-8062 [PMID: 36159514 DOI: 10.12998/wjcc.v10.i23.8057]
50 **Rana SS**, Gupta R. Early transluminal drainage of pancreatic necrotic collections. *Gastrointest Endosc* 2020; **92**: 1136 [PMID: 33160492 DOI: 10.1016/j.gie.2020.05.038]
51 **Trikudanathan G**, Tawfik P, Amateau SK, Munigala S, Arain M, Attam R, Beilman G, Flanagan S, Freeman ML, Mallery S. Early (< 4 Weeks) Versus Standard (≥ 4 Weeks) Endoscopically Centered Step-Up Interventions for Necrotizing Pancreatitis. *Am J Gastroenterol* 2018; **113**: 1550-1558 [PMID: 30279466 DOI: 10.1038/s41395-018-0232-3]
52 **Walter D**, Will U, Sanchez-Yague A, Brenke D, Hampe J, Wollny H, López-Jamar JM, Jechart G, Vilmann P, Gornals JB, Ullrich S, Fähndrich M, de Tejada AH, Junquera F, Gonzalez-Huix F, Siersema PD, Vleggaar FP. A novel lumen-apposing metal stent for endoscopic ultrasound-guided drainage of pancreatic fluid collections: a prospective cohort study. *Endoscopy* 2015; **47**: 63-67 [PMID: 25268308 DOI: 10.1055/s-0034-1378113]
53 **Guzmán-Calderón E**, Chacaltana A, Díaz R, Li B, Martinez-Moreno B, Aparicio JR. Head-to-head comparison between endoscopic ultrasound guided lumen apposing metal stent and plastic stents for the treatment of pancreatic fluid collections: A systematic review and meta-analysis. *J Hepatobiliary Pancreat Sci* 2022; **29**: 198-211 [PMID: 34107170 DOI: 10.1002/jhbp.1008]
54 **Lakhtakia S**. The endoscopic ultrasound features of pancreatic fluid collections: appearances can be deceptive! *Endoscopy* 2022; **54**: 563-564 [PMID: 35381602 DOI: 10.1055/a-1782-7437]
55 **Abu Dayyeh BK**, Mukewar S, Majumder S, Zaghlol R, Vargas Valls EJ, Bazerbachi F, Levy MJ, Baron TH, Gostout CJ, Petersen BT, Martin J, Gleeson FC, Pearson RK, Chari ST, Vege SS, Topazian MD. Large-caliber metal stents versus plastic stents for the management of pancreatic walled-off necrosis. *Gastrointest Endosc* 2018; **87**: 141-149 [PMID: 28478030 DOI: 10.1016/j.gie.2017.04.032]
56 **Parsa N**, Nieto JM, Powers P, Mitsuhashi S, Abdelqader A, Hadzinakos G, Anderloni AA, Fugazza A, James TW, Arlt A, Ellrichmann M, Aparicio JR, Trindade AJ, Stevens TK, Chahal P, Shah SL, Messallam AA, Lang G, Fejleh MP, Benias PC, Sejpal DV, Jones J, Mir FF, Aghaie Meybodi M, Ichkhanian Y, Vosoughi K, Novikov AA, Irani SS, Pawa R, Ahmed AM, Sedarat A, Hsueh W, Hampe J, Sharaiha RZ, Berzin TM, Willingham FF, Kushnir VM, Brewer Gutierrez OI, Ngamruengphong S, Huggett MT, Baron TH, Repici A, Adler DG, Nasr JT, Kowalski TE, Kumbhari V, Singh VK, Khashab MA. Endoscopic ultrasound-guided drainage of pancreatic walled-off necrosis using 20-mm versus 15-mm lumen-apposing metal stents: an international, multicenter, case-matched study. *Endoscopy* 2020; **52**: 211-219 [PMID: 32000275 DOI: 10.1055/a-1096-3299]
57 **Park SW**, Lee SS. Which Are the Most Suitable Stents for Interventional Endoscopic Ultrasound? *J Clin Med* 2020; **9** [PMID: 33171627 DOI: 10.3390/jcm9113595]
58 **Nakai Y**, Oyama H, Kanai S, Noguchi K, Sato T, Hakuta R, Ishigaki K, Saito K, Saito T, Hamada T, Takahara N, Mizuno S, Kogure H, Isayama H, Koike K. Double Guidewire Technique Using an Uneven Double Lumen Catheter for Endoscopic Ultrasound-Guided Interventions. *Dig Dis Sci* 2021; **66**: 1540-1547 [PMID: 32436121 DOI: 10.1007/s10620-020-06345-9]
59 **Binmoeller KF**, Weilert F, Shah JN, Bhat YM, Kane S. Endosonography-guided transmural drainage of pancreatic pseudocysts using an exchange-free access device: initial clinical experience. *Surg Endosc* 2013; **27**: 1835-1839 [PMID: 23299130 DOI: 10.1007/s00464-012-2682-9]

60 **Lang GD**, Fritz C, Bhat T, Das KK, Murad FM, Early DS, Edmundowicz SA, Kushnir VM, Mullady DK. EUS-guided drainage of peripancreatic fluid collections with lumen-apposing metal stents and plastic double-pigtail stents: comparison of efficacy and adverse event rates. *Gastrointest Endosc* 2018; **87**: 150-157 [PMID: 28713067 DOI: 10.1016/j.gie.2017.06.029]

61 **Brimhall B**, Han S, Tatman PD, Clark TJ, Wani S, Brauer B, Edmundowicz S, Wagh MS, Attwell A, Hammad H, Shah RJ. Increased Incidence of Pseudoaneurysm Bleeding With Lumen-Apposing Metal Stents Compared to Double-Pigtail Plastic Stents in Patients With Peripancreatic Fluid Collections. *Clin Gastroenterol Hepatol* 2018; **16**: 1521-1528 [PMID: 29474970 DOI: 10.1016/j.cgh.2018.02.021]

62 **Bang JY**, Hasan MK, Navaneethan U, Sutton B, Frandah W, Siddique S, Hawes RH, Varadarajulu S. Lumen-apposing metal stents for drainage of pancreatic fluid collections: When and for whom? *Dig Endosc* 2017; **29**: 83-90 [PMID: 27199157 DOI: 10.1111/den.12681]

63 **Wang Z**, Zhao S, Meng Q, Wang S, Chen Y, Wang F, Li Q, Yao J, Du Y, Jin Z, Bai Y, Li Z, Wang D. Comparison of three different stents for endoscopic ultrasound-guided drainage of pancreatic fluid collection: A large retrospective study. *J Gastroenterol Hepatol* 2019; **34**: 791-798 [PMID: 30475420 DOI: 10.1111/jgh.14557]

64 **Shamah SP**, Sahakian AB, Chapman CG, Buxbaum JL, Muniraj T, Aslanian HA, Villa E, Cho J, Haider HI, Waxman I, Siddiqui UD. Double pigtail stent placement as an adjunct to lumen-apposing metal stentsfor drainage of pancreatic fluid collections may not affect outcomes: A multicenter experience. *Endosc Ultrasound* 2022; **11**: 53-58 [PMID: 35102901 DOI: 10.4103/EUS-D-21-00030]

65 **Chen YI**, Barkun AN, Adam V, Bai G, Singh VK, Bukhari M, Gutierrez OB, Elmunzer BJ, Moran R, Fayad L, El Zein M, Kumbhari V, Repici A, Khashab MA. Cost-effectiveness analysis comparing lumen-apposing metal stents with plastic stents in the management of pancreatic walled-off necrosis. *Gastrointest Endosc* 2018; **88**: 267-276.e1 [PMID: 29614262 DOI: 10.1016/j.gie.2018.03.021]

66 **Varadarajulu S**, Christein JD, Tamhane A, Drelichman ER, Wilcox CM. Prospective randomized trial comparing EUS and EGD for transmural drainage of pancreatic pseudocysts (with videos). *Gastrointest Endosc* 2008; **68**: 1102-1111 [PMID: 18640677 DOI: 10.1016/j.gie.2008.04.028]

67 **Kahaleh M**, Shami VM, Conaway MR, Tokar J, Rockoff T, De La Rue SA, de Lange E, Bassignani M, Gay S, Adams RB, Yeaton P. Endoscopic ultrasound drainage of pancreatic pseudocyst: a prospective comparison with conventional endoscopic drainage. *Endoscopy* 2006; **38**: 355-359 [PMID: 16680634 DOI: 10.1055/s-2006-925249]

68 **Yoo J**, Yan L, Hasan R, Somalya S, Nieto J, Siddiqui AA. Feasibility, safety, and outcomes of a single-step endoscopic ultrasonography-guided drainage of pancreatic fluid collections without fluoroscopy using a novel electrocautery-enhanced lumen-apposing, self-expanding metal stent. *Endosc Ultrasound* 2017; **6**: 131-135 [PMID: 28440239 DOI: 10.4103/2303-9027.204814]

69 **Mukai S**, Itoi T, Tsuchiya T, Tonozuka R, Yamamoto K, Sofuni A. New deployment techniques of the lumen-apposing metal stent in walled-off necrosis filled with necrotic tissue: Chick opening its mouth (with video). *Dig Endosc* 2021; **33**: 985-989 [PMID: 33991135 DOI: 10.1111/den.14016]

70 **De Angelis CG**, Venezia L, Cortegoso Valdivia P, Rizza S, Bruno M, Pellicano R. Lumen-apposing metal stents in management of pancreatic fluid collections: The nobody's land of removal timing. *Saudi J Gastroenterol* 2019; **25**: 335-340 [PMID: 31823862 DOI: 10.4103/sjg.SJG_166_19]

71 **Yasuda I**, Takahashi K. Endoscopic management of walled-off pancreatic necrosis. *Dig Endosc* 2021; **33**: 335-341 [PMID: 32306430 DOI: 10.1111/den.13699]

72 **Arvanitakis M**, Delhaye M, Bali MA, Matos C, De Maertelaer V, Le Moine O, Devière J. Pancreatic-fluid collections: a randomized controlled trial regarding stent removal after endoscopic transmural drainage. *Gastrointest Endosc* 2007; **65**: 609-619 [PMID: 17324413 DOI: 10.1016/j.gie.2006.06.083]

73 **Trevino JM**, Tamhane A, Varadarajulu S. Successful stenting in ductal disruption favorably impacts treatment outcomes in patients undergoing transmural drainage of peripancreatic fluid collections. *J Gastroenterol Hepatol* 2010; **25**: 526-531 [PMID: 20074158 DOI: 10.1111/j.1440-1746.2009.06109.x]

74 **Donatsky AM**. Assessing transgastric Natural Orifice Transluminal Endoscopic Surgery prior to clinical implementation. *Dan Med J* 2014; **61**: B4903 [PMID: 25162448]

75 **Yang J**, Zeng Y, Zhang J. Endoscopic submucosal dissection-based suture combined with medical adhesive for complicated tuberculous bronchoesophageal fistula: a case report. *J Int Med Res* 2022; **50**: 3000605221080723 [PMID: 35225721 DOI: 10.1177/03000605221080723]

76 **Manrai M**, Kochhar R, Gupta V, Yadav TD, Dhaka N, Kalra N, Sinha SK, Khandelwal N. Outcome of Acute Pancreatic and Peripancreatic Collections Occurring in Patients With Acute Pancreatitis. *Ann Surg* 2018; **267**: 357-363 [PMID: 27805963 DOI: 10.1097/SLA.0000000000002065]

77 **Mouli VP**, Sreenivas V, Garg PK. Efficacy of conservative treatment, without necrosectomy, for infected pancreatic necrosis: a systematic review and meta-analysis. *Gastroenterology* 2013; **144**: 333-340.e2 [PMID: 23063972 DOI: 10.1053/j.gastro.2012.10.004]

78 **Sarathi Patra P**, Das K, Bhattacharyya A, Ray S, Hembram J, Sanyal S, Dhali GK. Natural resolution or intervention for fluid collections in acute severe pancreatitis. *Br J Surg* 2014; **101**: 1721-1728 [PMID: 25329330 DOI: 10.1002/bjs.9666]

79 **Iwashita T**, Iwata K, Hamada T, Saito T, Shiomi H, Takenaka M, Maruta A, Uemura S, Masuda A, Matsubara S, Mukai T, Takahashi S, Hayashi N, Isayama H, Yasuda I, Nakai Y. Supportive treatment during the periprocedural period of endoscopic treatment for pancreatic fluid collections: a critical review of current knowledge and future perspectives. *J Gastroenterol* 2023; **58**: 98-111 [PMID: 36342540 DOI: 10.1007/s00535-022-01935-y]

80 **Fabbri C**, Luigiano C, Lisotti A, Cennamo V, Virgilio C, Caletti G, Fusaroli P. Endoscopic ultrasound-guided treatments: are we getting evidence based--a systematic review. *World J Gastroenterol* 2014; **20**: 8424-8448 [PMID: 25024600 DOI: 10.3748/wjg.v20.i26.8424]

81 **Rattner DW**, Hawes R, Schwaitzberg S, Kochman M, Swanstrom L. The Second SAGES/ASGE White Paper on natural orifice transluminal endoscopic surgery: 5 years of progress. *Surg Endosc* 2011; **25**: 2441-2448 [PMID: 21359881 DOI: 10.1007/s00464-011-1605-5]

82 **Abdelhafez M**, Elnegouly M, Hasab Allah MS, Elshazli M, Mikhail HM, Yosry A. Transluminal retroperitoneal endoscopic necrosectomy with the use of hydrogen peroxide and without external irrigation: a novel approach for the treatment of walled-off pancreatic necrosis. *Surg Endosc* 2013; **27**: 3911-3920 [PMID: 23584819 DOI: 10.1007/s00464-013-2948-x]

83 **van Brunschot S**, van Grinsven J, Voermans RP, Bakker OJ, Besselink MG, Boermeester MA, Bollen TL, Bosscha K, Bouwense SA, Bruno MJ, Cappendijk VC, Consten EC, Dejong CH, Dijkgraaf MG, van Eijck CH, Erkelens GW, van Goor H, Hadithi M, Haveman JW, Hofker SH, Jansen JJ, Laméris JS, van Lienden KP, Manusama ER, Meijssen MA, Mulder CJ, Nieuwenhuis VB, Poley JW, de Ridder RJ, Rosman C, Schaapherder AF, Scheepers JJ, Schoon EJ, Seerden T, Spanier BW, Straathof JW, Timmer R, Venneman NG, Vleggaar FP, Witteman BJ, Gooszen HG, van Santvoort HC, Fockens P; Dutch Pancreatitis Study Group. Transluminal endoscopic step-up approach versus minimally invasive surgical step-up approach in patients with infected necrotising pancreatitis (TENSION trial): design and rationale of a randomised controlled multicenter trial [ISRCTN09186711]. *BMC Gastroenterol* 2013; **13**: 161 [PMID: 24274589 DOI: 10.1186/1471-230X-13-161]

84 **van Brunschot S**, Hollemans RA, Bakker OJ, Besselink MG, Baron TH, Beger HG, Boermeester MA, Bollen TL, Bruno MJ, Carter R, French JJ, Coelho D, Dahl B, Dijkgraaf MG, Doctor N, Fagenholz PJ, Farkas G, Castillo CFD, Fockens P, Freeman ML, Gardner TB, Goor HV, Gooszen HG, Hannink G, Lochan R, McKay CJ, Neoptolemos JP, Oláh A, Parks RW, Peev MP, Raraty M, Rau B, Rösch T, Rovers M, Seifert H, Siriwardena AK, Horvath KD, van Santvoort HC. Minimally invasive and endoscopic versus open necrosectomy for necrotising pancreatitis: a pooled analysis of individual data for 1980 patients. *Gut* 2018; **67**: 697-706 [PMID: 28774886 DOI: 10.1136/gutjnl-2016-313341]

85 **Boxhoorn L**, Besselink MG, Voermans RP; Dutch Pancreatitis Study Group. Surgery Versus Endoscopy for Infected Necrotizing Pancreatitis: A Fair Comparison? *Gastroenterology* 2019; **157**: 583-584 [PMID: 31103626 DOI: 10.1053/j.gastro.2019.03.073]

86 **Bang JY**, Wilcox CM, Hawes R, Varadarajulu S. Outcomes of a Structured, Stepwise Approach to Endoscopic Necrosectomy. *J Clin Gastroenterol* 2021; **55**: 631-637 [PMID: 32657959 DOI: 10.1097/MCG.0000000000001392]

87 **Sleeman D**, Levi DM, Cheung MC, Rahnemai-Azar A, Parisek S, Casillas V, Echenique A, Yrizarri J, Guerra JJ, Levi JU, Livingstone AS. Percutaneous lavage as primary treatment for infected pancreatic necrosis. *J Am Coll Surg* 2011; **212**: 748-52; discussion 752 [PMID: 21463827 DOI: 10.1016/j.jamcollsurg.2010.12.019]

88 **Schmidt PN**, Novovic S, Roug S, Feldager E. Endoscopic, transmural drainage and necrosectomy for walled-off pancreatic and peripancreatic necrosis is associated with low mortality--a single-center experience. *Scand J Gastroenterol* 2015; **50**: 611-618 [PMID: 25648776 DOI: 10.3109/00365521.2014.946078]

89 **Mukai S**, Itoi T, Sofuni A, Itokawa F, Kurihara T, Tsuchiya T, Ishii K, Tsuji S, Ikeuchi N, Tanaka R, Umeda J, Tonozuka R, Honjo M, Gotoda T, Moriyasu F. Expanding endoscopic interventions for pancreatic pseudocyst and walled-off necrosis. *J Gastroenterol* 2015; **50**: 211-220 [PMID: 24756577 DOI: 10.1007/s00535-014-0957-8]

90 **Gornals JB**, Consiglieri CF, Busquets J, Salord S, de-la-Hera M, Secanella L, Redondo S, Pelaez N, Fabregat J. Endoscopic necrosectomy of walled-off pancreatic necrosis using a lumen-apposing metal stent and irrigation technique. *Surg Endosc* 2016; **30**: 2592-2602 [PMID: 26335077 DOI: 10.1007/s00464-015-4505-2]

91 **Thompson CC**, Kumar N, Slattery J, Clancy TE, Ryan MB, Ryou M, Swanson RS, Banks PA, Conwell DL. A standardized method for endoscopic necrosectomy improves complication and mortality rates. *Pancreatology* 2016; **16**: 66-72 [PMID: 26748428 DOI: 10.1016/j.pan.2015.12.001]

92 **Lariño-Noia J**, de la Iglesia-García D, González-Lopez J, Díaz-Lopez J, Macías-García F, Mejuto R, Quiroga A, Mauriz V, Jardí A, Iglesias-García J, Domínguez-Muñoz JE. Endoscopic drainage with local infusion of antibiotics to avoid necrosectomy of infected walled-off necrosis. *Surg Endosc* 2021; **35**: 644-651 [PMID: 32076856 DOI: 10.1007/s00464-020-07428-4]

93 **Powers PC**, Siddiqui A, Sharaiha RZ, Yang G, Dawod E, Novikov AA, Javia A, Edirisuriya C, Noor A, Mumtaz T, Iqbal U, Loren DE, Kowalski TE, Cosgrove N, Alicea Y, Tyberg A, Andalib I, Kahaleh M, Adler DG. Discontinuation of proton pump inhibitor use reduces the number of endoscopic procedures required for resolution of walled-off pancreatic necrosis. *Endosc Ultrasound* 2019; **8**: 194-198 [PMID: 30719997 DOI: 10.4103/eus.eus_59_18]

94 **Garg R**, Gupta S, Singh A, Simonson MT, Rustagi T, Chahal P. Hydrogen peroxide assisted endoscopic necrosectomy for walled-off pancreatic necrosis: A systematic review and meta-analysis. *Pancreatology* 2021; **21**: 1540-1547 [PMID: 34565668 DOI: 10.1016/j.pan.2021.09.007]

95 **Günay S**, Paköz B, Çekiç C, Çamyar H, Alper E, Yüksel ES, Topal F, Binicier ÖB. Evaluation of hydrogen peroxide-assisted endoscopic ultrasonography-guided necrosectomy in walled-off pancreatic necrosis: A single-center experience. *Medicine (Baltimore)* 2021; **100**: e23175 [PMID: 33545925 DOI: 10.1097/MD.0000000000023175]

96 **Maharshi S**, Sharma SS, Ratra S, Sapra B, Sharma D. Management of walled-off necrosis with nasocystic irrigation with hydrogen peroxide versus biflanged metal stent: randomized controlled trial. *Endosc Int Open* 2021; **9**: E1108-E1115 [PMID: 34222637 DOI: 10.1055/a-1480-7115]

97 **Bhargava MV**, Rana SS, Gorsi U, Kang M, Gupta R. Assessing the Efficacy and Outcomes Following Irrigation with Streptokinase Versus Hydrogen Peroxide in Necrotizing Pancreatitis: A Randomized Pilot Study. *Dig Dis Sci* 2022; **67**: 4146-4153 [PMID: 34405362 DOI: 10.1007/s10620-021-07201-0]

98 **Brand M**, Hofmann N, Ho CN, Meining A. The over-the-scope grasper (OTSG). *Endoscopy* 2021; **53**: 152-155 [PMID: 32458998 DOI: 10.1055/a-1187-0178]

99 **Stassen PMC**, de Jonge PJF, Bruno MJ, Koch AD, Trindade AJ, Benias PC, Sejpal DV, Siddiqui UD, Chapman CG, Villa E, Tharian B, Inamdar S, Hwang JH, Barakat MT, Andalib I, Gaidhane M, Sarkar A, Shahid H, Tyberg A, Binmoeller K, Watson RR, Nett A, Schlag C, Abdelhafez M, Friedrich-Rust M, Schlachterman A, Chiang AL, Loren D, Kowalski T, Kahaleh M. Safety and efficacy of a novel resection system for direct endoscopic necrosectomy of walled-off pancreas necrosis: a prospective, international, multicenter trial. *Gastrointest Endosc* 2022; **95**: 471-479 [PMID: 34562471 DOI: 10.1016/j.gie.2021.09.025]

100 **Yachimski P**, Landewee CA, Campisano F, Valdastri P, Obstein KL. The waterjet necrosectomy device for endoscopic management of pancreatic necrosis: design, development, and preclinical testing (with videos). *Gastrointest Endosc* 2020;

92: 770-775 [PMID: 32334018 DOI: 10.1016/j.gie.2020.04.024]
101 **Case BM**, Jensen KK, Bakis G, Enestvedt BK, Shaaban AM, Foster BR. Endoscopic Interventions in Acute Pancreatitis: What the Advanced Endoscopist Wants to Know. *Radiographics* 2018; **38**: 2002-2018 [PMID: 30265612 DOI: 10.1148/rg.2018180066]
102 **Jiang TA**, Xie LT. Algorithm for the multidisciplinary management of hemorrhage in EUS-guided drainage for pancreatic fluid collections. *World J Clin Cases* 2018; **6**: 308-321 [PMID: 30283794 DOI: 10.12998/wjcc.v6.i10.308]
103 **Wang BH**, Xie LT, Zhao QY, Ying HJ, Jiang TA. Balloon dilator controls massive bleeding during endoscopic ultrasound-guided drainage for pancreatic pseudocyst: A case report and review of literature. *World J Clin Cases* 2018; **6**: 459-465 [PMID: 30294611 DOI: 10.12998/wjcc.v6.i11.459]
104 **Simons-Linares CR**, Chittajallu V, Chahal P. Stent gone rogue: endoscopic removal of a 3-year-old embedded cystogastrostomy stent. *VideoGIE* 2020; **5**: 548-551 [PMID: 33204913 DOI: 10.1016/j.vgie.2020.06.003]
105 **Bomman S**, Sanders D, Coy D, La Selva D, Pham Q, Zehr T, Law J, Larsen M, Irani S, Kozarek RA, Ross A, Krishnamoorthi R. Safety and clinical outcomes of early dual modality drainage (< 28 days) compared to later drainage of pancreatic necrotic fluid collections: a propensity score-matched study. *Surg Endosc* 2023; **37**: 902-911 [PMID: 36038648 DOI: 10.1007/s00464-022-09561-8]
106 **Bang JY**, Hawes RH, Varadarajulu S. Lumen-apposing metal stent placement for drainage of pancreatic fluid collections: predictors of adverse events. *Gut* 2020; **69**: 1379-1381 [PMID: 32066622 DOI: 10.1136/gutjnl-2019-320539]
107 **Holmes I**, Shinn B, Mitsuhashi S, Boortalary T, Bashir M, Kowalski T, Loren D, Kumar A, Schlachterman A, Chiang A. Prediction and management of bleeding during endoscopic necrosectomy for pancreatic walled-off necrosis: results of a large retrospective cohort at a tertiary referral center. *Gastrointest Endosc* 2022; **95**: 482-488 [PMID: 34678298 DOI: 10.1016/j.gie.2021.10.015]
108 **Facciorusso A**, Amato A, Crinò SF, Sinagra E, Maida M, Fugazza A, Binda C, Repici A, Tarantino I, Anderloni A, Fabbri C; i-EUS Group. Nomogram for prediction of adverse events after lumen-apposing metal stent placement for drainage of pancreatic fluid collections. *Dig Endosc* 2022; **34**: 1459-1470 [PMID: 35599610 DOI: 10.1111/den.14354]
109 **Smith ZL**, Gregory MH, Elsner J, Alajlan BA, Kodali D, Hollander T, Sayuk GS, Lang GD, Das KK, Mullady DK, Early DS, Kushnir VM. Health-related quality of life and long-term outcomes after endoscopic therapy for walled-off pancreatic necrosis. *Dig Endosc* 2019; **31**: 77-85 [PMID: 30152143 DOI: 10.1111/den.13264]
110 **Elmunzer BJ**. Endoscopic Drainage of Pancreatic Fluid Collections. *Clin Gastroenterol Hepatol* 2018; **16**: 1851-1863.e3 [PMID: 29601903 DOI: 10.1016/j.cgh.2018.03.021]
111 **Rosenberg A**, Steensma EA, Napolitano LM. Necrotizing pancreatitis: new definitions and a new era in surgical management. *Surg Infect (Larchmt)* 2015; **16**: 1-13 [PMID: 25761075 DOI: 10.1089/sur.2014.123]
112 **Maatman TK**, Zyromski NJ. Management of Necrotizing Pancreatitis. *Adv Surg* 2022; **56**: 13-35 [PMID: 36096565 DOI: 10.1016/j.yasu.2022.02.010]
113 **Qiu J**, Wei T. Immediate or Postponed Intervention for Infected Necrotizing Pancreatitis. *N Engl J Med* 2022; **386**: 402-403 [PMID: 35081290 DOI: 10.1056/NEJMc2117813]

World Journal of Clinical Cases

Submit a Manuscript: https://www.f6publishing.com

World J Clin Cases 2023 March 26; 11(9): 1903-1917

DOI: 10.12998/wjcc.v11.i9.1903

ISSN 2307-8960 (online)

MINIREVIEWS

Functional role of frontal electroencephalogram alpha asymmetry in the resting state in patients with depression: A review

Yu-Hong Xie, Ye-Min Zhang, Fan-Fan Fan, Xi-Yan Song, Lei Liu

Specialty type: Psychiatry

Provenance and peer review: Invited article; Externally peer reviewed.

Peer-review model: Single blind

Peer-review report's scientific quality classification

Grade A (Excellent): A
Grade B (Very good): B
Grade C (Good): 0
Grade D (Fair): D
Grade E (Poor): 0

P-Reviewer: Radhakrishnan R, New Zealand; Sobanski T, Germany; Zhao X, China

Received: November 23, 2022
Peer-review started: November 23, 2022
First decision: January 17, 2023
Revised: February 10, 2023
Accepted: March 1, 2023
Article in press: March 1, 2023
Published online: March 26, 2023

Yu-Hong Xie, Ye-Min Zhang, Fan-Fan Fan, Xi-Yan Song, Lei Liu, Psychology College of Teacher Education, Center of Group Behavior and Social Psychological Service, Ningbo University, Ningbo 315211, Zhejiang Province, China

Corresponding author: Lei Liu, PhD, Associate Professor, Psychology College of Teacher Education, Center of Group Behavior and Social Psychological Service, Ningbo University, No. 818 Fenghua Street, Ningbo 315211, Zhejiang Province, China. liulei@nbu.edu.cn

Abstract

Depression is a psychological disorder that affects the general public worldwide. It is particularly important to make an objective and accurate diagnosis of depression, and the measurement methods of brain activity have gradually received increasing attention. Resting electroencephalogram (EEG) alpha asymmetry in patients with depression shows changes in activation of the alpha frequency band of the left and right frontal cortices. In this paper, we review the findings of the relationship between frontal EEG alpha asymmetry in the resting state and depression. Based on worldwide studies, we found the following: (1) Compared with individuals without depression, those with depression showed greater right frontal EEG alpha asymmetry in the resting state. However, the pattern of frontal EEG alpha asymmetry in the resting state in depressive individuals seemed to disappear with age; (2) Compared with individuals without maternal depression, those with maternal depression showed greater right frontal EEG alpha asymmetry in the resting state, which indicated that genetic or experience-based influences have an impact on frontal EEG alpha asymmetry at rest; and (3) Frontal EEG alpha asymmetry in the resting state was stable, and little or no change occurred after antidepressant treatment. Finally, we concluded that the contrasting results may be due to differences in methodology, clinical characteristics, and participant characteristics.

Key Words: Depression; Frontal electroencephalogram alpha asymmetry; Frontal asymmetry; Resting state; Neurological indicator

Core Tip: Researchers have paid more attention to the functional role of frontal electroencephalogram alpha asymmetry (FAA) in the resting state in individuals with depression. In this paper, we review the findings of the relationship between FAA in the resting state and depression. Individuals with clinical depression showed greater right FAA in the resting state. The pattern of FAA in the resting state in individuals with clinical depression seemed to disappear with age. Individuals with maternal depression showed greater right FAA in the resting state. There was little or no change in FAA in the resting state after antidepressant treatment.

Citation: Xie YH, Zhang YM, Fan FF, Song XY, Liu L. Functional role of frontal electroencephalogram alpha asymmetry in the resting state in patients with depression: A review. *World J Clin Cases* 2023; 11(9): 1903-1917
URL: https://www.wjgnet.com/2307-8960/full/v11/i9/1903.htm
DOI: https://dx.doi.org/10.12998/wjcc.v11.i9.1903

INTRODUCTION

Depression is a leading cause of disability worldwide and contributes greatly to the global burden of disease. It is characterized by persistent sadness and a lack of interest or pleasure in previously rewarding or enjoyable activities, affecting daily life and even suicide in extreme cases[1]. Currently, depression affects more than 350 million people worldwide, and the growth rate of patients with depression has been approximately 18% in the past decade[1]. There are currently 95 million people suffering from depression in China, and approximately 280000 people commit suicide each year, 40% of whom suffer from depression[2]. The diagnosis rate of depression among adolescents in 2020 was 24.6%; the proportion of major depression was 7.4%[3]. The diagnosis of depression is usually carried out using clinical interviews conducted around the diagnostic classification system, such as the 11th edition of the International Classification of Diseases (ICD-11) and the 5th edition of the Diagnostic and Statistical Manual of Mental Disorders (DSM-V). These diagnostic criteria are usually based on oral reports from patients or their families and direct observations by clinicians because each disease type has its own symptoms, including behavioural, cognitive, emotional, or physical disorders. However, these diagnostic methods incorporate a "yes or no" approach in the diagnosis of depression, and self-reporting and clinical observation methods are highly subjective, which leads to errors in the diagnosis of depression. Therefore, there is currently a lack of objective examination methods for depression.

Objective measurement of depression has always been a focus of researchers, and the measurement methods of brain activity have gradually received increasing attention[4]. Among these methods, frontal electroencephalogram (EEG) alpha asymmetry is a promising measurement method[5]. In the past 30 years, research on the relationship between frontal EEG alpha asymmetry and mood, personality, and neuropsychological diseases has developed rapidly. There are two types of frontal EEG alpha asymmetry: frontal EEG alpha asymmetry in the resting state and frontal EEG alpha asymmetry during tasking conditions with emotional challenges[6]. The frontal EEG alpha asymmetry at rest is associated with various trait-like individual differences. It is also called trait frontal EEG alpha asymmetry. Frontal EEG alpha asymmetry in tasking conditions is related to the operation that is designed to affect the individual's emotional state and is labelled state frontal EEG alpha asymmetry[7]. According to previous studies, researchers have paid more attention to the functional role of frontal EEG alpha asymmetry in the resting state in individuals with depression[8].

Frontal EEG alpha asymmetry at rest shows differences in activation of the alpha frequency band of the left and right frontal cortices[9,10]. Related studies have shown that there is an inverse relationship between the activity of the alpha wave and the activity of the cerebral cortex. For example, research has shown that when the underlying cortex system is active, the alpha wave tends to decrease[11,12]. Frontal EEG alpha asymmetries are usually calculated by subtracting the EEG power in the right frontal cortices from the EEG power in the left frontal cortices. However, different researchers may use different methods of calculation. The first equation uses the channel "F4" and "F3" to refer to the levels of alpha power on the right and left frontal areas of the scalp, respectively, around the F4 and F3 positions on the 10-20 electrode placement system. These equations are used to compute frontal alpha asymmetry (FAA) by determining the difference or ratio between alpha power values at F3 and F4. There are two commonly used equations to calculate FAA in the literature. The majority of developmental studies employ the difference between the natural logarithm (ln) of absolute power at F4 and F3, which is expressed as ln(F4) – ln(F3)[13]. The second equation commonly used for computing frontal alpha asymmetry (FAA) involves taking the ratio of the difference between the alpha power levels in the left and right frontal hemispheres to their sum, expressed as (F4 - F3)/(F3 + F4). This approach is believed to normalize the difference value[14]. A less common third method is to log-transform the ratio, yielding [ln(F4)–ln(F3)]/[ln(F3) + ln(F4)][15]. Another approach to FAA calculation involves using relative frontal alpha power, which is determined by computing the percentage of alpha band power relative to

the total power across all frequency bands[16]. Relative power may have advantages over absolute power in evaluating paediatric populations due to its improved test-retest reliability[17] and ability to detect changes in the frequency composition of EEGs during development[18]. Recently, Harrewijn *et al* [19] introduced a fourth method to calculate FAA, which involves computing the difference between the natural logarithm of the relative power in both hemispheres, expressed as ln[rel(F4)] - ln[rel(F3)].

To explore whether frontal EEG alpha asymmetry in the resting state is a reliable and useful index for understanding depression, this article reviews the research on the relationship between frontal EEG alpha asymmetry in the resting state and depression. First, we reviewed the pattern of frontal EEG alpha asymmetry in the resting state of clinically depressed individuals. Second, we reviewed the pattern of frontal EEG alpha asymmetry in the resting state of children inherited from generation to generation (parents suffering from depression). Third, we discussed whether frontal EEG alpha asymmetry in the resting state can be used as an effective indicator of depression intervention. Finally, we summarized the reasons for the inconsistent results.

CLINICAL RESEARCH

Table 1 provides the comparison of methods in studies on the pattern of frontal EEG alpha asymmetry in the resting state of clinically depressed individuals. Many studies have investigated the pattern of frontal EEG alpha asymmetry in the resting state in depressed individuals compared with nondepressed individuals. For example, Henriques and Davidson revealed that participants who have depression at early ages have greater right frontal lobe activation than nondepressed participants[20]. Furthermore, many studies have found that there was less left frontal lobe activation in participants with depression [21-34], in previously depressed subjects[28], and in a sample of individuals with a history of childhood-onset depression compared to that in healthy controls[35]. However, there were also some contradictory results over the years. For example, asymmetry differences were not found between depressed individuals and nondepressed individuals[36-38]. In addition, Quinn *et al*[39] examined the pattern of frontal EEG alpha asymmetry in the resting state of depressed patients with nonmelancholia, depressed patients with melancholia and control participants. The results found that compared with depressed patients with melancholia and healthy participants, depressed patients with nonmelancholia showed larger left frontal lobe activation. Smith *et al*[32] examined the frontal EEG alpha asymmetry patterns in patients with lifetime depression, current depression, and healthy controls in the resting state. The results indicated that reduced relative activity in the left frontal brain region may be associated with an increased risk of major depressive disorder (MDD). These findings extend previous research by demonstrating that the sources of surface asymmetry associated with a history of depression are likely linked to asymmetry in the dorsal-lateral frontal regions of the brain. Furthermore, decreased motivation for activating motor scripts in the premotor regions and the precentral gyrus may be pertinent to depression, and decreased left frontal brain activity can predict a lifetime history of depression[33].

Furthermore, some studies have examined whether frontal EEG alpha asymmetry in the resting state is a stable measurement index in depressed individuals. Allen *et al*[11] investigated the short-term stability of frontal EEG alpha asymmetry in the resting state in female patients with depression. The results showed that in an 8-wk and 16-wk interval, the score of frontal EEG alpha asymmetry at resting state had high internal consistency and stability, and changes in asymmetry scores were not related to changes in clinical depression. Moreover, Vuga *et al*[40] compared the long-term stability (1 to 3 years) of frontal EEG alpha asymmetry at rest between depression patients and healthy individuals. The results demonstrated that for depression patients and healthy individuals, frontal EEG alpha asymmetry at rest was moderately stable, in which gender, the history of individual depression, the severity of depression characteristics in the post-test, and the degree of change in the severity of depression were not related to the stability of frontal EEG alpha asymmetry. In addition, Gold *et al*[41] aimed to investigate the extent to which frontal EEG alpha asymmetry at rest was an effective and reliable neurological indicator for diagnosing the severity of depression in adults. The results showed that in a 3-month interval, the correlation between the scores of frontal EEG alpha asymmetry in the resting state and psychiatric examination was mostly small and not statistically significant. Similarly, McFarland *et al*[42] also found that frontal EEG alpha asymmetry in the resting state did not predict the course of depression at six months. Therefore, these results concluded that frontal EEG alpha asymmetry in the resting state was stable over time, and its potential as a predictive biomarker for depressive symptoms remains unclear.

Most people with depression suffer from depression in childhood[43]. The study of frontal EEG alpha asymmetry in the resting state in children with major depression may reveal the biological relevance of the early development of the underlying chronic disease. Kentgen *et al*[44] investigated frontal EEG alpha asymmetry at rest in adolescents with depression compared to developing controls. The results showed that there was no significant difference in frontal EEG alpha asymmetry in the resting state between adolescents with depression and developing controls. Feldmann *et al*[45] aimed to extend previous findings and assess frontal EEG alpha asymmetry in the resting state in a major depressive

Table 1 The comparison of methods in studies on asymmetry pattern at resting state of clinically depressed individuals

Ref.	Sample		Age (yr)		% female	Diagnosis of depression	EEG detail			
	Experimental group	Control group	Experimental group	Control group			Reference montage	EO/EC	Recording length (min)	Alpha range (Hz)
Henriques *et al* [20], 1991	EG: 15 depressed subjects	CG: 13 healthy controls	M = 40.40 (depressed subjects)	M = 40.61 (HCs)	60.7	SADS	CZ; AE; AR	E0+EC	1	8–13
Baehr *et al*[21], 1998	EG: 13 MDD	CG: 11 healthy controls	M = 43.50 (MDD)	M = 44.20 (HCs)		DSM-IV; BDI	Cz	EC	5	8–13
Beeney *et al* [22], 2014	EG: 13 MDD	CG: 21 healthy controls	M = 32.12 (MDD)	M = 27.78 (HCs)	100	DSM–IV; SCID	AL	E0+EC	8	8–13
Bruder *et al* [23], 1997	EG: 44 MDD (19 with and 25 without an anxiety disorder)	CG: 26 healthy controls	MDD with an anxiety disorder: M = 36.70; MDD without an anxiety disorder: M = 41.30	M = 32.90 (HCs)	50	DSM-III-R	NR	E0+EC	6	7.8–12.5
Cantisani *et al* [24], 2016	EG: 20 depressed subjects	CG: 19 healthy controls	M = 43.30 (depressed subjects)	M = 41.05 (HCs)	53.8	SCID; DSM-IV-TR	CA		6	8–12.5
Dharmadhikari *et al*[25], 2019	EG: 24 MDD	CG: 17 healthy controls	M = 34.82 (MDD)	M = 29.52 (HCs)	63.4	DSM-IV	auricle	EC	10	8--13
Gordon *et al* [26], 2010	EG: 92 MDD	CG: 1908 healthy controls			58.7	DSM-IV	AR	E0+EC	4	8–13
Gotlib[27], 1998	EG: 16 currently depressed, 31 previously depressed	CG: 30 never depressed				SCID	Cz	E0+EC	8	8–13
Jaworska *et al* [28], 2012	EG: 53 MDD	CG: 43 healthy controls				DSM-IV-TR; SCID-IV-I/P; HAMD; MADRS	AM; CZ; AR	E0+EC	6	8–13
Kemp *et al*[29], 2010	EG: 15 MDD	CG: 15 healthy controls	M = 39.90 (MDD)	M = 42.40 (HCs)	60	MINI; DASS	AM	EC	2	8–13
Koo *et al*[30], 2019	EG: 20 MDD	CG: 20 healthy controls	M = 51.05 (MDD)	M = 47.15 (HCs)		ICD-10/DSM IV	AE	EC	10	8–13
Roh *et al*[31], 2020	EG: 44 MDD without Suicidal ideation, 23 MDD with suicidal ideation	CG: 60 healthy controls	M = 39.30 (MDD); M = 37.48 (MDD with SI)	M = 34.83 (HCs)	85	DSM-IV	ECC	EO	3	8–12
Stewart *et al* [32], 2010	EG: 143 MDD	CG: 163 healthy controls	M = 19.10 (MDD)		69	DSM-IV	CSD; Cz; LM	E0+EC	8	8–13
Cai *et al*[34], 2020	EG: 24 MDD	CG: 22 healthy controls				DSM-IV; MINI	Cz	EC	5	8–14
Nusslock *et al* [35], 2018	EG: 37 depression, 18 anxiety + depression	CG: 69 healthy controls				SCID	AM	E0+EC	6	8–13
Brzezicka *et al* [36], 2017	EG: 26 MDD	CG: 26 healthy controls	M = 28.00 (MDD)	M = 24.90 (HCs)			CSD	EC	5	8–13

Jang *et al*[37], 2020	EG: 20 MDD, 18 patients with schizophrenia	CG: 16 healthy controls	M = 42.60 (MDD); M = 32.00 (MDD with schizophrenia)	M = 37.75 (HCs)	48.1	DSM-IV; MINI	BM	E0+EC	5	8–12
Segrave *et al* [38], 2011	EG: 16 MDD	CG: 18 healthy controls	M = 40.75 (MDD)	M = 42.11 (HCs)	100	DSM-IV	Cz; CA	E0+EC	6	8–13
Quinn *et al*[39], 2014	EG: 117 MDD	CG: 120 healthy controls				MINI; DSM-IV	AR; ER	EC	2	8–13
Smith *et al*[99], 2018	EG:143 lifetime MDD, 62 current MDD	CG: 163 healthy control			69	BDI; SCID	Cz	E0+EC	8	8–13
Vuga *et al*[40], 2006	EG: 49 childhood onset MDD	CG: 50 healthy controls	19-34	19-39	66.7	DSM-IV	Cz	E0+EC	6	7.5–12.5; alpha 1 (7.5–10.5); alpha 2 (10.5–12.5)
Gold *et al*[41], 2013	EG: 79 adults with depression		M= 35.60		78.5	DSM-III-R; SCID; MADRS	ALM	EC	5	8–12
McFarland *et al* [42], 2006	EG: 67 MDD		M = 34.64		65.7	SCID	LE	E0+EC	6	8–13
Kentgen *et al* [44], 2000	EG: 25 right-handed female outpatients	CG: 10 healthy controls			100	DSM-IV	NR	E0+EC	6	7.8--12.5
Feldmann *et al* [45], 2018	EG: 16 adolescents with depression	CG: 34 healthy controls	M = 16.08	M = 15.67	72.6	ICD-10; BDI	Cz; Mastoids; AE	E0+EC	8	7.5–13
Grünewald *et al* [46], 2018	EG: 20 adolescents (12–17 yr) with unipolar depression (12 with fifirst episode, 8 with recurrent depression)	CG: 31 healthy controls	M = 14.85 (unipolar depression)	M = 14.16 (HCs)	60.8	DSM-IV; ICD-10	AR		5	7.5–13.5
Deslandes *et al* [89], 2008	EG: 22 depressed subjects	CG: 14 healthy controls	M = 71.60 (depressed subjects)	M = 72.40 (HCs)	94	DSM-IV	ER	E0+EC	8	8–13
Kaiser *et al*[50], 2018	EG: 14 depression, 11 anxiety + depression	CG: 14 healthy controls	M = 78.60 (anxiety + depression); m = 80.50 (depression)	M = 80.90 (HCs)	100	GDS; HADS	RLMB	E0+EC	4	6.9–12.9
Carvalho *et al* [51], 2011	EG: 12 depressed subjects, 8 remitted subjects	CG: 7 non-depresse elderly subjects			66.7	DSM-IV	Earlobes	EC	8	8–12.9

EC: Eyes closed; EO: Eyes open; EEG: Electroencephalogram; HCs: Healthy controls; MDD: Major depressive disorder.

Diagnosis of depression: BDI: Beck Depression Inventory; DASS: Depression, Anxiety and Stress Scales; DSM-IIIR: Diagnostic and Statistical Manual of Mental Disorders, Third edition, Revised; DSM-IV: Diagnostic and Statistical Manual of Mental Disorders, Fourth edition; GDS: Geriatric depression scale; HAMD: Hamilton Rating Scale for Depression; HADS: Hospital anxiety and depression scale-depression; ICD-11: 11th edition of the International Classification of Diseases; MADRS: Montgomery and Asberg Depression Rating Scale; MINI: Mini International Neuropsychiatric Interview; SADS: The Schedule for Affective Disorders and Schizophrenia; SCID: Structured Clinical Interview for DSM IIIR; SCID-IV-I/P: Structured Clinical Interview for DSM-IV, Axis I, Patient Version.

Reference montage: AE: The average across all 31 electrodes; AL: The average of all EEG leads; ALM: Averaged linked mastoids; AM: Averaged mastoids; AR: Average reference; BM: Both mastoids; CA: Common average montage; CA: Common average; CSD: Current source densities; ECC: The reference electrode was predefined; ER: Ear reference; LE: Linked ear; LM: Linked mastoids; NR: Nose reference; RLMB: The right and left mastoid bone.

adolescent sample while considering possible extraneous variables, such as comorbid anxiety and disease state. They repeated the results of Kentgen *et al*[44] and found that there was no significant difference between major depressive adolescents without comorbid anxiety disorder and healthy

controls. However, major depressive adolescents with comorbid anxiety disorder demonstrated greater right frontal lobe activation than healthy controls. The results show that frontal EEG alpha asymmetry in the resting state itself has nothing to do with adolescent depression and emphasize the importance of considering comorbid anxiety disorder when examining adolescents' asymmetry patterns[45]. In addition, Grünewald *et al*[46] analysed frontal EEG alpha asymmetry at rest in adolescents with depression and healthy controls. They found that adolescents with depression had less left-sided frontal alpha power, while healthy controls exhibited no asymmetry. For healthy controls, more left frontal alpha was associated with a higher depression score, which was not observed in adolescents with depression.

The diagnosis of depression in the elderly is often more difficult because the symptoms of depression may be confused by factors such as the individual's own physical condition[47]. In addition, depression in the elderly is connected with cognitive deficits and physical disability, which increases the difficulty of distinguishing depression from dementia[48]. At present, many studies have explored the relationship between frontal EEG alpha asymmetry in the resting state and depression in young people, but few studies have focused on frontal EEG alpha asymmetry in the resting state in elderly individuals with depression. Recently, Deslandes *et al*[49] found that depressed elderly patients showed relatively greater right frontal activity than healthy elderly patients; however, the difference was not significant. This was consistent with the results of Kaiser *et al*[50], who found that there was no significant difference in frontal EEG alpha asymmetry in the resting state between depressed elderly individuals and healthy elderly individuals. Carvalho and Hopko analysed frontal EEG alpha asymmetry in the resting state in depressed, remitted and nondepressed elderly subjects. There was no difference in frontal EEG alpha asymmetry at rest among the groups. Moreover, the results showed no evidence of a relationship between frontal EEG alpha asymmetry in the resting state, quality of life and depression in the elderly[51]. Therefore, frontal EEG alpha asymmetry at rest seemed to disappear with age. Future research on frontal EEG alpha asymmetry in the resting state should consider the influences of age.

INTERGENERATIONAL INHERITANCE RESEARCH

Table 2 provides the comparison of methods in studies on the inherited pattern of frontal EEG alpha asymmetry at rest in children over generations. Research has shown that the offspring of parents with depression are at increased risk of depression[52,53]. Considering that there was a close relationship between frontal EEG alpha asymmetry in the resting state and depression, frontal EEG alpha asymmetry may be affected by the early social environment, such as maternal depression. To date, extensive literature has exploited the relationship between maternal depression and frontal EEG alpha asymmetry in the resting state in infants and young children. A number of studies have found that compared with nondepressed mothers, infants of depressed mothers have greater right frontal EEG alpha asymmetry[54-59], and similar results were also found in the youth group[60,61]. In a meta-analysis study, Peltola *et al*[62] found that frontal EEG alpha asymmetry at rest is affected by psychosocial risk factors, such as child abuse or parental depression, which is manifested by greater activation of the right frontal cortex, with a significant effect size. Moreover, their results showed that the relationship between parental depressive symptoms and greater right frontal lobe activity was moderated by gender, in which girls were more affected by psychosocial risk factors than boys. Additionally, the effects of this long-term exposure to parental depression diminish with age.

Furthermore, in an effort to understand the earliest origin of frontal EEG alpha asymmetry in the resting state, which was considered to reflect a vulnerability to depression, some studies examined their consistency and their association with the mother's prenatal and postnatal depression symptoms. Goodman *et al*[63] demonstrated that the mother's prenatal depression symptom (nonpostpartum or concurrent) levels are related to the baby's right frontal EEG alpha asymmetry. This was consistent with the results of Wen *et al*[64]. They found that in a subsample in which the infant spent at least 50% of his or her daytime hours with his or her mother, a higher mother's postpartum depression level and lower maternal sensitivity predicted the baby's greater relative right frontal EEG asymmetry[63]. In addition, Lusby *et al*[65] found that mothers' prenatal and postpartum depression symptoms can predict the frontal EEG asymmetry scores of 3-month-old and 6-month-old infants. However, Goldstein *et al*[66] assessed frontal EEG alpha asymmetry twice, at ages 3 and 6, in never-depressed children. The study revealed that offspring of depressed mothers displayed a decline in relative activity in the left frontal alpha region during early childhood, while offspring of non-depressed mothers showed relatively consistent and symmetrical levels of frontal alpha activity during both assessments[66]. Although most studies have found that maternal depression has an important influence on determining the direction and degree of frontal EEG alpha asymmetry in the resting state in children[56,59,67], others have found no significant differences between offspring of nondepressed mothers and depressed mothers[68,69]. Future research needs to investigate the genetic mechanism that connects psychosocial risk and frontal EEG alpha asymmetry at rest. That is, whether genetic or experience-based influence has an impact on frontal EEG alpha asymmetry at resting state. In addition, as discussed above, a large number of studies have observed abnormal patterns of frontal EEG alpha asymmetry in the resting state in newborns of

Table 2 The comparison of methods in studies on asymmetry pattern at resting state of children inherited from generation to generation

Ref.	Sample		Age (yr)		% female	Diagnosis of depression	EEG detail			
	Experimental group	Control group	Experimentalgroup	Control group			Reference montage	EO/EC	Recording length (min)	Alpha range (Hz)
Dawson *et al*[54], 1997	EG: 117 mothers and their 13-15-mo-old infants		13.74		44.4	DSM-IIIR; SCID; CES-D	ME		1	6–9
Diego *et al* [56], 2006	EG: 38 depressed	CG: 28 non-depressed	3-6 mo			CES-D	Cz			3–13
Field *et al* [57], 1995	EG: 17 depressed adolescent mothers	CG: 15 non-depressed mothers	3-6 mo		50	DISC; BDI	Cz		3	3–12
Jones *et al* [58], 1997	EG: 20 depressed group	CG: 24 non-depressed group	M = 18.00	M = 18.70		CES-D; SCID	Cz		3	2–6
Jones *et al* [59], 1998	EG: 35 mothers with depressive symptom	CG: 28 non-depressive symptom	M = 38.80	M = 39.50	48	CES-D	Cz		3	8.5–125
Tomarken *et al*[60], 2004	EG: 23 high risk	CG: 13 low risk	M = 13.10	M = 13.00	52.6	SCID	Cz	E0+EC	8	8.5–12.5
Lopez-Duran *et al* [61], 2012	EG: 90 high risk	CG: 45 low risk	M = 7.36	M = 7.93	46.6	DSM-IV; SCID	CA	E0+EC	3	7.5–11.5
Goodman *et al*[63], 2020	EG: 136 total infants.		M = 12 mo			DSM-IV	ARC		3	6–9
Wen *et al* [64], 2017	EG: 111 infants		6 mo of age (± 2 wk)			EPDS	Cz		2	6–9
Lusby *et al* [65], 2014	EG: 83 mother–infant dyads participated		3 mo and 6 mo only			DSM-IV	ARC		3	6–9
Dawson *et al*[69], 1992	EG: 31 infants		M = 14.21 (mo)		59.1	CES-D	Cz		1	6–9
Bruder *et al*[68], 2007	EG: 19 both parent and grandparent having MDD; 14 either parent or grandparent having MDD	CG: 16 neither having MDD	M = 15.40; M = 10.60	M = 13.60	53		LE	E0+EC	2	7–12.5

EC: Eyes closed; EO: Eyes open; EEG: Electroencephalogram; HCs: Healthy controls; MDD: Major depressive disorder.

Diagnosis of depression: BDI: Beck Depression Inventory; CES-D: Center for Epidemiological Studies-Depression Scale; DSM-IIIR: Diagnostic and Statistical Manual of Mental Disorders, Third edition, Revised; DSM-IV: 4th edition of the Diagnostic and Statistical Manual of Mental Disorder; EPDS: Edinburgh Postnatal Depression Scale; SCID: Structured Clinical Interview for DSM IIIR.

Reference montage: ARC: Average reference configuration; AS: Average signal; CA: Common average; Cz: The midline central position; LE: Linked ears reference; ME: Mastoid electrodes; NR: Nose reference.

depressed mothers, indicating a genetic disposition to greater right-sided asymmetry across cross-sectional assessment. Future research can focus on longitudinal investigations to examine whether there are long-term and lasting changes in the psychosocial risks faced by children.

FRONTAL EEG ALPHA ASYMMETRY IN THE RESTING STATE AND ANTIDEPRESSANT TREATMENT

Table 3 provides the comparison of methods in studies on frontal EEG alpha asymmetry in response to antidepressant treatment. There are some studies suggesting that frontal EEG alpha asymmetry in the

Table 3 The comparison of methods in studies on frontal electroencephalogram alpha asymmetry of response to antidepressant treatment

Ref.	Sample		Age (yr)		Intervention time	% female	Diagnosis of depression	EEG detail			
	Experimental group	Control group	Experimental group	Control group				Reference montage	EO/EC	Recording length (min)	Alpha range (Hz)
Arns *et al* [70], 2016	EG: 236 Escitalopram, 251 Sertraline, 235 Venlafaxine-XR	CG: 336 controls	M = 38.85 (Escitalopram), M = 38.34 (Sertraline), M = 38.46 (Venlafaxine-XR), M = 37.84 (MDD)	M = 36.99 (Controls)	8 wk	57.03	DSM–IV; MINI; HRSD	AM	E0+EC	2	8–13
Vinne *et al*[71], 2019	EG: 136 treatment with escitalo pram, 169 treatment with sertraline, 188 treatment with venlafaxine-extended release				8 wk	54.47	MINI; HRSD; VQIDS-SR	AM	E0+EC	4	8–13
Bares *et al* [72], 2019	EG: 57 SSRIs, 46 SNRIs		M = 46.04 (SSRIs), M = 44.83 (SNRIs)		1 wk	74.76	DSM IV; MADRS; CGI	Cz	EC	10	8–13
Szumska *et al*[73], 2021	EG: 12 Mindfulness group	CG: 8 control group	M = 32.40 (Mindfulness group)	M = 35.00 (Control group)	8 wk	55	CES-D; MINI	Cz	E0+EC	3	8–13
Keune *et al*[74], 2011	EG: 78 MDD; 40 MBCT group	CG: 37 a wait-list condition	M = 48.93 (MBCT group)	M = 45.24 (wait-list group)	8 wk	74.03	DSM-IV	AM	E0+EC	8	8--13
Barnhofer *et al*[75], 2007	EG: 10 MBCT	CG: 12 treatment-as-usual	M = 48.00 (MBCT)	M = 38.60 (treatment-as-usual)	8 wk	50	MINI	AE	E0+EC	8	8–13
Gollan *et al*[77], 2014	EG: 37 MDD; Behavioral activation	CG: 35 non-MDD			16 wk	62.50	DSM-IV; IDS-C	AM	E0+EC	8	8–13
Allen *et al* [14], 2004	EG: 30 nonpharmacological intervention				8 wk	100	DSM–IV; HRSD	Cz; AM, AR	E0+EC	8	8–13
Spronk *et al*[78], 2008	EG: 8 MDD; rTMS Treatment		M = 42.60 (rTMS Treatment)			37.50	BDI; SCI	AM	E0+EC	2	alpha 1 (8–11); alpha 2 (11–13)
Wang *et al*[80], 2016	EG: 7 neurofeedback group		M = 47.43		6 wk	78.57	DSM-IV	Cz	EC	5	8–12
Vlcek *et al*[79], 2020	EG: 9 LF rTMS responder	CG: 16 LF rTMS non-responders			4 wk	80	MINI; MADRS; CGI	Cz	EC	10	8–12; 8–10; 10–12

EC: Eyes closed; EO: Eyes open; EEG: Electroencephalogram; HCs: Healthy controls; LF rTMS: Low-frequency Rtms; MBCT: Mindfulness-Based Cognitive Therapy; MDD: Major depressive disorder; rTMS: Repeated transcranial magnetic stimulation; SNRIs: Serotonin norepinephrine reuptake inhibitors; SSRIs: Selective serotonin reuptake inhibitors.

Diagnosis of depression: BDI: Beck Depression Inventory; CES-D: Centre for Epidemiological Studies Depression scale; CGI: Clinical Global Impression; HRSD: Hamilton rating scale for depression; MADRS: Montgomery and Asberg Depression Rating Scale; IDS-C: Inventory of Depressive Symptomatology–Clinician-Rated; MINI: Mini International Neuropsychiatric Interview; SCI: Structural clinical interview; VQIDS-SR: Very Quick Inventory of Depressive Symptomatology–Self Report.

Reference montage: AM: Averaged mastoids; AR: Average reference; Cz: The midline central position.

resting state may be more promising as an indicator of prognosis rather than diagnosis. This means that frontal EEG alpha asymmetry at resting state may be used as a biomarker for the stability and robust response of depression treatment. To date, some studies have tested the correlation between frontal EEG alpha asymmetry in the resting state and antidepressant treatment, including medical treatment, mindfulness treatment, behavioural activation treatment, acupuncture treatment, neurofeedback treatment, and transcranial magnetic stimulation (TMS) treatment.

Medical treatment

Arns *et al*[70] investigated whether frontal EEG alpha asymmetry in the resting state predicted antidepressant treatment outcome for depressive disorder; 1008 depressed participants were randomized to eight weeks treatment with escitalopram, sertraline or venlafaxine-extended release. The results showed that there were no significant differences in frontal EEG alpha asymmetry in the resting state between depressed participants and healthy controls. This was consistent with the results of van der Vinne *et al*[71]. Their results found that frontal EEG alpha asymmetry in the resting state did not change significantly after eight weeks of escitalopram, sertraline, or venlafaxine treatment. Moreover, Bares *et al*[72] investigated the effectiveness of frontal EEG alpha asymmetry at baseline and its changes at week 1 in predicting the response to antidepressants. Both groups who were treated with selective serotonin reuptake inhibitors or the serotonin norepinephrine reuptake inhibitor showed no differences at baseline or change in frontal EEG alpha asymmetry at week 1. These findings suggested that antidepressant medication has no effects on frontal EEG alpha asymmetry in the resting state.

Mindfulness treatment

Mindfulness training has been proven to be effective in reducing the recurrence rate of depression patients. Szumska *et al*[73] evaluated the impact of mindfulness training on depression and anxiety symptoms in individuals with depression and further evaluated whether the effect of mindfulness training in improving depression would be reflected by changes in frontal EEG alpha asymmetry in the resting state. Consistent with the results of previous studies, the depression and anxiety symptoms of the mindfulness training group were reduced, but there was no significant change in the average scores of frontal EEG alpha asymmetry in the resting state. Similarly, Keune *et al*[74] examined the effect of mindfulness training on residual depressive symptoms in patients with recurrent depression. The results showed that residual depressive symptoms and trait contemplation decreased, while trait mindfulness increased after mindfulness training, but this change did not occur in the waiting list control group. On the other hand, the average scores of frontal EEG alpha asymmetry in the resting state are not affected by training. These results provide strong support for the beneficial effects of mindfulness training in the treatment of depression. However, they do not support the hypothesis that asymmetric changes in the alpha band are used as the neural relevance of improvement in major depression. In addition, Barnhofer *et al*[75] investigated the effect of 8 wk of mindfulness training on preventing the recurrence of depression in individuals who were previously suicidal. The results showed that the relative activation of the left frontal lobe in the normal treatment group decreased, but there was no significant change in the mindfulness training group. The results suggested that mindfulness training can help suicidal depression patients maintain a balanced brain activation pattern.

Behavioural activation treatment

Behavioural activation treatment is an evidence-based treatment for depression[76]. Gollan *et al*[77] examined frontal EEG alpha asymmetry in the resting state in depressed and healthy subjects undergoing behavioural activation therapy and assessed the predictive effect of frontal EEG alpha asymmetry at rest in remission of depression. The results showed that there were no significant changes in frontal EEG alpha asymmetry before and after treatment for participants with depression and healthy participants.

Acupuncture treatment

Allen *et al*[11] examined the temporal stability of frontal EEG alpha asymmetry in the resting state in a sample of depressed women undergoing acupuncture treatment. The results showed that the asymmetrical frontal score generally showed good internal consistency and moderate stability over the 8- and 16-wk assessment intervals. In addition, changes in resting frontal asymmetry scores were not significantly associated with changes in depressive status between 8 and 16 wk.

TMS treatment

Repeated transcranial magnetic stimulation (rTMS) is an effective treatment method for depression that has been found to respond in nearly 45%-55% of patients and in remission in 30%-40% of patients. Spronk *et al*[78] examined the clinical effectiveness of rTMS in treating depression. The results showed that all subjects showed complete remission within 20 sessions, significantly reduced depressive symptoms (BDI score) and neuroticism scores, and increased scores on the extraversion scale of the (NEO)-Five Factor Inventory (NEO-FFI) personality questionnaire. However, there was no significant change in the frontal EEG alpha asymmetry. More recently, Vlcek *et al*[79] investigated whether there

were different frontal asymmetry patterns between low-frequency rTMS (LF rTMS) responders and nonresponders. The results showed that there was no significant difference in frontal EEG alpha asymmetry in the resting state between LF rTMS responders and nonresponders.

Neurofeedback treatment

Neurofeedback is a clinical intervention program designed to regulate brain activity and modulate frontal EEG alpha asymmetry. Wang *et al*[80] investigated the therapeutic effect of neurofeedback on patients with major depression. The results showed that the frontal EEG alpha asymmetry scores in the resting state decreased in the control group and increased in the neurofeedback group after the intervention. Depression and anxiety scores were significantly lower in MDD patients who received neurofeedback training than in those who did not. Furthermore, the results suggested that neurofeedback techniques can reduce right frontal lobe activation or increase left frontal lobe activation in patients with major depression.

In summary, most studies found that frontal EEG alpha asymmetry in the resting state in depressed patients consists mainly of trait-like features, and frontal EEG alpha asymmetry at rest was stable with little or no change between baseline and later assessment in depressed patients, although few studies suggest otherwise.

LIMITATIONS

Based on a review of the previous literature, it is clear that the relationship between frontal EEG lateralization and depression is not well defined, and there are a large number of inconsistent results. The results of a recent meta-analysis of the relationship between emotion regulation and frontal EEG asymmetry in depressed patients did not find frontal EEG asymmetry but rather a slight tendency towards left lateralization in the depressed group[81]. The study highlighted individual aspects of a study such as sample size and age group of participants as variables that influence effect size and disagreement between studies[38]. Consequently, inconsistent results about the studies on the relationship between frontal EEG alpha asymmetry in the resting state and depression may be due to differences in methodology (*e.g.*, reference electrode, alpha band), clinical characteristics (*e.g.*, diagnostic subtype, recruitment strategy), and participant characteristics (*e.g.*, gender, sample size). These issues have been discussed previously[19,34,50,82]. Therefore, this section provides a brief discussion.

Methodological differences

One reason for the inconsistent results is that different types of reference points were used in the EEG space. Most studies use linked ears, average reference, and mastoid as references, and a few studies use earlobes, Cz, and nose as references. Moreover, Stewart *et al*[83] suggested the use of current source density as a reference, which could lead to more consistent results in resting-state EEG studies, and Jesulola *et al*[84] concluded that the use of a common average reference was beneficial in reducing noise and improving signal quality.

In previous studies, there was a wide variability in the specific frequency range of the alpha band. Most studies consider the alpha band between 8 Hz and 13 Hz, while some studies consider other alpha band frequency ranges, such as 7.5 Hz-12.5 Hz, 8 Hz-12 Hz, and so on. These differences in the frequency range of the alpha band may lead to inconsistent results.

Clinical characteristics

Scales used for diagnosis vary across researchers, with the most common ones being the Diagnostic and Statistical Manual of Mental Disorders, followed by the Beck Depression Inventory[85]. Different scales may focus on different aspects of depression; therefore, the use of different scales may lead to difficulties in comparing the results of clinical depression diagnosis between studies.

In addition, although the clinical heterogeneity of depression is well known, few studies have examined its impact on frontal EEG alpha asymmetry in the resting state. Moreover, the results may be different when considering drug use and diagnosis. On the one hand, medication and drugs can affect the functionality of the brain; on the other hand, medication may have unknown interactions among themselves, changing the EEG signal even more.

Participant characteristics

In many studies, there have been large differences in the proportion of male to female subjects in the sample. For example, some studies used only female subjects[19,38,44,50,86,87] or samples with significantly more females than males[32,88-90]. Related studies have found gender-related brain mechanisms and brain asymmetry that contribute to emotional processing[91-93]. This suggests that gender variables may play an important role in cognitive function and the possible organization of the cerebral hemispheres; therefore, samples should be more evenly proportioned between males and females.

Effect size

Regarding effect size, the sample size of previous studies varied. For example, the sample size of most studies was generally less than 20 individuals[31,73,78,80,94-96], and some studies enrolled more than 100 individuals[35,97-99], but few had more than 200 individuals[27,82]. van der Vinne *et al*[82] suggested that a minimum of 300 participants is required to reveal patterns of frontal EEG alpha asymmetry in depressed individuals. Therefore, in these other studies that explored the patterns of alpha asymmetry in depressed individuals, the sample size may have been too small to be statistically significant.

CONCLUSION

From the studies reviewed, frontal EEG alpha asymmetry in the resting state was related to depression. First, studies from clinical research showed that compared with individuals without depression, those with depression showed greater right frontal EEG alpha asymmetry in the resting state. However, the pattern of frontal EEG alpha asymmetry at rest in depressive individuals seemed to disappear with age. Future research on frontal EEG alpha asymmetry in the resting state should consider the influences of age and research on frontal EEG alpha asymmetry in the resting state to determine whether it can be used to quantify the degree of depression. Second, studies of intergenerational inheritance showed that compared with individuals without maternal depression, those with maternal depression showed greater right frontal EEG alpha asymmetry in the resting state, which indicated a genetic disposition towards greater right-sided asymmetry across cross-sectional assessments. Future research can focus on longitudinal investigations to examine whether there are long-term and lasting changes in the psychosocial risks faced by children. Third, studies of antidepressant treatment revealed that frontal EEG alpha asymmetry in the resting state was stable and there was little or no change after antidepressant treatment. Future studies could use frontal EEG alpha asymmetry in the resting state as an indicator of treatment effectiveness to examine the efficacy of other antidepressant therapies, such as the use of frontal EEG alpha asymmetry in the resting state as an indicator to investigate the relationship between ECT and depression. Finally, there were contrasting results regarding the relationship between frontal EEG alpha asymmetry in the resting state and depression, and these results may be due to differences in methodology, clinical characteristics, and participant characteristics.

FOOTNOTES

Author contributions: Xie YH and Liu L wrote the paper; Zhang YM, Fan FF, and Song XY revised the paper.

Conflict-of-interest statement: All the author declare no conflict of interests for this article.

Country/Territory of origin: China

ORCID number: Yu-Hong Xie 0000-0003-1807-9602; Ye-Min Zhang 0000-0003-0961-8395; Fan-Fan Fan 0000-0001-7513-9080; Xi-Yan Song 0000-0001-6313-2156; Lei Liu 0000-0002-1666-8991.

S-Editor: Liu JH
L-Editor: A
P-Editor: Liu JH

REFERENCES

1 Organization World Health, Depression and other common mental disorders: global health estimates 2020; World Health Organization
2 Blue Book on National Depression 2022. Available from: https://mp.weixin.qq.com/s/DH5igAKDTuOwxusXfTWW_w
3 Chinese National Mental Health Development Report (2019~2020). Available from: http://ir.psych.ac.cn/handle/311026/40614
4 **Kalat J**, Shiota M. Emotion: Classification of Emotions. Thomson Wadsworth, Canada 2007
5 **Allen JJ**, Reznik SJ. Frontal EEG Asymmetry as a Promising Marker of Depression Vulnerability: Summary and

Methodological Considerations. *Curr Opin Psychol* 2015; **4**: 93-97 [PMID: 26462291 DOI: 10.1016/j.copsyc.2014.12.017]
6 **Smith EE**, Reznik SJ, Stewart JL, Allen JJ. Assessing and conceptualizing frontal EEG asymmetry: An updated primer on recording, processing, analyzing, and interpreting frontal alpha asymmetry. *Int J Psychophysiol* 2017; **111**: 98-114 [PMID: 27865882 DOI: 10.1016/j.ijpsycho.2016.11.005]
7 **Coan JA**, Allen JJ. Frontal EEG asymmetry as a moderator and mediator of emotion. *Biol Psychol* 2004; **67**: 7-49 [PMID: 15130524 DOI: 10.1016/j.biopsycho.2004.03.002]
8 **Bruder GE**, Tenke CE, Kayser J. Electrophysiological predictors of clinical response to antidepressants. *The Clinical Handbook for the Management of Mood Disorders* 2013; 380-393 [DOI: 10.1017/CBO9781139175869.030]
9 **Davidson RJ**. Cerebral Asymmetry, Emotion, and Affective Style. *Brain asymmetry* 1996; 361
10 **Laufs H**, Kleinschmidt A, Beyerle A, Eger E, Salek-Haddadi A, Preibisch C, Krakow K. EEG-correlated fMRI of human alpha activity. *Neuroimage* 2003; **19**: 1463-1476 [PMID: 12948703 DOI: 10.1016/s1053-8119(03)00286-6]
11 **Allen JJ**, Urry HL, Hitt SK, Coan JA. The stability of resting frontal electroencephalographic asymmetry in depression. *Psychophysiology* 2004; **41**: 269-280 [PMID: 15032992 DOI: 10.1111/j.1469-8986.2003.00149.x]
12 **Davidson RJ**. Anterior electrophysiological asymmetries, emotion, and depression: conceptual and methodological conundrums. *Psychophysiology* 1998; **35**: 607-614 [PMID: 9715104 DOI: 10.1017/S0048577298000134]
13 **Fox NA**, Rubin KH, Calkins SD, Marshall TR, Coplan RJ, Porges SW, Long JM, Stewart S. Frontal activation asymmetry and social competence at four years of age. *Child Dev* 1995; **66**: 1770-1784 [PMID: 8556898 DOI: 10.1111/j.1467-8624.1995.tb00964.x]
14 **Allen JJ**, Coan JA, Nazarian M. Issues and assumptions on the road from raw signals to metrics of frontal EEG asymmetry in emotion. *Biol Psychol* 2004; **67**: 183-218 [PMID: 15130531 DOI: 10.1016/j.biopsycho.2004.03.007]
15 **O'Reilly MA**, Bathelt J, Sakkalou E, Sakki H, Salt A, Dale NJ, de Haan M. Frontal EEG asymmetry and later behavior vulnerability in infants with congenital visual impairment. *Clin Neurophysiol* 2017; **128**: 2191-2199 [PMID: 28950152 DOI: 10.1016/j.clinph.2017.08.016]
16 **Marshall PJ**, Bar-Haim Y, Fox NA. Development of the EEG from 5 months to 4 years of age. *Clin Neurophysiol* 2002; **113**: 1199-1208 [PMID: 12139998 DOI: 10.1016/s1388-2457(02)00163-3]
17 **John ER**, Ahn H, Prichep L, Trepetin M, Brown D, Kaye H. Developmental equations for the electroencephalogram. *Science* 1980; **210**: 1255-1258 [PMID: 7434026 DOI: 10.1126/science.7434026]
18 **Clarke AR**, Barry RJ, McCarthy R, Selikowitz M. Age and sex effects in the EEG: development of the normal child. *Clin Neurophysiol* 2001; **112**: 806-814 [PMID: 11336896 DOI: 10.1016/s1388-2457(01)00488-6]
19 **Harrewijn A**, Buzzell GA, Debnath R, Leibenluft E, Pine DS, Fox NA. Frontal alpha asymmetry moderates the relations between behavioral inhibition and social-effect ERN. *Biol Psychol* 2019; **141**: 10-16 [PMID: 30599209 DOI: 10.1016/j.biopsycho.2018.12.014]
20 **Henriques JB**, Davidson RJ. Left frontal hypoactivation in depression. *J Abnorm Psychol* 1991; **100**: 535-545 [PMID: 1757667 DOI: 10.1037/0021-843x.100.4.535]
21 **Baehr E**, Rosenfeld JP, Baehr R, Earnest C. Comparison of two EEG asymmetry indices in depressed patients vs. normal controls. *Int J Psychophysiol* 1998; **31**: 89-92 [PMID: 9934624 DOI: 10.1016/s0167-8760(98)00041-5]
22 **Beeney JE**, Levy KN, Gatzke-Kopp LM, Hallquist MN. EEG asymmetry in borderline personality disorder and depression following rejection. *Personal Disord* 2014; **5**: 178-185 [PMID: 24364503 DOI: 10.1037/per0000032]
23 **Bruder GE**, Fong R, Tenke CE, Leite P, Towey JP, Stewart JE, McGrath PJ, Quitkin FM. Regional brain asymmetries in major depression with or without an anxiety disorder: a quantitative electroencephalographic study. *Biol Psychiatry* 1997; **41**: 939-948 [PMID: 9110099 DOI: 10.1016/s0006-3223(96)00260-0]
24 **Cantisani A**, Koenig T, Stegmayer K, Federspiel A, Horn H, Müller TJ, Wiest R, Strik W, Walther S. EEG marker of inhibitory brain activity correlates with resting-state cerebral blood flow in the reward system in major depression. *Eur Arch Psychiatry Clin Neurosci* 2016; **266**: 755-764 [PMID: 26590845 DOI: 10.1007/s00406-015-0652-7]
25 **Dharmadhikari AS**, Jaiswal SV, Tandle AL, Sinha D, Jog N. Study of Frontal Alpha Asymmetry in Mild Depression: A Potential Biomarker or Not? *J Neurosci Rural Pract* 2019; **10**: 250-255 [PMID: 31001013 DOI: 10.4103/jnrp.jnrp_293_18]
26 **Gordon E**, Palmer DM, Cooper N. EEG alpha asymmetry in schizophrenia, depression, PTSD, panic disorder, ADHD and conduct disorder. *Clin EEG Neurosci* 2010; **41**: 178-183 [PMID: 21077569 DOI: 10.1177/155005941004100404]
27 **Gotlib IH**. EEG alpha asymmetry, depression, and cognitive functioning. *Cognition & Emotion* 1998; **12** 449-478 DOI: 10.1080/026999398379673
28 **Jaworska N**, Blier P, Fusee W, Knott V. α Power, α asymmetry and anterior cingulate cortex activity in depressed males and females. *J Psychiatr Res* 2012; **46**: 1483-1491 [PMID: 22939462 DOI: 10.1016/j.jpsychires.2012.08.003]
29 **Kemp AH**, Griffiths K, Felmingham KL, Shankman SA, Drinkenburg W, Arns M, Clark CR, Bryant RA. Disorder specificity despite comorbidity: resting EEG alpha asymmetry in major depressive disorder and post-traumatic stress disorder. *Biol Psychol* 2010; **85**: 350-354 [PMID: 20708650 DOI: 10.1016/j.biopsycho.2010.08.001]
30 **Koo PC**, Berger C, Kronenberg G, Bartz J, Wybitul P, Reis O, Hoeppner J. Combined cognitive, psychomotor and electrophysiological biomarkers in major depressive disorder. *Eur Arch Psychiatry Clin Neurosci* 2019; **269**: 823-832 [PMID: 30392042 DOI: 10.1007/s00406-018-0952-9]
31 **Roh SC**, Kim JS, Kim S, Kim Y, Lee SH. Frontal Alpha Asymmetry Moderated by Suicidal Ideation in Patients with Major Depressive Disorder: A Comparison with Healthy Individuals. *Clin Psychopharmacol Neurosci* 2020; **18**: 58-66 [PMID: 31958906 DOI: 10.9758/cpn.2020.18.1.58]
32 **Smith EE**, Cavanagh JF, Allen JJB. Intracranial source activity (eLORETA) related to scalp-level asymmetry scores and depression status. *Psychophysiology* 2018; **55** [PMID: 29023805 DOI: 10.1111/psyp.13019]
33 **Stewart JL**, Bismark AW, Towers DN, Coan JA, Allen JJ. Resting frontal EEG asymmetry as an endophenotype for depression risk: sex-specific patterns of frontal brain asymmetry. *J Abnorm Psychol* 2010; **119**: 502-512 [PMID: 20677839 DOI: 10.1037/a0019196]
34 **Cai H**, Yuan Z, Gao Y, Sun S, Li N, Tian F, Xiao H, Li J, Yang Z, Li X, Zhao Q, Liu Z, Yao Z, Yang M, Peng H, Zhu J, Zhang X, Gao G, Zheng F, Li R, Guo Z, Ma R, Yang J, Zhang L, Hu X, Li Y, Hu B. A multi-modal open dataset for

mental-disorder analysis. *Sci Data* 2022; **9**: 178 [PMID: 35440583 DOI: 10.1038/s41597-022-01211-x]
35 **Nusslock R**, Shackman AJ, McMenamin BW, Greischar LL, Davidson RJ, Kovacs M. Comorbid anxiety moderates the relationship between depression history and prefrontal EEG asymmetry. *Psychophysiology* 2018; **55** [PMID: 28755454 DOI: 10.1111/psyp.12953]
36 **Brzezicka A**, Kamiński J, Kamińska OK, Wołyńczyk-Gmaj D, Sedek G. Frontal EEG alpha band asymmetry as a predictor of reasoning deficiency in depressed people. *Cogn Emot* 2017; **31**: 868-878 [PMID: 27089304 DOI: 10.1080/02699931.2016.1170669]
37 **Jang KI**, Lee C, Lee S, Huh S, Chae JH. Comparison of frontal alpha asymmetry among schizophrenia patients, major depressive disorder patients, and healthy controls. *BMC Psychiatry* 2020; **20**: 586 [PMID: 33302919 DOI: 10.1186/s12888-020-02972-8]
38 **Segrave RA**, Cooper NR, Thomson RH, Croft RJ, Sheppard DM, Fitzgerald PB. Individualized alpha activity and frontal asymmetry in major depression. *Clin EEG Neurosci* 2011; **42**: 45-52 [PMID: 21309442 DOI: 10.1177/155005941104200110]
39 **Quinn CR**, Rennie CJ, Harris AW, Kemp AH. The impact of melancholia versus non-melancholia on resting-state, EEG alpha asymmetry: electrophysiological evidence for depression heterogeneity. *Psychiatry Res* 2014; **215**: 614-617 [PMID: 24467874 DOI: 10.1016/j.psychres.2013.12.049]
40 **Vuga M**, Fox NA, Cohn JF, George CJ, Levenstein RM, Kovacs M. Long-term stability of frontal electroencephalographic asymmetry in adults with a history of depression and controls. *Int J Psychophysiol* 2006; **59**: 107-115 [PMID: 16002168 DOI: 10.1016/j.ijpsycho.2005.02.008]
41 **Gold C**, Fachner J, Erkkilä J. Validity and reliability of electroencephalographic frontal alpha asymmetry and frontal midline theta as biomarkers for depression. *Scand J Psychol* 2013; **54**: 118-126 [PMID: 23278257 DOI: 10.1111/sjop.12022]
42 **McFarland BR**, Shankman SA, Tenke CE, Bruder GE, Klein DN. Behavioral activation system deficits predict the six-month course of depression. *J Affect Disord* 2006; **91**: 229-234 [PMID: 16487598 DOI: 10.1016/j.jad.2006.01.012]
43 **Pine DS**, Cohen P, Gurley D, Brook J, Ma Y. The risk for early-adulthood anxiety and depressive disorders in adolescents with anxiety and depressive disorders. *Arch Gen Psychiatry* 1998; **55**: 56-64 [PMID: 9435761 DOI: 10.1001/archpsyc.55.1.56]
44 **Kentgen LM**, Tenke CE, Pine DS, Fong R, Klein RG, Bruder GE. Electroencephalographic asymmetries in adolescents with major depression: influence of comorbidity with anxiety disorders. *J Abnorm Psychol* 2000; **109**: 797-802 [PMID: 11196007 DOI: 10.1037//0021-843x.109.4.797]
45 **Feldmann L**, Piechaczek CE, Grünewald BD, Pehl V, Bartling J, Frey M, Schulte-Körne G, Greimel E. Resting frontal EEG asymmetry in adolescents with major depression: Impact of disease state and comorbid anxiety disorder. *Clin Neurophysiol* 2018; **129**: 2577-2585 [PMID: 30415151 DOI: 10.1016/j.clinph.2018.09.028]
46 **Grünewald BD**, Greimel E, Trinkl M, Bartling J, Großheinrich N, Schulte-Körne G. Resting frontal EEG asymmetry patterns in adolescents with and without major depression. *Biol Psychol* 2018; **132**: 212-216 [PMID: 29305876 DOI: 10.1016/j.biopsycho.2018.01.003]
47 **Chapman DP**, Perry GS. Depression as a major component of public health for older adults. *Prev Chronic Dis* 2008; **5**: A22 [PMID: 18082011]
48 **Bierman EJ**, Comijs HC, Jonker C, Beekman AT. Symptoms of anxiety and depression in the course of cognitive decline. *Dement Geriatr Cogn Disord* 2007; **24**: 213-219 [PMID: 17690554 DOI: 10.1159/000107083]
49 **Oliveira BRR**, Santos TM, Kilpatrick M, Pires FO, Deslandes AC. Affective and enjoyment responses in high intensity interval training and continuous training: A systematic review and meta-analysis. *PLoS One* 2018; **13**: e0197124 [PMID: 29874256 DOI: 10.1371/journal.pone.0197124]
50 **Kaiser AK**, Gnjezda MT, Knasmüller S, Aichhorn W. Electroencephalogram alpha asymmetry in patients with depressive disorders: current perspectives. *Neuropsychiatr Dis Treat* 2018; **14**: 1493-1504 [PMID: 29928121 DOI: 10.2147/NDT.S137776]
51 **Carvalho JP**, Hopko DR. Behavioral theory of depression: reinforcement as a mediating variable between avoidance and depression. *J Behav Ther Exp Psychiatry* 2011; **42**: 154-162 [PMID: 21315876 DOI: 10.1016/j.jbtep.2010.10.001]
52 **Warner V**, Mufson L, Weissman MM. Offspring at high and low risk for depression and anxiety: mechanisms of psychiatric disorder. *J Am Acad Child Adolesc Psychiatry* 1995; **34**: 786-797 [PMID: 7608053 DOI: 10.1097/00004583-199506000-00020]
53 **Weissman MM**, Warner V, Wickramaratne P, Moreau D, Olfson M. Offspring of depressed parents. 10 Years later. *Arch Gen Psychiatry* 1997; **54**: 932-940 [PMID: 9337774 DOI: 10.1001/archpsyc.1997.01830220054009]
54 **Dawson G**, Frey K, Panagiotides H, Osterling J, Hessl D. Infants of depressed mothers exhibit atypical frontal brain activity: a replication and extension of previous findings. *J Child Psychol Psychiatry* 1997; **38**: 179-186 [PMID: 9232464 DOI: 10.1111/j.1469-7610.1997.tb01852.x]
55 **Dawson G**, Panagiotides H, Klinger LG, Spieker S. Infants of depressed and nondepressed mothers exhibit differences in frontal brain electrical activity during the expression of negative emotions. *Dev Psychol* 1997; **33**: 650-656 [PMID: 9232380 DOI: 10.1037/0012-1649.33.4.650]
56 **Diego MA**, Field T, Jones NA, Hernandez-Reif M. Withdrawn and intrusive maternal interaction style and infant frontal EEG asymmetry shifts in infants of depressed and non-depressed mothers. *Infant Behav Dev* 2006; **29**: 220-229 [PMID: 17138277 DOI: 10.1016/j.infbeh.2005.12.002]
57 **Field T**, Fox NA, Pickens J, Nawrocki T. Relative right frontal EEG activation in 3-to 6-month-old infants of "depressed" mothers. *Developmental psychology* 1995; **31**: 358 [DOI: 10.1037/0012-1649.31.3.358]
58 **Jones NA**, Field T, Fox NA, Lundy B, Davalos M. EEG activation in 1-month-old infants of depressed mothers. *Dev Psychopathol* 1997; **9**: 491-505 [PMID: 9327235 DOI: 10.1017/s0954579497001260]
59 **Jones NA**, Field T, Davalos M. Massage therapy attenuates right frontal EEG asymmetry in one-month-old infants of depressed mothers. *Infant behavior and Development* 1998; **21**: 527-530 [DOI: 10.1016/S0163-6383(98)90025-X]
60 **Tomarken AJ**, Dichter GS, Garber J, Simien C. Resting frontal brain activity: linkages to maternal depression and socio-

economic status among adolescents. *Biol Psychol* 2004; **67**: 77-102 [PMID: 15130526 DOI: 10.1016/j.biopsycho.2004.03.011]

61 **Lopez-Duran NL**, Nusslock R, George C, Kovacs M. Frontal EEG asymmetry moderates the effects of stressful life events on internalizing symptoms in children at familial risk for depression. *Psychophysiology* 2012; **49**: 510-521 [PMID: 22220930 DOI: 10.1111/j.1469-8986.2011.01332.x]

62 **Peltola MJ**, Bakermans-Kranenburg MJ, Alink LR, Huffmeijer R, Biro S, van IJzendoorn MH. Resting frontal EEG asymmetry in children: meta-analyses of the effects of psychosocial risk factors and associations with internalizing and externalizing behavior. *Dev Psychobiol* 2014; **56**: 1377-1389 [PMID: 24863548 DOI: 10.1002/dev.21223]

63 **Goodman SH**, Simon HFM, Shamblaw AL, Kim CY. Parenting as a Mediator of Associations between Depression in Mothers and Children's Functioning: A Systematic Review and Meta-Analysis. *Clin Child Fam Psychol Rev* 2020; **23**: 427-460 [PMID: 32734498 DOI: 10.1007/s10567-020-00322-4]

64 **Wen DJ**, Soe NN, Sim LW, Sanmugam S, Kwek K, Chong YS, Gluckman PD, Meaney MJ, Rifkin-Graboi A, Qiu A. Infant frontal EEG asymmetry in relation with postnatal maternal depression and parenting behavior. *Transl Psychiatry* 2017; **7**: e1057 [PMID: 28291259 DOI: 10.1038/tp.2017.28]

65 **Lusby CM**, Goodman SH, Bell MA, Newport DJ. Electroencephalogram patterns in infants of depressed mothers. *Dev Psychobiol* 2014; **56**: 459-473 [PMID: 23852456 DOI: 10.1002/dev.21112]

66 **Goldstein BL**, Shankman SA, Kujawa A, Torpey-Newman DC, Olino TM, Klein DN. Developmental changes in electroencephalographic frontal asymmetry in young children at risk for depression. *J Child Psychol Psychiatry* 2016; **57**: 1075-1082 [PMID: 27138464 DOI: 10.1111/jcpp.12567]

67 **Miskovic V**, Schmidt LA, Georgiades K, Boyle M, MacMillan HL. Stability of resting frontal electroencephalogram (EEG) asymmetry and cardiac vagal tone in adolescent females exposed to child maltreatment. *Dev Psychobiol* 2009; **51**: 474-487 [PMID: 19629997 DOI: 10.1002/dev.20387]

68 **Bruder GE**, Tenke CE, Warner V, Weissman MM. Grandchildren at high and low risk for depression differ in EEG measures of regional brain asymmetry. *Biol Psychiatry* 2007; **62**: 1317-1323 [PMID: 17481594 DOI: 10.1016/j.biopsych.2006.12.006]

69 **Dawson G**, Klinger LG, Panagiotides H, Hill D, Spieker S. Frontal lobe activity and affective behavior of infants of mothers with depressive symptoms. *Child Dev* 1992; **63**: 725-737 [PMID: 1600832 DOI: 10.1111/j.1467-8624.1992.tb01657.x]

70 **Arns M**, Bruder G, Hegerl U, Spooner C, Palmer DM, Etkin A, Fallahpour K, Gatt JM, Hirshberg L, Gordon E. EEG alpha asymmetry as a gender-specific predictor of outcome to acute treatment with different antidepressant medications in the randomized iSPOT-D study. *Clin Neurophysiol* 2016; **127**: 509-519 [PMID: 26189209 DOI: 10.1016/j.clinph.2015.05.032]

71 **van der Vinne N**, Vollebregt MA, van Putten MJAM, Arns M. Stability of frontal alpha asymmetry in depressed patients during antidepressant treatment. *Neuroimage Clin* 2019; **24**: 102056 [PMID: 31795035 DOI: 10.1016/j.nicl.2019.102056]

72 **Bares M**, Novak T, Vlcek P, Hejzlar M, Brunovsky M. Early change of prefrontal theta cordance and occipital alpha asymmetry in the prediction of responses to antidepressants. *Int J Psychophysiol* 2019; **143**: 1-8 [PMID: 31195067 DOI: 10.1016/j.ijpsycho.2019.06.006]

73 **Szumska I**, Gola M, Rusanowska M, Krajewska M, Żygierewicz J, Krejtz I, Nezlek JB, Holas P. Mindfulness-based cognitive therapy reduces clinical symptoms, but do not change frontal alpha asymmetry in people with major depression disorder. *Int J Neurosci* 2021; **131**: 453-461 [PMID: 32223344 DOI: 10.1080/00207454.2020.1748621]

74 **Keune PM**, Bostanov V, Hautzinger M, Kotchoubey B. Mindfulness-based cognitive therapy (MBCT), cognitive style, and the temporal dynamics of frontal EEG alpha asymmetry in recurrently depressed patients. *Biol Psychol* 2011; **88**: 243-252 [PMID: 21884751 DOI: 10.1016/j.biopsycho.2011.08.008]

75 **Barnhofer T**, Duggan D, Crane C, Hepburn S, Fennell MJ, Williams JM. Effects of meditation on frontal alpha-asymmetry in previously suicidal individuals. *Neuroreport* 2007; **18**: 709-712 [PMID: 17426604 DOI: 10.1097/WNR.0b013e3280d943cd]

76 **Dimidjian S**, Barrera M Jr, Martell C, Muñoz RF, Lewinsohn PM. The origins and current status of behavioral activation treatments for depression. *Annu Rev Clin Psychol* 2011; **7**: 1-38 [PMID: 21275642 DOI: 10.1146/annurev-clinpsy-032210-104535]

77 **Gollan JK**, Hoxha D, Chihade D, Pflieger ME, Rosebrock L, Cacioppo J. Frontal alpha EEG asymmetry before and after behavioral activation treatment for depression. *Biol Psychol* 2014; **99**: 198-208 [PMID: 24674708 DOI: 10.1016/j.biopsycho.2014.03.003]

78 **Spronk D**, Arns M, Bootsma A, van Ruth R, Fitzgerald PB. Long-term effects of left frontal rTMS on EEG and ERPs in patients with depression. *Clin EEG Neurosci* 2008; **39**: 118-124 [PMID: 18751560 DOI: 10.1177/155005940803900305]

79 **Vlcek P**, Bares M, Novak T, Brunovsky M. Baseline Difference in Quantitative Electroencephalography Variables Between Responders and Non-Responders to Low-Frequency Repetitive Transcranial Magnetic Stimulation in Depression. *Front Psychiatry* 2020; **11**: 83 [PMID: 32174854 DOI: 10.3389/fpsyt.2020.00083]

80 **Wang S-Y**, Lin I-M, Peper E, Chen Y-T, Tang T-C, Yeh Y-C, Tsai Y-C, Chu C-C. The efficacy of neurofeedback among patients with major depressive disorder: Preliminary study. *Neuro Regulation* 2016; **3**: 127-127 [DOI: 10.15540/nr.3.3.127]

81 **Horato N**, Quagliato LA, Nardi AE. The relationship between emotional regulation and hemispheric lateralization in depression: a systematic review and a meta-analysis. *Transl Psychiatry* 2022; **12**: 162 [PMID: 35429989 DOI: 10.1038/s41398-022-01927-9]

82 **van der Vinne N**, Vollebregt MA, van Putten MJAM, Arns M. Frontal alpha asymmetry as a diagnostic marker in depression: Fact or fiction? *Neuroimage Clin* 2017; **16**: 79-87 [PMID: 28761811 DOI: 10.1016/j.nicl.2017.07.006]

83 **Stewart JL**, Coan JA, Towers DN, Allen JJ. Resting and task-elicited prefrontal EEG alpha asymmetry in depression: support for the capability model. *Psychophysiology* 2014; **51**: 446-455 [PMID: 24611480 DOI: 10.1111/psyp.12191]

84 **Jesulola E**, Sharpley CF, Agnew LL. The effects of gender and depression severity on the association between alpha asymmetry and depression across four brain regions. *Behav Brain Res* 2017; **321**: 232-239 [PMID: 28042006 DOI: 10.1016/j.bbr.2016.12.035]

85 **Beck AT**, Steer RA, Brown G. Beck depression inventory–II. *Psychological assessment* 1996 [DOI: 10.1037/t00742-000]

86 **Tomarken AJ**, Davidson RJ, Henriques JB. Resting frontal brain asymmetry predicts affective responses to films. *J Pers Soc Psychol* 1990; **59**: 791-801 [PMID: 2254854 DOI: 10.1037//0022-3514.59.4.791]

87 **Wheeler RE**, Davidson RJ, Tomarken AJ. Frontal brain asymmetry and emotional reactivity: a biological substrate of affective style. *Psychophysiology* 1993; **30**: 82-89 [PMID: 8416065 DOI: 10.1111/j.1469-8986.1993.tb03207.x]

88 **Solomon B**, Hong M, Klimova A, Powers A, Dennis TA. Child exuberance moderates the impact of EEG asymmetry on attention performance. *PSYCHOPHYSIOLOGY* 2010 [DOI: 10.1016/j.paid.2009.10.001]

89 **Deslandes AC**, de Moraes H, Pompeu FA, Ribeiro P, Cagy M, Capitão C, Alves H, Piedade RA, Laks J. Electroencephalographic frontal asymmetry and depressive symptoms in the elderly. *Biol Psychol* 2008; **79**: 317-322 [PMID: 18761052 DOI: 10.1016/j.biopsycho.2008.07.008]

90 **Mikolajczak M**, Bodarwé K, Laloyaux O, Hansenne M, Nelis D. Association between frontal EEG asymmetries and emotional intelligence among adults. *Personality and Individual Differences* 2010; **48**: 177-181

91 **Arnone B**, Pompili A, Tavares MC, Gasbarri A. Sex-related memory recall and talkativeness for emotional stimuli. *Front Behav Neurosci* 2011; **5**: 52 [PMID: 21909326 DOI: 10.3389/fnbeh.2011.00052]

92 **Gasbarri A**, Arnone B, Pompili A, Marchetti A, Pacitti F, Calil SS, Pacitti C, Tavares MC, Tomaz C. Sex-related lateralized effect of emotional content on declarative memory: an event related potential study. *Behav Brain Res* 2006; **168**: 177-184 [PMID: 16443292 DOI: 10.1016/j.bbr.2005.07.034]

93 **Gasbarri A**, Arnone B, Pompili A, Pacitti F, Pacitti C, Cahill L. Sex-related hemispheric lateralization of electrical potentials evoked by arousing negative stimuli. *Brain Res* 2007; **1138**: 178-186 [PMID: 17274960 DOI: 10.1016/j.brainres.2006.12.073]

94 **Acharya UR**, Oh SL, Hagiwara Y, Tan JH, Adeli H, Subha DP. Automated EEG-based screening of depression using deep convolutional neural network. *Comput Methods Programs Biomed* 2018; **161**: 103-113 [PMID: 29852953 DOI: 10.1016/j.cmpb.2018.04.012]

95 **Putnam KM**, McSweeney LB. Depressive symptoms and baseline prefrontal EEG alpha activity: a study utilizing Ecological Momentary Assessment. *Biol Psychol* 2008; **77**: 237-240 [PMID: 18079035 DOI: 10.1016/j.biopsycho.2007.10.010]

96 **Santangeli O**, Porkka-Heiskanen T, Virkkala J, Castaneda AE, Marttunen M, Paunio T, Urrila AS. Sleep and slow-wave activity in depressed adolescent boys: a preliminary study. *Sleep Med* 2017; **38**: 24-30 [PMID: 29031752 DOI: 10.1016/j.sleep.2017.06.029]

97 **Bedwell JS**, Spencer CC, Chan CC, Butler PD, Sehatpour P, Schmidt J. The P1 visual-evoked potential, red light, and transdiagnostic psychiatric symptoms. *Brain Res* 2018; **1687**: 144-154 [PMID: 29510142 DOI: 10.1016/j.brainres.2018.03.002]

98 **Goodman SH**, Liu R, Lusby CM, Park JS, Bell MA, Newport DJ, Stowe ZN. Consistency of EEG asymmetry patterns in infants of depressed mothers. *Dev Psychobiol* 2021; **63**: 768-781 [PMID: 33067826 DOI: 10.1002/dev.22046]

99 **Smith J**, Browning M, Conen S, Smallman R, Buchbjerg J, Larsen KG, Olsen CK, Christensen SR, Dawson GR, Deakin JF, Hawkins P, Morris R, Goodwin G, Harmer CJ. Vortioxetine reduces BOLD signal during performance of the N-back working memory task: a randomised neuroimaging trial in remitted depressed patients and healthy controls. *Mol Psychiatry* 2018; **23**: 1127-1133 [PMID: 28533517 DOI: 10.1038/mp.2017.104]

World Journal of Clinical Cases

Submit a Manuscript: https://www.f6publishing.com

World J Clin Cases 2023 March 26; 11(9): 1918-1929

DOI: 10.12998/wjcc.v11.i9.1918

ISSN 2307-8960 (online)

MINIREVIEWS

COVID-19 related liver injuries in pregnancy

Metodija Sekulovski, Simona Bogdanova-Petrova, Monika Peshevska-Sekulovska, Tsvetelina Velikova, Tsvetoslav Georgiev

Specialty type: Gastroenterology and hepatology

Provenance and peer review: Invited article; Externally peer reviewed.

Peer-review model: Single blind

Peer-review report's scientific quality classification

Grade A (Excellent): 0
Grade B (Very good): 0
Grade C (Good): C, C
Grade D (Fair): 0
Grade E (Poor): 0

P-Reviewer: Papalexis PG, Greece; Rotondo JC, Italy

Received: November 22, 2022
Peer-review started: November 22, 2022
First decision: January 3, 2023
Revised: January 17, 2023
Accepted: February 21, 2023
Article in press: February 21, 2023
Published online: March 26, 2023

Metodija Sekulovski, Department of Anesthesiology and Intensive Care, University Hospital Lozenetz, Sofia 1407, Bulgaria

Metodija Sekulovski, Monika Peshevska-Sekulovska, Tsvetelina Velikova, Medical Faculty, Sofia University St. Kliment Ohridski, Sofia 1407, Bulgaria

Simona Bogdanova-Petrova, Tsvetoslav Georgiev, First Department of Internal Medicine, Medical University-Varna, Varna 9010, Bulgaria

Simona Bogdanova-Petrova, Tsvetoslav Georgiev, Clinic of Rheumatology, University Hospital "St. Marina", Varna 9010, Bulgaria

Monika Peshevska-Sekulovska, Department of Gastroenterology, University Hospital Lozenetz, Sofia 1407, Bulgaria

Tsvetelina Velikova, Department of Clinical Immunology, University Hospital Lozenetz, Sofia 1407, Bulgaria

Corresponding author: Tsvetoslav Georgiev, MD, PhD, Associate Professor, First Department of Internal Medicine, Medical University-Varna, 1 Hristo Smirnenski str., Varna 9010, Bulgaria. tsetso@medfaculty.org

Abstract

While severe acute respiratory syndrome coronavirus 2 (SARS-CoV-2) quickly spread across the globe, our understanding of its pathogenic mechanisms evolved. Importantly, coronavirus disease 2019 (COVID-19) is now considered a syndromic multisystem inflammatory disease involving not only the respiratory system but also the cardiovascular, excretory, nervous, musculoskeletal, and gastrointestinal systems. Moreover, a membrane-bound form of angiotensin-converting enzyme 2, the entry receptor for SARS-CoV-2, is expressed on the surface of cholangiocytes and hepatocytes, suggesting the potential of COVID-19 to involve the liver. With the widespread distribution of SARS-CoV-2 throughout the population, infection during pregnancy is no longer a rare occurrence; however, little is known about the course of hepatic injuries and related outcomes in pregnant SARS-CoV-2-positive women. Thus, the understudied topic of COVID-related liver disease during pregnancy poses a great challenge for the consulting gynecologist and hepatologist. In this review, we aim to describe and summarize potential liver injuries in pregnant women with COVID-19.

Key Words: COVID-19; Liver injury; Pregnancy; SARS-CoV-2; Angiotensin-converting

enzyme 2 receptors

Core Tip: Angiotensin-converting enzyme 2 receptors are expressed in hepatocytes and cholangiocytes, suggesting the potential for liver involvement by coronavirus disease 2019 (COVID-19). Liver dysfunction is mainly observed in patients with severe or critical disease. However, little is known about the course of liver involvement and its sequelae in pregnant women positive for severe acute respiratory syndrome coronavirus 2. Several cases of hepatic injury in pregnant women with severe COVID-19 have been reported, making the liver the second most commonly affected organ following the lung.

Citation: Sekulovski M, Bogdanova-Petrova S, Peshevska-Sekulovska M, Velikova T, Georgiev T. COVID-19 related liver injuries in pregnancy. *World J Clin Cases* 2023; 11(9): 1918-1929
URL: https://www.wjgnet.com/2307-8960/full/v11/i9/1918.htm
DOI: https://dx.doi.org/10.12998/wjcc.v11.i9.1918

INTRODUCTION

The end of 2019 was marked by the emergence of a novel disease caused by the severe acute respiratory syndrome coronavirus 2 (SARS-CoV-2). Unprecedentedly, modern societies have faced the threat of coronavirus disease (COVID-19), resulting in over 649 million confirmed cases and 6.5 million deaths worldwide as of 18 Dec 2022[1]. While COVID-19 quickly spread across the globe, our understanding of its pathogenic mechanisms began to evolve. Considered a flu-like illness initially, the pathogenesis of this disease underwent a radical change[2]. As of now, COVID-19 is perceived as a syndromic multisystem inflammatory disease involving primarily the respiratory and cardiovascular systems, but also the endocrine, nervous, gastrointestinal, and hepatobiliary systems.

SARS-CoV-2 utilizes the angiotensin-2 converting enzyme (ACE2) receptor protein to attack the host system[3]. The cell entry receptor, ACE2, is widely expressed in the human body, including in the lungs (type II alveolar cells), the gastrointestinal tract (esophageal epithelial cells and absorptive enterocytes of the ileum and colon)[4], the hepatobiliary system (hepatocytes and cholangiocytes), the cardiovascular system (myocardial cells), the renal system (proximal tubule cells and bladder urothelial cells), and the pancreas[3].

SARS-CoV-2 can directly bind to ACE2 on the surface of cholangiocytes and hepatocytes to exert a cytopathic effect[5]. In fact, several studies have reported injury to the hepatobiliary system[6], making it one of the most commonly affected systems aside from the respiratory system[7].

With the widespread distribution of SARS-CoV-2 throughout the population, infection during pregnancy is no longer a rare event. However, liver disease during pregnancy is relatively poorly studied, and poses a challenge for consulting gynecologists and hepatologists[8].

There are many physiological, mechanical, and immunologic changes that occur during pregnancy that may influence susceptibility to and severity of COVID-19. Ever-accumulating evidence suggests that SARS-CoV-2 infection during pregnancy, especially in women with severe COVID-19, is linked to various adverse outcomes, including preeclampsia (PE), preterm delivery, and stillbirth[9]. Pregnant women are also prone to involvement of several organs and organ systems with severe COVID-19 infection, including the gastrointestinal tract and the liver. Therefore, we aimed to describe and summarize potential liver injuries in pregnant women with COVID-19.

SEARCH STRATEGY

Our search methodology follows predefined rules for writing a narrative biomedical review[10]. A comprehensive search was performed on 15 August 2022 in the LitCovid (PubMed) and Scopus databases. These databases were queried using the keywords "COVID-19" or "coronavirus" or "SARS-CoV" AND "liver" OR "hepat*" OR "cholang*" and articles were extracted from inception to 15 August 2022. Bibliographies of retrieved publications were also hand-searched for important information. Relevant data were also included from preprints, papers, and guidelines of relevant professional associations to provide contextual background. Only case reports, original articles, reviews, and considerations of official societies written in English were included. Relevant papers were selected according to the professional expertise, experience, and opinions of the authors in preparation of this narrative review[10].

LIVER INJURIES IN COVID-19 PATIENTS

ACE2 receptors are expressed in hepatocytes and cholangiocytes, suggesting the potential for liver involvement by COVID-19. Liver dysfunction is mainly observed in patients with severe or critical disease[11] or in those with altered liver biochemistry tests [*e.g.*, elevated total bilirubin, gamma-glutamyl transferase (GGT), aspartate aminotransferase/alanine aminotransferase (AST/ALT)][12]. Aberrations in other commonly-performed laboratory tests such as alkaline phosphatase and ferritin may also suggest liver injury[13]. Pathoanatomically, microvesicular steatosis has been observed, with mild lobular and portal inflammation[14]. Liver injury in COVID-19 is likely related to the immune response, including cytokine storm development[15]. Hepatic damage during SARS-CoV-2 infection is very diverse, ranging from mild and harmless elevation of transaminases to acute liver failure. To encompass the whole spectrum of liver disease, the clinical entity "COVID-19-associated liver injury" was recently introduced[16,17].

ACE2 expression in cholangiocyte clusters has been reported to be significantly higher than that in the hepatocytes (59.7% *vs* 2.6%)[5]. Cholangiocytes are involved in many aspects of liver physiology, including regeneration mechanisms, adaptive immune response; disruption of cholangiocyte function can cause hepatobiliary injury. This injury is detected by monitoring for any increase in cholestatic markers (*e.g.*, including gamma-glutamyl transferase), and is observed in about 54% of COVID-19 cases [12,18]. In addition, SARS-CoV-2 can lead to disruption of the barrier and bile acid (BA) transport functions of cholangiocytes *via* dysregulation of genes involved in BA formation and transport[19].

Four potential causes of liver damage have been proposed. The first is the direct invasion of hepatocytes by SARS-CoV-2, leading to abnormal levels of liver enzymes. Although this hypothesis is the most accepted, hepatocytes have not been shown to express a high level of ACE2, making the liver itself an unlikely target for infection by SARS-CoV-2[20]. However, other studies have shown a high level of ACE2 expression in cholangiocytes, suggesting an indirect cause of elevated liver enzymes *via* cholangiocyte dysfunction[5]. Furthermore, elevated alkaline phosphatase levels have not been consistently demonstrated in patients with COVID-19, supporting the hypothesis of indirect liver injury. As of now, pathoanatomic data provide no evidence of direct SARS-CoV-2 infection of hepatocytes, suggesting this is an unlikely cause of liver damage[21]. The second possible mechanism of liver damage in COVID-19 is the hepatotoxicity of drugs used to treat the disease. Abnormal liver tests may occur in women treated with multiple medications including systemic glucocorticoids, antiviral, anti-inflammatory and anticoagulant drugs during pregnancy[22]. Nonsteroidal anti-inflammatory drugs, antipyretics, and analgesics are often used in COVID-19 patients for symptomatic control in the acute phase of the disease. Antibiotics are also frequently used. Additionally, the systemic inflammatory response and multiorgan dysfunction seen with severe COVID-19 may contribute to the development of a cytokine storm, which is associated with liver damage. Finally, the occurrence of severe acute respiratory syndrome can lead to severe hypoxia, which can also contribute to liver dysfunction[18]. An essential role is also played by the body's overwhelming and often life-threatening response to infection [23].

Cases of severe hepatitis with pronounced hepatocytolysis leading to acute liver failure have also been described[24]. The prognosis in these cases is poor; the more severe the disease, the greater the probability of liver involvement and impairment.

There are few reports and little research on COVID-19 infection in children who already have chronic liver disease. It is unclear whether infections in the pediatric population are linked to decompensation of cirrhosis and the onset of acute or chronic liver failure, which alone is a risk factor for a severe COVID-19 course. Furthermore, comorbidities in adults such as diabetes, hypertension, and obesity frequently result in non-alcoholic hepatosteatosis (fatty liver disease), but this has not been reported in children. Recently, liver involvement has been added to the many factors scrutinized in determining the severity of COVID-19 or multisystem inflammatory syndrome in children. Indeed, the use of liver enzymes as a predictive indicator for the prognosis of these diseases has been proposed[25].

PREGNANCY AS A RISK FACTOR FOR SEVERE COVID-19

The prevalence of SARS-CoV-2 infection among pregnant women presenting for management of labor and delivery is estimated at 3%-20%, depending on patient age and reproductive and socioeconomic settings[26,27]. Even after controlling for age, race, and sex, the risk of asymptomatic infection in obstetric patients was 15 times greater than in surgical patients[28].

In one study, pregnant women with COVID-19 were 3 times more likely than nonpregnant women with COVID-19 to be admitted to an intensive care unit (10.5 per 1000 cases *vs* 3.9 per 1000 cases), 2.9 times more likely to require invasive ventilation (2.9 per 1000 cases *vs* 1.1 per 1000 cases), 2.4 times more likely to require extracorporeal membrane oxygenation (0.7 per 1000 cases *vs* 0.3 per 1000 cases), and 1.7 times more likely to die (1.5 per 1000 cases *vs* 1.2 per 1000 cases)[29].

Underlying medical conditions, such as obesity, chronic lung disease (*e.g.*, asthma), and chronic hypertension were related to more severe COVID-19 in pregnancy. Contributing factors that are

exacerbated by comorbidities include inflammation, altered immune system function, and decreased ability to combat infection[30,31]. Susceptibility to respiratory viral infections has been demonstrated in pregnant women[32], attributed in part to the phenomenon of immune modulation occurring during pregnancy[33]. The most important factors related to severe COVID-19 in pregnant women and pregnancy outcomes are presented in Figure 1.

In general, the clinical management of COVID-19 in pregnancy is comparable to that in nonpregnant women, and effective medications should not be delayed based on pregnancy status[34]. However, in addition to the direct effective of COVID-19 on pregnancy outcomes, the pandemic and its impact on healthcare systems have had negative pregnancy-related consequences, including higher rates of stillbirth and maternal death[9,35]. Furthermore, SARS-CoV-2 infection during the first trimester of pregnancy is related to a higher risk of miscarriage[36].

LIVER INJURIES IN PREGNANT COVID-19 PATIENTS

Immunological reactions and cardiovascular changes brought on by pregnancy may accelerate the progression of COVID-19. However, little is known about the course of liver disease and its associated outcomes in pregnant SARS-CoV-2-positive women. Cases of severe COVID-19 disease and associated hepatic injury have been reported[6,37-39], making the liver the second most commonly affected organ following the lung. Transient elevations in serum aminotransferases are common. Several factors, including severe hypoxemia due to acute respiratory failure, drug interactions, septic shock, and multiorgan dysfunction have been linked to acute liver damage in severe COVID-19[6].

Much of the research on COVID-19 and its effects on pregnant patients with hepatic injury is currently under investigation. One study by Deng *et al*[40] compared pregnant patients without liver injury following SARS-CoV-2 infection to those with liver injury. This study demonstrated higher levels of procalcitonin, interleukin-6, liver enzymes, and lactate dehydrogenase in pregnant patients with hepatic involvement by the disease. There were no statistical differences between the two groups with respect to the severity of COVID-19, time from disease onset to hospitalization, length of hospital stay, radiological findings, or obstetric management. Four patients with liver injury in the third trimester voluntarily chose cesarean section, two had a vaginal delivery, and the rest did not deliver. The 6 live births resulted in no fetal death, neonatal death, or asphyxia. The authors found a 29.7% prevalence of liver injury in pregnant COVID-19 patients, with worse inflammation than those who did not have liver injury[40]. Another interesting case was reported by Anness *et al*[41] in which a pregnant woman at 28 wk gestation had COVID-19 complicated by hepatic dysfunction. However, in this case, the authors did find a correlation between the severity of COVID-19 disease and liver injury. After excluding PE and intrahepatic cholestasis (IHC) during pregnancy, because of the anamnesis of gestational diabetes and past history of IHC in the first pregnancy, they concluded that the abnormal liver tests were attributable to severe COVID-19. The normalization of liver function tests in the patient accompanied her clinical improvement in terms of viral symptoms, confirming the viral etiology of the liver disease. Another enduring hypothesis with respect to COVID-19 and hepatic injury with abnormal liver function tests is presented in a retrospective cohort study by Can *et al*[42]. This study considered that the aminotransferase elevation in COVID-19 pregnant women might be drug-induced, as the use of lopinavir/ritonavir and hydroxychloroquine were significantly higher at the beginning of pandemic and duration of treatment was longer in pregnant women with abnormal aminotransferases. Hence, liver function in SARS-CoV-2 infected pregnant women who received antiviral treatment should be closely monitored.

A similar case of drug-induced liver cytolysis in a pregnant woman with COVID-19 was reported by Lamazou *et al*[43]. This study presented a case of severe SARS-CoV-2 infection in the first trimester in a patient treated with hydroxychloroquine. Due to history of multiple implantation failure, an immunological treatment, aspirin, enoxaparin and filgrastim were used daily for 10 mo before an embryo transfer. The patient had no pregestational comorbidities such as hypertension, diabetes, or cardiovascular disease. In the 7th gestational wk (GW), the patient was noted to have abnormal liver function tests (AST, ALT and GGT 3, 5, and 2 times the upper limit of normal, respectively). Despite ruling out viral etiology (*e.g.*, viral hepatitis, cytomegalovirus, or Epstein-Barr virus), the patient's liver function deteriorated and improved only after stopping hydroxychloroquine. This case raises concerns regarding the possible association between COVID-19, prolonged usage of hydroxychloroquine, and drug-induced hepatitis[43].

Managing liver injury during pregnancy is a significant challenge and requires a multispecialty approach. Established classifications help obstetric specialists diagnose and treat pregnancy-related liver diseases efficiently. Among the most common of these are hyperemesis gravidarum, IHC during pregnancy, PE, HELLP (hemolysis, elevated liver enzymes, low platelets) syndrome and last but not least, acute fatty liver of pregnancy (AFLP)[44].

However, as mentioned above, although COVID-19 infection is gaining momentum as a possible factor contributing to hepatic dysfunction, little is known about its influence on women with pregnancy-related liver diseases.

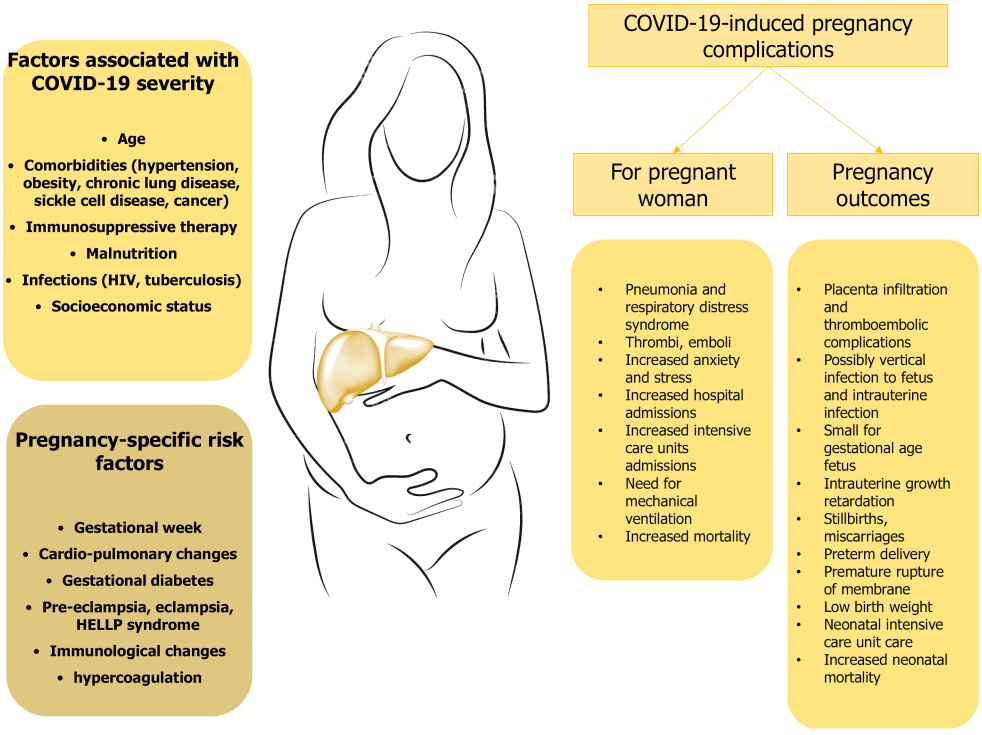

DOI: 10.12998/wjcc.v11.i9.1918

Figure 1 Severe coronavirus disease 2019 in pregnancy and associated complications for mother and fetus. COVID-19: Coronavirus disease 2019; HELLP: Hemolysis, elevated liver enzymes, low platelets; HIV: Human immunodeficiency virus.

PE

According to current data, it is clear that pregnant women with COVID-19 have an increased risk of hypertensive disorders, and the characteristics of these disorders are similar to those of non-pregnant hypertensive patients[45]. There is a growing body of evidence that raises concerns regarding the significant percentage of PE in pregnant COVID-19 patients. One of the most common complications in pregnant COVID-19 patients is PE[46]. Like the lungs and gastrointestinal tract, the placenta also has high expression of ACE2 receptors; therefore, SARS-CoV-2 infection could lead to placental dysregulation. This is in line with the fact that both PE and COVID-19 can affect the microcirculation, resulting in thrombotic incidents. High rates of PE have been reported in cases of severe and critical COVID-19 in pregnant women[47]. Among the most promising diagnostic markers for PE are soluble endoglin, pregnancy-associated plasma protein-A, soluble fms-like tyrosine kinase 1 (sFlt-1), and placental growth factor (PlGF). Because of placental hypoxia, a common finding in PE, there is often sFlt-1 overproduction with inhibition of PlGF. This can be observed in the circulation 5 wk or more before the onset of PE symptoms. Furthermore, the sFlt-1/PlGF ratio might also be affected by various infectious agents, including SARS-CoV-2. Unregulated levels of these mediators are related to placental insufficiency[48].

Another study by Mendoza *et al*[49] found that 11.9% of pregnant COVID-19 patients develop signs of PE and that these signs were only observed in severe COVID-19 pneumonia cases. However, the authors suspected that the signs and symptoms consistent with PE, which were present in 4 of 5 PE cases, may have resulted from the use of complex pharmacotherapy or the renal and cardiovascular dysfunction associated with SARS-CoV-2 infection. Abnormal angiogenic status (sFlt-1/PlGF ratio), increased lactate dehydrogenase (LDH), and poor placental perfusion typical of PE were confirmed in only 1 of the patients, indicating that this case was probably an actual case of PE, while the others were classified as PE-like syndrome. Cesarean section was performed on only this single patient with definitive PE. In contrast, the PE-like syndrome was not considered an absolute indication for earlier delivery due to the potential for spontaneous resolution of the syndrome after recovery from severe pneumonia. In summary, pregnant women with COVID-19 may develop a PE-like syndrome that, despite the similarities, can be appropriately differentiated from true PE by angiogenic markers to avoid unnecessary interventions such as preterm induction of labor.

AFLP

AFLP is a rare, potentially fatal complication that occurs in the peripartum period. The Swansea criteria are widely used for the diagnosis of AFLP and include results from both clinical and instrumental findings as well as pathological examination[50]. Choudhary *et al*[51] reported an interesting case of a PE patient with COVID-19 whose condition deteriorated after diagnosis of AFLP by Swansea criteria.

The patient also exhibited renal failure and severe COVID-19 pneumonia. The authors pointed out that the symptoms of COVID-19 might mimic those of HELLP syndrome, viral hepatitis, or IHC. Therefore, the best diagnostic approach includes first ruling out these other causes. Compared to HELLP syndrome, AFLP is associated with higher degrees of liver enzyme derangement and coagulation abnormalities. In addition, it is known that COVID-19 is frequently associated with hepatic dysfunction [52]. These findings are supported by a case report by Morton *et al*[53] in which a pregnant woman with influenza hepatitis developed AFLP. In this study, the authors elucidated a possible mechanism linking the 2 diseases: impaired hepatic fatty acid oxidation mediated by Kupffer cell cytokine release, hepatic oxidative stress, and hepatocyte injury as a result of viral infection. Following this mechanism, it is conceivable that COVID-19 could trigger a similar response and contribute to the development of PE. So far, available data have shown that pregnant women with severe COVID-19 disease could develop PE-like syndrome[49]. Therefore, it is of great significance for healthcare providers to be aware of the existence of this syndrome and carefully monitor pregnant patients with suspected AFLP.

IHC in pregnancy

Due to its effect on the liver, COVID-19 is associated with higher aminotransferase levels, especially in pregnant patients with IHC[54]. Increased levels of serum BA are the most sensitive diagnostic marker of IHC, likely due in part to its impaired resorption as a result of increased estrogen. However, in the case of SARS-CoV-2 infection, there is doubt as to whether hepatic dysfunction is due to IHC, SARS-CoV-2, or both[55]. Liver injury may result from direct infection of hepatocytes or from a byproduct of hypoxic cellular injury. Rabiei *et al*[56] reported a case of a 38-year-old COVID-19 patient pregnant with triplets. The patient also exhibited IHC of pregnancy and was treated with ursodeoxycholic acid. Due to worsening of her condition, she had preterm delivery in the 29th GW with a good outcome for her and 1 of 3 infants. However, 2 of the infants died due to severe pulmonary insufficiency and sepsis[56]. It is reasonable to speculate that in pregnant women with concurrent IHC and COVID-19, the obstetric cholestasis and viral infection act synergistically to worsen hepatic function. Based on available data, it appears that the simultaneous presence of IHC and COVID-19 does not affect maternal and fetal outcomes more than in women with cholestasis alone. However, there is still a lack of evidence regarding whether increasing degrees of hepatic dysfunction are related to an increased risk of adverse pregnancy outcomes such as spontaneous and iatrogenic preterm delivery, meconium-stained amniotic fluid, neonatal respiratory distress syndrome, and stillbirth. Furthermore, it is unclear if established COVID-19 prognostic markers can be used in this cohort of patients.

HELLP, HELLP-like syndrome, and hepatic rupture

Because of the serious nature of the pandemic, the research community has focused on the complex pathogenesis of COVID-19 disease. Many studies have described the multifactorial nature of COVID-19, and have demonstrated thrombocytopenia, endothelial damage, impaired aggregation, impaired bone marrow function, and decreased megakaryocyte activity[57,58].

It is also known that many of the factors mentioned above, such as endothelial damage, platelet activation, and thrombosis, are also the hidden villains behind the physiopathology of HELLP syndrome and PE[59]. HELLP syndrome is a multisystemic disorder seen in 0.5%-0.9% of all pregnancies, mostly in the last trimester (70%), in multiparous women, and in advanced cases that are not diagnosed or treated early. HELLP syndrome has been associated with impaired renal function, intracranial hemorrhage, intrahepatic hemorrhage, coagulopathy, and disseminated intravascular coagulation[59]. Unfortunately, similar symptoms are often also present in pregnant COVID-19 patients, which makes the diagnosis challenging. Nevertheless, early recognition of the diagnosis could be life-saving, as mentioned in a study by Arslan *et al*[60]. The authors reported a case of a 30-year-old primigravida woman with COVID-19 and severe HELLP syndrome with a fatal outcome for mother and baby. Despite definitive evidence, given the sequence of events in this case, it is reasonable to speculate that COVID-19 may be a contributing factor in the development HELLP syndrome. Čivrná *et al*[61] reported another interesting case series describing the differences between HELLP and HELLP-like syndromes associated with COVID-19. In this study, 1 patient was noted to have elevated liver enzymes, elevated LDH, and a low ratio of angiogenic biomarkers, but did not have pregnancy complications. Laboratory findings in this patient normalized after recovering from SARS-CoV-2 infection. Hence, the authors diagnosed this patient with HELLP-like syndrome. In contrast, another patient in this case series did meet the criteria for HELLP syndrome, and her condition deteriorated resulting in respiratory failure and hepatic rupture. Proper early diagnosis of HELLP syndrome in severe COVID-19 in pregnancy could pose a diagnostic dilemma due to the similarity in presentations of these conditions [61].

Ronnje *et al*[62] reported a case of a 26-year-old woman with atypical HELLP syndrome and severe COVID-19, highlighting the similarities between the two conditions and the fact that prompt diagnosis may be delayed. This study also proposed that COVID-19 infection during pregnancy is linked to an increased risk of maternal thrombotic incidents, given that pregnancy itself induces a hypercoagulable state. In this case report, the conclusion that the severe COVID-19 infection caused the patient's liver injury and coagulation dysfunction was supported by detection of high D-dimer levels and elevated liver enzymes[62]. Misdiagnosis might lead to unnecessary intervention and iatrogenic prematurity or

underestimation of the severity of HELLP syndrome, causing delayed therapeutic intervention. As such, further investigation into this topic is of paramount importance to clarify the exact mechanisms, design an adequate therapeutic strategy, and avoid adverse outcomes.

As a late pregnancy-related liver disease, HELLP syndrome is a well-known culprit implicated in various complications. Among the most life-threatening of these is liver rupture with or without infarction[63]. Hepatic rupture has a low incidence rate (approximately 1 per 200000 pregnancies). It is primarily associated with AFLP or HELLP syndrome, and rarely occurs without associated liver disease. After excluding all non-pregnancy-related liver diseases, clinicians should consider 3 other possible causes of liver rupture in pregnancy: HELLP syndrome, severe PE, and rupture of hemangioma. Current reports assessing the pathogenetic mechanism of hepatic rupture in pregnant patients focus largely on HELLP syndrome. However, with the growing impact of COVID-19 and the millions of affected patients globally, among which are a significant percentage of pregnant women, the question arises whether SARS-CoV-2 could contribute to such a serious complication. One of the first to associate COVID-19 and hepatic rupture was a case of a 32-year-old pregnant patient reported by Ambrož *et al*[64]. This patient was found with SARS-CoV-2 infection in the third trimester; her condition deteriorated resulting in bilateral pneumonia and hemoperitoneum as a result of hepatic rupture. Vascular effects (*e.g.*, endotheliitis, procoagulation, or thrombosis) seem to be essential contributors to the worsening of hepatopathy during pregnancy, possibly through changes affecting the endothelium occurring during severe inflammatory response. These changes are thought to underlie liver rupture in the setting of pregnancy. In another study by Ahmed *et al*[65], a case of hemorrhage with intraabdominal hematoma was reported in a patient with severe COVID-19, PE, and HELLP syndrome.

Finally, high rates of infant and maternal mortality have been reported, 42% and 39%, respectively. These data underscore the need for close collaboration between the obstetrician and the surgeon[66,67]. As such, COVID-19 complications in pregnant patients including severe hepatopathy require further research.

PREGNANCY OUTCOMES AFTER LIVER INJURY

We reviewed available literature regarding COVID-19 in women with pregnancy-related hepatic injury. In total, 34 pregnant COVID-19 patients and 37 infants were included in our review[49,50,54,56,60-62,65,68]. We determined that the most common reported liver disease in pregnancy was IHC, followed by HELLP syndrome, and AFLP (61.7%, 32.3% and 2.9%, respectively). Most patients reported flu-like symptoms (n = 27), and 6 patients (17.65%) were diagnosed with pneumonia or acute respiratory distress syndrome (ARDS). Two pregnant women reported abdominal pain, and only one was diagnosed with intraabdominal hemorrhage. Only 1 patient presented with sepsis and multiorgan failure. A significant percentage (88.2%) of the women underwent C-section (Table 1).

With respect to maternal mortality rates, 2 (5.88%) pregnant women in the reviewed cases died; both cases were significant for HELLP syndrome (1 in week 22 and 1 in week 32 of gestation). Neonatal or fetal death were found in 4 cases (10.81%). Two babies were delivered at week 29 by mothers with IHC, while the other two were delivered at week by mothers with HELLP syndrome (Table 1). With respect to maternal medical history and treatment strategies employed, we cannot accurately report the data as they were not reported in the reviewed studies. Another limitation of our research was inability to assess the maternal age and gestational ages of fetuses with preterm delivery due to lack available data.

To our knowledge, this literature review is among the few that have addressed COVID-19 in pregnant patients with associated liver injury. However, despite review of the available data on the topic, there are still some missing points in etiopathogenetic mechanisms and the outcomes of COVID-19-related liver injury in pregnancy. The relevant available studies are summarized in Table 1.

Taken together, the results of available literature have shown that liver injury should be considered in pregnant patients with COVID-19. To this end, active follow-up and treatment of COVID-19 is mandatory. However, not a single laboratory or a clinical marker could be established as definitive for COVID-19-related liver injury. Usually, liver enzymes are elevated in these cases; however, this finding may be a consequence of pharmacotherapy (*e.g.*, systemic glucocorticoids or antiviral, anti-inflammatory, or anticoagulant drugs). Comorbidities such as established liver disease, diabetes, hypertension, and obesity frequently result in non-alcoholic hepatosteatosis and may also impact the onset and severity of liver injury caused by SARS-CoV-2 during pregnancy. Pregnancy itself is a risk factor for severe COVID-19; therefore, managing liver injury during pregnancy is a significant challenge and requires a multispecialty approach.

VACCINATION FOR PREGNANT WOMEN TO AVOID COMPLICATIONS

Similar to those with autoimmune diseases, pregnant women have generally been excluded from clinical trials of novel drugs and vaccinations due to worries regarding fetal consequences. This has also been true of COVID-19 vaccines thus far[69].

Table 1 Coronavirus disease 2019-related liver injuries in pregnant women

Ref.	Number of patients	Type of disease	Concomitant disease	Past disease	Age	Gestational week	Symptoms	Treatment	Outcome
Ronnje *et al* [62]	1	HELLP	HT; OO	Appendectomy; cholecystectomy	26	32	Flu-like (myalgia, arthralgia, cough); abdominal pain; fever	CS paracetamol; Morphine; dalteparin 7500 UI/d; betamethasone; cefotaxime	M + B: alive
Mendoza *et al*[49]	5	PE; HELLP	NR	NR	39.4 (34.2-44.5)	28.6 (22.3-32.4)	Severe pneumonia	1 CS, hypertensive therapy; 4 no delivery	M + B: alive
Rabiei *et al* [56]	1	IHCP	HT; GDM	Primary infertility	38	29 + 2	Flu-like (myalgia, arthralgia, cough)	UDCA; CS	M and 2nd baby: alive; 1st and 3rd baby: death
Ahmed *et al* [65]	1	HELLP	NR	NR	26	NR	Confusion; intraabdominal hematoma	Surgery; CS	M + B: Alive
Čivrná *et al* [61]	2	HELLP; HR	NR	NR	NR	NR	1st flu-like (myalgia, arthralgia, cough); 2nd ARDS, HR	CS	1st M + B: alive; 2nd: NR
Choudhary *et al*[51]	1	PE; AFLP	NR	NR	27	35	Icteric fever; flu-like (myalgia, arthralgia, cough); renal failure	Labetalol 200 mg/d; Mg sulfate; CS	M + Both babies: alive
Arslan *et al* [60]	1	HELLP	NR	NR	30	32	Flu-like (myalgia, arthralgia, cough); fever; pneumonia; renal failure; sepsis	CS	M + B: death
D'Ambrosi *et al*[54]	20	IHCP	NR	NR	30.5 ± 5.7		Flu-like (myalgia, arthralgia, cough); fever	NR	M + B: alive
Futterman *et al*[68]	2	HELLP	NR	NR	NR	22; 29	NR	NR	1st M + B: death; 2nd M + B: alive

AFLP: Acute fatty liver of pregnancy; ARDS: Acute hypoxemic respiratory failure; B: Baby; CS: Corticosteroids; GDM: Gestational diabetes mellitus; GW: Gestational week; HELLP: Hemolysis, elevated liver enzymes and low platelets; HR: Hepatic rupture; HT: Hypothyroidism; IHCP: Intrahepatic cholestasis of pregnancy; M: Mother; M + B: Mother and baby; Mg: Magnesium; NR: Not reported, OO: Overweight and obese; PE: Preeclampsia; UDCA: Ursodeoxycholic acid.

Although there are limited data on the efficacy and safety in pregnant women, the Centers for Disease Control and Prevention, the American College of Obstetricians and Gynecologists, and the Society for Maternal-Fetal Medicine have each issued guidelines for the use of COVID-19 vaccines in pregnant women[70]. These guidelines are supported by data suggesting that vaccines reduce mortality and complications in SARS-CoV-2 infected people, especially those at high risk for severe disease.

LIMITATIONS

Our narrative review has been conducted by using a search strategy that is adequate to retrieve relevant studies. Although we presented a thorough review of available literature, we acknowledge some limitations. First, liver disease associated with SARS-CoV-2 infection during pregnancy is still understudied. This has resulted in a relatively small number of available case reports, original articles, reviews, and considerations of official societies. Second, despite all the collected data on the topic, there are still some missing points in etiopathogenetic mechanisms and the outcomes associated with COVID-19-related hepatic injury in pregnancy. Most authors did not report data on maternal medical history and treatment strategies utilized; therefore, we cannot present accurate information these topics. Another disadvantage we faced during review of the available literature was that maternal and gestational ages at the time of preterm delivery were also often not reported. Finally, the narrative

nature of our review did not allow us to make conclusions based on statistical analyses. However, we believe that these limitations are minor and represent opportunities to inform future research. Our aim to describe and summarize potential liver injuries in pregnant women with COVID-19 will hopefully be of tremendous help to consulting gynecologists and hepatologists who may encounter this scenario.

FUTURE DIRECTIONS

Many questions regarding how to promptly diagnose COVID-19-related liver injury in pregnant women remain. An algorithm that includes a diagnostic approach for these patients, including laboratory testing, clinical and imaging investigations, and most importantly, management (treatment and follow-up), is needed. Since pregnancy, underlying liver conditions, and others are risk factors for severe COVID-19 and adverse outcomes, liver injury is a highly unfavorable prognostic marker. More studies that include pregnant women with COVID-19 could help close the gap in knowledge and will improve the recommendations for clinical practice.

CONCLUSION

It is accepted that immunological reactions and cardiovascular changes brought on by pregnancy may accelerate the progression of COVID-19. However, little is known about the course of liver disease and associated outcomes in pregnant COVID-19 patients. Several factors, including severe hypoxemia due to acute respiratory failure, drug interactions, septic shock, and multiorgan dysfunction have been linked to acute liver damage in severe COVID-19 disease. Transient elevations in serum aminotransferases are common. Much of the research on COVID-19 and its effects on pregnant patients with hepatic injury is still ongoing. The management of liver injury during pregnancy is a significant challenge and requires a multispecialty approach that should utilize established classifications set forth by various professional obstetric organizations. Among the most common pregnancy- and liver-related complications are hyperemesis gravidarum, IHC, PE, HELLP syndrome, and AFLP. Finally, vaccination in pregnant women may reduce the risk of severe COVID-19 during pregnancy and help to avoid adverse delivery outcomes.

FOOTNOTES

Author contributions: Georgiev T and Sekulovski M contributed to the conceptualization; Georgiev T Sekulovski M, Bogdanova-Petrova S and Peshevska-Sekulovska M contributed to the resources and literature review; Georgiev T, Sekulovski M, Bogdanova-Petrova S and Peshevska-Sekulovska M contributed to the preparation of original draft; Georgiev T, Sekulovski M, Velikova T contributed to the review and editing; Georgiev T, and Velikova T contributed to the supervision; All authors revised and approved the final version of the manuscript.

Conflict-of-interest statement: The authors declare they have no conflicts of interest.

Country/Territory of origin: Bulgaria

ORCID number: Metodija Sekulovski 0000-0001-8374-7756; Simona Bogdanova-Petrova 0000-0002-2601-2021; Monika Peshevska-Sekulovska 0000-0002-8468-0132; Tsvetelina Velikova 0000-0002-0593-1272; Tsvetoslav Georgiev 0000-0002-1652-4648.

S-Editor: Chang KL
L-Editor: Filipodia
P-Editor: Chang KL

REFERENCES

1 **World Health Organization**. Weekly epidemiological update on COVID-19 - 21 December 2022. [cited 4 January 2023]. Available from: https://www.who.int/publications/m/item/covid-19-weekly-epidemiological-update---21-december-2022

2 **Georgiev T**, Angelov AK. Complexities of diagnosis and management of COVID-19 in autoimmune diseases: Potential benefits and detriments of immunosuppression. *World J Clin Cases* 2020; **8**: 3669-3678 [PMID: 32953843 DOI: 10.12998/wjcc.v8.i17.3669]

3 **Hoffmann M**, Kleine-Weber H, Schroeder S, Krüger N, Herrler T, Erichsen S, Schiergens TS, Herrler G, Wu NH, Nitsche A, Müller MA, Drosten C, Pöhlmann S. SARS-CoV-2 Cell Entry Depends on ACE2 and TMPRSS2 and Is Blocked by a Clinically Proven Protease Inhibitor. *Cell* 2020; **181**: 271-280.e8 [PMID: 32142651 DOI: 10.1016/j.cell.2020.02.052]

4 **Velikova T**, Snegarova V, Kukov A, Batselova H, Mihova A, Nakov R. Gastrointestinal mucosal immunity and COVID-19. *World J Gastroenterol* 2021; **27**: 5047-5059 [PMID: 34497434 DOI: 10.3748/wjg.v27.i30.5047]

5 **Chai X**, Hu L, Zhang Y, Han W, Lu Z, Ke A, Zhou J, Shi G, Fang N, Fan J, Cai J, Lan F. Specific ACE2 expression in cholangiocytes may cause liver damage after 2019-nCoV infection. 2020 Preprint. Available from: bioRxiv:2020.02.03.931766 [DOI: 10.1101/2020.02.03.931766]

6 **Li J**, Fan JG. Characteristics and Mechanism of Liver Injury in 2019 Coronavirus Disease. *J Clin Transl Hepatol* 2020; **8**: 13-17 [PMID: 32274341 DOI: 10.14218/JCTH.2020.00019]

7 **Velikova TV**, Kotsev SV, Georgiev DS, Batselova HM. Immunological aspects of COVID-19: What do we know? *World J Biol Chem* 2020; **11**: 14-29 [PMID: 33024515 DOI: 10.4331/wjbc.v11.i2.14]

8 **Mikolasevic I**, Filipec-Kanizaj T, Jakopcic I, Majurec I, Brncic-Fischer A, Sobocan N, Hrstic I, Stimac T, Stimac D, Milic S. Liver Disease During Pregnancy: A Challenging Clinical Issue. *Med Sci Monit* 2018; **24**: 4080-4090 [PMID: 29905165 DOI: 10.12659/MSM.907723]

9 **Jamieson DJ**, Rasmussen SA. An update on COVID-19 and pregnancy. *Am J Obstet Gynecol* 2022; **226**: 177-186 [PMID: 34534497 DOI: 10.1016/j.ajog.2021.08.054]

10 **Gasparyan AY**, Ayvazyan L, Blackmore H, Kitas GD. Writing a narrative biomedical review: considerations for authors, peer reviewers, and editors. *Rheumatol Int* 2011; **31**: 1409-1417 [PMID: 21800117 DOI: 10.1007/s00296-011-1999-3]

11 **Shi H**, Han X, Jiang N, Cao Y, Alwalid O, Gu J, Fan Y, Zheng C. Radiological findings from 81 patients with COVID-19 pneumonia in Wuhan, China: a descriptive study. *Lancet Infect Dis* 2020; **20**: 425-434 [PMID: 32105637 DOI: 10.1016/S1473-3099(20)30086-4]

12 **Zhang C**, Shi L, Wang FS. Liver injury in COVID-19: management and challenges. *Lancet Gastroenterol Hepatol* 2020; **5**: 428-430 [PMID: 32145190 DOI: 10.1016/S2468-1253(20)30057-1]

13 **Georgakopoulou VE**, Bali T, Adamantou M, Asimakopoulou S, Makrodimitri S, Samara S, Triantafyllou M, Voutsinas PM, Eliadi I, Karamanakos G, Basoulis D, Chatzipanagiotou O, Adamopoulou E, Alevizou A, Athanasiadis M, Spandidos DA, Papalexis P, Tarantinos K, Sipsas NV, Samarkos M, Cholongitas E. Acute hepatitis and liver injury in hospitalized patients with COVID-19 infection. *Exp Ther Med* 2022; **24**: 691 [PMID: 36277149 DOI: 10.3892/etm.2022.11627]

14 **Yao X**, Ye F, Zhang M, Cui C, Huang B, Niu P, Liu X, Zhao L, Dong E, Song C, Zhan S, Lu R, Li H, Tan W, Liu D. In Vitro Antiviral Activity and Projection of Optimized Dosing Design of Hydroxychloroquine for the Treatment of Severe Acute Respiratory Syndrome Coronavirus 2 (SARS-CoV-2). *Clin Infect Dis* 2020; **71**: 732-739 [PMID: 32150618 DOI: 10.1093/cid/ciaa237]

15 **Taneva G**, Dimitrov D, Velikova T. Liver dysfunction as a cytokine storm manifestation and prognostic factor for severe COVID-19. *World J Hepatol* 2021; **13**: 2005-2012 [PMID: 35070004 DOI: 10.4254/wjh.v13.i12.2005]

16 **Cooper KM**, Colletta A, Asirwatham AM, Moore Simas TA, Devuni D. COVID-19 associated liver injury: A general review with special consideration of pregnancy and obstetric outcomes. *World J Gastroenterol* 2022; **28**: 6017-6033 [PMID: 36405386 DOI: 10.3748/wjg.v28.i42.6017]

17 **Mohammed SA**, Eid KM, Anyiam FE, Wadaaallah H, Muhamed MAM, Morsi MH, Dahman NBH. Liver injury with COVID-19: laboratory and histopathological outcome-systematic review and meta-analysis. *Egypt Liver J* 2022; **12**: 9 [PMID: 35096428 DOI: 10.1186/s43066-022-00171-6]

18 **Yu D**, Du Q, Yan S, Guo XG, He Y, Zhu G, Zhao K, Ouyang S. Liver injury in COVID-19: clinical features and treatment management. *Virol J* 2021; **18**: 121 [PMID: 34108015 DOI: 10.1186/s12985-021-01593-1]

19 **Zhao B**, Ni C, Gao R, Wang Y, Yang L, Wei J, Lv T, Liang J, Zhang Q, Xu W, Xie Y, Wang X, Yuan Z, Zhang R, Lin X. Recapitulation of SARS-CoV-2 infection and cholangiocyte damage with human liver ductal organoids. *Protein Cell* 2020; **11**: 771-775 [PMID: 32303993 DOI: 10.1007/s13238-020-00718-6]

20 **Du M**, Cai G, Chen F, Christiani DC, Zhang Z, Wang M. Multiomics Evaluation of Gastrointestinal and Other Clinical Characteristics of COVID-19. *Gastroenterology* 2020; **158**: 2298-2301.e7 [PMID: 32234303 DOI: 10.1053/j.gastro.2020.03.045]

21 **Yao XH**, Li TY, He ZC, Ping YF, Liu HW, Yu SC, Mou HM, Wang LH, Zhang HR, Fu WJ, Luo T, Liu F, Guo QN, Chen C, Xiao HL, Guo HT, Lin S, Xiang DF, Shi Y, Pan GQ, Li QR, Huang X, Cui Y, Liu XZ, Tang W, Pan PF, Huang XQ, Ding YQ, Bian XW. A pathological report of three COVID-19 cases by minimal invasive autopsies. *Zhonghua Bing Li Xue Za Zhi* 2020; **49**: 411-417 [PMID: 32172546 DOI: 10.3760/cma.j.cn112151-20200312-00193]

22 **Karlafti E**, Paramythiotis D, Pantazi K, Georgakopoulou VE, Kaiafa G, Papalexis P, Protopapas AA, Ztriva E, Fyntanidou V, Savopoulos C. Drug-Induced Liver Injury in Hospitalized Patients during SARS-CoV-2 Infection. *Medicina (Kaunas)* 2022; **58** [PMID: 36557050 DOI: 10.3390/medicina58121848]

23 **Mao R**, Qiu Y, He JS, Tan JY, Li XH, Liang J, Shen J, Zhu LR, Chen Y, Iacucci M, Ng SC, Ghosh S, Chen MH. Manifestations and prognosis of gastrointestinal and liver involvement in patients with COVID-19: a systematic review and meta-analysis. *Lancet Gastroenterol Hepatol* 2020; **5**: 667-678 [PMID: 32405603 DOI: 10.1016/S2468-1253(20)30126-6]

24 **Wander P**, Epstein M, Bernstein D. COVID-19 Presenting as Acute Hepatitis. *Am J Gastroenterol* 2020; **115**: 941-942 [PMID: 32301760 DOI: 10.14309/ajg.0000000000000660]

25 **Lazova S**, Alexandrova T, Gorelyova-Stefanova N, Atanasov K, Tzotcheva I, Velikova T. Liver Involvement in Children with COVID-19 and Multisystem Inflammatory Syndrome: A Single-Center Bulgarian Observational Study. *Microorganisms* 2021; **9** [PMID: 34576853 DOI: 10.3390/microorganisms9091958]

26 **LaCourse SM**, Kachikis A, Blain M, Simmons LE, Mays JA, Pattison AD, Salerno CC, McCartney SA, Kretzer NM, Resnick R, Shay RL, Savitsky LM, Curtin AC, Huebner EM, Ma KK, Delaney S, Delgado C, Schippers A, Munson J, Pottinger PS, Cohen S, Neme S, Bourassa L, Bryan A, Greninger A, Jerome KR, Roxby AC, Lokken E, Cheng E, Adams

Waldorf KM, Hitti J. Low Prevalence of Severe Acute Respiratory Syndrome Coronavirus 2 Among Pregnant and Postpartum Patients With Universal Screening in Seattle, Washington. *Clin Infect Dis* 2021; **72**: 869-872 [PMID: 32472688 DOI: 10.1093/cid/ciaa675]

27 **Vintzileos WS**, Muscat J, Hoffmann E, John NS, Vertichio R, Vintzileos AM, Vo D. Screening all pregnant women admitted to labor and delivery for the virus responsible for coronavirus disease 2019. *Am J Obstet Gynecol* 2020; **223**: 284-286 [PMID: 32348743 DOI: 10.1016/j.ajog.2020.04.024]

28 **Kelly JC**, Raghuraman N, Carter EB, Palanisamy A, Stout MJ. Preprocedural asymptomatic coronavirus disease 2019 cases in obstetrical and surgical units. *Am J Obstet Gynecol* 2021; **224**: 114-116 [PMID: 32971011 DOI: 10.1016/j.ajog.2020.09.023]

29 **Zambrano LD**, Ellington S, Strid P, Galang RR, Oduyebo T, Tong VT, Woodworth KR, Nahabedian JF 3rd, Azziz-Baumgartner E, Gilboa SM, Meaney-Delman D; CDC COVID-19 Response Pregnancy and Infant Linked Outcomes Team. Update: Characteristics of Symptomatic Women of Reproductive Age with Laboratory-Confirmed SARS-CoV-2 Infection by Pregnancy Status - United States, January 22-October 3, 2020. *MMWR Morb Mortal Wkly Rep* 2020; **69**: 1641-1647 [PMID: 33151921 DOI: 10.15585/mmwr.mm6944e3]

30 **Galang RR**, Newton SM, Woodworth KR, Griffin I, Oduyebo T, Sancken CL, Olsen EO, Aveni K, Wingate H, Shephard H, Fussman C, Alaali ZS, Silcox K, Siebman S, Halai UA, Lopez CD, Lush M, Sokale A, Barton J, Chaudhary I, Patrick PH, Schlosser L, Reynolds B, Gaarenstroom N, Chicchelly S, Read JS, de Wilde L, Mbotha D, Azziz-Baumgartner E, Hall AJ, Tong VT, Ellington S, Gilboa SM; Centers for Disease Control and Prevention COVID-19 Response Pregnancy and Infant Linked Outcomes Team. Risk Factors for Illness Severity Among Pregnant Women With Confirmed Severe Acute Respiratory Syndrome Coronavirus 2 Infection-Surveillance for Emerging Threats to Mothers and Babies Network, 22 State, Local, and Territorial Health Departments, 29 March 2020-5 March 2021. *Clin Infect Dis* 2021; **73**: S17-S23 [PMID: 34021332 DOI: 10.1093/cid/ciab432]

31 **Metz TD**, Clifton RG, Hughes BL, Sandoval G, Saade GR, Grobman WA, Manuck TA, Miodovnik M, Sowles A, Clark K, Gyamfi-Bannerman C, Mendez-Figueroa H, Sehdev HM, Rouse DJ, Tita ATN, Bailit J, Costantine MM, Simhan HN, Macones GA; Eunice Kennedy Shriver National Institute of Child Health and Human Development (NICHD) Maternal-Fetal Medicine Units (MFMU) Network. Disease Severity and Perinatal Outcomes of Pregnant Patients With Coronavirus Disease 2019 (COVID-19). *Obstet Gynecol* 2021; **137**: 571-580 [PMID: 33560778 DOI: 10.1097/AOG.0000000000004339]

32 **Longman RE**, Johnson TR. Viral respiratory disease in pregnancy. *Curr Opin Obstet Gynecol* 2007; **19**: 120-125 [PMID: 17353679 DOI: 10.1097/GCO.0b013e328028fdc7]

33 **Mazziotta C**, Pellielo G, Tognon M, Martini F, Rotondo JC. Significantly Low Levels of IgG Antibodies Against Oncogenic Merkel Cell Polyomavirus in Sera From Females Affected by Spontaneous Abortion. *Front Microbiol* 2021; **12**: 789991 [PMID: 34970247 DOI: 10.3389/fmicb.2021.789991]

34 **American College of Obstetricians and Gynecologists**. COVID-19 Vaccination Considerations for Obstetric–Gynecologic Care. [cited 20 September 2022]. Available from: https://www.acog.org/clinical/clinical-guidance/practice-advisory/articles/2020/12/covid-19-vaccination-considerations-for-obstetric-gynecologic-care

35 **Chmielewska B**, Barratt I, Townsend R, Kalafat E, van der Meulen J, Gurol-Urganci I, O'Brien P, Morris E, Draycott T, Thangaratinam S, Le Doare K, Ladhani S, von Dadelszen P, Magee L, Khalil A. Effects of the COVID-19 pandemic on maternal and perinatal outcomes: a systematic review and meta-analysis. *Lancet Glob Health* 2021; **9**: e759-e772 [PMID: 33811827 DOI: 10.1016/S2214-109X(21)00079-6]

36 **Balachandren N**, Davies MC, Hall JA, Stephenson JM, David AL, Barrett G, O'Neill HC, Ploubidis GB, Yasmin E, Mavrelos D. SARS-CoV-2 infection in the first trimester and the risk of early miscarriage: a UK population-based prospective cohort study of 3041 pregnancies conceived during the pandemic. *Hum Reprod* 2022; **37**: 1126-1133 [PMID: 35389480 DOI: 10.1093/humrep/deac062]

37 **Zu ZY**, Jiang MD, Xu PP, Chen W, Ni QQ, Lu GM, Zhang LJ. Coronavirus Disease 2019 (COVID-19): A Perspective from China. *Radiology* 2020; **296**: E15-E25 [PMID: 32083985 DOI: 10.1148/radiol.2020200490]

38 **Mao R**, Liang J, Shen J, Ghosh S, Zhu LR, Yang H, Wu KC, Chen MH; Chinese Society of IBD, Chinese Elite IBD Union; Chinese IBD Quality Care Evaluation Center Committee. Implications of COVID-19 for patients with pre-existing digestive diseases. *Lancet Gastroenterol Hepatol* 2020; **5**: 425-427 [PMID: 32171057 DOI: 10.1016/S2468-1253(20)30076-5]

39 **Guan WJ**, Ni ZY, Hu Y, Liang WH, Ou CQ, He JX, Liu L, Shan H, Lei CL, Hui DSC, Du B, Li LJ, Zeng G, Yuen KY, Chen RC, Tang CL, Wang T, Chen PY, Xiang J, Li SY, Wang JL, Liang ZJ, Peng YX, Wei L, Liu Y, Hu YH, Peng P, Wang JM, Liu JY, Chen Z, Li G, Zheng ZJ, Qiu SQ, Luo J, Ye CJ, Zhu SY, Zhong NS; China Medical Treatment Expert Group for Covid-19. Clinical Characteristics of Coronavirus Disease 2019 in China. *N Engl J Med* 2020; **382**: 1708-1720 [PMID: 32109013 DOI: 10.1056/NEJMoa2002032]

40 **Deng G**, Zeng F, Zhang L, Chen H, Chen X, Yin M. Characteristics of pregnant patients with COVID-19 and liver injury. *J Hepatol* 2020; **73**: 989-991 [PMID: 32569609 DOI: 10.1016/j.jhep.2020.06.022]

41 **Anness A**, Siddiqui F. COVID-19 complicated by hepatic dysfunction in a 28-week pregnant woman. *BMJ Case Rep* 2020; **13** [PMID: 32878840 DOI: 10.1136/bcr-2020-237007]

42 **Can E**, Oğlak SC, Ölmez F. Abnormal liver function tests in pregnant patients with COVID-19 - a retrospective cohort study in a tertiary center. *Ginekol Pol* 2022 [PMID: 35072238 DOI: 10.5603/GP.a2021.0182]

43 **Lamazou F**, Oger P, Dieli-Crimi R, Guerin A, Letouzey V, Octernaud S, Place V, Calès P, Descamps P, Delaroche L. COVID-19 infection in first trimester of pregnancy marked by a liver cytolysis in a woman previously treated by hydroxychloroquine for repeated implantation failure: a case report. *BMC Infect Dis* 2020; **20**: 845 [PMID: 33198681 DOI: 10.1186/s12879-020-05551-0]

44 **Sharma AV**, John S. Liver Disease In Pregnancy. 2022 Jun 21. In: StatPearls [Internet]. Treasure Island (FL): StatPearls Publishing; 2022 Jan- [PMID: 29489187]

45 **Chornock R**, Iqbal SN, Wang T, Kodama S, Kawakita T, Fries M. Incidence of Hypertensive Disorders of Pregnancy in Women with COVID-19. *Am J Perinatol* 2021; **38**: 766-772 [PMID: 33940651 DOI: 10.1055/s-0041-1727167]

46 **Antoun L**, Taweel NE, Ahmed I, Patni S, Honest H. Maternal COVID-19 infection, clinical characteristics, pregnancy, and neonatal outcome: A prospective cohort study. *Eur J Obstet Gynecol Reprod Biol* 2020; **252**: 559-562 [PMID: 32732059 DOI: 10.1016/j.ejogrb.2020.07.008]

47 **Li Y**, Zhou W, Yang L, You R. Physiological and pathological regulation of ACE2, the SARS-CoV-2 receptor. *Pharmacol Res* 2020; **157**: 104833 [PMID: 32302706 DOI: 10.1016/j.phrs.2020.104833]

48 **Sathiya R**, Rajendran J, Sumathi S. COVID-19 and Preeclampsia: Overlapping Features in Pregnancy. *Rambam Maimonides Med J* 2022; **13** [PMID: 35089126 DOI: 10.5041/RMMJ.10464]

49 **Mendoza M**, Garcia-Ruiz I, Maiz N, Rodo C, Garcia-Manau P, Serrano B, Lopez-Martinez RM, Balcells J, Fernandez-Hidalgo N, Carreras E, Suy A. Pre-eclampsia-like syndrome induced by severe COVID-19: a prospective observational study. *BJOG* 2020; **127**: 1374-1380 [PMID: 32479682 DOI: 10.1111/1471-0528.16339]

50 **Ch'ng CL**, Morgan M, Hainsworth I, Kingham JG. Prospective study of liver dysfunction in pregnancy in Southwest Wales. *Gut* 2002; **51**: 876-880 [PMID: 12427793 DOI: 10.1136/gut.51.6.876]

51 **Choudhary A**, Singh V, Bharadwaj M, Barik A. Pregnancy With SARS-CoV-2 Infection Complicated by Preeclampsia and Acute Fatty Liver of Pregnancy. *Cureus* 2021; **13**: e15645 [PMID: 34306855 DOI: 10.7759/cureus.15645]

52 **Cai Q**, Huang D, Yu H, Zhu Z, Xia Z, Su Y, Li Z, Zhou G, Gou J, Qu J, Sun Y, Liu Y, He Q, Chen J, Liu L, Xu L. COVID-19: Abnormal liver function tests. *J Hepatol* 2020; **73**: 566-574 [PMID: 32298767 DOI: 10.1016/j.jhep.2020.04.006]

53 **Morton A**. Presumed acute fatty liver of pregnancy following influenza A hepatitis. *Obstet Med* 2017; **10**: 186-188 [PMID: 29225680 DOI: 10.1177/1753495X17695173]

54 **D'Ambrosi F**, Di Maso M, Viscardi A, Ossola MW, Soldavini CM, Cetera GE, Erra R, Ferrazzi E. Serum hepatic biomarkers in women with obstetric cholestasis and a concurrent SARS-CoV-2 infection. *J Obstet Gynaecol Res* 2022; **48**: 2713-2720 [PMID: 35915565 DOI: 10.1111/jog.15383]

55 **Geenes V**, Chappell LC, Seed PT, Steer PJ, Knight M, Williamson C. Association of severe intrahepatic cholestasis of pregnancy with adverse pregnancy outcomes: a prospective population-based case-control study. *Hepatology* 2014; **59**: 1482-1491 [PMID: 23857305 DOI: 10.1002/hep.26617]

56 **Rabiei M**, Soori T, Abiri A, Farsi Z, Shizarpour A, Pirjani R. Maternal and fetal effects of COVID-19 virus on a complicated triplet pregnancy: a case report. *J Med Case Rep* 2021; **15**: 87 [PMID: 33602315 DOI: 10.1186/s13256-020-02643-y]

57 **Lippi G**, Plebani M, Henry BM. Thrombocytopenia is associated with severe coronavirus disease 2019 (COVID-19) infections: A meta-analysis. *Clin Chim Acta* 2020; **506**: 145-148 [PMID: 32178975 DOI: 10.1016/j.cca.2020.03.022]

58 **Zulfiqar AA**, Lorenzo-Villalba N, Hassler P, Andrès E. Immune Thrombocytopenic Purpura in a Patient with Covid-19. *N Engl J Med* 2020; **382**: e43 [PMID: 32294340 DOI: 10.1056/NEJMc2010472]

59 **Mihu D**, Costin N, Mihu CM, Seicean A, Ciortea R. HELLP syndrome - a multisystemic disorder. *J Gastrointestin Liver Dis* 2007; **16**: 419-424 [PMID: 18193124]

60 **Arslan E**. COVID-19: A Cause of HELLP Syndrome? *Int J Womens Health* 2022; **14**: 617-623 [PMID: 35506047 DOI: 10.2147/IJWH.S362877]

61 **Čivrná Jana**, Skanderová Daniela, Ehrmann Jiří, Pilka Radovan. HELLP syndrome and HELLP-like syndrome in pregnancies with covid-19 - case reports. *Ceska Gynekol* 2021; **86**: 236-241 [PMID: 34493047 DOI: 10.48095/cccg2021236]

62 **Ronnje L**, Länsberg JK, Vikhareva O, Hansson SR, Herbst A, Zaigham M. Complicated COVID-19 in pregnancy: a case report with severe liver and coagulation dysfunction promptly improved by delivery. *BMC Pregnancy Childbirth* 2020; **20**: 511 [PMID: 32887569 DOI: 10.1186/s12884-020-03172-8]

63 **Westbrook RH**, Dusheiko G, Williamson C. Pregnancy and liver disease. *J Hepatol* 2016; **64**: 933-945 [PMID: 26658682 DOI: 10.1016/j.jhep.2015.11.030]

64 **Ambrož R**, Stašek M, Molnár J, Špička P, Klos D, Hambálek J, Skanderová D. Spontaneous liver rupture following SARS-CoV-2 infection in late pregnancy: A case report. *World J Clin Cases* 2022; **10**: 5042-5050 [PMID: 35801049 DOI: 10.12998/wjcc.v10.i15.5042]

65 **Ahmed I**, Eltaweel N, Antoun L, Rehal A. Severe pre-eclampsia complicated by acute fatty liver disease of pregnancy, HELLP syndrome and acute kidney injury following SARS-CoV-2 infection. *BMJ Case Rep* 2020; **13** [PMID: 32784239 DOI: 10.1136/bcr-2020-237521]

66 **Marsh FA**, Kaufmann SJ, Bhabra K. Surviving hepatic rupture in pregnancy--a literature review with an illustrative case report. *J Obstet Gynaecol* 2003; **23**: 109-113 [PMID: 12745549 DOI: 10.1080/0144361031000074583]

67 **Reck T**, Bussenius-Kammerer M, Ott R, Müller V, Beinder E, Hohenberger W. Surgical treatment of HELLP syndrome-associated liver rupture -- an update. *Eur J Obstet Gynecol Reprod Biol* 2001; **99**: 57-65 [PMID: 11604187 DOI: 10.1016/s0301-2115(01)00358-x]

68 **Futterman I**, Toaff M, Navi L, Clare CA. COVID-19 and HELLP: Overlapping Clinical Pictures in Two Gravid Patients. *AJP Rep* 2020; **10**: e179-e182 [PMID: 32566368 DOI: 10.1055/s-0040-1712978]

69 **Velikova T**, Georgiev T. SARS-CoV-2 vaccines and autoimmune diseases amidst the COVID-19 crisis. *Rheumatol Int* 2021; **41**: 509-518 [PMID: 33515320 DOI: 10.1007/s00296-021-04792-9]

70 **Rasmussen SA**, Kelley CF, Horton JP, Jamieson DJ. Coronavirus Disease 2019 (COVID-19) Vaccines and Pregnancy: What Obstetricians Need to Know. *Obstet Gynecol* 2021; **137**: 408-414 [PMID: 33370015 DOI: 10.1097/AOG.0000000000004290]

World Journal of Clinical Cases

Submit a Manuscript: https://www.f6publishing.com

World J Clin Cases 2023 March 26; 11(9): 1930-1938

DOI: 10.12998/wjcc.v11.i9.1930

ISSN 2307-8960 (online)

MINIREVIEWS

Examined lymph node count for gastric cancer patients after curative surgery

Yi Zeng, Lu-Chuan Chen, Zai-Sheng Ye, Jing-Yu Deng

Specialty type: Gastroenterology and hepatology

Provenance and peer review: Invited article; Externally peer reviewed.

Peer-review model: Single blind

Peer-review report's scientific quality classification

Grade A (Excellent): 0
Grade B (Very good): 0
Grade C (Good): C
Grade D (Fair): D
Grade E (Poor): 0

P-Reviewer: Aurello P, Italy; Imai Y, Japan

Received: November 28, 2022
Peer-review started: November 28, 2022
First decision: January 14, 2023
Revised: January 29, 2023
Accepted: February 21, 2023
Article in press: February 21, 2023
Published online: March 26, 2023

Yi Zeng, Lu-Chuan Chen, Zai-Sheng Ye, Department of Gastrointestinal Surgical Oncology, Clinical Oncology School of Fujian Medical University, Fujian Cancer Hospital, Fuzhou 350014, Fujian Province, China

Jing-Yu Deng, Department of Gastric Surgery, Tianjin Medical University Cancer Institute and Hospital, National Clinical Research Center for Cancer, Key Laboratory of Cancer Prevention and Therapy, Tianjin 300202, China

Corresponding author: Jing-Yu Deng, MD, PhD, Chief Doctor, Professor, Department of Gastric Surgery, Tianjin Medical University Cancer Institute and Hospital, National Clinical Research Center for Cancer, Key Laboratory of Cancer Prevention and Therapy, Huanhu West Road, Tianjin 300202, China. dengery@126.com

Abstract

Lymph node (LN) metastasis is the most common form of metastasis in gastric cancer (GC). The status and stage of LN metastasis are important indicators that reflect the progress of GC. The number of LN metastases is still the most effective index to evaluate the prognosis of patients in all stages of LN metastasis. Examined LN (ELN) count refers to the number of LNs harvested from specimens by curative gastrectomy for pathological examination. This review summarizes the factors that influence ELN count, including individual and tumor factors, intraoperative dissection factors, postoperative sorting factors, and pathological examination factors. Different ELN counts will lead to prognosis-related stage migration. Fine LN sorting and regional LN sorting are the two most important LN sorting technologies. The most direct and effective way to harvest a large number of LNs is for surgeons to perform *in vitro* fine LN sorting.

Key Words: Stomach; Neoplasm; Lymph node; Metastasis; Prognosis

Core Tip: Examined lymph node (ELN) count refers to the number of lymph nodes harvested from specimens by curative gastrectomy for pathological examination. We herein discussed the factors influencing ELN count and their roles in stage migration and sorting methods.

Citation: Zeng Y, Chen LC, Ye ZS, Deng JY. Examined lymph node count for gastric cancer patients after curative surgery. *World J Clin Cases* 2023; 11(9): 1930-1938
URL: https://www.wjgnet.com/2307-8960/full/v11/i9/1930.htm
DOI: https://dx.doi.org/10.12998/wjcc.v11.i9.1930

INTRODUCTION

Metastasis is one of the lethal biological characteristics of malignant tumor cells. Lymph node (LN) metastasis is the most common form of metastasis in gastric cancer (GC). The proportion of LN metastasis can reach more than 50% in GC with deep submucosal invasion[1]. The status and stage of LN metastasis are important indicators that reflect the progress of GC. LN metastasis can remarkably affect therapeutic effect and clinical prognosis[2]. LN metastasis staging methods that are used to evaluate the prognosis of patients with GC after radical resection include the range of LN metastasis, the number of LN metastases, LN ratio, the maximum diameter of LN metastasis, and the log odds of positive LNs[3-6]. A number of clinical analysis and research results for prognosis evaluation have shown that the number of LN metastases is still the most effective index for the evaluation of the prognosis of patients in all stages of LN metastasis[7-9]. The criteria of LN metastasis (pN) staging of GC in the Union for International Cancer Control and American Joint Commission for Cancer (AJCC) are constantly changing and updating. Therefore, how to accurately evaluate the number of LN metastases is still the focus of clinical attention. The examined LNs (ELNs) used to determine the number of LN metastases are from dissected LNs (DLNs). ELN count refers to the number of LNs harvested from specimens by curative gastrectomy for pathological examination.

This article summarizes the implication of ELN count for patients with GC after curative surgery.

INFLUENCING FACTORS OF ELN COUNT AFTER CURATIVE GASTRECTOMY

The accuracy of the evaluation of LN metastasis depends on standardized LN harvesting and subsequent detailed pathological examination. Therefore, ELN count is affected by the following factors (Table 1).

Individual and tumor factors

Individual differences in immune status, disease stage, and the biological behavior of tumor cells in different patients can lead to a certain difference in the number of perigastric LNs. LNs are derived from the differentiation and development of endothelial cells in lymphatic vessels or lymphatic sac and their surrounding mesenchymal cells in the embryonic period; that is, in theory, LNs can be formed in areas where lymphatic vessels are located. This localization can also be considered a potential reason for the recurrence of local LN metastasis after standardized LN dissection for GC. A variety of tumor-derived driving factors, including multiple antigens, cytokine growth factors and exosomes, can be drained to tumor regional LNs through the lymphatic duct system and then regulate the immune response, remodel lymphatic vessels, and induce microenvironment adaptation and the metastasis and colonization of cancer cells[10]. Dikken *et al*[11] showed that ELN count in female patients with GC after surgery is higher than that in male patients. The difference between the two sexes may be related to the difference in their immune system status. They also showed that ELN count in young patients is higher than that in elderly patients because elderly patients have a weak immune response to tumor; thus, the elderly may be subjected to a more conservative strategy of intraoperative dissection. Kodera *et al*[12] showed that obesity can affect ELN count in patients with GC. ELN count was considerably reduced in surgical patients with body mass index (BMI) ≥ 27 kg/m^2 compared with male patients with BMI < 25 kg/m^2 and female patients with BMI < 22 kg/m^2. Obesity may have a negative impact on ELN count by increasing the difficulty of surgical dissection and LN identification. Tumor stage is also one of the factors that affect the detection of LNs. The T stage of a tumor affects ELN count after surgery[13]. A higher T stage is related to more harvested LNs. Although preoperative chemotherapy can inhibit tumor cells in perigastric LNs to a certain extent and even achieve N-stage downregulation, no evidence shows that it can remarkably affect ELN count[12].

Intraoperative dissection factors

DLN refers to the number of LNs included in the surgical specimens removed from the abdominal cavity of a patient according to the radical range determined by the GC staging of the patient. DLN count is determined by the extent of LN dissection and the number of LNs around the stomach during surgery. D1+ LN dissection is currently the main choice for early GC, and D2 LN dissection should be necessary for advanced resectable GC. The number of LNs around the stomach in total gastrectomy is more than that in subtotal gastrectomy. Therefore, more LNs can be dissected for postoperative

Table 1 Influencing factors of examined lymph node count after curative gastrectomy

Classifications	Factors	Specific
Lymph node harvesting	Individual and tumor factors	Immune status (active/inhibited)[10], sex (female/male)[11], age (young/elderly)[11], body mass index (emaciation/obesity)[12], disease stage (early/advanced)[13], *etc*
	Intraoperative dissection factors	Extent of lymph node dissection (D1/D2)[14], scope of gastrectomy (total/subtotal/partial)[14], operation mode (laparoscopic/open)[15-16], qualification of the surgeons[17-19], *etc*
Examination detail	Postoperative sorting factors	Omission of small lymph nodes[21-22], persons (surgeons/pathologists)[23-24], lymph node sorting methods (fine/regional)[55-56], *etc*
	Pathological examination factors	Special metastasis (extranodal soft tissue/skip metastasis)[25-28], fat clearance technology (alcohol/coniferous oil/formaldehyde)[30-35], dye marker (methylene blue, nanocarbon)[36-38], *etc*

pathological examination. Lu *et al*[14] reported that the average number of LNs removed by subtotal gastrectomy and total gastrectomy are 26 ± 9.6 and 29 ± 10.7 ($P < 0.01$), respectively. In the same way, the total number of LNs dissected in patients with early GC who underwent partial gastrectomy and with preserved function may be decreased because parts of the perigastric LNs do not need to be dissected. With the development of minimally invasive technology, laparoscopic gastrectomy can reduce intraoperative blood loss, accelerate postoperative recovery, and shorten hospital stay. Bouras *et al*[15] showed that the number of LNs detected in laparoscopic surgery is less than that in open surgery (26.7 *vs* 31.4; $P < 0.05$) at the same tumor-node-metastasis (TNM) stage possibly because the extent of LN dissection in laparoscopic surgery is often less than that in open surgery. However, a meta-analysis of 12 studies comparing minimally invasive surgery with open surgery showed that laparoscopic surgery does not reduce the number of LNs detected compared with open surgery[16]. Therefore, the effect of laparoscopic surgery on DLN count needs to be further studied. In addition, qualification of the surgeon has a direct impact on DLN count[17-19].

Postoperative sorting factors

Theoretically, ELN count should not exceed DLN count. A trained person needs to sort the LNs from each group in the perigastric region one by one from the surgical specimens of GC and make corresponding records before sending the harvested LNs for examination. Different sorting methods may lead to different LN counts. Almost all oncologists agree that postoperative factors can directly affect the follow-up diagnosis and treatment of cancer[20]. In the postoperative sample processing, the omission of small LNs will likely cause an error in metastatic LN count, which will directly lead to the downgrading of TNM staging based on the number of metastatic LNs and cannot objectively reflect the actual situation. Noda *et al*[21] showed that 37.9% of LNs with metastasis have a maximum diameter of less than 5 mm; hence, 37.9% of metastatic LNs in GC specimens may be missed if 5 mm LNs are not found. Downstaging will occur in 14.9% and 4.2% of the cases if all nodes less than 6 and 4 mm, respectively, are ignored. Hanna *et al*[22] pointed out that the proportion of smaller LNs in ELNs showed an upward trend with the increase in ELN count. Different countries have differences regarding whether surgeons or pathologists carry out the sorting work after surgery. This work is done by pathologists in most European and American countries, whereas the procedure is done by surgeons in Japan. Bunt *et al*[23] compared the differences in LN detection in Europe, America, and Japan and suggested that the sorting of LNs should be done by surgeons immediately after surgery. The average number of LNs harvested by surgeons after D2 gastrectomy is 60 ± 24.1, which is significantly higher than that (31 ± 16.4) harvested by pathologists ($P < 0.001$). In Japan, the LNs of different groups in the perigastric region are sorted by experienced surgeons immediately after curative resection; therefore, the number of LNs harvested for GC surgery in Japan has always been in the leading position in the world with an average of 39.4[24]. By contrast, some Western pathologists object to post-operative LN sorting because it will destroy the edge of the tumor[22].

Pathological examination factors

LNs are fixed in neutral formaldehyde solution, embedded in paraffin, and sectioned in the pathology department prior to the assessment of LN metastasis. This routine postoperative procedure can directly affect ELN count. The discovery of extranodal soft tissue and skip metastases has led to some controversy on the pathological diagnosis of LN metastasis. Some studies suggest that extranodal soft tissue nodule is a risk factor for the prognosis of patients with GC, and the postoperative survival rate of patients decreases considerably with the increase in the number of extranodal-positive soft tissue nodule[25,26]. Several extranodal soft tissue nodules can be found microscopically. In fact, the structure of LNs is partially or completely destroyed by the proliferation of metastatic GC cells, which makes it impossible to identify them correctly. Therefore, pathologists can only judge them as soft tissue nodules. A similar situation can also be seen in the destruction of LN structure after multiple preoperative radiotherapy. Although the impact of skip metastasis on the prognosis of GC remains controversial, it is still a negative factor affecting the survival of patients. The occurrence of skip metastasis is related to

low DLN count; hence, the number of LNs in a pathological section is difficult to determine[27]. In theory, LNs have occult tumor cells (including micrometastases and isolated tumor cells), but serial sections of LNs are difficult to carried out[28]. Many clinical reports still support that LN micrometastasis should be considered an unfavorable factor affecting the prognosis of patients[29].

In addition, fat clearance technology can also improve the detection rate of pathological LNs[30-33]. Candela *et al*[34] reported a fat clearance technique applied to the treatment of GC specimens after operation. The average ELN count was increased from 20 to 36 by using different concentrations of alcohol and coniferous oil as pretreatment before staining, which improved the accuracy of staging. The ELN count by this method is higher than that reported by Japanese scholars in the same period, and this method has obvious advantages in detecting smaller LNs. Aoyama *et al*[35] treated samples with 10% formaldehyde aqueous solution containing methylene blue for 48 h. The LNs and lymphatic network were clearly displayed; therefore, the ELN count was increased (43.4 *vs* 33.6; $P = 0.005$), and the efficiency of LN detection was improved (1.49/min *vs* 1.12/min; $P = 0.010$). A meta-analysis included 27 studies on the application of fat clearance and methylene blue staining in the detection of LNs in gastrointestinal tumor samples[36]. The results showed that compared with the traditional manual method, the two techniques could increase ELN count, harvest more metastatic-positive LNs and improve the identification of small LNs. Carbon nanoparticles can be selectively absorbed by lymphatic vessels. Li *et al*[37] applied nanocarbon to the surgery of advanced GC, which could increase ELN count (38.33 in the nanocarbon group and 28.27 in the control group, $P = 0.041$) and identify smaller LNs (the maximum diameters of LNs in the nanocarbon and control groups were 3.32 and 4.30 mm, respectively [$P = 0.023$]). In addition, indocyanine green can be used as a tracer for LNs in GC[38]. However, indocyanine green depends on special laparoscopic equipment during the surgery and cannot develop color in pathological sorting.

ELN COUNT AND LN STAGE MIGRATION

The depth of primary invasion (pT) and distant metastasis (M) can be directly determined by pathologists under a high-power microscope in the current AJCC postoperative pathological staging (pTNM) system. The final pathological report of LN metastasis stage may have errors, such as the Will–Roger phenomenon, due to the existence of LN dissection range, ELN count, disease stage, patient individuality, and other factors[39]. Will–Roger phenomenon refers to the positive correlation between the number of LN metastases and the range of LN dissection. LN stage migration can be gradually reduced or avoided through an increase in LN dissection range. Therefore, ELN count for curative gastrectomy is closely related to LN stage migration. The clinical data of a large sample of patients undergoing radical gastrectomy in a single center in China showed that the number of metastatic LNs is positively correlated with an increase in ELN count[40]. The survival data of 7620 patients with GC from three centers in China suggest a substantial migration of postoperative LN stage (pN stage), especially in early-stage patients with less than 15 LNs (pT1NanyM0 stage) and advanced-stage patients with less than 35 LNs (pT2–4NanyM0 stage); hence, the 5-year survival rate of patients with different stages in China is obviously lower than that in Japan, South Korea, and other medical centers[7]. Sano *et al*[24] found that the proportion of patients with pN3b (8.7%) from East Asian countries except Japan and South Korea (including 979 patients in China) with a low number of LNs (24.8 per case) is almost twice as high as those in Japan and South Korea. Some studies have shown that the survival rate of patients with positive LN metastasis whose ELN count is more than 30 is the highest in the same subgroup of patients with pN stage; this prognosis-related stage migration is also caused by difference in ELN count[41].

In 2005, Smith used the Surveillance, Epidemiology and End Results database to analyze 3814 patients with GC with equal staging of T1–2N0, T1–2N1, T3N0, and T3N1[42]. The survival time of patients with more than 15 LNs detected was better than that of patients with less than 15 LNs detected at the same stage. The 5-year survival rate increased by 5.7%–10.9% for every 10 additional LNs. Volpe *et al*[43] analyzed 114 patients who underwent proximal gastrectomy (including D1, D1+, D2, and D2+) and found no remarkable relationship between ELN count and overall survival. However, for patients who underwent extended radical gastrectomy (D2 or D2+), the median survival time of patients with more than 15 LNs detected increased from 25 to 42 mo. In 2009, the authors also found that according to the 6th edition of TNM staging of GC, patients with no less than 15 LNs have remarkably longer postoperative overall survival time, disease-free survival time, or survival time than patients with less than 15 LNs after recurrence[44]. We also found that increased ELN count is an independent factor affecting the survival time of patients with GC who only have perigastric LN metastasis (only LN metastasis on the greater curvature and lesser curvature side)[45]. Therefore, in the 7th edition of the TNM staging of GC, the recommended number of LNs was changed to no less than 16. The reason is that patients with pN3b stage need at least 16 LN metastases confirmed by pathology.

However, 16 LNs are not the ultimate limit. Kim *et al*[46] pointed out that for patients with advanced differentiated GC, the prognosis when 25 and 40 LNs were used as the cut-off values of ELN count was also different. The study group with more ELN count had a longer average survival time compared

with patients with less than 25 and 40 LNs detected. Chen *et al*[47] analyzed 1363 patients with curative gastrectomy and found that ELN count and N stage are independent prognostic factors. The 5-year survival rates of N2 and N3 patients with more than 25 LNs detected are 58.59% and 32.77%, respectively, which are remarkably better than 52.48% and 21.67% of patients, respectively, with 15–24 LNs detected in the same period. The clinical data of 7620 patients with GC undergoing curative gastrectomy in three medical centers in China showed that for the same pN stage (except pN0 stage), the 5-year survival rate of patients with GC who have more than 30 LNs is 8%–15% higher than that of patients with less than 30 LNs[7].

For patients with negative LNs, we demonstrated that insufficient ELN count may be a potential risk factor for the postoperative recurrence of GC[48]. An ELN count less than 16 means higher local recurrence rate and peritoneal metastasis rate[49]. Several studies have confirmed that ELN count can affect the prognosis of patients with pN0[49-51]. ELN count is an independent prognostic factor particularly for patients with stage III pN0 GC[52,53]. In 2017, authors compared the clinicopathological data of pN0 patients in Tianjin Medical University Cancer Institute and Hospital (TJMUCH) and Tokyo Medical University Hospital (TMUH) in the past 10 years and found that ELN count in patients with pN0 GC in TMUH reached 34.84, which was much higher than that in TJMUCH, and the postoperative survival rate of patients was also significantly higher than that in TJMUCH ($P < 0.001$)[8]. Further analysis showed that the postoperative survival rate of patients with pN0 GC in TMUH, also increased by 57% with the increase of ELN count. In addition, we also confirmed that increased ELN count can reduce or prevent stage migration in pN0 patients[41].

LN SORTING TECHNOLOGY

LNs need to be sorted out from the whole specimen obtained by radical gastrectomy according to the location of LN regions in each group for postoperative pathological examination, which can provide fine information for the number and location of LN metastases. The most important factor that can reflect ELN count is the operation of LN sorting. Sorting LNs from fresh specimens during or immediately after surgery requires a detailed understanding and affirmation of the whole scope of surgical dissection. Detailed records of LNs after sorting can provide clear information for postoperative pathology to detect the location of LN metastasis. In addition, perigastric LNs are easier to harvest from fresh samples, especially in fat and soft tissue specimens, than LNs isolated after neutral formaldehyde immersion.

The two main sorting methods are fine LN sorting and regional LN sorting. ELN count in the fine LN sorting group is much higher than that in the regional LN sorting group with the same pT, pN, or pTNM stage ($P < 0.001$). The number of metastatic LNs in the fine LN sorting group was significantly higher than that in the regional LN sorting group ($P < 0.001$)[54].

Fine LN sorting

Japanese scholars have been following "fine sorting," that is, LNs are separated from GC samples and then separated from the soft tissue one by one according to the location of each group of LNs around the stomach and the surrounding soft tissue. This method can harvest a larger number of LNs, which helps in judging the extent of the local invasion of the disease and also provides objective evidence for postoperative pathology report to evaluate the quality of surgery. Schmidt *et al*[55] pointed out that on the basis of D2 LN dissection, the fine sorting of LNs from postoperative *ex vivo* specimens can make the average ELN count in each GC patient reach 40; thus, accurate LN staging can be obtained for the prognosis evaluation of patients. According to the latest research results of the Sloan Caitlin Memorial Cancer Centre, ELN count by the fine LN sorting of *ex vivo* specimens by surgeons can be significantly increased (30 *vs* 21; $P < 0.0001$) compared with regional sorting or sorting by pathologists[56]. Many scholars have explored a series of methods, including fat clearance and intraoperative marker staining, to achieve more precise LN sorting[34,57-61]. These methods provide more comprehensive information for the postoperative evaluation of patients with LN metastasis; however, they take a long time, may require toxic reagents, and need to be completed in the fume hood and could be difficult for beginners. In general, the most direct and effective way to harvest a large number of LNs is for surgeons to perform *in vitro* fine LN sorting.

Regional LN sorting

Some scholars in other countries directly separate and label each group of LNs around the stomach from the GC samples together with the surrounding soft tissues instead of separating each group of LNs from the soft tissues one by one. This method saves time. However, the pathologist needs to separate the LNs one by one. Theoretically, a certain stage migration occurs in postoperative LNs metastasis. Hanna *et al* [22] reported a systematic fat blocking and microscopic search method for regional LN sorting to improve the number of regional LNs. In this method, the pathologist obtains all the perigastric, periesophageal, and periduodenal fat from the specimen (the fat in the greater omentum is not treated); removes the larger LNs; divides the remaining fat into blocks and obtains single stained hematoxylin

and eosin slices from each block to examine the LNs under a light microscope. This method can detect more LNs compared with the ordinary manual LN sorting method (66 ± 21 *vs* 50 ± 20; $P < 0.05$), but it also has obvious disadvantages. It increases the cost of pathological examination and cannot determine the number of LNs in each group; therefore, its popularization and application are limited.

CONCLUSION

At present, the number of LN metastases is still the most effective index to evaluate the prognosis of patients. Accuracy of the evaluation of LN metastasis depends on the standardized harvesting of LNs and subsequent detailed pathological analysis. Different ELN counts will lead to prognosis-related stage migration. Fine LN sorting and regional LN sorting are the two most important LN sorting technologies. Although ELN count is affected by many factors, the most direct and effective way to harvest a large number of LNs is for surgeons to perform *in vitro* fine LN sorting.

FOOTNOTES

Author contributions: Zeng Y collected the data and wrote the paper; Chen L, Ye Z, and Deng J conceived and reviewed the paper.

Conflict-of-interest statement: The authors have no conflicts of interest to declare.

Country/Territory of origin: China

ORCID number: Yi Zeng 0000-0001-9144-8414; Lu-Chuan Chen 0000-0003-3362-447X; Zai-Sheng Ye 0000-0001-9881-6400; Jing-Yu Deng 0000-0003-4299-1327.

S-Editor: Liu JH
L-Editor: Filipodia
P-Editor: Liu JH

REFERENCES

1 **Wang J**, Dang P, Raut CP, Pandalai PK, Maduekwe UN, Rattner DW, Lauwers GY, Yoon SS. Comparison of a lymph node ratio-based staging system with the 7th AJCC system for gastric cancer: analysis of 18,043 patients from the SEER database. *Ann Surg* 2012; **255**: 478-485 [PMID: 22330040 DOI: 10.1097/SLA.0b013e31824857e2]
2 **Nitti D**, Marchet A, Olivieri M, Ambrosi A, Mencarelli R, Belluco C, Lise M. Ratio between metastatic and examined lymph nodes is an independent prognostic factor after D2 resection for gastric cancer: analysis of a large European monoinstitutional experience. *Ann Surg Oncol* 2003; **10**: 1077-1085 [PMID: 14597447 DOI: 10.1245/aso.2003.03.520]
3 **Cheong O**, Oh ST, Kim BS, Yook JH, Kim JH, Im JT, Park GC. Large metastatic lymph node size, especially more than 2 cm: independent predictor of poor prognosis in node-positive gastric carcinoma. *World J Surg* 2008; **32**: 262-266 [PMID: 18064519 DOI: 10.1007/s00268-007-9158-4]
4 **Deng J**, Liang H. Discussion of the applicability of positive lymph node ratio as a proper N-staging for predication the prognosis of gastric cancer after curative surgery plus extended lymphadenectomy. *Ann Surg* 2012; **256**: e35-6; author reply e37 [PMID: 23154399 DOI: 10.1097/SLA.0b013e3182769545]
5 **Deng J**, Liang H, Sun D, Pan Y. The prognostic analysis of lymph node-positive gastric cancer patients following curative resection. *J Surg Res* 2010; **161**: 47-53 [PMID: 19783008 DOI: 10.1016/j.jss.2008.12.019]
6 **Liu H**, Deng J, Zhang R, Hao X, Jiao X, Liang H. The RML of lymph node metastasis was superior to the LODDS for evaluating the prognosis of gastric cancer. *Int J Surg* 2013; **11**: 419-424 [PMID: 23541652 DOI: 10.1016/j.ijsu.2013.03.009]
7 **Deng J**, Liu J, Wang W, Sun Z, Wang Z, Zhou Z, Xu H, Liang H. Validation of clinical significance of examined lymph node count for accurate prognostic evaluation of gastric cancer for the eighth edition of the American Joint Committee on Cancer (AJCC) TNM staging system. *Chin J Cancer Res* 2018; **30**: 477-491 [PMID: 30510359 DOI: 10.21147/j.issn.1000-9604.2018.05.01]
8 **Deng J**, Yamashita H, Seto Y, Liang H. Increasing the Number of Examined Lymph Nodes is a Prerequisite for Improvement in the Accurate Evaluation of Overall Survival of Node-Negative Gastric Cancer Patients. *Ann Surg Oncol* 2017; **24**: 745-753 [PMID: 27770340 DOI: 10.1245/s10434-016-5513-8]
9 **Dong Y**, Qiu Y, Deng J, Wang W, Sun Z, Wang Z, Zhou Z, Xu H, Liang H. Insufficient examined lymph node count

underestimates staging in pN3a patients after curative gastrectomy: a multicenter study with external validation. *J Cancer Res Clin Oncol* 2020; **146**: 515-528 [PMID: 31813005 DOI: 10.1007/s00432-019-03081-0]

10 **Sleeman JP**. The lymph node pre-metastatic niche. *J Mol Med (Berl)* 2015; **93**: 1173-1184 [PMID: 26489604 DOI: 10.1007/s00109-015-1351-6]

11 **Dikken JL**, van Grieken NC, Krijnen P, Gönen M, Tang LH, Cats A, Verheij M, Brennan MF, van de Velde CJ, Coit DG. Preoperative chemotherapy does not influence the number of evaluable lymph nodes in resected gastric cancer. *Eur J Surg Oncol* 2012; **38**: 319-325 [PMID: 22261085 DOI: 10.1016/j.ejso.2011.12.016]

12 **Kodera Y**, Ito S, Yamamura Y, Mochizuki Y, Fujiwara M, Hibi K, Ito K, Akiyama S, Nakao A. Obesity and outcome of distal gastrectomy with D2 lymphadenectomy for carcinoma. *Hepatogastroenterology* 2004; **51**: 1225-1228 [PMID: 15239284]

13 **Cunningham D**, Allum WH, Stenning SP, Thompson JN, Van de Velde CJ, Nicolson M, Scarffe JH, Lofts FJ, Falk SJ, Iveson TJ, Smith DB, Langley RE, Verma M, Weeden S, Chua YJ, MAGIC Trial Participants. Perioperative chemotherapy versus surgery alone for resectable gastroesophageal cancer. *N Engl J Med* 2006; **355**: 11-20 [PMID: 16822992 DOI: 10.1056/NEJMoa055531]

14 **Lu J**, Wang W, Zheng CH, Fang C, Li P, Xie JW, Wang JB, Lin JX, Chen QY, Cao LL, Lin M, Huang CM, Zhou ZW. Influence of Total Lymph Node Count on Staging and Survival After Gastrectomy for Gastric Cancer: An Analysis From a Two-Institution Database in China. *Ann Surg Oncol* 2017; **24**: 486-493 [PMID: 27619942 DOI: 10.1245/s10434-016-5494-7]

15 **Bouras G**, Lee SW, Nomura E, Tokuhara T, Tsunemi S, Tanigawa N. Comparative analysis of station-specific lymph node yield in laparoscopic and open distal gastrectomy for early gastric cancer. *Surg Laparosc Endosc Percutan Tech* 2011; **21**: 424-428 [PMID: 22146165 DOI: 10.1097/SLE.0b013e3182367dee]

16 **Straatman J**, van der Wielen N, Cuesta MA, de Lange-de Klerk ES, Jansma EP, van der Peet DL. Minimally Invasive Versus Open Total Gastrectomy for Gastric Cancer: A Systematic Review and Meta-analysis of Short-Term Outcomes and Completeness of Resection : Surgical Techniques in Gastric Cancer. *World J Surg* 2016; **40**: 148-157 [PMID: 26350821 DOI: 10.1007/s00268-015-3223-1]

17 **Kang SY**, Lee SY, Kim CY, Yang DH. Comparison of Learning Curves and Clinical Outcomes between Laparoscopy-assisted Distal Gastrectomy and Open Distal Gastrectomy. *J Gastric Cancer* 2010; **10**: 247-253 [PMID: 22076193 DOI: 10.5230/jgc.2010.10.4.247]

18 **Zhao LY**, Zhang WH, Sun Y, Chen XZ, Yang K, Liu K, Chen XL, Wang YG, Song XH, Xue L, Zhou ZG, Hu JK. Learning curve for gastric cancer patients with laparoscopy-assisted distal gastrectomy: 6-year experience from a single institution in western China. *Medicine (Baltimore)* 2016; **95**: e4875 [PMID: 27631257 DOI: 10.1097/MD.0000000000004875]

19 **Zhou D**, Quan Z, Wang J, Zhao M, Yang Y. Laparoscopic-assisted versus open distal gastrectomy with D2 lymph node resection for advanced gastric cancer: effect of learning curve on short-term outcomes. a meta-analysis. *J Laparoendosc Adv Surg Tech A* 2014; **24**: 139-150 [PMID: 24625347 DOI: 10.1089/lap.2013.0481]

20 **Ajani JA**. Operate on my stomach cancer? *J Clin Oncol* 2004; **22**: 1763-4; author reply 1764 [PMID: 15118003 DOI: 10.1200/JCO.2004.99.277]

21 **Noda N**, Sasako M, Yamaguchi N, Nakanishi Y. Ignoring small lymph nodes can be a major cause of staging error in gastric cancer. *Br J Surg* 1998; **85**: 831-834 [PMID: 9667718 DOI: 10.1046/j.1365-2168.1998.00691.x]

22 **Hanna GB**, Amygdalos I, Ni M, Boshier PR, Mikhail S, Lloyd J, Goldin R. Improving the standard of lymph node retrieval after gastric cancer surgery. *Histopathology* 2013; **63**: 316-324 [PMID: 23837447 DOI: 10.1111/his.12167]

23 **Bunt AM**, Hermans J, van de Velde CJ, Sasako M, Hoefsloot FA, Fleuren G, Bruijn JA. Lymph node retrieval in a randomized trial on western-type versus Japanese-type surgery in gastric cancer. *J Clin Oncol* 1996; **14**: 2289-2294 [PMID: 8708719 DOI: 10.1200/JCO.1996.14.8.2289]

24 **Sano T**, Coit DG, Kim HH, Roviello F, Kassab P, Wittekind C, Yamamoto Y, Ohashi Y. Proposal of a new stage grouping of gastric cancer for TNM classification: International Gastric Cancer Association staging project. *Gastric Cancer* 2017; **20**: 217-225 [PMID: 26897166 DOI: 10.1007/s10120-016-0601-9]

25 **Guo J**, Pan Y, Guo X, Sun C, Jin J, Zhang N, Liang H, Deng J. Effect of the number of positive niduses in extranodal soft tissues on the overall survival of gastric cancer patients. *Int J Clin Exp Pathol* 2017; **10**: 11090-11097 [PMID: 31966457]

26 **Jiang N**, Deng JY, Ding XW, Ke B, Liu N, Liang H. Node-extranodal soft tissue stage based on extranodal metastasis is associated with poor prognosis of patients with gastric cancer. *J Surg Res* 2014; **192**: 90-97 [PMID: 24953988 DOI: 10.1016/j.jss.2014.05.053]

27 **Choi YY**, An JY, Guner A, Kang DR, Cho I, Kwon IG, Shin HB, Hyung WJ, Noh SH. Skip lymph node metastasis in gastric cancer: is it skipping or skipped? *Gastric Cancer* 2016; **19**: 206-215 [PMID: 25708370 DOI: 10.1007/s10120-015-0472-5]

28 **Tavares A**, Monteiro-Soares M, Viveiros F, Maciel Barbosa J, Dinis-Ribeiro M. Occult Tumor Cells in Lymph Nodes of Patients with Gastric Cancer: A Systematic Review on Their Prevalence and Predictive Role. *Oncology* 2015; **89**: 245-254 [PMID: 26160338 DOI: 10.1159/000433543]

29 **Lee CM**, Cho JM, Jang YJ, Park SS, Park SH, Kim SJ, Mok YJ, Kim CS, Kim JH. Should lymph node micrometastasis be considered in node staging for gastric cancer? *Ann Surg Oncol* 2015; **22**: 765-771 [PMID: 25201506 DOI: 10.1245/s10434-014-4073-z]

30 **Cohen SM**, Wexner SD, Schmitt SL, Nogueras JJ, Lucas FV. Effect of xylene clearance of mesenteric fat on harvest of lymph nodes after colonic resection. *Eur J Surg* 1994; **160**: 693-697 [PMID: 7888471]

31 **Koren R**, Paz A, Konichezsky M, Sadikov E, Klein B, Livne P, Gal R. Lymph node revealing solution: a rapid method for the fixation of cystectomy specimens. *Pathol Res Pract* 1999; **195**: 77-80 [PMID: 10093825 DOI: 10.1016/S0344-0338(99)80074-0]

32 **Prabhudesai AG**, Dalton R, Kumar D, Finlayson CJ. Mechanised one-day fat clearance method to increase the lymph node yield in rectal cancer specimens. *Br J Biomed Sci* 2005; **62**: 120-123 [PMID: 16196457 DOI: 10.1080/09674845.2005.11732697]

33 **Scott KW**, Grace RH. Detection of lymph node metastases in colorectal carcinoma before and after fat clearance. *Br J Surg* 1989; **76**: 1165-1167 [PMID: 2688803 DOI: 10.1002/bjs.1800761118]

34 **Candela FC**, Urmacher C, Brennan MF. Comparison of the conventional method of lymph node staging with a comprehensive fat-clearing method for gastric adenocarcinoma. *Cancer* 1990; **66**: 1828-1832 [PMID: 2208038 DOI: 10.1002/1097-0142(19901015)66:8<1828::aid-cncr2820660830>3.0.co;2-z]

35 **Aoyama T**, Fujikawa H, Cho H, Ogata T, Shirai J, Hayashi T, Rino Y, Masuda M, Oba MS, Morita S, Yoshikawa T. A methylene blue-assisted technique for harvesting lymph nodes after radical surgery for gastric cancer: a prospective, randomized, controlled study. *Am J Surg Pathol* 2015; **39**: 266-273 [PMID: 25356528 DOI: 10.1097/PAS.0000000000000336]

36 **Abbassi-Ghadi N**, Boshier PR, Goldin R, Hanna GB. Techniques to increase lymph node harvest from gastrointestinal cancer specimens: a systematic review and meta-analysis. *Histopathology* 2012; **61**: 531-542 [PMID: 23551433 DOI: 10.1111/j.1365-2559.2012.04357.x]

37 **Li Z**, Ao S, Bu Z, Wu A, Wu X, Shan F, Ji X, Zhang Y, Xing Z, Ji J. Clinical study of harvesting lymph nodes with carbon nanoparticles in advanced gastric cancer: a prospective randomized trial. *World J Surg Oncol* 2016; **14**: 88 [PMID: 27009101 DOI: 10.1186/s12957-016-0835-3]

38 **Takahashi N**, Nimura H, Fujita T, Yamashita S, Mitsumori N, Yanaga K. Quantitative assessment of visual estimation of the infrared indocyanine green imaging of lymph nodes retrieved at sentinel node navigation surgery for gastric cancer. *BMC Surg* 2016; **16**: 35 [PMID: 27245664 DOI: 10.1186/s12893-016-0152-3]

39 **de Manzoni G**, Verlato G, Roviello F, Morgagni P, Di Leo A, Saragoni L, Marrelli D, Kurihara H, Pasini F. The new TNM classification of lymph node metastasis minimises stage migration problems in gastric cancer patients. *Br J Cancer* 2002; **87**: 171-174 [PMID: 12107838 DOI: 10.1038/sj.bjc.6600432]

40 **Deng J**, Liang H, Sun D, Wang D, Pan Y. Suitability of 7th UICC N stage for predicting the overall survival of gastric cancer patients after curative resection in China. *Ann Surg Oncol* 2010; **17**: 1259-1266 [PMID: 20217252 DOI: 10.1245/s10434-010-0939-x]

41 **Gu P**, Deng J, Wang W, Wang Z, Zhou Z, Xu H, Liang H. Impact of the number of examined lymph nodes on stage migration in node-negative gastric cancer patients: a Chinese multi-institutional analysis with propensity score matching. *Ann Transl Med* 2020; **8**: 938 [PMID: 32953738 DOI: 10.21037/atm-19-4727]

42 **Smith DD**, Schwarz RR, Schwarz RE. Impact of total lymph node count on staging and survival after gastrectomy for gastric cancer: data from a large US-population database. *J Clin Oncol* 2005; **23**: 7114-7124 [PMID: 16192595 DOI: 10.1200/JCO.2005.14.621]

43 **Volpe CM**, Driscoll DL, Douglass HO Jr. Outcome of patients with proximal gastric cancer depends on extent of resection and number of resected lymph nodes. *Ann Surg Oncol* 2000; **7**: 139-144 [PMID: 10761793 DOI: 10.1007/s10434-000-0139-1]

44 **Deng JY**, Liang H, Sun D, Pan Y, Zhang RP, Wang BG, Zhan HJ. Outcome in relation to numbers of nodes harvested in lymph node-positive gastric cancer. *Eur J Surg Oncol* 2009; **35**: 814-819 [PMID: 19111430 DOI: 10.1016/j.ejso.2008.11.007]

45 **Deng J**, Liang H, Sun D, Pan Y, Liu Y, Wang D. Extended lymphadenectomy improvement of overall survival of gastric cancer patients with perigastric node metastasis. *Langenbecks Arch Surg* 2011; **396**: 615-623 [PMID: 21380618 DOI: 10.1007/s00423-011-0753-3]

46 **Kim YI**. Does the retrieval of at least 15 lymph nodes confer an improved survival in patients with advanced gastric cancer? *J Gastric Cancer* 2014; **14**: 111-116 [PMID: 25061538 DOI: 10.5230/jgc.2014.14.2.111]

47 **Chen HN**, Chen XZ, Zhang WH, Chen XL, Yang K, Liu JP, Zhang B, Chen ZX, Chen JP, Zhou ZG, Hu JK. Necessity of harvesting at least 25 lymph nodes in patients with stage N2-N3 resectable gastric cancer: a 10-year, single-institution cohort study. *Medicine (Baltimore)* 2015; **94**: e620 [PMID: 25761190 DOI: 10.1097/MD.0000000000000620]

48 **Deng J**, Liang H, Sun D, Zhang R, Zhan H, Wang X. Prognosis of gastric cancer patients with node-negative metastasis following curative resection: outcomes of the survival and recurrence. *Can J Gastroenterol* 2008; **22**: 835-839 [PMID: 18925308 DOI: 10.1155/2008/761821]

49 **Jiao XG**, Deng JY, Zhang RP, Wu LL, Wang L, Liu HG, Hao XS, Liang H. Prognostic value of number of examined lymph nodes in patients with node-negative gastric cancer. *World J Gastroenterol* 2014; **20**: 3640-3648 [PMID: 24707149 DOI: 10.3748/wjg.v20.i13.3640]

50 **Baiocchi GL**, Tiberio GA, Minicozzi AM, Morgagni P, Marrelli D, Bruno L, Rosa F, Marchet A, Coniglio A, Saragoni L, Veltri M, Pacelli F, Roviello F, Nitti D, Giulini SM, De Manzoni G. A multicentric Western analysis of prognostic factors in advanced, node-negative gastric cancer patients. *Ann Surg* 2010; **252**: 70-73 [PMID: 20562605 DOI: 10.1097/SLA.0b013e3181e4585e]

51 **Xu D**, Huang Y, Geng Q, Guan Y, Li Y, Wang W, Yuan S, Sun X, Chen Y, Li W, Zhou Z, Zhan Y. Effect of lymph node number on survival of patients with lymph node-negative gastric cancer according to the 7th edition UICC TNM system. *PLoS One* 2012; **7**: e38681 [PMID: 22723875 DOI: 10.1371/journal.pone.0038681]

52 **Zhang N**, Bai H, Deng J, Wang W, Sun Z, Wang Z, Xu H, Zhou Z, Liang H. Impact of examined lymph node count on staging and long-term survival of patients with node-negative stage III gastric cancer: a retrospective study using a Chinese multi-institutional registry with Surveillance, Epidemiology, and End Results (SEER) data validation. *Ann Transl Med* 2020; **8**: 1075 [PMID: 33145294 DOI: 10.21037/atm-20-1358a]

53 **Zhang N**, Deng J, Wang W, Sun Z, Wang Z, Xu H, Zhou Z, Liang H. Negative lymph node count as an independent prognostic factor in stage III patients after curative gastrectomy: A retrospective cohort study based on a multicenter database. *Int J Surg* 2020; **74**: 44-52 [PMID: 31874262 DOI: 10.1016/j.ijsu.2019.12.018]

54 **Zhang N**, Deng J, He W, Liu Y, Wang X, Ding X, Zhang R, Liang H. Clinical value of standardized procedures of fine lymph node sorting from gastric cancer samples after curative resection: a study of 727 cases. *Chin J Clin Oncol* 2019; **46**: 22-27 [DOI: 10.3969/j.issn.1000-8179.2019.01.911]

55 **Schmidt B**, Chang KK, Maduekwe UN, Look-Hong N, Rattner DW, Lauwers GY, Mullen JT, Yang HK, Yoon SS. D2 lymphadenectomy with surgical ex vivo dissection into node stations for gastric adenocarcinoma can be performed safely in

Western patients and ensures optimal staging. *Ann Surg Oncol* 2013; **20**: 2991-2999 [PMID: 23760588 DOI: 10.1245/s10434-013-3019-1]

56 **Afaneh C**, Levy A, Selby L, Ku G, Tang L, Yoon SS, Coit D, Strong VE. Ex Vivo Lymphadenectomy During Gastrectomy for Adenocarcinoma Optimizes Lymph Node Yield. *J Gastrointest Surg* 2016; **20**: 165-71; discussion 171 [PMID: 26403717 DOI: 10.1007/s11605-015-2948-3]

57 **Iversen LH**, Laurberg S, Hagemann-Madsen R, Dybdahl H. Increased lymph node harvest from colorectal cancer resections using GEWF solution: a randomised study. *J Clin Pathol* 2008; **61**: 1203-1208 [PMID: 18755719 DOI: 10.1136/jcp.2008.060210]

58 **Kerwel TG**, Spatz J, Anthuber M, Wünsch K, Arnholdt H, Märkl B. Injecting methylene blue into the inferior mesenteric artery assures an adequate lymph node harvest and eliminates pathologist variability in nodal staging for rectal cancer. *Dis Colon Rectum* 2009; **52**: 935-941 [PMID: 19502859 DOI: 10.1007/DCR.0b013e31819f28c9]

59 **Märkl B**, Moldovan AI, Jähnig H, Cacchi C, Spatz H, Anthuber M, Oruzio DV, Kretsinger H, Arnholdt HM. Combination of ex vivo sentinel lymph node mapping and methylene blue-assisted lymph node dissection in gastric cancer: a prospective and randomized study. *Ann Surg Oncol* 2011; **18**: 1860-1868 [PMID: 21503792 DOI: 10.1245/s10434-011-1713-4]

60 **Märkl B**, Wünsch K, Hebick KU, Anthuber M, Probst A, Arnholdt HM, Spatz H. Methylene blue-assisted lymph node dissection in combination with ex vivo sentinel lymph node mapping in gastric cancer. *Histopathology* 2009; **54**: 433-441 [PMID: 19309395 DOI: 10.1111/j.1365-2559.2009.03243.x]

61 **Wilkinson EJ**, Hause L. Probability in lymph node sectioning. *Cancer* 1974; **33**: 1269-1274 [PMID: 4823479 DOI: 10.1002/1097-0142(197405)33:5<1269::aid-cncr2820330512>3.0.co;2-x]

World Journal of Clinical Cases

Submit a Manuscript: https://www.f6publishing.com

World J Clin Cases 2023 March 26; 11(9): 1939-1950

DOI: 10.12998/wjcc.v11.i9.1939

ISSN 2307-8960 (online)

MINIREVIEWS

Laparoscopic common bile duct exploration to treat choledocholithiasis in situs inversus patients: A technical review

Bo-Ya Chiu, Shu-Hung Chuang, Shih-Chang Chuang, Kung-Kai Kuo

Specialty type: Medicine, research and experimental

Provenance and peer review: Invited article; Externally peer reviewed.

Peer-review model: Single blind

Peer-review report's scientific quality classification

Grade A (Excellent): 0
Grade B (Very good): B
Grade C (Good): 0
Grade D (Fair): D
Grade E (Poor): 0

P-Reviewer: Atqiaee K, Iran; Miao G, China

Received: December 6, 2022
Peer-review started: December 6, 2022
First decision: December 26, 2022
Revised: January 18, 2023
Accepted: February 27, 2023
Article in press: February 27, 2023
Published online: March 26, 2023

Bo-Ya Chiu, School of Post-baccalaureate Medicine, College of Medicine, Kaohsiung Medical University, Kaohsiung 80708, Taiwan

Shu-Hung Chuang, Shih-Chang Chuang, Kung-Kai Kuo, Division of General and Digestive Surgery, Department of Surgery, Kaohsiung Medical University Hospital, Kaohsiung Medical University, Kaohsiung 80708, Taiwan

Shu-Hung Chuang, Shih-Chang Chuang, Kung-Kai Kuo, School of Medicine, College of Medicine, Kaohsiung Medical University, Kaohsiung 80708, Taiwan

Corresponding author: Shu-Hung Chuang, MD, PhD, Assistant Professor, Doctor, Surgeon, Surgical Oncologist, Division of General and Digestive Surgery, Department of Surgery, Kaohsiung Medical University Hospital, Kaohsiung Medical University, No. 100 Shih-Chuan 1st Road, Sanmin District, Kaohsiung 80708, Taiwan. atreecsw@hotmail.com

Abstract

Situs inversus (SI) is a rare congenital condition characterized by a mirror-image transposition of the major visceral organs. Since the 1990s, more than one hundred SI patients have been reported to have successfully undergone laparoscopic cholecystectomy. In these cases, the major problem is to overcome is the left-right condition for right-handed surgeons. Laparoscopic common bile duct exploration (LCBDE), an alternative to treat patients with bile duct stones, has shown equivalent efficacy and is less likely to cause pancreatitis than endoscopic retrograde cholangiopancreatography. Recent updated meta-analyses revealed that a shorter postoperative hospital stay, fewer procedural interventions, cost-effectiveness, a higher stone clearance rate, and fewer perioperative complications are additional advantages of LCBDE. However, the technique is technically demanding, even for skilled laparoscopic surgeons. Conducting LCBDE in patients with difficult situations, such as SI, is more complex than usual. We herein review published SI patients with choledocholithiasis treated by LCBDE, including our own experience, and this paper focuses on the technical aspects.

Key Words: Choledocholithiasis; Choledochotomy; Laparoscopic common bile duct exploration; Single incision; Situs inversus; Transcystic

Core Tip: Laparoscopic common bile duct exploration (LCBDE) is an alternative option to treat choledocholithiasis. Compared to endoscopic retrograde cholangiopancreatography, it has been demonstrated that LCBDE has resulted in shorter hospital stays, fewer procedures, and greater cost-effectiveness in recent studies. Nevertheless, LCBDE is a technically demanding procedure. It is even more challenging in difficult circumstances such as situs inversus (SI). Herein, we present an analysis of published SI patients with choledocholithiasis treated by LCBDE and our own case, and this paper focuses on the technical aspects.

Citation: Chiu BY, Chuang SH, Chuang SC, Kuo KK. Laparoscopic common bile duct exploration to treat choledocholithiasis in situs inversus patients: A technical review. *World J Clin Cases* 2023; 11(9): 1939-1950
URL: https://www.wjgnet.com/2307-8960/full/v11/i9/1939.htm
DOI: https://dx.doi.org/10.12998/wjcc.v11.i9.1939

INTRODUCTION

For more than two decades, laparoscopic common bile duct exploration (LCBDE) and endoscopic retrograde cholangiopancreatography (ERCP) with stone removal have been widely accepted techniques for managing common bile duct (CBD) stones[1-3]. As LCBDE is a technically demanding procedure, ERCP has gradually become mainstream in clinical practice. In 2018, an updated network meta-analysis including 13 trials and 1757 patients revealed that laparoscopic cholecystectomy (LC) plus LCBDE had better outcomes than LC plus ERCP in terms of not only length of hospital stay but also stone clearance rate and perioperative complications[4]. Other studies exhibited inconsistent results[3,5,6]. The trend in favor of ERCP resulted in decreased familiarity with LCBDE by surgeons. The complex steps and delicate tools used in LCBDE also make it challenging to perform.

Situs inversus (SI) is a rare condition causing left-right positioning of thoracic and abdominal organs [7]. Clinically, SI by itself is asymptomatic; however, when it is associated with CBD stones, the diagnosis can be challenging due to the reversed anatomical location[8]. This is also true for LC and LCBDE. As LC in SI has been studied in two meta-analyses[9,10], LCBDE in SI is limited to a small number of case reports. This review is aimed at assessing published SI patients treated by LCBDE and shares our own experience in the technical aspects.

LITERATURE REVIEW AND OUR OWN EXPERIENCE

Data collection

A search for all articles regarding CBD exploration in patients with SI was conducted in The Cochrane Library, PubMed, Embase, and Web of Science without language restriction until October 5, 2022. The keywords used were "Situs inversus" plus "laparoscopic bile duct exploration", "choledocholithotripsy", "choledocholithotomy", "choledocholithiasis", and "bile duct stone". All relevant studies reporting one or more cases of CBD stone exploration in SI that were found as full texts, structured abstracts or conference reports were included. Studies that described procedures conducted in open surgery or other than CBD exploration were excluded. Duplications of the same patient reported in different studies were also excluded. A total of 12 records were identified by the literature search. In accordance with the study exclusion criteria, two articles were excluded for reporting the same patient [11,12], and the other two articles were excluded for open surgery[13,14]. Finally, eight case reports were included in this review[8,15-21]. The detailed information is presented in Tables 1-3.

Our own experience

A 79-year-old female with SI had underlying hypertension, type II diabetes mellitus, dyslipidemia, and an operation history of ectopic pregnancy 50 years prior. This time, she suffered from postprandial epigastric pain accompanied by a jaundice episode 5 d before her medical seeking. At the emergency room, physical examination was unremarkable. Laboratory values showed white blood cell 7,200/mm (normal range: 4000–10000), C-reactive protein 33.31 mg/dL (0–8), total bilirubin 1.17 mg/dL (1.0–2.0), direct bilirubin 0.5 mg/dL (0.2–1), alanine transaminase 39 IU/L (10–40), aspartate aminotransferase 89 IU/L (10–42), and alkaline phosphatase 147 IU/L (28–94). Abdominal computed tomography (CT) showed cholelithiasis and choledocholithiasis in the distal CBD (Figure 1A and B). Other anomalies included distal CBD draining into the duodenal 3rd portion, duplication of the right ureter, and right hydroureteronephrosis (Figure 1A and C). Under the impression of acute calculous cholecystitis and choledocholithiasis with obstructive jaundice and liver function impairment, she was admitted for single-incision LC and LCBDE. The detailed surgical procedure is discussed below, and the patient's

Table 1 Preoperative characteristics of situs inversus patients treated by laparoscopic bile duct exploration in the literature review

Ref.	Year	Age	Sex	Medical history	Presentation	Diagnostic tools for CBD stone	Preoperative intervention
Kang *et al*[21]	2004	64	F	Atrial fibrillation	Jaundice, abnormal liver function	Echo, CT, MRCP	Nil
Tai *et al*[20]	2004	NA	F	Arrhythmia with pacemaker implantation	NA	NA	ERCP
Weber-Sánchez *et al*[15]	2011	60	M	NA	Jaundice, cholecystitis	NA	NA
Han *et al*[16]	2012	71	F	NA	NA	CT	ERCP
Liu *et al*[8]	2017	51	F	Nil	Cholecystitis, abnormal liver function	CT, MRCP	Nil
Senthilnathan *et al*[17]	2017	76	F	Gallbladder stone s/p open cholecystectomy	NA	NA	ERCP
Takalkar *et al*[19]	2018	50	F	NA	Jaundice, abnormal liver function, cholecystitis	Echo, MRCP	ERCP + ERBD
Simkhada *et al*[18]	2021	63	F	HTN, hypothyroidism, CKD	NA	MRCP	ERCP
Our case	2022	79	F	HTN, hyperlipidemia, DM, CKD, ectopic pregnancy	Jaundice, abnormal liver function, cholecystitis	CT	Nil

F: Female; M: Male; s/p: Status post; HTN: Hypertension; DM: Diabetes mellitus; CKD: Chronic kidney disease; CT: Computed tomography; MRCP: Magnetic resonance cholangiopancreatography; ERCP: Endoscopic retrograde cholangiopancreatography; ERBD: Endoscopic retrograde biliary drainage; NA: Not available; CBD: Common bile duct.

postoperative recovery was uneventful. She was discharged on the 3rd postoperative day. No complications occurred after a 24.5-mo follow-up.

The single-incision LCBDE (SILCBDE) technique has been described in detail previously[22,23]. The patient was given general anesthesia and placed in the reverse Trendelenburg position. The surgeon and the assistant stood on the right side of the patient owing to the mirror positioning of the intraabdominal organs. The surgery began with the insertion of a commercial multichannel port through a 2 cm left paraumbilical incision. A 5-mm atraumatic grasper was inserted through the left 5-mm port to retract the gallbladder to the 2 o'clock direction. A 5-mm 50-cm-long 30-degree laparoscope was passed through the lower 12-mm port to provide visualization. The working ports were served by the upper 12-mm and right 5-mm ports. After dissecting Calot's triangle (Figure 2A) and securing the proximal cystic duct, a small incision was made into the cystic duct, and a 5 French feeding tube was passed into the nondilated cystic duct (Figure 2B and C). We conducted a diagnostic intraoperative cholangiogram (IOC), and distal CBD stones were confirmed (Figure 3A). Then, we used a modified technique named "basket-in-catheter"(BIC)[24]: The Dormia basket was inserted into a six French feeding tube and then went forward to the predestined distance. After entering the distal CBD, the basket was opened to trap the stone (Figures 2B and 3B). After stone clearance, completion IOC was performed to confirm that there were no retained stones (Figure 3C). Finally, the cystic duct was closed, and the gallbladder was detached from the liver bed (Figure 2D) with a closed suction drain left in the subhepatic space. The surgery took 152 min with an estimated blood loss of 5 ml. The details of the operation are shown in the Video.

ACUTE BILIARY TRACT DISEASE IN SITUS INVERSUS PATIENTS

Overview of Situs inversus

SI is a rare defect of situs orientation. As SI fails to generate normal left-right asymmetry, it results in a spectrum of laterality disturbances[25]. The most common of these is immotile cilia syndrome, known as Kartagener syndrome[26-28]. Ivemark's syndrome, cardiac malformation and biliary atresia are also found in patients with SI[29-31]. In our case, duplication of the right ureter and abnormal insertion of the distal CBD into the 3rd portion of the duodenum were found on CT (Figures 1 and 3C). Although their association with SI remains unclear[32,33], we should always pay attention to SI patients to identify possible anomalies in preoperative surveys.

Table 2 Intraoperative characteristics of situs inversus patients treated by laparoscopic bile duct exploration in the literature review

Ref.	Year	IOC	Incision number	Style	Position	Surgeon site	Working hand	Choledochoscopy	CBDE route	Approach technique
Kang *et al*[21]	2004	N	4	MirA	NA	Right side	Left	Yes	Choledochotomy with T-tube closure	Choledochoscopy
Tai *et al*[20]	2004	N	4[a]	NA	NA	NA	NA	NA	NA	NA
Weber-Sánchez *et al*[15]	2011	N	4[a]	NA	NA	NA	NA	NA	NA	NA
Han *et al*[16]	2012	N	4	MirCon	NA	NA	NA	Yes	Choledochotomy	Choledochoscopy
Liu *et al*[8]	2017	N	4[a]	NA	NA	NA	NA	NA	NA	NA
Senthilnathan *et al*[17]	2017	Y	4	MirCon	Supine, split legs	Between legs	NA	No	Choledochotomy with CDD[b]	Balloon and saline sweep
Takalkar *et al*[19]	2018	N	4	MirA	NA	NA	NA	No	Choledochotomy with CDD[c]	NA
Simkhada *et al*[18]	2021	N	4	MirA	Lithotomy	Right side	Left	Yes	Choledochotomy with primary closure	Endo-forceps
Our case	2022	Y	1	SP	Reverse Trendelenburg	Right side	Right	No	Transcystic approach	Basket in catheter

[a]Defined as conventional in study.
[b]Underwent laparoscopic cholecystectomy six months prior. Found common bile duct stone and small residual gallbladder containing stone this time.
[c]Due to significant dilation of the common bile duct (> 2 cm).
IOC: Intraoperative cholangiogram; MirA: Mirrored American; MirCon: Mirrored conventional; SP: Single-port. CDD: Choledochoduodenostomy; CBDE: Common bile duct exploration; NA: Not available; N: No; Y: Yes.

Table 3 Operative results of situs inversus patients treated by laparoscopic bile duct exploration in the literature review

Ref.	Year	OP time (min)	Conversion	PLOS (d)	Complication	Mortality	Follow-up (mo)
Kang *et al*[21]	2004	240	No	NA	NA	Nil	Nil
Tai *et al*[20]	2004	NA	No	NA	Nil	Nil	Nil
Weber-Sánchez *et al*[15]	2011	NA	No	NA	NA	Nil	Nil
Han *et al*[16]	2012	129	No	NA	Nil	Nil	Nil
Liu *et al*[8]	2017	NA	No	5	Nil	Nil	Nil
Senthilnathan *et al*[17]	2017	NA	No	7	Nil	Nil	Nil
Takalkar *et al*[19]	2018	NA	No	NA	NA	Nil	Nil
Simkhada *et al*[18]	2021	NA	No	NA	NA	Nil	Nil
Our case	2022	152	No	3	Nil	Nil	24.5

OP: Operative; PLOS: Postoperative length of hospital stay; NA: Not available.

Diagnosis

A total of 9 case reports including our case, was comprised of eight women and one man with ages ranging from 50 to 79 years of age, as detailed in Table 1. Systemic disease was reported in four patients [18,20,21], and one of them was equipped with a pacemaker[20]. One patient had an ectopic pregnancy history. Also, one patient had undergone LC before, but residual gallbladder and CBD stones were found six months later[17]. The presentation in four of these patients was jaundice[15,19,21], while four patients developed cholecystitis[8,15,19]. Additional high-resolution imaging was used to assess the abdominal anatomy in six patients: Two patients underwent abdominal CT only[16], magnetic resonance cholangiopancreatography (MRCP) was used in two cases[18,19], and two patients underwent both CT and MRCP[8,21].

Due to the left-right presentation of SI, a timely diagnosis of acute abdominal diseases in SI patients is difficult for emergency physicians[34,35]. Liu *et al*[8] reported a 15-d delay diagnosis of acute cholangitis

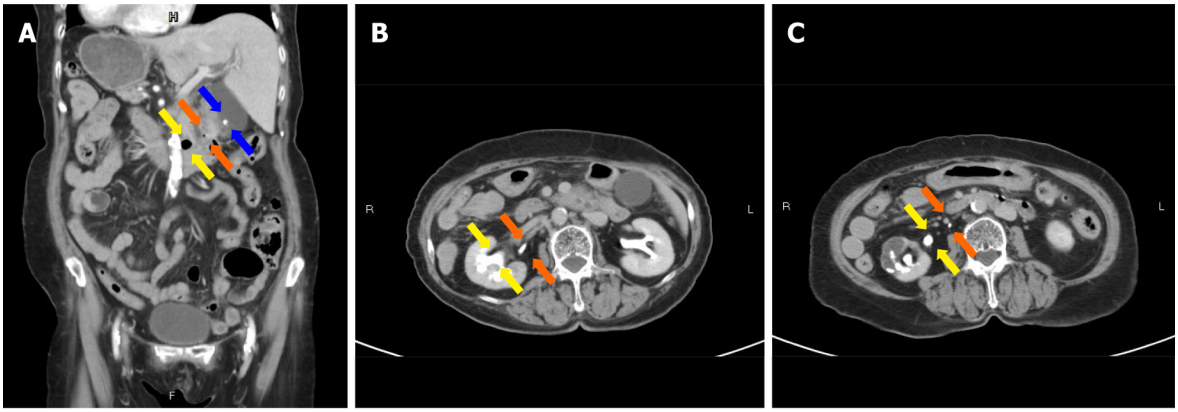

DOI: 10.12998/wjcc.v11.i9.1939

Figure 1 Preoperative computed tomography showed situs inversus, stones in the gallbladder and the common bile duct, and associated anomalies. A: A gallbladder stone (blue arrows), a common bile duct stone (orange arrows) and a diverticulum at the 3rd portion of the duodenum (yellow arrows); B: Right upper ureter of the duplication (orange arrows) and lower pelvis of the duplication (yellow arrows); C: Right upper ureter (orange arrows) and right lower ureter (yellow arrows).

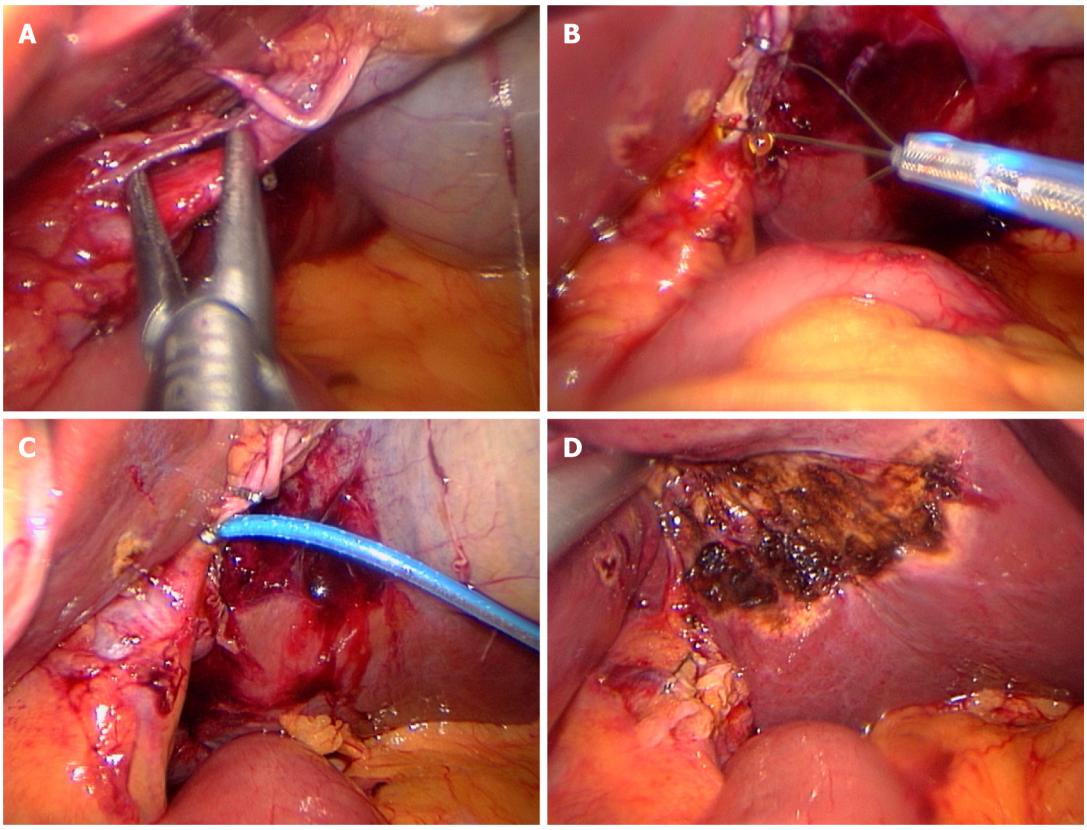

DOI: 10.12998/wjcc.v11.i9.1939

Figure 2 Intraoperative photos during single-incision laparoscopic transcystic common bile duct exploration in a patient with situs inversus. A: Dissection of the hepatocystic triangle; B: An opened retrieval basket in a 6 French feeding tube; C: Cystic duct cannulation for intraoperative cholangiography; D: Completion of choledocholithotripsy and cholecystectomy.

[8]. For patients with postprandial left upper abdominal pain, physical examination is needed to reveal a heartbeat in the right hemithorax and hepatic dullness in the left upper abdomen so that cholelithiasis associated with SI can be considered in addition to acute myocardial infarction or a peptic ulcer. In patients with uncertain features, a careful physical examination with radiological investigations plays a significant role in SI diagnosis[36,37]. Here, we propose a practical algorithm for the diagnosis and management of cholelithiasis and choledocholithiasis in SI patients (Figure 4).

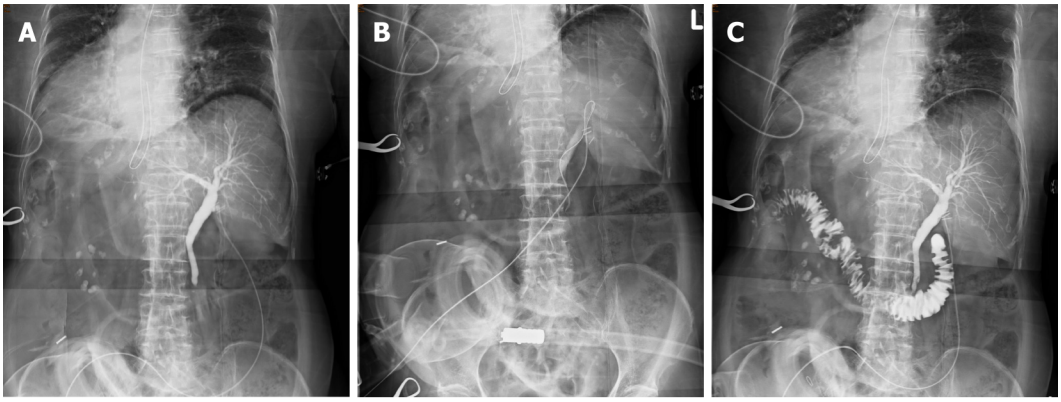

DOI: 10.12998/wjcc.v11.i9.1939

Figure 3 Intraoperative cholangiograms during transcystic choledocholithotripsy using a modified "basket in catheter" technique. A: The diagnostic cholangiogram showed an obstructive biliary tree; B: Transcystic basket trawling; C: The completion cholangiogram revealed stone clearance and a patent distal common bile duct.

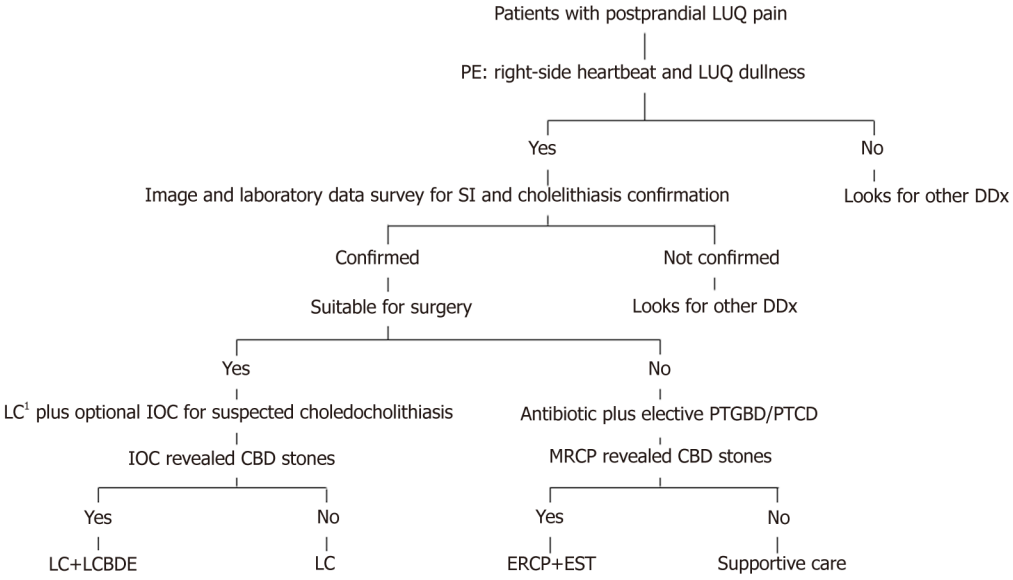

DOI: 10.12998/wjcc.v11.i9.1939

Figure 4 A practical algorithm for diagnosis and management to treat cholelithiasis and choledocholithiasis in situs inversus patients. [1]Laparoscopic cholecystectomy can be performed with four ports or a single port based on the surgeon's discretion. LUQ: Left upper quadrant; PE: Physical examination; SI: Situs inversus; DDx: Differential diagnosis; LC: Laparoscopic cholecystectomy; IOC: Intraoperative cholangiography; MRCP: Magnetic resonance cholangiopancreatography; PTGBD: Percutaneous transhepatic gallbladder drainage; PTCD: Percutaneous transhepatic cholangiography and drainage; CBD: Common bile duct; LCBDE: Laparoscopic common bile duct exploration; ERCP: Endoscopic retrograde cholangiopancreatography; EST: Endoscopic sphincterotomy.

Endoscopic retrograde cholangiopancreatography vs laparoscopic common bile duct exploration

Patients with SI also pose significant challenges to endoscopists and surgeons[38-42]. ERCP is one of the most challenging procedures in SI patients. Given the reversed anatomy, a 180-degree clockwise rotation in the duodenum is often required[43-47]. Furthermore, cannulation to the bile duct is difficult because of the lack of visualization and the ectopic location of the ampulla of Vater in SI patients[7]. In 2022, Ding *et al*[48] published a case series containing 14 patients with SI undergoing ERCP. The rate of successful cannulation was 85.7% (12/14), while difficult cannulation occurred in 71.4% (10/14) of those patients[48]. Although the literature review until 2021 revealed a 100% cannulation success of 41 patients[48], one of five cases reported in 2022 failed[49-52]. Plus there were 5 failed cases in our literature review, and the overall success rate was 87.7%. Compared to ERCP, LCBDE provides full intraperitoneal visualization. In the five case reports of our literature review, all the patients had successful LCBDE after failed ERCP, and the former might be a better option to treat choledocholithiasis in SI patients.

LAPAROSCOPIC COMMON BILE DUCT EXPLORATION IN SITUS INVERSUS PATIENTS

Outcome

In addition to our case, the operative time was only shown in two more patients: 240 min[21] and 129 min[16]. Postoperative hospital stay was also recorded in two other patients as five days[8] and seven days[17]. While we spent 152 min to complete the SILCBDE, the postoperative hospital stay was only three days. Of these patients, no conversion, complication, or mortality was recorded. The detailed operative results are presented in Table 3.

Trocar positioning

Conducting laparoscopic surgery in SI patients is also difficult owing to the transposed organs[53-55]. The first consideration is trocar positioning. There are essentially two types of laparoscopic port placements in SI patients: The "American mirror technique" and the "French mirror technique"[9,10]. Surgeons can choose either of them depending on their discretion. In most of the case reports in our review, the "American mirror technique" was used, while some authors ambiguously described it as a "conventional technique" that could be the "American mirror technique" or "French mirror technique". The handedness of the surgeons is the second problem[56,57]. Surgeons use their left hand for dissection *via* the epigastric port and use the right hand for the midclavicular port. As most surgeons are right-handed, using the left hand will not be precise and may pose danger. In using the right hand, however, the surgeon will have to cross the patient's body to perform the dissection[10]. To address this dilemma, a systemic review showed that left-handed surgeons yielded shorter intervention times than right-handed surgeons during LC of SI patients[9]. However, there were only seven left-handed surgeons in 121 cases in this study. While most surgical procedures are designed for right-handed surgeons, it is not uncommon for left-handed surgeons to use their right hand as the working hand in daily practice[58, 59]. Using a nondominant hand might not have much impact on the surgical outcome.

In our literature review of LCBDE in SI patients (Table 2), although some of the patients ambiguously described their operative technique as "conventional"[8,15,20], most of them reported a four-port technique with the American mirror style[18,19,21]. Our patient is the only case treated by SILCBDE.

Single-incision laparoscopic common bile duct exploration

Compared with the difficulty in LCBDE for SI patients, SILCBDE seems to have some advantages. We developed this novel technique in July 2012, and it soon became our standard of care for choledocholithiasis, including difficult situations such as Mirizzi syndrome Csendes type II-IV[22,23,60]. In addition to a 5-mm 50-cm-long 30-degree laparoscope and a 5-mm flexible fiber choledochosope set, only conventional straight laparoscopic instruments were needed. Either the single-incision multiple-port longitudinal-array technique[61] or a commercial multichannel port could be used at the surgeon's discretion (Figure 5). This procedure is indicated for every patient with choledocholithiasis who can tolerate regular laparoscopic surgery. While SILCBDE is selected for SI patients, the mirror position of trocars is unnecessary because only one single port was used. The handedness problem is invalid, as dissection can be performed by the right hand, and the left hand can be used for gallbladder traction[62-65]. It has little adverse effect in our technique as well, while gallbladder traction is usually carried out by the assistant[22,23,66]. Additionally, SILCBDE decreases incisional trauma and postoperative pain, speeds recovery and provides favorable cosmesis. The only modification needed is the positions of operators and assistants, which should be moved from the patient's left side to the right side. Since our surgeon is an experienced surgeon who has performed more than 100 SILCBDEs[22], the risk of major complications is minimal. Our patient also attained the shortest postoperative stay in this review.

Choledochotomy and transcystic approach

Another issue in SI undergoing LCBDE is the approach route. The laparoscopic approach for CBD stones can be categorized into transcystic exploration and choledochotomy[67]. The location, number, and size of the CBD stones along with the anatomy of the cystic duct and the CBD influence the choice between these two techniques[68]. For example, small distal stones (≤ 6 mm diameter) are more suitable for the transcystic approach; choledochotomy can be considered if the CBD is larger than 7 mm or intrahepatic duct stones exist[67]. In our literature review, choledochoscopy was used in three patients to conduct bile duct exploration[16,18,21]. Five patients underwent choledochotomy that closed by one T-tube drainage[21], one patient had primary closure[18], two patients had choledochoduodenostomies [17,19], and the remaining one patient had an unmentioned repair[16]. The only transcystic approach was applied in our case. Balloon and saline sweeping was used in one case[17], and we used a basket in a catheter to remove the bile duct stone (Table 2).

Although many studies have reported that transcystic approaches have shorter postoperative hospital stays and fewer bile leaks than choledochotomies[69-72], in most of the cases in our review, the latter was used. Senthilnathan *et al*[17] mentioned that a residual gallbladder containing small calculi was found six months after LC in an SI patient[17]. CBD stones were also exhibited at the same time, which might have migrated from the cystic duct. In this situation, a transcystic approach might be a better option to detect and remove retained cystic duct stones that could be missed by choledochotomy. Our

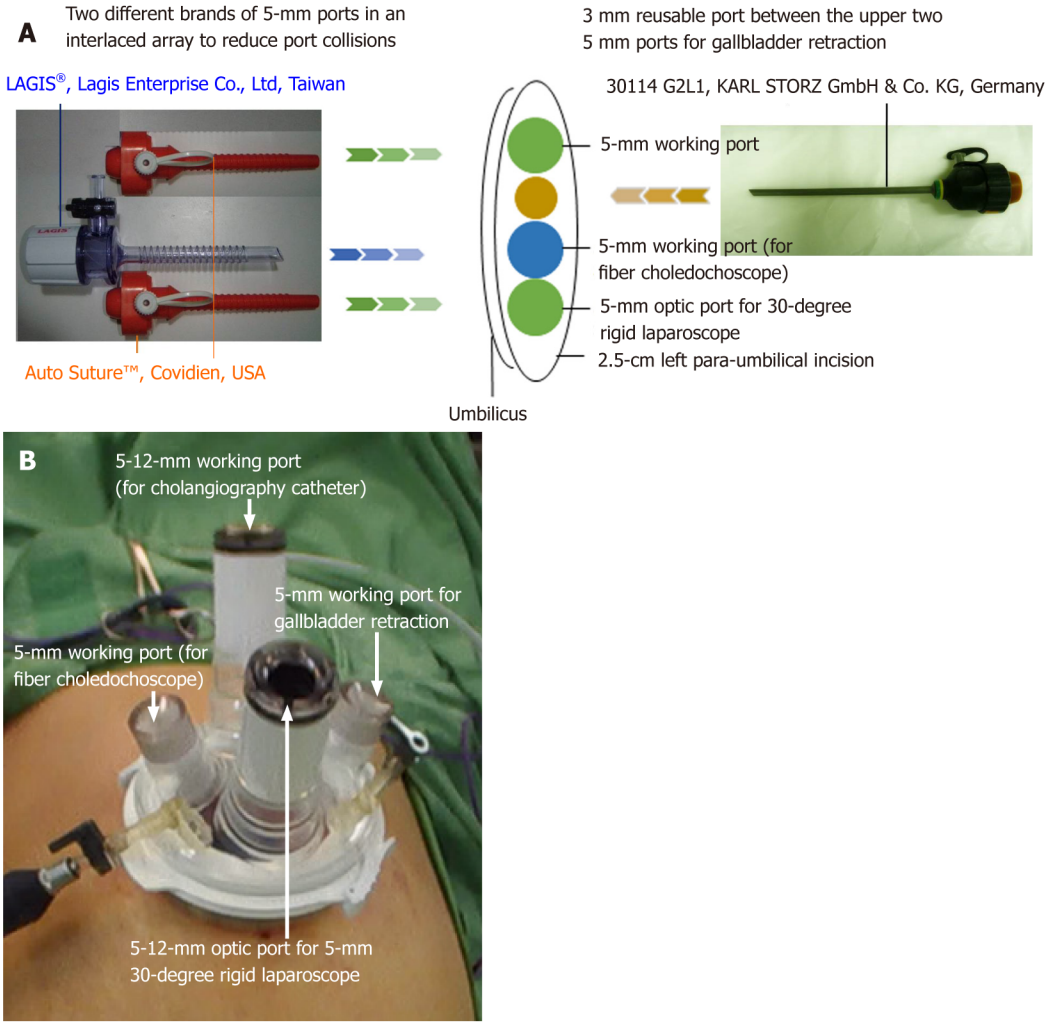

DOI: 10.12998/wjcc.v11.i9.1939

Figure 5 Port design in single-incision laparoscopic common bile duct exploration. A: The single-incision multiple-port longitudinal-array technique; B: A commercial multichannel port.

patient is the only case in which a transcystic approach was applied in this review. We showed that SILCBDE with a transcytic approach can be performed successfully in an SI patient. In addition, we used a modified technique named BIC[24]. As choledochoscopy is a delicate device and could be under repair at times, BIC can be performed easily by using a small feeding tube and a stone basket. In our experience, it could achieve stone clearance in nearly half of simple CBD stone cases (data unpublished). With these novel techniques, an SI patient with choledocholithiasis can experience the least invasive LCBDE approach. In our case, SILCBDE *via* a transcystic approach using a modified BIC technique took 152 min to complete, similar to other cases in this review. After a 24.5-mo follow-up, no late complications or stone recurrence were identified.

Limitation

There are several limitations to our study that must be acknowledged. First, due to the rarity of such cases, the number of included cases is very limited. The conclusion might be considered expert opinions, relatively low-quality evidence. Second, cases included in our review were published between 2004 and 2022. Bias could occur because of the advances in techniques and instruments used, which results in consistent cohort heterogeneity. Finally, missing data were encountered in most of the patients, and therefore, some important issues were difficult to address. For example, information on the postoperative length of hospital stay and complications was only available for three (33.3%) and five (55.6%) patients, respectively.

CONCLUSION

Both ERCP and LCBDE are valid options to treat choledocholithiasis by experienced endoscopists and

surgeons. Although there are no related comparative studies, LCBDE seems to be superior to ERCP for SI patients in terms of better intraperitoneal visualization and a lower failure rate. In SI patients, some difficulties of conventional multiport laparoscopic surgical techniques could be overcome by SILCBDE. The transcystic approach and a modified BIC technique are also feasible and safe with many benefits, as we described in our report.

FOOTNOTES

Author contributions: Chiu BY and Chuang SH drafted the manuscript; Chuang SH, Chuang SC, and Kuo KK revised the manuscript; All authors have read and approved the final manuscript.

Conflict-of-interest statement: All the authors report no relevant conflicts of interest for this article.

Country/Territory of origin: Taiwan

ORCID number: Shu-Hung Chuang 0000-0002-2007-0415; Shih-Chang Chuang 0000-0003-1481-1632.

S-Editor: Li L
L-Editor: A
P-Editor: Li L

REFERENCES

1 **European Association for the Study of the Liver (EASL)**. EASL Clinical Practice Guidelines on the prevention, diagnosis and treatment of gallstones. *J Hepatol* 2016; **65**: 146-181 [PMID: 27085810 DOI: 10.1016/j.jhep.2016.03.005]
2 **Park CH**. The Management of Common Bile Duct Stones. *Korean J Gastroenterol* 2018; **71**: 260-263 [PMID: 29791984 DOI: 10.4166/kjg.2018.71.5.260]
3 **Zhang J**, Ling X. Risk factors and management of primary choledocholithiasis: a systematic review. *ANZ J Surg* 2021; **91**: 530-536 [PMID: 32815266 DOI: 10.1111/ans.16211]
4 **Pan L**, Chen M, Ji L, Zheng L, Yan P, Fang J, Zhang B, Cai X. The Safety and Efficacy of Laparoscopic Common Bile Duct Exploration Combined with Cholecystectomy for the Management of Cholecysto-choledocholithiasis: An Up-to-date Meta-analysis. *Ann Surg* 2018; **268**: 247-253 [PMID: 29533266 DOI: 10.1097/SLA.0000000000002731]
5 **Parra-Membrives P**, Martínez-Baena D, Lorente-Herce J, Jiménez-Riera G. Comparative Study of Three Bile Duct Closure Methods Following Laparoscopic Common Bile Duct Exploration for Choledocholithiasis. *J Laparoendosc Adv Surg Tech A* 2018; **28**: 145-151 [PMID: 28976804 DOI: 10.1089/lap.2017.0433]
6 **Morton A**, Cralley A, Brooke-Sanchez M, Pieracci FM. Laparoscopic common bile duct exploration by acute care surgeons saves time and money compared to ERCP. *Am J Surg* 2022; **224**: 116-119 [PMID: 35351289 DOI: 10.1016/j.amjsurg.2022.03.026]
7 **Eitler K**, Bibok A, Telkes G. Situs Inversus Totalis: A Clinical Review. *Int J Gen Med* 2022; **15**: 2437-2449 [PMID: 35264880 DOI: 10.2147/IJGM.S295444]
8 **Liu Y**, Wu L, Chen Y, Li D, Jiang J, Zhong W, Cao Y. Delayed diagnosis of abdominal pain in patient with situs inversus totalis in emergency department: A case report. *Medicine (Baltimore)* 2017; **96**: e9028 [PMID: 29245291 DOI: 10.1097/MD.0000000000009028]
9 **Enciu O**, Toma EA, Tulin A, Georgescu DE, Miron A. Look beyond the Mirror: Laparoscopic Cholecystectomy in Situs Inversus Totalis-A Systematic Review and Meta-Analysis (and Report of New Technique). *Diagnostics (Basel)* 2022; **12** [PMID: 35626419 DOI: 10.3390/diagnostics12051265]
10 **Chaouch MA**, Jerraya H, Dougaz MW, Nouira R, Dziri C. A Systematic Review of Laparoscopic Cholecystectomy in Situs Inversus. *J Invest Surg* 2021; **34**: 324-333 [PMID: 31164015 DOI: 10.1080/08941939.2019.1622822]
11 **Wong J**, Tang CN, Chau CH, Luk YW, Li MK. Laparoscopic cholecystectomy and exploration of common bile duct in a patient with situs inversus. *Surg Endosc* 2001; **15**: 218 [PMID: 12200663 DOI: 10.1007/s004640040037]
12 **Tang CN**, Tsui KK, Ha JP, Siu WT, Li MK. Laparoscopic exploration of the common bile duct: 10-year experience of 174 patients from a single centre. *Hong Kong Med J* 2006; **12**: 191-196 [PMID: 16760546]
13 **Emmanuel J**, Sriram N, Muthukaruppan R. Endoscopic retrograde cholangiopancreatography in a patient with complete situs inversus viscerum: A case report and literature review. *DEN Open* 2022; **2**: e17 [PMID: 35310748 DOI: 10.1002/deo2.17]
14 **Alzahrani HA**, Yamani NM. Gallbladder agenesis with a primary choledochal stone in a patient with situs inversus totalis. *Am J Case Rep* 2014; **15**: 185-188 [PMID: 24803979 DOI: 10.12659/AJCR.890523]
15 **Weber-Sánchez A**, Bravo-Torreblanca C, Garteiz-Martínez D, Carbó-Romano R, Vega-Rivera F, Hernández R. Case

report: laparoscopic cholecystectomy and common bile duct exploration in a 60 year-old patient with situs inversus. *Rev Gastroenterol Mex* 2011; **76**: 255-259 [PMID: 22041317]
16 **Han SJ**, Chun KS, Song IS. Laparoscopic cbd exploration in patient with situs inversus totalis. *HPB* 2012; **14**: 328 [DOI: 10.1111/j.1477-2574.2012.00512.x]
17 **Senthilnathan P**, Parthasarathi R, Rajapandian S, Praveen Raj P, Vijai A, Nalankilli VP, Srivatsan G, Sabnis S, Palanivelu C. Laparoscopic CBD exploration with choledochoduodenostomy for bileduct stones in a patient with situs inversus totalis. *Surgical Endoscopy and Other Interventional Techniques* 2017; **31**: S95 [DOI: 10.1007/s00464-017-5448-6]
18 **Simkhada S**, Malla B, Shrestha R. Laparoscopic Cholecystectomy and Common Bile Duct Exploration in Situs Inversus Patients. *Kathmandu Univ Med J (KUMJ)* 2021; **19**: 271-274 [PMID: 34819450]
19 **Takalkar YP**, Koranne MS, Vashist KS, Khedekar PG, Garale MN, Rege SA, Dalvi AN. Laparoscopic cholecystectomy with choledochoduodenostomy in a patient with situs inversus totalis. *J Minim Access Surg* 2018; **14**: 241-243 [PMID: 29882522 DOI: 10.4103/jmas.JMAS_122_17]
20 **Tai CK**, Tang CN, Ha JP, Chau CH, Siu WT, Li MK. Laparoscopic exploration of common bile duct in difficult choledocholithiasis. *Surg Endosc* 2004; **18**: 910-914 [PMID: 15095079 DOI: 10.1007/s00464-003-8216-8]
21 **Kang SB**, Han HS. Laparoscopic exploration of the common bile duct in a patient with situs inversus totalis. *J Laparoendosc Adv Surg Tech A* 2004; **14**: 103-106 [PMID: 15107220 DOI: 10.1089/109264204322973880]
22 **Chuang SH**, Hung MC, Huang SW, Chou DA, Wu HS. Single-incision laparoscopic common bile duct exploration in 101 consecutive patients: choledochotomy, transcystic, and transfistulous approaches. *Surg Endosc* 2018; **32**: 485-497 [PMID: 28643057 DOI: 10.1007/s00464-017-5658-y]
23 **Chuang SH**, Chen PH, Chang CM, Tsai YF, Lin CS. Single-incision laparoscopic common bile duct exploration with conventional instruments: an innovative technique and a comparative study. *J Gastrointest Surg* 2014; **18**: 737-743 [PMID: 24347312 DOI: 10.1007/s11605-013-2420-1]
24 **Qandeel H**, Zino S, Hanif Z, Nassar MK, Nassar AH. Basket-in-catheter access for transcystic laparoscopic bile duct exploration: technique and results. *Surg Endosc* 2016; **30**: 1958-1964 [PMID: 26198157 DOI: 10.1007/s00464-015-4421-5]
25 **Soofi M**, Alpert MA, Barbadora J, Mukerji B, Mukerji V. Human Laterality Disorders: Pathogenesis, Clinical Manifestations, Diagnosis, and Management. *Am J Med Sci* 2021; **362**: 233-242 [PMID: 34052215 DOI: 10.1016/j.amjms.2021.05.020]
26 **Zurcher K**, Kawashima A. Kartagener's Syndrome. *N Engl J Med* 2021; **384**: e45 [PMID: 33764707 DOI: 10.1056/NEJMicm2028152]
27 **Wallmeier J**, Nielsen KG, Kuehni CE, Lucas JS, Leigh MW, Zariwala MA, Omran H. Motile ciliopathies. *Nat Rev Dis Primers* 2020; **6**: 77 [PMID: 32943623 DOI: 10.1038/s41572-020-0209-6]
28 **Lucas JS**, Davis SD, Omran H, Shoemark A. Primary ciliary dyskinesia in the genomics age. *Lancet Respir Med* 2020; **8**: 202-216 [PMID: 31624012 DOI: 10.1016/S2213-2600(19)30374-1]
29 **Chen W**, Guo Z, Qian L, Wang L. Comorbidities in situs inversus totalis: A hospital-based study. *Birth Defects Res* 2020; **112**: 418-426 [PMID: 31994846 DOI: 10.1002/bdr2.1652]
30 **Masiwal P**, Chenthil KS, Priyadarsini B, Gnanaprakasam J, Srihari I. Ivemark Syndrome. *J Assoc Physicians India* 2016; **64**: 73-75 [PMID: 27735157]
31 **Nair R**, Muthukuru SR. Dextrocardia. 2022 Sep 19. In: StatPearls [Internet]. *StatPearls Publishing*2022 Jan- [PMID: 32310534]
32 **Munshi FI**, Polotti CF, Elsamra SE. Robot-Assisted Radical Cystectomy with Intracorporeal Ileal Conduit in a Patient with Situs Inversus Totalis. *J Endourol Case Rep* 2020; **6**: 135-138 [PMID: 33102709 DOI: 10.1089/cren.2019.0137]
33 **Miheţiu AF**, Bratu DG, Popescu OM, Juravle C, Dumitrean IE, Chicea R. A rare case of situs inversus totalis associated with sigmoid diverticulitis and appendicular agenesis. Embryological, clinical considerations and literature review. *Rom J Morphol Embryol* 2021; **62**: 861-867 [PMID: 35263418 DOI: 10.47162/RJME.62.3.27]
34 **Di Buono G**, Maienza E, Buscemi S, Randisi B, Romano G, Agrusa A. Acute appendicitis in a patient with situs viscerum inversus totalis: Role of laparoscopic approach. A case report and brief literature review. *Int J Surg Case Rep* 2020; **77S**: S29-S33 [PMID: 33208280 DOI: 10.1016/j.ijscr.2020.10.047]
35 **Herrera Ortiz AF**, Lacouture JC, Sandoval Medina D, Gómez Meléndez LJ, Uscategui R. Acute Cholecystitis in a Patient With Situs Inversus Totalis: An Unexpected Finding. *Cureus* 2021; **13**: e15799 [PMID: 34306867 DOI: 10.7759/cureus.15799]
36 **Evola G**, Ferrara F, Di Fede GF, Patanè M, Sarvà S, Piazza L. Left-sided acute appendicitis in a patient with situs viscerum inversus totalis: A case report. *Int J Surg Case Rep* 2022; **90**: 106658 [PMID: 34915437 DOI: 10.1016/j.ijscr.2021.106658]
37 **Umar UA**, Alremeithi AN, Qayyum H. Incidental diagnosis of situs inversus totalis: a perspective from an emergency department attendance. *BMJ Case Rep* 2021; **14** [PMID: 33837038 DOI: 10.1136/bcr-2021-242337]
38 **Abbey E**, Yang F, Qi L, Wu JJ, Tong L, Zhen Z. Situs inversus totalis patients with gastric cancer: Robotic surgery the standard of treatment? *Int J Surg Case Rep* 2021; **81**: 105818 [PMID: 33887833 DOI: 10.1016/j.ijscr.2021.105818]
39 **Kasai S**, Hino H, Shiomi A, Kagawa H, Manabe S, Yamaoka Y, Kato S, Hanaoka M, Kinugasa Y. Robotic-assisted surgery for rectal cancer with situs inversus totalis: A case report. *Asian J Endosc Surg* 2021; **14**: 803-806 [PMID: 33797194 DOI: 10.1111/ases.12937]
40 **Li X**, Liu Z, Kong R, Zhang C, Ge S. Robot-assisted beating-heart surgery for atrial septal defect repair in a case of situs inversus totalis with dextrocardia. *Int J Med Robot* 2021; **17**: e2304 [PMID: 34197045 DOI: 10.1002/rcs.2304]
41 **Yeom SS**, Kim KH, Lee SY, Kim CH, Kim HR, Kim YJ. Reduced-Port Laparoscopic Surgery for Patients With Proximal Transverse Colon Cancer With Situs Inversus Totalis: A Case Report. *Ann Coloproctol* 2018; **34**: 322-325 [PMID: 30630305 DOI: 10.3393/ac.2018.05.29.1]
42 **Jomaa S**, Deeb H, Alshaar D, Alahmar FO. Surgical challenges during open pancreaticoduodenectomy in a patient with situs inversus totalis: A rare case report and literature review. *Ann Med Surg (Lond)* 2022; **82**: 104610 [PMID: 36268427 DOI: 10.1016/j.amsu.2022.104610]
43 **Hu L**, Chai Y, Yang X, Wu Z, Sun H, Wang Z. Duodenoscope combined with laparoscopy in treatment of biliary stones for a patient with situs inversus totalis: A case report. *Medicine (Baltimore)* 2019; **98**: e14272 [PMID: 30762727 DOI:

10.1097/MD.0000000000014272]
44 **de la Serna-Higuera C**, Perez-Miranda M, Flores-Cruz G, Gil-Simón P, Caro-Patón A. Endoscopic retrograde cholangiopancreatography in situs inversus partialis. *Endoscopy* 2010; **42** Suppl 2: E98 [PMID: 20306407 DOI: 10.1055/s-0029-1214968]
45 **Yoshida A**, Minaga K, Takeda O, Hanno H, Takayanagi S, Dozaiku T, Kudo M. Successful biliary cannulation using a novel rotatable sphincterotome in a patient with situs inversus totalis. *Endoscopy* 2020; **52**: E333-E334 [PMID: 32131093 DOI: 10.1055/a-1122-8416]
46 **Tanisaka Y**, Ryozawa S, Sudo K, Fujita A, Mizuide M, Nonaka K, Tashima T. Successful endoscopic retrograde cholangiopancreatography using pancreatic guidewire placement for biliary cannulation in a patient with situs inversus and Billroth-I gastrectomy (with video). *JGH Open* 2019; **3**: 540-541 [PMID: 31832558 DOI: 10.1002/jgh3.12163]
47 **Shimoda F**, Satoh A, Asonuma S, Umemura K, Shimosegawa T. Successful removal of multiple bile duct stones using a papillary large balloon dilation in a very elderly woman with situs inversus totalis. *Clin J Gastroenterol* 2021; **14**: 309-313 [PMID: 32772241 DOI: 10.1007/s12328-020-01198-1]
48 **Ding B**, Wang J, Wei X, Du Y, Xia L, Sun C, Han K, Yang X, Guo X, Pan Y, Wang X. Efficacy and safety of ERCP in patients with situs inversus totalis: multicenter case series and literature review. *BMC Gastroenterol* 2022; **22**: 497 [PMID: 36451092 DOI: 10.1186/s12876-022-02593-3]
49 **Gao YK**, Liu SH, Xie SA, Wen HP, Cao LQ. Successful endoscopic drainage of malignant obstructive jaundice in patients with situs inversus totalis: Two cases report. *Int J Surg Case Rep* 2022; **93**: 106873 [PMID: 35290847 DOI: 10.1016/j.ijscr.2022.106873]
50 **Naser J**, Sarmini MT, Vozzo C, Saleh MA, Chahal P. ERCP and EUS technique in situs inversus totalis: preparing for a left-sided plot twist. *VideoGIE* 2022; **7**: 367-370 [PMID: 36238805 DOI: 10.1016/j.vgie.2022.05.008]
51 **Oh CH**. Successful endoscopic retrograde cholangiopancreatography and bilateral stenting in a patient with situs inversus totalis. *Dig Liver Dis* 2022; **54**: 136-137 [PMID: 33067158 DOI: 10.1016/j.dld.2020.09.019]
52 **Valdivielso Cortázar E**, Porto Fuentes Ó, González Peñas L, Couto Wörner I, Souto Ruzo J, González Conde B, Estévez Prieto E, Alonso Aguirre P. ERCP and situs inversus. *Rev Esp Enferm Dig* 2022; **114**: 176-177 [PMID: 34696595 DOI: 10.17235/reed.2021.8374/2021]
53 **Atwez A**, Keilani Z. Laparoscopic Roux-en-Y gastric bypass in a patient with situs inversus totalis: Case report, technical tips and review of the literature. *Int J Surg Case Rep* 2018; **45**: 56-62 [PMID: 29573597 DOI: 10.1016/j.ijscr.2018.03.004]
54 **Sagawa H**, Ito S, Hayakawa S, Ueno S, Okubo T, Tanaka T, Ogawa R, Takahashi H, Matsuo Y, Mitsui A, Kimura M, Takiguchi S. Robotic distal gastrectomy for gastric cancer in a patient with situs inversus totalis and a vascular anomaly. *Int Cancer Conf J* 2022; **11**: 253-260 [PMID: 36186219 DOI: 10.1007/s13691-022-00554-x]
55 **Zavalza JF**, Molina GA, Paipilla OA, Gil M, Rosales K. Situs inversus and bariatric surgery: A challenge for the surgical team. *Ann Med Surg (Lond)* 2021; **72**: 102972 [PMID: 34840772 DOI: 10.1016/j.amsu.2021.102972]
56 **Patle NM**, Tantia O, Sasmal PK, Khanna S, Sen B. Laparoscopic cholecystectomy in situs inversus-our experience of 6 cases. *Indian J Surg* 2010; **72**: 391-394 [PMID: 21966139 DOI: 10.1007/s12262-010-0159-4]
57 **García-Núñez LM**, Soto-Ortega LE, Payró-Hernández LE, Cabello-Pasini R. Laparoscopic cholecystectomy in situs inversus: the disadvantage of being right-handed. *Rev Gastroenterol Mex* 2008; **73**: 149-152 [PMID: 19671501]
58 **Tchantchaleishvili V**, Myers PO. Left-handedness--a handicap for training in surgery? *J Surg Educ* 2010; **67**: 233-236 [PMID: 20816359 DOI: 10.1016/j.jsurg.2010.06.001]
59 **Prasad NK**, Kvasnovsky C, Wise ES, Kavic SM. The Right Way to Teach Left-Handed Residents: Strategies for Training by Right Handers. *J Surg Educ* 2018; **75**: 271-277 [PMID: 28756969 DOI: 10.1016/j.jsurg.2017.07.004]
60 **Chuang SH**, Kuo KK, Chuang SC, Wang SN, Chang WT, Su WL, Huang JW, Wu PH, Chan HM, Kuok CH. Single-incision versus four-incision laparoscopic transfistulous bile duct exploration for Mirizzi syndrome type II. *Surg Endosc* 2022; **36**: 8672-8683 [PMID: 35697855 DOI: 10.1007/s00464-022-09369-6]
61 **Chuang SH**, Yang WJ, Chang CM, Lin CS, Yeh MC. Is routine single-incision laparoscopic cholecystectomy feasible? *Am J Surg* 2015; **210**: 315-321 [PMID: 25916613 DOI: 10.1016/j.amjsurg.2014.12.032]
62 **Khiangte E**, Newme I, Patowary K, Phukan P. Single-port laparoscopic cholecystectomy in situs inversus totalis using the E.K. glove port. *J Minim Access Surg* 2013; **9**: 180-182 [PMID: 24250066 DOI: 10.4103/0972-9941.118838]
63 **Deguchi Y**, Mitamura K, Omotaka S, Eguchi J, Sakuma D, Sato M, Nomura N, Ito T, Grimes KL, Inoue H. Single-incision cholecystectomy in a patient with situs inversus totalis presenting with cholelithiasis: A case report. *Asian J Endosc Surg* 2015; **8**: 347-349 [PMID: 26303735 DOI: 10.1111/ases.12180]
64 **Jhobta RS**, Gupta A, Negi B, Negi K. Single-incision laparoscopic cholecystectomy using conventional instruments in situs inversus totalis. *BMJ Case Rep* 2018; **11** [PMID: 30567103 DOI: 10.1136/bcr-2018-226404]
65 **Jang EJ**, Roh YH. Single Port Laparoscopic Cholecystectomy in a Patient with Situs Inversus Totalis: A Case Report. *J Minim Invasive Surg* 2019; **22**: 81-84 [PMID: 35602771 DOI: 10.7602/jmis.2019.22.2.81]
66 **Chuang SH**, Lin CS. Single-incision laparoscopic surgery for biliary tract disease. *World J Gastroenterol* 2016; **22**: 736-747 [PMID: 26811621 DOI: 10.3748/wjg.v22.i2.736]
67 **Gupta N**. Role of laparoscopic common bile duct exploration in the management of choledocholithiasis. *World J Gastrointest Surg* 2016; **8**: 376-381 [PMID: 27231516 DOI: 10.4240/wjgs.v8.i5.376]
68 **Zerey M**, Haggerty S, Richardson W, Santos B, Fanelli R, Brunt LM, Stefanidis D. Laparoscopic common bile duct exploration. *Surg Endosc* 2018; **32**: 2603-2612 [PMID: 29273878 DOI: 10.1007/s00464-017-5991-1]
69 **Navaratne L**, Martinez Isla A. Transductal versus transcystic laparoscopic common bile duct exploration: an institutional review of over four hundred cases. *Surg Endosc* 2021; **35**: 437-448 [PMID: 32246237 DOI: 10.1007/s00464-020-07522-7]
70 **Bekheit M**, Smith R, Ramsay G, Soggiu F, Ghazanfar M, Ahmed I. Meta-analysis of laparoscopic transcystic versus transcholedochal common bile duct exploration for choledocholithiasis. *BJS Open* 2019; **3**: 242-251 [PMID: 31183439 DOI: 10.1002/bjs5.50132]
71 **Feng Q**, Huang Y, Wang K, Yuan R, Xiong X, Wu L. Laparoscopic Transcystic Common Bile Duct Exploration: Advantages over Laparoscopic Choledochotomy. *PLoS One* 2016; **11**: e0162885 [PMID: 27668730 DOI: 10.1371/journal.pone.0162885]

72 **Guan H**, Jiang G, Mao X. Primary duct closure combined with transcystic drainage versus T-tube drainage after laparoscopic choledochotomy. *ANZ J Surg* 2019; **89**: 885-888 [PMID: 31067598 DOI: 10.1111/ans.15163]

World Journal of Clinical Cases

Submit a Manuscript: https://www.f6publishing.com

World J Clin Cases 2023 March 26; 11(9): 1951-1962

DOI: 10.12998/wjcc.v11.i9.1951

ISSN 2307-8960 (online)

MINIREVIEWS

Airway ultrasound for patients anticipated to have a difficult airway: Perspective for personalized medicine

Harumasa Nakazawa, Kohji Uzawa, Joho Tokumine, Alan Kawarai Lefor, Akira Motoyasu, Tomoko Yorozu

Specialty type: Anesthesiology

Provenance and peer review: Invited article; Externally peer reviewed.

Peer-review model: Single blind

Peer-review report's scientific quality classification

Grade A (Excellent): 0
Grade B (Very good): B
Grade C (Good): C, C
Grade D (Fair): 0
Grade E (Poor): 0

P-Reviewer: Beyoglu MA, Turkey; Sivanand N, India; Sun P, China

Received: December 14, 2022
Peer-review started: December 14, 2022
First decision: January 19, 2023
Revised: January 28, 2023
Accepted: February 27, 2023
Article in press: February 27, 2023
Published online: March 26, 2023

Harumasa Nakazawa, Kohji Uzawa, Joho Tokumine, Akira Motoyasu, Tomoko Yorozu, Department of Anesthesiology, Kyorin University School of Medicine, Mitaka 181-8611, Tokyo, Japan

Alan Kawarai Lefor, Department of Surgery, Jichi Medical University, Shimotsuke 329-0498, Tochigi, Japan

Corresponding author: Joho Tokumine, MD, PhD, Professor, Department of Anesthesiology, Kyorin University School of Medicine, 6-20-2 Sinkawa, Mitaka 181-8611, Tokyo, Japan. dg274825@cf6.so-net.ne.jp

Abstract

Airway ultrasound allows for precise airway evaluation, particularly for assessing the difficult airway and the potential for front of neck access. Many studies have shown that identification of the cricothyroid membrane by airway ultrasound is more accurate than digital palpation. However, no reports to date have provided clinical evidence that ultrasound identification of the cricothyroid membrane increases the success rate of cricothyroidotomy. This is a narrative review which describes patients with difficult airways for whom airway ultrasound may have been useful for clinical decision making. The role of airway ultrasound for the evaluation of difficult airways is summarized and an approach to the use of ultrasound for airway management is proposed. The goal of this review is to present practical applications of airway ultrasound for patients predicted to have a difficult airway and who undergo cricothyroidotomy.

Key Words: Airway ultrasound; Difficult airway; Point-of-care ultrasound; Cricothyroidotomy; Intubation; Mask ventilation

Core Tip: Airway ultrasound may provide a simpler and more accurate prediction of the difficult airway, especially to distinguish difficult mask ventilation from difficult tracheal intubation. Accurate cricothyroid membrane identification may provide a landmark for securing a surgical airway in clinical practice.

Citation: Nakazawa H, Uzawa K, Tokumine J, Lefor AK, Motoyasu A, Yorozu T. Airway ultrasound for patients anticipated to have a difficult airway: Perspective for personalized medicine. *World J Clin Cases* 2023; 11(9): 1951-1962
URL: https://www.wjgnet.com/2307-8960/full/v11/i9/1951.htm
DOI: https://dx.doi.org/10.12998/wjcc.v11.i9.1951

INTRODUCTION

Point-of-care ultrasound (POCUS) is a quickly used and repeatable tool for bedside clinical evaluation. Today, POCUS supports perioperative decision making in all phases and settings of clinical care[1]. POCUS is achieving results for diagnosis and treatment in emergency medicine and intensive care[2-4].

Airway ultrasound is one form of POCUS. Although it is thought to hold great potential, there is no evidence to date whether airway ultrasound has a significant impact on clinical decision making. This narrative review and perspective discuss what is known about the efficacy of airway ultrasound from existing studies and then reflect on this information with clinical insight from individual patients. Airway ultrasound is considered useful because it provides insights that can facilitate decision-making for securing the airway in patients with an anticipated difficult airway.

The literature search in the present study was conducted using PubMed, Medline, and Scopus with the key words "airway ultrasound" "difficult airway" and "point-of-care ultrasound." Meta-analyses were cited whenever possible to answer clinical questions, and other citations were used when deemed necessary to answer clinical questions.

WHAT CAN AIRWAY ULTRASOUND TELL US?

Airway ultrasound is useful for pre-anesthetic airway evaluation, particularly to assess the potential for requiring front of neck access, confirmation of tracheal intubation, prediction of optimal tracheal tube size, and evaluation of vocal cord motion and function[1,5-7]. Among these possible applications of airway ultrasound, prediction and treatment of the difficult airway is expected to be the most important clinically.

CAN AIRWAY ULTRASOUND PREDICT A DIFFICULT AIRWAY?

A report on the management of patients with a difficult airway from the United Kingdom described the importance of airway assessment to avoid airway accidents[8]. It has also been noted that current airway evaluations are not adequate[9]. The modified Mallampati classification, mandibular protrusion, neck circumstance and other factors to predict the presence of a difficult airway are traditionally based on observations and measurements on the surface of the patient's body. Studies to predict the presence of a difficult airway using airway ultrasound have begun. This is not a conventional prediction based on information from the body surface, but from information obtained about the internal anatomy, and belongs to the same family of predictions using information from internal structures such those made with images from computed tomography (CT) scans[10]. The ability to predict the difficult airway by airway ultrasound will likely never exceed that of predicting the difficult airway using information from a CT scan, because CT scans present more information and can reconstruct three-dimensional structures, while airway ultrasound is always limited to two-dimensional information. CT scans have associated problems, such as radiation exposure and high cost as well as the need to usually transport the patient to a dedicated CT scanner location. Even if those problems are ignored, the clinical utility of airway ultrasound may exceed that available with a CT scan. Airway ultrasound is characterized by mobility and repeatability to get the information needed instantly, at the point of care.

Measurements to predict the presence of a difficult airway fall into two categories. The first is the distance from the skin to the airway. There is a hypothesis that an increase in anterior neck thickness restricts the mobility of pharyngeal structures and thereby affects direct laryngoscopy[11]. However, Komatsu *et al*[11] found no association between the presence of a difficult airway and anterior neck thickness at the level of the vocal cords. In a recent meta-analysis, anterior neck thickness at the vocal cord level or at the cricothyroid membrane is not a predictor for the presence of a difficult airway[12]. However, the distance from the skin to the epiglottis, or hyoid bone, may be a predictor of difficult intubation[12,13]. For direct laryngoscopy, the tongue, epiglottis, and mandible are considered obstacles anterior to the oral airway space[14]. Based on this concept, the thickness of the oropharynx and hypopharynx can be assumed to have more effect on the performance of direct laryngoscopy than the thickness of the anterior larynx.

The second category of measurements to predict the presence of a difficult airway is based on the significance of measuring the hyomental distance. When performing direct laryngoscopy, important obstacles are not only located anteriorly. The posterior obstacles refer to the upper teeth, maxilla, head, and others[14]. The key to overcoming posterior obstacles is the mobility of the upper cervical spine [14]. Mobility of the upper cervical spine, especially at the occipital-atlantoaxial joint, is important, and the ratio of the neutral position to the head extended position of the hyomental distance is reported to be a good indicator as a substitute for radiographic measurement of occipital-atlantoaxial joint extension [15]. In a meta-analysis, hyomental distance did not differ significantly between patients with and without intubation difficulties[12]. However, there was a significant difference in the ratio of hyomental distance between the neutral position and extension, referred to as the hyomental distance ratio. The difference in results for hyomental distance and the hyomental distance ratio may be due to large individual differences in hyomental distance. Ultrasound measurement of hyomental distance does not require x-rays. Therefore, use of the hyomental distance ratio is facilitated in clinical practice.

Studies to predict the presence of a difficult airway in terms of whether direct laryngoscopy is possible may have to be reconsidered in the future due to improvements in, and the widespread use of videolaryngoscopy, which is partially overcoming problems associated with the difficult airway[16,17]. Difficult airways include difficult intubation and difficult mask ventilation. Difficult mask ventilation is even more dangerous than difficult tracheal intubation. Li *et al*[18] reported that measurement of the submental portion by ultrasound is predictive of difficult mask ventilation. Bianchini *et al*[19] reported that tongue base thickness is predictive of difficult mask ventilation. Enlargement of the tongue base or submental portion can cause airway narrowing. The Mallampati score reflects the size of the tongue in the oropharyngeal space[20]. There is a belief that ultrasonic measurement of tongue base thickness is a more accurate measure of the property embodied in the Mallampati classification[21]. This idea is anatomically quite reasonable and deserves further study.

Table 1 shows cutoff values for difficult airway predictors that are considered important[12]. Each predictor can be classified based on its anatomical significance. Skin to epiglottis distance is a highly evaluated index with excellent sensitivity and specificity for predicting the difficult airway[22]. Skin to epiglottis distance is anatomically considered to reflect the distance from the skin to the airway[22]. A longer distance is associated with increasing difficultly when performing direct laryngoscopy[22]. Anatomical reasons are explained by the three column model of the upper airway described by Greenland[23]. Briefly, the increase in skin to epiglottis distance makes the orientation of the tracheal axis (secondary curve of the three column model) to be downward. The skin to epiglottis distance may be an indicator of the difficulty for both mask ventilation and direct laryngoscopy. The hyomental distance ratio is as a predictor of difficult direct laryngoscopy[24], and tongue base thickness is a predictor of difficult mask ventilation[25].

The measurement of anterior neck thickness may make sense based on the anterior obstacles of the oral airway space theory[14]. These measurement points are the distance from the skin to the hyoid bone, the distance from the skin to the anterior commissure, and the thickness of the anterior neck soft tissues at the level of the hyoid bone. The authors speculate that anterior cervical thickness would be associated with obesity, which is clearly a predictor of an airway difficulty. In this paper, three predictors were chosen based on anatomical considerations. However, there is still the potential for more accurate prediction by combining anterior neck thickness with other independent predictors.

Figure 1 illustrates the evaluation of each difficult airway predictor and its measurement in a man with sleep apnea syndrome who is anticipated to have a difficult airway based on a traditional predictor, the modified Mallampati score, Class IV. The distance from the skin to the epiglottis is 3.42 cm, which is more than the cutoff value of 2.54 (Table 1). The hyomental distance ratio is 6.42/5.77 = 1.11, which is larger than the cutoff value of 1.085. Tongue base thickness is 8.31, which is more than the cutoff value of 5.87. Taken together, the evaluation of these parameters suggest that this man is at high risk for difficult in mask ventilation but not direct laryngoscopy. Administration of anesthesia required an oral airway and two-person bag-valve mask ventilation to secure the airway after inducing general anesthesia, but intubation was performed by a resident with a Macintosh laryngoscope with modified Cormack-Lehane classification grade 2a.

Thus, each difficult airway predictor can be used to predict when difficult airways might be present in a patient and allow the clinician to devise a strategy to safely secure the patient's airway.

DOES OBSERVATION OF THE VOCAL CORDS FAIL TO PREDICT AN AIRWAY DIFFICULTY?

As previously mentioned, anterior neck thickness at the vocal cord level is not a satisfactory predictor for the presence of a difficult airway[12]. Since the vocal cords are located inside the thyroid cartilage, the ultrasound probe must be manipulated to provide an image through the cricothyroid membrane toward the head to observe the vocal cords. The ultrasound beam for viewing the vocal cords crosses the anterior cervical surface at an angle, not vertically. Therefore, evaluating the thickness of the anterior neck with the thickness of the anterior neck soft tissue at the level of the vocal cords is of questionable

Table 1 Cutoff values for predictors of a difficult airway

Predictor[12]	DDL or DMV	Cutoff value (sensitivity, specificity)
Distance from skin to epiglottis[22]	DDL, DMV	> 2.54 cm (82.0, 91.0)
Hyomental distance ratio[23] (extension/neutral position)	DDL	< 1.085 (75.0, 85.3)
Tongue base thickness	DMV	> 5.87 cm (85.0, 91.0)

DDL: Difficult direct laryngoscopy; DMV: Difficult mask ventilation.

value. However, observation of the vocal cords is important when performing airway ultrasound. This is because undiagnosed lesions in the glottis can lead to an otherwise unrecognized difficult airway. In 2016, we reported a patient with a difficult airway due to an undiagnosed subglottic tumor, which could have been identified with airway ultrasound[26]. Recently, Adi *et al*[27] reported the use of airway ultrasound to diagnose a mass lesion in the glottis which resulted in airway narrowing. If one suspects airway stenosis, we recommend airway ultrasound to observe the vocal cords as the first step.

Case 1: A 93-year-old woman was planned to undergo repair of a femoral neck fracture. She developed a "cannot intubate cannot oxygenate" emergency after induction of general anesthesia, and the anesthesiologist let her awaken. Airway compromise was caused by undiagnosed subglottic tumors (Figure 2).

IS AIRWAY ULTRASONOGRAPHY AN EFFECTIVE ADJUNCT FOR CRICOTHYROIDOTOMY?

The Fourth National Airways Project in the United Kingdom showed that emergency cricothyroidotomy has a failure rate of 64%[8]. The cause of this high failure rate has not been determined[8]. Identification of the cricothyroid membrane may hold the key to successful emergency cricothyroidotomy. Numerous studies have addressed whether airway ultrasound facilitates accurate cricothyroid membrane identification[28-36]. Other studies have evaluated the accuracy of identifying this membrane by airway ultrasound in pregnant women[37,38], obese patients[39-41], and children[42-45]. Most studies concluded that identification of the cricothyroid membrane by airway ultrasound is more accurate than by digital palpation. However, the results of these studies should be interpreted with caution, because there are no clinical reports showing that ultrasound identification of the cricothyroid membrane increases the success rate of cricothyroidotomy. Furthermore, airway ultrasound is not recommended once securing the airway has failed, as it is more time-consuming than digital palpation [46]. Nevertheless, airway ultrasound is expected to be useful for strategy planning in patients with an anticipated difficult airway.

IS CRICOTHYROIDOTOMY AN ANATOMICALLY VALID FRONT-OF-NECK ACCESS TARGET?

There are various descriptions of the size and shape of the cricothyroid membrane[47]. Reported length and width ranges (minimum-maximum) of the cricothyroid membrane are 3-12 and 6-18 mm, respectively. The shape of the cricothyroid membrane has been reported to be rhombic, triangular, and trapezoidal. First, it is important to understand that not all of the space between the thyroid and cricoid cartilages is covered solely by the cricothyroid ligament. The cricothyroid membrane is formed mainly by the central median cricothyroid ligament and by the lateral part of a ligament named the conus elasticus on both sides (Figure 3). Most of the conus elasticus is covered by the cricothyroid muscles, and the caudal part of the central median cricothyroid ligament is also covered by the cricothyroid muscles. The cricothyroid muscle attaches to the cricoid cartilage anterolaterally and to the lower lamina of the thyroid cartilage. In cricothyroidotomy, the cricothyroid muscle would give high resistance to needle puncture or surgical incision and is also an obstacle to digital palpation of the cricothyroid membrane for identification due to decreased dimpling of the cricothyroid membrane.

It is necessary to understand the distribution of blood vessels around the cricothyroid membrane since it relates to hemorrhagic complications. The vascular distribution around the cricothyroid membrane exists both inside and outside the membrane (Figure 3). Incision or puncture along the lateral side of the cricothyroid membrane may damage the superior thyroid artery, resulting in rather significant bleeding[48]. The cricothyroid artery runs anterior and cephalad to the cricothyroid membrane and is easily damaged during cricothyroidotomy. Incision or puncture of the cricothyroid membrane is more safely performed in the central to caudal area[49].

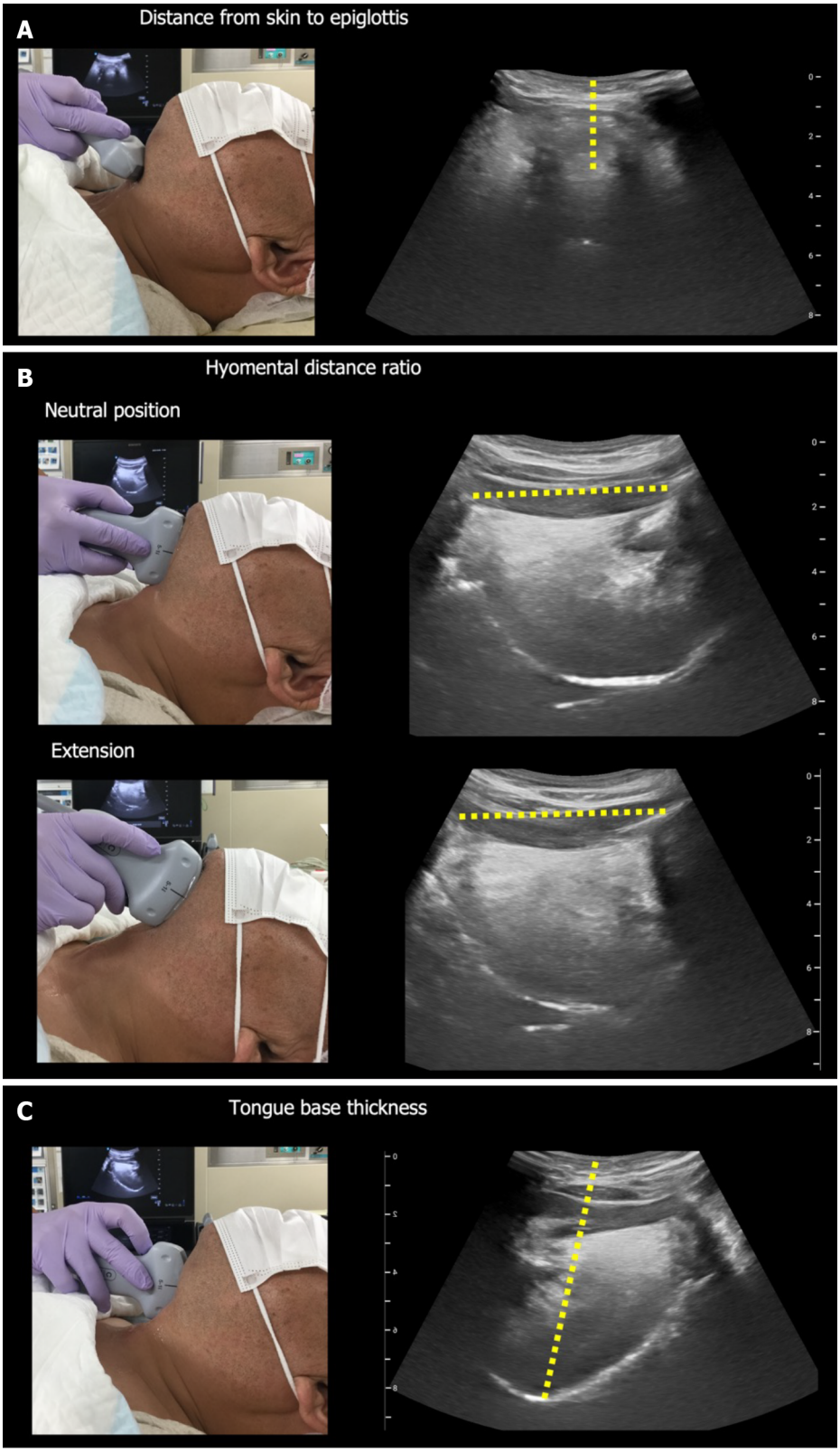

DOI: 10.12998/wjcc.v11.i9.1951

Figure 1 Predicting a difficult airway using airway ultrasound. A: Ultrasound measurement of the distance from skin to epiglottis; B: Ultrasound measurement of the hyomental distance in the neutral and maximal extended neck positions; C: Ultrasound measurement of the distance from skin to tongue base.

Posterior tracheal wall injury, tracheal laceration, and esophageal perforation are among the complications of cricothyroidotomy[50]. Complications can be caused by applying too much force or the use of unnecessarily long needles during needle cricothyroidotomy and by inserting the blade too deeply during surgical cricothyroidotomy[50-52].

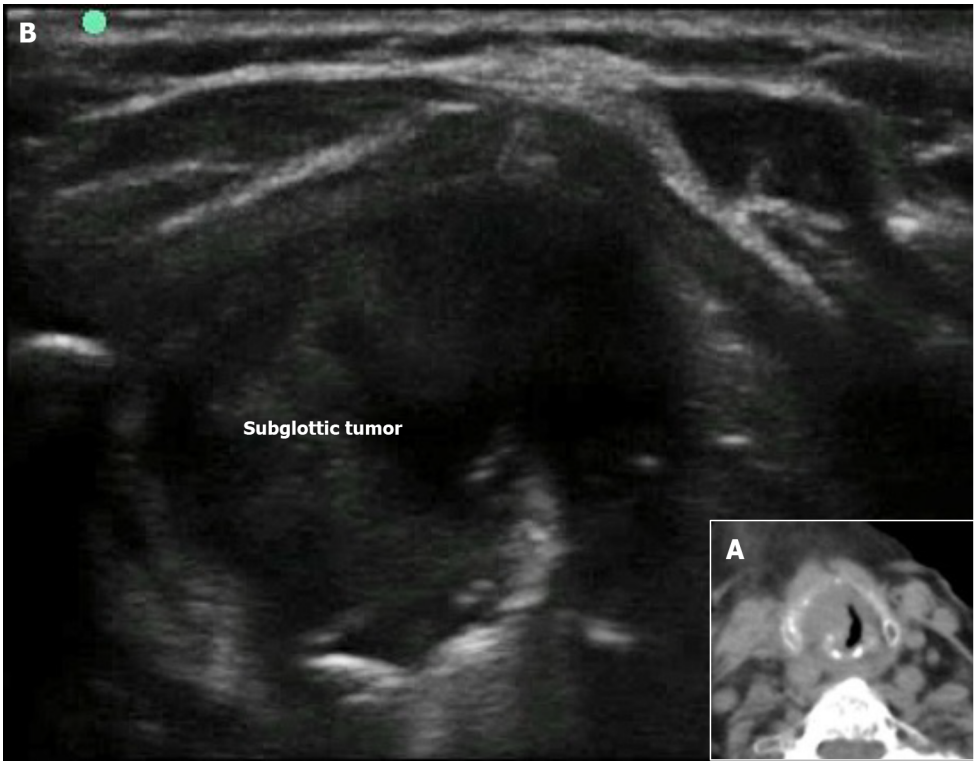

Figure 2 Subglottic tumor (reproduced from Figure 1 of Falcetta *et al*[22], with the permission of the copyright holder). A: Transverse image from the computed tomography scan shows a subglottic mass; B: Ultrasound view at the level of the cricothyroid membrane shows a mass (subglottic tumor). Citation: Falcetta S, Cavallo S, Gabbanelli V, Pelaia P, Sorbello M, Zdravkovic I, Donati A. Evaluation of two neck ultrasound measurements as predictors of difficult direct laryngoscopy: A prospective observational study. *Eur J Anaesthesiol* 2018; 35: 605-612. Copyright© The Authors 2018. Published by Wolters Kluwer. The authors have obtained the permission for figure using (Supplementary material).

In summary, it should be recognized that the safe target for a cricothyroidotomy is very small, about 5.5 mm long and 6.9 mm wide[47]. The instrumentation used for puncture and the technique of incision are important to avoid complications.

IDENTIFYING THE CRICOTHYROID MEMBRANE BY AIRWAY ULTRASOUND

The longitudinal technique and the transverse technique have been reported to aid in identification of the cricothyroid membrane[28,38]. The transverse technique can identify the cricothyroid membrane more quickly than the longitudinal technique, but the transverse technique is not superior to the longitudinal technique in terms of accuracy of identification[39,53]. Kristensen *et al*[39] recommend that the technique used for identification of the cricothyroid membrane should be chosen by the patient.

LONGITUDINAL TECHNIQUE

The longitudinal technique is called the "string of pearls" technique. It is so called because when the ultrasound probe is placed in a sagittal line from the thyroid cartilage to the caudal side, the cricoid and tracheal cartilages appear to be arranged in a bead-like pattern. The cricothyroid membrane is easily identified between the cricoid cartilage and the thyroid cartilage is widely open, compared to the space between the cricoid cartilage and the tracheal cartilage (Figure 3A and B).

TRANSVERSE TECHNIQUE

The transverse technique is also known as TACA technique. The name is derived from the method of performing the procedure. T and C stand for the initials of thyroid cartilage and cricoid cartilage, respectively, and A for the air interface line. The transverse ultrasound view of the thyroid cartilage is easily identified because it looks like a triangular roof. When the probe is moved caudally and the triangular thyroid cartilage disappears, a bright white line appears in the midline. This is the

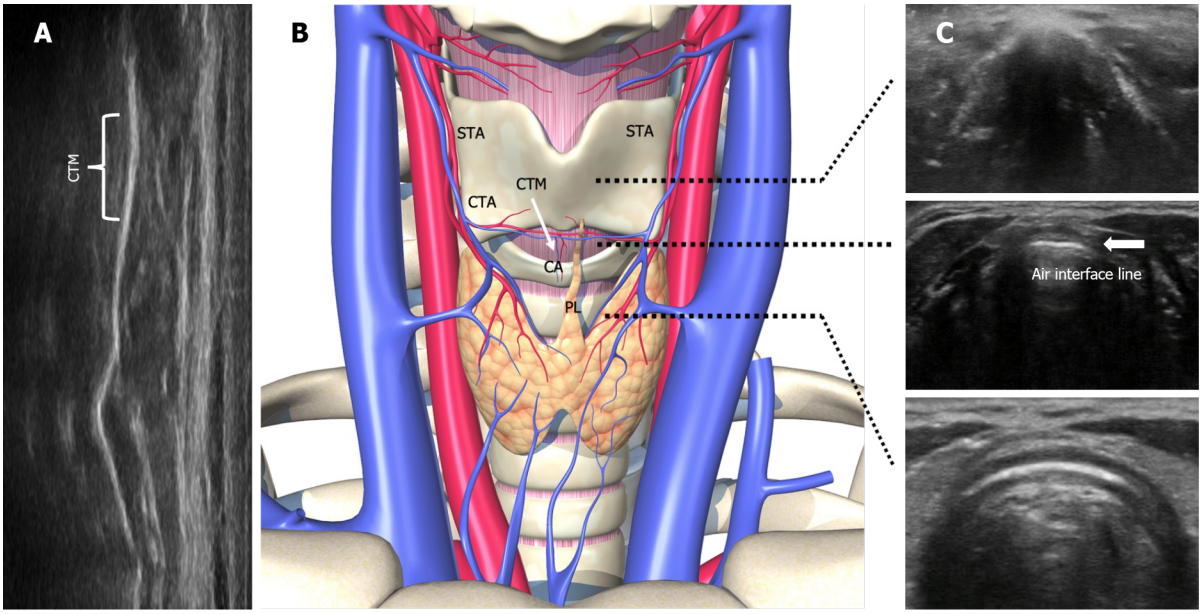

DOI: 10.12998/wjcc.v11.i9.1951

Figure 3 Anatomy and sonographic appearance of the cricothyroid membrane. A: Longitudinal view for identifying the cricothyroid membrane; B: The thyroid, cricoid, and tracheal cartilages are strung together and appear like a string of pearls. Anatomy of the cricothyroid membrane; C: Transverse view for identifying the cricothyroid membrane. Air interface line indicates the cricothyroid membrane. CTM: Cricothyroid membrane; STA: Superior thyroid artery; CTA: Cricothyroid artery; CA: Common artery; PL: Pyramidal lobe of the thyroid gland.

cricothyroid membrane, and the white line is due to the reflection of ultrasound waves from the air on the inner surface of the trachea just below the cricothyroid membrane (the air interface line). The cricoid cartilage is recognized because it is shaped like a black horseshoe. The TACA technique scans the thyroid cartilage – air interface line - cricoid cartilage from cephalad to caudal sides, and then scans the cephalad side again to identify the air interface line (cricothyroid membrane) (Figure 3B and C).

Case 2: We cared for a patient with an anticipated difficult airway[54]. A neck abscess pointing to the left side gave the illusion that the center of the neck was at the location marked by the asterisk in Figure 4. The surgeon believed that this region contained the cricothyroid membrane based on digital palpation. However, the trachea was displaced and rotated to the opposite side. The actual cricothyroid membrane was located to the right of the expected location.

IS AIRWAY ULTRASOUND USEFUL TO DEVISE A STRATEGY FOR PATIENTS ANTICIPATED TO HAVE A DIFFICULT AIRWAY?

There are several approaches to secure an airway in a patient anticipated to have a difficult airway. These include awake tracheal intubation, anesthetized tracheal intubation, and supraglottic ventilation. However, planning the optimal strategy varies and depends on the degree and reason for difficulty in securing the airway, the preference of the medical practitioner, and the constraints of the equipment available. If the prediction of the presence of a difficult airway using airway ultrasound is correct, anesthetized tracheal intubation can be performed in patients with predicted to have difficult tracheal intubation but easy mask ventilation, because video-laryngoscopy and fiberoptic intubation will be attempted between episodes of intermitted ventilation with a mask. Even if tracheal intubation is not possible, the patient can be awakened by stopping the administration of general anesthesia. However, patients with difficult mask ventilation but easy tracheal intubation should be intubated immediately after rapid sequence induction. In many cases, overlap of different degrees of difficult tracheal intubation and difficult mask ventilation are present.

The American Society of Anesthesiologists' Task Force on Management of the Difficult Airway states that awake intubation should be selected when there is a high risk of difficult mask ventilation and difficult tracheal intubation, a high risk of aspiration, and a high risk of oxyhemoglobin desaturation[55, 56]. In patients anticipated to have a difficult airway, making a plan to safely secure the airway is the most important issue. Usually, awake intubation or surgical front-of-neck access should be considered as possible alternatives. In particular, awake intubation will require a back-up plan, referred to as "double setup airway intervention," which implies preparing simultaneously for both awake intubation and surgical cricothyroidotomy[57].

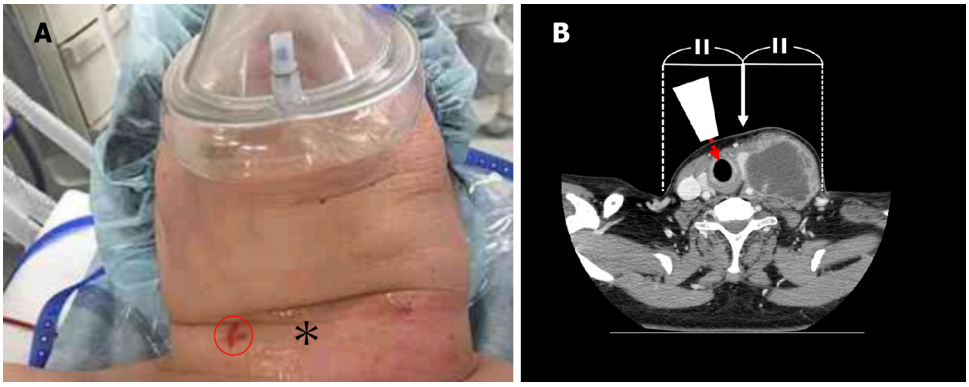

Figure 4 Identification of the cricothyroid membrane by airway ultrasound (reproduced from Figures 1 and 3 of Katayama *et al*[52], with the permission of the copyright holder). A: The patient's neck: The asterisk indicates the area palpated by the surgeon to find the cricothyroid membrane. The red circle shows the cricothyroid membrane identified by ultrasound; B: Cervical computed tomography scan image: The white arrow points to the apparent center of the neck. The true center (sagittal line) of the neck is shifted to the right. The ultrasound probe (white trapezoid) is placed perpendicularly to the skin and the ultrasound beam (red dashed arrow) is directed toward the cricothyroid membrane. Citation: Katayama A, Watanabe K, Tokumine J, Lefor AK, Nakazawa H, Jimbo I, Yorozu T. Cricothyroidotomy needle length is associated with posterior tracheal wall injury: A randomized crossover simulation study (CONSORT). *Medicine (Baltimore)* 2020; 99: e19331. Copyright© The Authors 2020. Published by MDPI. The authors have obtained the permission for figure using (Supplementary material).

CAN AIRWAY ULTRASOUND BE USED TO PREDICT TRACHEAL TUBE SIZE?

Tracheal intubation in a pediatric patient may also present difficulty securing the airway for the physician because determination of the optimal diameter of the tracheal tube is difficult. In pediatric patients, the cross-sectional shape of the trachea is circular at the cricothyroid level and oval at the subglottic level[58]. The narrowest part of the trachea is the transverse diameter at the subglottic level [58]. Using airway ultrasound, the subglottic diameter can be directly measured[59]. A recent meta-analysis showed that airway ultrasound can accurately predict tracheal tube size estimates, unlike the usual age or height-based formulas used in pediatric patients[60]. The minimal transverse diameter of the cricoid cartilage level was reported to be important to select the tracheal size for ventilation setting [61]. The ultrasound measurement points for determining tube size vary slightly among investigators, which include the narrowest part of the subglottic airway, the middle or most caudal part of the cricoid cartilage, and so on[62]. Although the usefulness of ultrasound in selecting tube size in pediatric tracheal intubation is unquestioned, further research is needed to standardize this approach.

LIMITATIONS OF AIRWAY ULTRASOUND

POCUS is influenced by factors such as skill of the operator and the measurement environment. Therefore, airway ultrasonography is also influenced by several factors. To overcome this weak point of airway ultrasound, development and standardization of an educational program is needed[63]. Bowness *et al* showed that the location of the cricothyroid membrane identified by a skilled operator did not change when returned to the extended neck position after moving the neck transiently for tracheal intubation[64]. The study showed that airway ultrasound may provide reproducible and reliable results with sufficient operator proficiency. In the future, as education becomes standardized and acquisition of appropriate airway ultrasound skills becomes more widespread, airway ultrasound will be the best means of assessing the ever-changing airways of patients.

CONCLUSION

Airway ultrasound may provide a simpler and more accurate prediction of the difficult airway compared with traditionally used indicators, especially to distinguish between difficult mask ventilation and difficult tracheal intubation. In addition, accurate cricothyroid membrane identification may provide a benchmark for securing a surgical airway in clinical practice. In conclusion, airway ultrasound has great potential to facilitate airway assessment and make it accurate, however further studies are needed to demonstrate clinical benefits in a variety of situations.

ACKNOWLEDGEMENTS

We thank Mr. Takashi Nozawa (Department of Clinical Engineering, Kyorin University School of Medicine) for his kind support.

FOOTNOTES

Author contributions: Nakazawa H, Uzawa K, Motoyasu A and Tokumine J helped with literature acquisition and contributed in writing the original daft; Lefor AK contributed in editing the draft; Yorozu T helped in the conceptualization and data validation.

Conflict-of-interest statement: Authors declare no conflict of interests for this article.

Country/Territory of origin: Japan

ORCID number: Harumasa Nakazawa 0000-0002-3258-9310; Kohji Uzawa 0000-0002-1000-9485; Joho Tokumine 0000-0003-3481-2085; Alan Kawarai Lefor 0000-0001-6673-5630; Akira Motoyasu 0000-0003-1610-0631; Tomoko Yorozu 0000-0002-2161-4525.

S-Editor: Yan JP
L-Editor: A
P-Editor: Yan JP

REFERENCES

1 **Zieleskiewicz L**, Ortner C, Bruckert V, Via G, Bouvet L. Point of care ultrasonography: And now, where shall we go in perioperative medicine? *Anaesth Crit Care Pain Med* 2022; **41**: 101014 [PMID: 34954222 DOI: 10.1016/j.accpm.2021.101014]
2 **Bobbia X**, Zieleskiewicz L, Pradeilles C, Hudson C, Muller L, Claret PG, Leone M, de La Coussaye JE; Winfocus France Group. The clinical impact and prevalence of emergency point-of-care ultrasound: A prospective multicenter study. *Anaesth Crit Care Pain Med* 2017; **36**: 383-389 [PMID: 28412493 DOI: 10.1016/j.accpm.2017.02.008]
3 **Zieleskiewicz L**, Lopez A, Hraiech S, Baumstarck K, Pastene B, Di Bisceglie M, Coiffard B, Duclos G, Boussuges A, Bobbia X, Einav S, Papazian L, Leone M. Bedside POCUS during ward emergencies is associated with improved diagnosis and outcome: an observational, prospective, controlled study. *Crit Care* 2021; **25**: 34 [PMID: 33482873 DOI: 10.1186/s13054-021-03466-z]
4 **Zieleskiewicz L**, Muller L, Lakhal K, Meresse Z, Arbelot C, Bertrand PM, Bouhemad B, Cholley B, Demory D, Duperret S, Duranteau J, Guervilly C, Hammad E, Ichai C, Jaber S, Langeron O, Lefrant JY, Mahjoub Y, Maury E, Meaudre E, Michel F, Muller M, Nafati C, Perbet S, Quintard H, Riu B, Vigne C, Chaumoitre K, Antonini F, Allaouchiche B, Martin C, Constantin JM, De Backer D, Leone M; CAR'Echo and AzuRea Collaborative Networks. Point-of-care ultrasound in intensive care units: assessment of 1073 procedures in a multicentric, prospective, observational study. *Intensive Care Med* 2015; **41**: 1638-1647 [PMID: 26160727 DOI: 10.1007/s00134-015-3952-5]
5 **You-Ten KE**, Siddiqui N, Teoh WH, Kristensen MS. Point-of-care ultrasound (POCUS) of the upper airway. *Can J Anaesth* 2018; **65**: 473-484 [PMID: 29349733 DOI: 10.1007/s12630-018-1064-8]
6 **Gottlieb M**, Holladay D, Burns KM, Nakitende D, Bailitz J. Ultrasound for airway management: An evidence-based review for the emergency clinician. *Am J Emerg Med* 2020; **38**: 1007-1013 [PMID: 31843325 DOI: 10.1016/j.ajem.2019.12.019]
7 **Osman A**, Sum KM. Role of upper airway ultrasound in airway management. *J Intensive Care* 2016; **4**: 52 [PMID: 27529028 DOI: 10.1186/s40560-016-0174-z]
8 **Cook TM**, Woodall N, Frerk C; Fourth National Audit Project. Major complications of airway management in the UK: results of the Fourth National Audit Project of the Royal College of Anaesthetists and the Difficult Airway Society. Part 1: anaesthesia. *Br J Anaesth* 2011; **106**: 617-631 [PMID: 21447488 DOI: 10.1093/bja/aer058]
9 **Nørskov AK**, Rosenstock CV, Wetterslev J, Astrup G, Afshari A, Lundstrøm LH. Diagnostic accuracy of anaesthesiologists' prediction of difficult airway management in daily clinical practice: a cohort study of 188 064 patients registered in the Danish Anaesthesia Database. *Anaesthesia* 2015; **70**: 272-281 [PMID: 25511370 DOI: 10.1111/anae.12955]
10 **Ji C**, Ni Q, Chen W. Diagnostic accuracy of radiology (CT, X-ray, US) for predicting difficult intubation in adults: A meta-analysis. *J Clin Anesth* 2018; **45**: 79-87 [PMID: 29306118 DOI: 10.1016/j.jclinane.2017.12.023]
11 **Komatsu R**, Sengupta P, Wadhwa A, Akça O, Sessler DI, Ezri T, Lenhardt R. Ultrasound quantification of anterior soft tissue thickness fails to predict difficult laryngoscopy in obese patients. *Anaesth Intensive Care* 2007; **35**: 32-37 [PMID:

17323663 DOI: 10.1177/0310057X0703500104]
12 **Sotoodehnia M**, Rafiemanesh H, Mirfazaelian H, Safaie A, Baratloo A. Ultrasonography indicators for predicting difficult intubation: a systematic review and meta-analysis. *BMC Emerg Med* 2021; **21**: 76 [PMID: 34217221 DOI: 10.1186/s12873-021-00472-w]
13 **Carsetti A**, Sorbello M, Adrario E, Donati A, Falcetta S. Airway Ultrasound as Predictor of Difficult Direct Laryngoscopy: A Systematic Review and Meta-analysis. *Anesth Analg* 2022; **134**: 740-750 [PMID: 34914641 DOI: 10.1213/ANE.0000000000005839]
14 **Isono S**. Common practice and concepts in anesthesia: time for reassessment: is the sniffing position a "gold standard" for laryngoscopy? *Anesthesiology* 2001; **95**: 825-827 [PMID: 11605919 DOI: 10.1097/00000542-200110000-00007]
15 **Takenaka I**, Iwagaki T, Aoyama K, Ishimura H, Kadoya T. Preoperative evaluation of extension capacity of the occipitoatlantoaxial complex in patients with rheumatoid arthritis: comparison between the Bellhouse test and a new method, hyomental distance ratio. *Anesthesiology* 2006; **104**: 680-685 [PMID: 16571962 DOI: 10.1097/00000542-200604000-00011]
16 **Stroumpoulis K**, Pagoulatou A, Violari M, Ikonomou I, Kalantzi N, Kastrinaki K, Xanthos T, Michaloliakou C. Videolaryngoscopy in the management of the difficult airway: a comparison with the Macintosh blade. *Eur J Anaesthesiol* 2009; **26**: 218-222 [PMID: 19237983 DOI: 10.1097/EJA.0b013e32831c84d1]
17 **Lewis SR**, Butler AR, Parker J, Cook TM, Smith AF. Videolaryngoscopy versus direct laryngoscopy for adult patients requiring tracheal intubation. *Cochrane Database Syst Rev* 2016; **11**: CD011136 [PMID: 27844477 DOI: 10.1002/14651858.CD011136.pub2]
18 **Lin HY**, Tzeng IS, Hsieh YL, Kao MC, Huang YC. Submental Ultrasound Is Effective in Predicting Difficult Mask Ventilation but Not in Difficult Laryngoscopy. *Ultrasound Med Biol* 2021; **47**: 2243-2249 [PMID: 34020847 DOI: 10.1016/j.ultrasmedbio.2021.04.004]
19 **Bianchini A**, Nardozi L, Nardi E, Scuppa MF. Airways ultrasound in predicting difficult face mask ventilation. *Minerva Anestesiol* 2021; **87**: 26-34 [PMID: 33054014 DOI: 10.23736/S0375-9393.20.14455-9]
20 **Mallampati SR**, Gatt SP, Gugino LD, Desai SP, Waraksa B, Freiberger D, Liu PL. A clinical sign to predict difficult tracheal intubation: a prospective study. *Can Anaesth Soc J* 1985; **32**: 429-434 [PMID: 4027773 DOI: 10.1007/BF03011357]
21 **Deriy L**, Gerstein NS. Moving past Mallampati: airway ultrasound in predicting difficult face mask ventilation. *Minerva Anestesiol* 2021; **87**: 4-6 [PMID: 33538414 DOI: 10.23736/S0375-9393.20.15283-0]
22 **Falcetta S**, Cavallo S, Gabbanelli V, Pelaia P, Sorbello M, Zdravkovic I, Donati A. Evaluation of two neck ultrasound measurements as predictors of difficult direct laryngoscopy: A prospective observational study. *Eur J Anaesthesiol* 2018; **35**: 605-612 [PMID: 29889671 DOI: 10.1097/EJA.0000000000000832]
23 **Greenland KB**. Airway assessment based on a three column model of direct laryngoscopy. *Anaesth Intensive Care* 2010; **38**: 14-19 [PMID: 20191771 DOI: 10.1177/0310057X1003800104]
24 **Rana S**, Verma V, Bhandari S, Sharma S, Koundal V, Chaudhary SK. Point-of-care ultrasound in the airway assessment: A correlation of ultrasonography-guided parameters to the Cormack-Lehane Classification. *Saudi J Anaesth* 2018; **12**: 292-296 [PMID: 29628843 DOI: 10.4103/sja.SJA_540_17]
25 **Xu L**, Dai S, Sun L, Shen J, Lv C, Chen X. Evaluation of 2 ultrasonic indicators as predictors of difficult laryngoscopy in pregnant women: A prospective, double blinded study. *Medicine (Baltimore)* 2020; **99**: e18305 [PMID: 32011432 DOI: 10.1097/MD.0000000000018305]
26 **Uzawa K**, Tokumine J, Lefor AK, Takagi T, Watanabe K, Yorozu T. Difficult Airway Due to an Undiagnosed Subglottic Tumor: A Case Report. *Medicine (Baltimore)* 2016; **95**: e3383 [PMID: 27082606 DOI: 10.1097/MD.0000000000003383]
27 **Adi O**, Fong CP, Sum KM, Ahmad AH. Usage of airway ultrasound as an assessment and prediction tool of a difficult airway management. *Am J Emerg Med* 2021; **42**: 263.e1-263.e4 [PMID: 32994082 DOI: 10.1016/j.ajem.2020.09.011]
28 **Kristensen MS**, Teoh WH, Rudolph SS. Ultrasonographic identification of the cricothyroid membrane: best evidence, techniques, and clinical impact. *Br J Anaesth* 2016; **117** Suppl 1: i39-i48 [PMID: 27432055 DOI: 10.1093/bja/aew176]
29 **Kristensen MS**, Teoh WH. Ultrasound identification of the cricothyroid membrane: the new standard in preparing for front-of-neck airway access. *Br J Anaesth* 2021; **126**: 22-27 [PMID: 33131758 DOI: 10.1016/j.bja.2020.10.004]
30 **Rai Y**, You-Ten E, Zasso F, De Castro C, Ye XY, Siddiqui N. The role of ultrasound in front-of-neck access for cricothyroid membrane identification: A systematic review. *J Crit Care* 2020; **60**: 161-168 [PMID: 32836091 DOI: 10.1016/j.jcrc.2020.07.030]
31 **Lamb A**, Zhang J, Hung O, Flemming B, Mullen T, Bissell MB, Arseneau I. Accuracy of identifying the cricothyroid membrane by anesthesia trainees and staff in a Canadian institution. *Can J Anaesth* 2015; **62**: 495-503 [PMID: 25637060 DOI: 10.1007/s12630-015-0326-y]
32 **Hung KC**, Chen IW, Lin CM, Sun CK. Comparison between ultrasound-guided and digital palpation techniques for identification of the cricothyroid membrane: a meta-analysis. *Br J Anaesth* 2021; **126**: e9-e11 [PMID: 32896429 DOI: 10.1016/j.bja.2020.08.012]
33 **Mallin M**, Curtis K, Dawson M, Ockerse P, Ahern M. Accuracy of ultrasound-guided marking of the cricothyroid membrane before simulated failed intubation. *Am J Emerg Med* 2014; **32**: 61-63 [PMID: 24475485 DOI: 10.1016/j.ajem.2013.07.004]
34 **Altun D**, Ali A, Koltka K, Buget M, Çelik M, Doruk C, Çamcı AE. Role of ultrasonography in determining the cricothyroid membrane localization in the predicted difficult airway. *Ulus Travma Acil Cerrahi Derg* 2019; **25**: 355-360 [PMID: 31297781 DOI: 10.14744/tjtes.2019.65250]
35 **Aslani A**, Ng SC, Hurley M, McCarthy KF, McNicholas M, McCaul CL. Accuracy of identification of the cricothyroid membrane in female subjects using palpation: an observational study. *Anesth Analg* 2012; **114**: 987-992 [PMID: 22366848 DOI: 10.1213/ANE.0b013e31824970ba]
36 **Siddiqui N**, Yu E, Boulis S, You-Ten KE. Ultrasound Is Superior to Palpation in Identifying the Cricothyroid Membrane in Subjects with Poorly Defined Neck Landmarks: A Randomized Clinical Trial. *Anesthesiology* 2018; **129**: 1132-1139 [PMID: 30260895 DOI: 10.1097/ALN.0000000000002454]

37 **Zieleskiewicz L**, Bouvet L, Einav S, Duclos G, Leone M. Diagnostic point-of-care ultrasound: applications in obstetric anaesthetic management. *Anaesthesia* 2018; **73**: 1265-1279 [PMID: 30047997 DOI: 10.1111/anae.14354]

38 **You-Ten KE**, Desai D, Postonogova T, Siddiqui N. Accuracy of conventional digital palpation and ultrasound of the cricothyroid membrane in obese women in labour. *Anaesthesia* 2015; **70**: 1230-1234 [PMID: 26186092 DOI: 10.1111/anae.13167]

39 **Kristensen MS**, Teoh WH, Rudolph SS, Hesselfeldt R, Børglum J, Tvede MF. A randomised cross-over comparison of the transverse and longitudinal techniques for ultrasound-guided identification of the cricothyroid membrane in morbidly obese subjects. *Anaesthesia* 2016; **71**: 675-683 [PMID: 27037981 DOI: 10.1111/anae.13465]

40 **Lavelle A**, Drew T, Fennessy P, McCaul C, Shannon J. Accuracy of cricothyroid membrane identification using ultrasound and palpation techniques in obese obstetric patients: an observational study. *Int J Obstet Anesth* 2021; **48**: 103205 [PMID: 34280884 DOI: 10.1016/j.ijoa.2021.103205]

41 **Gadd K**, Wills K, Harle R, Terblanche N. Relationship between severe obesity and depth to the cricothyroid membrane in third-trimester non-labouring parturients: a prospective observational study. *Br J Anaesth* 2018; **120**: 1033-1039 [PMID: 29661380 DOI: 10.1016/j.bja.2018.02.010]

42 **Walsh B**, Fennessy P, Ni Mhuircheartaigh R, Snow A, McCarthy KF, McCaul CL. Accuracy of ultrasound in measurement of the pediatric cricothyroid membrane. *Paediatr Anaesth* 2019; **29**: 744-752 [PMID: 31063634 DOI: 10.1111/pan.13658]

43 **Fennessy P**, Walsh B, Laffey JG, McCarthy KF, McCaul CL. Accuracy of pediatric cricothyroid membrane identification by digital palpation and implications for emergency front of neck access. *Paediatr Anaesth* 2020; **30**: 69-77 [PMID: 31746536 DOI: 10.1111/pan.13773]

44 **Basaran B**, Egilmez AI, Alatas N, Yilbas AA, Sargin M. Accuracy of identifying the cricothyroid membrane in children using palpation. *J Anesth* 2018; **32**: 768-773 [PMID: 30054717 DOI: 10.1007/s00540-018-2538-0]

45 **Daniel SJ**, Bertolizio G, McHugh T. Airway ultrasound: Point of care in children-The time is now. *Paediatr Anaesth* 2020; **30**: 347-352 [PMID: 31901216 DOI: 10.1111/pan.13823]

46 **Alerhand S**. Ultrasound for identifying the cricothyroid membrane prior to the anticipated difficult airway. *Am J Emerg Med* 2018; **36**: 2078-2084 [PMID: 30025948 DOI: 10.1016/j.ajem.2018.07.027]

47 **Develi S**, Yalcin B, Yazar F. Topographical anatomy of cricothyroid membrane and its relation with invasive airway access. *Clin Anat* 2016; **29**: 949-954 [PMID: 27481637 DOI: 10.1002/ca.22750]

48 **Dover K**, Howdieshell TR, Colborn GL. The dimensions and vascular anatomy of the cricothyroid membrane: relevance to emergent surgical airway access. *Clin Anat* 1996; **9**: 291-295 [PMID: 8842535 DOI: 10.1002/(SICI)1098-2353(1996)9:5<291::AID-CA1>3.0.CO;2-G]

49 **Boon JM**, Abrahams PH, Meiring JH, Welch T. Cricothyroidotomy: a clinical anatomy review. *Clin Anat* 2004; **17**: 478-486 [PMID: 15300867 DOI: 10.1002/ca.10231]

50 **Hsiao J**, Pacheco-Fowler V. Videos in clinical medicine. Cricothyroidotomy. *N Engl J Med* 2008; **358**: e25 [PMID: 18509116 DOI: 10.1056/NEJMvcm0706755]

51 **Abbrecht PH**, Kyle RR, Reams WH, Brunette J. Insertion forces and risk of complications during cricothyroid cannulation. *J Emerg Med* 1992; **10**: 417-426 [PMID: 1430978 DOI: 10.1016/0736-4679(92)90270-4]

52 **Katayama A**, Watanabe K, Tokumine J, Lefor AK, Nakazawa H, Jimbo I, Yorozu T. Cricothyroidotomy needle length is associated with posterior tracheal wall injury: A randomized crossover simulation study (CONSORT). *Medicine (Baltimore)* 2020; **99**: e19331 [PMID: 32118765 DOI: 10.1097/MD.0000000000019331]

53 **Jimbo I**, Uzawa K, Tokumine J, Mitsuda S, Watanabe K, Yorozu T. Ultrasonographic identification of the cricothyroid membrane in a patient with a difficult airway as a result of cervical hematoma caused by hemophilia: a case report. *BMC Anesthesiol* 2019; **19**: 124 [PMID: 31288737 DOI: 10.1186/s12871-019-0798-3]

54 **Okano H**, Uzawa K, Watanabe K, Motoyasu A, Tokumine J, Lefor AK, Yorozu T. Ultrasound-guided identification of the cricothyroid membrane in a patient with a difficult airway: a case report. *BMC Emerg Med* 2018; **18**: 5 [PMID: 29422029 DOI: 10.1186/s12873-018-0156-7]

55 **Apfelbaum JL**, Hagberg CA, Connis RT, Abdelmalak BB, Agarkar M, Dutton RP, Fiadjoe JE, Greif R, Klock PA, Mercier D, Myatra SN, O'Sullivan EP, Rosenblatt WH, Sorbello M, Tung A. 2022 American Society of Anesthesiologists Practice Guidelines for Management of the Difficult Airway. *Anesthesiology* 2022; **136**: 31-81 [PMID: 34762729 DOI: 10.1097/ALN.0000000000004002]

56 **Rosenblatt WH**, Yanez ND. A Decision Tree Approach to Airway Management Pathways in the 2022 Difficult Airway Algorithm of the American Society of Anesthesiologists. *Anesth Analg* 2022; **134**: 910-915 [PMID: 35171880 DOI: 10.1213/ANE.0000000000005930]

57 **Law JA**, Duggan LV, Asselin M, Baker P, Crosby E, Downey A, Hung OR, Kovacs G, Lemay F, Noppens R, Parotto M, Preston R, Sowers N, Sparrow K, Turkstra TP, Wong DT, Jones PM; Canadian Airway Focus Group. Canadian Airway Focus Group updated consensus-based recommendations for management of the difficult airway: part 2. Planning and implementing safe management of the patient with an anticipated difficult airway. *Can J Anaesth* 2021; **68**: 1405-1436 [PMID: 34105065 DOI: 10.1007/s12630-021-02008-z]

58 **Mizuguchi S**, Motomura Y, Maki J, Baba R, Ichimiya Y, Tokuda K, Kaku N, Takada H, Maehara Y, Ohga S. Tracheal Size and Morphology on the Reconstructed CT Imaging. *Pediatr Crit Care Med* 2019; **20**: e366-e371 [PMID: 31162371 DOI: 10.1097/PCC.0000000000001996]

59 **Bharathi BM**, Somayaji S, Tulasi T, Sheriff NK, Bagliker JS. Prediction of Endotracheal Tube Size in Pediatric Population Using Ultrasonographic Subglottic Diameter and Age-Related Formulas: A Comparative Study. *Anesth Essays Res* 2022; **16**: 1-6 [PMID: 36249135 DOI: 10.4103/aer.aer_11_22]

60 **Gupta B**, Ahluwalia P. Prediction of endotracheal tube size in the pediatric age group by ultrasound: A systematic review and meta-analysis. *J Anaesthesiol Clin Pharmacol* 2022; **38**: 371-383 [PMID: 36505227 DOI: 10.4103/joacp.JOACP_650_20]

61 **Schramm C**, Eisleben LS, Kessler J, Jensen K, Plaschke K. Role of ultrasound measuring position and ventilation pressure in determining correct tube size in children. *Paediatr Anaesth* 2017; **27**: 1241-1246 [PMID: 29063711 DOI: 10.1111/pan.13267]

62 **Park S**, Shin SW, Kim HJ, Byeon GJ, Yoon JU, Kim EJ, Kim HY. Choice of the correct size of endotracheal tube in pediatric patients. *Anesth Pain Med (Seoul)* 2022; **17**: 352-360 [PMID: 36317427 DOI: 10.17085/apm.22215]
63 **Li L**, Yong RJ, Kaye AD, Urman RD. Perioperative Point of Care Ultrasound (POCUS) for Anesthesiologists: an Overview. *Curr Pain Headache Rep* 2020; **24**: 20 [PMID: 32200432 DOI: 10.1007/s11916-020-0847-0]
64 **Bowness J**, Teoh WH, Kristensen MS, Dalton A, Saint-Grant AL, Taylor A, Crawley S, Chisholm F, Varsou O, McGuire B. A marking of the cricothyroid membrane with extended neck returns to correct position after neck manipulation and repositioning. *Acta Anaesthesiol Scand* 2020; **64**: 1422-1425 [PMID: 32698252 DOI: 10.1111/aas.13680]

World Journal of Clinical Cases

Submit a Manuscript: https://www.f6publishing.com

World J Clin Cases 2023 March 26; 11(9): 1963-1973

DOI: 10.12998/wjcc.v11.i9.1963

ISSN 2307-8960 (online)

ORIGINAL ARTICLE

Observational Study

Clinicopathological features and expression of regulatory mechanism of the Wnt signaling pathway in colorectal sessile serrated adenomas/polyps with different syndrome types

Dan Qiao, Xiao-Yan Liu, Lie Zheng, Ya-Li Zhang, Ren-Ye Que, Bing-Jing Ge, Hong-Yan Cao, Yan-Cheng Dai

Specialty type: Gastroenterology and hepatology

Provenance and peer review: Invited article; Externally peer reviewed.

Peer-review model: Single blind

Peer-review report's scientific quality classification

Grade A (Excellent): 0
Grade B (Very good): 0
Grade C (Good): C, C
Grade D (Fair): 0
Grade E (Poor): 0

P-Reviewer: Belder N, Turkey; Kumar A, India

Received: November 22, 2022
Peer-review started: November 22, 2022
First decision: February 7, 2023
Revised: February 12, 2023
Accepted: March 3, 2023
Article in press: March 3, 2023
Published online: March 26, 2023

Dan Qiao, Xiao-Yan Liu, Ren-Ye Que, Bing-Jing Ge, Hong-Yan Cao, Yan-Cheng Dai, Department of Gastroenterology, Shanghai Traditional Chinese Medicine-Integrated Hospital, Shanghai University of Traditional Chinese Medicine, Shanghai 200082, China

Lie Zheng, Department of Gastroenterology, Traditional Chinese Medicine Hospital of Xi'an, Xi'an 730000, Shaanxi Province, China

Ya-Li Zhang, Institute of Digestive Diseases, Longhua Hospital, Shanghai University of Traditional Chinese Medicine, Shanghai 200032, China

Corresponding author: Yan-Cheng Dai, PhD, Associate Chief Physician, Department of Gastroenterology, Shanghai Traditional Chinese Medicine-Integrated Hospital, Shanghai University of Traditional Chinese Medicine, No. 230 Baoding Road, Hongkou District, Shanghai 200082, China. daiyancheng2005@126.com

Abstract

BACKGROUND

Colorectal cancer (CRC) is the third most common cancer worldwide, with the fourth highest mortality among all cancers. Reportedly, in addition to adenomas, serrated polyps, which account for 15%-30% of CRCs, can also develop into CRCs through the serrated pathway. Sessile serrated adenomas/polyps (SSAs/Ps), a type of serrated polyps, are easily misdiagnosed during endoscopy.

AIM

To observe the difference in the Wnt signaling pathway expression in SSAs/Ps patients with different syndrome types.

METHODS

From January 2021 to December 2021, patients with SSAs/Ps were recruited from the Endoscopy Room of Shanghai Traditional Chinese Medicine-Integrated Hospital, affiliated with Shanghai University of Traditional Chinese Medicine. Thirty cases each of large intestine damp-heat (Da-Chang-Shi-Re, DCSR) syndrome and spleen-stomach weakness (Pi-Wei-Xu-Ruo) syndrome were reported. Baseline comparison of the general data, typical tongue coating, colonoscopy findings, and hematoxylin and eosin findings was performed in each group. The expression of the Wnt pathway-related proteins, namely β-catenin,

adenomatous polyposis coli, and mutated in colorectal cancer, were analyzed using immunohistochemistry.

RESULTS

Significant differences were observed with respect to the SSAs/Ps size between the two groups of patients with different syndrome types (P = 0.001). The other aspects did not differ between the two groups. The Wnt signaling pathway was activated in patients with SSAs/Ps belonging to both groups, which was manifested as β-catenin protein translocation into the nucleus. However, SSAs/Ps patients with DCSR syndrome had more nucleation, higher β-catenin expression, and negative regulatory factor (adenomatous polyposis coli and mutated in colorectal cancer) expression (P < 0.0001) than SSA/P patients with Pi-Wei-Xu-Ruo syndrome. In addition, the SSA/P size was linearly correlated with the related protein expression.

CONCLUSION

Patients with DCSR syndrome had a more obvious Wnt signaling pathway activation and a higher risk of carcinogenesis. A high-quality colonoscopic diagnosis was essential. The thorough assessment of clinical diseases can be improved by combining the diseases of Western medicine with the syndromes of traditional Chinese medicine.

Key Words: Sessile serrated adenomas/polyps; Wnt signaling pathway; Large intestine damp-heat syndrome; Spleen-stomach weakness syndrome

Core Tip: We aimed to observe the difference in the Wnt signaling pathway expression in sessile serrated adenoma/polyp patients with large intestine damp-heat (Da-Chang-Shi-Re) syndrome and spleen-stomach weakness (Pi-Wei-Xu-Ruo) syndrome. We observed that patients with Da-Chang-Shi-Re syndrome had a more obvious Wnt signaling pathway activation and a higher risk of carcinogenesis. A high-quality colonoscopic diagnosis was essential. The thorough assessment of clinical diseases can be improved by combining the diseases of Western medicine with the syndromes of traditional Chinese medicine.

Citation: Qiao D, Liu XY, Zheng L, Zhang YL, Que RY, Ge BJ, Cao HY, Dai YC. Clinicopathological features and expression of regulatory mechanism of the Wnt signaling pathway in colorectal sessile serrated adenomas/polyps with different syndrome types. *World J Clin Cases* 2023; 11(9): 1963-1973
URL: https://www.wjgnet.com/2307-8960/full/v11/i9/1963.htm
DOI: https://dx.doi.org/10.12998/wjcc.v11.i9.1963

INTRODUCTION

Colorectal cancer (CRC) is the third most common cancer worldwide, with the fourth highest mortality among all cancers. Every year, CRC causes approximately 900000 cancer-related deaths and accounts for 10% of all cancer diagnoses[1]. Precancerous colorectal lesions include colorectal polys, with the classic adenoma CRC pathway being the commonest carcinogenic pathway. Reportedly, in addition to adenomas, serrated polyps, which account for 15%-30% of CRC, can also develop into CRCs through the serrated pathway[2,3]. Serrated polyps are characterized by serrated crypt structures. According to the World Health Organization classification in 2010, serrated polyps can be divided into three subtypes, which are as follows: Hyperplastic polyps (HPs), sessile serrated adenomas/polyps (SSAs/Ps), and traditional serrated adenomas[4]. Similar endoscopic manifestations are observed for SSAs/Ps and HPs; hence, they are easily misdiagnosed under endoscopy. Endoscopists must therefore deepen their expertise in SSAs/Ps to improve the rate of diagnosis[5]. As per traditional Chinese medicine (TCM), SSAs/Ps are "enteromas," referring to single or multiple vegetations in the colorectal mucosa, characterized by abdominal pain or abdominal fullness and discomfort, loose or mucinous stools, or hematochezia and constipation[6]. The large intestine damp-heat (Da-Chang-Shi-Re, DCSR) syndrome and spleen-stomach weakness (Pi-Wei-Xu-Ruo, PWXR) syndrome are commonly observed in patients with "enteromas"[7]. The Wnt signaling pathway plays a crucial role in homeostatic renewal, cell proliferation, and colorectal epithelium differentiation. The sporadic occurrence of an enteroma is brought about by the abnormal activation of the Wnt signaling pathway[8]. Abnormal activation of the classical Wnt signaling pathway with β-catenin as the core in serrated polyps might be an early event of carcinogenesis[9]. TCM is based on syndrome differentiation and treatment. Whether the Wnt signaling

pathway through β-catenin, adenomatous polyposis coli (APC), and mutated in CRC (MCC) protein expression vary in SSA/Ps patients with different syndrome types warrants research. This study aimed to provide new ideas and a theoretical basis for differentiating "enteromas" using TCM, guide clinical treatment and evaluate prognosis, and enrich the scientific connotation of "treating the same disease with different methods" in TCM by observing the difference in the Wnt pathway expression in SSA/Ps patients with different syndrome types.

MATERIALS AND METHODS

Design

This was a single-center, parallel, controlled trial conducted at Shanghai TCM-Integrated Hospital, affiliated with Shanghai University of TCM and registered in the Chinese Clinical Trial Registry (ChiCTR2000038536). Informed consent was obtained from all participants before the trial. The Ethics Committee of Shanghai TCM-Integrated Hospital (2020-091-1) approved the experimental protocol, and the research method was not significantly modified during the study.

Selection criteria

Inclusion criteria: The inclusion criteria were as follows: (1) A diagnosis consistent with that of SSA/Ps; (2) The TCM syndrome differentiation conforms to "enteroma" DCSR or PWXR; (3) Age ranging from 18 to 70 years; and (4) Voluntary participation in the study, along with signed informed consent. DCSR syndrome was defined as follows: (1) Main symptoms included increased stool frequency, yellow-brown stools with a foul odor, a feeling of incomplete evacuation with a burning sensation around the anus, and red tongue with a yellow coating; and (2) Secondary symptoms included abdominal pain, urgent defecation, thirst and scanty urine, constipation or a feeling of incomplete evacuation, feverish sensations, yellow urine, a clouded heavy head and body, and a soft, rapid, or slippery pulse. PWXR syndrome was defined as follows: (1) Main symptoms included abdominal distension, particularly after consuming greasy food, recurrent loose stools, lassitude, shortness of breath and lazy words, and a pale tongue with a thin, white coating; and (2) Secondary symptoms included gastric or abdominal distension, cold limbs and cold intolerance, lusterless face, poor appetite, loose stools, and a weak and thready pulse. The syndrome was determined if two main symptoms and more than three secondary symptoms were present.

Exclusion criteria: The exclusion criteria were as follows: (1) Patients aged < 18 years or > 70 years and pregnant and lactating women; (2) Patients without a pathological diagnosis of SSA/Ps; (3) Patients in whom colonoscopy was contraindicated or those who could not undergo colonoscopy for other reasons; (4) A colonoscopic diagnosis of enteritis, intestinal ulcer, or non-colorectal polyps; (5) Digestive tract tumors; (6) Patients with serious primary diseases, such as cardiovascular and cerebrovascular diseases, liver and kidney diseases, hematological diseases, and psychosis; and (7) Syndrome type established without the presence of superficial symptoms. An attending physician with 5 years of experience diagnosed the TCM syndrome type based on the patient's symptoms, signs, tongue coating, and pulse. Another attending physician with 5 years of experience then reviewed the diagnosis. If the two TCM doctors had varying opinions on the syndrome differentiation, a deputy director with ≥ 10 years of experience differentiated and classified the syndromes, and the final diagnosis was based on a majority in terms of opinion.

Observed indicators

General information: The general information comprised data on sex, age, the SSA/P site (right colon, left colon, or rectum), clinical symptoms (constipation, diarrhea, abdominal pain, abdominal distension, or mild or no symptoms), tongue coating, and pulse condition.

Colonoscopy and histological staining: An attending physician or an associate chief physician with >3 years of experience performed the colonoscopy using an Olympus GIF HQ290 colonoscope with a preoperative Boston bowel preparation scale score of ≥ 7 and a withdrawal time of ≥ 6 min[10]. The specimen was obtained by colonoscopy, following which it was fixed with 10% neutral buffered formalin and stained using hematoxylin and eosin. Two pathologists who were blinded to the endoscopic results of the patient established the pathological diagnosis. Multiple adenomas/polyps with the largest diameter were recorded, and the pathological records revealed the highest degree of malignancy.

Immunohistochemical analysis: The β-catenin, APC, and MCC protein expression in the colonic mucosa were detected using immunohistochemistry (the streptavidin-peroxidase-biotin method). We used β-catenin (ab223075; Abcam, Cambridge, MA, United States), APC (ab40778; Abcam, Cambridge, MA, United States), and MCC (PA5-57934; Thermo Fisher Scientific, Waltham, MA, United States). Three pictures were randomly taken from each slice under × 200 magnification, and Image Pro Plus 6.0

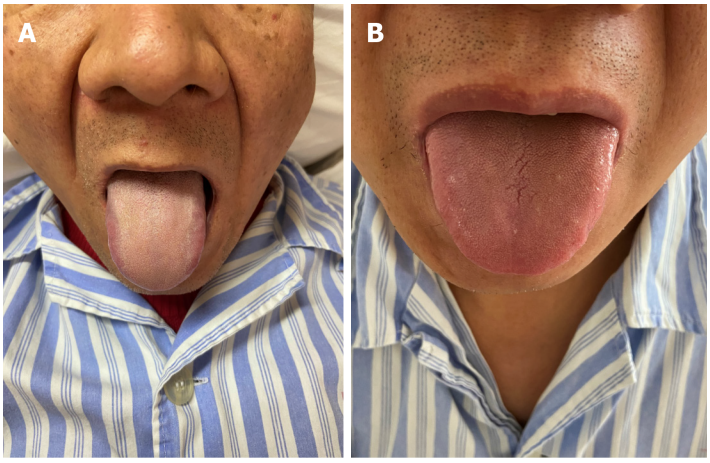

DOI: 10.12998/wjcc.v11.i9.1963

Figure 1 Classification of the tongue coating. A: Patients with large intestine damp-heat (Da-Chang-Shi-Re) syndrome showed a thick yellow coating; B: Patients with spleen-stomach weakness (Pi-Wei-Xu-Ruo) syndrome showed a thin white coating.

was used to semi-quantitatively analyze the protein expression area, after which its average optical density was measured (average optical density = integrated optical density/area of the target distribution area).

Statistical analysis

Statistical Package for the Social Sciences 24.0 was used to perform statistical analysis (IBM Corp., Armonk, NY, United States). The χ^2 test was used for count data, and the mean ± standard deviation was used for measurement data. One-way analysis of variance was used for measurement data between groups, and the least significant difference test was used for comparison between groups. Wilcoxon's rank-sum test was used for non-normally distributed data. Pearson's method was used for the correlation analysis. Statistical significance was set at $P < 0.05$.

RESULTS

Case source and baseline data comparison

From January 2021 to December 2021, patients with SSAs/Ps were recruited from the Endoscopy Room of Shanghai TCM-Integrated Hospital, affiliated with the Shanghai University of TCM. Thirty cases each of DCSR syndrome and PWXR syndrome were recruited. Baseline comparison of general data (Table 1), typical tongue coatings (Figure 1), colonoscopic findings (Figure 2), and the hematoxylin and eosin findings (Figure 3) of each group are presented in the respective tables/figures. Significant differences in the SSA/Ps size were observed between the two groups, while no differences were observed in terms of the other aspects.

Protein expression of β-catenin, APC, and MCC in each group

The protein expression of β-catenin, APC, and MCC in each group and the results of the statistical analysis are presented in Figure 4 and Table 2. The cell membrane generally demonstrated positive β-catenin expression, while β-catenin overexpression was observed in the cytoplasm or nucleus, which is referred to as ectopic expression. The positive expression area of β-catenin in patients with DCSR syndrome significantly increased compared with that of the patients with PWXR syndrome, with more nucleation observed in patients with DCSR syndrome. APC and MCC positive cells were observed in the cytoplasm as brown-yellow particles. The positive expression areas of APC and MCC in patients with DCSR syndrome significantly decreased compared with those of the patients with PWXR syndrome. The SSA/Ps size in patients with DCSR and PWXR was positively correlated with the β-catenin expression, with the results being statistically different ($P = 0.0002$ *vs* $P < 0.0001$), while the SSA/Ps size in patients with DCSR and PWXR was negatively correlated with APC and MCC expression ($P = 0.0259$ *vs* $P = 0.0034$ and $P < 0.0001$ *vs* $P = 0.0029$) (Figure 5).

Table 1 Comparison of the general data of sessile serrated adenoma/polyp patients with large intestine damp-heat (Da-Chang-Shi-Re) syndrome and spleen-stomach weakness (Pi-Wei-Xu-Ruo) syndrome

	DCSR syndrome, *n* = 30		PWXR syndrome, *n* = 30	*P* value
Sex				0.791
Male	19		18	
Female	11		12	
Age in yr	58.800 ± 9.290		58.900 ± 7.097	0.578
Size in cm	0.800 ± 0.435		0.520 ± 0.219	0.001
Location				0.158
Right half of the colon	9		4	
Left half of the colon	13		20	
Rectum	8		6	
Clinical symptoms				0.435
Constipation	4		6	
Diarrhea	2		6	
Abdominal pain	2		4	
Abdominal distension	4		5	
Mild symptoms or asymptomatic	18	11		

DCSR: Large intestine damp-heat (Da-Chang-Shi-Re); PWXR: Spleen-stomach weakness (Pi-Wei-Xu-Ruo).

Table 2 Protein expression of β-catenin, adenomatous polyposis coli, and mutated in colorectal cancer in patients with large intestine damp-heat (Da-Chang-Shi-Re) syndrome and spleen-stomach weakness (Pi-Wei-Xu-Ruo) syndrome

	DCSR syndrome, *n* = 30	PWXR syndrome, *n* = 30	*P* value
β-catenin	0.32 ± 0.03	0.20 ± 0.02	$P < 0.0001$
APC	0.17 ± 0.01	0.23 ± 0.02	$P < 0.0001$
MCC	0.18 ± 0.01	0.24 ± 0.01	$P < 0.0001$

APC: Adenomatous polyposis coli; DCSR: Large intestine damp-heat (Da-Chang-Shi-Re); MCC: Mutated in colorectal cancer; PWXR: Spleen-stomach weakness (Pi-Wei-Xu-Ruo).

DISCUSSION

Colonoscopy is a valuable tool for identifying SSAs/Ps; however, the detection rate using endoscopy remains low (0%-23%). Therefore, it is crucial to increase the understanding of endoscopists in terms of the endoscopic characteristics of SSAs/Ps. SSAs/Ps are flat protuberances without pedicles, with a hidden shape and pale surface, similar to the mucosal color, making it challenging to detect under conventional endoscopy, resulting in a missed diagnosis. The endoscopic features mainly include a mucus cap or a "red cap sign," ambiguous boundaries, irregular shape, cumulus-like surface structure, glandular duct expansion, black spots in crypts, and glandular duct openings in type II-0 or II-d[11,12]. The main characteristics of SSAs/Ps are an abnormal crypt structure, including crypt expansion, irregular branch recess, the horizontal extension of the recess, and an L-shaped or inverted T-shaped basal recess[3].

Wnt signaling activation is a significant early event in most cases of CRC. Abnormal Wnt signaling pathway activation results in β-catenin translocation from the cytoplasm into the nucleus and activates the transcription of several genes with pro-proliferation effects. Simultaneously, chromosome instability occurs owing to abnormal chromosomal separation during mitosis. Studies have reported abnormal Wnt signaling activation in serrated adenomas[13]. The *APC* gene is located on chromosome 5q21-22 and is a negative regulator of the Wnt signaling pathway. APC could be associated with β-catenin for promoting β-catenin degradation. β-catenin, as a tumor suppressor gene, is involved in two relatively independent processes. It plays a crucial structural role in intercellular adhesion junctions and is the key

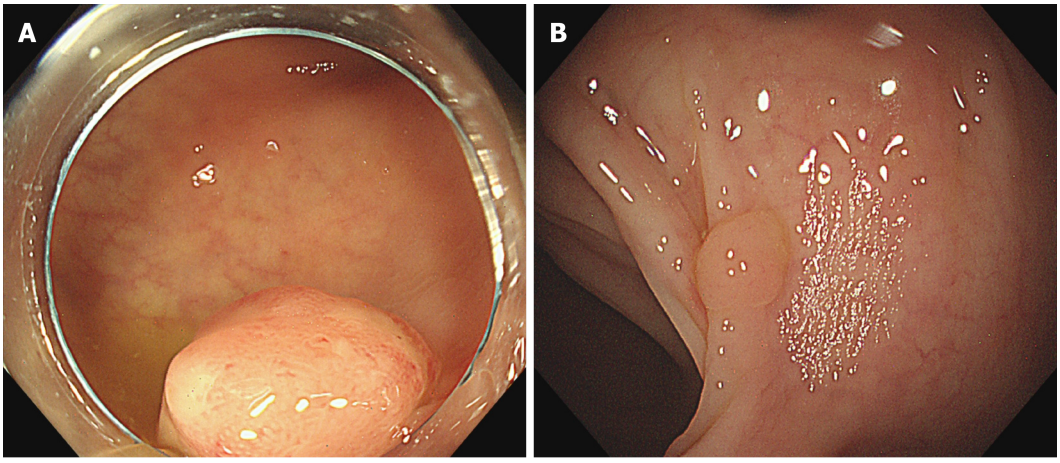

DOI: 10.12998/wjcc.v11.i9.1963

Figure 2 Endoscopic features. A: Adenoma in a patient with large intestine damp-heat (Da-Chang-Shi-Re) syndrome. Close observation revealed a dilated branched vessel and an open II pit; B: Polyp in a patient with spleen-stomach weakness (Pi-Wei-Xu-Ruo) syndrome. The surface was smooth, with a small amount of attached hyaline mucus. The color was similar to that of the background mucosa.

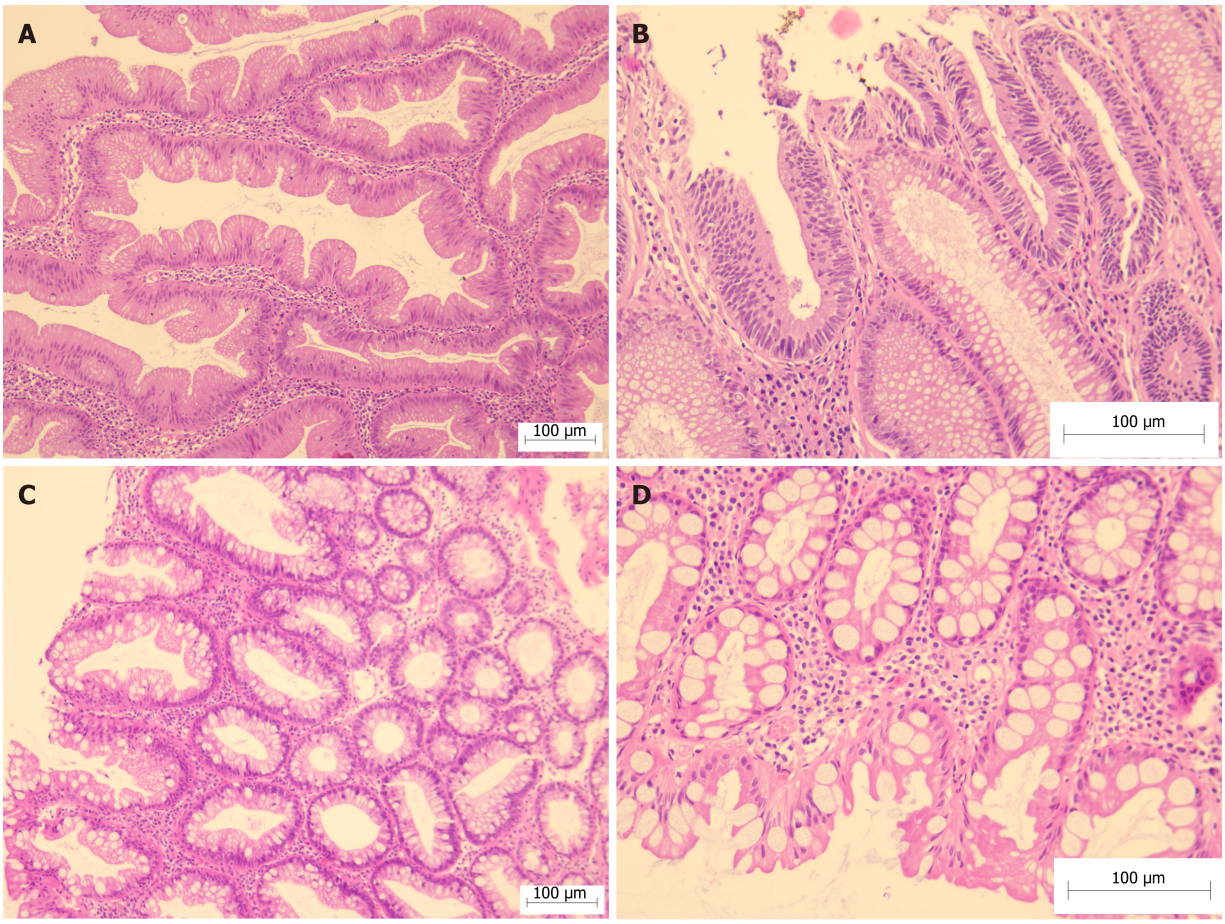

DOI: 10.12998/wjcc.v11.i9.1963

Figure 3 Hematoxylin and eosin staining in each group. A and B: Patient with large intestine damp-heat (Da-Chang-Shi-Re) syndrome. A: The crypt epithelium was serrated, and interstitial oedema was observed (× 100); B: Goblet cells were absent in the crypts of the adenoma, and the nuclei were pencil-rod-shaped (× 200). C and D: Patient with spleen-stomach weakness (Pi-Wei-Xu-Ruo) syndrome. C: The epithelium was serrated, and the crypts are evenly distributed and undifferentiated, comprising several goblet cells (× 100); D: The upper part of the crypt was serrated, and the base was not expanded (× 200).

component of the APC-β-catenin-T cell transcription factor signaling pathway. β-catenin primarily binds to cadherin on the cell membrane surface and participates in homogenous adhesion in normal mature cells. However, the free β-catenin in the cytoplasm is ubiquitinated by phosphate and can be degraded by the proteasome at a low level. However, the β-catenin level in the cytoplasm increases with impaired

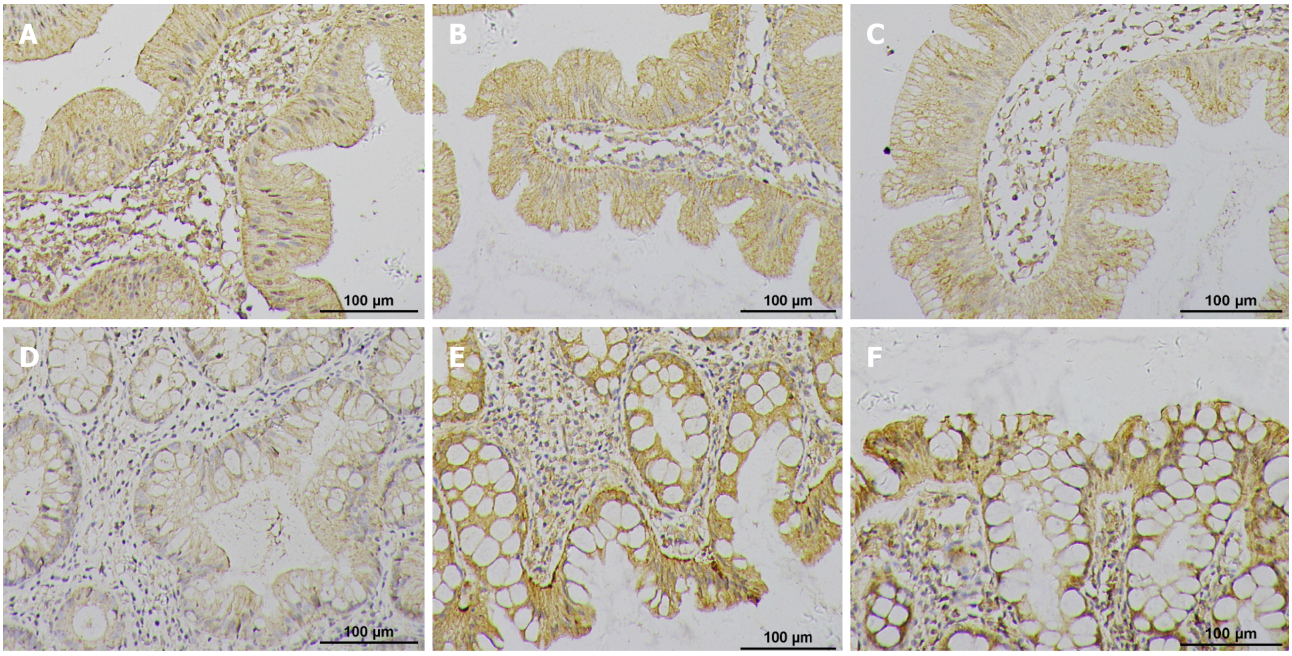

DOI: 10.12998/wjcc.v11.i9.1963

Figure 4 Protein expression of β-catenin, adenomatous polyposis coli, and mutated in colorectal cancer in each group (× 200). A, B, and C: Patient with large intestine damp-heat (Da-Chang-Shi-Re) syndrome; D, E, and F: Patient with spleen-stomach weakness (Pi-Wei-Xu-Ruo) syndrome.

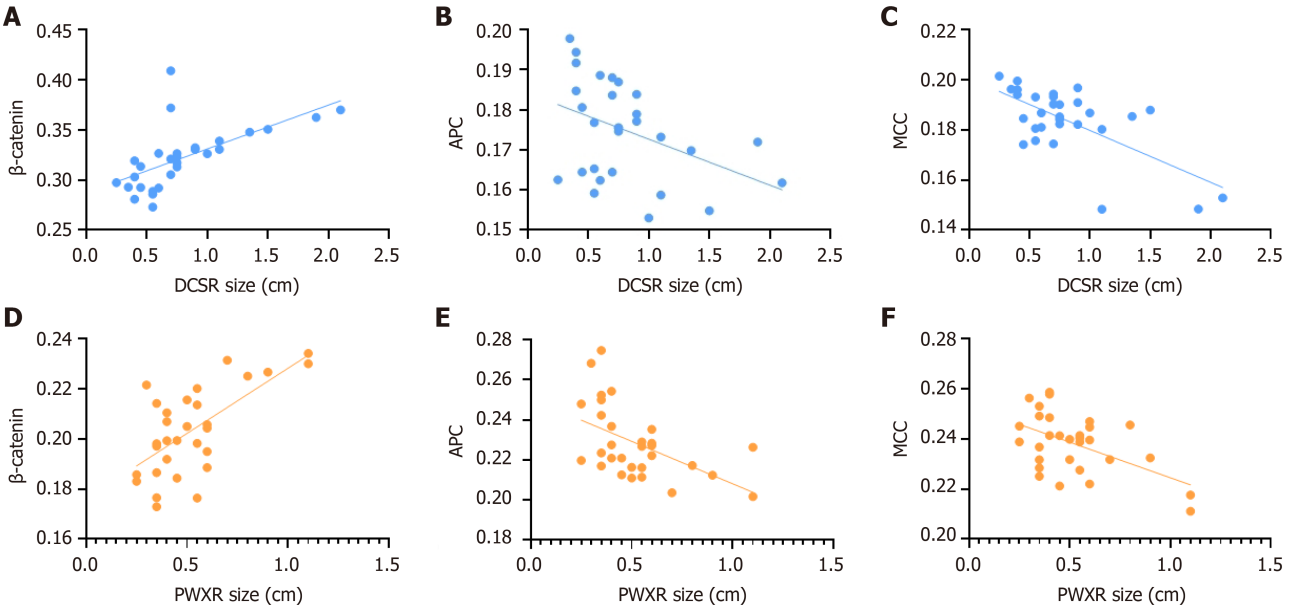

DOI: 10.12998/wjcc.v11.i9.1963

Figure 5 Correlation analysis between the related protein expression and the sessile serrated adenomas/polyps size. A, B, and C: Patient with large intestine damp-heat (Da-Chang-Shi-Re) syndrome; D, E, and F: Patient with spleen-stomach weakness (Pi-Wei-Xu-Ruo) syndrome. APC: Adenomatous polyposis coli; DCSR: Large intestine damp-heat (Da-Chang-Shi-Re); MCC: Mutated in colorectal cancer; PWXR: Spleen-stomach weakness (Pi-Wei-Xu-Ruo).

degradation, resulting in β-catenin translocation into the nucleus and T cell transcription factor binding to initiate the transcription of downstream target genes, thereby initiating tumor growth[14]. *MCC* is a susceptibility gene for familial colonic polyps. Studies have reported that *MCC* might be a significant tumor suppressor gene in the serrate carcinogenesis pathway. MCC can directly interact with β-catenin and inhibit the Wnt signaling pathway through different mechanisms in a manner similar to APC[15].

Unlike HPs, SSAs/Ps are associated with CRC risk and are considered precancerous colorectal lesions. Studies have reported that SSAs/Ps with cell dysplasia or carcinogenesis often carry the v-raf murine sarcoma viral oncogene homolog B1 mutant gene, and Wnt/β-catenin activation of the catenin pathway promotes SSA/P development compared with atypical hyperplasia or invasive cancer[16,17].

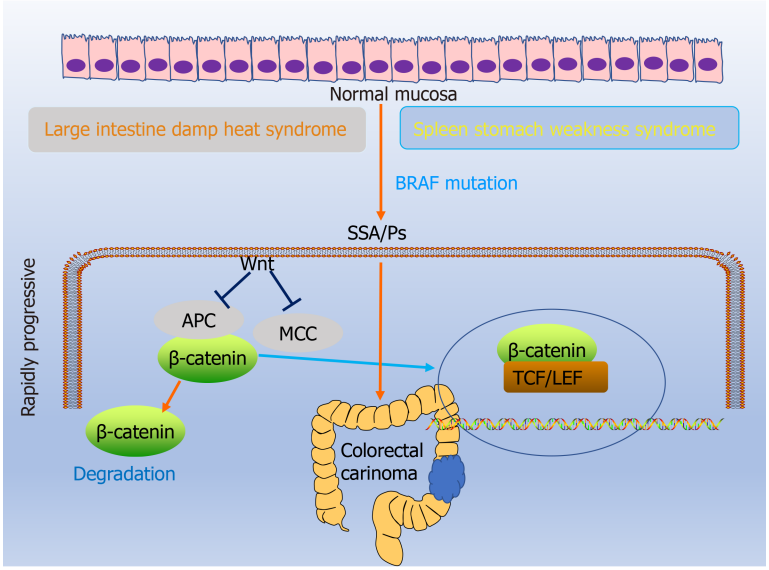

DOI: 10.12998/wjcc.v11.i9.1963

Figure 6 Abnormal Wnt signaling pathway activation in sessile serrated adenomas/polyps. APC: Adenomatous polyposis coli; LEF: Lymphoid enhancing factor; MMC: Mutated in colorectal cancer; SSA/P: Sessile serrated adenoma/polyp; TCF: T cell transcription factor.

Herein, the endoscopic manifestations and pathological features of SSAs/Ps were combined with TCM macro syndrome differentiation, broadening the depth and scope of TCM observation and thereby helping to understand the disease more comprehensively.

A comparison of the baseline data revealed that the SSA/P size in patients with DCSR syndrome was significantly larger than that in patients with PWXR syndrome. Dampness and heat were diverted into the intestinal tract, forming polyps with turbid qi. Therefore, large adenomas were more common. However, long-term eating disorders affect transportation in the spleen and stomach. The essence of grain was not refined, and the blood and qi were passive. Qi deficiency and blood stasis were observed, and the phlegm was internally bound, resulting in polyps. Therefore, small polyps were more common. In terms of the clinical manifestations, some patients had constipation, diarrhea, abdominal pain, abdominal distension, and other symptoms, while some patients had no discomfort, which further highlights the importance of early gastrointestinal cancer screening.

Traditional white light endoscopy is the simplest method for diagnosing SSAs/Ps. Herein, we preliminarily confirmed the lesion location and size by white light endoscopy, following with other diagnostic methods based on the specific conditions of the lesion. Certain narrow-band imaging techniques were also used[18,19]. Moy *et al*[20] analyzed the endoscopic features of 147 cases of colonic polyposis and concluded that the surfaces covered with mucus caps and vascular thickening were important predictive features of SSAs/Ps. If endoscopy revealed polyps covered with mucus caps and thickened vessels, SSAs/Ps could be suspected, and further measures were taken to confirm the diagnosis.

The Wnt pathway-related protein expression (β-catenin, APC, and MCC) was analyzed by immunohistochemistry considering the malignant potential of SSAs/Ps[21]. The results revealed that Wnt signaling activation in the patients with SSAs/Ps belonging to both groups was manifested as β-catenin protein translocation into the nucleus. However, SSA/Ps patients with DCSR syndrome had more nucleation, higher β-catenin expression, and less expression of negative regulatory factors (APC and MCC). In addition, the SSA/P size was linearly correlated with the related protein expression in patients with DCSR and PWXR. The results suggested that SSA/P patients with DCSR syndrome might be at high risk for carcinogenesis and accelerated malignant transformation (Figure 6).

We chose conventional endoscopic treatment, including cold forceps polypectomy, cold snare polypectomy, endoscopic mucosal resection, and endoscopic submucosal dissection techniques, targeted drugs (probiotics, different Chinese herbal medicines according to the clinical symptoms based on syndrome differentiation), and diet and lifestyle modifications for such patients with SSAs/Ps. We also referred to the Japanese Digestive Association guidelines for managing colorectal polyps and the British Digestive Association guidelines for post-polypectomy surveillance[22,23]. Colonoscopy was planned 1 year after surgery in SSAs/Ps patients with DCSR syndrome with adenomas/polyps measuring > 10 mm in diameter[24].

CONCLUSION

The Wnt/β-catenin signaling pathway and its related factors serve as diagnostic and prognostic CRC indicators. Therefore, targeting the Wnt/β-catenin pathway now serves as a treatment strategy for CRC and is constantly being studied[25]. SSA/P patients with DCSR syndrome had a more obvious Wnt signaling pathway activation and a higher risk of carcinogenesis compared with SSA/P patients with PWXR syndrome. A high-quality colonoscopic diagnosis was essential. The thorough assessment of clinical diseases can be improved by combining the diseases of Western medicine with the syndromes of TCM.

ARTICLE HIGHLIGHTS

Research background

Colorectal cancer (CRC) is the third most common cancer worldwide, with the fourth highest mortality among all cancers. Reportedly, in addition to adenomas, serrated polyps, which account for 15%-30% of CRCs, can also develop into CRCs through the serrated pathway. Sessile serrated adenomas/polyps (SSAs/Ps) are a type of serrated polyps that are easily misdiagnosed under endoscopy.

Research motivation

Traditional Chinese medicine is based on syndrome differentiation and treatment. Whether the Wnt signaling pathway through β-catenin, adenomatous polyposis coli (APC), and mutated CRC (MCC) protein expression are different in SSAs/Ps patients with different syndrome types warrants research.

Research objectives

We aimed to observe the difference in the Wnt signaling pathway expression in SSA/P patients with different syndrome types.

Research methods

Thirty cases each of large intestine damp-heat (Da-Chang-Shi-Re, DCSR) syndrome and spleen-stomach weakness (Pi-Wei-Xu-Ruo) syndrome were reported. Baseline comparison of general data, typical tongue coatings, colonoscopic findings, the hematoxylin and eosin findings, and the β-catenin, APC, and MCC protein expression in the colonic mucosa of each group were analyzed.

Research results

Significant differences were observed between the two groups of patients with different syndrome types ($P = 0.001$) with respect to the SSA/P size. The other aspects did not differ between the groups. The Wnt signaling pathway was activated in patients with SSAs/Ps belonging to both groups, which was manifested as β-catenin protein translocation into the nucleus. However, SSA/P patients with DCSR syndrome had more nucleation, higher β-catenin expression, and decreased negative regulatory factor (APC and MCC) expression ($P < 0.0001$) than SSA/P patients with Pi-Wei-Xu-Ruo syndrome. In addition, the SSA/P size was linearly correlated with the related protein expression.

Research conclusions

Patients with DCSR syndrome had a more obvious Wnt signaling pathway activation and a higher risk of carcinogenesis.

Research perspectives

A high-quality colonoscopic diagnosis was essential. The thorough assessment of clinical diseases can be improved by combining the diseases of Western medicine with the syndromes of traditional Chinese medicine.

FOOTNOTES

Author contributions: Qiao D and Liu XY contributed equally to this work, and both collected cases and analyzed data; Zheng L and Zhang YL performed pathological examination; Que RY, Ge BJ, and Cao HY prepared the figures and tables; Qiao D and Dai YC wrote and reviewed the manuscript; Dai YC conceived and supervised the study; all authors contributed to the article and approved the submitted version.

Supported by the National Natural Science Foundation of China, No. 81873253; the Shanghai Natural Science Foundation, No. 22ZR1458800; the Hongkou District Health Committee, No. HKZK2020A01; and the Xinglin Scholar Program of Shanghai University of Traditional Chinese Medicine, No. [2020]23.

Institutional review board statement: The Ethics Committee of Shanghai Traditional Chinese Medicine-Integrated Hospital (2020-091-1) approved the experimental protocol.

Conflict-of-interest statement: All authors declare that they have no conflicts of interest.

Data sharing statement: The data analyzed during this study can be obtained from the corresponding author upon reasonable request.

Country/Territory of origin: China

ORCID number: Dan Qiao 0000-0002-5699-904X; Lie Zheng 0000-0002-8243-3736; Ya-Li Zhang 0000-0002-8987-3558; Ren-Ye Que 0000-0002-6467-5950; Bing-Jing Ge 0000-0002-8781-2399; Hong-Yan Cao 0000-0002-1515-1181; Yan-Cheng Dai 0000-0002-3571-077X.

S-Editor: Xing YX
L-Editor: Filipodia
P-Editor: Xing YX

REFERENCES

1 **Dekker E**, Tanis PJ, Vleugels JLA, Kasi PM, Wallace MB. Colorectal cancer. *Lancet* 2019; **394**: 1467-1480 [PMID: 31631858 DOI: 10.1016/S0140-6736(19)32319-0]
2 **Murakami T**, Sakamoto N, Nagahara A. Clinicopathological features, diagnosis, and treatment of sessile serrated adenoma/polyp with dysplasia/carcinoma. *J Gastroenterol Hepatol* 2019; **34**: 1685-1695 [PMID: 31158302 DOI: 10.1111/jgh.14752]
3 **Murakami T**, Sakamoto N, Nagahara A. Endoscopic diagnosis of sessile serrated adenoma/polyp with and without dysplasia/carcinoma. *World J Gastroenterol* 2018; **24**: 3250-3259 [PMID: 30090005 DOI: 10.3748/wjg.v24.i29.3250]
4 **Kim ER**, Chang DK. How to Detect Sessile Serrated Adenoma/Polyps. *Clin Endosc* 2018; **51**: 313-314 [PMID: 30078302 DOI: 10.5946/ce.2018.108]
5 **Lui RN**, Sung JJY. Sessile serrated adenoma/polyps: Why we should be working flat out to understand more about these flat lesions? *J Gastroenterol Hepatol* 2019; **34**: 1667-1668 [PMID: 31726488 DOI: 10.1111/jgh.14891]
6 **Xie JQ**, Ming DL, Han CP. Chinese Internal Medicine. *PMPH* 2013; 487-497
7 **Tuo LY**, Du WZ, Lyu K, Xu W. Analysis of Traditional Chinese Medicine Syndrome Types in 97 Cases of Inflammatory Polyps. *World Chinese Medicine* 2019; **14**: 224-227
8 **Cheng X**, Xu X, Chen D, Zhao F, Wang W. Therapeutic potential of targeting the Wnt/β-catenin signaling pathway in colorectal cancer. *Biomed Pharmacother* 2019; **110**: 473-481 [PMID: 30530050 DOI: 10.1016/j.biopha.2018.11.082]
9 **Fu X**, Li L, Peng Y. Wnt signalling pathway in the serrated neoplastic pathway of the colorectum: possible roles and epigenetic regulatory mechanisms. *J Clin Pathol* 2012; **65**: 675-679 [PMID: 22412046 DOI: 10.1136/jclinpath-2011-200602]
10 **Tseng CW**, Hsieh YH, Koo M, Leung FW. Comparing right colon adenoma detection rate during water exchange and air insufflation: a double-blind randomized controlled trial. *Tech Coloproctol* 2022; **26**: 35-44 [PMID: 34705136 DOI: 10.1007/s10151-021-02537-1]
11 **Hazewinkel Y**, López-Cerón M, East JE, Rastogi A, Pellisé M, Nakajima T, van Eeden S, Tytgat KM, Fockens P, Dekker E. Endoscopic features of sessile serrated adenomas: validation by international experts using high-resolution white-light endoscopy and narrow-band imaging. *Gastrointest Endosc* 2013; **77**: 916-924 [PMID: 23433877 DOI: 10.1016/j.gie.2012.12.018]
12 **Uraoka T**, Higashi R, Horii J, Harada K, Hori K, Okada H, Mizuno M, Tomoda J, Ohara N, Tanaka T, Chiu HM, Yahagi N, Yamamoto K. Prospective evaluation of endoscopic criteria characteristic of sessile serrated adenomas/polyps. *J Gastroenterol* 2015; **50**: 555-563 [PMID: 25270966 DOI: 10.1007/s00535-014-0999-y]
13 **Hashimoto T**, Yamashita S, Yoshida H, Taniguchi H, Ushijima T, Yamada T, Saito Y, Ochiai A, Sekine S, Hiraoka N. WNT Pathway Gene Mutations Are Associated With the Presence of Dysplasia in Colorectal Sessile Serrated Adenoma/Polyps. *Am J Surg Pathol* 2017; **41**: 1188-1197 [PMID: 28614199 DOI: 10.1097/PAS.0000000000000877]
14 **Xiao J**, Lv D, Zhou J, Bei Y, Chen T, Hu M, Zhou Q, Fu S, Huang Q. Therapeutic Inhibition of miR-4260 Suppresses Colorectal Cancer *via* Targeting MCC and SMAD4. *Theranostics* 2017; **7**: 1901-1913 [PMID: 28638476 DOI: 10.7150/thno.19168]
15 **Luo XS**, Wang HP, Zhu XJ, Li SG, Long XK, Jiang SY, Zhang QQ. Correlation between positive KRAS mutation and P53 and MCC in colorectal cancer. *J Dig Oncol* 2021; **13**: 125-129
16 **Ashktorab H**, Delker D, Kanth P, Goel A, Carethers JM, Brim H. Molecular Characterization of Sessile Serrated Adenoma/Polyps From a Large African American Cohort. *Gastroenterology* 2019; **157**: 572-574 [PMID: 31004568 DOI: 10.1053/j.gastro.2019.04.015]

17 **Murakami T**, Akazawa Y, Yatagai N, Hiromoto T, Sasahara N, Saito T, Sakamoto N, Nagahara A, Yao T. Molecular characterization of sessile serrated adenoma/polyps with dysplasia/carcinoma based on immunohistochemistry, next-generation sequencing, and microsatellite instability testing: a case series study. *Diagn Pathol* 2018; **13**: 88 [PMID: 30458818 DOI: 10.1186/s13000-018-0771-3]

18 **Parikh ND**, Chaptini L, Njei B, Laine L. Diagnosis of sessile serrated adenomas/polyps with image-enhanced endoscopy: a systematic review and meta-analysis. *Endoscopy* 2016; **48**: 731-739 [PMID: 27223636 DOI: 10.1055/s-0042-107592]

19 **Suzuki Y**, Ohata K, Matsuhashi N. Delineating sessile serrated adenomas/polyps with acetic acid spray for a more accurate piecemeal cold snare polypectomy. *VideoGIE* 2020; **5**: 519-521 [PMID: 33204905 DOI: 10.1016/j.vgie.2020.05.030]

20 **Moy BT**, Forouhar F, Kuo CL, Devers TJ. Endoscopic Features of Mucous Cap Polyps: A Way to Predict Serrated Polyps. *Clin Endosc* 2018; **51**: 368-374 [PMID: 29699379 DOI: 10.5946/ce.2017.155]

21 **Neary PM**, Schwartzberg DM, Bora Cengiz T, Kalady MF, Church JM. Aspects of the Natural History of Sessile Serrated Adenomas/Polyps: Risk Indicators for Carcinogenesis in the Colorectal Mucosa? *Dis Colon Rectum* 2018; **61**: 1380-1385 [PMID: 30346367 DOI: 10.1097/DCR.0000000000001208]

22 **Tanaka S**, Saitoh Y, Matsuda T, Igarashi M, Matsumoto T, Iwao Y, Suzuki Y, Nishida H, Watanabe T, Sugai T, Sugihara K, Tsuruta O, Hirata I, Hiwatashi N, Saito H, Watanabe M, Sugano K, Shimosegawa T; Japanese Society of Gastroenterology. Evidence-based clinical practice guidelines for management of colorectal polyps. *J Gastroenterol* 2015; **50**: 252-260 [PMID: 25559129 DOI: 10.1007/s00535-014-1021-4]

23 **Rutter MD**, East J, Rees CJ, Cripps N, Docherty J, Dolwani S, Kaye PV, Monahan KJ, Novelli MR, Plumb A, Saunders BP, Thomas-Gibson S, Tolan DJM, Whyte S, Bonnington S, Scope A, Wong R, Hibbert B, Marsh J, Moores B, Cross A, Sharp L. British Society of Gastroenterology/Association of Coloproctology of Great Britain and Ireland/Public Health England post-polypectomy and post-colorectal cancer resection surveillance guidelines. *Gut* 2020; **69**: 201-223 [PMID: 31776230 DOI: 10.1136/gutjnl-2019-319858]

24 **Shichijo S**, Yamaguchi S, Nakamatsu D, Inoue T, Nakahara M, Ogiyama H, Yamada T, Kinoshita K, Ishihara R, Michida T, Nishida T, Tsujii Y, Hayashi Y, Shinzaki S, Fukui K, Ito Y, Kitamura M, Honma K, Morii E, Takehara T; Osaka Gut Forum. Local recurrence after endoscopic resection of sessile serrated lesions: A multicenter prospective study by the Osaka Gut Forum. *J Gastroenterol Hepatol* 2022; **37**: 2306-2312 [PMID: 36266771 DOI: 10.1111/jgh.16032]

25 **Bian Y**, Wang G, Zhou J, Yin G, Liu T, Liang L, Yang X, Zhang W, Ni K, Tang D, Yu Y. Astragalus membranaceus (Huangqi) and Rhizoma curcumae (Ezhu) decoction suppresses colorectal cancer *via* downregulation of Wnt5/β-Catenin signal. *Chin Med* 2022; **17**: 11 [PMID: 34991661 DOI: 10.1186/s13020-021-00564-6]

World Journal of Clinical Cases

Submit a Manuscript: https://www.f6publishing.com

World J Clin Cases 2023 March 26; 11(9): 1974-1984

DOI: 10.12998/wjcc.v11.i9.1974

ISSN 2307-8960 (online)

ORIGINAL ARTICLE

Randomized Controlled Trial

Effects of individual shock wave therapy *vs* celecoxib on hip pain caused by femoral head necrosis

Jun-Yu Zhu, Jun Yan, Jian Xiao, Hai-Guang Jia, Hao-Jun Liang, Geng-Yan Xing

Specialty type: Orthopedics

Provenance and peer review: Unsolicited article; Externally peer reviewed.

Peer-review model: Single blind

Peer-review report's scientific quality classification

Grade A (Excellent): 0
Grade B (Very good): 0
Grade C (Good): C, C
Grade D (Fair): 0
Grade E (Poor): 0

P-Reviewer: Bianchi J, United States; Verlaan JJ, Netherlands

Received: November 19, 2022
Peer-review started: November 19, 2022
First decision: January 30, 2023
Revised: February 7, 2023
Accepted: March 3, 2023
Article in press: March 3, 2023
Published online: March 26, 2023

Jun-Yu Zhu, Geng-Yan Xing, Orthopedic Department, The Third Medical Center of Chinese People's Liberation Army General Hospital, The Armed Police Clinical College, Anhui Medical University, Hefei 230022, Anhui Province, China

Jun-Yu Zhu, Jun Yan, Jian Xiao, Hai-Guang Jia, Hao-Jun Liang, Orthopedic Department, The Third Medical Center of Chinese People's Liberation Army General Hospital, Beijing 100039, China

Corresponding author: Geng-Yan Xing, PhD, Additional Professor, Orthopedic Department, The Third Medical Center of Chinese People's Liberation Army General Hospital, The Armed Police Clinical College, Anhui Medical University, No. 81 Meishan Road, Hefei 230022, Anhui Province, China. jyzhu@ihep.ac.cn

Abstract

BACKGROUND

Celecoxib has been used to treat hip discomfort and functional difficulties associated with osteonecrosis of the femoral head (ONFH), although significant adverse reactions often follow long-term use. Extracorporeal shock wave therapy (ESWT) can delay the progression of ONFH, alleviate the pain and functional limitations it causes, and avoid the adverse effects of celecoxib.

AIM

To investigate the effects of individual ESWT, a treatment alternative to the use of celecoxib, in alleviating pain and dysfunction caused by ONFH.

METHODS

This was a randomized, controlled, double-blinded, non-inferiority trial. We examined 80 patients for eligibility in this study; 8 patients were excluded based on inclusion and exclusion criteria. A total of 72 subjects with ONFH were randomly assigned to group A (n = 36; celecoxib + alendronate + sham-placebo shock wave) or group B (n = 36; individual focused shock wave [ESWT based on magnetic resonance imaging three-dimensional (MRI-3D) reconstruction] + alendronate). The outcomes were assessed at baseline, at the end of treatment, and at an 8-wk follow-up. The primary outcome measure was treatment efficiency after 2 wk of intervention using the Harris hip score (HHS) (improvement of 10 points or more from the baseline was deemed sufficient). Secondary outcome measures were post-treatment HHS, visual analog scale (VAS), and Western Ontario and McMaster Universities Osteoarthritis Index (WOMAC) scores.

RESULTS

After treatment, the pain treatment efficiency of group B was greater than that of group A (69% *vs* 51%; 95%CI: 4.56% to 40.56%), with non-inferiority thresholds of -4.56% and -10%, respectively. Furthermore, the HHS, WOMAC, and VAS scores in group B dramatically improved during the follow-up period as compared to those in group A ($P < 0.001$). After therapy, the VAS and WOMAC in group A were significantly improved from the 2nd to 8th wk ($P < 0.001$), although HHS was only significantly altered at the 2 wk point ($P < 0.001$). On the 1st d and 2nd wk after treatment, HHS and VAS scores were different between groups, with the difference in HHS lasting until week 4. Neither group had severe complications such as skin ulcer infection or lower limb motor-sensory disturbance.

CONCLUSION

Individual shock wave therapy (ESWT) based on MRI-3D reconstruction was not inferior to celecoxib in managing hip pain and restrictions associated with ONFH.

Key Words: Extracorporeal shockwave therapy; Osteonecrosis of femoral head; Pain; Magnetic resonance imaging three-dimensional reconstruction; Celecoxib

Core Tip: This is a randomized, controlled, and non-inferiority trial. To the best of our knowledge, the present study is the first to investigate the short-term effectiveness of extracorporeal shock wave therapy (ESWT) in the management of osteonecrosis of the femoral head (ONFH). Traditional ESWT was innovated by magnetic resonance imaging three-dimensional (MRI-3D) reconstruction technology. The final results demonstrate that ESWT based on MRI-3D reconstruction is not inferior to celecoxib in treating hip discomfort and restrictions associated with ONFH.

Citation: Zhu JY, Yan J, Xiao J, Jia HG, Liang HJ, Xing GY. Effects of individual shock wave therapy *vs* celecoxib on hip pain caused by femoral head necrosis. *World J Clin Cases* 2023; 11(9): 1974-1984
URL: https://www.wjgnet.com/2307-8960/full/v11/i9/1974.htm
DOI: https://dx.doi.org/10.12998/wjcc.v11.i9.1974

INTRODUCTION

Osteonecrosis of the femoral head (ONFH) is a prevalent condition in orthopedic clinics, characterized by the gradual loss of bone cellularity and structure. Ischemia, necrosis, and collapse are characteristic pathological processes associated with ONFH[1,2]. The hip is one of the most important weight-bearing joints in the human body[3], and structural and pathological changes of this joint often lead to pain, dysfunction, and even disability[4]. Those suffering from ONFH are mostly young or middle-aged[5]. In the United States, more than 20000 individuals are afflicted by ONFH annually, and the prevalence continues to rise[6,7]. In China, it is estimated that more than 8 million individuals have suffered from ONFH[2].

Currently, the treatment of ONFH mainly includes the following: (1) Surgical treatment (artificial hip arthroplasty and drilling decompression); (2) Drug therapy [nonsteroidal anti-inflammatory drugs (NSAIDs) and alendronate]; (3) Physical therapies [extracorporeal shock wave therapy (ESWT) or high-pressure oxygen therapy]; and (4) Lifestyle changes (weight control and reduction of weight-bearing activities)[2,8,9]. Because of the limited life of the artificial joint in hip arthroplasty, the difficulties of secondary revision, the inadequate impact of hip preservation surgery, and considerable trauma, most patients prefer oral pharmacotherapy to alleviate symptoms[10]. The main goal of pharmacotherapy is to relieve hip pain and improve joint function. It has achieved some success in the management of ONFH, but long-term use of certain drugs is often accompanied by severe side effects[11-13]. Therefore, exploring a noninvasive treatment that can reduce side effects and replace traditional drug therapy is urgently needed. In treating ONFH, the biological effects of ESWT include analgesia, improvement of microcirculation, and promotion of osteocyte proliferation and differentiation[14-16]. A clinical study by Wang *et al*[17] in 2008 demonstrated that ESWT delays the progression of necrosis, alleviates hip joint pain, and promotes recovery of hip joint function.

In terms of analgesia and improving activity, ESWT avoids the side effects of drugs and dramatically decreases the trauma and economic burden associated with surgery[18,19]. However, the effects of ESWT often cannot be maximized due to acetabular obstruction during the transmission of shock wave

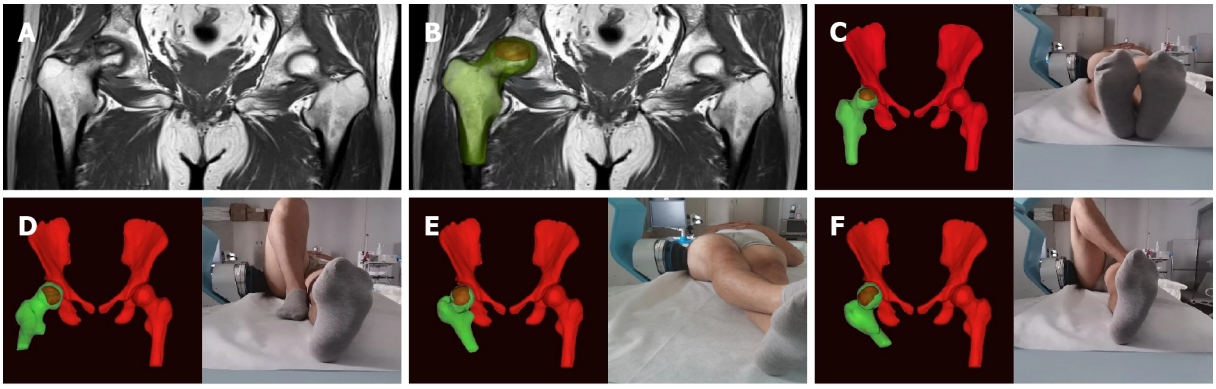

DOI: 10.12998/wjcc.v11.i9.1974

Figure 1 Personalized extracorporeal shock wave therapy based on magnetic resonance imaging three-dimensional reconstruction. A: Magnetic resonance imaging (MRI) image; B: Three-dimensional (3D) reconstructed MRI images; C-F: Personalized posture + MRI-3D image + extracorporeal shock wave = personalized extracorporeal shock wave therapy.

energy and its attenuation in bone conduction[20-22]. Magnetic resonance imaging three-dimensional (MRI-3D) reconstruction to strengthen extracorporeal shock wave (ESW) targeting may be a reasonable solution for this issue[23]. Thus, the primary aim of this prospective, randomized study was to determine whether ESWT based on MRI-3D reconstruction was as effective as NSAIDs in improving pain and dysfunction associated with ONFH.

MATERIALS AND METHODS

Design and patients

This study was a prospective, double-blinded, non-inferiority randomized controlled trial designed per the principles of the Declaration of Helsinki. It was approved by the Ethics Committee of The Third Medical Center of Chinese People's Liberation Army General Hospital (ID: 001-R1) and registered on the Chinese Clinical Trial Registry (ChiCTR2100047844).

The study was conducted at the outpatient rehabilitation medicine department of The Third Medical Center of Chinese People's Liberation Army General Hospital. All consecutive subjects affected by ONFH associated with hip pain and dysfunction referred to the hospital from June 2021 to October 2021 were screened for inclusion in an outpatient rehabilitative setting. The recruitment procedure was performed by 2 specialists and included clinical examination of the affected hip, an MRI of the pelvis, an X-ray of the pelvis, and assessment of patient disease history and general condition.

Eligibility criteria were as follows: (1) Adult age (18-75 years); (2) Diagnosed as ONFH and Association Research Circulation Osseous staging I-IV, confirmed with plain radiograph and MRI; (3) Patient unwillingness to accept surgical treatment and agreement not to use any other non-study treatment for hip pain during the study period; and (4) Voluntary participation in the clinical trial, compliance with the requirements of the trial, and signing of an informed consent form.

General contraindications to shock wave therapy were considered, including use of a pacemaker, pregnancy, bleeding disorder, anticoagulant drug use, or cancer in the focal area, and use of immunosuppressive agents. Patients with any of these contraindications were excluded.

Seventy-two patients were recruited and randomly divided into two groups. All participants provided written informed consent after a detailed understanding of the objectives and procedures of the study. The randomization was performed using the IWRS central random system (https://iwrs.ymedical.net/#/projects/157/dashboard), generating group A and group B. A flow diagram of the trial profile is shown in Figure 1.

Interventions

In group A, 200 mg celecoxib was used once daily for 9 consecutive days. Using sham focused ESWT, the protocol was the same as that used in group B, except that the energy level was a single grade (0.07 mJ/mm^2) and no coupling gel was used on the treatment site. Instead, thick gauze was placed between the skin and the transmitter, with no energy applied. In group B, using personalized focused extracorporeal shockwave therapy (fESWT), the shock wave was generated by a focused shock wave generator (HK.SWT-007; Huikan AG, China) with a penetration depth between 0 and 70 mm and a focus diameter of 7.5 mm. All ESWT procedures were performed without general or regional anesthesia. First, raw MRI data from imaging of both hip joints (Digital Imaging and Communication in Medicine coronal T1-weighted MRI) were imported to the interactive medical imaging control system software (Mimics; Materialise Company, Laueven, Belgium). A three-dimensional (3D) view of the femoral head and its

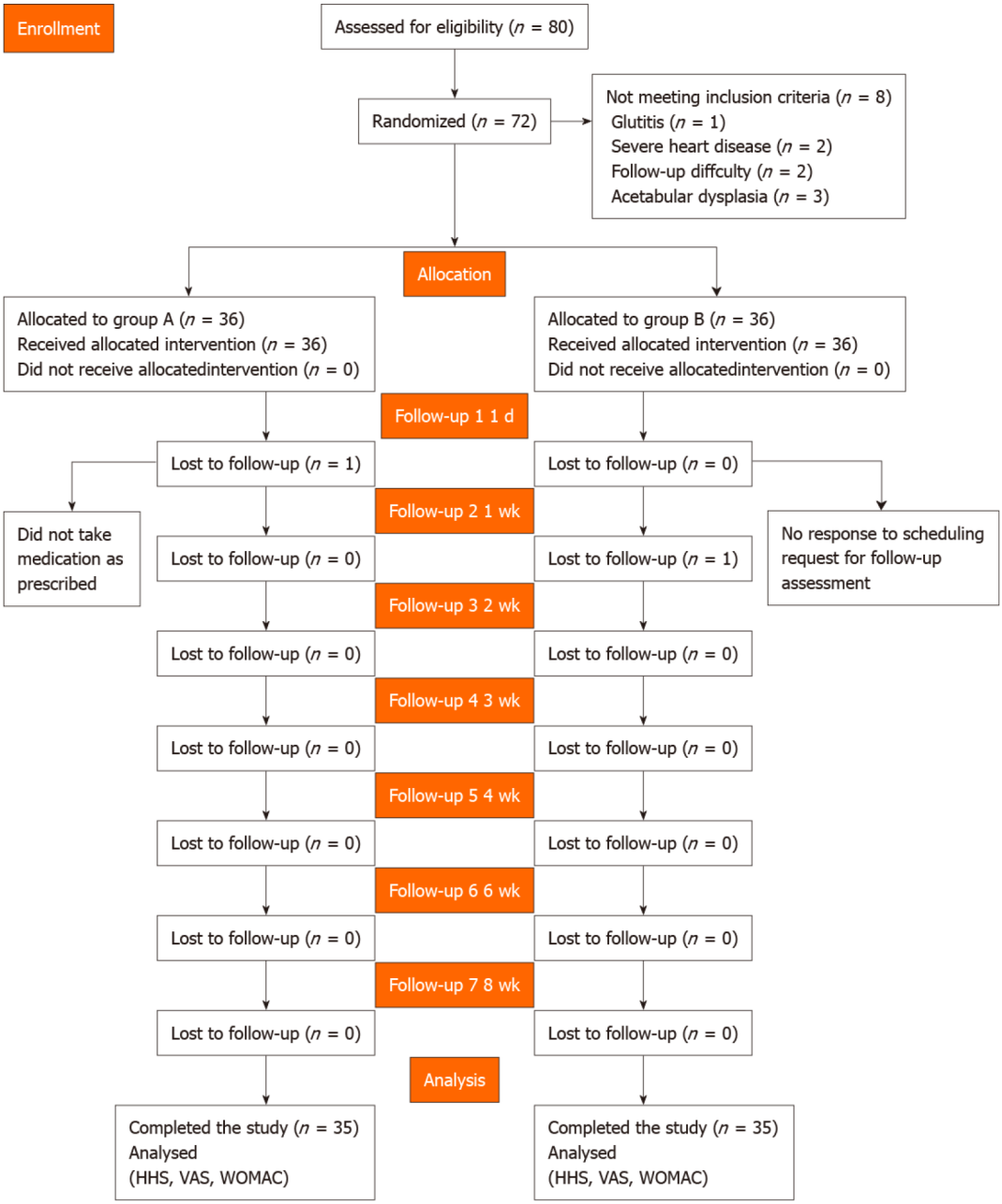

DOI: 10.12998/wjcc.v11.i9.1974

Figure 2 Study flow diagram. HHS: Harris hip score; VAS: Visual analog scale; WOMAC: Western Ontario and McMaster Universities Osteoarthritis Index.

necrotic area was obtained by image segmentation, visualization, registration, and other functions. The size and spatial location of the necrotic area were determined using the 3D perspective of the reconstructed necrotic area. The junctional zone between normal and necrotic bone within the femoral head was delineated under MRI-3D image guidance. Within the junctional zone, 2 or 3 points approximately 1.0 cm apart were chosen under MRI-3D imaging guidance and the corresponding locations were marked on the skin in the groin area. Next, physicians adjusted the treatment points according to personalized posture with the subjects in different lying positions. Furthermore, they placed the treatment head at the surface of the hip corresponding to the necrotic area (with avoidance of keep essential blood vessels and nerves) (Figure 2). Next, the water sac was adjusted to the appropriate position, and the proper amount of medical coupling agent was applied to the surface of the water in contact with the human body. Finally, when using 5-10 grade energy therapy (energy flow density: 0.20-0.6 mJ/mm^2), the energy was increased from low to high according to the subject's sensitivity to pain. Simultaneously, to ensure exact targeting, the position was monitored throughout treatment, and the drift of the treatment point was adjusted in real-time.

The clinicians administering ESWT had extensive experience using this treatment to treat various musculoskeletal disorders. Each treatment cycle included 5 sessions with 1000 impulses per point, each administered at a frequency of 60 times per minute, at 48-72 h intervals.

During the trial, all the subjects were treated with basic treatment (70 mg oral alendronate sodium once per wk).

Outcome measurements

The primary outcome measure was treatment efficacy after the 2nd wk of treatment. Harris hip score (HHS) improved by 10 points after therapy, which was deemed sufficient. The secondary outcome measures [HHS, visual analog scale (VAS), and Western Ontario and McMaster Universities Osteoarthritis Index (WOMAC) scores] were improved on the 1st d and the 2nd, 4th, and 8th wk after treatment as compared to baseline. After completing therapy, pain recurrence was evaluated if the subject's VAS pain score was equal to or higher than baseline during the follow-up period. Each subject was instructed to record his or her VAS score at the following timepoints following therapy: day 1, week 1, week 2, week 3, week 4, week 6, and week 8.

Sample size

A sample size of 64 patients was computed given an alpha error of 5% (two-sided) and a power of 80%, assuming that the pain improvement rate of group A and group B was 65% and 85%, respectively, with a non-inferiority limit of -10%. Thus, non-inferiority would be demonstrated if the lower boundary of the 95%CI for the difference was higher than -10%. After considering the potential for patient dropout (estimated at 10%), the final sample was 72 patients (36 per group).

Randomization and blinding

Patients were randomized to group A or group B after providing written informed consent. Randomization was performed by a person not involved in the study, and a computer-generated list of random numbers was used. Patients and investigators were blinded to allocation. After intervention, results were recorded by a specialized physician. To maintain blinding, statistical analyses were conducted by independent statisticians, and results were not shared with the patients or other participants before the end of the study.

Statistical analysis

This experiment was a non-inferiority test. Statistical analysis was performed using Graphpad5.0 software (La Jolla, CA, United States). All statistical tests were bilateral, and $P < 0.05$ was considered statistically significant. Quantitative data were normally distributed by mean ± SD, and the skewed distribution was described by median or interquartile range. A paired sample *t*-test was used to compare the mean change of each evaluation indicator between the pre-treatment and scheduled follow-up time points. Two-sample independent *t*-test or Wilcoxon rank-sum test was used to compare the groups. The classified data distribution was described by rate or composition ratio. The main curative effect used the normal approximation method, and the 95%CI of the rate difference between the two groups was compared with the non-inferiority boundary value of -10%.

Data availability

The datasets are available from the corresponding author upon reasonable request.

RESULTS

We examined 80 patients for study eligibility and 8 patients were excluded per inclusion and exclusion criteria. Seventy-two patients were randomized into two groups, which received treatment predefined for each group. All patients completed the designated interventions, which was monitored and reported at the end of the treatment period by physiotherapists. Two participants were lost to follow-up. All others were analyzed at each of the assessment points (Figure 1). There were no differences in age, sex, height, weight, BMI, or symptom duration between the groups ($P > 0.05$) (Table 1).

The findings of the Harris, VAS, and WOMAC score analyses were documented over the follow-up period (Table 2). The analysis found no statistical significance in the baseline data of the two groups of patients. With respect to the continuous changes in VAS, the downward trend in group B was faster than in group A (Figure 3).

The treatment efficacy observed in group A (18/35) and group B (24/35) were 51% and 69%, respectively (95%CI: -4.56% to 40.56%. The non-inferiority thresholds according to the primary outcome measure for group A and group B were -4.56% and -10%, respectively. In addition, the Harris, WOMAC, and VAS scores in group B were significantly improved at day 1, week 2, week 4, and week 8 following treatment (Table 2). In group A, the VAS and WOMAC scores were significantly improved at day 1, week 2, week 4, and week 8 following treatment ($P < 0.001$), while changes in HHS significant only at week 2 following treatment ($P < 0.001$). On day 1 and week 2 following treatment, HHS and VAS scores were significantly different between groups, with the difference in HHS lasting until week 4 (Table 2).

Table 1 Patient characteristics, mean ± SD

Characteristic	Group A	Group B	*P* value
Patients, *n*	35	35	
Sex, male/female	26/10	18/17	
Age in yr	40.06 ± 13.48	43.72 ± 13.69	0.256[1]
Weight in kg	71.82 ± 11.02	67.79 ± 10.93	0.124[1]
Height in cm	171.6 ± 7.71	168.4 ± 8.22	0.099[1]
BMI in kg/m^2	24.4 ± 3.59	23.8 ± 2.85	0.424[1]
Pain duration in mo	14.8 ± 7.99	13.7 ± 7.89	0.564[1]

[1]Paired-samples t-test data are expressed as mean ± SD or *n* (%).
Data were analyzed using unpaired *t*-test. BMI: Body mass index.

Table 2 Outcome assessment before and after treatment

Parameter	Baseline	1 d	2 wk	4 wk	8 wk
Group A					
Patients, *n*	35	35	35	35	35
HHS range 0-100, mean ± SD	51.8 ± 11.8	51.8 ± 11.6	57.9 ± 12.5	52.9 ± 11.5	52.7 ± 11.2
Difference *vs* baseline		0.962[1]	< 0.001[1]	0.218[1]	0.315[1]
Difference *vs* group B		< 0.001[2]	0.004[2]	0.047[2]	0.147[2]
VAS (0-10), mean ± SD	5.3 ± 1.1	5.0 ± 1.0	3.9 ± 1.0	4.1 ± 1.0	4.4 ± 1.0
Difference *vs* baseline		0.003[1]	< 0.001[1]	< 0.001[1]	< 0.001[1]
Difference *vs* group B		< 0.001[2]	< 0.001[2]	0.257[2]	0.166[2]
WOMAC range 0-240, mean ± SD	93.7 ± 32.4	92.3 ± 31.8	87.6 ± 31.5	89.3 ± 31.4	90.2 ± 31.2
Difference *vs* baseline		0.022[1]	< 0.001[1]	< 0.001[1]	< 0.001[1]
Difference *vs* group B		0.196[2]	0.447[2]	0.596[2]	0.651[2]
Group B					
Patients, *n*	35	35	35	35	35
HHS range 0-100, mean ± SD	53.9 ± 13.3	62.4 ± 11.6	62.9 ± 12.1	58.5 ± 12.0	56.9 ± 12.9
Difference *vs* baseline		< 0.001[1]	< 0.001[1]	< 0.001[1]	< 0.001[1]
VAS range 0-10, mean ± SD	5.0 ± 1.2	3.1 ± 1.1	3.0 ± 1.0	3.9 ± 1.1	4.1 ± 1.1
Difference *vs* baseline		< 0.001[1]	< 0.001[1]	< 0.001[1]	< 0.001[1]
WOMAC range 0-240, mean ± SD	91.0 ± 25.1	83.5 ± 23.9	82.5 ± 24.0	86.0 ± 24.3	87.1 ± 24.7
Difference *vs* baseline		< 0.001[1]	< 0.001[1]	< 0.001[1]	< 0.001[1]

[1]Paired-sample *t*-test.
[2]Two-sample independent *t*-test statistical significance at $P < 0.05$.
HHS: Harris hip score; VAS: Visual analog scale; WOMAC: Western Ontario and McMaster Universities Osteoarthritis Index.

Short-term side effects such as discomfort, edema, and bruising were similar in both groups. Heart rate, blood pressure, body temperature, and routine blood tests were unaffected by treatment. Patients from either group experienced no serious complication such as skin ulceration infection or lower extremity motor-sensory impairment.

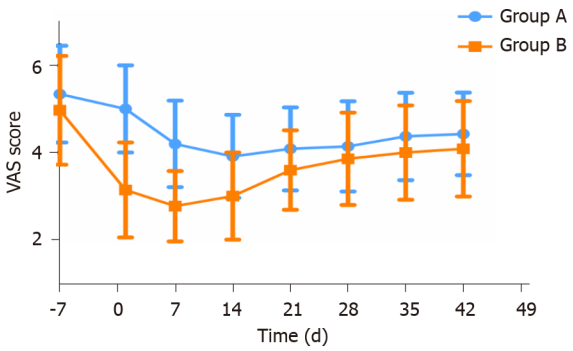

DOI: 10.12998/wjcc.v11.i9.1974

Figure 3 Changing trend of the visual analog scale in groups A and B. VAS: Visual analog scale.

DISCUSSION

This study demonstrated that fESWT can effectively and safely treat hip pain and functional restrictions associated with ONFH. The treatment efficacy observed in group B was significantly higher than that of group A. Moreover, most secondary outcomes, including composite scores and response criteria, showed improvements favoring the use of fESWT.

ONFH causes the collapse of the femoral head with severe pain and limited mobility[24]. Hip pain and functional limitations are the typical clinical manifestations of this condition[25]. Therefore, symptom alleviation and recovery of hip joint function are essential in determining the effectiveness of short-term treatment[1]. In this study, we proposed that individualized fESWT could be used for short-term symptomatic treatment of ONFH and it is as effective as NSAIDs (*e.g.*, celecoxib) with respect to analgesia and improvement of joint function[26]. After an 8-wk follow-up, we found that individualized fESWT was effective in alleviating hip joint pain and promoting recovery of hip joint function during short-term applications. The therapeutic effect peaked 1 wk after the intervention and was superior to celecoxib in both therapeutic and analgesic efficacy.

ONFH is more likely to occur in young and active patients as compared to osteoarthritis[4,27]. Therefore, most patients choose non-surgical treatments. In the short term, many non-operative treatments for ONFH are designed to relieve hip pain and improve joint function, while long-term treatments largely aim to prevent the progression of necrosis[28]. Recent studies recommend the use of osteoclast inhibitors and NSAIDs for symptomatic treatment[2,29]. In 2009, a nationwide cohort study conducted in Denmark showed that NSAIDs were associated with increased relative risks of cardiovascular events and death, even in the low-risk population[30]. At the same time, Singh *et al*[31] showed that NSAIDs had severe gastrointestinal toxicity, highlighting the significant adverse reactions associated with pharmacotherapy.

ESWT represents mechanical stimulation of the joint and has great potential in treating ONFH as it avoids the adverse effects of drug therapy. In 2 clinical studies, Wang *et al*[32] and Vulpiani *et al*[33] separately explored the long-term dose effects of ESWT in the treatment of ONFH. These studies demonstrated that ESWT could stimulate the growth of new bone at the site of necrosis and delay the progression of ONFH with long-term application[33]. Other studies have also indicated that ESWT might relieve pain by suppressing the release of inflammatory factors and downregulating the expression of pain-related, calcitonin gene-related peptides in dorsal root ganglion[34,35]. Additionally, it can directly act on peripheral sensory nerve endings, improving the pain threshold and preventing the production and propagation of pain signals[36]. These data suggest that ESWT may be useful as short-term, symptomatic supportive treatment in the management of ONFH.

To the best of our knowledge, this is the first investigation of the efficacy of ESWT in the short-term management of ONFH. Our results showed that the Harris, WOMAC, and VAS scores of group B improved significantly at day 1, week 2, week 4, and week 8 following treatment ($P < 0.001$). In group A, the VAS and WOMAC scores were significantly improved at week 2, week 4, and week 8 following treatment ($P < 0.001$), while Harris scores differed significantly only at week 2 ($P < 0.001$). These data suggest that both fESWT and celecoxib are effective in improving hip pain and promoting joint function in patients with ONFH. However, fESWT was superior to celecoxib in speed of onset and analgesic effect (a comparison of the two groups found significant differences in HHS and VAS at day 1 and week 2 following treatment, with the difference in HHS lasting until week 4). This finding suggests that, as compared to pharmacotherapy, ESWT avoids the lack of targeted treatment and limits bone marrow edema induced by early ONFH. During treatment, fESWT promotes blood circulation and reduces inflammation, thereby limiting pain associated with ONFH[14,37,38]. Treatment with traditional NSAIDs does not exhibit these features.

Additionally, based on our prior experience with ESWT, we noted that the acetabulum frequently blocks the incoming shock wave and reduces the therapeutic impact as a result of the uniqueness of hip joint anatomy. In a study of the energy decay of shock waves utilizing the femoral heads of pigs, ESW attenuated by 50% for every 10 mm of penetration into the femoral head[20]. Coupled with acetabular blocking, traditional ESWT often fails to maximize function[21]. Therefore, to reduce unnecessary energy attenuation in ESW transmission, our team designed an individual fESWT treatment for each patient according to MRI-3D reconstruction combined with posture adjustment (Figure 1). The 3D picture of the MRI, as opposed to the conventional X-ray localization, better reflected the spatial location and size of the necrotic area, increasing the accuracy of ESWT targeting and improving the curative impact. This supports the idea that MRI is the gold standard for diagnosing early stage ONFH, whereas X-ray and computed tomography less effective in diagnosing this condition[1,2,39].

Study limitations

Our study does have some limitations. Because the trial used a new treatment method (ESWT) based on MRI-3D reconstruction, we performed only a conservative non-inferiority test. Furthermore, due to ethical concerns and a lack of relevant pathology and other objective markers, the study could not investigate the exact causes of pain induced by ONFH. As a result, the lack of this objective evaluation may have led to bias in interpretation of the experimental results. Therefore, our goals in the next phase of study are optimization of the treatment regimen and exploration of the mechanism of ESWT to improve treatment of pain associated with ONFH. Finally, this study only included patients from a single medical center, and recruitment of subjects was somewhat limited.

CONCLUSION

Short-term ESWT based on MRI-3D reconstruction can relieve hip pain caused by ONFH, and is not inferior to celecoxib in terms of treatment efficacy and continuous analgesic effect. It also shows significant efficacy in improving the function of the hip joint, indicating that ESWT is a promising alternative for the short-term management of ONFH.

ARTICLE HIGHLIGHTS

Research background

Hip pain and functional joint limitations are the major symptoms associated with osteonecrosis of the femoral head (ONFH). The long-term use of nonsteroidal anti-inflammatory drugs (NSAIDs) such as celecoxib are often associated with severe adverse effects.

Research motivation

The motivation of this study was to explore a new treatment, extracorporeal shock wave therapy (ESWT) to replace pharmacotherapy in the treatment of ONFH.

Research objectives

This study investigated the efficacy of ESWT in improving pain and joint dysfunction associated with ONFH as compared to that of NSAID therapy.

Research methods

The eligible 72 ONFH patients were randomly assigned to two groups: the experiment group and the control group. All patients underwent clinical assessment and analysis during pre- and post-treatment periods.

Research results

The Harris hip score, Western Ontario and McMaster Universities Arthritis Index, and visual analog scale scores in both the experiment and control groups were significantly improved, but those of the experimental group improved to a greater degree.

Research conclusions

ESWT based on magnetic resonance imaging three-dimensional reconstruction was not inferior to celecoxib in controlling hip pain and function associated with ONFH.

Research perspectives

The findings of this study indicate that individual shock wave therapy represents an alternative to pharmacotherapy in effectively alleviating pain associated with ONFH.

ACKNOWLEDGEMENTS

We are grateful to the patients who participated in our study. We thank our research team, Geng-Yan Xing, Jun Yan, Hao-Jun Liang, Hai-Guan Jia, Li Tong, Jian Xiao, Fan Hu, Hao Li, and Fu-Jin Li, for their assistance with data collection and management, and the occupational therapists who provided the intervention.

FOOTNOTES

Author contributions: Xing GY designed this study; Yan J and Jia HG collected the data; Liang HJ analyzed the data; Zhu JY and Xiao J drafted the manuscript and gave final approval of the version to be published.

Institutional review board statement: The research protocol was approved by the Ethics Committee of The Third Medical Center of Chinese People's Liberation Army General Hospital (ID: 001-R1).

Clinical trial registration statement: This study was registered on the Chinese Clinical Trial Registry (ChiCTR2100047844).

Informed consent statement: Informed written consent was obtained from the patients to publish this report and any accompanying images.

Conflict-of-interest statement: The authors declare that they have no conflicts of interest.

Data sharing statement: The datasets used and/or analyzed in the current study are available from the corresponding author upon reasonable request.

CONSORT 2010 statement: The manuscript was prepared and revised according to the CONSORT 2010 statement.

Country/Territory of origin: China

ORCID number: Jun-Yu Zhu 0000-0002-7826-2516; Hai-Guang Jia 0000-0003-4313-3586; Geng-Yan Xing 0000-0001-5412-9692.

S-Editor: Zhang H
L-Editor: Filipodia
P-Editor: Zhang H

REFERENCES

1 **Microsurgery Department of the Orthopedics Branch of the Chinese Medical Doctor Association**; Group from the Osteonecrosis and Bone Defect Branch of the Chinese Association of Reparative and Reconstructive Surgery; Microsurgery and Reconstructive Surgery Group of the Orthopedics Branch of the Chinese Medical Association. Chinese Guideline for the Diagnosis and Treatment of Osteonecrosis of the Femoral Head in Adults. *Orthop Surg* 2017; **9**: 3-12 [PMID: 28371498 DOI: 10.1111/os.12302]

2 **Zhao D**, Zhang F, Wang B, Liu B, Li L, Kim SY, Goodman SB, Hernigou P, Cui Q, Lineaweaver WC, Xu J, Drescher WR, Qin L. Guidelines for clinical diagnosis and treatment of osteonecrosis of the femoral head in adults (2019 version). *J Orthop Translat* 2020; **21**: 100-110 [PMID: 32309135 DOI: 10.1016/j.jot.2019.12.004]

3 **Li Z**, Zhuang Z, Hong Z, Chen L, He W, Wei Q. Avascular necrosis after femoral neck fracture in children and adolescents: poor prognosis and risk factors. *Int Orthop* 2021; **45**: 2899-2907 [PMID: 34549321 DOI: 10.1007/s00264-021-05210-2]

4 **Hauzeur JP**, Malaise M, de Maertelaer V. A prospective cohort study of the clinical presentation of non-traumatic osteonecrosis of the femoral head: spine and knee symptoms as clinical presentation of hip osteonecrosis. *Int Orthop* 2016; **40**: 1347-1351 [PMID: 26728612 DOI: 10.1007/s00264-015-3079-x]

5 **Yoon BH**, Jones LC, Chen CH, Cheng EY, Cui Q, Drescher W, Fukushima W, Gangji V, Goodman SB, Ha YC, Hernigou P, Hungerford M, Iorio R, Jo WL, Khanduja V, Kim H, Kim SY, Kim TY, Lee HY, Lee MS, Lee YK, Lee YJ, Mont MA, Sakai T, Sugano N, Takao M, Yamamoto T, Koo KH. Etiologic Classification Criteria of ARCO on Femoral Head Osteonecrosis Part 1: Glucocorticoid-Associated Osteonecrosis. *J Arthroplasty* 2019; **34**: 163-168.e1 [PMID: 30348552 DOI: 10.1016/j.arth.2018.09.005]

6 **Hungerford DS**. Osteonecrosis: avoiding total hip arthroplasty. *J Arthroplasty* 2002; **17**: 121-124 [PMID: 12068421 DOI: 10.1054/arth.2002.33300]

7 **Mont MA**, Salem HS, Piuzzi NS, Goodman SB, Jones LC. Nontraumatic Osteonecrosis of the Femoral Head: Where Do We Stand Today? *J Bone Joint Surg Am* 2020; **102**: 1084-1099 [PMID: 32282421 DOI: 10.2106/JBJS.19.01271]

8 **Puljak L**, Marin A, Vrdoljak D, Markotic F, Utrobicic A, Tugwell P. Celecoxib for osteoarthritis. *Cochrane Database Syst Rev* 2017; **5**: CD009865 [PMID: 28530031 DOI: 10.1002/14651858.CD009865.pub2]

9 **Lai KA**, Shen WJ, Yang CY, Shao CJ, Hsu JT, Lin RM. The use of alendronate to prevent early collapse of the femoral head in patients with nontraumatic osteonecrosis. A randomized clinical study. *J Bone Joint Surg Am* 2005; **87**: 2155-2159 [PMID: 16203877 DOI: 10.2106/JBJS.D.02959]

10 **Tsukanaka M**, Halvorsen V, Nordsletten L, EngesæTer IØ, EngesæTer LB, Marie Fenstad A, Röhrl SM. Implant survival and radiographic outcome of total hip replacement in patients less than 20 years old. *Acta Orthop* 2016; **87**: 479-484 [PMID: 27435903 DOI: 10.1080/17453674.2016.1212180]

11 **Dahlberg LE**, Holme I, Høye K, Ringertz B. A randomized, multicentre, double-blind, parallel-group study to assess the adverse event-related discontinuation rate with celecoxib and diclofenac in elderly patients with osteoarthritis. *Scand J Rheumatol* 2009; **38**: 133-143 [PMID: 19165648 DOI: 10.1080/03009740802419065]

12 **Mallen SR**, Essex MN, Zhang R. Gastrointestinal tolerability of NSAIDs in elderly patients: a pooled analysis of 21 randomized clinical trials with celecoxib and nonselective NSAIDs. *Curr Med Res Opin* 2011; **27**: 1359-1366 [PMID: 21561397 DOI: 10.1185/03007995.2011.581274]

13 **Moore RA**, Derry S, Makinson GT, McQuay HJ. Tolerability and adverse events in clinical trials of celecoxib in osteoarthritis and rheumatoid arthritis: systematic review and meta-analysis of information from company clinical trial reports. *Arthritis Res Ther* 2005; **7**: R644-R665 [PMID: 15899051 DOI: 10.1186/ar1704]

14 **Sung PH**, Yin TC, Chai HT, Chiang JY, Chen CH, Huang CR, Yip HK. Extracorporeal Shock Wave Therapy Salvages Critical Limb Ischemia in B6 Mice through Upregulating Cell Proliferation Signaling and Angiogenesis. *Biomedicines* 2022; **10** [PMID: 35052796 DOI: 10.3390/biomedicines10010117]

15 **Li B**, Wang R, Huang X, Ou Y, Jia Z, Lin S, Zhang Y, Xia H, Chen B. Extracorporeal Shock Wave Therapy Promotes Osteogenic Differentiation in a Rabbit Osteoporosis Model. *Front Endocrinol (Lausanne)* 2021; **12**: 627718 [PMID: 33841330 DOI: 10.3389/fendo.2021.627718]

16 **Alshihri A**, Niu W, Kämmerer PW, Al-Askar M, Yamashita A, Kurisawa M, Spector M. The effects of shock wave stimulation of mesenchymal stem cells on proliferation, migration, and differentiation in an injectable gelatin matrix for osteogenic regeneration. *J Tissue Eng Regen Med* 2020; **14**: 1630-1640 [PMID: 32885906 DOI: 10.1002/term.3126]

17 **Wang CJ**, Wang FS, Yang KD, Huang CC, Lee MS, Chan YS, Wang JW, Ko JY. Treatment of osteonecrosis of the hip: comparison of extracorporeal shockwave with shockwave and alendronate. *Arch Orthop Trauma Surg* 2008; **128**: 901-908 [PMID: 18060419 DOI: 10.1007/s00402-007-0530-5]

18 **Wang CJ**, Huang CC, Wang JW, Wong T, Yang YJ. Long-term results of extracorporeal shockwave therapy and core decompression in osteonecrosis of the femoral head with eight- to nine-year follow-up. *Biomed J* 2012; **35**: 481-485 [PMID: 23442361 DOI: 10.4103/2319-4170.104413]

19 **Ludwig J**, Lauber S, Lauber HJ, Dreisilker U, Raedel R, Hotzinger H. High-energy shock wave treatment of femoral head necrosis in adults. *Clin Orthop Relat Res* 2001; 119-126 [PMID: 11400872 DOI: 10.1097/00003086-200106000-00016]

20 **Hausdorf J**, Lutz A, Mayer-Wagner S, Birkenmaier C, Jansson V, Maier M. Shock wave therapy for femoral head necrosis-Pressure measurements inside the femoral head. *J Biomech* 2010; **43**: 2065-2069 [PMID: 20451206 DOI: 10.1016/j.jbiomech.2010.04.009]

21 **Tsutsumi M**, Nimura A, Akita K. New insight into the iliofemoral ligament based on the anatomical study of the hip joint capsule. *J Anat* 2020; **236**: 946-953 [PMID: 31867743 DOI: 10.1111/joa.13140]

22 **Tsutsumi M**, Yamaguchi I, Nimura A, Utsunomiya H, Akita K, Kudo S. In vivo magnetic resonance imaging study of the hip joint capsule in the flexion abduction external rotation position. *Sci Rep* 2022; **12**: 6656 [PMID: 35459931 DOI: 10.1038/s41598-022-10718-7]

23 **Derry S**, Moore RA. Single dose oral celecoxib for acute postoperative pain in adults. *Cochrane Database Syst Rev* 2013; **2013**: CD004233 [PMID: 24150982 DOI: 10.1002/14651858.CD004233.pub4]

24 **Ikeuchi K**, Hasegawa Y, Seki T, Takegami Y, Amano T, Ishiguro N. Epidemiology of nontraumatic osteonecrosis of the femoral head in Japan. *Mod Rheumatol* 2015; **25**: 278-281 [PMID: 25036228 DOI: 10.3109/14397595.2014.932038]

25 **Wang P**, Wang C, Meng H, Liu G, Li H, Gao J, Tian H, Peng J. The Role of Structural Deterioration and Biomechanical Changes of the Necrotic Lesion in Collapse Mechanism of Osteonecrosis of the Femoral Head. *Orthop Surg* 2022; **14**: 831-839 [PMID: 35445585 DOI: 10.1111/os.13277]

26 **Luan S**, Wang S, Lin C, Fan S, Liu C, Ma C, Wu S. Comparisons of Ultrasound-Guided Platelet-Rich Plasma Intra-Articular Injection and Extracorporeal Shock Wave Therapy in Treating ARCO I-III Symptomatic Non-Traumatic Femoral Head Necrosis: A Randomized Controlled Clinical Trial. *J Pain Res* 2022; **15**: 341-354 [PMID: 35153512 DOI: 10.2147/JPR.S347961]

27 **Seki T**, Hasegawa Y, Masui T, Yamaguchi J, Kanoh T, Ishiguro N, Kawabe K. Quality of life following femoral osteotomy and total hip arthroplasty for nontraumatic osteonecrosis of the femoral head. *J Orthop Sci* 2008; **13**: 116-121 [PMID: 18392915 DOI: 10.1007/s00776-007-1208-0]

28 **Petek D**, Hannouche D, Suva D. Osteonecrosis of the femoral head: pathophysiology and current concepts of treatment. *EFORT Open Rev* 2019; **4**: 85-97 [PMID: 30993010 DOI: 10.1302/2058-5241.4.180036]

29 **Luyten FP**, Geusens P, Malaise M, De Clerck L, Westhovens R, Raeman F, Vander Mijnsbrugge D, Mathy L, Hauzeur JP, De Keyser F, Van den Bosch F. A prospective randomised multicentre study comparing continuous and intermittent treatment with celecoxib in patients with osteoarthritis of the knee or hip. *Ann Rheum Dis* 2007; **66**: 99-106 [PMID: 16815864 DOI: 10.1136/ard.2006.052308]

30 **Fosbøl EL**, Gislason GH, Jacobsen S, Folke F, Hansen ML, Schramm TK, Sørensen R, Rasmussen JN, Andersen SS, Abildstrom SZ, Traerup J, Poulsen HE, Rasmussen S, Køber L, Torp-Pedersen C. Risk of myocardial infarction and death associated with the use of nonsteroidal anti-inflammatory drugs (NSAIDs) among healthy individuals: a nationwide cohort study. *Clin Pharmacol Ther* 2009; **85**: 190-197 [PMID: 18987620 DOI: 10.1038/clpt.2008.204]

31 **Singh G**. Recent considerations in nonsteroidal anti-inflammatory drug gastropathy. *Am J Med* 1998; **105**: 31S-38S

[PMID: 9715832 DOI: 10.1016/S0002-9343(98)00072-2]

32 **Wang CJ**, Huang CC, Yip HK, Yang YJ. Dosage effects of extracorporeal shockwave therapy in early hip necrosis. *Int J Surg* 2016; **35**: 179-186 [PMID: 27664561 DOI: 10.1016/j.ijsu.2016.09.013]

33 **Vulpiani MC**, Vetrano M, Trischitta D, Scarcello L, Chizzi F, Argento G, Saraceni VM, Maffulli N, Ferretti A. Extracorporeal shock wave therapy in early osteonecrosis of the femoral head: prospective clinical study with long-term follow-up. *Arch Orthop Trauma Surg* 2012; **132**: 499-508 [PMID: 22228278 DOI: 10.1007/s00402-011-1444-9]

34 **Murata R**, Nakagawa K, Ohtori S, Ochiai N, Arai M, Saisu T, Sasho T, Takahashi K, Moriya H. The effects of radial shock waves on gene transfer in rabbit chondrocytes in vitro. *Osteoarthritis Cartilage* 2007; **15**: 1275-1282 [PMID: 17537650 DOI: 10.1016/j.joca.2007.04.001]

35 **Hausdorf J**, Lemmens MA, Kaplan S, Marangoz C, Milz S, Odaci E, Korr H, Schmitz C, Maier M. Extracorporeal shockwave application to the distal femur of rabbits diminishes the number of neurons immunoreactive for substance P in dorsal root ganglia L5. *Brain Res* 2008; **1207**: 96-101 [PMID: 18371941 DOI: 10.1016/j.brainres.2008.02.013]

36 **Takahashi N**, Ohtori S, Saisu T, Moriya H, Wada Y. Second application of low-energy shock waves has a cumulative effect on free nerve endings. *Clin Orthop Relat Res* 2006; **443**: 315-319 [PMID: 16462457 DOI: 10.1097/01.blo.0000188064.56091.a7]

37 **Zhao W**, Gao Y, Zhang S, Liu Z, He L, Zhang D, Li W, Meng Q. Extracorporeal shock wave therapy for bone marrow edema syndrome in patients with osteonecrosis of the femoral head: a retrospective cohort study. *J Orthop Surg Res* 2021; **16**: 21 [PMID: 33413520 DOI: 10.1186/s13018-020-02159-7]

38 **Sukubo NG**, Tibalt E, Respizzi S, Locati M, d'Agostino MC. Effect of shock waves on macrophages: A possible role in tissue regeneration and remodeling. *Int J Surg* 2015; **24**: 124-130 [PMID: 26291028 DOI: 10.1016/j.ijsu.2015.07.719]

39 **Hopkins C**, Genant HK. Editorial for Guidelines for clinical diagnosis and treatment of osteonecrosis of the femoral head in adults (2019 version). *J Orthop Translat* 2020; **21**: A1 [PMID: 32309141 DOI: 10.1016/j.jot.2020.01.009]

World Journal of Clinical Cases

Submit a Manuscript: https://www.f6publishing.com

World J Clin Cases 2023 March 26; 11(9): 1985-1991

DOI: 10.12998/wjcc.v11.i9.1985

ISSN 2307-8960 (online)

CASE REPORT

Very low calorie ketogenic diet and common rheumatic disorders: A case report

Mariangela Rondanelli, Zaira Patelli, Clara Gasparri, Francesca Mansueto, Cinzia Ferraris, Mara Nichetti, Tariq A Alalwan, Ignacio Sajoux, Roberto Maugeri, Simone Perna

Specialty type: Medicine, research and experimental

Provenance and peer review: Unsolicited article; Externally peer reviewed.

Peer-review model: Single blind

Peer-review report's scientific quality classification

Grade A (Excellent): 0
Grade B (Very good): 0
Grade C (Good): C, C
Grade D (Fair): 0
Grade E (Poor): 0

P-Reviewer: Kotlyarov S, Russia; Xie Y, China

Received: October 20, 2022
Peer-review started: October 20, 2022
First decision: October 31, 2022
Revised: November 10, 2022
Accepted: January 9, 2023
Article in press: January 9, 2023
Published online: March 26, 2023

Mariangela Rondanelli, Department of Public Health, Experimental and Forensic Medicine, Unit of Human and Clinical Nutrition, IRCCS Mondino Foundation, Pavia 27100, Italy

Zaira Patelli, Clara Gasparri, Francesca Mansueto, Mara Nichetti, Endocrinology and Nutrition Unit, Azienda di Servizi alla Persona ''Istituto Santa Margherita'', University of Pavia, Pavia 27100, Italy

Cinzia Ferraris, Food Education and Sport Nutrition Laboratory, Department of Public Health, Experimental and Forensic Medicine, University of Pavia, Pavia 27100, Italy

Tariq A Alalwan, Simone Perna, Department of Biology, College of Science, University of Bahrain, Sakhir 32038, Bahrain

Ignacio Sajoux, Chief Scientific Office, Medical Department Pronokal Group, Barcelona 08001, Spain

Roberto Maugeri, Medical Direction, PronoKal Group, Savigliano 12038, Italy

Corresponding author: Clara Gasparri, MSc, Research Fellow, Endocrinology and Nutrition Unit, Azienda di Servizi alla Persona ''Istituto Santa Margherita'', University of Pavia, Via Emila 12, Pavia 27100, Italy. clara.gasparri01@universitadipavia.it

Abstract

BACKGROUND

The scientific literature provides evidence that nutritional ketosis can be an important support in the treatment of pathologies in which inflammation is present, as recent studies have shown that ketone bodies have anti-inflammatory activity in numerous diseases, including rheumatic diseases. We report the case of a 22-year-old woman with class I obesity and juvenile idiopathic arthritis who started treatment with a very low calorie ketogenic diet (VLCKD).

CASE SUMMARY

The patient was a 22-year-old woman diagnosed with juvenile idiopathic arthritis at age 4 years and with a body mass index (BMI) of 30.8 kg/m^2, waist circumference (WC) 80 cm, fat mass (FM) 28.1 kg, free FM 45.7 kg, and visceral adipose tissue (VAT) 3.5 kg, assessed on bioimpedance analysis. She was treated using a commercial VLCKD weight-loss program (PNK® method); this program provides high-biological-value protein preparations and natural foods. Each protein

preparation contains 15 g protein, 4 g carbohydrate, 3 g fat, and 50 mg omega-3 docosahexaenoic acid, with an energy content of 90–120 kcal. After four months on the program, the BMI was 28.6 kg/m^2, WC 73 cm, FM 23.2 kg, free FM 41.9 kg, and VAT 2.9 kg.

CONCLUSION

VLCKD enabled the patient to reach her target weight and to reduce her joint pain and headaches. Laboratory inflammatory indices also normalized.

Key Words: Very low calorie ketogenic diet; Inflammation; PNK® method; Weight loss; Obesity; Rheumatic disorders; Case report

Core Tip: A commercial weight-loss program (PNK® method) was used, based on a very low calorie ketogenic diet (VLCKD). VLCKD allowed the patient to achieve weight goal, better management of joint pain, headache episodes and normalization of inflammatory indices.

Citation: Rondanelli M, Patelli Z, Gasparri C, Mansueto F, Ferraris C, Nichetti M, Alalwan TA, Sajoux I, Maugeri R, Perna S. Very low calorie ketogenic diet and common rheumatic disorders: A case report. *World J Clin Cases* 2023; 11(9): 1985-1991

URL: https://www.wjgnet.com/2307-8960/full/v11/i9/1985.htm

DOI: https://dx.doi.org/10.12998/wjcc.v11.i9.1985

INTRODUCTION

Nutritional ketosis has been used since the 1920s as a treatment for refractory epilepsy[1] and the very low calorie ketogenic diet (KD) is currently gaining popularity as a potential therapy for obesity and metabolic disorders[2].

The Italian Association of Dietetics and Clinical Nutrition gives the following indications for very low calorie ketogenic diet (VLCKD): Morbid obesity or obesity with comorbidities (including type 2 diabetes, dyslipidemia, hypertension, metabolic syndrome, obstructive sleep apnea syndrome, bone disease or severe arthropathy); the preoperative period of severe obesity with an indication for bariatric surgery; patients with severe comorbidities and overweight, necessitating rapid weight loss; non-alcoholic fatty liver disease; and drug-resistant epilepsy[3,4].

In addition to these established indications, the scientific literature advocates the use of nutritional ketosis in the treatment of chronic inflammatory diseases, as recent studies have shown that ketone bodies have anti-inflammatory activity in numerous diseases[5,6].

The ketone body β-hydroxybutyrate (βOHB) is elevated during VLCKD treatment, and there is increasing evidence that βOHB acts not only as an energy substrate but also as a signaling molecule[6]. βOHB is a ligand for G protein-coupled receptors that bind short-chain fatty acids, including hydroxy-carboxylic acid receptor 2 and free fatty acid receptor 3. It can attenuate oxidative stress in the spinal cord and kidney by suppressing class I histone deacetylases[6] and has been shown to suppress NOD-like receptor family pyrin domain containing 3 inflammasome-mediated inflammatory disease[6-10].

Inflammatory rheumatic disorders induce chronic inflammation in joints and other tissues[11] and are characterized by an increased expression of several proinflammatory cytokines, including interleukin (IL)-1, IL-6, tumour necrosis factor-α, IL-23, and IL-17[12].

A more recent review by Ciaffi *et al*[13] suggests that the KD could play a role in the treatment of patients with rheumatic musculoskeletal diseases as the KD can facilitate weight loss and modulate systemic inflammation, resulting in a rapid response to systemic therapy[13].

In obese patients, the VLCKD was significantly more effective than a standard low-calorie diet in terms of weight loss[14,15]. It has also been demonstrated that a VLCKD supplemented with omega-3 docosahexaenoic acid (DHA) has a significantly superior anti-inflammatory effect, despite non-significant differences in weight loss and metabolic improvement[16].

Given the potential benefits, a 22-year-old woman with a body mass index (BMI) of 30.8 kg/m^2 and who had been diagnosed with juvenile idiopathic arthritis at the age of 4 years, was started on a VLCKD.

CASE PRESENTATION

Chief complaints

A 22-year-old woman attended outpatients at the Santa Margherita Nutritional Rehabilitation Institute, Pavia, Italy, for an endocrinology and dietary consultation. The patient reported gradual and persistent weight gain from the age of 10 years.

History of present illness

She had been diagnosed with juvenile idiopathic arthritis at age of 4 years, and occasionally presented headache and alternating episodes of constipation and diarrhea.

At the time of her first consultation at this outpatients, she was on estrogen-progestogen therapy and had been prescribed naproxen 550 mg or 7.5 mg meloxicam as required.

Physical examination

Weight (kg) was measured to an accuracy of ± 0.05 kg, and BMI was calculated as weight in kilograms divided by height in meters squared (kg/m^2). Bioimpedance analysis (Zeus, Cosmed, Italy) provided whole-body and compartmentalized values for fat mass (FM) and fat-free mass, visceral adipose tissue (VAT), and intra- and extracellular water analysis for estimating hydration status.

Additionally, waist circumference (WC) was measured by a trained dietician at the level of the umbilicus at the end of normal expiration using a non-elastic measuring tape.

The patient's baseline basal metabolic rate (BMR) was assessed by indirect calorimetry (Cosmed Q-NRG) at the first anthropometric and nutritional evaluation.

The patient never had significant limitations in physical activity.

FINAL DIAGNOSIS

The patient had juvenile idiopathic arthritis and I grade obesity.

TREATMENT

The initial dietary approach was a balanced, low-calorie diet based on World Health Organization (WHO) criteria (WHO, Washington, DC, United States)[17] adapted to the BMR calculated by indirect calorimetry.

Then, the patient was started on a commercial weight-loss program based on a VLCKD (PNK® method, Barcelona, Spain). This program consists of high-biological-value protein products and whole natural foods. Each protein food provides 90-120 kcal and it's composed by 15 g protein, 4 g carbohydrate, 3 g fat, and 50 mg omega-3 DHA. The program consists of three phases: Intervention, dietary re-education, and maintenance (Table 1).

The intervention phase consists of a very low calorie diet (600–800 kcal/day), with a low content of carbohydrate (20–50 g/day), and fat (10 g/day of olive oil). The intake of high-biological-value protein is fixed around 0.8 and 1.2 g *per* kg ideal body weight *per* day, in order to ensure the coverage of protein requirements. The intervention phase is composed by 3 steps. In step 1, patients consume 5 protein servings at high-biological-value and 2 portions of vegetables. The permitted vegetables are divided into two groups. Vegetables in group A have a very low glycemic index and include chard, celery, watercress, borage, broccoli, soybean sprouts, zucchini, lamb's lettuce, cauliflower, chicory, spinach, turnip greens, fennel, lettuce, cucumber, pickled gherkins, green peppers, mushrooms, radishes, and rocket; consumption of these vegetables is not limited. Vegetables in group B have a low glycemic index and include artichoke, eggplant, cabbage, asparagus, green beans, turnip, yellow and red peppers, leeks, and tomatoes; consumption is limited to 100 g *per* day.

During step 2, a natural protein serving (100-150 g of meat, poultry, fish, or seafood, canned tuna in brine or two eggs) is consumed in place of one of the protein preparation, at lunch or dinner. Patients will therefore be consuming four high-biological-value protein preparations *per* day.

In step 3, a fresh source of protein is introduced at both lunch and dinner, choosing between 100-150 g of meat, poultry, fish, seafood, canned tuna in brine, or two eggs. In step 3, patients are therefore eating three high-biological-value protein preparations *per* day.

During the intervention phase, vitamin and mineral supplementation is provided in accordance with international requirements[18]. The composition is shown in Table 2.

During the dietary treatment, the patient followed a specially recommended physical activity program. During step 1, 2, and 3 the recommended physical activity is anaerobic, with toning exercises to be performed preferably in the morning, at least 2 or 3 times a week; each exercise should be performed for 3 sets, with one minute of rest between sets, for a total of 30 min of physical activity. In steps 4 and 5, in addition to toning exercises to be performed at least 2-3 times a week, cardiovascular

Table 1 Structure of the PronoKal PnK method

Intervention (80% of the target weight loss)			Dietary re-education (20% of the target weight loss)		Maintenance
Weight loss					New lifestyle
Step 1: 40% of the target weight loss	Step 2: 20% of the target weight loss	Step 3: 20% of the target weight loss	Step 4: 10% of the target weight loss	Step 5: 10% of the target weight loss	
Very low calorie ketogenic diet (630-700 kcal/day)			Low-calorie diet (800-1500 kcal/day)		Balanced diet (1500-2000 kcal/day)

Table 2 Composition of the vitamin and mineral supplementation during the very low calorie ketogenic diet

	In 2 sachets
Vitamin A (μg)	800
Vitamin D (μg)	5
Vitamin E (mg)	12
Vitamin K (μg)	75
Vitamin C (mg)	80
Thiamine (mg)	1.1
Riboflavin (mg)	1.4
Niacin (mg)	16
Vitamin B6 (mg)	1.4
Folic acid (μg)	200
Vitamin B12 (μg)	2.5
Biotin (μg)	50
Pantothenic acid (mg)	6
Potassium (mg)	2000
Calcium (mg)	800
Magnesium (mg)	375
Iron (g)	14
Zinc (mg)	10
Copper (mg)	1
Manganese (mg)	1
Selenium (μg)	55
Chrome (μg)	40
Molybdenum (μg)	50
Iodine (μg)	150

activity, such as walking or exercise bike of gentle or moderate intensity, is planned for about 50-60 min, twice a week.

During the VLCKD the patient didn't need to take the recommended medications.

OUTCOME AND FOLLOW-UP

After the VLCKD period, the patient has been administered with a low-calorie diet; she reduced her BMI from I class obesity to overweight. Telephone contacts with the patient continue and new check-ups will be scheduled in order to monitor body weight.

DISCUSSION

After two months, at the first follow-up visit, body weight remained unchanged (Table 3) and the patient reported increasing joint pain, for which the rheumatological team introduced hydroxychloroquine 200 mg/day. The patient was not satisfied with either the treatment or the dietary plan.

Given the failure of the low-calorie balanced diet, the nutrition team decided to switch to a VLCKD (the PNK® method). The patient received multidisciplinary support from doctors, physical activity instructors, and nutritionist-coaches throughout follow-up.

The VLCKD intervention was started in early 2022, with a body weight of 79.9 kg. In step 1, the patient lost 8 kg, from 79.9 kg to 72 kg, the WC decreased from 82 cm to 75 cm, and the body composition improved, with a reduction in FM, from 29.4 kg (36.9%) to 25.3 kg (35.1%), and VAT, from 3.8 kg to 3.0 kg. At the follow-up visit at the end of step 1, the patient reported a subjective feeling of well-being and the headaches had ceased.

Step 2 started in February 2022 and led to a further loss of about 4 kg (Table 3). At the follow-up visit at the end of step 2, the patient reported tolerance of the dietary plan and that she performed the physical activity as defined in the PNK program. Her sleep pattern and quality had improved, as had her joint pain, and there had been no recurrence of the headaches. Body weight was 69 kg and the WC 72 cm; FM and the VAT decreased to 23.2 kg and 2.7 kg, respectively (Table 3).

The patient next moved to step 3 in April 2022. Body weight remained unchanged (69 kg) (Table 3). Contact with the patient took place by telephone, hence body composition measurements were not possible.

The patient did not lose weight during two weeks of step 3, and the nutrition team therefore decided to progress to step 4 (dietary re-education phase), moving the patient to a low-calorie diet to favor dietary compliance. During this stage the patient regained some of the weight she had lost, reaching a weight of 72.8 kg (Table 3).

Step 5 was initiated in June 2022 after the patient had completed step 4 and during this final step of the weight-loss phase, the weight remained practically unchanged (Table 3). Contact was by telephone, so again it was not possible to perform body composition analysis. The patient reported a feeling of well-being and good sleep quality, and there was no sensation of hunger.

Despite slight weight regain, the patient reported feeling better than before undertaking the VLCKD. We consider that this effect may be due as much to the beneficial effects of the nutritional ketosis or even the anti-inflammatory effect of the omega-3 DHA supplementation as to the weight loss. The serum inflammatory markers before and during the VLCKD are shown in Table 4.

A blood test was taken during the VLCKD and showed the following: Lupus anticoagulant, negative; silica clotting time ratio, 0.96; Russel's viper venom time ratio, 1.05; ferritin, 10 ng/mL; erythrocyte sedimentation rate (ESR), 31 mm/h; complement component C3, 1.15 g/L; complement component C4, 0.19 g/L; rheumatoid factor, < 20 IU/mL, and C-reactive protein (CRP), < 5 mg/L. Protein electrophoresis trace did not reveal the presence of abnormal monoclonal components and the interferon-gamma release assay was negative.

The administration of a VLCKD would appear to improve all the parameters evaluated in order to assess inflammatory profile. In particular it's noteworthy the reduction of CRP values from 17 mg/L up to the normal range. Similar results were obtained by previous studies conducted in obese[14] and overweight subjects[18].

Anthropometric parameters at baseline and their changes during the dietary treatment are shown in Table 3.

Considering the entire weight loss diet therapy program, from the beginning to the end of the ketogenic phase, the patient lost 5.3 kg (from 78.3 to 73), with a greater weight loss at the end of steps 2 and 3 (-9.3 kg), always going to improve her wellbeing. In steps 4 and 5 the patient gained 4 kg but it is very interesting to note how the improvement in body composition obtained during weight loss phase (with reduction of FM and preservation of fat free mass) has been maintained over time (step 4 and 5).

Finally, also the VAT, which is a well-known cardiovascular risk factor producing chronic low-grade inflammation[19], has significantly reduced (-600 g) from the beginning to the end of dietary program.

The goal of healthy weight loss was therefore achieved, since weight reduction has mainly affected FM, while lean mass was mostly preserved.

CONCLUSION

The VLCKD allowed the patient to achieve her target body weight (reducing from class I obesity to overweight), with an improvement in her joint pain and the episodes of headache, and an improvement in serum inflammatory markers (reduction in CRP from 17 mg/L to 5 mg/L and ESR from 95 mm/h to 31 mm/h).

Table 3 Changes in the anthropometric parameters during dietary treatment

	Base-line	First follow-up visit during LCD	Second follow-up visit during LCD	VLCKD, end Step 1	VLCKD, end Step 2	End of step 3 of intervention phase	End of step 4 of intervention phase	End of step 5 of intervention phase
Body weight (kg)	78.3	78	79.9	72	69	69	72.8	73
BMI (kg/m^2)	30.8	30.7	31.3	28.3	27.1	27.1	28.6	28.7
Waist circum-ference (cm)	80	80	82	75	72	/	73	73
Fat mass (%)	35.9	35.6	36.9	35.1	33.6	/	33.7	/
Fat mass (kg)	28.1	27.8	29.4	25.3	23.2	/	24.5	/
Fat free mass (kg)	45.7	45.8	45.7	42.6	41.9	/	44.2	/
VAT (kg)	3.5	3.4	3.8	3.0	2.7	/	2.9	/

LCD: Low-calorie diet; VLCKD: Very low calorie ketogenic diet; VAT: Visceral adipose tissue.

Table 4 Serum inflammatory markers during dietary treatment

	During the LCD	During the VLCKD	Laboratory reference range
Erythrocyte sedimentation rate (mm/h)	95	31	< 15
C-reactive protein (mg/L)	17	< 5	< 5
Complement component C3 (g/L)	1.34	1.15	0.90-1.80
Complement component C4 (g/L)	0.26	0.19	0.10-0.40
Silica clotting time (ratio)	1.08	0.96	≤ 1.16
Russell's viper venom time (ratio)	1.24	1.05	< 1.20

LCD: Low-calorie diet; VLCKD: Very low calorie ketogenic diet.

FOOTNOTES

Author contributions: Rondanelli M, Sajoux I, and Maugeri R are responsible for conceptualization; Patelli Z, Gasparri C, and Mansueto F are responsible for the investigation; Alalwan TA, and Perna S contributed to the data curation; Patelli Z, and Gasparri C wrote the original draft preparation; Ferraris C, and Nichetti M wrote the review and editing; Rondanelli M is responsible for visualization and project administration; Rondanelli M, Sajoux I, and Maugeri R contributed to the supervision; All authors have read and agreed to the published version of the manuscript.

Informed consent statement: Informed consent was obtained from the participant in the study.

Conflict-of-interest statement: I.S. and R.M. are employed by PronoKal Group. The remaining authors declare no conflict of interest.

CARE Checklist (2016) statement: The authors have read the CARE Checklist (2016), and the manuscript was prepared and revised according to the CARE Checklist (2016).

Country/Territory of origin: Italy

ORCID number: Mariangela Rondanelli 0000-0001-8336-4851; Clara Gasparri 0000-0002-1088-6648; Mara Nichetti 0000-0003-1902-817X; Simone Perna 0000-0002-2720-1473.

S-Editor: Fan JR
L-Editor: A
P-Editor: Fan JR

REFERENCES

1 **Cooder HR**. Epilepsy in Children: With Particular Reference to the Ketogenic Diet. *Cal West Med* 1933; **39**: 169-173 [PMID: 18742621]
2 **Caprio M**, Infante M, Moriconi E, Armani A, Fabbri A, Mantovani G, Mariani S, Lubrano C, Poggiogalle E, Migliaccio S, Donini LM, Basciani S, Cignarelli A, Conte E, Ceccarini G, Bogazzi F, Cimino L, Condorelli RA, La Vignera S, Calogero AE, Gambineri A, Vignozzi L, Prodam F, Aimaretti G, Linsalata G, Buralli S, Monzani F, Aversa A, Vettor R, Santini F, Vitti P, Gnessi L, Pagotto U, Giorgino F, Colao A, Lenzi A; Cardiovascular Endocrinology Club of the Italian Society of Endocrinology. Very-low-calorie ketogenic diet (VLCKD) in the management of metabolic diseases: systematic review and consensus statement from the Italian Society of Endocrinology (SIE). *J Endocrinol Invest* 2019; **42**: 1365-1386 [PMID: 31111407 DOI: 10.1007/s40618-019-01061-2]
3 **Muscogiuri G**, Barrea L, Laudisio D, Pugliese G, Salzano C, Savastano S, Colao A. The management of very low-calorie ketogenic diet in obesity outpatient clinic: a practical guide. *J Transl Med* 2019; **17**: 356 [PMID: 31665015 DOI: 10.1186/s12967-019-2104-z]
4 **Muscogiuri G**, El Ghoch M, Colao A, Hassapidou M, Yumuk V, Busetto L; Obesity Management Task Force (OMTF) of the European Association for the Study of Obesity (EASO). European Guidelines for Obesity Management in Adults with a Very Low-Calorie Ketogenic Diet: A Systematic Review and Meta-Analysis. *Obes Facts* 2021; **14**: 222-245 [PMID: 33882506 DOI: 10.1159/000515381]
5 **Puchalska P**, Crawford PA. Multi-dimensional Roles of Ketone Bodies in Fuel Metabolism, Signaling, and Therapeutics. *Cell Metab* 2017; **25**: 262-284 [PMID: 28178565 DOI: 10.1016/j.cmet.2016.12.022]
6 **Newman JC**, Verdin E. Ketone bodies as signaling metabolites. *Trends Endocrinol Metab* 2014; **25**: 42-52 [PMID: 24140022 DOI: 10.1016/j.tem.2013.09.002]
7 **Shimazu T**, Hirschey MD, Newman J, He W, Shirakawa K, Le Moan N, Grueter CA, Lim H, Saunders LR, Stevens RD, Newgard CB, Farese RV Jr, de Cabo R, Ulrich S, Akassoglou K, Verdin E. Suppression of oxidative stress by β-hydroxybutyrate, an endogenous histone deacetylase inhibitor. *Science* 2013; **339**: 211-214 [PMID: 23223453 DOI: 10.1126/science.1227166]
8 **Cheng CW**, Biton M, Haber AL, Gunduz N, Eng G, Gaynor LT, Tripathi S, Calibasi-Kocal G, Rickelt S, Butty VL, Moreno-Serrano M, Iqbal AM, Bauer-Rowe KE, Imada S, Ulutas MS, Mylonas C, Whary MT, Levine SS, Basbinar Y, Hynes RO, Mino-Kenudson M, Deshpande V, Boyer LA, Fox JG, Terranova C, Rai K, Piwnica-Worms H, Mihaylova MM, Regev A, Yilmaz ÖH. Ketone Body Signaling Mediates Intestinal Stem Cell Homeostasis and Adaptation to Diet. *Cell* 2019; **178**: 1115-1131.e15 [PMID: 31442404 DOI: 10.1016/j.cell.2019.07.048]
9 **Kong G**, Liu J, Li R, Lin J, Huang Z, Yang Z, Wu X, Zhu Q. Ketone Metabolite β-Hydroxybutyrate Ameliorates Inflammation After Spinal Cord Injury by Inhibiting the NLRP3 Inflammasome. *Neurochem Res* 2021; **46**: 213-229 [PMID: 33108630 DOI: 10.1007/s11064-020-03156-2]
10 **Kong G**, Huang Z, Ji W, Wang X, Liu J, Wu X, Li R, Zhu Q. The Ketone Metabolite β-Hydroxybutyrate Attenuates Oxidative Stress in Spinal Cord Injury by Suppression of Class I Histone Deacetylases. *J Neurotrauma* 2017; **34**: 2645-2655 [PMID: 28683591 DOI: 10.1089/neu.2017.5192]
11 **Korte SM**, Straub RH. Fatigue in inflammatory rheumatic disorders: pathophysiological mechanisms. *Rheumatology (Oxford)* 2019; **58**: v35-v50 [PMID: 31682277 DOI: 10.1093/rheumatology/kez413]
12 **Gabay C**, McInnes IB. The biological and clinical importance of the 'new generation' cytokines in rheumatic diseases. *Arthritis Res Ther* 2009; **11**: 230 [PMID: 19519923 DOI: 10.1186/ar2680]
13 **Ciaffi J**, Mitselman D, Mancarella L, Brusi V, Lisi L, Ruscitti P, Cipriani P, Meliconi R, Giacomelli R, Borghi C, Ursini F. The Effect of Ketogenic Diet on Inflammatory Arthritis and Cardiovascular Health in Rheumatic Conditions: A Mini Review. *Front Med (Lausanne)* 2021; **8**: 792846 [PMID: 34970568 DOI: 10.3389/fmed.2021.792846]
14 **Rondanelli M**, Perna S, Ilyas Z, Peroni G, Bazire P, Sajuox I, Maugeri R, Nichetti M, Gasparri C. Effect of very low-calorie ketogenic diet in combination with omega-3 on inflammation, satiety hormones, body composition, and metabolic markers. A pilot study in class I obese subjects. *Endocrine* 2022; **75**: 129-136 [PMID: 34532829 DOI: 10.1007/s12020-021-02860-5]
15 **Moreno B**, Bellido D, Sajoux I, Goday A, Saavedra D, Crujeiras AB, Casanueva FF. Comparison of a very low-calorie-ketogenic diet with a standard low-calorie diet in the treatment of obesity. *Endocrine* 2014; **47**: 793-805 [PMID: 24584583 DOI: 10.1007/s12020-014-0192-3]
16 **de Luis D**, Domingo JC, Izaola O, Casanueva FF, Bellido D, Sajoux I. Effect of DHA supplementation in a very low-calorie ketogenic diet in the treatment of obesity: a randomized clinical trial. *Endocrine* 2016; **54**: 111-122 [PMID: 27117144 DOI: 10.1007/s12020-016-0964-z]
17 **World Health Organization (WHO) Technical Report Series 894**. Obesity: preventing and managing the global epidemic. Report of a WHO consultation. [cited 10 October 2022]. Available from: https://www.who.int/
18 **Merra G**, Gratteri S, De Lorenzo A, Barrucco S, Perrone MA, Avolio E, Bernardini S, Marchetti M, Di Renzo L. Effects of very-low-calorie diet on body composition, metabolic state, and genes expression: a randomized double-blind placebo-controlled trial. *Eur Rev Med Pharmacol Sci* 2017; **21**: 329-345 [PMID: 28165552]
19 **Magnuson AM**, Fouts JK, Regan DP, Booth AD, Dow SW, Foster MT. Adipose tissue extrinsic factor: Obesity-induced inflammation and the role of the visceral lymph node. *Physiol Behav* 2018; **190**: 71-81 [PMID: 29501838 DOI: 10.1016/j.physbeh.2018.02.044]

World Journal of Clinical Cases

Submit a Manuscript: https://www.f6publishing.com

World J Clin Cases 2023 March 26; 11(9): 1992-2001

DOI: 10.12998/wjcc.v11.i9.1992

ISSN 2307-8960 (online)

CASE REPORT

Delayed versus immediate intervention of ruptured brain arteriovenous malformations: A case report

Andi Kurnia Bintang, Ashari Bahar, Muhammad Akbar, Gita Vita Soraya, Anthony Gunawan, Nurussyariah Hammado, Mochammad Erwin Rachman, Zulvikar Syambani Ulhaq

Specialty type: Neurosciences

Provenance and peer review: Unsolicited article; Externally peer reviewed.

Peer-review model: Single blind

Peer-review report's scientific quality classification

Grade A (Excellent): 0
Grade B (Very good): 0
Grade C (Good): C, C
Grade D (Fair): 0
Grade E (Poor): 0

P-Reviewer: Kumar S, India; Sidoti A

Received: October 7, 2022
Peer-review started: October 7, 2022
First decision: November 22, 2022
Revised: December 7, 2022
Accepted: February 22, 2023
Article in press: February 22, 2023
Published online: March 26, 2023

Andi Kurnia Bintang, Ashari Bahar, Muhammad Akbar, Gita Vita Soraya, Anthony Gunawan, Nurussyariah Hammado, Mochammad Erwin Rachman, Department of Neurology, Hasanuddin University, Makassar 90245, Indonesia

Gita Vita Soraya, Department of Biochemistry, Faculty of Medicine, Hasanuddin University, Makassar 90245, Indonesia

Nurussyariah Hammado, Faculty of Health and Sport Science, State University of Makassar, Makassar 90222, Indonesia

Mochammad Erwin Rachman, Faculty of Medicine, Muslim University of Indonesia, Makassar 90231, Indonesia

Zulvikar Syambani Ulhaq, Research Center for Preclinical and Clinical Medicine, National Research and Innovation Agency Republic of Indonesia, Cibinong 16911, Indonesia

Zulvikar Syambani Ulhaq, Laboratory of Developmental Disorders and Toxicology, Kyushu University, Fukuoka 8190395, Japan

Zulvikar Syambani Ulhaq, Department of Biomedical Science, Faculty of Medicine and Health Sciences, Maulana Malik Ibrahim State Islamic University, Malang 65144, Indonesia

Corresponding author: Ashari Bahar, MD, Consultant Physician-Scientist, Department of Neurology, Hasanuddin University, Jl. Perintis Kemerdekaan No.KM.10, Makassar 90245, Indonesia. asharibahar@med.unhas.ac.id

Abstract

BACKGROUND

Brain arteriovenous malformations (bAVMs) remains one of the most prevalent causes of intracranial hemorrhage and stroke-like syndromes in the young adult population. Although it has been agreed upon that definitive treatment using either single or multi-modal approach is warranted for successful bAVM management, much debate still revolves regarding the optimal timing of definitive treatment.

CASE SUMMARY

In this report, we present a case of delayed, definitive endovascular treatment for ruptured bAVM in a 21-year-old female, 3 mo post-ictus. The bAVM, with a left

pericallosal feeding artery and cortical draining veins, was successfully obliterated through embolization using the Onyx 18. On follow-up the patient has recommenced her daily activities and experiences only mild occasional headaches with mild motor deficits. The report leads to our review on an important issue regarding the optimal timing of ruptured bAVM definitive management and bring forward the current evidence available on delayed *vs* immediate definitive bAVM intervention. We also highlight current issues that need to be addressed for clearer guidelines on definitive therapy initiation.

CONCLUSION

Current treatment paradigms of ruptured bAVM remains elusive, with substantial heterogeneity in the current literature. A consensus on the definition of "acute" *vs* "delayed", management goal, follow-up length and outcome parameters are required to support formation of a clear paradigm.

Key Words: Brain arteriovenous malformation; Ruptured brain arteriovenous malformation; Definitive intervention; Endovascular treatment; Case report

Core Tip: In this case report, we present an example of successful delayed management of a ruptured brain arteriovenous malformation (bAVM) in a young female. The case is followed by an updated review regarding current "delayed" and "immediate" definitive interventions for bAVMs and problems associated with the current data on the effectivity of these paradigms.

Citation: Bintang AK, Bahar A, Akbar M, Soraya GV, Gunawan A, Hammado N, Rachman ME, Ulhaq ZS. Delayed versus immediate intervention of ruptured brain arteriovenous malformations: A case report. *World J Clin Cases* 2023; 11(9): 1992-2001

URL: https://www.wjgnet.com/2307-8960/full/v11/i9/1992.htm

DOI: https://dx.doi.org/10.12998/wjcc.v11.i9.1992

INTRODUCTION

Brain arteriovenous malformations (bAVMs) continue to be one of the most prevalent causes of intracranial hemorrhage and stroke-like syndromes in the young adult population. It is defined as an anomalous network or nidus occurring within the brain parenchyma, in which a high-flow shunt or bypass occurs between the feeding artery to the veins. A large majority of bAVMs manifest as intracranial hemorrhage as the presenting symptom, due to rupture of the malformation. Hemorrhagic bAVMs have been shown to result in a morbidity rate of 30%-50% and mortality rate of 10%-30%[1]. Additionally, hemorrhagic bAVMs have a re-rupture risk of more than 4.8% per year[2,3].

Definitive treatment of bAVMs consist of three main modalities, namely endovascular embolization, stereotactic radiotherapy, and microsurgical resection or extirpation of the malformation, with the goal of complete nidus obliteration and minimized hemorrhage recurrence. Although it has been agreed upon that definitive treatment using either single or multi-modal approach is warranted for successful bAVM management, much debate still revolves regarding the optimal timing of definitive treatment.

Some indications warrant immediate definitive treatment, such as massive hemorrhage that implies a life-threatening mass effect, rapid neurological deterioration, or the presence of high-risk aneurysms, in which surgical evacuation can be performed in conjunction with definitive resection of small, superficial bAVMs. However, other cases may fall into the category of gray areas for immediate treatment. In fact, many interventionists and surgeons prefer delayed definitive treatment, when possible, due to easier visualization and high success rates. The current guideline on the management of bAVMs has acknowledged the lack of evidence to direct decisions in this setting[2], although some reports have suggested an ideal interval of 2-6 wk from rupture for removal of the bAVM[2,4,5], and that immediate removal may be associated with larger mortality and morbidity risk[5]. Unfortunately, more data is needed to prove either the benefits or disadvantages of both approaches.

Here we present a case report of a successful, delayed, exclusively endovascular management in a young, 21-year-old female with a ruptured bAVM of 3 mo onset. We then emphasize on this highly debatable topic with an updated literature review on the current evidence regarding outcomes of definitive treatment using either of the three modalities.

CASE PRESENTATION

Chief complaints

A 21-year-old female presented to Dr. Wahidin Sudirohusodo General Hospital, Makassar, Indonesia, in September 2021 with a chief complaint of weakness on the right side of her body, in addition to right-sided hypoesthesia and occasional headaches.

History of present illness

The complaints were first experienced 3 mo prior, with sudden onset, while the patient was performing her daily activities as a college student. She also recalled other symptoms upon onset, such as headache, transient vision loss, slurred speech, and vomiting. At the time, she experienced a brief period of loss of consciousness and was treated conservatively at her local health care center due to lack of imaging modalities.

History of past illness

The patient had no prior history of trauma, infection, hypertension, diabetes, or stroke.

Personal and family history

The patient had no significant personal or family history to disclose.

Physical examination

On presentation at our center, her vital signs were normal. The neurological bedside examination revealed a GCS score of 15, no meningeal signs, and good cognitive function. Her cranial nerve assessment was within normal limits. The motor strength assessment showed weakness on the right side with a strength score of 4 on the right upper and lower extremities. The right extremities also showed increased tone and physiologic reflexes. No pathologic reflexes were observed. The exam also showed right sided hypoesthesia. Autonomic function was within normal limits.

Laboratory examinations

Laboratory tests, chest X-rays, and electrocardiography exams showed no abnormal findings.

Imaging examinations

The first imaging examination was a non-contrast head computed tomography (CT) scan performed a few days after the onset, at the patient's regional hospital. The exam revealed an intracerebral hematoma of the left cerebral hemisphere (Figure 1). Due to the rise in COVID-19 cases at the time, her referral to Dr. Wahidin Sudirohusodo General Hospital for further investigation and definitive therapy was delayed based on her family's decision, and she was given conservative treatment.

A head CT angiography (Figure 2) was performed approximately 2 mo after onset, revealing the presence of an arteriovenous malformation (AVM) on the left frontal lobe with a feeding artery from the left anterior cerebral artery, draining into the superior sagittal sinus.

We performed a digital subtraction angiography (DSA) on the patient a few days after her admission in our center (Figure 3). The DSA confirmed that the bAVM fed off the left pericallosal artery, with two draining veins, one towards the cortical vein while the other has undergone stenosis. We graded the AVM as a Spetzler-Martin Grade II AVM.

FINAL DIAGNOSIS

Based on the clinical findings, the patient was diagnosed with bAVM.

TREATMENT

The patient was subjected to a definitive therapy of embolization on the left pericallosal artery using the Onyx 18 until the nidus and draining vein can no longer be visualized (Figure 4). The patient was tolerant of the whole procedure, and no additional deficits were experienced throughout her care, and was discharged from the hospital a few days following embolization.

OUTCOME AND FOLLOW-UP

The patient returned 3 mo after the procedure for a follow-up visit to the Neurology Outpatient Clinic of Dr. Wahidin Sudirohusodo General Hospital. Her follow-up CT-scan revealed encephalomalacia of

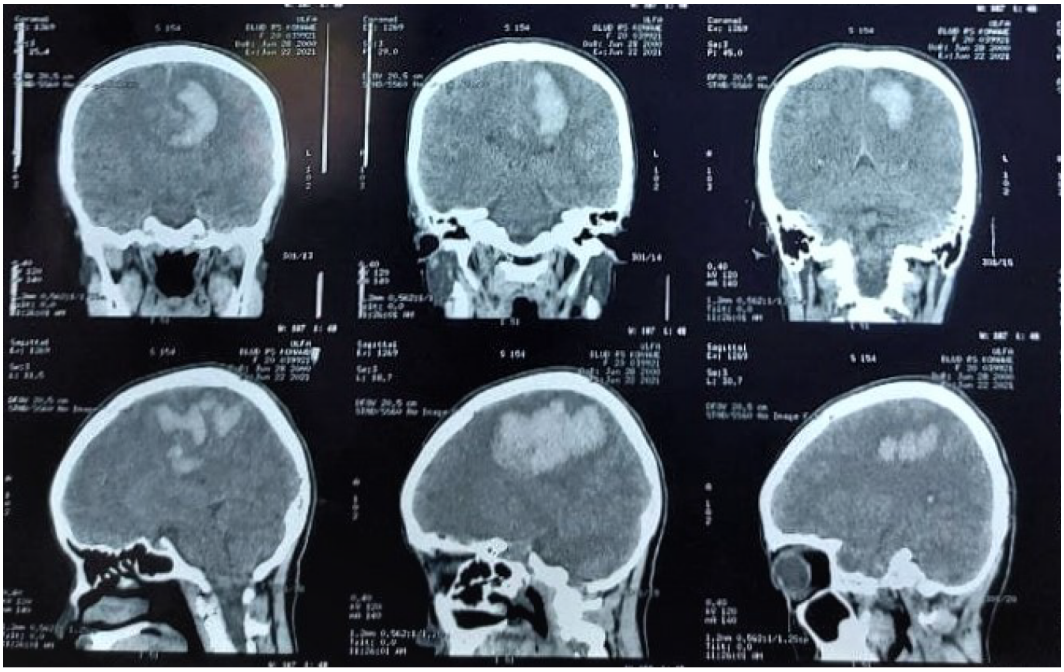

DOI: 10.12998/wjcc.v11.i9.1992

Figure 1 Head non-contrast computed tomography scan on onset (3 mo prior to presentation at our center), revealing extensive intracerebral hematoma of the left cerebral hemisphere.

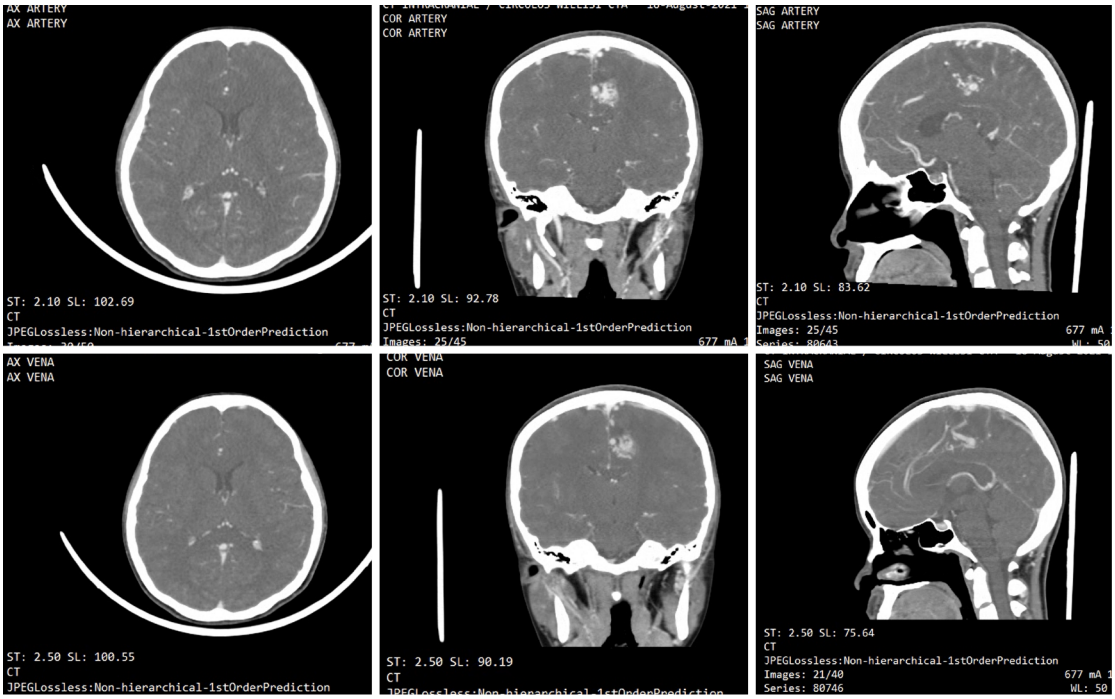

DOI: 10.12998/wjcc.v11.i9.1992

Figure 2 Subsequent head computed tomography angiography was performed 2 mo after onset, revealing the brain arteriovenous malformation, with a feeding artery from the left anterior cerebral artery, draining into the superior sagittal sinus.

the parasagittal region at the left frontal and parietal lobes with mild dilatation of the left lateral ventricle (Figure 5). And to date, approximately 1 year after the procedure, the patient has experienced no rebleeding. She currently lives with minor motor deficit resulting in abnormal gait, and experiences occasional headaches which are manageable with over-the-counter therapy (Glasgow Outcome Scale Score = 2).

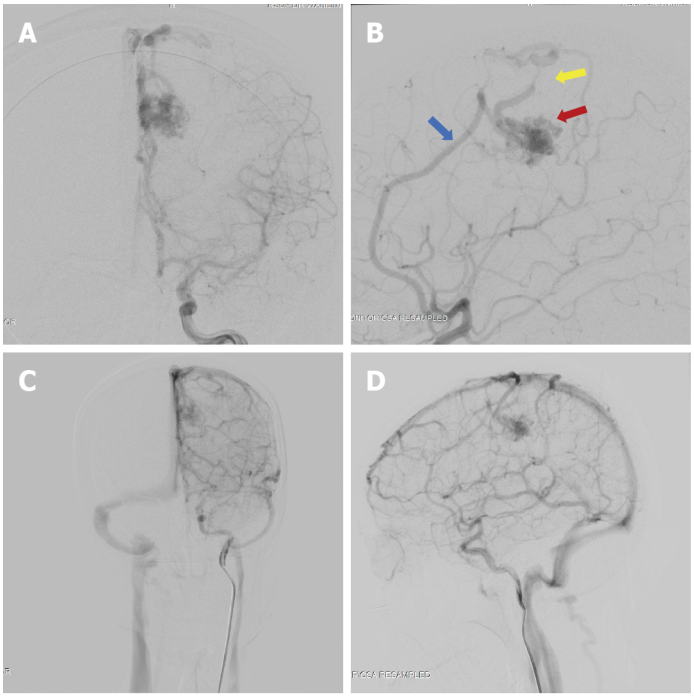

DOI: 10.12998/wjcc.v11.i9.1992

Figure 3 Digital subtraction angiography results of the patient. The digital subtraction angiography image revealed the presence of an arteriovenous malformation (red arrow) feeding off the left pericallosal artery (blue arrow) and draining towards the cortical vein and a stenotic vein (yellow arrow). A: Late arterial phase anterior-posterior view; B: Late arterial phase, lateral view; C: Late venous phase, antero-posterior view; D: Late venous phase, lateral view.

DISCUSSION

The case we presented is one of the many ruptured bAVM cases encountered in our center that was successfully managed using delayed definitive treatment. The 21-year-old female experienced an intracerebral hematoma due to the bAVM rupture, leading to neurological deficits in the form of right-sided weakness and hypoesthesia. The bAVM was visualized on CT-angiography, then gold-standard DSA and definitive endovascular treatment was performed 3 mo after the rupture. The bAVM was treated successfully and the patient was able to recommence her daily activities.

In this instance, the delay to definitive investigations and therapy was coincidental, due to the high wave of the COVID-19 pandemic. But on many occasions, the delay is more deliberate, with interventionists arguing against immediate definitive intervention due to difficulties associated with vascular visualization during acute stages of hematoma. Despite the ongoing approach of either delayed or immediate treatment, there still is insufficient evidence to provide definite recommendations.

In this section, we present the current evidence regarding immediate and delayed treatment of bAVMs. Whilst there is currently a lack of studies comparing the two paradigm approaches, we have summarized individual studies looking at either of the two approaches when feasible, with results summarized in Table 1[6-15]. Traditionally, indications for emergency or immediate intervention of ruptured bAVMs include patients with life-threatening hematoma and its associated mass effects, deteriorating neurological status, and the presence of aneurysms[5,8]. In a state of emergency described above, there is no ambiguity, and the decision for immediate evacuation or decompressive craniectomy is clear. In conjunction with the emergency evacuation, extirpation of small superficial bAVMs is typically performed. The question that remains is whether immediate resection or obliteration of the bAVM is more beneficial in patients that do not have any life-threatening indications. Some experts have stated that acute definitive management is required for a good outcome, arguing that treatment delay require patients to recover twice, both from the hemorrhage and from the subsequent definitive intervention[16]. Some centers have argued that early surgery can achieve better rebleeding protection, reduce length-of-stay, and allow earlier initiation of rehabilitation.

On the other hand, arguments supporting delayed definitive treatment state that surgical management of bAVMs should be performed following recovery of the brain from injury and to wait for stabilization of the patient's general condition. A highly variable rest period of 1-6 wk between hemorrhage and definitive treatment is generally advocated in several literatures[4,15,17]. There are several other issues associated with acute interventions such as secondary edema and challenging visualization of compressed vessels, and therefore, delaying the intervention allows edema reduction that is most pronounced in the early days post hemorrhage[5]. There are also concerning observations regarding the hazardous consequences of early intervention, that have led to preventable neurological

Table 1 Summary of the current evidence on delayed versus immediate treatment of ruptured brain arteriovenous malformations

Ref.	Time from ictus (rupture)	bAVM type and SMG	Modality of definitive treatments	Number of subjects	Age	Outcome	Follow-up period	Result
Bartolomeo *et al*[6], 2021	48 h; > 48 h	I-IV	Surgery; multimodal evacuation of hematoma	25	Mean age 38 and 45.55	mRS score	3 mo and 1 yr	Surgery after rest period is better, but early surgery seems reasonable for young patients
Mansur *et al* [7], 2021	48 h; > 48 h	I-IV	Targeted embolization; surgery; combination of delayed therapy; observation	32 acute; 284 non-acute	Mean age of acute: 32; non acute: 284	Change in mRS score and clinical outcome/re-rupture	Mean 3.2 ± 1.4 yr	Delayed curative treatment preferred. Acute targeted embolization warranted for weak points
Beecher *et al* [8], 2017	Delayed only: Minimal 4 wk post-hemorrhage	N/A	Radiation; surgery; embolization	102	N/A	Time to treatment failure (re-hemorrhage or neurological decline)	Median 248 d	6 (5.8%) new hemorrhage. Authors in support of delaying treatment for at least weeks to allow for neurologic improvement prior to intervention
Bir *et al*[9], 2016	< 24 h; 24-48 h; > 48 h	I-IV	Embolization; GK SRS; microsurgical resection	78	Median age 45	Mean mRS grading	Mean mo 45.17 (1-223)	Significant difference in mean mRS: Group < 24h *vs* > 48h ($P = 0.01$); Group 24-48 h *vs* > 48 h ($P = 0.03$)
Todnem *et al* [10], 2019	Immediate embolization (time not defined) followed by delayed GK-SRS	III-IV	Embolization and SRS combination	16	Mean age 46.63 yr	mRS score	45.4 21.43 mo	Improvement of mRS score and no recurrent hemorrhage
van Rooij *et al* [11], 2012	Acute phase: Within 10 d of ictus	N/A	Embolization with either coils or Onyx	23	Mean age 42 yr	Obliteration status; hemorrhage recurrence; mortality	21 mo mean	1 death (following surgical evacuation of frontal hematoma); 13 patients had complete obliteration; No new hemorrhage
Andreou *et al* [12], 2008	Median 2 wk after ictus (range 1-28 wk)	Micro-AVM; SMG N/A	Embolization	25	N/A	Procedure-related complic-ations; obliteration status; re-hemorrhage	6 mo	3 complications; 22 complete obliterations; 2 recurrences
Stemer *et al* [13], 2013	Acute phaseMedian 4 d after ictus(Range 8-75)	I-VI	Embolization (Onyx only)	21	Mean age 38 yr	Procedure-related complic-ations; obliteration status; re-hemorrhage; GOS	7.5 mo mean	2 asymptomatic complications; 0 new hemorrhage; 7 complete obliterations after the first procedure; mean GOS improvement from 4.0 on presentation to 4.4 after first procedure
Pavesi *et al* [14], 2009	Acute phase (within 6 d of ictus)	I-II	Radical AVM surgical removal + hematoma evacuation	27	Mean age 41.3 yr	GOS; rehemorrhage; mortality	22 mo mean	85% favorable functional outcome (GOS: good recovery – moderate disability); 2 re-hemorrhages; 7.4% mortality
Kuhmonen *et al*[[15], 2005	Acute phase (within 4 d of ictus)	1-V	Craniotomy and extirpation; ventricular drainage; embolization	49	Mean age 32.8	GOS; mortality	2-3 mo	More than half of the patients had a good functional outcome; Mortality 12.2 %

bAVM: Brain arteriovenous malformation; GOS: Glasgow outcome scale; GK-SRS: Gamma-knife stereotactic radiation surgery; SMG: Spletzer-Martin Grade.

deficits[5]. And finally, several unique conditions may place the patient as a candidate for delayed definitive treatment, such as bAVMs in pregnancy that typically require delay of intervention until post-gestation[18].

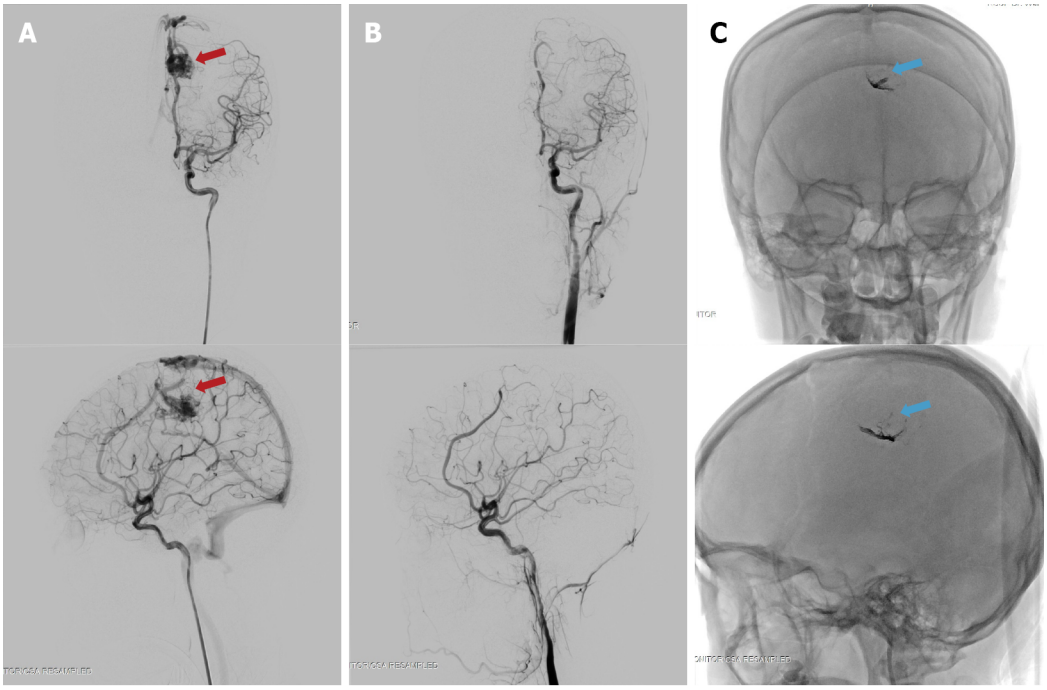

DOI: 10.12998/wjcc.v11.i9.1992

Figure 4 Digital subtraction angiography images before and after the embolization procedure on the brain arteriovenous malformation at approximately 3 mo post-ictus. The embolization procedure was performed on the left pericallosal artery using the Onyx 18 until the nidus and draining vein can no longer be visualized. A: The nidus, before embolization (red arrow) on antero-posterior (top) and lateral (bottom) view of arterial phase; B: Complete obliteration of the nidus after embolization on the arterial phase, antero-posterior (top) and lateral (bottom) view; C: The onyx cast visible through fluoroscopy, on antero-posterior (top) and lateral (bottom) view, indicated with blue arrow.

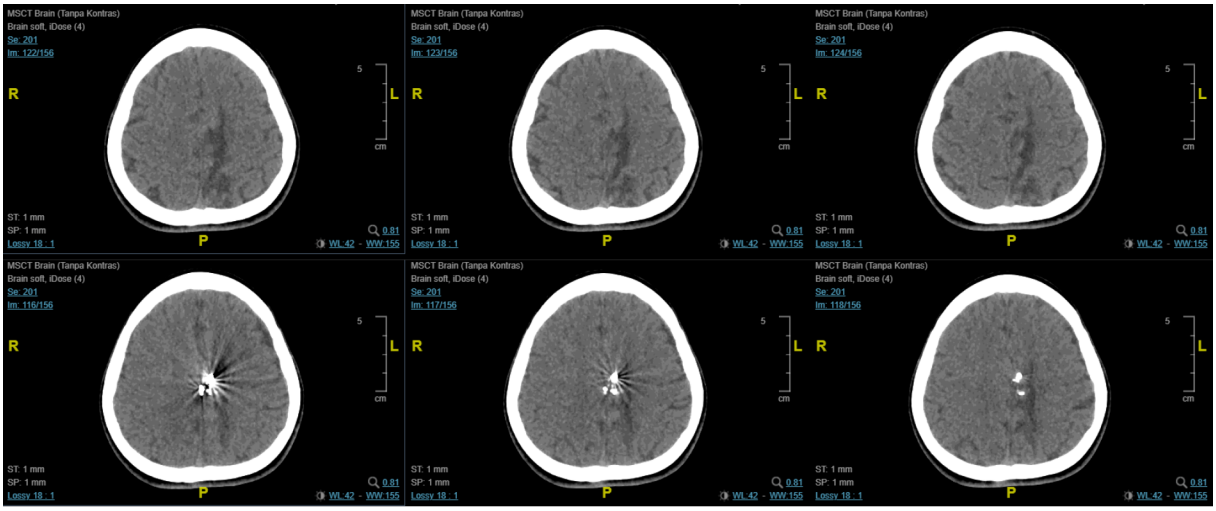

DOI: 10.12998/wjcc.v11.i9.1992

Figure 5 Follow-up computed tomography-scan revealed encephalomalacia of the parasagittal region at the left frontal and parietal lobes with mild dilatation of the left lateral ventricle. A hyperdense blooming artefact is visualized due to the Onyx cast.

Despite the ongoing debate of early *vs* delayed definitive bAVM management, there remains a lack of studies comparing the two approaches and its outcome, especially those performed in a single cohort. The spontaneous supratentorial lobar intracerebral hematomas trial has demonstrated that relative to early surgery, delayed hematoma surgery leads to deterioration. However, its sample population did not include those with hematoma due to AVM associated bleeding[19].

In order to pave the way for more definitive recommendations on the management of AVM ruptures, we propose that several urgent matters need to be addressed. Firstly, a clear consensus on the definition of immediate and delayed definitive treatment in bAVM management is urgently needed. In other words, when is a procedure considered immediate and when is it considered delayed? Most of the included studies in this report had varying time frames of patient inclusion. Additionally, a systematic

approach to this topic is still hindered by the complexity of the management of bAVMs. Until today, intervention of ruptured bAVM is highly multidisciplinary, varies on a case-by-case basis, and is highly dependent on the clinical status, the size and location of the bAVM and the feeding-drainage pattern. This leads to the large heterogeneity in the literature of bAVM investigations. Current clinical trials on bAVM is highly limited, with the largest known trial only focusing on unruptured bAVM (A Randomized Trial of Unruptured Brain AVMs or the ARUBA trial)[20]. Even so, the trial continues to be criticized due to methodological deficiences[21], only further emphasizing the complexity of bAVM management and investigations into the management.

Outcomes of treatment success also needs to be more strictly defined. Commonly measured outcomes include nidus obliteration (which requires additional radiographic evidence in the follow-up period), hemorrhage recurrence, functional status or neurological sequelae, and mortality. A consensus on defined parameters, in addition to a pre-defined length of follow-up will greatly assist in the acquirement of homogenous data that is urgently needed to answer the current questions in regard to which time approach is more superior, with an end goal of a clear treatment paradigm for ruptured bAVM.

Recurrent hemorrhage itself is an important issue in bAVM management, and was shown to occur at an annual rate of 33% for males and 10% for females[22]. Beecher *et al*[8] identified obesity as the main predictor of AVM re-bleeding (P = 0.048). Meanwhile studies focusing on early intervention has identified age as a factor that significantly affects outcome[15]. While it remains unclear whether late or immediate approaches differ in re-hemorrhage rates, early intervention studies have claimed that the approach minimizes complications from delayed venous occlusion and is more efficient as it does not require multiple anesthetics or hospital admissions.

The decision to delay treatment may be supported by the difficulties associated with performing gold-standard angiography in the hyperacute phase. To illustrate, in a cohort described by Andreou *et al*[12], of all 25 patients with acute presentation of micro-bAVM ruputure, only 17 was diagnostic of the AVM. In the acute phase, cerebral lumens undergo compression or destruction due to the surrounding hematoma. Additionally, patients may also experience vascular thrombosis or spasm, further complicating clear visualization of the lesion. Some other reasons include delayed cross-institutional referral, need for additional diagnostic imaging, patient preference, or pregnancy[8].

A recent retrospective study has shown that delayed conclusive treatment yields more favorable functional outcome[6], and that both approaches are influenced by different factors, wherein early intervention is influenced by the ICH score, while the delayed intervention is influenced by the bAVM microarchitecture as defined by the Spetzler-Martin grades. In said study, the mortality rate between the early and delayed group was also significantly different, although this should be interpreted with caution, due to the higher likelihood of high-risk emergency comorbidities accompanying cases of early treatment. Another recent study comparing delayed *vs* acute approaches showed that delayed treatment had significantly higher nidus obliteration rates and were less likely to require multiple treatments[7]. No significant difference was observed in the re-rupture rate or mortality. Interestingly, the study stated that in patients with the acute targeted approach, it's not the acute timing itself rather than the targeted approach that provided a protective effect on the acutely managed patients.

Although this review has focused mainly on the timing of treatment, there has been some interesting development of molecular investigations into bAVM pathomechanism using high-throughput next-generation sequencing and pathway analysis, which may have future implications in the future personalized management of bAVM[23,24]. An example is the recent discovery on the importance of TGF- β signaling in bAVM pathogenesis[24,25]. In the future, as more exploration into bAVM mechanism will be needed to improve personalized management of bAVM.

To our knowledge, this is the first review to summarize the current literature on the topic of delayed *vs* immediate definitive intervention for ruptured bAVMs. Clearly, unless a consensus is reached on the questions raised above, heterogeneity will continue to exist, and a clear paradigm on the timing of definitive treatment of bAVM will continue to be delayed.

CONCLUSION

In this case report and review, we illustrate a common scenario of a delayed approach to bAVM definitive treatment using an endovascular approach. The current treatment paradigm of ruptured bAVM remains elusive, with many interventionists favoring either a delayed or acute treatment approach. There is substantial heterogeneity in the current literature, rendering it highly difficult to determine which of the following time-based approach is more superior. We believe that a consensus on the definition of acute *vs* delayed, the goal of management in ruptured bAVM, the follow-up length and outcome parameters need to be determined in order to acquire homogenous data that can support the formation of a clear treatment paradigm.

ACKNOWLEDGEMENTS

We would like to thank the patient who has participated in this study.

FOOTNOTES

Author contributions: Bahar A and Bintang AK conceptualized and supervised the study, performed the data collection and finalized the manuscript; Bahar A, Soraya GV and Bintang AK drafted the manuscript and revised the manuscript; Ulhaq ZS and Soraya GV performed the systematic review; Gunawan A, Akbar M, Hammado N, Rachman ME, and Ulhaq ZS revised the manuscript and provided substantial input; all authors have read and approved the final manuscript.

Informed consent statement: The subject described in the case report has provided written consent for publication.

Conflict-of-interest statement: The authors declare no conflict of interest.

CARE Checklist (2016) statement: The authors have read the CARE Checklist (2016), and the manuscript was prepared and revised according to the CARE Checklist (2016).

Country/Territory of origin: Indonesia

ORCID number: Ashari Bahar 0000-0001-8994-1816; Gita Vita Soraya 0000-0002-2656-4176; Zulvikar Syambani Ulhaq 0000-0002-2659-1940.

S-Editor: Chang KL
L-Editor: A
P-Editor: Chang KL

REFERENCES

1 **Stapf C**, Mast H, Sciacca RR, Choi JH, Khaw AV, Connolly ES, Pile-Spellman J, Mohr JP. Predictors of hemorrhage in patients with untreated brain arteriovenous malformation. *Neurology* 2006; **66**: 1350-1355 [PMID: 16682666 DOI: 10.1212/01.wnl.0000210524.68507.87]
2 **Derdeyn CP**, Zipfel GJ, Albuquerque FC, Cooke DL, Feldmann E, Sheehan JP, Torner JC; American Heart Association Stroke Council. Management of Brain Arteriovenous Malformations: A Scientific Statement for Healthcare Professionals From the American Heart Association/American Stroke Association. *Stroke* 2017; **48**: e200-e224 [PMID: 28642352 DOI: 10.1161/STR.0000000000000134]
3 **Kim H**, Al-Shahi Salman R, McCulloch CE, Stapf C, Young WL; MARS Coinvestigators. Untreated brain arteriovenous malformation: patient-level meta-analysis of hemorrhage predictors. *Neurology* 2014; **83**: 590-597 [PMID: 25015366 DOI: 10.1212/WNL.0000000000000688]
4 **Zacharia BE**, Vaughan KA, Jacoby A, Hickman ZL, Bodmer D, Connolly ES Jr. Management of ruptured brain arteriovenous malformations. *Curr Atheroscler Rep* 2012; **14**: 335-342 [PMID: 22623087 DOI: 10.1007/s11883-012-0257-9]
5 **Aoun SG**, Bendok BR, Batjer HH. Acute management of ruptured arteriovenous malformations and dural arteriovenous fistulas. *Neurosurg Clin N Am* 2012; **23**: 87-103 [PMID: 22107861 DOI: 10.1016/j.nec.2011.09.013]
6 **Di Bartolomeo A**, Scafa AK, Giugliano M, Dugoni DE, Ruggeri AG, Delfini R. Ruptured Brain Arteriovenous Malformations: Surgical Timing and Outcomes-A Retrospective Study of 25 Cases. *J Neurosci Rural Pract* 2021; **12**: 4-11 [PMID: 33551615 DOI: 10.1055/s-0040-1716792]
7 **Mansur A**, Kostynskyy A, Krings T, Agid R, Radovanovic I, Mendes Pereira V. The safety profile and angioarchitectural changes after acute targeted embolization of ruptured arteriovenous malformations. *J Neurosurg* 2021; 1-10 [PMID: 33962377 DOI: 10.3171/2020.9.JNS201558]
8 **Beecher JS**, Lyon K, Ban VS, Vance A, McDougall CM, Whitworth LA, White JA, Samson D, Batjer HH, Welch BG. Delayed treatment of ruptured brain AVMs: is it ok to wait? *J Neurosurg* 2018; **128**: 999-1005 [PMID: 28686111 DOI: 10.3171/2017.1.JNS16745]
9 **Bir SC**, Maiti TK, Konar S, Nanda A. Overall outcomes following early interventions for intracranial arteriovenous malformations with hematomas. *J Clin Neurosci* 2016; **23**: 95-100 [PMID: 26321303 DOI: 10.1016/j.jocn.2015.05.041]
10 **Todnem N**, Ward A, Nahhas M, Vender JR, Alleyne CH, Rahimi SY. A Retrospective Cohort Analysis of Hemorrhagic Arteriovenous Malformations Treated with Combined Endovascular Embolization and Gamma Knife Stereotactic Radiosurgery. *World Neurosurg* 2019; **122**: e713-e722 [PMID: 30394359 DOI: 10.1016/j.wneu.2018.10.125]

11 **van Rooij WJ**, Jacobs S, Sluzewski M, Beute GN, van der Pol B. Endovascular treatment of ruptured brain AVMs in the acute phase of hemorrhage. *AJNR Am J Neuroradiol* 2012; **33**: 1162-1166 [PMID: 22282446 DOI: 10.3174/ajnr.A2995]

12 **Andreou A**, Ioannidis I, Lalloo S, Nickolaos N, Byrne JV. Endovascular treatment of intracranial microarteriovenous malformations. *J Neurosurg* 2008; **109**: 1091-1097 [PMID: 19035724 DOI: 10.3171/JNS.2008.109.12.1091]

13 **Stemer AB**, Bank WO, Armonda RA, Liu AH, Herzig DW, Bell RS. Acute embolization of ruptured brain arteriovenous malformations. *J Neurointerv Surg* 2013; **5**: 196-200 [PMID: 22406978 DOI: 10.1136/neurintsurg-2011-010214]

14 **Pavesi G**, Rustemi O, Berlucchi S, Frigo AC, Gerunda V, Scienza R. Acute surgical removal of low-grade (Spetzler-Martin I-II) bleeding arteriovenous malformations. *Surg Neurol* 2009; **72**: 662-667 [PMID: 19604554 DOI: 10.1016/j.surneu.2009.03.035]

15 **Kuhmonen J**, Piippo A, Väärt K, Karatas A, Ishii K, Winkler P, Niemelä M, Porras M, Hernesniemi J. Early surgery for ruptured cerebral arteriovenous malformations. *Acta Neurochir Suppl* 2005; **94**: 111-114 [PMID: 16060249 DOI: 10.1007/3-211-27911-3_17]

16 **Hafez A**, Oulasvirta E, Koroknay-Pál P, Niemelä M, Hernesniemi J, Laakso A. Timing of surgery for ruptured supratentorial arteriovenous malformations. *Acta Neurochir (Wien)* 2017; **159**: 2103-2112 [PMID: 28894970 DOI: 10.1007/s00701-017-3315-9]

17 **Ogilvy CS**, Stieg PE, Awad I, Brown RD Jr, Kondziolka D, Rosenwasser R, Young WL, Hademenos G; Stroke Council, American Stroke Association. Recommendations for the management of intracranial arteriovenous malformations: a statement for healthcare professionals from a special writing group of the Stroke Council, American Stroke Association. *Circulation* 2001; **103**: 2644-2657 [PMID: 11382737 DOI: 10.1161/01.cir.103.21.2644]

18 **Salvati A**, Ferrari C, Chiumarulo L, Medicamento N, Dicuonzo F, De Blasi R. Endovascular treatment of brain arteriovenous malformations ruptured during pregnancy--a report of two cases. *J Neurol Sci* 2011; **308**: 158-161 [PMID: 21719029 DOI: 10.1016/j.jns.2011.06.015]

19 **Mendelow AD**, Gregson BA, Fernandes HM, Murray GD, Teasdale GM, Hope DT, Karimi A, Shaw MD, Barer DH; STICH investigators. Early surgery versus initial conservative treatment in patients with spontaneous supratentorial intracerebral haematomas in the International Surgical Trial in Intracerebral Haemorrhage (STICH): a randomised trial. *Lancet* 2005; **365**: 387-397 [PMID: 15680453 DOI: 10.1016/S0140-6736(05)17826-X]

20 **Mohr JP**, Parides MK, Stapf C, Moquete E, Moy CS, Overbey JR, Al-Shahi Salman R, Vicaut E, Young WL, Houdart E, Cordonnier C, Stefani MA, Hartmann A, von Kummer R, Biondi A, Berkefeld J, Klijn CJ, Harkness K, Libman R, Barreau X, Moskowitz AJ; international ARUBA investigators. Medical management with or without interventional therapy for unruptured brain arteriovenous malformations (ARUBA): a multicentre, non-blinded, randomised trial. *Lancet* 2014; **383**: 614-621 [PMID: 24268105 DOI: 10.1016/S0140-6736(13)62302-8]

21 **Meling TR**, Proust F, Gruber A, Niemela M, Regli L, Roche PH, Vajkoczy P. On apples, oranges, and ARUBA. *Acta Neurochir (Wien)* 2014; **156**: 1775-1779 [PMID: 24890935 DOI: 10.1007/s00701-014-2140-7]

22 **Mast H**, Young WL, Koennecke HC, Sciacca RR, Osipov A, Pile-Spellman J, Hacein-Bey L, Duong H, Stein BM, Mohr JP. Risk of spontaneous haemorrhage after diagnosis of cerebral arteriovenous malformation. *Lancet* 1997; **350**: 1065-1068 [PMID: 10213548 DOI: 10.1016/s0140-6736(97)05390-7]

23 **Scimone C**, Donato L, Marino S, Alafaci C, D'Angelo R, Sidoti A. Vis-à-vis: a focus on genetic features of cerebral cavernous malformations and brain arteriovenous malformations pathogenesis. *Neurol Sci* 2019; **40**: 243-251 [PMID: 30523548 DOI: 10.1007/s10072-018-3674-x]

24 **Scimone C**, Donato L, Alafaci C, Granata F, Rinaldi C, Longo M, D'Angelo R, Sidoti A. High-Throughput Sequencing to Detect Novel Likely Gene-Disrupting Variants in Pathogenesis of Sporadic Brain Arteriovenous Malformations. *Front Genet* 2020; **11**: 146 [PMID: 32184807 DOI: 10.3389/fgene.2020.00146]

25 **Scimone C**, Granata F, Longo M, Mormina E, Turiaco C, Caragliano AA, Donato L, Sidoti A, D'Angelo R. Germline Mutation Enrichment in Pathways Controlling Endothelial Cell Homeostasis in Patients with Brain Arteriovenous Malformation: Implication for Molecular Diagnosis. *Int J Mol Sci* 2020; **21** [PMID: 32560555 DOI: 10.3390/ijms21124321]

World Journal of Clinical Cases

Submit a Manuscript: https://www.f6publishing.com

World J Clin Cases 2023 March 26; 11(9): 2002-2008

DOI: 10.12998/wjcc.v11.i9.2002

ISSN 2307-8960 (online)

CASE REPORT

Children with infectious pneumonia caused by *Ralstonia insidiosa*: A case report

Shuang-Zhu Lin, Mei-Jia Qian, Yan-Wei Wang, Qian-Dui Chen, Wan-Qi Wang, Jia-Yi Li, Rui-Tong Yang, Xin-Yao Wang, Chun-Yu Mu, Kai Jiang

Specialty type: Medicine, research and experimental

Provenance and peer review: Unsolicited article; Externally peer reviewed.

Peer-review model: Single blind

Peer-review report's scientific quality classification

Grade A (Excellent): 0
Grade B (Very good): 0
Grade C (Good): C
Grade D (Fair): 0
Grade E (Poor): E

P-Reviewer: Chiu H, Taiwan; Karunanayake A, Sri Lanka

Received: November 8, 2022
Peer-review started: November 8, 2022
First decision: November 25, 2022
Revised: December 2, 2022
Accepted: February 21, 2023
Article in press: February 21, 2023
Published online: March 26, 2023

Shuang-Zhu Lin, Mei-Jia Qian, Kai Jiang, Diagnosis and Treatment Center for Children, Affiliated Hospital of Changchun University of Chinese Medicine, Changchun 130021, Jilin Province, China

Yan-Wei Wang, Department of Imaging, Affiliated Hospital of Changchun University of Chinese Medicine, Changchun 130021, Jilin Province, China

Qian-Dui Chen, Rui-Tong Yang, Xin-Yao Wang, College of Integrated Chinese and Western Medicine, Changchun University of Chinese Medicine, Changchun 130117, Jilin Province, China

Wan-Qi Wang, Jia-Yi Li, Chun-Yu Mu, College of Traditional Chinese Medicine, Changchun University of Chinese Medicine, Changchun 130117, Jilin Province, China

Corresponding author: Kai Jiang, MD, Chief Physician, Professor, Diagnosis and Treatment Center for Children, Affiliated Hospital of Changchun University of Chinese Medicine, No. 1478 Gongnong Road, Chaoyang District, Changchun 130021, Jilin Province, China. 2835221172@qq.com

Abstract

BACKGROUND

Ralstonia is a Gram-negative non-fermentative bacterium widespread in nature, and includes four species, *Ralstonia pickettii*, *Ralstonia solanacearum*, *Ralstonia mannitolilytica*, and *Ralstonia insidiosa*, which were proposed in 2003. *Ralstonia* is mainly found in the external water environment, including municipal and medical water purification systems. This bacterium has low toxicity and is a conditional pathogen. It has been reported in recent years that infections due to *Ralstonia* are increasing. Previous studies have shown that most cases of infection are caused by *Ralstonia pickettii*, a few by *Ralstonia mannitolilytica*, and infections caused by *Ralstonia insidiosa* are rare.

CASE SUMMARY

A 2-year-old Chinese child suffered from intermittent fever and cough for 20 d and was admitted to hospital with bronchial pneumonia. Bronchoscopy and alveolar lavage fluid culture confirmed *Ralstonia insidiosa* pneumonia. The infection was well controlled after treatment with meropenem and azithromycin.

CONCLUSION

Ralstonia infections are increasing, and we report a rare case of *Ralstonia insidiosa* infection in a child. Clinicians should be vigilant about *Ralstonia* infections.

Key Words: Children; Infections; Ralstonia insidiosa; Pneumonia; Treatment; Case report

Core Tip: *Ralstonia* is a rare type of conditionally pathogenic bacterium found in nature, and its infection incidents have been increasing in recent years. We describe a 2-year-old male baby, who was diagnosed with *Ralstonia insidiosa* infection after culture of alveolar lavage fluid. The infection was controlled with a combination of two antibiotics. Our report adds to the case reports of rare *Ralstonia insidiosa* infections and warns doctors to be aware of this rare infection.

Citation: Lin SZ, Qian MJ, Wang YW, Chen QD, Wang WQ, Li JY, Yang RT, Wang XY, Mu CY, Jiang K. Children with infectious pneumonia caused by *Ralstonia insidiosa*: A case report. *World J Clin Cases* 2023; 11(9): 2002-2008
URL: https://www.wjgnet.com/2307-8960/full/v11/i9/2002.htm
DOI: https://dx.doi.org/10.12998/wjcc.v11.i9.2002

INTRODUCTION

Ralstonia is a non-fermentative species widespread in nature, it is a Gram-negative bacterium, which was first isolated in 1973 and incorporated into *Burkholderia* (*Burkholderia pickettii* and *Burkholderia solanacearum*). The genus *Ralstonia* was named separately in 1995 by Yabuuchi *et al*[1], and it includes *Ralstonia pickettii*, *Ralstonia solanacearum*, *Ralstonia mannitolilytica*, and *Ralstonia insidiosa*, which were newly introduced in 2003[2]. *Ralstonia* reproduces in wet conditions and can survive long-term in harsh environments, mainly in external water environments, including municipal water and medical water purification systems[3,4]. Previous reports indicated that the bacterium was less virulent and was an opportunistic pathogen. However, human infections with *Ralstonia* without exposure to a contaminated solution are rare, thus the bacterium was not considered a major pathogen[5].

However, the incidence of *Ralstonia* infection is increasing in recent years. Previous studies have shown that most cases of infection are caused by *Ralstonia pickettii*, and a few by *Ralstonia mannitolilytica*; these pathogens can cause bloodstream infections, pneumonia, prostatitis, and many other diseases[6]. *Ralstonia pickettii*, has been isolated from various clinical specimens, such as sputum, blood, infected wounds, urine, ears, nasal swabs, and cerebrospinal fluid[5].

Ralstonia insidiosa is a new species proposed in 2003[7], which is closest to *Ralstonia pickettii*, and it has been reported to be isolated from the respiratory tract of patients with cystic fibrosis. In addition, *Ralstonia insidiosa* has been detected in water distribution and laboratory-purified water systems[8]. However, due to the low incidence of this bacterium infection and insufficient clinical awareness, reports of *Ralstonia insidiosa* infection are infrequent.

CASE PRESENTATION

Chief complaints

A boy aged 2 years and 6 mo presented with intermittent fever and cough for 20 d and attended hospital on January 27, 2019.

History of present illness

The child had a fever without apparent cause which started 20 d previously. His fever was persistent, with yellow-colored sputum but no blood-stained sputum. The clinical diagnosis was bronchial pneumonia, and azithromycin, erythromycin and other drugs were administered for 19 d, and the effect was not satisfactory. On admission, the child still had a fever, and cough with sputum.

History of past illness

The child had previously been physically fit. Family members denied contact with contaminated water in the endemic area or history of surgery and invasive procedures.

Personal and family history

The child was gravida 1, para 1, delivered by cesarean section at term, and had no history of related infections, infectious diseases, or history of genetic diseases in the family.

Physical examination

The child's weight was 16 kg, height 91 cm, admission temperature 39.6 °C, pulse rate 120 bpm, and respiratory rate 28 breaths/min. He had good nutritional status, normal development, no rash on the skin or mucous membranes throughout the body, no pharyngeal hyperemia, and no enlargement and purulent discharge of tonsils, and superficial lymph nodes in the entire body were not palpable. Breath was regular and orderly, breath sounds in both lungs were rough, and crackles could be heard. The heart rhythm was aligned. Pericardial rub, additional heart sounds, and pathological murmur were not heard on auscultation. The abdominal examination was normal. The liver, gallbladder and spleen were not palpable, percussion pain in both kidney areas was negative, and neurological examination was normal.

Laboratory examinations

On January 27, 2019, routine blood tests showed white blood cell count (WBC) 7.15 × 10^9/L, neutrophil (NEU) 59.90%, lymphocyte (LYM) 31.20%, monocyte (MON) ratio 8.50%, red blood cell count (RBC) 4.37 × 10^{12}/L, platelet (PLT) count 159 × 10^9/L, abnormal LYM (YX) < 10%, and high-sensitivity C-reactive protein (hs-CRP) < 0.50 mg/L.

On January 28, 2019, procalcitonin was < 0.1 ng/mL, immunoglobulin A 0.693 g/L, and complement C3 0.720 g/L. No abnormalities were found in myocardial enzymes, liver and kidney function, and various viral antibody tests. Tuberculosis antibodies, antinuclear antibodies, rheumatoid factor detection and the anti-O test were normal.

On January 30, 2019, thyroid function tests showed T3 0.877 nmol/L, T4 52.92 nmol/L, free triiodothyronine 2.39 pmol/L, free thyroxine 9.43 pmol/L, A-thrombopoietin 96.34 IU/mL, and A-thyroglobulin 328.80 IU/mL.

On February 1, 2019, routine blood tests showed WBC 7.60 × 10^9/L, NEU 45.80%, LYM 36.70%, MON 8.30%, RBC 4.45 × 10^{12}/L, PLT 253 × 10^9/L, and hs-CRP 11 mg/L, and D-dimer 932 μg/L. Fungal-D glucan was higher than 162 pg/mL (normal values were < 100.5 pg/mL). No abnormalities in tuberculosis-infected T cells and respiratory virus antibodies were detected.

On February 2, 2019, a blood culture was tested on the next day after admission, and the result was negative on the 7th d.

On February 4, 2019, routine blood tests showed WBC 6.42 × 10^9/L, NEU 38.64%, LYM 51.44%, MON 6.24%, RBC 4.20 × 10^{12}/L, PLT 277 × 10^9/L, and hs-CRP < 0.50 mg/L.

On February 7, 2019, routine blood tests showed WBC 6.61 × 10^9/L, NEU 47.44%, LYM 39.34%, MON 8.04%, RBC 4.39 × 10^{12}/L, PLT 272 × 10^9/L, and hs-CRP < 0.50 mg/L.

According to the "National Clinical Laboratory Operating Procedures" compiled by the Department of Medical Administration, Ministry of Health, China, The usual WBC count range is (4.0-10.0) × 10^9, the normal value for the percentage of NEUs is 50%-70%, the normal value for the LYM percentage is 20%-40%, the normal value of the percentage of monocytes is 3%-8%, the normal value of RBCs is (3.5-5.5) × 10^{12}/L, the normal value of PLTs is (100-300) × 10^9/L, the normal value for the hypersensitive CRP is 0-3 mg/L.

Imaging examinations

Computed tomography (CT) scanning of the lungs was performed, with the following findings.

On January 27, 2019, the texture of both lungs was enhanced, the bronchial vascular bundle was thickened and disordered, multiple fuzzy cord shadows were seen, and the lower lobe of the right lung showed patchy dense opacity, with smooth edges and an uneven internal density (Figure 1A).

On January 31, 2019, compared with the previous CT images on January 27, 2019, the density of the lower lobe of the right lung had increased significantly, the edges were blurred, and an irregular cavity was seen inside. A small amount of fluid was noted in the right thorax (Figure 1B).

FINAL DIAGNOSIS

The patient was eventually diagnosed with *Ralstonia insidiosa* pneumonia.

TREATMENT

The patient was started on conventional empirical medication with amoxicillin sodium-clavulanate potassium 30 mg/kg 3 times daily and adenosine monophosphate 5 mg/kg once a day. On the third day of admission, the child had increased fever and was given meropenem 20 mg/kg 3 times daily and

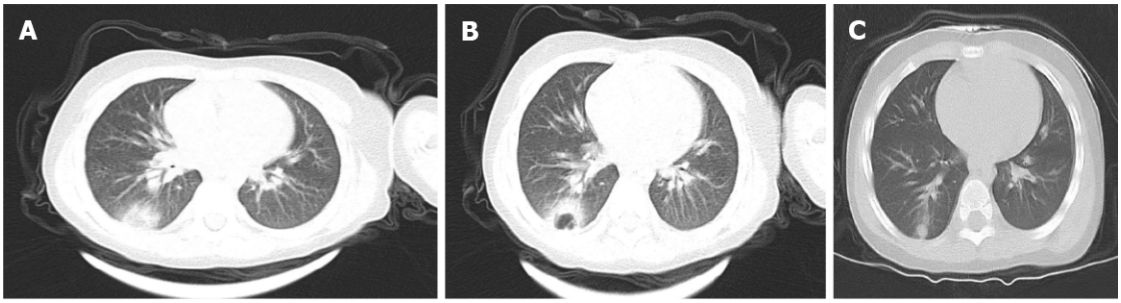

DOI: 10.12998/wjcc.v11.i9.2002

Figure 1 Computed tomography images. A: Computed tomography (CT) images of the lungs in the child on the 19th d of infection onset and the day of admission; B: CT scan of the lungs on day 4 after admission; C: CT scan of the lungs more than 1 mo after discharge.

immunoglobulin 1 g/kg once a day intravenously. Subsequently, meropenem 20 mg/kg was administered 3 times daily combined with azithromycin 10 mg/kg once a day. Based on the timeline of the onset of the infection, a chart of the child's fever trend (Figure 2) and WBC count (Figure 3) was prepared for comparison.

OUTCOME AND FOLLOW-UP

The child has been followed up, and no disease recurrence has been observed. A pulmonary CT performed 42 d after discharge on March 21, 2019, showed texture enhancement in both lungs. The lower lobe of the right lung showed patchy and cord-like high-density opacities with blurred edges (Figure 1C).

DISCUSSION

With regard to *Ralstonia* infections, a review of previous literature showed that the majority of cases were nosocomial infections, with evidence that *Ralstonia* enters the hospital environment primarily through a contaminated water supply system[9]. Infections are primarily caused by contaminated solutions, including blood products, sterile water, saline, respiratory therapeutic fluids[10-13], and that the most common infected items are blood collection tubes, dialysis machines, and nebulizers, which may eventually lead to different diseases such as bacteremia, sepsis, respiratory infections, and pneumonia[14], with human infections unrelated to contaminated solutions being rare. Infections occur predominantly in weak or immunosuppressed individuals, mainly in the elderly or neonates who are immunocompromised.

The child in the present report was admitted to hospital with intermittent fever and cough for 20 d, with no history of surgery or invasive procedures which excluded contact with medical devices such as ventilators and dialysis machines. The child had a long course of the disease and received antibiotics for 19 d before admission to the hospital (exact dose was unknown). After admission, we ruled out febrile illnesses such as tuberculosis, infectious mononucleosis, Kawasaki disease, rheumatic fever, and epidemic hemorrhagic fever. Physical and chemical examinations showed lower values of immunoglobulin A, complement C3, and serum T3 and T4, suggesting that the child was immunocompromised. On admission, CT showed a patchy dense shadow in the lower lobe of the right lung. A blood culture was tested on the next day after admission, and the result was negative on the 7th d. This also made the diagnosis difficult. The child was initially considered to have lobar pneumonia and was given amoxicillin sodium-clavulanate potassium, immunoglobulin, and meropenem as empirical treatment against infection. The child's condition did not improve, and a second CT scan showed a significant increase in the hyperdense shadow in the lower lobe of the right lung and a small amount of pleural effusion. The child was also tested for fungal-D glucan, which was higher than 162 mg/L. This also led us to consider the possibility of specific flora infectious pneumonia and fungal pneumonia at the time of diagnosis. As fungal pneumonia does not have characteristic imaging, bronchoalveolar lavage is used for diagnosis[15]. During follow-up, the child underwent bronchoscopy, and an alveolar lavage fluid culture was performed, which eventually confirmed the diagnosis of *Ralstonia insidiosa* infection based on the lavage fluid culture results.

Reliable therapeutic data on *Ralstonia insidiosa* infection are lacking. Studies related to drug resistance in *Ralstonia insidiosa* have shown that this bacterium is highly resistant to the aminoglycoside gentamicin and the β-lactam antibiotic aztreonam, with different drug resistance to ticarcillin-clavulanic acid mixtures[16]. Studies by Ryan and Adley[16] have shown that most *Ralstonia* strains are sensitive to

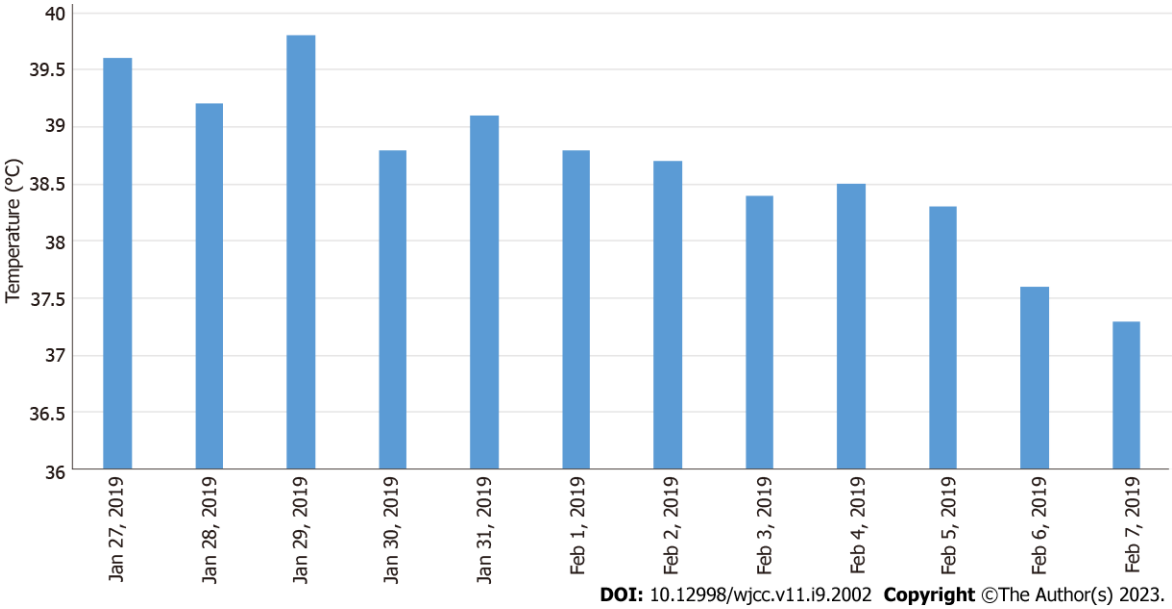

Figure 2 The body temperature in the figure is the highest daily body temperature of the child.

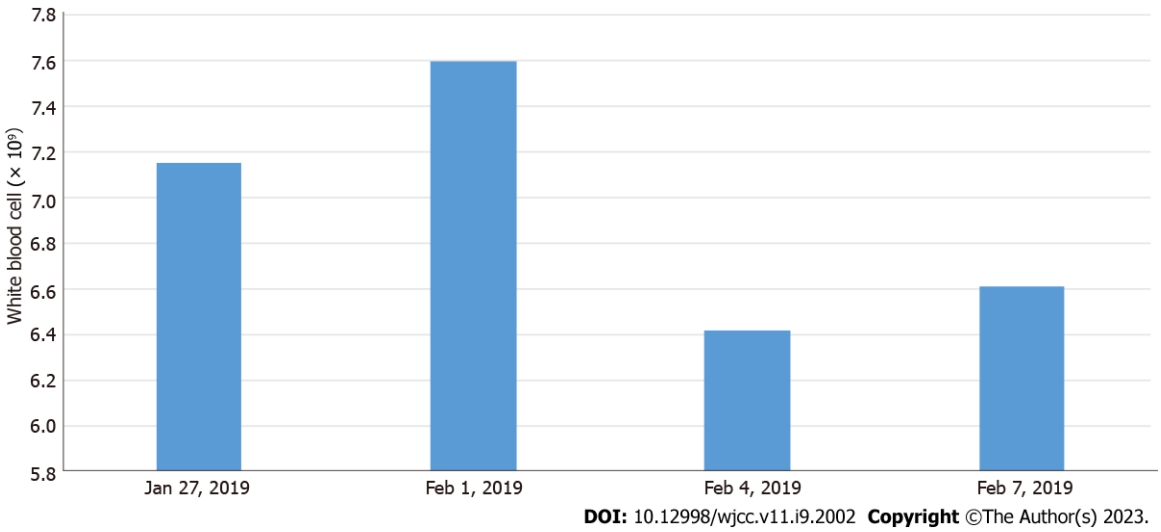

Figure 3 A chart of the child's fever trend and white blood cell count. The usual white blood cell count range is (4.0-10.0) × 10^9 according to the "National Clinical Laboratory Operating Procedures" compiled by the Department of Medical Administration, Ministry of Health, China.

carbapenem antibiotics. All isolates were sensitive to quinolones (ciprofloxacin and ofloxacin), tetracyclines (tetracycline and minocycline), cephalosporins (cefotaxime and ceftazidime), folate pathway inhibitors (meperidine/sulfamethoxazole) and uropipexicillin broad-spectrum-lactam antibiotics (piperacillin)[17]. Our patient, after 3 d of anti-infective treatment with azithromycin 10 mg/kg once daily combined with meropenem 20 mg/kg three times daily prior to the diagnosis of *Ralstonia insidiosa* infection, showed a significant reduction in fever and a significant improvement in clinical signs. Therefore, this regimen was continued for 4 d after diagnosis and the infection eventually improved and was controlled.

CONCLUSION

Ralstonia infections are becoming increasingly common in clinical practice. The reasons for this may be associated with the massive clinical use and partial misuse of antibiotics, the insidious nature of the bacterium, which is easily overlooked in the early stages of infection, and its multi-drug resistance, which makes the infection difficult to control. Our report presents a rare case of childhood *Ralstonia insidiosa* pneumonia. Clinicians should be vigilant about *Ralstonia* infections, especially in immunocom-

promised patients and those with a history of invasive procedures such as ventilators and dialysis machines.

ACKNOWLEDGEMENTS

We would like to thank the patient and his family members for their contributions to this report.

FOOTNOTES

Author contributions: Lin SZ and Qian MJ are the attending doctors at the Diagnosis and Treatment Center for Children, Affiliated Hospital of Changchun University of Chinese Medicine, and provided this case; Wang YW and Chen QD reviewed the literature, and wrote and revised the manuscript; Wang WQ, Yang RT and Wang XY compiled the literature review, conducted the preliminary translation of the report and the subsequent submission; Jiang K provided guidance on the article; and all authors issued final approval for the version to be submitted.

Informed consent statement: We have obtained informed consent from the parents of the child.

Conflict-of-interest statement: All the authors report no relevant conflicts of interest for this article.

CARE Checklist (2016) statement: We have read and followed the CARE Checklist (2016) to prepare this report.

Country/Territory of origin: China

ORCID number: Shuang-Zhu Lin 0000-0001-5333-2138; Mei-Jia Qian 0000-0002-3847-4194; Yan-Wei Wang 0000-0003-1606-4255; Qian-Dui Chen 0000-0002-8593-4077; Wan-Qi Wang 0000-0002-8247-7616; Jia-Yi Li 0000-0002-7729-4479; Rui-Tong Yang 0000-0003-0923-3444; Xin-Yao Wang 0000-0002-9066-5887; Chun-Yu Mu 0000-0002-5966-3322; Kai Jiang 0000-0002-0194-9934.

S-Editor: Wang JJ
L-Editor: A
P-Editor: Wang JJ

REFERENCES

1 **Yabuuchi E**, Kosako Y, Yano I, Hotta H, Nishiuchi Y. Transfer of two Burkholderia and an Alcaligenes species to Ralstonia gen. Nov.: Proposal of Ralstonia pickettii (Ralston, Palleroni and Doudoroff 1973) comb. Nov., Ralstonia solanacearum (Smith 1896) comb. Nov. and Ralstonia eutropha (Davis 1969) comb. Nov. *Microbiol Immunol* 1995; **39**: 897-904 [PMID: 8657018 DOI: 10.1111/j.1348-0421.1995.tb03275.x]

2 **Sharma D**, Sharma P, Soni P, Gupta B. Ralstonia picketti neonatal sepsis: a case report. *BMC Res Notes* 2017; **10**: 28 [PMID: 28061799 DOI: 10.1186/s13104-016-2347-1]

3 **Chen YY**, Huang WT, Chen CP, Sun SM, Kuo FM, Chan YJ, Kuo SC, Wang FD. An Outbreak of Ralstonia pickettii Bloodstream Infection Associated with an Intrinsically Contaminated Normal Saline Solution. *Infect Control Hosp Epidemiol* 2017; **38**: 444-448 [PMID: 28115025 DOI: 10.1017/ice.2016.327]

4 **Vincenti S**, Quaranta G, De Meo C, Bruno S, Ficarra MG, Carovillano S, Ricciardi W, Laurenti P. Non-fermentative gram-negative bacteria in hospital tap water and water used for haemodialysis and bronchoscope flushing: prevalence and distribution of antibiotic resistant strains. *Sci Total Environ* 2014; **499**: 47-54 [PMID: 25173861 DOI: 10.1016/j.scitotenv.2014.08.041]

5 **Pan W**, Zhao Z, Dong M. Lobar pneumonia caused by Ralstonia pickettii in a sixty-five-year-old Han Chinese man: a case report. *J Med Case Rep* 2011; **5**: 377 [PMID: 21843320 DOI: 10.1186/1752-1947-5-377]

6 **Fang Q**, Feng Y, Feng P, Wang X, Zong Z. Nosocomial bloodstream infection and the emerging carbapenem-resistant pathogen Ralstonia insidiosa. *BMC Infect Dis* 2019; **19**: 334 [PMID: 31014269 DOI: 10.1186/s12879-019-3985-4]

7 **Coenye T**, Goris J, De Vos P, Vandamme P, LiPuma JJ. Classification of Ralstonia pickettii-like isolates from the environment and clinical samples as Ralstonia insidiosa sp. nov. *Int J Syst Evol Microbiol* 2003; **53**: 1075-1080 [PMID: 12892129 DOI: 10.1099/ijs.0.02555-0]

8 **Ryan MP**, Pembroke JT, Adley CC. Genotypic and phenotypic diversity of Ralstonia pickettii and Ralstonia insidiosa isolates from clinical and environmental sources including High-purity Water. Diversity in Ralstonia pickettii. *BMC Microbiol* 2011; **11**: 194 [PMID: 21878094 DOI: 10.1186/1471-2180-11-194]

9 **Tayeb LA**, Lefevre M, Passet V, Diancourt L, Brisse S, Grimont PA. Comparative phylogenies of Burkholderia, Ralstonia, Comamonas, Brevundimonas and related organisms derived from rpoB, gyrB and rrs gene sequences. *Res Microbiol* 2008; **159**: 169-177 [PMID: 18280706 DOI: 10.1016/j.resmic.2007.12.005]

10 **Moreira BM**, Leobons MB, Pellegrino FL, Santos M, Teixeira LM, de Andrade Marques E, Sampaio JL, Pessoa-Silva CL. Ralstonia pickettii and Burkholderia cepacia complex bloodstream infections related to infusion of contaminated water for injection. *J Hosp Infect* 2005; **60**: 51-55 [PMID: 15823657 DOI: 10.1016/j.jhin.2004.09.036]

11 **Labarca JA**, Trick WE, Peterson CL, Carson LA, Holt SC, Arduino MJ, Meylan M, Mascola L, Jarvis WR. A multistate nosocomial outbreak of Ralstonia pickettii colonization associated with an intrinsically contaminated respiratory care solution. *Clin Infect Dis* 1999; **29**: 1281-1286 [PMID: 10524976 DOI: 10.1086/313458]

12 **McNeil MM**, Solomon SL, Anderson RL, Davis BJ, Spengler RF, Reisberg BE, Thornsberry C, Martone WJ. Nosocomial Pseudomonas pickettii colonization associated with a contaminated respiratory therapy solution in a special care nursery. *J Clin Microbiol* 1985; **22**: 903-907 [PMID: 4066922 DOI: 10.1128/jcm.22.6.903-907.1985]

13 **Yoneyama A**, Yano H, Hitomi S, Okuzumi K, Suzuki R, Kimura S. Ralstonia pickettii colonization of patients in an obstetric ward caused by a contaminated irrigation system. *J Hosp Infect* 2000; **46**: 79-80 [PMID: 11023730 DOI: 10.1053/jhin.2000.0791]

14 **Ryan MP**, Pembroke JT, Adley CC. Ralstonia pickettii: a persistent gram-negative nosocomial infectious organism. *J Hosp Infect* 2006; **62**: 278-284 [PMID: 16337309 DOI: 10.1016/j.jhin.2005.08.015]

15 **Fortún J**. Diagnostic and therapeutic approach to fungal pneumonia in the critically ill patient. *Rev Esp Quimioter* 2022; **35** Suppl 1: 97-103 [PMID: 35488836 DOI: 10.37201/req/s01.21.2022]

16 **Ryan MP**, Adley CC. The antibiotic susceptibility of water-based bacteria Ralstonia pickettii and Ralstonia insidiosa. *J Med Microbiol* 2013; **62**: 1025-1031 [PMID: 23579396 DOI: 10.1099/jmm.0.054759-0]

17 **Girlich D**, Naas T, Nordmann P. OXA-60, a chromosomal, inducible, and imipenem-hydrolyzing class D beta-lactamase from Ralstonia pickettii. *Antimicrob Agents Chemother* 2004; **48**: 4217-4225 [PMID: 15504844 DOI: 10.1128/AAC.48.11.4217-4225.2004]

World Journal of Clinical Cases

Submit a Manuscript: https://www.f6publishing.com

World J Clin Cases 2023 March 26; 11(9): 2009-2014

DOI: 10.12998/wjcc.v11.i9.2009

ISSN 2307-8960 (online)

CASE REPORT

Transient ischemic attack induced by pulmonary arteriovenous fistula in a child: A case report

Jun Zheng, Qi-Yue Wu, Xia Zeng, Du-Fei Zhang

Specialty type: Medicine, research and experimental

Provenance and peer review: Unsolicited article; Externally peer reviewed.

Peer-review model: Single blind

Peer-review report's scientific quality classification

Grade A (Excellent): 0
Grade B (Very good): B, B
Grade C (Good): 0
Grade D (Fair): 0
Grade E (Poor): 0

P-Reviewer: Khouzam RN, United States; Suwanto D, Indonesia

Received: November 12, 2022
Peer-review started: November 12, 2022
First decision: January 30, 2023
Revised: February 1, 2023
Accepted: March 3, 2023
Article in press: March 3, 2023
Published online: March 26, 2023

Jun Zheng, Qi-Yue Wu, Xia Zeng, Du-Fei Zhang, Department of Pediatrics, Hainan Women and Children's Medical Center, Haikou 570000, Hainan Province, China

Corresponding author: Du-Fei Zhang, MBBS, Chief Physician, Director, Department of Pediatrics, Hainan Women and Children's Medical Center, No. 17 Changbin Road, Xiuying District, Haikou 570000, Hainan Province, China. freezdfei@163.com

Abstract

BACKGROUND

Cerebral ischemic stroke is attributed to paradoxical cerebral embolism. Pulmonary arteriovenous fistula (PAVF) is a rare potential cause of cerebral ischemic stroke, and cerebral ischemic stroke induced by PAVF in children is rare.

CASE SUMMARY

We report a case of right PAVF that presented as a transient ischemic attack (TIA) in a 13-year-old boy. The patient underwent embolization therapy and remained clinically stable for 2 years after treatment.

CONCLUSION

TIA induced by PAVF in children is rare, lacks typical clinical manifestations, and should not be ignored.

Key Words: Pulmonary arteriovenous fistula; Transient ischemic attack; Paradoxical cerebral embolism; Children; Case report

Core Tip: Pulmonary arteriovenous fistula (PAVF) is a rare potential cause of cerebral ischemic stroke. Children with PAVF have atypical clinical presentations, and even present with cerebral ischemic stroke or transient ischemic attack as the only clinical finding. If a PAVF is suspected, we recommend that appropriate examinations should be performed for early detection, and then active treatment and follow-up should be offered.

Citation: Zheng J, Wu QY, Zeng X, Zhang DF. Transient ischemic attack induced by pulmonary arteriovenous fistula in a child: A case report. *World J Clin Cases* 2023; 11(9): 2009-2014
URL: https://www.wjgnet.com/2307-8960/full/v11/i9/2009.htm
DOI: https://dx.doi.org/10.12998/wjcc.v11.i9.2009

INTRODUCTION

Cases of cerebral ischemic stroke induced by pulmonary arteriovenous fistula (PAVF) are mostly reported in adults, and are largely attributed to paradoxical cerebral embolism (PCE)[1-5]. Due to congenital or acquired arteriovenous communications, PCE can be caused by emboli transferring from a vein to an artery, or transferring from the right heart system to the left heart system. PCE is most commonly induced *via* a patent foramen ovale (PFO)[6], and PAVF is a rare potential cause. Cerebral ischemic stroke induced by PAVF in children is rare. We report the case of a 13-year-old boy with a transient ischemic attack (TIA) induced *via* PAVF. We aim to bring attention to this rare cause of PCE with the goal of decreasing the rate of missed diagnosis.

CASE PRESENTATION

Chief complaints

A 13-year-old boy was admitted to our hospital on September 2, 2020 due to intermittent dizziness for 2 d.

History of present illness

The patient presented with intermittent dizziness and bilateral limb weakness for 2 d. During the attack, he fainted and then recovered spontaneously approximately 5 min later. He had no dyspnea, nausea, vomiting, tinnitus, hearing loss, or convulsions.

History of past illness

The patient had a no previous medical history.

Personal and family history

The patient had no relevant personal or family history.

Physical examination

Physical examination showed no neurological or cardiorespiratory abnormalities. His vital signs were stable.

Laboratory examinations

The results of laboratory examinations were normal.

Imaging examinations

Subsequent chest x-ray showed a mass shadow in the right upper lung (Figure 1). Cardiac color ultrasound showed no obvious abnormalities and no PFO was seen. Cardiovascular computed tomography (CT) angiography (CTA) showed that the right upper pulmonary artery (diameter 7.4 mm) had expanded. Its branching vessels were thickened and twisted into an abnormal vascular nest with direct reflux into the right upper pulmonary posterior vein, and the artery finally merged into the right upper pulmonary vein (Figure 2). Brain magnetic resonance imaging and cerebral artery magnetic resonance angiography showed no obvious abnormalities (Figure 3). Contrast-enhanced transcranial Doppler (c-TCD) ultrasound was remarkable for a large right-to-left shunt (RLS) (Figure 4).

FINAL DIAGNOSIS

The patient was diagnosed with TIA and PAVF. TIA induced *via* PAVF was considered.

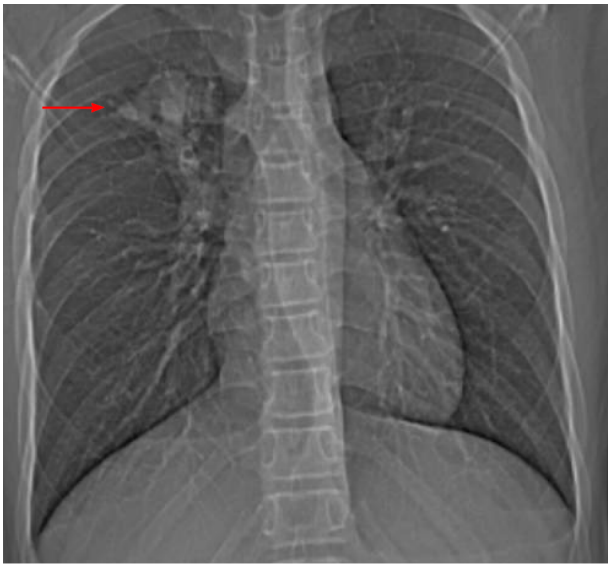

DOI: 10.12998/wjcc.v11.i9.2009

Figure 1 Chest x-ray. A mass shadow in the right upper lung (red arrow).

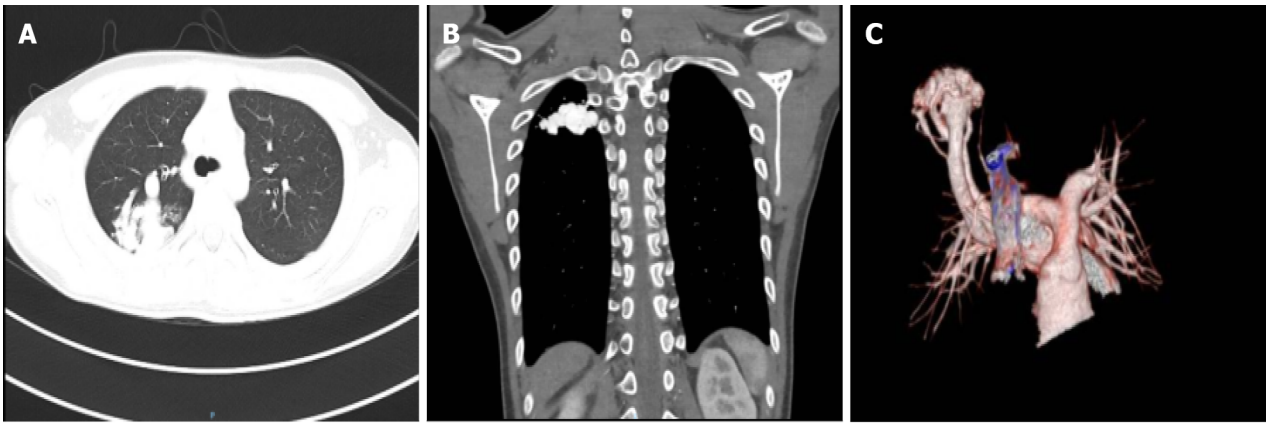

DOI: 10.12998/wjcc.v11.i9.2009

Figure 2 Cardiovascular computed tomography angiography. A and B: Representative images showing the abnormal vascular nest in the right upper lung; C: Expansion of the right upper pulmonary artery with thickened and twisted branching vessels to form an abnormal vascular nest with direct reflux into the right upper pulmonary posterior vein. The artery finally merged into the right upper pulmonary vein.

TREATMENT

The patient underwent embolization therapy of the PAVF under general anesthesia on the day 3 of hospitalization. Intraoperative angiography showed that the PAVF originated from the right upper pulmonary branch artery (Figure 5A and B), which was no longer detected after embolization with a vascular plug (Figure 5C and D).

OUTCOME AND FOLLOW-UP

At the 10 mo postoperative follow-up, a chest x-ray showed that the position of the vascular plug was stable (Figure 6A), and a CT scan showed that the PAVF had markedly shrunk (Figure 6B). At the 1 year and 2 years postoperative follow-up points, the patient remained clinically stable without symptoms of dizziness, limb weakness, or fainting.

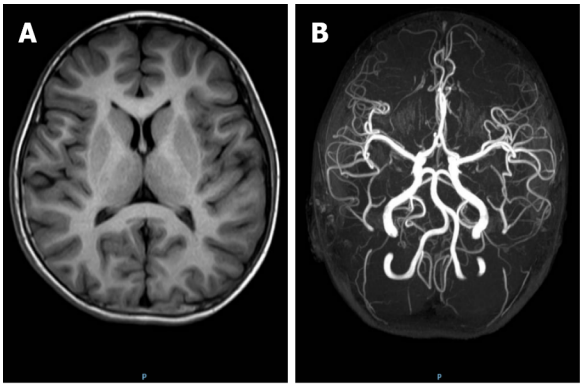

DOI: 10.12998/wjcc.v11.i9.2009

Figure 3 Brain magnetic resonance imaging and cerebral magnetic resonance angiography. A: Magnetic resonance imaging showed no obvious abnormalities; B: Magnetic resonance angiography showed no obvious abnormalities.

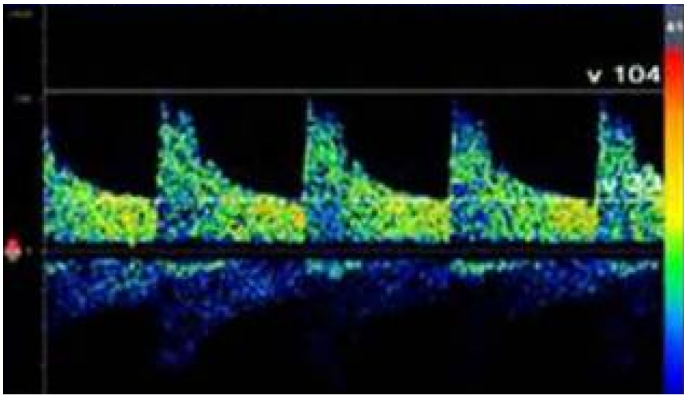

DOI: 10.12998/wjcc.v11.i9.2009

Figure 4 Contrast-enhanced transcranial Doppler ultrasound. Significant embolus signals appeared in the middle cerebral artery within 10 s after Valsalva maneuver.

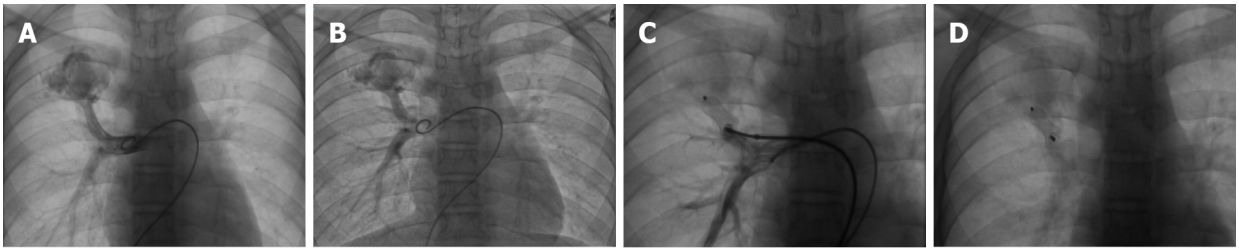

DOI: 10.12998/wjcc.v11.i9.2009

Figure 5 Angiography and embolization treatment. A and B: Representative angiography images showing a pulmonary arteriovenous fistula (PAVF) originating from the right upper pulmonary branch artery; C and D: Representative images showing the PAVF was no longer detected after embolization with a vascular plug.

DISCUSSION

The presence of a RLS, which can result in paradoxical brain embolism, is an important etiology of ischemic stroke especially in young adults. PFO and PAVF are the most important causes of RLS. TCD ultrasound is currently reported to be a noninvasive and useful method for detecting RLS. The gold standard for detecting RLS is contrast-enhanced transesophageal echocardiography. It is recommended that these examinations be carried out immediately after onset of stroke[7]. A previous report showed that the prevalence of PAVF is 0.026%[8], and TIA is a clinical manifestation of PAVF in up to 20% of cases[1]. At present, it is believed that the risk factors for cerebral ischemic stroke in patients with PAVF are as follows: (1) Feeding artery diameter > 3 mm; and (2) existence of multiple PAV malformations[9]. Whether patients with PAVF present with clinical manifestations depends on the level of the RLS. There

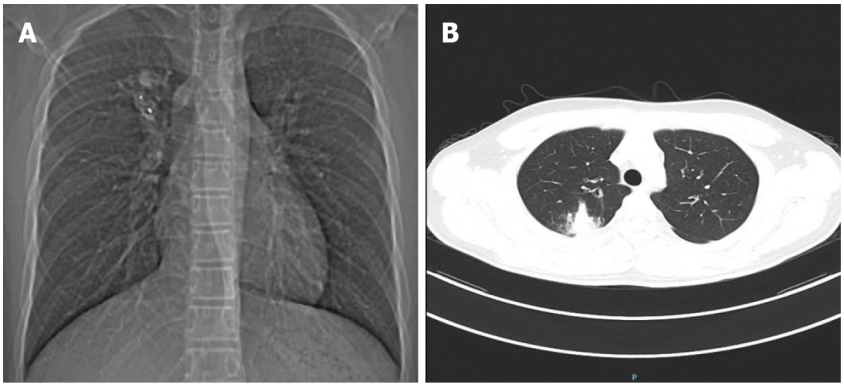

DOI: 10.12998/wjcc.v11.i9.2009

Figure 6 Postoperative follow-up imaging. A: Chest x-ray showed that the position of the vascular plug was stable; B: Computed tomography showed that the pulmonary arteriovenous fistula markedly shrank after embolization therapy.

are intrapulmonary and extrapulmonary manifestations in patients with PAVF. The intrapulmonary manifestations include dyspnea after activity, dizziness, easy fatigability, and others[10-12]. Physical examination may reveal cyanosis, clubbing of fingers or toes, or continuous chest murmur. Some patients may only present with abnormal arterial blood gas analysis. The extrapulmonary manifestations include migraine, TIA, ischemic stroke, brain abscess, epilepsy, and others[10-12].

Espejo-Herrero *et al*[1] reported a patient with TIA presenting with a short-term (30 min) right limb paralysis, with subsequent pulmonary arteriography showing a PAVF. Pulmonary digital subtraction angiography (DSA) is the gold standard for the diagnosis of PAVF, which can determine fistula size, feeding artery, draining vein, and other conditions[10]. However, DSA is an invasive examination. As a noninvasive procedure, CTA can not only show the lesions (even mild lesions) and the blood vessels involved in PAVF, but can also accurately judge peripheral and complex PAVF anatomy, which is more helpful in diagnosis[10]. At present, c-TCD is widely used for RLS screening, which can observe the dynamics of emboli entering the intracranial arteries and the changes of cerebral blood flow in real time [13]. In our case, c-TCD ultrasound revealed a large RLS, which was in line with the diagnosis of PAVF.

Most PAVFs will gradually enlarge and rarely shrink spontaneously, which may cause serious complications. The mortality rate in untreated patients with PAVF is as high as 50%, which can be reduced to 3% after treatment. It is currently recommended that active treatment should be pursued in patients with symptomatic or asymptomatic PAVF if the lesion diameter exceeds 3 mm. PAVF treatments mainly include surgery and interventional embolization, both of which can improve the symptoms of hypoxia and prevent the occurrence of central nervous system complications[10,11]. Todo *et al*[14] reported a patient with recurrent ischemic stroke caused by PAVF with a feeding artery diameter of 1.80 mm, and embolic events were successfully prevented after fistula embolization. Our patient was treated with interventional embolization of PAVF in our hospital. The patient had no recurrent seizure or TIA symptoms for 2 years, further suggesting that recurrent TIA symptoms are indeed associated with PAVF.

CONCLUSION

Although PAVF is a rare cause of abnormal embolism, it should not be ignored. Most patients with PAVF have atypical clinical presentations, and can even present with cerebral ischemic stroke or TIA as the only clinical finding. Therefore, in patients with cryptogenic stroke, especially children, appropriate examinations should be performed to determine whether a PAVF may be present. If a PAVF is discovered, active treatment and follow-up should be pursued.

FOOTNOTES

Author contributions: Zheng J and Zhang DF drafted the manuscript; Wu QY and Zeng X collected the clinical data; Zheng J and Zhang DF revised the manuscript for intellectual content; All authors read and approved the final manuscript.

Supported by Scientific Research Project of Hainan Provincial Health Industry, China, No. 20A200081; and Clinical Medical Center Project of Hainan Province, China, No. QWYH202175.

Informed consent statement: Written informed consent was obtained from the patient for publication of this case

report.

Conflict-of-interest statement: All the authors report having no relevant conflicts of interest for this article.

CARE Checklist (2016) statement: The authors have read the CARE Checklist (2016), and the manuscript was prepared and revised according to the CARE Checklist (2016).

Country/Territory of origin: China

ORCID number: Du-Fei Zhang 0000-0003-4611-1825.

S-Editor: Fan JR
L-Editor: Filipodia
P-Editor: Fan JR

REFERENCES

1 **Espejo-Herrero JJ**, Bravo-Rodríguez F, Triviño-Tarradas F, Ysamat-Marfá R, Zurera-Tendero LJ, Canis-López M. [Transient ischemic attack as the presenting symptom of a pulmonary arteriovenous fistula]. *Rev Neurol* 2005; **40**: 163-165 [PMID: 15750902]
2 **Roshanali F**, Mandegar MH, Oraii S. Traumatic pulmonary arteriovenous fistula may be misdiagnosed with residual shunt after patent foramen ovale closure. *BMJ Case Rep* 2012; **2012** [PMID: 23001101 DOI: 10.1136/bcr-2012-006802]
3 **Wozniak L**, Mielczarek M, Sabiniewicz R. Paradoxical brain embolism in a young man: is it only a patent foramen ovale? *Neurol Neurochir Pol* 2015; **49**: 61-64 [PMID: 25666776 DOI: 10.1016/j.pjnns.2014.12.003]
4 **Tomelleri G**, Bovi P, Carletti M, Mazzucco S, Bazzoli E, Casilli F, Onorato E, Moretto G. Paradoxical brain embolism in a young man with isolated pulmonary arteriovenous fistula. *Neurol Sci* 2008; **29**: 169-171 [PMID: 18612765 DOI: 10.1007/s10072-008-0930-5]
5 **Cortes M**, Mayeda GS, Liu MW. Recurrent minor strokes/TIA with a right to left shunt. *BMJ Case Rep* 2018; **2018** [PMID: 29991544 DOI: 10.1136/bcr-2018-224862]
6 **Vindiš D**, Hutyra M, Šaňák D, Král M, Čecháková E, Littnerová S, Adam T, Přeček J, Hudec Š, Ječmenová M, Táborský M. Patent Foramen Ovale and the Risk of Cerebral Infarcts in Acute Pulmonary Embolism-A Prospective Observational Study. *J Stroke Cerebrovasc Dis* 2018; **27**: 357-364 [PMID: 29031497 DOI: 10.1016/j.jstrokecerebrovasdis.2017.09.004]
7 **Matsuoka H**. [Paradoxical brain embolism]. *Rinsho Shinkeigaku* 2005; **45**: 849-851 [PMID: 16447743]
8 **Ma X**, Li LL, Yu D, Jie B, Jiang S. Management of pulmonary arteriovenous malformations involves additional factors aside from the diameter of feeding arteries: a 3-year case-case retrospective analysis. *Respir Res* 2022; **23**: 107 [PMID: 35501913 DOI: 10.1186/s12931-022-02030-9]
9 **Holzer RJ**, Cua CL. Pulmonary Arteriovenous Malformations and Risk of Stroke. *Cardiol Clin* 2016; **34**: 241-246 [PMID: 27150172 DOI: 10.1016/j.ccl.2016.01.001]
10 **Tellapuri S**, Park HS, Kalva SP. Pulmonary arteriovenous malformations. *Int J Cardiovasc Imaging* 2019; **35**: 1421-1428 [PMID: 30386957 DOI: 10.1007/s10554-018-1479-x]
11 **Majumdar S**, McWilliams JP. Approach to Pulmonary Arteriovenous Malformations: A Comprehensive Update. *J Clin Med* 2020; **9** [PMID: 32575535 DOI: 10.3390/jcm9061927]
12 **Kramdhari H**, Valakkada J, Ayyappan A. Diagnosis and endovascular management of pulmonary arteriovenous malformations. *Br J Radiol* 2021; **94**: 20200695 [PMID: 34038182 DOI: 10.1259/bjr.20200695]
13 **Wessler BS**, Kent DM, Thaler DE, Ruthazer R, Lutz JS, Serena J. The RoPE Score and Right-to-Left Shunt Severity by Transcranial Doppler in the CODICIA Study. *Cerebrovasc Dis* 2015; **40**: 52-58 [PMID: 26184495 DOI: 10.1159/000430998]
14 **Todo K**, Moriwaki H, Higashi M, Kimura K, Naritomi H. A small pulmonary arteriovenous malformation as a cause of recurrent brain embolism. *AJNR Am J Neuroradiol* 2004; **25**: 428-430 [PMID: 15037468]

World Journal of Clinical Cases

Submit a Manuscript: https://www.f6publishing.com

World J Clin Cases 2023 March 26; 11(9): 2015-2020

DOI: 10.12998/wjcc.v11.i9.2015

ISSN 2307-8960 (online)

CASE REPORT

Motor cortex transcranial magnetic stimulation to reduce intractable postherpetic neuralgia with poor response to other threapies: Report of two cases

Huan Wang, Yu-Zhong Hu, Xian-Wei Che, Liang Yu

Specialty type: Clinical neurology

Provenance and peer review: Unsolicited article; Externally peer reviewed.

Peer-review model: Single blind

Peer-review report's scientific quality classification

Grade A (Excellent): 0
Grade B (Very good): 0
Grade C (Good): C, C
Grade D (Fair): 0
Grade E (Poor): 0

P-Reviewer: Higa K, Japan; Shelat VG, Singapore

Received: November 14, 2022
Peer-review started: November 15, 2022
First decision: December 26, 2022
Revised: January 5, 2023
Accepted: February 21, 2023
Article in press: February 21, 2023
Published online: March 26, 2023

Huan Wang, Yu-Zhong Hu, Liang Yu, Department of Anesthesiology, Zhejiang Chinese Medicine University, Hangzhou 310000, Zhejiang Province, China

Xian-Wei Che, Transcranial Magnetic Stimulation Centre, Deqing Hospital of Hangzhou Normal University, Hangzhou 310000, Zhejiang Province, China

Liang Yu, Department of Pain, Hangzhou First People's Hospital, Hangzhou 310000, Zhejiang Province, China

Corresponding author: Liang Yu, MD, Chief Physician, Department of Anesthesiology, Zhejiang Chinese Medicine University, No. 548 Binwen Road, Hangzhou 310000, Zhejiang Province, China. yuliang0601@zju.edu.cn

Abstract

BACKGROUND

Postherpetic neuralgia (PHN) is a typical neuropathic pain condition that appears in the lesioned skin regions following the healing of shingles. The pain condition tends to persist, which is often accompanied by negative emotions (*e.g.*, anxiety and depression) and substantially reduces the quality of life. In addition to analgesia (*e.g.*, pregabalin and gabapentin), nerve radiofrequency technology is an effective treatment for intractable PHN. However, there is still a significant portion of patients who do not benefit from this treatment. As a non-invasive form of brain stimulation, repetitive transcranial magnetic stimulation (rTMS) targeting the motor cortex is able to reduce neuropathic pain with grade A evidence.

CASE SUMMARY

Here we report two cases in which motor cortex rTMS was used to treat intractable PHN that did not respond to initial drug and radiofrequency therapies. Moreover, we specifically investigated rTMS efficacy at 3 mo following treatment.

CONCLUSION

Motor cortex rTMS can treat intractable PHN that did not respond to initial drug and radiofrequency therapies.

Key Words: Post herpetic neuralgia; Repetitive transcranial magnetic stimulation; Radiofrequency; Case report

Core Tip: Postherpetic neuralgia (PHN) is a kind of refractory neuropathic pain, which seriously affects the quality of life. Repetitive transcranial magnetic stimulation can be used as an effective complement to the treatment of patients with refractory PHN.

Citation: Wang H, Hu YZ, Che XW, Yu L. Motor cortex transcranial magnetic stimulation to reduce intractable postherpetic neuralgia with poor response to other threapies: Report of two cases. *World J Clin Cases* 2023; 11(9): 2015-2020
URL: https://www.wjgnet.com/2307-8960/full/v11/i9/2015.htm
DOI: https://dx.doi.org/10.12998/wjcc.v11.i9.2015

INTRODUCTION

Postherpetic neuralgia (PHN) is a typical neuropathic pain condition that appears in the lesioned skin regions following the healing of shingles[1]. The pain condition tends to persist, which is often accompanied by negative emotions (*e.g.*, anxiety and depression) and substantially reduces the quality of life[1]. In addition to analgesia (*e.g.*, pregabalin and gabapentin), nerve radiofrequency technology is a effective treatment for intractable PHN[2,3]. However, there is still a significant portion of patients who do not benefit from this treatment.

As a non-invasive form of brain stimulation, repetitive transcranial magnetic stimulation (rTMS) targeting the motor cortex (M1) is able to reduce neuropathic pain with grade A evidence[4]. Here we report two cases in which motor cortex rTMS was used to treat intractable PHN that did not respond to initial drug and radiofrequency therapies. Moreover, we specifically investigated rTMS efficacy at 3 mo following treatment[4].

CASE PRESENTATION

Chief complaints

Case 1: A 65-year-old woman was admitted with persistent pain in the left chest and back (T5/T6) for 6 mo after herpes zoster.

Case 2: A 75-year-old woman was admitted with left lower back pain (T11/12) for 4 mo after herpes zoster.

History of present illness

Case 1: The patient's pain was characterized by persistent tingling and burning sensations, with a visual analog scale (VAS) score of 8. She was prescribed pregabalin 150 mg bid, but she did not want to continue increasing the dose of the drug because of the side effect of dizziness, and received a spinal nerve radiofrequency surgery. However, there was no clear analgesia following these treatments.

Case 2: The patient was prescribed gabapentin 0.6 g tid. However, she had renal insufficiency so the drug dose was not increased further, as well as a spinal nerve radiofrequency surgery. The patient reported slight pain relief after treatment but still with a VAS score of 6.

History of past illness

Case 1: The patient claimed no history of past illness.

Case 2: The patient had a history of renal insufficiency for 5 years and was on drugs regularly.

Personal and family history

Neither patient had any relevant personal or family history.

Physical examination
Physical examination of both patients revealed no abnormalities.

Laboratory examinations
Laboratory examination of both patients revealed no abnormalities.

Imaging examinations
Imaging examination of both patients revealed no abnormalities.

FINAL DIAGNOSIS

Cases 1 and 2
PHN.

TREATMENT

Both patients provided written informed consent for rTMS treatment. rTMS was delivered to the contralateral motor cortex once daily for 10 consecutive days using an RT-50 stimulation system connected to a figure-of-eight coil (Sichuan Junjian Wanfeng Medical Equipment Co.). Each rTMS session delivered 3000 pulses at 10 Hz with 5-sec trains and 25-sec intervals at 100% resting motor threshold. Patients were assessed at baseline, the fifth treatment, the end of treatment, and 2 wk, 1 mo, and 3 mo after treatment. Clinical assessment included VAS, McGill Pain Questionnaire (McGill), Pittsburgh Sleep Quality Index (PSQI), Hamilton Depression Scale (24 items), Hamilton Anxiety Scale (17 items), Mini-mental State Examination (MMSE), and Perceived Deficits Questionnaire-Depression (PDQ-D). Drug dose remained the same as that before this treatment.

OUTCOME AND FOLLOW-UP

Both patients demonstrated a promising analgesia effect, with pain experience changing from severe to mild-to-moderate level (Figure 1). There was also a protect effect on negative emotions, especially in the first case with an initial mild depressive symptom. We also observed a significant improvement in sleep quality in both cases. More importantly, the protective effects of motor cortex rTMS lasted for 3 mo following treatment (Figure 2).

DISCUSSION

Here we report two cases in which motor cortex rTMS was able to significantly reduce intractable PHN that did respond to first-line drug and radiofrequency therapies. Drugs and radiofrequency therapies are first-line treatments in clinical settings for PHN[5]. Our results indicated that motor cortex rTMS could be considered when the pain become intractable and/or the patient does not seem to benefit from regular drug and radiofrequency therapies. Some studies have shown that rTMS treatment is safe for patients with PHN and has better efficacy at 10 Hz[6], which is the frequency that we chose for these two patients. More importantly, our results indicated a long-term analgesic effect for 3 mo. Most previous studies have shown that pain relief from neuroplasticity can last for several days, usually a week to a month, after transcranial magnetic stimulation treatment[4]. This long-term 3-mo effect was potentially associated with a relatively large dose of pulses in daily treatment[7]. Previous studies tended to deliver approximately 1500 daily pulses whereby the number of pulses was doubled in these two cases.

TMS is a non-invasive stimulation technique that produces analgesic effects similar to those of invasive techniques by targeting rTMS to M1[8]. High-frequency rTMS delivered to M1 areas obtains analgesic effects by modulating several distant brain regions involved in the processing or control of nociceptive information. This pain relief can last for several weeks beyond the duration of stimulation, especially during repetition, and may be related to the process of long-term synaptic plasticity[9]. rTMS is now mainly used for the treatment of neuropathic pain and requires a trained physician or nurse to perform this procedure, which is a technique that can be widely used. The most common side effects are dizziness and scalp discomfort, which are transient and disappear after the treatment.

The mechanism of rTMS analgesia remains an open question. There is evidence that motor cortex rTMS could drive top-down pain modulation[10]. In addition, motor cortex stimulation is also able to activate cortical and subcortical regions (*e.g.*, insular and cingulate cortex) involved in the processing of

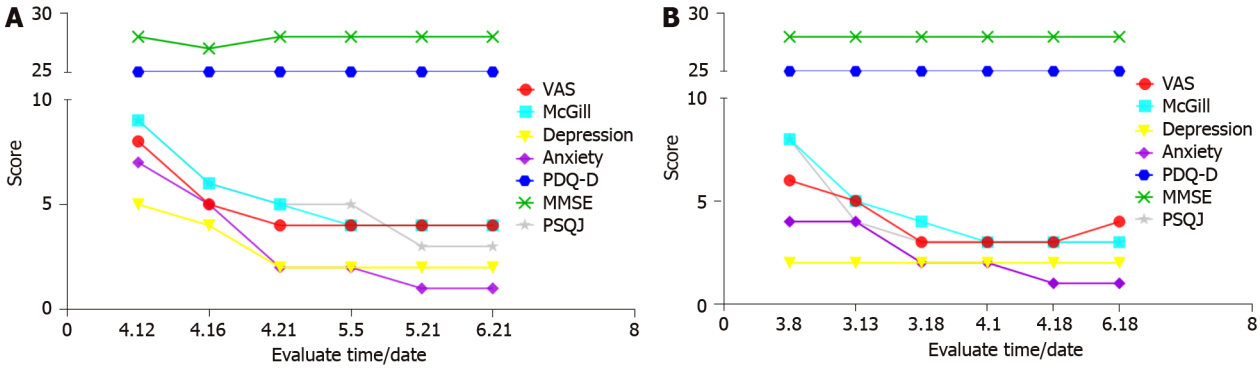

DOI: 10.12998/wjcc.v11.i9.2015

Figure 1 Case results. A: Case 1; B: Case 2. Motor cortex rTMS is able to reduce pain conditions, negative emotions, as well as sleep quality in two cases with intractable postherpetic neuralgia when first-line drug and radiofrequency therapies had no clear benefits. VAS: Visual analogue scale; McGill: McGill Pain Questionnaire; Depression: Hamilton Depression Scale (24 items); Anxiety: Hamilton Anxiety Scale (17 items); PDQ-D: Perceived Deficits Questionnaire-Depression; MMSE: Mini-mental State Examination; PSQI: Pittsburgh Sleep Quality Index.

DOI: 10.12998/wjcc.v11.i9.2015

Figure 2 A patient treated by repetitive transcranial magnetic stimulation.

affective-emotional aspects of pain[11]. In either case, cortical and/or subcortical responses to rTMS may help explain the poor response to radiofrequency therapies, in which spinal nerves may not be well damaged by the surgery or become recurrent following surgery.

We have also observed a promising effect on negative emotions in these two cases. This is in line with the finding of a study that rTMS treatment had a significant effect on the whole brain functional network in PHN patients with inhibited sensory-motor functions and improvements in mood, cognitive, emotional, and memory functions[12]. rTMS has been approved by the United States Food and Drug Administration to treat depression by targeting the dorsolateral prefrontal cortex. Recent studies have also tried to manage comorbid pain and depression with rTMS in one setting[13]. In addition, we provide an interesting finding that motor cortex rTMS is able to improve sleep quality in the two cases, which has been rarely investigated compared to evidence on depression and neuropathic pain[14,15].

CONCLUSION

To conclude, we provide two cases in which motor cortex rTMS is able to reduce pain sensations in intractable PHN when first-line drug and radiofrequency therapies had no clear benefits. These findings need to be further validated in large, randomized controlled trials.

FOOTNOTES

Author contributions: Wang H contributed to literature search, and manuscript drafting and writing; Che XW contributed to supervision and writing of the manuscript; Hu YZ and Yu L contributed to literature search; all authors made substantial contributions to conception and design and data acquisition, analysis, or interpretation; took part in drafting the article or revising it critically for important intellectual content; gave final approval of the version to be published; and agree to be accountable for all aspects of the work.

Informed consent statement: Informed written consent was obtained from the patients for publication of this report and any accompanying images.

Conflict-of-interest statement: All the authors declare that they have no conflict of interest to disclose.

CARE Checklist (2016) statement: The authors have read the CARE Checklist (2016), and the manuscript was prepared and revised according to the CARE Checklist (2016).

Country/Territory of origin: China

ORCID number: Liang Yu 0000-0001-9810-2838.

S-Editor: Liu JH
L-Editor: Wang TQ
P-Editor: Liu JH

REFERENCES

1 **Gross GE**, Eisert L, Doerr HW, Fickenscher H, Knuf M, Maier P, Maschke M, Müller R, Pleyer U, Schäfer M, Sunderkötter C, Werner RN, Wutzler P, Nast A. S2k guidelines for the diagnosis and treatment of herpes zoster and postherpetic neuralgia. *J Dtsch Dermatol Ges* 2020; **18**: 55-78 [DOI: 10.1111/ddg.14013]
2 **Makharita MY**, El Bendary HM, Sonbul ZM, Ahmed SES, Latif MA. Ultrasound-guided Pulsed Radiofrequency in the Management of Thoracic Postherpetic Neuralgia: A Randomized, Double-blinded, Controlled Trial. *Clin J Pain* 2018; **34**: 1017-1024 [PMID: 29757758 DOI: 10.1097/AJP.0000000000000629]
3 **Huang X**, Ma Y, Wang W, Guo Y, Xu B, Ma K. Efficacy and safety of pulsed radiofrequency modulation of thoracic dorsal root ganglion or intercostal nerve on postherpetic neuralgia in aged patients: a retrospective study. *BMC Neurol* 2021; **21**: 233 [PMID: 34162352 DOI: 10.1186/s12883-021-02286-6]
4 **Lefaucheur JP**, André-Obadia N, Antal A, Ayache SS, Baeken C, Benninger DH, Cantello RM, Cincotta M, de Carvalho M, De Ridder D, Devanne H, Di Lazzaro V, Filipović SR, Hummel FC, Jääskeläinen SK, Kimiskidis VK, Koch G, Langguth B, Nyffeler T, Oliviero A, Padberg F, Poulet E, Rossi S, Rossini PM, Rothwell JC, Schönfeldt-Lecuona C, Siebner HR, Slotema CW, Stagg CJ, Valls-Sole J, Ziemann U, Paulus W, Garcia-Larrea L. Evidence-based guidelines on the therapeutic use of repetitive transcranial magnetic stimulation (rTMS). *Clin Neurophysiol* 2014; **125**: 2150-2206 [PMID: 25034472 DOI: 10.1016/j.clinph.2014.05.021]
5 **Finnerup NB**, Attal N, Haroutounian S, McNicol E, Baron R, Dworkin RH, Gilron I, Haanpää M, Hansson P, Jensen TS, Kamerman PR, Lund K, Moore A, Raja SN, Rice AS, Rowbotham M, Sena E, Siddall P, Smith BH, Wallace M. Pharmacotherapy for neuropathic pain in adults: a systematic review and meta-analysis. *Lancet Neurol* 2015; **14**: 162-173 [PMID: 25575710 DOI: 10.1016/S1474-4422(14)70251-0]
6 **Pei Q**, Wu BS, Tang YZ, Yang XH, Song LP, Wang N, Li Y, Sun CL, Ma SM, Ni JX. Repetitive transcranial magnetic stimulation at different Frequencies for postherpetic neuralgia: a double-bind, sham-controlled, randomized trial. *Pain Physician* 2019; **22**: E303-E313 [DOI: 10.36076/ppj/2019.22.E303]
7 **Cruccu G**, Garcia-Larrea L, Hansson P, Keindl M, Lefaucheur JP, Paulus W, Taylor R, Tronnier V, Truini A, Attal N. EAN guidelines on central neurostimulation therapy in chronic pain conditions. *Eur J Neurol* 2016; **23**: 1489-1499 [PMID: 27511815 DOI: 10.1111/ene.13103]
8 **Lefaucheur JP**, Drouot X, Keravel Y, Nguyen JP. Pain relief induced by repetitive transcranial magnetic stimulation of precentral cortex. *Neuroreport* 2001; **12**: 2963-2965 [PMID: 11588611 DOI: 10.1097/00001756-200109170-00041]
9 **Hosomi K**, Sugiyama K, Nakamura Y, Shimokawa T, Oshino S, Goto Y, Mano T, Shimizu T, Yanagisawa T, Saitoh Y; TEN-P11-01 investigators. A randomized controlled trial of 5 daily sessions and continuous trial of 4 weekly sessions of repetitive transcranial magnetic stimulation for neuropathic pain. *Pain* 2020; **161**: 351-360 [PMID: 31593002 DOI: 10.1097/j.pain.0000000000001712]
10 **Lefaucheur JP**, Drouot X, Menard-Lefaucheur I, Zerah F, Bendib B, Cesaro P, Keravel Y, Nguyen JP. Neurogenic pain relief by repetitive transcranial magnetic cortical stimulation depends on the origin and the site of pain. *J Neurol Neurosurg Psychiatry* 2004; **75**: 612-616 [PMID: 15026508 DOI: 10.1136/jnnp.2003.022236]

11 **Moisset X**, de Andrade DC, Bouhassira D. From pulses to pain relief: an update on the mechanisms of rTMS-induced analgesic effects. *Eur J Pain* 2016; **20**: 689-700 [PMID: 26471248 DOI: 10.1002/ejp.811]

12 **Pei Q**, Zhuo Z, Jing B, Meng Q, Ma X, Mo X, Liu H, Liang W, Ni J, Li H. The effects of repetitive transcranial magnetic stimulation on the whole-brain functional network of postherpetic neuralgia patients. *Medicine (Baltimore)* 2019; **98**: e16105 [PMID: 31232955 DOI: 10.1097/MD.0000000000016105]

13 **Leung A**, Shirvalkar P, Chen R, Kuluva J, Vaninetti M, Bermudes R, Poree L, Wassermann EM, Kopell B, Levy R; and the Expert Consensus Panel. Transcranial Magnetic Stimulation for Pain, Headache, and Comorbid Depression: INS-NANS Expert Consensus Panel Review and Recommendation. *Neuromodulation* 2020; **23**: 267-290 [PMID: 32212288 DOI: 10.1111/ner.13094]

14 **Nardone R**, Sebastianelli L, Versace V, Brigo F, Golaszewski S, Pucks-Faes E, Saltuari L, Trinka E. Effects of repetitive transcranial magnetic stimulation in subjects with sleep disorders. *Sleep Med* 2020; **71**: 113-121 [PMID: 32173186 DOI: 10.1016/j.sleep.2020.01.028]

15 **Guo J**, Chen X, Lyu Z, Xiu H, Lin S, Liu F. Repetitive transcranial magnetic stimulation (rTMS) for post-stroke sleep disorders: a systematic review of randomized controlled trials. *Neurol Sci* 2022; **43**: 6783-6794 [PMID: 35980480 DOI: 10.1007/s10072-022-06349-5]

World Journal of Clinical Cases

Submit a Manuscript: https://www.f6publishing.com

World J Clin Cases 2023 March 26; 11(9): 2021-2028

DOI: 10.12998/wjcc.v11.i9.2021

ISSN 2307-8960 (online)

CASE REPORT

Small bowel adenocarcinoma in neoterminal ileum in setting of stricturing Crohn's disease: A case report and review of literature

Shruthi Karthikeyan, Jeanne Shen, Kian Keyashian, John Gubatan

Specialty type: Gastroenterology and hepatology

Provenance and peer review: Invited article; Externally peer reviewed.

Peer-review model: Single blind

Peer-review report's scientific quality classification

Grade A (Excellent): A
Grade B (Very good): 0
Grade C (Good): 0
Grade D (Fair): D
Grade E (Poor): 0

P-Reviewer: Knudsen T, Denmark; Tajra JBM, Brazil

Received: November 14, 2022
Peer-review started: November 14, 2022
First decision: January 12, 2023
Revised: January 25, 2023
Accepted: March 3, 2023
Article in press: March 3, 2023
Published online: March 26, 2023

Shruthi Karthikeyan, Kian Keyashian, John Gubatan, Department of Medicine, Division of Gastroenterology and Hepatology, Stanford University School of Medicine, Stanford, CA 94306, United States

Jeanne Shen, Department of Pathology, Stanford University School of Medicine, Stanford, CA 94306, United States

Corresponding author: John Gubatan, MD, Doctor, Department of Medicine, Division of Gastroenterology and Hepatology, Stanford University School of Medicine, 300 Pasteur Drive, Alway M211 MC 5187, Stanford, CA 94306, United States. jgubatan@stanford.edu

Abstract

BACKGROUND

Small bowel adenocarcinomas (SBA) are rare malignancies with exceedingly low survival rates, with different presentation in Crohn's disease (CD). CD-induced SBA poses diagnostic challenges given overlapping presentation with stricturing CD and lack of diagnostics for early detection. Moreover, guidance is lacking on the impact of recently approved therapeutics in CD on SBA management. Here, we aim to highlight the future of CD-induced SBA management and discuss the potential merit of balloon enteroscopy and genetic testing for earlier detection.

CASE SUMMARY

We report the case of a 60-year-old female with longstanding Crohn's ileitis, presenting with acute obstructive symptoms attributed to stricturing phenotype. Her obstructive symptoms were refractory to intravenous (IV) steroids, with further investigation *via* computed tomography enterography not providing additional diagnostic yield. Ultimately, surgical resection revealed SBA in the neoterminal ileum, with oncologic therapy plan created. However, this therapy plan could not be initiated due to continued obstructive symptoms attributed to active CD. Ultimately, infused biologic therapy was initiated, but her obstructive symptoms continued to remain dependent on IV corticosteroids. Review of diagnostics by a multidisciplinary care team suggested metastatic disease in the peritoneum, lending to a shift in the goals of care to comfort.

CONCLUSION

With the diagnostic and therapeutic challenges of concurrent SBA and CD, multidisciplinary care and algorithmic management can optimize outcomes.

Key Words: Crohn's disease; Small bowel adenocarcinoma; Management; Diagnosis; Case report

Core Tip: The prognosis of Crohn's disease-induced small bowel adenocarcinomas (SBA) depends largely on staging at diagnosis, with early detection resulting in potentially improved outcomes. A multidisciplinary approach with gastroenterology, colorectal surgery, and radiology is key to this early diagnosis. Initially, a thorough family history can aid in decision-making with earlier intervention in those with stricturing phenotype and suggestion of higher colorectal cancer risk or syndrome. If imaging shows atypical features such as a mass, retrograde balloon enteroscopy should not be delayed. Finally, when surgical resection is considered in strictures refractory to medical therapy, lymph node sampling can aid in surgical staging of the SBA.

Citation: Karthikeyan S, Shen J, Keyashian K, Gubatan J. Small bowel adenocarcinoma in neoterminal ileum in setting of stricturing Crohn's disease: A case report and review of literature. *World J Clin Cases* 2023; 11(9): 2021-2028
URL: https://www.wjgnet.com/2307-8960/full/v11/i9/2021.htm
DOI: https://dx.doi.org/10.12998/wjcc.v11.i9.2021

INTRODUCTION

Small bowel adenocarcinomas (SBA) are rare malignancy that originate from the epithelial lining of the small intestine and progressively invade deeper layers of tissue. A systematic review and meta-analysis [1] of eight studies comprising 7344 patients with Crohn's disease (CD) estimated the standardized incidence ratio of small bowel cancer to be 22.01. Risk factors for SBA include hereditary mutations, celiac disease, and inflammatory bowel disease (IBD)[1-3]. More recent work suggests CD-induced SBA may be a separate entity than *de novo* SBA, driven by mutations of different genes and presenting in younger populations.

Patients with CD-induced SBA typically present with intermittent abdominal pain, weight loss, and nausea, but delays in diagnosis result in 33% of patients presenting with an intestinal obstruction[4]. Diagnostic challenges arise given the similar presentation to fibrostenotic CD. Highly specific and sensitive radiological methods can detect SBA but typically once it has caused an obstruction late in the disease course, greatly diminishing prognosis[5]. The current mainstay approach for both SBA and fibrostenotic CD remains surgical resection with histopathology.

CD-induced SBA is a rare phenomenon, and as the therapeutic landscape for CD expands, there presents more opportunity for variation in phenotype, progression, and therapy. Here we present a case of CD-induced SBA in a 60-year-old female with a history of Crohn's ileitis refractory to intravenous (IV) steroids and biologic therapy, presenting with neoterminal ileal obstructions and hepatic consolidation. Through a literature review of previous cases we investigate clinical features and prognostic factors and subsequently propose the use of novel diagnostic techniques for early detection of malignancy.

CASE PRESENTATION

Chief complaints

A 60-year-old female with a 30-year history of poorly controlled stricturing small bowel CD (Montreal L1B2) presented with abdominal pain and nausea.

History of present illness

She was admitted with several weeks of increasing nausea and vomiting, abdominal pain, inability to pass gas or stool. She denies fevers, chills, change in bowel movements, or hematochezia.

History of past illness

The patient was diagnosed with CD 30 years ago, managed largely with mesalamine and courses of corticosteroids. About 15 years after her initial diagnosis, she presented with small bowel obstruction and underwent an exploratory surgery with small bowel resection. She was subsequently treated with corticosteroids with plans for biologic-based treatment which was cost-prohibitive. She was lost to

follow-up until she presented more recently with recurrent obstructive symptoms.

Personal and family history

She denied family history of malignant tumors, including small and large bowel malignancy.

Physical examination

On physical exam, she was afebrile and well-developed, well-nourished. She was clearly uncomfortable with distension. She had diffused abdominal tenderness without rebound or guarding. Her exam was otherwise unremarkable.

Laboratory examinations

Initial labs most notable for an elevated fecal calprotectin 448 (normal < 50 mcg/mg) and normal C-reactive protein. Stool tests (Clostridium difficile and gastrointestinal polymerase chain reaction (PCR) were negative for infection.

Imaging examinations

The patient underwent a computed tomography (CT) enterography which demonstrated multifocal stricturing, predominantly of the ileum, with progressive partial small bowel obstruction. There was no clear intra-luminal or submucosal mass visualized in the small bowel (Figure 1). Given longstanding untreated small bowel CD and elevated calprotectin, the presentation was concerning for small bowel obstruction in the setting of mixed inflammatory and fibrostenotic strictures.

FINAL DIAGNOSIS

The final diagnosis was metastatic CD-SBA.

TREATMENT

Her case was managed in a multidisciplinary fashion, with input from gastroenterology, colorectal surgery, and radiology. Despite IV corticosteroids, she continued to have obstructive symptoms and, ten days later, the decision was made for a repeat ileocecectomy with end ileostomy. Histopathologic examination of the background ileum showed severe chronic active ileitis with cryptitis (Figure 2) consistent with active Crohn's disease. Histopathologic examination of the resected ileocolic anastomosis revealed a poorly-differentiated adenocarcinoma comprised of sheets of single malignant cells with signet-ring morphology. Well-differentiated areas (tubules with small rigid lumina and polarized tumor cell clusters without a distinct lumina) were also identified (Figure 3). The ileum proximal to the tumor displayed a background of chronic active ileitis. Metastatic carcinoma was also found in 6/235 lymph nodes. She was subsequently discharged home with outpatient follow-up.

The patient was readmitted with recurrent obstructive symptoms with CT imaging showing a partial small bowel obstruction with a transition point in the proximal jejunum. The patient had a response to IV methylprednisolone but had recurrence of symptoms after transitioning to oral prednisone. Her case was discussed at a multidisciplinary conference, with a focus on risks and benefits of escalation to biologic therapy. After shared decision-making, infliximab was initiated, and the patient obtained two doses taken alongside IV solumedrol. She continues to remain dependent on IV corticosteroids.

OUTCOME AND FOLLOW-UP

Subsequent CT and positron emission tomography scan demonstrated metastatic hepatic involvement, loculated ascites, and omental nodularity concerning for peritoneal carcinomatosis, and the focus of care was transitioned to comfort measures only. Patient's perspective was not available.

DISCUSSION

Neoplasms of the small bowel comprise 2.4%[6] of all gastrointestinal cancers and the rarity in comparison to CRC is thought to be due to the fluid, alkaline and immunoglobulin A rich nature of the small intestine[7]. SBA describes the malignant transformation of glandular epithelia and is the most prevalent malignancy of the types of small intestine cancers[8]. The incidence of small bowel cancers in the United States have risen from 1.18/100000 in 1973[3] to 2.5/100000 in 2021[9], and are 1.5 to 2 times more common in males than females[9]. Known risk factors include consumption of alcohol, smoked

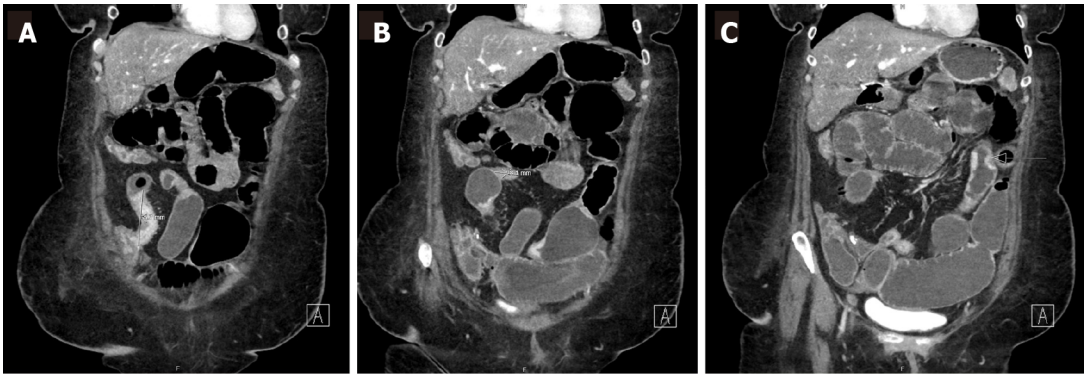

DOI: 10.12998/wjcc.v11.i9.2021

Figure 1 Computed tomography enterography demonstrating multifocal stricturing Crohn's disease. A: Persistent areas of mucosal hyperenhancement and segments of stricturing throughout the small bowel. This included an approximately 6.5 cm area of stricturing of the terminal ileum just proximal to the ileocecal valve; B: Additional smaller segments of stricturing of the terminal ileum proximal to this measuring approximately 2.8 cm and 1.8 cm; C: Additional more proximal 4.5 cm segment of stricturing. Possible short segments of stricturing of jejunum in the left hemiabdomen. No fistulas visualized.

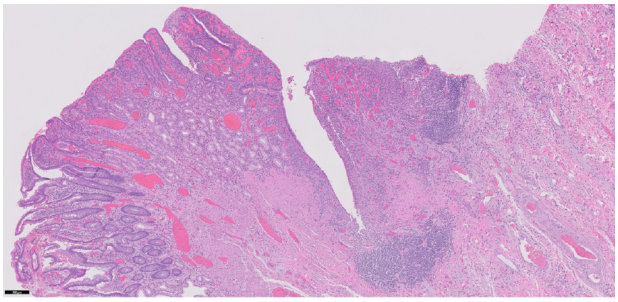

DOI: 10.12998/wjcc.v11.i9.2021

Figure 2 Resected ileum with severe chronic active Crohn's ileitis. The background ileum showed severe chronic active ileitis with cryptitis, crypt abscess formation, fissuring ulceration (center), architectural distortion, pyloric metaplasia, and lymphoid aggregates (5 × objective magnification).

foods and refined carbohydrates, a background of hereditary cancer syndromes including familial adenomatous polyposis and hereditary nonpolyposis CRC or IBD[10]. SBA tends to localize to the duodenum and jejunum, while a small percentage localize to the ileum[11]. This is in contrast to CD-induced SBA, where the ileum is most commonly involved.

The prevalence of SBA is markedly higher in CD patients, at 1.15 per 1000 CD patients[12], A study done by Yu *et al*[13] determined the standardized infection ratio (SIR) of SBA in CD to be 8.3, with the SIR for stricturing CD being 14.7 per 100000 person years. The eight-fold increase in risk for SBA in a background of CD warrants active surveillance methods and development of an effective algorithm for the detection and diagnosis of SBA.

Recent work suggests major differences in the pathogenesis of *de novo* SBA and CD-induced SBA[8]. CD-induced SBA thought to be caused by a predisposed gastrointestinal environment of chronic inflammation[14,15]. The environment increases permeability of carcinogens and promotes malabsorption of anti-carcinogenic compounds[16]. Longstanding CD results in cycles of inflammation and scar tissue formation, resulting in mutagenesis of genes implicated in tumor suppression and chromatin remodeling leading to an increased risk of carcinogenesis. Molecular differences between de novo SBA and CD-induced SBA indicate the implication of different carcinogenic pathways[15]. A prospective analysis reveals CD-induced SBA is predominantly driven by mutations of CDKN2A/B, CASP8 and ATRX[9].

There is little information directing management of the disease, resulting in many cases being treated as an extrapolation from CRC due to overlap in the drivers of molecular pathogenesis and lack of knowledge surrounding the progression of SBA[17]. The presentation is nonspecific lending to an average delay in diagnosis of 6 to 12 mo. In light of this delay in diagnosis, SBA has a markedly decreased 5-year survival rate at 34.9% and increase in prevalence, as opposed to the 51.5% 5 year survival rate in CRC and decline in prevalence[18].

Risk factors

A prior study using the National Cancer Database[19] involving 493 patients with CD-associated SBA and 2175 with sporadic SBA demonstrated that CD-associated SBA were more likely to present at a

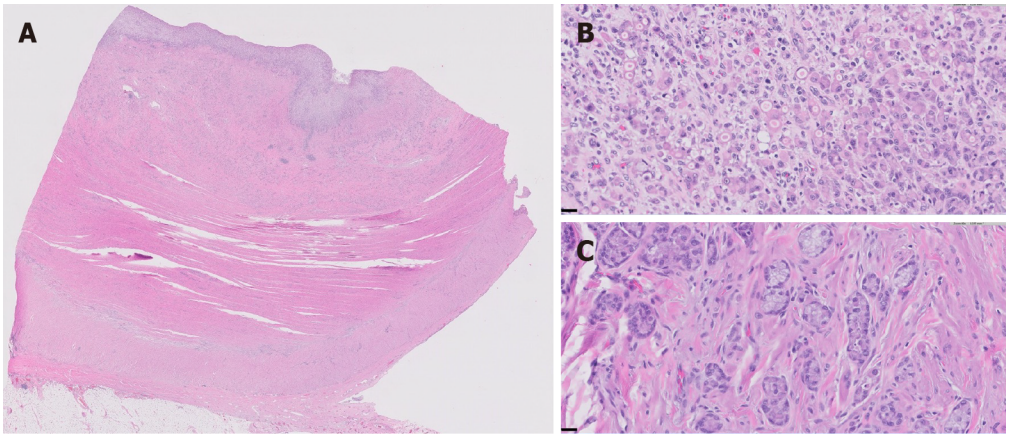

DOI: 10.12998/wjcc.v11.i9.2021

Figure 3 Small bowel adenocarcinoma in resected neoterminal ileum. A: Cross section of the ileum near the anastomosis, showing complete effacement of the mucosa and infiltration of the underlying ileal wall by the adenocarcinoma (0.5 × objective magnification); B: Representative high-magnification view of the poorly-differentiated adenocarcinoma, comprised of sheets of single malignant cells and cell clusters with signet ring morphology (40 × objective magnification); C: Representative high-magnification view of a well-differentiated region of the adenocarcinoma, characterized by well-defined tubules with small, rigid lumina, mimicking intestinal crypts, as well as tumor cells arranged in well-polarized clusters without distinct lumina (40 × objective magnification).Tumor was noted in 6/35 lymph nodes and showed serosal involvement and lymphovascular and perineural invasion. Immunohistochemistry revealed intact expression of DNA mismatch proteins MLH1, MSH2, MSH6 and PMS2.

younger age, have tumors located in the ileum, and have poorly differentiated tumors compared to sporadic SBA. The typical age of diagnosis of *de novo* SBA is 60-69 years, whereas CD-induced SBA is 45-55 years, with diagnosis of CD usually predating diagnosis of SBA by 20 years[20]. SBA is also more likely to affect males (62.5%-80%)[21]. Family history of colorectal cancer (CRC) and potential cancer syndromes are also important risk factors, highlighting the need for a thorough family history. In addition, a prior multi-center case-control study[22] suggested that a prior small bowel resection and prolonged salicylate treatment (> 2 years) were associated with decreased risk of SBA in CD.

In contrast to these known risk factors, our patient's gender and age did not fit typical demographics of CD-induced SBA and her symptoms were readily attributable to stricturing CD, signifying the need to broaden conceptualizations regarding demographic trends. In addition she developed SBA despite having a prior small bowel resection and being on long-term mesalamine therapy.

Diagnostics

The pathogenesis of CD-induced SBA suggests the prospect of genetic testing in refractory CD to investigate potential risk factors for malignancy development. Advances in liquid biopsy allow for the detection of tumor related markers through analysis of ctDNA, cfDNA and circulating tumor derived endothelial cells in samples of biological fluids[23]. Recent work describes the merits of this method in the detection and real time monitoring of CRC, allowing repeated temporal sampling for detection at curable stages[24-26]. A study done by Zhong *et al*[27] found that mesenchymal cell marker vimentin (M-CTC) in liquid biopsy directly correlated with tumor size, tumor, node and metastasis stage and vascular invasion. Unfortunately, the cost of liquid biopsy[26] outweighs its feasibility as a screening method, warranting discovery of affordable techniques that serve the same purpose for SBA. Nevertheless, these techniques could be applied to high-risk phenotypes, such as stricturing CD.

Resection is an invasive process with several associated risks, posing the need to explore novel less invasive diagnostic techniques. Currently CT and magnetic resonance enterography provide high specificity and sensitivity in the detection of stricturing malignant lesions at lesions at 98% and 95%[28] respectively. If a mass is seen on these imaging modalities, further diagnostics could be pursued. However, the shortcomings of cross-sectional imaging include lack of ability to distinguish CD-related stricturing from malignancy; neither of these methods can allow for examination of cellular morphology like histopathology, which is why both methods must be combined for definitive diagnosis of malignancy.

Independent of imaging finding of a mass, a method that is able to evaluate the investigate a significant length of the gastrointestinal tract and the strictured area whilst allowing for biopsy, delivery of therapy and tattooing the lesion as a marking for subsequent surgery double balloon enteroscopy (DBE)[29]. DBE has a 85.9% positive rate of diagnosis opposed to the 72.9% of CT[30]. A case in 2021 was able to harness DBE to diagnose SBA presence and progression prior to surgery[31], allowing for early confirmation of peritoneal dissemination *via* laparoscopy prior to resection.

Survival and effect of biologics on disease progression

The mainstay treatment for SBA remains to be surgical resection of the primary tumor and loco-regional lymph node resection. This may be accompanied with chemotherapy in between surgeries if multiple surgeries are required to resect the mass. In the case that the final ileal loop is affected, an ileocecal or right hemicolectomy with ligation of the ileocolic artery is recommended[14].

Patients with lymph node involvement have a 32% 5-year overall survival (OS) compared to the 52% of patients without lymph node involvement[14]. Moreover, patients with over 75% lymph node involvements had a 12% 5-year OS as opposed to 51% in patients with less than 75% lymph node involvement[14]. 5-year OS for resected *vs* non resected tumors are 40-60% and 15-30% respectively[14]. Recent work has shown very minimal improvement in prognosis when adjuvant chemotherapy such as fluoropyrimidine and oxaliplatin are used in conjunction with surgery for stage 3 disease[14]. However, retrospective studies do indicate the efficacy of chemotherapy in non-surgically treated patients, showing an OS of 12 mo *vs* 2 mo for chemotherapy treated and non-treated respectively[12]. Generally, when chemotherapy is pursued, patients with concomitant IBD stop biologic treatments until the course of chemotherapy is complete due to increased risk of carcinogenesis with immunosuppression[13].

Our patient was started on infliximab alongside IV steroids, prior to development of ascites and metastatic hepatic involvement representative of peritoneal carcinomatosis. While there have been some small studies that have correlated infliximab therapy to either development or rapid progression of colorectal adenocarcinoma, larger studies show similar progression as a basline population[32-34]. Further larger studies can clarify the association between the usage of anti-TNF therapy and incidence of malignancy to justify the merit of anti-TNF biologics to treat CD in patients with risk factors for small bowel cancer progression or recurrence.

Multidisciplinary care

This case is unique regarding the patient's demographics which challenge what is currently expected in patients with CD induced SBA, making diagnosis difficult, especially when paired with insignificant imaging. Our case highlights the need for multidisciplinary care for management of CD-induced SBA. Medical gastroenterologists, colorectal surgeons, radiologist, specialized pathologists, and medical oncologists are key elements of the team to expedite diagnosis and delineate treatment.

Proposal of a novel algorithm

Through this case, we propose an approach for earlier detection of SBA in CD patients. First, identification of a CRC risk or syndrome in the setting of stricturing ileal CD warrants evaluation of the stricture DBE. Furthermore, symptomatic strictures unresponsive to therapy should head to surgery early in the course of hospitalization. Finally, during the surgical approach, sampling of the lymph nodes to understand the staging of SBA. These different stages should be approached in a multidisciplinary fashion.

Although this study provides insight into a novel presentation of CD induced SBA, this case report is limited primarily by clinical follow up and sample size. While we provide one algorithm to treatment, a prospective multicenter trial would be needed to validate the recommendations and conclusions made in this study. Moreover, the limited clinical follow up may have skewed results.

CONCLUSION

Our case highlights the challenges of diagnosing and managing SBA in longstanding CD. It emphasizes that the absence of an apparent mass on cross-sectional imaging in a patient with CD and bowel obstruction does not rule out malignancy, underlining the importance of maintaining a broad differential diagnosis in patients with nonrefractory, obstructive CD. SBA is a recognized complication of CD. Studies identifying clinical factors to risk stratify patients who will develop small bowel malignancy in CD are lacking. Future studies are needed to explore strategies for early detection and prevention of SBA among patients with CD.

FOOTNOTES

Author contributions: Karthikeyan S reviewed the literature, prepared case report, and wrote the manuscript; Shen J provided the gastrointestinal pathology interpretation and images and feedback regarding the manuscript; Keyashian K and Gubatan J provided critical feedback and drafted the manuscript.

Informed consent statement: All study participants provided informed written consent prior to study enrollment.

Conflict-of-interest statement: All the authors report no relevant conflicts of interest for this article.

CARE Checklist (2016) statement: The authors have read the CARE Checklist (2016), and the manuscript was

prepared and revised according to the CARE Checklist (2016).

Country/Territory of origin: United States

ORCID number: John Gubatan 0000-0001-6037-2883.

S-Editor: Zhang H
L-Editor: A
P-Editor: Zhang H

REFERENCES

1 **Annese V**. Small Bowel Adenocarcinoma in Crohn's Disease: An Underestimated Risk? *J Crohns Colitis* 2020; **14**: 285-286 [PMID: 32167150 DOI: 10.1093/ecco-jcc/jjz168]
2 **Occhipinti M**, Botticell A, Onesti CE, Ghidini M, Righini R, Pizzo C, Milano A, Tomasello G, Di Pietro FR, Toppo L. Treatment and outcome for small bowel adenocarcinoma (SBA): a real life experience of two Italian centres. *Ann Oncol* 2017; **28**: vi50 [DOI: 10.1093/annonc/mdx425.022]
3 **Palascak-Juif V**, Bouvier AM, Cosnes J, Flourié B, Bouché O, Cadiot G, Lémann M, Bonaz B, Denet C, Marteau P, Gambiez L, Beaugerie L, Faivre J, Carbonnel F. Small bowel adenocarcinoma in patients with Crohn's disease compared with small bowel adenocarcinoma de novo. *Inflamm Bowel Dis* 2005; **11**: 828-832 [PMID: 16116317 DOI: 10.1097/01.mib.0000179211.03650.b6]
4 **Dasari BV**, Gardiner KR. Management of adenocarcinoma of the small intestine. *Gastrointest Cancer Res* 2009; **3**: 121-122 [PMID: 19626156]
5 **Li J**, Wang Z, Liu N, Hao J, Xu X. Small bowel adenocarcinoma of the jejunum: a case report and literature review. *World J Surg Oncol* 2016; **14**: 177 [PMID: 27402105 DOI: 10.1186/s12957-016-0932-3]
6 **Paski SC**, Semrad CE. Small bowel tumors. *Gastrointest Endosc Clin N Am* 2009; **19**: 461-479 [PMID: 19647652 DOI: 10.1016/j.giec.2009.04.012]
7 **Calman KC**. Why are small bowel tumours rare? *Gut* 1974; **15**: 552-554 [PMID: 4609841 DOI: 10.1136/gut.15.7.552]
8 Cancer.Net. Small Bowel Cancer. Introduction. [cited 9 November 2022]. Available from: https://www.cancer.net/cancer-types/small-bowel-cancer/introduction
9 SEER Cancer. Cancer Stat Facts: Small Intestine Cancer. [cited 28 June 2022]. Available from: https://seer.cancer.gov/statfacts/html/smint.html
10 **Quinones GAO**, Suheb MZK, Woolf A. Small Bowel Cancer. In: StatPearls [Internet]. Treasure Island (FL): StatPearls Publishing, 2022
11 **Halfdanarson TR**, McWilliams RR, Donohue JH, Quevedo JF. A single-institution experience with 491 cases of small bowel adenocarcinoma. *Am J Surg* 2010; **199**: 797-803 [PMID: 20609724 DOI: 10.1016/j.amjsurg.2009.05.037]
12 **Chin YH**, Jain SR, Lee MH, Ng CH, Lin SY, Mai AS, Muthiah MD, Foo FJ, Sundar R, Ong DEH, Leow WQ, Leong R, Chan WPW. Small bowel adenocarcinoma in Crohn's disease: a systematic review and meta-analysis of the prevalence, manifestation, histopathology, and outcomes. *Int J Colorectal Dis* 2022; **37**: 239-250 [PMID: 34704127 DOI: 10.1007/s00384-021-04050-1]
13 **Yu J**, Refsum E, Perrin V, Helsingen LM, Wieszczy P, Løberg M, Bretthauer M, Adami HO, Ye W, Blom J, Kalager M. Inflammatory bowel disease and risk of adenocarcinoma and neuroendocrine tumors in the small bowel. *Ann Oncol* 2022; **33**: 649-656 [PMID: 35276334 DOI: 10.1016/j.annonc.2022.02.226]
14 **Aparicio T**, Zaanan A, Svrcek M, Laurent-Puig P, Carrere N, Manfredi S, Locher C, Afchain P. Small bowel adenocarcinoma: epidemiology, risk factors, diagnosis and treatment. *Dig Liver Dis* 2014; **46**: 97-104 [PMID: 23796552 DOI: 10.1016/j.dld.2013.04.013]
15 **Pandya K**, Overman MJ, Gulhati P. Molecular Landscape of Small Bowel Adenocarcinoma. *Cancers (Basel)* 2022; **14** [PMID: 35267592 DOI: 10.3390/cancers14051287]
16 **Caio G**, Volta U, Ursini F, Manfredini R, De Giorgio R. Small bowel adenocarcinoma as a complication of celiac disease: clinical and diagnostic features. *BMC Gastroenterol* 2019; **19**: 45 [PMID: 30917787 DOI: 10.1186/s12876-019-0964-6]
17 **Pedersen KS**, Raghav K, Overman MJ. Small Bowel Adenocarcinoma: Etiology, Presentation, and Molecular Alterations. *J Natl Compr Canc Netw* 2019; **17**: 1135-1141 [PMID: 31487680 DOI: 10.6004/jnccn.2019.7344]
18 **Young JI**, Mongoue-Tchokote S, Wieghard N, Mori M, Vaccaro GM, Sheppard BC, Tsikitis VL. Treatment and Survival of Small-bowel Adenocarcinoma in the United States: A Comparison With Colon Cancer. *Dis Colon Rectum* 2016; **59**: 306-315 [PMID: 26953989 DOI: 10.1097/DCR.0000000000000562]
19 **Fields AC**, Hu FY, Lu P, Irani J, Bleday R, Goldberg JE, Melnitchouk N. Small Bowel Adenocarcinoma: Is There a Difference in Survival for Crohn's Versus Sporadic Cases? *J Crohns Colitis* 2020; **14**: 303-308 [PMID: 31541248 DOI: 10.1093/ecco-jcc/jjz157]
20 **Kodaira C**, Osawa S, Mochizuki C, Sato Y, Nishino M, Yamada T, Takayanagi Y, Takagaki K, Sugimoto K, Kanaoka S,

Furuta T, Ikuma M. A case of small bowel adenocarcinoma in a patient with Crohn's disease detected by PET/CT and double-balloon enteroscopy. *World J Gastroenterol* 2009; **15**: 1774-1778 [PMID: 19360924 DOI: 10.3748/wjg.15.1774]

21 **Lech G**, Korcz W, Kowalczyk E, Chaber A, Słodkowski M. The risk of small bowel adenocarcinoma in patients with Crohn's disease. *Prz Gastroenterol* 2020; **15**: 309-313 [PMID: 33777270 DOI: 10.5114/pg.2020.101559]

22 **Piton G**, Cosnes J, Monnet E, Beaugerie L, Seksik P, Savoye G, Cadiot G, Flourie B, Capelle P, Marteau P, Lemann M, Colombel JF, Khouri E, Bonaz B, Carbonnel F. Risk factors associated with small bowel adenocarcinoma in Crohn's disease: a case-control study. *Am J Gastroenterol* 2008; **103**: 1730-1736 [PMID: 18564124 DOI: 10.1111/j.1572-0241.2008.01847.x]

23 **Zhou H**, Zhu L, Song J, Wang G, Li P, Li W, Luo P, Sun X, Wu J, Liu Y, Zhu S, Zhang Y. Liquid biopsy at the frontier of detection, prognosis and progression monitoring in colorectal cancer. *Mol Cancer* 2022; **21**: 86 [PMID: 35337361 DOI: 10.1186/s12943-022-01556-2]

24 **Mauri G**, Vitiello PP, Sogari A, Crisafulli G, Sartore-Bianchi A, Marsoni S, Siena S, Bardelli A. Liquid biopsies to monitor and direct cancer treatment in colorectal cancer. *Br J Cancer* 2022; **127**: 394-407 [PMID: 35264786 DOI: 10.1038/s41416-022-01769-8]

25 **Broccard SP**, Kasbi AA, Bagaria SP, Jones J, Shoudry M, Gabriel EM. Liquid biopsies for colorectal cancer: a narrative review of ongoing clinical trials and the current use of this technology at a comprehensive cancer center. *J Gastrointest Oncol* 2022; **13**: 438-449 [PMID: 35284120 DOI: 10.21037/jgo-21-470]

26 **Raza A**, Khan AQ, Inchakalody VP, Mestiri S, Yoosuf ZSKM, Bedhiafi T, El-Ella DMA, Taib N, Hydrose S, Akbar S, Fernandes Q, Al-Zaidan L, Krishnankutty R, Merhi M, Uddin S, Dermime S. Dynamic liquid biopsy components as predictive and prognostic biomarkers in colorectal cancer. *J Exp Clin Cancer Res* 2022; **41**: 99 [PMID: 35292091 DOI: 10.1186/s13046-022-02318-0]

27 **Zhong Y**, Ma T, Qiao T, Hu H, Li Z, Luo K, Wang Y, Tang Q, Wang G, Huang R, Wang X. Role of Phenotypes of Circulating Tumor Cells in the Diagnosis and Treatment of Colorectal Cancer. *Cancer Manag Res* 2021; **13**: 7077-7085 [PMID: 34531685 DOI: 10.2147/CMAR.S316544]

28 **Coco D**, Leanza S, Boccoli G. Small bowel adenocarcinoma (SBA) three years after colonic adenocarcinoma in an elderly patient: Case report in a National Institute of Health and Aging (INRCA) and review of the literature. *Int J Surg Case Rep* 2014; **5**: 939-943 [PMID: 25460441 DOI: 10.1016/j.ijscr.2014.07.011]

29 **Safatle-Ribeiro AV**, Ribeiro U Jr. Impact of enteroscopy on diagnosis and management of small bowel tumors. *Chin J Cancer Res* 2020; **32**: 319-333 [PMID: 32694897 DOI: 10.21147/j.issn.1000-9604.2020.03.04]

30 **Chen WG**, Shan GD, Zhang H, Li L, Yue M, Xiang Z, Cheng Y, Wu CJ, Fang Y, Chen LH. Double-balloon enteroscopy in small bowel tumors: a Chinese single-center study. *World J Gastroenterol* 2013; **19**: 3665-3671 [PMID: 23801870 DOI: 10.3748/wjg.v19.i23.3665]

31 **Lee SC**. Minimally invasive surgery with adenocarcinoma of jejunum diagnosed pathologically before surgery: A case report. *Int J Surg Case Rep* 2021; **79**: 354-357 [PMID: 33508617 DOI: 10.1016/j.ijscr.2021.01.061]

32 **Xiao L**, Sun L, Zhao K, Pan YS. Crohn's disease with infliximab treatment complicated by rapidly progressing colorectal cancer: A case report. *World J Gastrointest Oncol* 2021; **13**: 305-311 [PMID: 33889281 DOI: 10.4251/wjgo.v13.i4.305]

33 **Egea-Valenzuela J**, Belchí-Segura E, Essouri N, Sánchez-Torres A, Carballo-Alvarez F. Adenocarcinoma of the rectum and anus in a patient with Crohn's disease treated with infliximab. *Rev Esp Enferm Dig* 2010; **102**: 501-504 [PMID: 20670073 DOI: 10.4321/s1130-01082010000800009]

34 **Smaali J**, Sekkach Y. Adénocarcinome ano-réctal après traitement par Infliximab pour une maladie de Crohn fistulisante [Anorectal adenocarcinoma after Infliximab treatment for fistulizing Crohn's disease]. *Pan Afr Med J* 2017; **26**: 172 [PMID: 28674565 DOI: 10.11604/pamj.2017.26.172.10218]

World Journal of Clinical Cases

Submit a Manuscript: https://www.f6publishing.com

World J Clin Cases 2023 March 26; 11(9): 2029-2035

DOI: 10.12998/wjcc.v11.i9.2029

ISSN 2307-8960 (online)

CASE REPORT

Novel combined endoscopic and laparoscopic surgery for advanced T2 gastric cancer: Two case reports

Jian-Hua Dai, Feng Qian, Lei Chen, Sen-Lin Xu, Xiao-Feng Feng, Hong-Bo Wu, Yao Chen, Zhi-Hong Peng, Pei-Wu Yu, Gui-Yong Peng

Specialty type: Gastroenterology and hepatology

Provenance and peer review: Unsolicited article; Externally peer reviewed.

Peer-review model: Single blind

Peer-review report's scientific quality classification

Grade A (Excellent): 0
Grade B (Very good): B
Grade C (Good): C
Grade D (Fair): 0
Grade E (Poor): 0

P-Reviewer: He YH, China; Murariu MS, Romania

Received: December 1, 2022
Peer-review started: December 1, 2022
First decision: January 2, 2023
Revised: January 14, 2023
Accepted: February 22, 2023
Article in press: February 22, 2023
Published online: March 26, 2023

Jian-Hua Dai, Lei Chen, Xiao-Feng Feng, Hong-Bo Wu, Yao Chen, Zhi-Hong Peng, Gui-Yong Peng, Department of Gastroenterology, Southwest Hospital, The Third Military Medical University, Chongqing 400038, China

Feng Qian, Pei-Wu Yu, Department of General Surgery, Southwest Hospital, The Third Military Medical University, Chongqing 400038, China

Sen-Lin Xu, Department of Pathology, Southwest Hospital, The Third Military Medical University, Chongqing 400038, China

Corresponding author: Gui-Yong Peng, MD, Chief Physician, Department of Gastroenterology, Southwest Hospital, The Third Military Medical University, No. 30 Gaotan Yanzheng Street, Shapingba District, Chongqing 400038, China. pgy63@163.com

Abstract

BACKGROUND

The standard treatment for advanced T2 gastric cancer (GC) is laparoscopic or surgical gastrectomy (either partial or total) and D2 lymphadenectomy. A novel combined endoscopic and laparoscopic surgery (NCELS) has recently been proposed as a better option for T2 GC. Here we describe two case studies demonstrating the efficacy and safety of NCELS.

CASE SUMMARY

Two T2 GC cases were both resected by endoscopic submucosal dissection and full-thickness resection and laparoscopic lymph nodes dissection. This method has the advantage of being more precise and minimally invasive compared to current methods. The treatment of these 2 patients was safe and effective with no complications. These cases were followed up for nearly 4 years without recurrence or metastasis.

CONCLUSION

This novel method provides a minimally invasive treatment option for T2 GC, and its potential indications, effectiveness and safety needs to be further evaluated in controlled studies.

Key Words: Novel combined endoscopic and laparoscopic surgery; T2 gastric cancer; Endoscopic submucosal dissection and full-thickness resection; Laparoscopic lymph nodes

dissection; Minimally invasive; Case report

Core Tip: We propose a new method of combining endoscopic local lesion resection and laparoscopic lymph node dissection for 2 cases of advanced T2 gastric cancer (GC). This new method has the advantages of precision and being minimally invasive with similar outcomes as surgical resection. It is a novel method providing a minimally invasive treatment option for T2 GC.

Citation: Dai JH, Qian F, Chen L, Xu SL, Feng XF, Wu HB, Chen Y, Peng ZH, Yu PW, Peng GY. Novel combined endoscopic and laparoscopic surgery for advanced T2 gastric cancer: Two case reports. *World J Clin Cases* 2023; 11(9): 2029-2035
URL: https://www.wjgnet.com/2307-8960/full/v11/i9/2029.htm
DOI: https://dx.doi.org/10.12998/wjcc.v11.i9.2029

INTRODUCTION

The standard treatment for advanced gastric cancer (GC) is laparoscopic or surgical gastrectomy (either partial or total) and D2 lymphadenectomy[1]. Here, we report 2 cases indicating that endoscopic local lesion resection combined with laparoscopic lymph node dissection may be an effective treatment for T2 GC. These cases included a 23-year-old male with a 2.0 cm × 2.0 cm T2 poorly differentiated gastric antrum adenocarcinoma and a 54-year-old female with a 2.0 cm × 2.5 cm T2 poorly differentiated gastric body adenocarcinoma. Both were resected by endoscopic submucosal dissection and full-thickness resection (ESDFTR) and laparoscopic lymph node dissection with good postoperative recovery. This method has the advantages of being more precise and minimally invasive compared to current methods. With this in mind, its potential indications, effectiveness and safety need to be further evaluated in controlled studies.

At present, partial or total gastrectomy is used in the minimally invasive treatment of advanced GC. However, this procedure has the drawback that it destroys the normal anatomical structure of the stomach seriously affecting its physiological function. It is often associated with substantial trauma, slower recovery, a higher complication rate and decreased postoperative quality of life. With advances in endoscopic resection technology, endoscopic submucosal dissection (ESD) or closed laparoscopic and endoscopic cooperative surgery is increasingly applied for T1 early cancer[2]. Endoscopic full-thickness resection technology can completely remove benign tumors of the muscularis propria[3]. For treatment of T2 GC, we reported a novel combined endoscopic and laparoscopic surgery (NCELS) to resect local lesions with ESDFTR (Figure 1) along with lymph node removal by laparoscope, which together achieved complete resection of the lesion and thorough clearing of the lymph nodes. This procedure also allowed preservation of the anatomical structure and physiological function of the stomach thereby enhancing the postoperative quality of life of the patients.

CASE PRESENTATION

Chief complaints

A 23-year-old male and a 54-year-old female were admitted to our hospital with poorly differentiated gastric adenocarcinoma.

Personal and family history

No specific medical history.

Laboratory examinations

Carcinoembryonic antigen (CEA) test values were in the normal range.

Imaging examinations

Gastroscopy revealed a 2.0 cm × 2.0 cm protuberant lesion on the greater curvature of the anterior wall of the gastric antrum in the male patient (Figure 2) and a 2.0 cm × 2.5 cm 0-IIa + IIc type lesion on the greater curvature of the lower gastric body in the female patient (Figure 3). Pathological examination showed poorly differentiated adenocarcinoma. Contrast-enhanced computed tomography (CT) of the

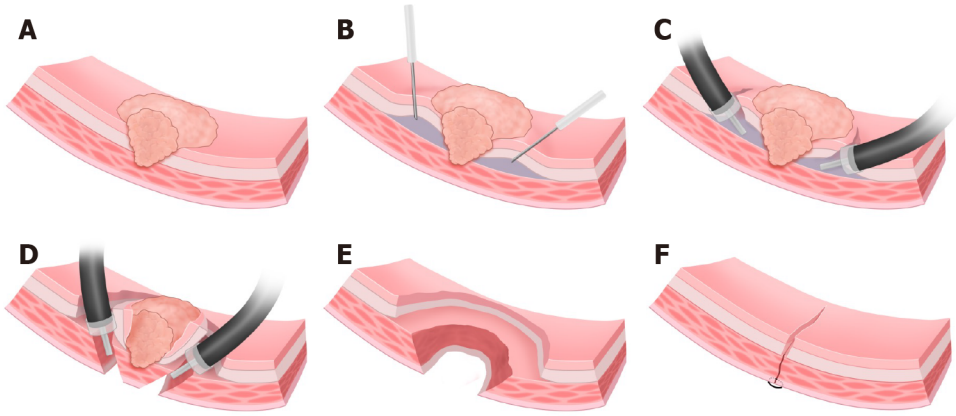

DOI: 10.12998/wjcc.v11.i9.2029

Figure 1 Endoscopic submucosal dissection and full-thickness resection. A: T2 gastric cancer lesion; B: Submucosal injection on the lateral side of the lesion; C: Endoscopic submucosal dissection; D: The circumferential full-thickness resection is performed at 0.5-1.0 cm lateral to the deep infiltration, and the resected lesion is removed; E: Gastric wall wound after endoscopic submucosal dissection and full-thickness resection. The serosal defect is smaller than the mucosal defect; F: The gastric wall wound is sutured by endoscope or laparoscope.

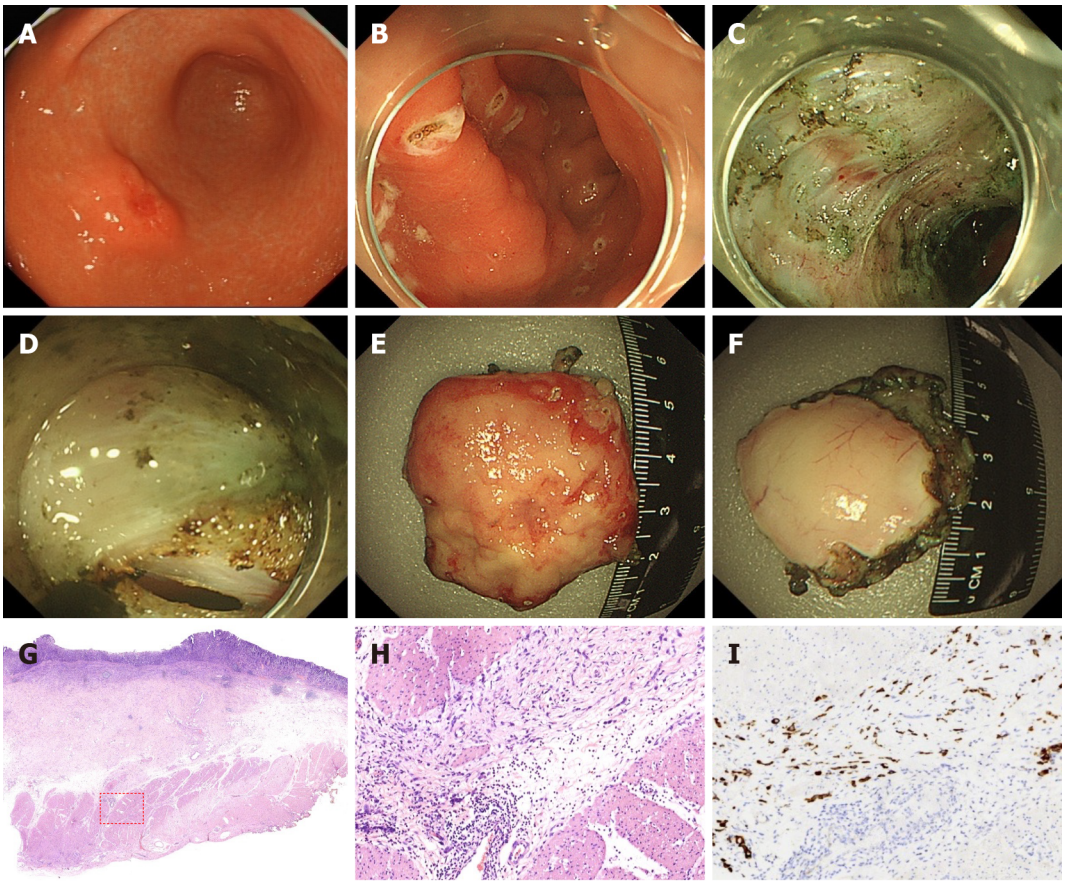

DOI: 10.12998/wjcc.v11.i9.2029

Figure 2 Case 1, minimally invasive endoscopic resection of T2 gastric cancer (endoscopic submucosal dissection and full-thickness resection) and pathology. A and B: Protuberant lesion on the greater curvature of the anterior wall of the gastric antrum, about 2.0 cm × 2.0 cm. The resection area was marked 1.5 cm outside the edge of the lesion, then endoscopic submucosal dissection (ESD) was performed along the outside of the marked point; C and D: ESD circumferentially peeled to the submucosa, which was thinned and unclear, indicating that the lesion was deeply infiltrated (SM3 or T2). At 0.5-1.0 cm outside the unclear portion of submucosa, the lesion was resected by ESD and full-thickness resection; E: Mucosal surface of resected lesion (3.2 cm × 3.5 cm); F: The serosa of the resected lesion revealed that the area of the resected mucosa (normal mucosa and the mucosa with shallow infiltration) was significantly larger than that of the serosa (location of deep infiltration); G and H: Poorly differentiated adenocarcinoma, infiltrating into the superficial layer of the muscularis propria (red box); scale bar, 500 μm; I: Immunohistochemical staining of cytokeratin expression at location of poorly differentiated adenocarcinoma.

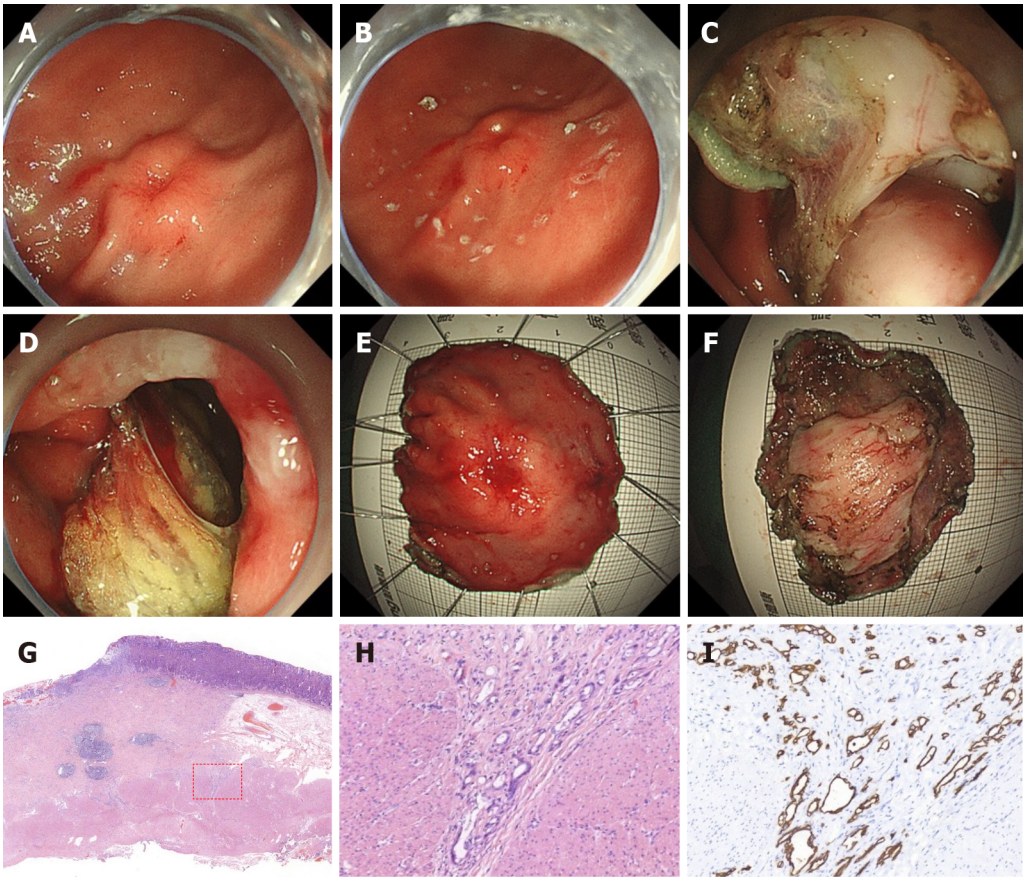

DOI: 10.12998/wjcc.v11.i9.2029

Figure 3 Case 2, minimally invasive endoscopic resection of T2 gastric cancer (endoscopic submucosal dissection and full-thickness resection) and pathology. A and B: Lesion on the greater curvature of the lower gastric body, central ulcer, marginal eminence, about 2.0 cm × 2.5 cm. The resection area was marked 1.5 cm outside the edge of the lesion, and endoscopic submucosal dissection (ESD) was performed along the outside of the marked point. ESD circumferentially peeled to the submucosa, which was thinned and unclear, indicating that the lesion was deeply infiltrated (SM3 or T2); C and D: At 0.5-1.0 cm outside the unclear portion of submucosa, the lesion was resected by ESD and full-thickness resection; E: Mucosal surface of resected lesion (3.8 cm × 4.0 cm); F: The serosa of the resected lesion showed that the area of the resected mucosa (normal mucosa and the mucosa with shallow infiltration) was significantly larger than that of the serosa (location with deep infiltration); G and H: Poorly differentiated adenocarcinoma, containing signet ring cells, infiltrating into the superficial layer of muscularis propria (red box); scale bar, 500 μm; I: Immunohistochemical staining of cytokeratin expression at location of poorly differentiated adenocarcinoma.

abdomen showed that areas of the antrum and gastric body were slightly thickened. No metastasis to the lymph nodes or other organs was observed on the chest and abdomen CT scans. Endoscopic ultrasonography revealed invasion of the muscularis propria.

FINAL DIAGNOSIS

The clinical diagnosis in both cases was T2 GC without lymph node and other organ metastasis. Postoperative pathological diagnosis was T2 GC for both cases.

TREATMENT

The patients were placed under general anesthesia with endotracheal intubation. The procedure included four steps as follows:

Step 1: Determine the demarcation line. Magnifying endoscopy with narrow band imaging was used to determine the demarcation line of the lesion. Marking was set to 1.5 cm outside the lesion.

Step 2: ESDFTR. After submucosal injection, the lesion was dissected by circumferential ESD until the tumor infiltrated deeper (the submucosa was thin or unclear), then dental floss was used to traction the lesion. A whole layer incision was performed at 0.5-1.0 cm lateral to the deep infiltration, followed by circumferential full-thickness resection, and the resected lesion was removed.

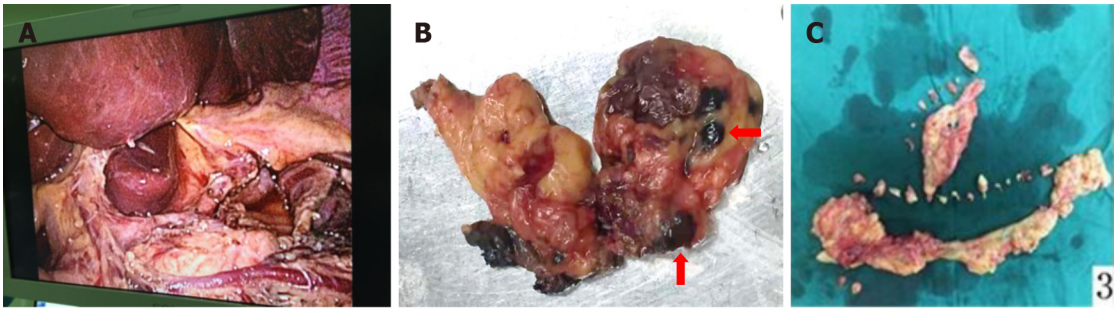

DOI: 10.12998/wjcc.v11.i9.2029

Figure 4 Novel combined endoscopic and laparoscopic surgery. A: Laparoscopic D2 lymphadenectomy can achieve skeletonization of common hepatic artery, proper hepatic artery and splenic artery; B and C: Dissection of lymph nodes (red arrow) and omentum.

Step 3: Gastric wound suture and lymph node dissection. The gastric wound was sutured with an endoscope or laparoscope. Then regional lymph nodes were radically dissected (Figure 4).

Step 4: Pathological examination. The resected gastric specimens and lymph nodes were pathologically examined to determine the depth of invasion and lymph node metastasis.

OUTCOME AND FOLLOW-UP

The 2 cases were characterized as poorly differentiated adenocarcinoma, infiltrating into the superficial layer of the muscularis propria. One case had negative lymph node metastasis, and the other case had nerve infiltration. Postoperative pathological diagnosis was T2 GC for both cases.

The patients were discharged 8 d and 10 d after operation. No local or metastatic recurrence of lymph nodes and organs were found in regular review of gastroscopy (Figure 5) and enhanced CT of the abdomen within 4 years for the male patient and 3 years for the female patient following the operation. CEA test values remained in the normal range. Their postoperative quality of life was good, with no significant gastrointestinal symptoms, and they retained a normal diet and weight.

DISCUSSION

At present, there are two main techniques for minimally invasive treatment of GC: endoscopic resection and laparoscopic radical resection. Both endoscopic and laparoscopic therapies have their own advantages and limitations in the treatment of T2 GC. The advantages of endoscopic resection are that the lesion can be observed under direct vision, the resection range of the lesion can be accurately determined, the lesion can be completely removed, and the normal gastric anatomy and gastric physiological function can be preserved, thus ensuring postoperative quality of life of the patient. However, the limitations are that the lymph nodes cannot be cleared and the risk of lymph node metastasis cannot be eliminated[4]. The advantage of laparoscopic surgery is that it can completely remove the lesion and thoroughly clear the lymph nodes. However, because T2 cancers grow in the lumen, the extent of the lesion cannot be accurately determined outside the gastric wall. Therefore, laparoscopic surgery alone requires partial or total gastrectomy, which destroys the normal anatomical structure of the stomach and affects the physiological function of the stomach, thus seriously affecting postoperative quality of life of the patient, combined with a risk of local residue and recurrence[5,6].

T2 GC often has deep infiltration in the central part of the lesion, while the surrounding region is shallow, with mucosal or submucosal infiltration. Using ESDFTR technology, submucosal dissection can be used to completely remove the mucosal and submucosal infiltrating lesion, followed by full-thickness resection to remove the lesion in the deep submucosa and muscularis propria, which can minimize the damage to the gastric anatomical structure providing a more precise and minimally invasive treatment option. In addition, laparoscopy is a more reliable procedure to seal the gastric wound. Furthermore, the lymph nodes can be thoroughly cleared of metastatic tumor tissue. Therefore, the NCELS can both provide a cure and be precise and minimally invasive. Compared with traditional surgery, NCELS for T2 GC achieved complete resection of the lesion, thorough clearing of the lymph nodes and preservation of the anatomical structure and physiological function of the stomach. It has the advantages of less trauma, fewer complications, lower cost and better postoperative quality of life.

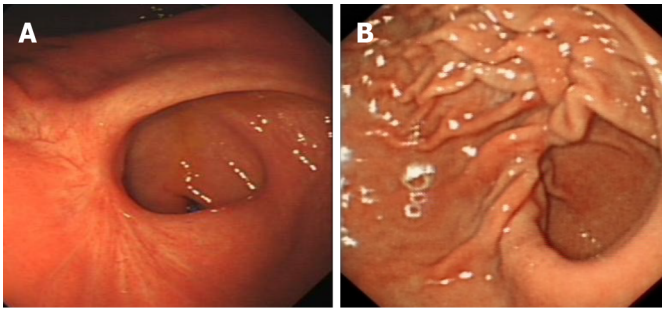

DOI: 10.12998/wjcc.v11.i9.2029

Figure 5 Endoscopy images after endoscopic submucosal dissection and full-thickness resection. A: Case 1 endoscopy image after endoscopic submucosal dissection and full-thickness resection (ESDFTR); B: Case 2 endoscopy image after ESDFTR.

CONCLUSION

The novel method described here provides a minimally invasive treatment option for T2 GC. However, the selection of standard indications, surgical methods, short-term and long-term complications, long-term recurrence rate and prognosis still need further evaluation.

FOOTNOTES

Author contributions: Dai JH, Qian F and Chen L contributed equally to this work, and they were involved in the patient treatment and postoperative management; Xu SL provided pathological data and corresponding analysis; Feng XF, Wu HB, Chen Y, Peng ZH and Yu PW analyzed the cases and postoperative management; Peng GY designed the research study, performed endoscopic treatments on patients and wrote the manuscript; All authors have read and approved the final manuscript.

Informed consent statement: All study participants provided informed written consent prior to study enrollment.

Conflict-of-interest statement: The authors declare that they have no conflicts of interest to disclose.

CARE Checklist (2016) statement: The authors have read the CARE Checklist (2016), and the manuscript was prepared and revised according to the CARE Checklist (2016).

Country/Territory of origin: China

ORCID number: Jian-Hua Dai 0000-0002-8792-7188; Feng Qian 0000-0002-4311-3705; Pei-Wu Yu 0000-0001-9717-0142; Gui-Yong Peng 0000-0002-6007-9481.

S-Editor: Zhang H
L-Editor: Filipodia
P-Editor: Zhang H

REFERENCES

1 **Japanese Gastric Cancer Association**. Japanese gastric cancer treatment guidelines 2018 (5th edition). *Gastric Cancer* 2021; **24**: 1-21 [PMID: 32060757 DOI: 10.1007/s10120-020-01042-y]
2 **Saito H**, Nishimura A, Sakimura Y, Tawara H, Hayashi K, Kato K, Tsuji T, Yamamoto D, Kitamura H, Kadoya S, Bando H. Closed laparoscopic and endoscopic cooperative surgery for early gastric cancer with difficulty in endoscopic submucosal dissection: a report of three cases. *Surg Case Rep* 2020; **6**: 235 [PMID: 32990798 DOI: 10.1186/s40792-020-01015-4]
3 **Bhagat VH**, Kim M, Kahaleh M. A Review of Endoscopic Full-thickness Resection, Submucosal Tunneling Endoscopic Resection, and Endoscopic Submucosal Dissection for Resection of Subepithelial Lesions. *J Clin Gastroenterol* 2021; **55**: 309-315 [PMID: 33606429 DOI: 10.1097/MCG.0000000000001500]
4 **Eisenberg D**, Bell R. Intraoperative endoscopy: a requisite tool for laparoscopic resection of unusual gastrointestinal lesions-

-a case series. *J Surg Res* 2009; **155**: 318-320 [PMID: 19482295 DOI: 10.1016/j.jss.2008.06.046]

5 **Matsuda T**, Hiki N, Nunobe S, Aikou S, Hirasawa T, Yamamoto Y, Kumagai K, Ohashi M, Sano T, Yamaguchi T. Feasibility of laparoscopic and endoscopic cooperative surgery for gastric submucosal tumors (with video). *Gastrointest Endosc* 2016; **84**: 47-52 [PMID: 26684599 DOI: 10.1016/j.gie.2015.11.040]

6 **Hu J**, Or BH, Hu K, Wang ML. Comparison of the post-operative outcomes and survival of laparoscopic versus open resections for gastric gastrointestinal stromal tumors: A multi-center prospective cohort study. *Int J Surg* 2016; **33** Pt A: 65-71 [PMID: 27475743 DOI: 10.1016/j.ijsu.2016.07.064]

World Journal of Clinical Cases

Submit a Manuscript: https://www.f6publishing.com

World J Clin Cases 2023 March 26; 11(9): 2036-2042

DOI: 10.12998/wjcc.v11.i9.2036

ISSN 2307-8960 (online)

CASE REPORT

Acromicric dysplasia caused by a mutation of fibrillin 1 in a family: A case report

Ren Shen, Jian-Hua Feng, Shan-Pu Yang

Specialty type: Medicine, research and experimental

Provenance and peer review: Unsolicited article; Externally peer reviewed.

Peer-review model: Single blind

Peer-review report's scientific quality classification

Grade A (Excellent): 0
Grade B (Very good): 0
Grade C (Good): C
Grade D (Fair): 0
Grade E (Poor): 0

P-Reviewer: Zhai JF, China

Received: November 29, 2022
Peer-review started: November 29, 2022
First decision: February 14, 2023
Revised: February 20, 2023
Accepted: March 3, 2023
Article in press: March 3, 2023
Published online: March 26, 2023

Ren Shen, Shan-Pu Yang, Department of Pediatrics, The People's Hospital of Yuhuan, Taizhou 317600, Zhejiang Province, China

Jian-Hua Feng, Department of Hematology, The First Affiliated Hospital of Wenzhou Medical University, Wenzhou 325000, Zhejiang Province, China

Corresponding author: Shan-Pu Yang, MBChB, Chief Physician, Department of Pediatrics, The People's Hospital of Yuhuan, No. 18 Changle Road, Yucheng Street, Taizhou 317600, Zhejiang Province, China. ysp6005@qq.com

Abstract

BACKGROUND

Acromicric dysplasia (AD) is a rare skeletal dysplasia. Its incidence is < 1/1000000, and only approximately 60 cases are reported worldwide. It is a disease characterized by severe short stature, short hands and feet, facial abnormalities, normal intelligence, and bone abnormalities. Unlike other skeletal dysplasia, AD has a mild clinical phenotype, mainly characterized by short stature. Extensive endocrine examination has not revealed a potential cause. The clinical effect of growth hormone therapy is still uncertain.

CASE SUMMARY

We report a clinical phenotype of AD associated with mutations in the fibrillin 1 (*FBN1*) (OMIM 102370) gene c.5183C>T (p. Ala1728Val) in three people from a Chinese family. A 4-year-old member of the family first visited the hospital because of slow growth and short stature for 2 years, but no abnormalities were found after a series of laboratory tests, echocardiography, pituitary magnetic resonance imaging, and ophthalmological examination. Recombinant human growth hormone (rhGH) was used to treat the patient for > 5 years. The efficacy of rhGH was apparent in the first year of treatment; the height increased from -3.64 standard deviation score (SDS) to -2.88 SDS, while the efficacy weakened from the second year. However, long-term follow-up is required to clarify the efficacy of rhGH.

CONCLUSION

FBN1-related AD has genetic heterogeneity and/or clinical variability, which brings challenges to the evaluation of clinical treatment. rhGH is effective for treatment of AD, but long-term follow-up is needed to clarify the effect.

Key Words: *Fibrillin 1*; Gene; Acromicric dysplasia; Short stature; Recombinant human growth hormone; Case report

Core Tip: Acromicric dysplasia (AD) is a rare skeletal dysplasia, and its incidence is < 1 in 1000000. Here, we report a clinical phenotype of AD associated with mutations in the *fibrillin 1* (OMIM 102370) gene c.5183C>T (p.Ala1728Val) in three people from a Chinese family. A 4-year-old boy was treated with recombinant human growth hormone (rhGH) for > 5 years. The efficacy of rhGH was clear in the first year of treatment; his height increased from -3.64 standard deviation score (SDS) to -2.88 SDS, while the efficacy weakened from the second year. However, long-term follow-up is required to clarify the efficacy of rhGH.

Citation: Shen R, Feng JH, Yang SP. Acromicric dysplasia caused by a mutation of fibrillin 1 in a family: A case report. *World J Clin Cases* 2023; 11(9): 2036-2042
URL: https://www.wjgnet.com/2307-8960/full/v11/i9/2036.htm
DOI: https://dx.doi.org/10.12998/wjcc.v11.i9.2036

INTRODUCTION

Geleophysic dysplasia (GD), acromicric dysplasia (AD), and Weill–Marchesani syndrome (WMS) are all acrodysplasia syndromes caused by mutations in the fibrillin 1 (*FBN1*) gene. AD is a rare heterogeneous skeletal dysplasia characterized by short stature, short hands and feet, stiff joints, thickened skin, facial abnormalities, normal intelligence, and skeletal abnormalities, with a prevalence of < 1 in 1000000[1-3]. Although these diseases are similar in physical features, each disease has its own unique clinical phenotype. GD is characterized by happy facial features, progressive valvular heart disease, progressive hepatomegaly, tracheal stenosis, and tiptoe gait. Although AD shows similar characteristics as GD, AD usually does not manifest heart valve abnormalities, hepatomegaly, tracheal stenosis, or eye disease[4]. WMS is distinguished from AD by ocular abnormalities, including lens myopia, lens ectopia, glaucoma, and spherical lenses. In contrast to the genetic heterogeneity of GD and WMS, AD is caused only by mutations in *FBN1* and is an autosomal dominant disorder[5]. Here, we report the clinical phenotype and genetic characteristics of three cases of AD associated with a mutation in the *FBN1* (OMIM 102370) gene c.5183C>T (p. Ala1728Val) in a Chinese family, to enhance clinicians' understanding of the disease and to share the experience of a young patient receiving long-term recombinant human growth hormone (rhGH) therapy.

CASE PRESENTATION

Chief complaints

A 4-year-old boy presented with slow growth and short stature for 2 years.

History of present illness

Two years ago, the patient was found to have short stature, normal mental capacity, liver enlargement, dyspnea, myopia, glaucoma, and other symptoms.

History of past illness

The patient was healthy in the past and had no history of skin, heart, lung, liver, kidney or eye diseases.

Personal and family history

The patient was born in Zhejiang Province of China, of Han nationality. The patient was the first birth of the second pregnancy, born by cesarean section at 40 wk' gestation, with a birth weight of 3500 g and length of 50 cm, and without a history of birth trauma asphyxia at birth. In the family, the height of the father was 140 cm [< -5 standard deviation score (SDS)][6] tall and the grandfather was 147 cm (< -4 SDS)[6] tall, the mother and grandmother were of normal height, and neither parents nor grandparents were consanguineous (Figure 1).

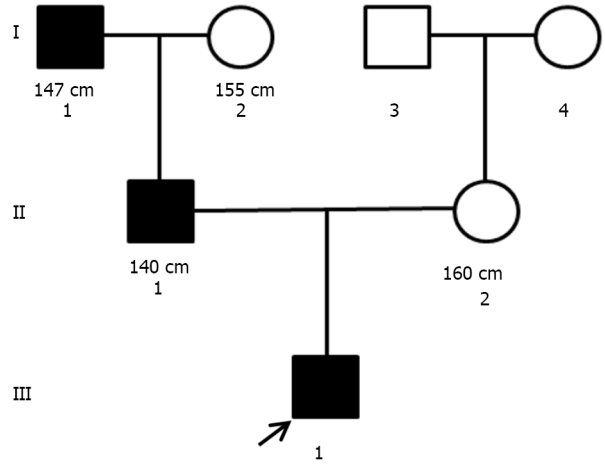

Patient (III.1), the paternal line is affected. The black means heterozygous, white means normal.

DOI: 10.12998/wjcc.v11.i9.2036

Figure 1 Pedigree map of the family.

Physical examination

The patient was short (90.5 cm, < -3 SDS)[6], with low weight (12.5 kg, < -2 SDS)[6], round face, stubby nose, forward-leaned nostrils, long eyelashes and thick lips (Figure 2).

Laboratory examinations

There were no obvious abnormalities in sex hormones, insulin-like growth factor (IGF)-1, IGF binding protein-3, thyroid function, biochemistry, trace elements, routine blood tests, routine urine tests, growth hormone challenge tests, cardiac ultrasound, pituitary-enhanced magnetic resonance imaging or karyotyping (550 bands, G bands).

Imaging examinations

Radiography showed delayed bone age (2.4 years) (Figure 3A). Plain pelvic radiography showed a beak-like femur head (Figure 3B), and the lumbar lateral radiograph showed lumbar lordosis (Figure 3C).

Further diagnostic work-up

The patient, his father and grandfather all showed significant familial short stature. We suspected the possibility of hereditary short stature and recommended that the patient, his parents and his grandfather underwent whole-exome sequencing. On October 17, 2019, whole-exome sequencing of the patient, his father and grandfather showed a mutation of the *FBN1* gene (OMIM 102370) c.5183C>T (p. Ala1728Val), while whole-exome sequencing of the patient's mother showed no abnormalities. The pathogenicity criteria of the mutation according to the American College of Medical Genetics and Genomics, and the pathogenicity rating was likely pathogenic[7].

FINAL DIAGNOSIS

Combined with the patient's medical history, physical examination and whole-exome sequencing, the final diagnosis was AD.

TREATMENT

Before whole-exome sequencing, the initial diagnosis was idiopathic short stature. From October 2016 to October 2019, rhGH at a dose of 0.12–0.15 IU/kg/d was used to treat the patient. After whole-exome sequencing, the final diagnosis was AD. Although the current case reports suggested that rhGH treatment had limited benefits on the final height of the children, the parents requested to continue rhGH treatment after informed consent was obtained. From October 2019 to present, rhGH at a dose of 0.15 IU/kg/d was used to treat the patient (it was suspended from July 2021 to February 2022) (Figure 4).

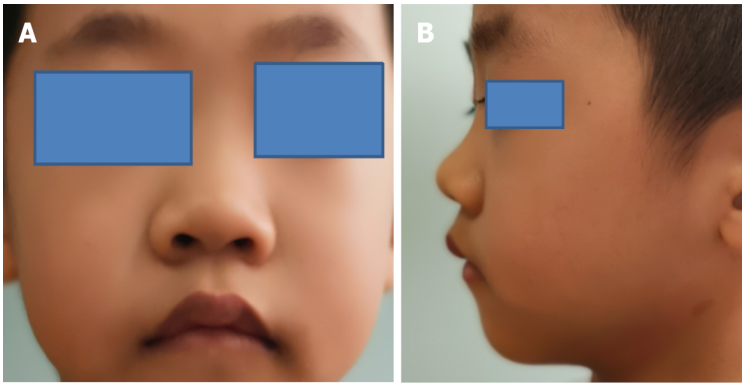

DOI: 10.12998/wjcc.v11.i9.2036

Figure 2 Distinctive facial features. A: Round face, stubby nose, forward-leaned nostrils and thick lips; B: Long eyelashes.

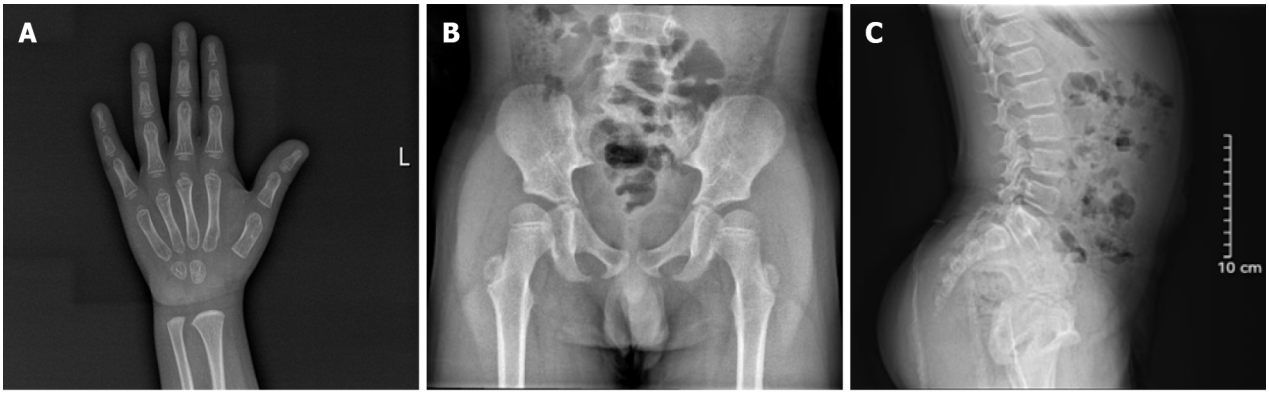

DOI: 10.12998/wjcc.v11.i9.2036

Figure 3 Representative radiographic images. A: Delayed bone age; B: Beak-like femur head; C: Lumbar lordosis.

OUTCOME AND FOLLOW-UP

The height at the beginning of treatment was 90.5 cm (-3.64 SDS), and the height after treatment in the first year (October 2016 to September 2017) was 99.5 cm (-2.88 SDS). Thus, the annual growth rate during the first year was 9.0 cm/year. The height after treatment in the second year (October 2017 to September 2018) was 106 cm (-2.60 SDS); thus, the annual growth rate during the second year was 6.5 cm/year. The height after treatment in the third year (October 2018 to September 2019) was 110.5 cm (-2.80 SDS); thus, the annual growth rate during the third year was 4.5 cm/year. The height after treatment in the fourth year (October 2019 to September 2020) was 114.1 cm (-3.04 SDS); thus, the annual growth rate during the fourth year was 3.6 cm/year. The height after treatment in the fifth year (October 2020 to July 2021) was 117.1 cm (-3.09 SDS), yielding an annual growth rate during the fifth year of 3.0 cm/year. Considering the poor efficacy, it is recommended to stop rhGH treatment. After stopping rhGH for 7 mo, the height was 118.5 cm (-3.17 SDS) in February 2022; thus, the annual growth rate was 2.4 cm/year. The parents requested reuse of rhGH. Afterward, the height was 119.6 cm (-3.20 SDS) in June 2022 and 121.7 cm (-3.11 SDS) in October 2022, indicating an annual growth rate of 4.8 cm/year. To date, the patient has been treated and followed up for 6 years (Figure 4). The efficacy of rhGH treatment was clear in the first year, and the height increased from -3.64 SDS to -2.88 SDS. However, the efficacy of the treatment weakened from the second year. At the request of the parents, the patients would continue to be treated with rhGH and be followed up.

DISCUSSION

In 1986, Maroteaux *et al*[8] first described a novel type of osteodysplasia in six children with short stature, short hands and feet, normal intelligence, mild facial deformities, and hand X-ray abnormalities. They called the disease AD and could not clarify the cause further because of the limitations of the genetic diagnostic technology at that time.

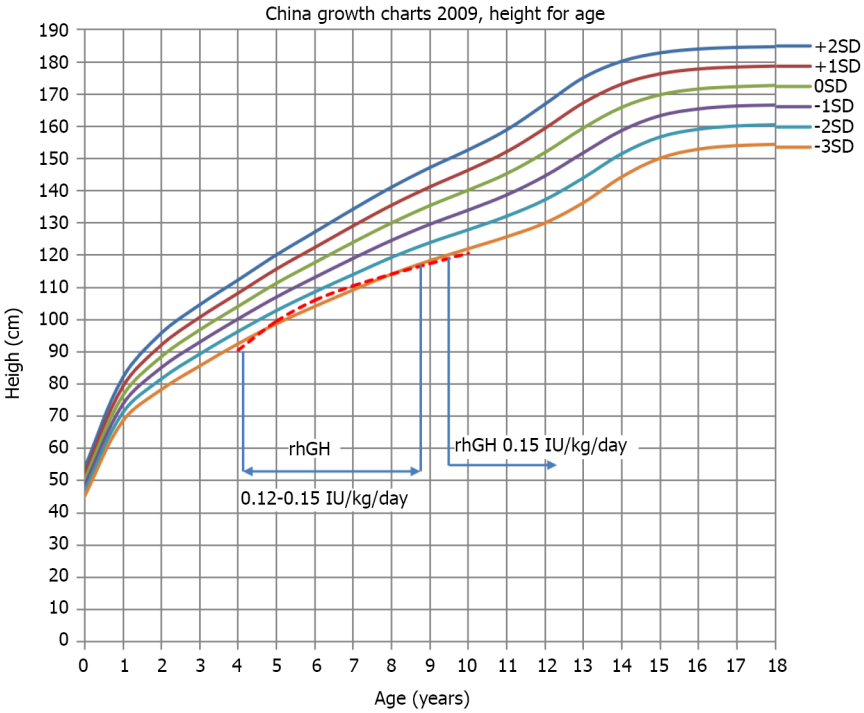

DOI: 10.12998/wjcc.v11.i9.2036

Figure 4 Age and height curve. rhGH: Recombinant human growth hormone; SD: Standard deviation.

In 1991, Dietz *et al*[9] first identified the *FBN1* gene as the causative gene of Marfan syndrome (MS). In 2011, Le Goff *et al*[10] found that the *FBN1* gene was associated with GD and AD autosomal dominant inheritance, which showed the opposite phenotype of MS. Both AD and MS have *FBN1* gene mutations, so why do the two diseases have opposite phenotypes? Mutations in *FBN1* leading to MS exist throughout the entire length of the gene (mainly in exon regions 13, 15, 24–28, 32 and 43)[11], while *FBN1* mutations that result in AD are mainly limited to the hotspot regions of exons 41 and 42[5]. These findings indicated that the clinical phenotype could be related to the type and location of the gene variant.

In the 2015 revision of the classification of hereditary bone diseases, acral dysplasia included 10 diseases, among which the *FBN1* gene mutation causes AD, GD, and WMS, and specific mutations in the *FBN1* gene have been found in AD, GD and WMS patients[1,4,12]. The *FBN1* gene is located in the long arm of human chromosome 15 (15q15–q21.1) and contains 66 exons, encoding a 2871-aa (350 kDa) structural protein called fibrillin (FBN)1[13]. FBN1 consists of 47 epidermal growth factor-like domains and seven transforming growth factor (TGF)-β1-binding-protein-like domains[14]. *FBN1* is the only gene associated with AD that is inherited in an autosomal dominant manner[5]. The *FBN1* gene can participate in the TGF-β signaling pathway by regulating the bioavailability and local activity of TGF-β, which is an important pathway for linear growth regulation. AD and GD2 (ADAMTSL2-negative) are caused by TGF-β5 region heterozygous missense mutations in the *FBN1* gene, and disruption of TGF-β signaling is a common underlying mechanism in different types of patients with acrodysplasia[15].

In the present case, the patient's father and grandfather all had mutations in the *FBN1* gene c.5183C>T (p. Ala1728Val). This gene mutation was first found in a GD patient with severe short stature and cardiac involvement[10]. We reviewed three previously reported AD cases associated with mutation of *FBN1* (OMIM 102370) gene c.5183C>T (p.Ala1728Val). A Brazilian boy developed severe dwarfism at the age of 10 years and 2 mo (-3.9 SDS). He was born with normal birth length, his mother was short at 131cm (-5 SDS), while his father and brothers were normal in height. Physical examination found that fingers and palms were short. His nose bridge was wide, the middle part of his nose was prominent, his lips were thick, and he had obvious genu varus, but his gait was normal. No abnormality was found in endocrine examination. The patient was diagnosed as idiopathic short stature and began to receive rhGH treatment (50-66 mg/kg/d) according to experience, but the overall effect was poor [15]. An African–American girl born in the United States was 107.5 cm (-4 SDS) tall at the age of 7 years. She was born at 37 wk of gestation, with a birth length of only 43 cm (-2.3 SDS) and a birth weight of 2580 g (-0.9 SDS). The height of both parents was normal. The physical examination found that the bridge of the nose was broad, and she had slight osteoporosis, thick lips, small hands and feet, but no other abnormalities. Endocrine examination was normal, and bone age was delayed by about 2 years. At the age of 8 years and 9 mo, recombinant IGF-1 was administered according to experience, and reached a maximum dose of 90 mg/kg/d. The growth rate increased significantly. However, this growth acceleration was confused with early puberty development at the age of 9 years and 1 mo. After the start

of leuprorelin treatment, the growth rate decreased to 4–5 cm/year before treatment. Treatment with recombinant IGF-1 was stopped at the age of 9 years and 4 mo[15]. A 5 years and 7 month old Chinese boy was 100.3 cm tall (< -3 SDS). The birth length was 49 cm. His father was 148 cm tall (< -4 SDS). His mother was 160 cm tall. Physical examination showed that the hands were wide and short, but there was no joint stiffness, and there were no abnormality in cardiovascular, abdominal or endocrine examination. The X-ray examination showed that the tubular bone of the hands were shortened and the femoral head was beaked[13]. Although these cases had the same gene mutation site, the clinical phenotypes varied. This site variant might be associated with the autosomal dominant AD (OMIM: 102370), GD (OMIM: 614185) and WMS (OMIM: 608328)[1]. In our case, the three patients showed severe short stature as the main manifestation, and none of them had hepatomegaly, heart valve disease, joint stiffness or eye disease. Meanwhile, the disease condition was milder compared with GD or WMS, neither the quality of the study or quality of life was affected, and the adults are doing well in their professions; thus, all the clinical conditions support the diagnosis of AD. The same mutation at the *FBN1* gene locus could lead to a variety of different clinical phenotypes, and the discovery of multiple phenotypes could help to conduct further research on the pathogenesis of the diseases.

GH therapy has not been widely used in patients with skeletal dysplasia because of genetic heterogeneity and/or clinical variability, which pose challenges in assessing treatment effectiveness. The efficacy of GH in the treatment of AD is still unclear. Faivre *et al*[16] reported one case of AD given rhGH treatment, but there was no significant effect on final height. Jin *et al*[17] found that a patient with AD received rhGH treatment of 0.1 IU/kg/d for 3.5 years, and during treatment, his growth rate remained at 5 cm/year, and his height was -2.23 SDS after 3.5 years. However, long-term follow-up is needed to verify the effect of rhGH treatment. The effects of GH treatment in our present case were similar to those in the patient just described. In our case, the patient's height increased by 9.0 cm in the first year of rhGH treatment, 6.5 cm in the second year, 4.5 cm in the third year, 3.6 cm in the fourth year, and 3 cm in the fifth year. In the first year of treatment, the annual growth rate was 9.0 cm/year, and the height increased from -3.64 SDS to -2.88 SDS, an increase of 0.76 SDS, suggesting that rhGH therapy was effective[18]. In the patient's family, the height of the father was 140 cm (< -5 SDS) tall and the grandfather was 147 cm (< -4 SDS) tall. In the first 5 years of treatment, the growth rate of the patient remained at 5.3 cm/year, and the height increased from -3.64 SDS to -3.09 SDS. It seems that the treatment had some effect, and the first year was the most significant. However, whether it would have a positive effect on the final height remains unclear, and long-term follow-up observation is needed.

CONCLUSION

AD is a rare skeletal dysplasia and an autosomal dominant disease. *FBN1* is the only gene related to AD. *FBN1*-related acral dysplasia has genetic heterogeneity and/or clinical variability, which brings challenges to the evaluation of clinical treatment. rhGH therapy appears to have some effect on growth, but long-term follow-up is needed to clarify the effect.

FOOTNOTES

Author contributions: Yang SP and Shen R were responsible for the diagnosis and treatment of the patient; Shen R prepared the manuscript; Yang SP and Feng JH participated in revision of the manuscript; All authors have read and approved the final manuscript.

Informed consent statement: Informed written consent was obtained from the patients for publication of this report and any accompanying images.

Conflict-of-interest statement: All the authors report no relevant conflicts of interest for this article.

CARE Checklist (2016) statement: The authors have read the CARE Checklist (2016), and the manuscript was prepared and revised according to the CARE Checklist (2016).

Country/Territory of origin: China

ORCID number: Ren Shen 0000-0001-7369-6692; Jian-Hua Feng 0000-0003-1570-7626; Shan-Pu Yang 0000-0003-3135-5165.

S-Editor: Fan JR

L-Editor: A
P-Editor: Fan JR

REFERENCES

1 **Bonafe L**, Cormier-Daire V, Hall C, Lachman R, Mortier G, Mundlos S, Nishimura G, Sangiorgi L, Savarirayan R, Sillence D, Spranger J, Superti-Furga A, Warman M, Unger S. Nosology and classification of genetic skeletal disorders: 2015 revision. *Am J Med Genet A* 2015; **167A**: 2869-2892 [PMID: 26394607 DOI: 10.1002/ajmg.a.37365]
2 **Globa E**, Zelinska N, Dauber A. The Clinical Cases of Geleophysic Dysplasia: One Gene, Different Phenotypes. *Case Rep Endocrinol* 2018; **2018**: 8212417 [PMID: 30057829 DOI: 10.1155/2018/8212417]
3 **Quitter F**, Flury M, Waldmueller S, Schubert T, Koehler K, Huebner A. Acromicric dysplasia due to a novel missense mutation in the fibrillin 1 gene in a three-generation family. *J Pediatr Endocrinol Metab* 2022; **35**: 1443-1447 [PMID: 35942587 DOI: 10.1515/jpem-2022-0287]
4 **Wang Y**, Zhang H, Ye J, Han L, Gu X. Three novel mutations of the FBN1 gene in Chinese children with acromelic dysplasia. *J Hum Genet* 2014; **59**: 563-567 [PMID: 25142510 DOI: 10.1038/jhg.2014.73]
5 **Sakai LY**, Keene DR, Renard M, De Backer J. FBN1: The disease-causing gene for Marfan syndrome and other genetic disorders. *Gene* 2016; **591**: 279-291 [PMID: 27437668 DOI: 10.1016/j.gene.2016.07.033]
6 **Li H**, Ji CY, Zong XN, Zhang YQ. [Height and weight standardized growth charts for Chinese children and adolescents aged 0 to 18 years]. *Zhonghua Er Ke Za Zhi* 2009; **47**: 487-492 [PMID: 19951507]
7 **Richards S**, Aziz N, Bale S, Bick D, Das S, Gastier-Foster J, Grody WW, Hegde M, Lyon E, Spector E, Voelkerding K, Rehm HL; ACMG Laboratory Quality Assurance Committee. Standards and guidelines for the interpretation of sequence variants: a joint consensus recommendation of the American College of Medical Genetics and Genomics and the Association for Molecular Pathology. *Genet Med* 2015; **17**: 405-424 [PMID: 25741868 DOI: 10.1038/gim.2015.30]
8 **Maroteaux P**, Stanescu R, Stanescu V, Rappaport R. Acromicric dysplasia. *Am J Med Genet* 1986; **24**: 447-459 [PMID: 3728563 DOI: 10.1002/ajmg.1320240307]
9 **Dietz HC**, Cutting GR, Pyeritz RE, Maslen CL, Sakai LY, Corson GM, Puffenberger EG, Hamosh A, Nanthakumar EJ, Curristin SM. Marfan syndrome caused by a recurrent de novo missense mutation in the fibrillin gene. *Nature* 1991; **352**: 337-339 [PMID: 1852208 DOI: 10.1038/352337a0]
10 **Le Goff C**, Mahaut C, Wang LW, Allali S, Abhyankar A, Jensen S, Zylberberg L, Collod-Beroud G, Bonnet D, Alanay Y, Brady AF, Cordier MP, Devriendt K, Genevieve D, Kiper PÖ, Kitoh H, Krakow D, Lynch SA, Le Merrer M, Mégarbane A, Mortier G, Odent S, Polak M, Rohrbach M, Sillence D, Stolte-Dijkstra I, Superti-Furga A, Rimoin DL, Topouchian V, Unger S, Zabel B, Bole-Feysot C, Nitschke P, Handford P, Casanova JL, Boileau C, Apte SS, Munnich A, Cormier-Daire V. Mutations in the TGFβ binding-protein-like domain 5 of FBN1 are responsible for acromicric and geleophysic dysplasias. *Am J Hum Genet* 2011; **89**: 7-14 [PMID: 21683322 DOI: 10.1016/j.ajhg.2011.05.012]
11 **Collod-Béroud G**, Le Bourdelles S, Ades L, Ala-Kokko L, Booms P, Boxer M, Child A, Comeglio P, De Paepe A, Hyland JC, Holman K, Kaitila I, Loeys B, Matyas G, Nuytinck L, Peltonen L, Rantamaki T, Robinson P, Steinmann B, Junien C, Béroud C, Boileau C. Update of the UMD-FBN1 mutation database and creation of an FBN1 polymorphism database. *Hum Mutat* 2003; **22**: 199-208 [PMID: 12938084 DOI: 10.1002/humu.10249]
12 **Le Goff C**, Cormier-Daire V. From tall to short: the role of TGFβ signaling in growth and its disorders. *Am J Med Genet C Semin Med Genet* 2012; **160C**: 145-153 [PMID: 22791552 DOI: 10.1002/ajmg.c.31337]
13 **Shan YC**, Yang ZC, Ma L, Ran N, Feng XY, Liu XM, Fu P, Yi MJ. A Review of Three Chinese Cases of Acromicric/Geleophysic Dysplasia with FBN1 Mutations. *Int J Gen Med* 2021; **14**: 1873-1880 [PMID: 34040419 DOI: 10.2147/IJGM.S306018]
14 **Sakai LY**, Keene DR. Fibrillin protein pleiotropy: Acromelic dysplasias. *Matrix Biol* 2019; **80**: 6-13 [PMID: 30219651 DOI: 10.1016/j.matbio.2018.09.005]
15 **de Bruin C**, Finlayson C, Funari MF, Vasques GA, Lucheze Freire B, Lerario AM, Andrew M, Hwa V, Dauber A, Jorge AA. Two Patients with Severe Short Stature due to a FBN1 Mutation (p.Ala1728Val) with a Mild Form of Acromicric Dysplasia. *Horm Res Paediatr* 2016; **86**: 342-348 [PMID: 27245183 DOI: 10.1159/000446476]
16 **Faivre L**, Le Merrer M, Baumann C, Polak M, Chatelain P, Sulmont V, Cousin J, Bost M, Cordier MP, Zackai E, Russell K, Finidori G, Pouliquen JC, Munnich A, Maroteaux P, Cormier-Daire V. Acromicric dysplasia: long term outcome and evidence of autosomal dominant inheritance. *J Med Genet* 2001; **38**: 745-749 [PMID: 11694546 DOI: 10.1136/jmg.38.11.745]
17 **Jin HS**, Song HY, Cho SY, Ki CS, Yang SH, Kim OH, Kim SJ. Acromicric Dysplasia Caused by a Novel Heterozygous Mutation of FBN1 and Effects of Growth Hormone Treatment. *Ann Lab Med* 2017; **37**: 92-94 [PMID: 27834076 DOI: 10.3343/alm.2017.37.1.92]
18 **Cohen P**, Rogol AD, Deal CL, Saenger P, Reiter EO, Ross JL, Chernausek SD, Savage MO, Wit JM; 2007 ISS Consensus Workshop participants. Consensus statement on the diagnosis and treatment of children with idiopathic short stature: a summary of the Growth Hormone Research Society, the Lawson Wilkins Pediatric Endocrine Society, and the European Society for Paediatric Endocrinology Workshop. *J Clin Endocrinol Metab* 2008; **93**: 4210-4217 [PMID: 18782877 DOI: 10.1210/jc.2008-0509]

World Journal of Clinical Cases

Submit a Manuscript: https://www.f6publishing.com

World J Clin Cases 2023 March 26; 11(9): 2043-2050

DOI: 10.12998/wjcc.v11.i9.2043

ISSN 2307-8960 (online)

CASE REPORT

Ultrasound-guided intra-articular corticosteroid injection in a patient with manubriosternal joint involvement of ankylosing spondylitis: A case report

Min-Hee Choi, In-Young Yoon, Won-Joong Kim

Specialty type: Medicine, research and experimental

Provenance and peer review: Unsolicited article; Externally peer reviewed.

Peer-review model: Single blind

Peer-review report's scientific quality classification

Grade A (Excellent): 0
Grade B (Very good): 0
Grade C (Good): C, C
Grade D (Fair): 0
Grade E (Poor): 0

P-Reviewer: Chiu CD, Taiwan; Cure E, Turkey

Received: November 25, 2022
Peer-review started: November 25, 2022
First decision: December 19, 2022
Revised: December 28, 2022
Accepted: February 15, 2023
Article in press: February 15, 2023
Published online: March 26, 2023

Min-Hee Choi, In-Young Yoon, Won-Joong Kim, Department of Anesthesiology and Pain Medicine, Ewha Womans University Mokdong Hospital, Seoul 07985, South Korea

Corresponding author: Won-Joong Kim, MD, PhD, Associate Professor, Department of Anesthesiology and Pain Medicine, Ewha Womans University Mokdong Hospital, 1071, Anyangcheon-ro, Yangcheon-gu, Seoul 07985, South Korea. ickypoo@naver.com

Abstract

BACKGROUND

Manubriosternal joint (MSJ) disease is a rare cause of anterior chest pain but can be a major sign of systemic arthritic involvement. In patients with ankylosing spondylitis (AS), a type of systemic arthritis, chest pain can be due to MSJ involvement and can be improved by ultrasound-guided corticosteroid injection into the joint.

CASE SUMMARY

A 64-year-old man visited our pain clinic complaining of anterior chest pain. There were no abnormal findings on lateral sternum X-ray, but arthritic changes in the MSJ were observed on single-photon emission computed tomography-computed tomography. We performed additional laboratory tests, and he was finally diagnosed with AS. For pain relief, we performed ultrasound-guided intra-articular (IA) corticosteroid injections into the MSJ. After the injections, his pain nearly resolved.

CONCLUSION

For patients complaining of anterior chest pain, AS should be considered, and single-photon emission computed tomography-computed tomography can be helpful in diagnosis. In addition, ultrasound-guided IA corticosteroid injections may be effective for pain relief.

Key Words: Ankylosing spondylitis; Anterior chest pain; Manubriosternal joint; Single-photon emission computed tomography-computed tomography; Case report

Core Tip: Manubriosternal joint (MSJ) disease is a rare cause of anterior chest pain but can be a major sign of systemic arthritic involvement. In patients with anterior chest pain, systemic arthritic diseases such as ankylosing spondylitis should be considered but are difficult to diagnose. This report suggests that single-photon emission computed tomography-computed tomography can be an effective diagnostic tool for evaluating musculoskeletal causes of anterior chest pain, and this pain can be controlled by ultrasound-guided intra-articular corticosteroid injections into the MSJ.

Citation: Choi MH, Yoon IY, Kim WJ. Ultrasound-guided intra-articular corticosteroid injection in a patient with manubriosternal joint involvement of ankylosing spondylitis: A case report. *World J Clin Cases* 2023; 11(9): 2043-2050
URL: https://www.wjgnet.com/2307-8960/full/v11/i9/2043.htm
DOI: https://dx.doi.org/10.12998/wjcc.v11.i9.2043

INTRODUCTION

Manubriosternal joint (MSJ) disease is an often undetected cause of anterior chest pain[1]. Diagnosis is difficult as it is based on exclusion of other causes[2]. Many diagnostic tools can be used to identify diseases that cause anterior chest pain. Particularly, single-photon emission computed tomography-computed tomography (SPECT-CT) can be helpful in differentiating the diagnosis due to musculoskeletal disorders such as arthritis.

Infection, trauma, crystal deposition disease, and inflammatory diseases such as ankylosing spondylitis (AS) and rheumatic arthritis (RA) can cause arthritis of the MSJ[3]. Although these diseases are often accompanied by systemic symptoms, in rare cases intermittent MSJ arthralgia can be a major sign of arthritic involvement.

We report a case in which a patient with anterior chest pain as the main symptom was diagnosed with AS through SPECT-CT, and the pain was relieved by ultrasound-guided intra-articular (IA) corticosteroid injections.

CASE PRESENTATION

Chief complaints

A 64-year-old man (180 cm, 81 kg) visited our pain clinic with intermittent anterior chest pain lasting 6 mo.

History of present illness

The patient's chest pain worsened when he engaged in exercises like pull-ups or changed position. This pain affected his ability to work and perform activities of daily living. He also had mild back pain, but it did not interfere with his daily activities and did not require treatment.

History of past illness

The patient had no history of trauma to his anterior chest. His symptoms worsened 3 mo prior to his visit, based on which an orthopedic doctor prescribed non-steroidal anti-inflammatory drugs (NSAIDs) and injected corticosteroids into the painful area. However, the pain did not improve.

Personal and family history

The patient had no family or personal history related to the symptom.

Physical examination

On physical examination, there was tenderness in the left anterior chest wall but no swelling or heat sensation. There was no back tenderness.

Laboratory examinations

Blood tests including complete blood count, inflammatory markers (C-reactive protein, erythrocyte sedimentation rate), blood biochemistry, and coagulation indices were within the normal ranges.

Imaging examinations

There were no abnormal findings on lateral sternum X-ray (Figure 1), but arthritic changes in the MSJ were observed on SPECT-CT (Figure 2). In bone scintigraphy, there was no active inflammation in the

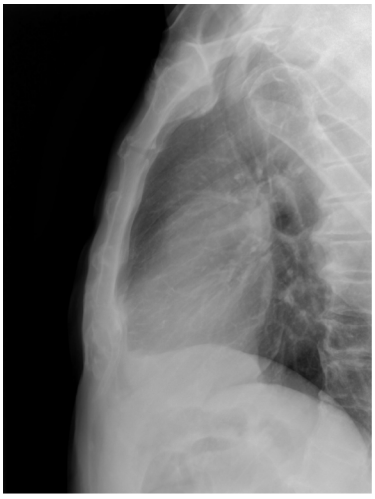

DOI: 10.12998/wjcc.v11.i9.2043

Figure 1 Lateral sternum X-ray. The X-ray showed normal findings.

sacroiliac joint (SIJ).

Further diagnostic workup

Rheumatoid factor, anti-cyclic citrullinated peptide antibody, uric acid, fluorescent anti-nuclear antibody, and human leukocyte antigen-B27 tests were performed, and human leukocyte antigen-B27 was positive. SIJ pain provocation tests (distraction, thigh thrust, compression, Patrick, and Gaenslen) and the Schober test were negative. X-rays of the lumbar spine and SIJ showed syndesmophytes and sacroiliitis (Figure 3). Subsequent magnetic resonance imaging (MRI) of the SIJ revealed bilateral sacroiliitis with active inflammation at the left SIJ (Figure 4).

FINAL DIAGNOSIS

According to the modified New York Classification Criteria, the patient was diagnosed with AS.

TREATMENT

Before visiting our clinic, the patient received NSAIDs and local corticosteroid injections, but the pain did not improve significantly. Therefore, we performed ultrasound-guided IA corticosteroid injections into the MSJ. In the supine position, we prepared the skin of the anterior chest wall aseptically. Then, a 12-Hz linear transducer ultrasound probe was placed parallel to the midsternum to identify the MSJ[4]. We inserted a 25 G needle using ultrasound guidance and injected 1 mL of 0.375% ropivacaine and 2.5 mg dexamethasone into the MSJ (Figure 5). With IA corticosteroid injection, we prescribed NSAIDs.

OUTCOME AND FOLLOW-UP

After 1 wk of treatment, the pain was significantly relieved, decreasing from Numeric Rating Scale (NRS) 6 to NRS 3. Because the pain persisted after the injection, although it was relieved significantly, we performed another ultrasound-guided IA corticosteroid injection. Two weeks after the second injection, his symptoms improved from NRS 3 to NRS 2. However, the patient continued to experience discomfort in his anterior chest and requested an additional injection. Two weeks after this third injection, his pain had nearly resolved, and the patient did not revisit after the final injection. During follow-up, we recommended continuing the prescribed medication.

DISCUSSION

This case report is an account of a patient who complained of localized pain in the anterior chest and was diagnosed with AS on SPECT-CT. He experienced effective pain reduction after ultrasound-guided

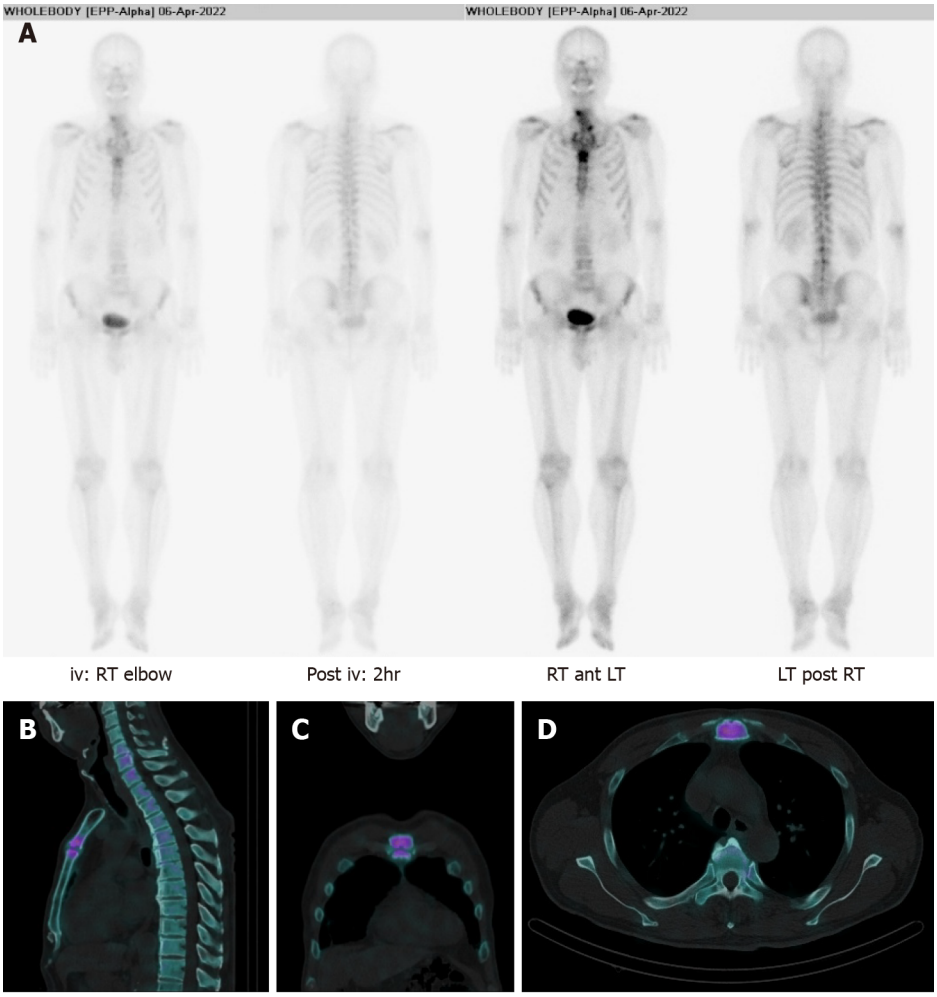

DOI: 10.12998/wjcc.v11.i9.2043

Figure 2 Bone scintigraphy and single-photon emission computed tomography-computed tomography of the manubriosternal joint. A: Bone scintigraphy; B: Sagittal; C: Coronal; D: Axial images of single-photon emission computed tomography-computed tomography indicated arthritic change in the manubriosternal joint. iv: Intravenous; RT: Right; LT: Left.

IA corticosteroid injections.

It is important to identify life-threatening diseases in a patient with chest pain, although such pain is benign in approximately 80% of cases, of which musculoskeletal chest pain accounts for almost 50%[5-8]. Musculoskeletal chest pain can be caused by a variety of factors, grouped into three categories of isolated musculoskeletal pain, rheumatic diseases, and non-rheumatic systemic causes. Even though critical causes of anterior chest pain might be ruled out, various diseases should be considered for differential diagnosis of benign anterior chest pain, such as costochondritis, Tietze syndrome (isolated musculoskeletal pain), fibromyalgia, RA, AS, septic arthritis, psoriatic arthritis (rheumatic disease), neoplasm, and osteoporotic fracture (non-rheumatic system causes)[9]. An MSJ problem is a possible cause of benign chest pains.

The MSJ is a complex joint between the manubrium and the body of the sternum[1]. This secondary cartilaginous joint (symphysis) may resemble a synovial joint susceptible to osteoarthritic degeneration, as 30% of patients undergo fibrocartilage disk absorption. Primary MSJ osteoarthritis (OA) has no identifiable etiology; secondary OA results from RA, AS, psoriatic arthritis, or gout[10]. In most cases, MSJ arthralgia due to secondary MSJ OA is accompanied by systemic symptoms, but it can be the main sign of systemic arthritis[11,12]. Our patient did not complain of systemic symptoms including back pain but only of anterior chest pain. Therefore, evaluation for systemic diseases should be considered when a patient complains of MSJ arthralgia even if there are no other symptoms.

AS is a systemic disease that can cause secondary OA of the MSJ and is a chronic inflammatory disease that mainly affects axial joints[13]. Baek *et al*[14] reported clinical features of AS in Korean patients, and chronic back pain was a presenting symptom in approximately 75% of AS patients. The most frequently affected extraspinal joints in AS are the hips and shoulders and are involved at presentation in up to 15% of cases. Other peripheral joint involvement presents in 10%-20% of patients. The proportion of patients with enthesis involvement at disease onset is about 1.5%[14]. The most characteristic clinical symptom of AS is inflammatory back pain. Pain and stiffness in the mid-thoracic

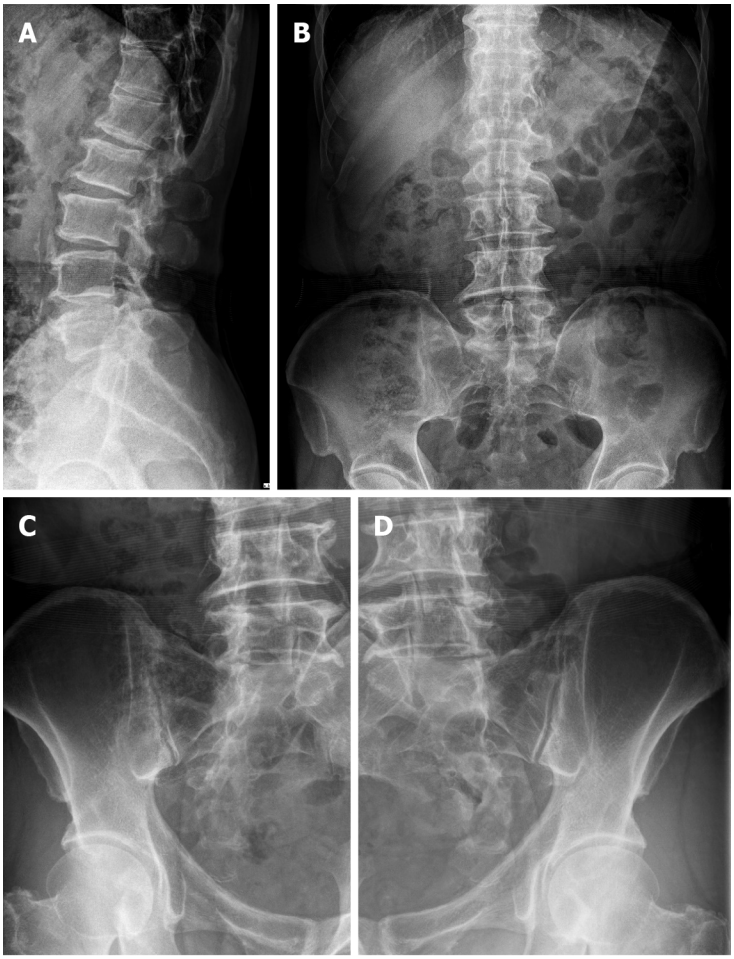

DOI: 10.12998/wjcc.v11.i9.2043

Figure 3 X-rays of the lumbar spine and sacroiliac joints. A and B: Syndesmophytes and degenerative spondylosis were shown; A: Lateral view; B: Anterior posterior (AP) view of the lumbar spine; C and D: Bilateral sacroiliitis was found; C: AP view of the left sacroiliac joint; D: AP view of right sacroiliitis.

or cervical region may be the initial symptom instead of the more common presentations of AS[15]. On the other hand, MSJ causing anterior chest pain is a rare presenting symptom[12,16]. In a retrospective study performed in 275 patients with spondyloarthritis, 37% experienced spondyloarthritis-associated chest pain[17]. However, anterior chest wall pain as the presenting symptom occurred in only 4%-6% of cases[18]. For this reason, it is difficult to suspect AS in patients with anterior chest pain, and diagnosis of AS can be delayed in patients with anterior chest pain.

The diagnosis of AS is based on radiologic evidence of sacroiliitis. Therefore, it may be essential to evaluate SIJ in patients with AS. Various physical examination tests have been advocated as diagnostic aids in patient with SIJ problems; however, reliability of SIJ provocation tests have been questioned[19,20]. Although the patient in this case had no symptom related to SIJ and SIJ provocation tests were negative, bilateral sacroiliitis was observed on MRI. Hence, if AS is suspected, imaging of SIJ should be performed even if there is no abnormality on physical examinations.

SPECT-CT offers functional information about increased bone turnover in combination with morphological details[21]. The modality can detect not only metastatic lesions but also benign lesions such as infective, inflammatory, or traumatic bony lesions[22]. The evidence base for the role of SPECT-CT in benign musculoskeletal pathology is emerging, and several studies have revealed the clinical significance of SPECT-CT in the diagnosis of benign musculoskeletal disease[23]. Some prospective studies suggested the usefulness of SPECT-CT as a diagnostic tool for benign musculoskeletal diseases [24,25]. In the present case, SPECT-CT revealed inflammatory arthritic change in the MSJ, although a simple X-ray showed normal findings. Likewise, in a patient complaining of pain in the focal area that is not easily determined with simple X-ray or other general imaging tests, SPECT-CT can be used as a diagnostic method. Since there are many structures in the thorax that can produce musculoskeletal pain such as the costoverterbral, sternocostal, costochondral, and MSJs, it is difficult to identify an exact lesion in the thorax. Considering this, SPECT-CT can be useful in locating the precise lesion in patients with musculoskeletal chest pain.

Oye *et al*[12] suggested anterior chest pain due to MSJ involvement as a presenting symptom of AS and MRI as a valuable diagnostic tool. MRI has been increasingly used as an imaging modality in

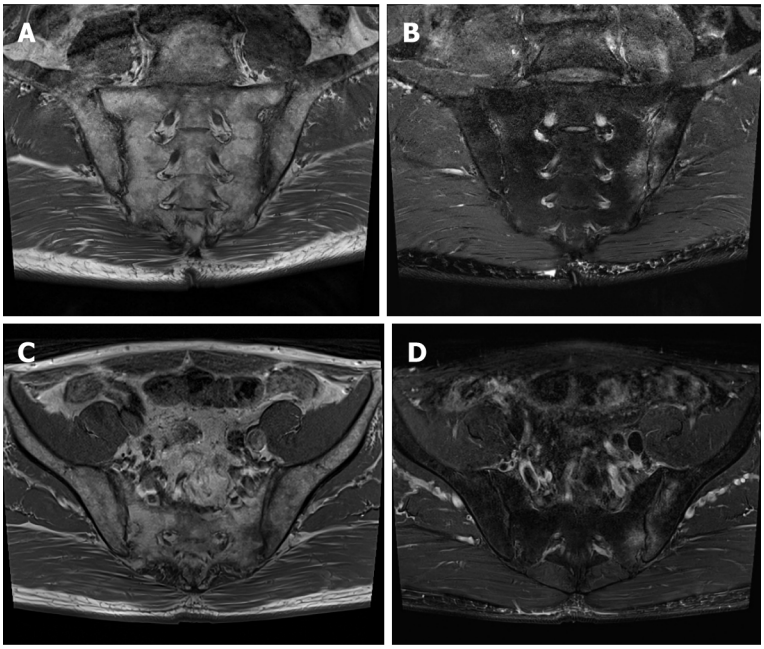

DOI: 10.12998/wjcc.v11.i9.2043

Figure 4 Magnetic resonance imaging scans of sacroiliac joints showed bilateral sacroiliitis with active inflammation at the left sacroiliac joint. A: T1-weighted image of sacroiliac joints, coronal view; B: T2-weighted image of sacroiliac joints, coronal view; C: T1-weighted image of sacroiliac joints, axial view; D: T2-weighted image of sacroiliac joints, axial view.

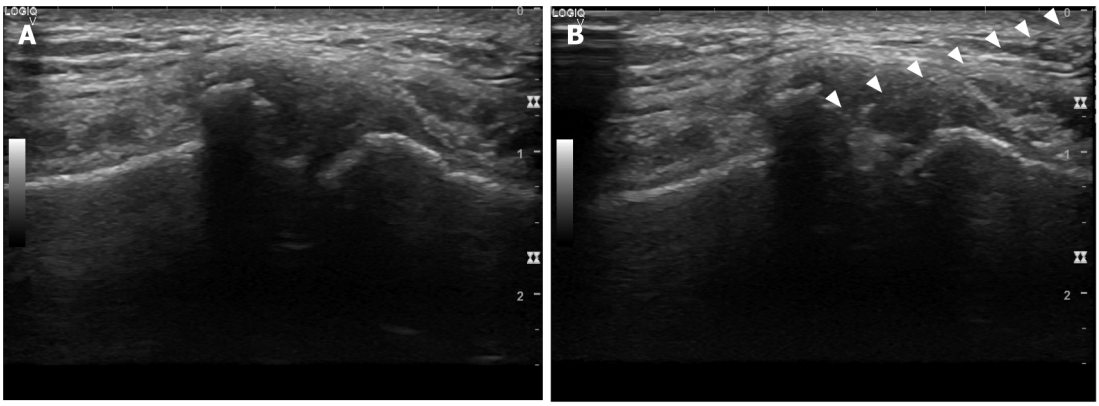

DOI: 10.12998/wjcc.v11.i9.2043

Figure 5 Ultrasound view of the manubriosternal joint. A: Manubriosternal joint view with a 12-Hz linear probe parallel to the midsternum; B: Ultrasound-guided intra-articular corticosteroid injection into the manubriosternal joint. Arrowheads: Points at needle.

patients with AS because of its capacity to identify both active inflammation and chronic structural changes in axial skeletal structures[26]. However, in patients with claustrophobia, pacemakers, or metal implant, use of MRI is limited[27]. SPECT-CT can be an alternative to MRI in these cases.

Systemic drugs like NSAIDs are the primary treatment of AS, but IA corticosteroid injections into the painful joint often satisfactorily ameliorate acute inflammatory pain[28]. Since the MSJ is a narrow space and it can be difficult to inject a corticosteroid, IA corticosteroid injection into the joint space can be performed more easily and accurately using ultrasound guidance. Therefore, in systemic diseases like AS, when symptoms are limited to specific joints, ultrasound-guided IA corticosteroid injections may be effective for pain relief.

CONCLUSION

Inflammatory arthritis including AS should be considered in patients complaining of anterior chest pain, and SPECT-CT can be helpful in differential diagnosis. Ultrasound-guided IA corticosteroid injections may be an effective treatment option.

FOOTNOTES

Author contributions: Choi MH contributed to manuscript writing and editing; Yoon IY examined the patient and contributed to data analysis; Kim WJ contributed to conceptualization and supervision; All authors have read and approved the final manuscript.

Informed consent statement: Written informed consent was obtained from the patient for publication of this report and any accompanying images.

Conflict-of-interest statement: All the authors report no relevant conflicts of interest for this article.

CARE Checklist (2016) statement: The authors have read CARE Checklist (2016), and the manuscript was prepared and revised according to CARE Checklist (2016).

Country/Territory of origin: South Korea

ORCID number: Min-Hee Choi 0000-0001-8795-8606; In-Young Yoon 0000-0002-7400-0797; Won-Joong Kim 0000-0003-2046-8690.

S-Editor: Li L
L-Editor: Filipodia
P-Editor: Li L

REFERENCES

1 **Sebes JI**, Salazar JE. The manubriosternal joint in rheumatoid disease. *AJR Am J Roentgenol* 1983; **140**: 117-121 [PMID: 6600299 DOI: 10.2214/ajr.140.1.117]
2 **Vaishya R**, Vijay V, Rai BK. Osteoarthritis of the Manubriosternal Joint: An Uncommon Cause of Chest Pain. *Cureus* 2015; **7**: e370 [PMID: 26677420 DOI: 10.7759/cureus.370]
3 **Ehara S**. Manubriosternal joint: imaging features of normal anatomy and arthritis. *Jpn J Radiol* 2010; **28**: 329-334 [PMID: 20585919 DOI: 10.1007/s11604-010-0438-9]
4 **Cho JY**, Park D. Ultrasound-Guided Corticosteroid Injection in a Patient With Tietze Syndrome Combined With Costochondral Joint Swelling. *Am J Phys Med Rehabil* 2019; **98**: e71-e73 [PMID: 30362978 DOI: 10.1097/PHM.0000000000001072]
5 **Stochkendahl MJ**, Christensen HW. Chest pain in focal musculoskeletal disorders. *Med Clin North Am* 2010; **94**: 259-273 [PMID: 20380955 DOI: 10.1016/j.mcna.2010.01.007]
6 **Klinkman MS**, Stevens D, Gorenflo DW. Episodes of care for chest pain: a preliminary report from MIRNET. Michigan Research Network. *J Fam Pract* 1994; **38**: 345-352 [PMID: 8163958]
7 **Svavarsdóttir AE**, Jónasson MR, Gudmundsson GH, Fjeldsted K. Chest pain in family practice. Diagnosis and long-term outcome in a community setting. *Can Fam Physician* 1996; **42**: 1122-1128 [PMID: 8704488]
8 **Verdon F**, Herzig L, Burnand B, Bischoff T, Pécoud A, Junod M, Mühlemann N, Favrat B; GMIRG. Chest pain in daily practice: occurrence, causes and management. *Swiss Med Wkly* 2008; **138**: 340-347 [PMID: 18561039 DOI: 10.4414/smw.2008.12123]
9 **Winzenberg T**, Jones G, Callisaya M. Musculoskeletal chest wall pain. *Aust Fam Physician* 2015; **44**: 540-544 [PMID: 26510139]
10 **Mitchell TA**, Alderete JF, Helsel BS. Manubriosternal arthrodesis: a novel surgical approach for refractory osteoarthritis. *J Thorac Cardiovasc Surg* 2014; **148**: e232-e233 [PMID: 25167982 DOI: 10.1016/j.jtcvs.2014.07.036]
11 **Becker JA**, Daily JP, Pohlgeers KM. Acute Monoarthritis: Diagnosis in Adults. *Am Fam Physician* 2016; **94**: 810-816 [PMID: 27929277]
12 **Oye M**, Ali AA, Wasserman PL, Kaeley GS, Thway M. Manubriosternal Joint Involvement as a Presenting Feature of Axial Spondyloarthritis. *Cureus* 2021; **13**: e20527 [PMID: 35070561 DOI: 10.7759/cureus.20527]
13 **Elsaman AM**, Hamed A, Radwan AR. Ultrasound-guided epidural block in axial spondyloarthritis patients with limited spine mobility: a randomized controlled trial. *Korean J Pain* 2021; **34**: 114-123 [PMID: 33380574 DOI: 10.3344/kjp.2021.34.1.114]
14 **Baek HJ**, Shin KC, Lee YJ, Kang SW, Lee EB, Yoo CD, Song YW. Clinical features of adult-onset ankylosing spondylitis in Korean patients: patients with peripheral joint disease (PJD) have less severe spinal disease course than those without PJD. *Rheumatology (Oxford)* 2004; **43**: 1526-1531 [PMID: 15316125 DOI: 10.1093/rheumatology/keh373]
15 **Kim Y**, Kim GT, Lee SG, Lee HN, Kang J, Ko TY. First Asian case of biopsy-confirmed manubriosternal joint involvement in rheumatoid arthritis. *Z Rheumatol* 2020; **79**: 389-392 [PMID: 32140801 DOI: 10.1007/s00393-020-00763-w]

16 **Wendling D**, Prati C, Demattei C, Loeuille D, Richette P, Dougados M. Anterior chest wall pain in recent inflammatory back pain suggestive of spondyloarthritis. data from the DESIR cohort. *J Rheumatol* 2013; **40**: 1148-1152 [PMID: 23678156 DOI: 10.3899/jrheum.121460]

17 **Ramonda R**, Lorenzin M, Lo Nigro A, Vio S, Zucchetta P, Frallonardo P, Campana C, Oliviero F, Modesti V, Punzi L. Anterior chest wall involvement in early stages of spondyloarthritis: advanced diagnostic tools. *J Rheumatol* 2012; **39**: 1844-1849 [PMID: 22798267 DOI: 10.3899/jrheum.120107]

18 **Elhai M**, Paternotte S, Burki V, Durnez A, Fabreguet I, Koumakis E, Meyer M, Payet J, Roure F, Dougados M, Gossec L. Clinical characteristics of anterior chest wall pain in spondyloarthritis: an analysis of 275 patients. *Joint Bone Spine* 2012; **79**: 476-481 [PMID: 22119315 DOI: 10.1016/j.jbspin.2011.10.003]

19 **Cohen SP**. Sacroiliac joint pain: a comprehensive review of anatomy, diagnosis, and treatment. *Anesth Analg* 2005; **101**: 1440-1453 [PMID: 16244008 DOI: 10.1213/01.ANE.0000180831.60169.EA]

20 **Spadaro A**, Iagnocco A, Baccano G, Ceccarelli F, Sabatini E, Valesini G. Sonographic-detected joint effusion compared with physical examination in the assessment of sacroiliac joints in spondyloarthritis. *Ann Rheum Dis* 2009; **68**: 1559-1563 [PMID: 18957488 DOI: 10.1136/ard.2008.093351]

21 **Bhure U**, Roos JE, Pérez Lago MDS, Steurer I, Grünig H, Hug U, Strobel K. SPECT/CT arthrography. *Br J Radiol* 2018; **91**: 20170635 [PMID: 29099611 DOI: 10.1259/bjr.20170635]

22 **Riaz S**, Bashir H, Hassan A, Nawaz MK. Musculoskeletal Spect-Ct: A Pictorial Review. *J Ayub Med Coll Abbottabad* 2016; **28**: 427-437 [PMID: 28718583]

23 **Saha S**, Burke C, Desai A, Vijayanathan S, Gnanasegaran G. SPECT-CT: applications in musculoskeletal radiology. *Br J Radiol* 2013; **86**: 20120519 [PMID: 24096590 DOI: 10.1259/bjr.20120519]

24 **Even-Sapir E**, Flusser G, Lerman H, Lievshitz G, Metser U. SPECT/multislice low-dose CT: a clinically relevant constituent in the imaging algorithm of nononcologic patients referred for bone scintigraphy. *J Nucl Med* 2007; **48**: 319-324 [PMID: 17268031]

25 **Linke R**, Kuwert T, Uder M, Forst R, Wuest W. Skeletal SPECT/CT of the peripheral extremities. *AJR Am J Roentgenol* 2010; **194**: W329-W335 [PMID: 20308478 DOI: 10.2214/AJR.09.3288]

26 **Zochling J**, Baraliakos X, Hermann KG, Braun J. Magnetic resonance imaging in ankylosing spondylitis. *Curr Opin Rheumatol* 2007; **19**: 346-352 [PMID: 17551364 DOI: 10.1097/BOR.0b013e32816a938c]

27 **Parghane RV**, Singh B, Sharma A, Singh H, Singh P, Bhattacharya A. Role of (99m)Tc-Methylene Diphosphonate SPECT/CT in the Detection of Sacroiliitis in Patients with Spondyloarthropathy: Comparison with Clinical Markers and MRI. *J Nucl Med Technol* 2017; **45**: 280-284 [PMID: 28798229 DOI: 10.2967/jnmt.117.193094]

28 **Golder W**, Karberg K, Sieper J. Fluoroscopy-guided application of corticosteroids for local control of manubriosternal joint pain in patients with spondyloarthropathies. *Clin Rheumatol* 2004; **23**: 481-484 [PMID: 15300467 DOI: 10.1007/s10067-004-0912-9]

World Journal of Clinical Cases

Submit a Manuscript: https://www.f6publishing.com

World J Clin Cases 2023 March 26; 11(9): 2051-2059

DOI: 10.12998/wjcc.v11.i9.2051

ISSN 2307-8960 (online)

CASE REPORT

Granulomatous prostatitis after bacille Calmette-Guérin instillation resembles prostate carcinoma: A case report and review of the literature

Yu Yao, Jun-Jie Ji, Hai-Yun Wang, Li-Jiang Sun, Gui-Ming Zhang

Specialty type: Infectious diseases

Provenance and peer review: Unsolicited article; Externally peer reviewed.

Peer-review model: Single blind

Peer-review report's scientific quality classification

Grade A (Excellent): A
Grade B (Very good): B
Grade C (Good): C
Grade D (Fair): 0
Grade E (Poor): 0

P-Reviewer: Crocetto F, Italy; Crocetto F, Italy; Koukoulaki M, Greece

Received: November 27, 2022
Peer-review started: November 27, 2022
First decision: January 12, 2023
Revised: January 15, 2023
Accepted: March 1, 2023
Article in press: March 1, 2023
Published online: March 26, 2023

Yu Yao, Jun-Jie Ji, Hai-Yun Wang, Li-Jiang Sun, Gui-Ming Zhang, Department of Urology, The Affiliated Hospital of Qingdao University, Qingdao 266003, Shandong Province, China

Corresponding author: Gui-Ming Zhang, MD, PhD, Doctor, Department of Urology, The Affiliated Hospital of Qingdao University, No.16 Jiangsu Road, Qingdao 266003, Shandong Province, China. zhangguiming9@126.com

Abstract

BACKGROUND

Bacille Calmette-Guérin (BCG) instillation is recommended in patients with non-muscle-invasive bladder cancer who have intermediate-risk and high-risk tumors. However, granulomatous prostatitis is a rare complication induced by BCG instillation, which can easily be misdiagnosed as prostate cancer. Here, we report a case of granulomatous prostatitis that resembled prostate cancer.

CASE SUMMARY

A 64-year-old Chinese man with bladder cancer received BCG instillation. Three days later, he stopped BCG instillation and received anti-infective therapy due to the urinary tract infection. Three months after BCG restart, he had rising total prostate-specific antigen (PSA) (9.14 ng/mL) and decreasing free PSA/total PSA (0.09). T2-weighted images of magnetic resonance imaging (MRI) showed a 28 mm × 20 mm diffuse low signal abnormality in the right peripheral zone, which was markedly hyperintense on high *b*-value diffusion-weighted MRI and hypointense on apparent diffusion coefficient map images. Considering Prostate Imaging Reporting and Data System score of 5 and possibility of prostate cancer, a prostate biopsy was conducted. Histopathology showed typical features of granulomatous prostatitis. The nucleic acid test for tuberculosis was positive. He was finally diagnosed with BCG-induced granulomatous prostatitis. Thereafter, he stopped BCG instillation and received anti-tuberculosis treatment. During 10 mo follow-up, he had no evidence of tumor recurrence or symptoms of tuberculosis.

CONCLUSION

Temporarily elevated PSA and high followed by low signal abnormality on diffusion-weighted MRI are important indicators of BCG-induced granulomatous prostatitis.

Key Words: Granulomatous prostatitis; Prostate cancer; Bacille Calmette-Guérin; Magnetic resonance imaging; Prostate-specific antigen; Case report

Core Tip: Granulomatous prostatitis is a rare complication of BCG instillation, which can easily be misdiagnosed as prostate cancer. Here, we report a 64-year-old Chinese man with BCG-induced granulomatous prostatitis that resembles prostate cancer. Although histopathology remains the gold standard to accurately differentiate between the two diagnoses, some clues such as temporarily elevated PSA levels and a high signal followed by a low-signal abnormality on high *b*-value diffusion-weighted MRI are important indicators of BCG-induced granulomatous prostatitis.

Citation: Yao Y, Ji JJ, Wang HY, Sun LJ, Zhang GM. Granulomatous prostatitis after bacille Calmette-Guérin instillation resembles prostate carcinoma: A case report and review of the literature. *World J Clin Cases* 2023; 11(9): 2051-2059
URL: https://www.wjgnet.com/2307-8960/full/v11/i9/2051.htm
DOI: https://dx.doi.org/10.12998/wjcc.v11.i9.2051

INTRODUCTION

Bladder cancer is the tenth most common malignancy worldwide and the sixth most common malignancy in men[1]. Approximately 75% of bladder cancer patients present with a disease confined to the mucosa or submucosa, which is defined as non-muscleinvasive bladder cancer (NMIBC)[2]. Compared with muscleinvasive bladder cancer, NMIBC is associated with better long-term survival and a lower risk of cancerspecific mortality[3,4]. Although transurethral resection of a bladder tumor (TURBT) can completely eradicate NMIBC, the high variability in the 3-month recurrence rate indicates that TURBT alone is inadequate[5]. Therefore, TURBT followed by intravesical chemotherapy or intravesical immunotherapy with bacille Calmette-Guérin (BCG) is recommended as a standard treatment for NMIBC[6].

Mycobacterium BCG, the sole tuberculosis vaccine that was first administered to a newborn baby in 1921, has saved tens of millions of lives over the past century[7]. BCG generates immunity and, therefore, has antitumor activity against tumors such as NMIBC[8]. BCG after TURBT was confirmed to be superior to TURBT plus chemotherapy or TURBT alone for preventing a recurrence of NMIBC in several recent meta-analyses[9-12]. A Cochrane systematic review also showed that mitomycin intravesical chemotherapy was less effective than BCG instillation in reducing the recurrence rate of NMIBC[13]. Therefore, intravesical BCG after TURBT is recommended in NMIBC patients with intermediate-risk and high-risk tumors.

However, BCG instillation is associated with more local and systemic side effects than intravesical chemotherapy, which may influence the treatment period[13,14]. Most patients only show mild local complications such as cystitis, urination frequency, and macroscopic hematuria[14]. The incidence of serious side effects is below 5% and nearly all cases can be treated effectively[15]. Only 1% of patients had a BCG infection in a registry-based cohort analysis[16]. One study that included BCG infection cases indicated that the top four sites of infection were the lungs, vascular tissue, the liver, and osteoarticular tissue[17]. Several cases of BCG infection after BCG instillation have been reported recently[18-21].

Compared with sites of infection such as the lungs and liver, genitourinary BCG infection is not common. Granulomatous prostatitis is a rare complication induced by BCG instillation and the exact incidence is unknown. Besides specific granulomatous prostatitis, it may be secondary to infections, surgery, associated to malacoplakia or to systemic granulomatous diseases such as sarcoidosis and Wegener's granulomatosis[22,23]. Several cases have reported that granulomatous prostatitis presents as increased serum levels of prostate-specific antigen (PSA) and a node with an abnormal signal detected by multiparametric prostate magnetic resonance imaging (MP-MRI). Furthermore, previous cases involved nodular or diffusely firm enlargement on digital rectal examination, which was suggestive of prostate cancer and only resulted in a diagnosis of granulomatous prostatitis after prostate biopsy[24-27]. Here, we present a case of granulomatous prostatitis induced by BCG instillation and describe how to differentiate between granulomatous prostatitis induced by BCG instillation and prostate cancer.

CASE PRESENTATION

Chief complaints

A 64-year-old Chinese man with weekly BCG instillation visited our center in January 2022 for routinely examination of bladder cancer complaining of rising total PSA level (9.14 ng/mL) and decreasing free PSA/total PSA (0.09) with no symptom.

History of present illness

The patient was diagnosed with high-grade NMIBC in March 2020 and scheduled for gemcitabine intravesical chemotherapy. Owing to a pathologically T1G3 bladder carcinoma on histopathology, TURBT was repeated 3 mo later. Cystoscopy showed necrosis attached to the surface of the scar, and pathology suggested inflammatory necrosis with no tumor. Two months after the second TURBT, weekly BCG instillations were recommended to replace the gemcitabine intravesical chemotherapy. Three days after the first BCG instillation, the patient experienced fever up to 39 °C, gross hematuria, lower abdomen pain, and perineal pain. The physical examination and scrotal B-ultrasound indicated left hydrocele testis and epididymitis. Routine laboratory blood results indicated that total leukocyte counts were elevated to 18.25 × 10^9/L with increasing neutrophil granulocyte count (10.62 × 10^9/L) and decreasing hemoglobin levels (114 g/L). In addition, urinary testing revealed pyuria, hematuria, and bacteriuria. The patient was diagnosed with a urinary tract infection and received piperacillin and tazobactam as anti-infective therapy for 6 d until his temperature returned to normal. His urinary testing also became normal 1 wk later. He stopped BCG instillation and restarted gemcitabine intravesical chemotherapy. Following the second TURBT, cystoscopies and urinary B-ultrasounds were performed every 3 mo. The results showed no evidence of tumor recurrence. Sixteen months after the second TURBT, BCG intravesical immunotherapy was restarted.

History of past illness

The patient had no history of tuberculosis.

Personal and family history

The patient and his family had no history of prostate cancer.

Physical examination

Digital rectal examination revealed a moderately enlarged, non-painful prostate gland with shallow central sulcus and normal density.

Laboratory examinations

Laboratory tests revealed a rising serum total PSA level (9.14 ng/mL) and a decreasing serum ratio of free PSA/total PSA (0.09).

Imaging examinations

MP-MRI was performed. Axial T2-weighted images showed a 28 mm × 20 mm low-signal, diffuse abnormality in the right peripheral zone (Figure 1A). On diffusion-weighted MRI with a *b*-value at 1500, the lesion was seen as a markedly hyperintense focus (Figure 1B), which was consistent with a lesion with a Prostate Imaging Reporting and Data System (PI-RADS) score of 5, with hypointense signal on an apparent diffusion coefficient map image (Figure 1C).

Further diagnostic work-up

Considering the increasing PSA results and abnormal focus in MP-MRI, the patient was primarily diagnosed with prostate cancer. A transperineal prostate needle biopsy was conducted. Levofloxacin was used as antibiotic prophylaxis. However, the histopathological findings showed benign prostate tissue with typical features of granulomatous prostatitis with multinucleated giant cells, epithelioid cells, fibroblasts, and infiltration lymphocytes (Figure 2). A nucleic acid test of tuberculosis was subsequently performed and the result was positive (Ct = 37.18).

FINAL DIAGNOSIS

Based on the patient's medical history, he was finally diagnosed with BCG-induced granulomatous prostatitis.

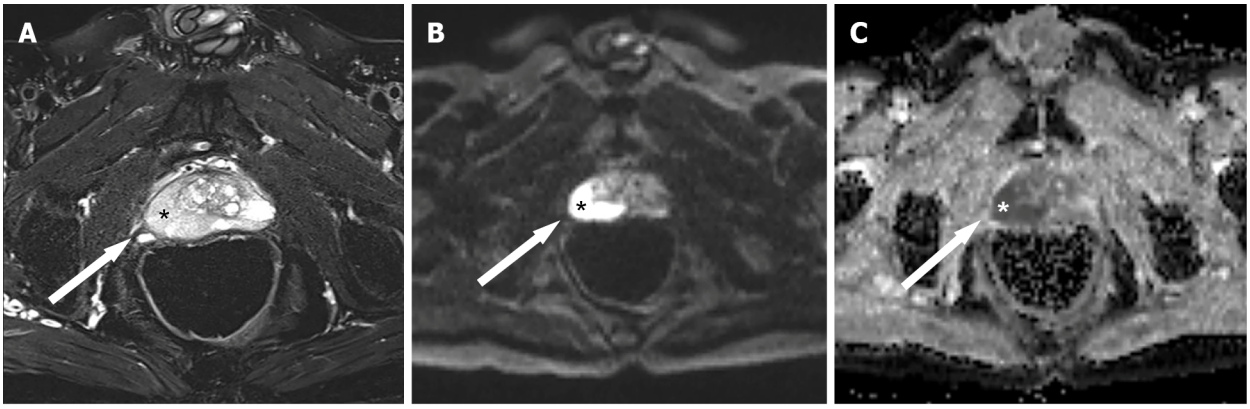

DOI: 10.12998/wjcc.v11.i9.2051

Figure 1 Multiparametric magnetic resonance imaging of the case patient. Axial T2-weighted images showed a 28 mm × 20 mm low-signal, diffuse abnormality in the right peripheral zone (A). Diffusion-weighted magnetic resonance imaging with a *b*-value at 1500 showed hyperintense focus (B), with a hypointense signal on an apparent diffusion coefficient map image (C).

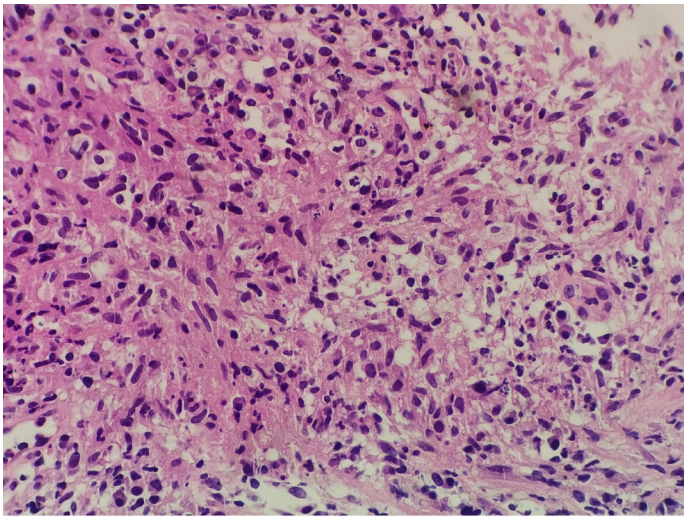

DOI: 10.12998/wjcc.v11.i9.2051

Figure 2 Hematoxylin and eosin staining slide from the prostate biopsy shows benign prostate tissue with typical features of granulomatous prostatitis with multinucleated giant cells, epithelioid cells, fibroblasts, and infiltration lymphocytes (magnification ×400).

TREATMENT

Thereafter, he received isoniazid, rifapentine, levofloxacin, and ethambutol as anti-tuberculosis treatment. The BCG instillation was stopped and replaced by epirubicin intravesical chemotherapy.

OUTCOME AND FOLLOW-UP

During a follow-up visit 10 mo after prostate biopsy, the patient had no evidence of tumor recurrence or symptoms of tuberculosis.

DISCUSSION

BCG instillation is used as standard immunotherapy in bladder cancer. As for complications, a tuberculosis infection in the urinary system is not common, as infection mostly occurs in the parenchymatous organs such as the testis, penis, kidneys, and prostate[17]. In recent articles, granulomatous prostatitis has been reported to account for 3.5% of BCG infections[28], and occurs in 1.06% of all bladder cancer patients who receive BCG instillation[29]. Most cases are asymptomatic and easily misdiagnosed as prostate cancer. Therefore, we present a case of granulomatous prostatitis induced by

BCG instillations in order to investigate useful strategies for the differential diagnosis of the condition.

In two recent cases, elevated PSA levels ranging from 6.1 ng/mL to 8.4 ng/mL in patients with granulomatous prostatitis after BCG instillation[24,30]. In our patient, increasing total PSA levels and a decreasing ratio of free PSA/total PSA was found, which complicated the differentiation between prostate cancer and granulomatous prostatitis. Wang *et al*[31] discovered that half of all patients with BCG-induced granulomatous prostatitis had elevated PSA, while the ratio of free PSA/total PSA decreased to less than 0.16 in all patients. Although PSA has increased during immunotherapy for bladder cancer in some studies, the PSA elevation has been self-limited, and only PSA elevations for over 3 to 12 mo have led to recommendations for prostate biopsy[32,33]. Another study also reported that 40% of bladder cancer patients had elevated PSA after intravesical BCG therapy, but the PSA reverted to normal within 3 mo[34]. It seems that prostate biopsy should be delayed in these patients while PSA is monitored. However, two patients whose PSA level was elevated after BCG instillations were pathologically diagnosed with both granulomatous prostatitis and prostate cancer [26,27]. In an epidemiological study, concomitant prostate cancer was reported in 35.9% of patients with granulomatous prostatitis[17]. In another article, prostate cancer detection after intravesical BCG occurred frequently in patients with elevated PSA and a bladder tumor located far from the bladder neck[35]. These findings together suggest the need to develop patterns or curves of PSA levels after BCG instillation that could be used to distinguish between granulomatous prostatitis and prostate cancer. This strategy could reduce the frequency of unnecessary biopsies.

MP-MRI is widely used in the diagnosis of prostate cancer because it has good sensitivity for the localization and detection of over International Society of Urological Pathology grade 2 carcinomas[36-38]. With the inability to differentiate between granulomatous prostatitis and prostate cancer on transrectal ultrasound[25], specific characteristics of BCG-induced granulomatous prostatitis on MP-MRI have been proposed recently. In the case patient, an abnormal focus showed low signal in T2-weighted images and an apparent diffusion coefficient in the peripheral zone, which has been reported previously[24,26,27,31,39]. These characteristics could occur because the histology of granulomatous prostatitis includes stromal infiltration of chronic inflammatory cells and extracellular fluid surrounding the prostatic cells. However, both prostate cancer and granulomatous prostatitis present as destruction of the prostate gland with weakened water diffusion capability, and this is visualized as lower apparent diffusion coefficient values. The decreased signal intensity in T2-weighted images is also caused by the decreased water content present in both prostate cancer and granulomatous prostatitis[39]. Moreover, both BCG-related granulomatous prostatitis and prostate cancer mostly occurs in the peripheral zone of the prostate, which creates challenges in diagnosis[40,41].

On high *b*-value diffusion-weighted MRI, the lesion of the case patient had a markedly hyperintense focus with a PI-RADS version 2 score of 5. Several other studies support our finding of a PI-RADS version 2 score of 5[24,31,41]. However, Gottlieb *et al*[39] reported five patients with granulomatous prostatitis whose abnormalities on high *b*-value diffusion-weighted MRI were of low signal. Matsushima *et al*[42] described computed-tomography-detected asymptomatic abnormalities in the prostate after BCG therapy that naturally disappeared during the follow-up period. Similarly, one patient was reported to have temporarily elevated PSA after BCG instillations. One article demonstrated three different imaging patterns of BCG-related granulomatous prostatitis on MP-MRI, and all hyperintense focus on diffusion-weighted MRI reverted to hypointense during the follow-up period [40]. Therefore, we hypothesize that the signal on high *b*-value diffusion-weighted MRI is high in acute BCG-related granulomatous prostatitis and low in chronic BCG-related granulomatous prostatitis. Patients with a PI-RADS score of 3 or less on MRI should be recommended for a follow-up radiologic examination instead of undergoing prostate biopsy[39]. In one patient, an abnormality with increased fluorodeoxyglucose activity was detected by positron emission tomography computed tomography and pathologically diagnosed as BCG-related granulomatous prostatitis[43]. In granulomatous prostatitis, dynamic contrast-enhanced persistent time of prostate lesions on enhanced MRI was longer than that of prostate cancer[44]. These discoveries provide new clues for differential diagnosis.

Granulomas are clusters of macrophages surrounded by a mononuclear leukocytes and plasma cells. While the pathogenesis of BCG-related granulomatous prostatitis is uncertain, some evidence exists. BCG instillation induces a massive increase in lymphocytes, especially in the proportion of CD4+ Th1 cells[45]; this increase is an inflammatory reaction to BCG in the bladder. Miyashita *et al*[46] and Butel *et al*[47] noticed that BCG-related granulomatous prostatitis often radiated from close to the prostatic urethra toward the gland periphery in a wedge-shaped area related to one or more duct systems. A hypothesis was put forward that granulomatous prostatitis was caused by the intra-prostatic reflux of urine contaminated with BCG in the bladder[48]. Therefore, hypersensitivity reactions to BCG antigens from refluxed urine may cause infectious complications, including BCG-induced granulomatous prostatitis[49,50]. Anatomically, ducts in the peripheral zone enter the urethra at less obtuse angles than those from other zones and are likely to be more prone to refluxed urine and damage from potential BCG infections[47]. This could explain why most granulomatous prostatitis occurs in the peripheral zone. A multivariable regression analysis indicated that prostate volume and body mass index were significant risk factors for BCG-induced granulomatous prostatitis[51]. Despite the low incidence of this disease, the mechanisms and predictors of BCG-induced granulomatous prostatitis should be further explored. And histological evaluation remains the gold standard to differentiate granulomatous

prostatitis from prostate cancer.

BCG-induced granulomatous prostatitis and prostatic abscesses tend to be intermediate complications that mostly occur 4 wk from the last instillation, whereas testicular and epididymal tuberculosis tend to be late complications (56 wk from the last instillation)[17]. However, our patient showed lower urinary tract symptoms, urinary hydrocele testis, and epididymitis only 3 d after the first instillation. Although he recovered after antibiotic treatment, we speculate that the BCG infection of the urogenital system occurred after the first instillation. BCG instillation was stopped, and the patient received anti-tuberculosis treatment after histopathological diagnosis with BCG-induced granulomatous prostatitis. Most BCG-induced granulomatous prostatitis is asymptomatic and does not require treatment[26,31]. The 4-quinolones and antituberculotics including isoniazid, rifapentine, pyrazinamide, and ethambutol are used in symptomatic BCG-induced granulomatous prostatitis and some BCG-induced prostatic abscesses[25,30,52-54]. If anti-tuberculosis treatment is ineffective, surgery such as transurethral resection of prostate is recommended[55]. The diagnosis and treatment of BCG-induced granulomatous prostatitis requires further study.

CONCLUSION

Granulomatous prostatitis is a rare complication of BCG instillation that can easily be misdiagnosed as prostate cancer. Although histopathology remains the gold standard to accurately differentiate between the two diagnoses, some clues such as temporarily elevated PSA levels and a high signal followed by a low-signal abnormality on high *b*-value diffusion-weighted MRI are important indicators of BCG-induced granulomatous prostatitis. High-quality studies should be designed to improve the diagnosis of BCG-induced granulomatous prostatitis.

FOOTNOTES

Author contributions: Zhang GM designed the study; Yao Y and Ji JJ collected, analyzed and interpreted the clinical data, and wrote the manuscript; Wang HY and Sun LJ collected part of the patients' clinical data; Zhang GM supervised the project and revised the manuscript; all authors vouch for the respective data and analysis, approved the final version, and agreed to publish the manuscript.

Supported by the Natural Science Foundation of Shandong Province, No. ZR2021MH354.

Informed consent statement: All procedures performed in studies involving human participants were in accordance with the ethical standards of the institutional and/or national research committee and with the 1964 Helsinki declaration and its later amendments or comparable ethical standards. This study is approved by Ethics Committee of the Affiliated Hospital of Qingdao University.

Conflict-of-interest statement: The authors declare no conflicts of interest.

CARE Checklist (2016) statement: The authors have read the CARE Checklist (2016), and the manuscript was prepared and revised according to the CARE Checklist (2016).

Country/Territory of origin: China

ORCID number: Li-Jiang Sun 0000-0001-5856-8270; Gui-Ming Zhang 0000-0002-5856-5325.

S-Editor: Chang KL
L-Editor: A
P-Editor: Chang KL

REFERENCES

1 **Sung H**, Ferlay J, Siegel RL, Laversanne M, Soerjomataram I, Jemal A, Bray F. Global Cancer Statistics 2020: GLOBOCAN Estimates of Incidence and Mortality Worldwide for 36 Cancers in 185 Countries. *CA Cancer J Clin* 2021; **71**: 209-249 [PMID: 33538338 DOI: 10.3322/caac.21660]

2 Bladder cancer: diagnosis and management of bladder cancer: © NICE (2015) Bladder cancer: diagnosis and management of bladder cancer. *BJU Int* 2017; **120**: 755-765 [PMID: 29168333 DOI: 10.1111/bju.14045]

3 **Burger M**, Catto JW, Dalbagni G, Grossman HB, Herr H, Karakiewicz P, Kassouf W, Kiemeney LA, La Vecchia C, Shariat S, Lotan Y. Epidemiology and risk factors of urothelial bladder cancer. *Eur Urol* 2013; **63**: 234-241 [PMID: 22877502 DOI: 10.1016/j.eururo.2012.07.033]

4 **Martini A**, Fallara G, Pellegrino F, Cirulli GO, Larcher A, Necchi A, Montorsi F, Capitanio U. Neoadjuvant and adjuvant immunotherapy in renal cell carcinoma. *World J Urol* 2021; **39**: 1369-1376 [PMID: 33386494 DOI: 10.1007/s00345-020-03550-z]

5 **Brausi M**, Collette L, Kurth K, van der Meijden AP, Oosterlinck W, Witjes JA, Newling D, Bouffioux C, Sylvester RJ; EORTC Genito-Urinary Tract Cancer Collaborative Group. Variability in the recurrence rate at first follow-up cystoscopy after TUR in stage Ta T1 transitional cell carcinoma of the bladder: a combined analysis of seven EORTC studies. *Eur Urol* 2002; **41**: 523-531 [PMID: 12074794 DOI: 10.1016/s0302-2838(02)00068-4]

6 **Babjuk M**, Burger M, Compérat EM, Gontero P, Mostafid AH, Palou J, van Rhijn BWG, Rouprêt M, Shariat SF, Sylvester R, Zigeuner R, Capoun O, Cohen D, Escrig JLD, Hernández V, Peyronnet B, Seisen T, Soukup V. European Association of Urology Guidelines on Non-muscle-invasive Bladder Cancer (TaT1 and Carcinoma In Situ) - 2019 Update. *Eur Urol* 2019; **76**: 639-657 [PMID: 31443960 DOI: 10.1016/j.eururo.2019.08.016]

7 **Lange C**, Aaby P, Behr MA, Donald PR, Kaufmann SHE, Netea MG, Mandalakas AM. 100 years of Mycobacterium bovis bacille Calmette-Guérin. *Lancet Infect Dis* 2022; **22**: e2-e12 [PMID: 34506734 DOI: 10.1016/S1473-3099(21)00403-5]

8 **Mukherjee N**, Julián E, Torrelles JB, Svatek RS. Effects of Mycobacterium bovis Calmette et Guérin (BCG) in oncotherapy: Bladder cancer and beyond. *Vaccine* 2021; **39**: 7332-7340 [PMID: 34627626 DOI: 10.1016/j.vaccine.2021.09.053]

9 **Malmström PU**, Sylvester RJ, Crawford DE, Friedrich M, Krege S, Rintala E, Solsona E, Di Stasi SM, Witjes JA. An individual patient data meta-analysis of the long-term outcome of randomised studies comparing intravesical mitomycin C *vs* bacillus Calmette-Guérin for non-muscle-invasive bladder cancer. *Eur Urol* 2009; **56**: 247-256 [PMID: 19409692 DOI: 10.1016/j.eururo.2009.04.038]

10 **Shelley MD**, Wilt TJ, Court J, Coles B, Kynaston H, Mason MD. Intravesical bacillus Calmette-Guérin is superior to mitomycin C in reducing tumour recurrence in high-risk superficial bladder cancer: a meta-analysis of randomized trials. *BJU Int* 2004; **93**: 485-490 [PMID: 15008714 DOI: 10.1111/j.1464-410x.2003.04655.x]

11 **Böhle A**, Jocham D, Bock PR. Intravesical bacillus Calmette-Guerin *vs* mitomycin C for superficial bladder cancer: a formal meta-analysis of comparative studies on recurrence and toxicity. *J Urol* 2003; **169**: 90-95 [PMID: 12478111 DOI: 10.1016/S0022-5347(05)64043-8]

12 **Shelley MD**, Kynaston H, Court J, Wilt TJ, Coles B, Burgon K, Mason MD. A systematic review of intravesical bacillus Calmette-Guérin plus transurethral resection *vs* transurethral resection alone in Ta and T1 bladder cancer. *BJU Int* 2001; **88**: 209-216 [PMID: 11488731 DOI: 10.1046/j.1464-410x.2001.02306.x]

13 **Schmidt S**, Kunath F, Coles B, Draeger DL, Krabbe LM, Dersch R, Kilian S, Jensen K, Dahm P, Meerpohl JJ. Intravesical Bacillus Calmette-Guérin *vs* mitomycin C for Ta and T1 bladder cancer. *Cochrane Database Syst Rev* 2020; **1**: CD011935 [PMID: 31912907 DOI: 10.1002/14651858.CD011935.pub2]

14 **Brausi M**, Oddens J, Sylvester R, Bono A, van de Beek C, van Andel G, Gontero P, Turkeri L, Marreaud S, Collette S, Oosterlinck W. Side effects of Bacillus Calmette-Guérin (BCG) in the treatment of intermediate- and high-risk Ta, T1 papillary carcinoma of the bladder: results of the EORTC genito-urinary cancers group randomised phase 3 study comparing one-third dose with full dose and 1 year with 3 years of maintenance BCG. *Eur Urol* 2014; **65**: 69-76 [PMID: 23910233 DOI: 10.1016/j.eururo.2013.07.021]

15 **van der Meijden AP**, Sylvester RJ, Oosterlinck W, Hoeltl W, Bono AV; EORTC Genito-Urinary Tract Cancer Group. Maintenance Bacillus Calmette-Guerin for Ta T1 bladder tumors is not associated with increased toxicity: results from a European Organisation for Research and Treatment of Cancer Genito-Urinary Group Phase III Trial. *Eur Urol* 2003; **44**: 429-434 [PMID: 14499676 DOI: 10.1016/s0302-2838(03)00357-9]

16 **Larsen ES**, Nordholm AC, Lillebaek T, Holden IK, Johansen IS. The epidemiology of bacille Calmette-Guérin infections after bladder instillation from 2002 through 2017: a nationwide retrospective cohort study. *BJU Int* 2019; **124**: 910-916 [PMID: 31054198 DOI: 10.1111/bju.14793]

17 **Cabas P**, Rizzo M, Giuffrè M, Antonello RM, Trombetta C, Luzzati R, Liguori G, Di Bella S. BCG infection (BCGitis) following intravesical instillation for bladder cancer and time interval between treatment and presentation: A systematic review. *Urol Oncol* 2021; **39**: 85-92 [PMID: 33308969 DOI: 10.1016/j.urolonc.2020.11.037]

18 **Zaza SI**, Ghasemzadeh A, Bennett KM. Mycobacterium Bovis Causing Mycotic Aneurysm Secondary to Intravesical Treatment with Bacillus Calmette-Guérin: A Case Report. *Ann Vasc Surg* 2022; **79**: 437.e1-437.e6 [PMID: 34644643 DOI: 10.1016/j.avsg.2021.07.032]

19 **Notghi AAA**, Hosseini F, Tsogas N. Severe diffuse proliferative bronchiolitis complicating culture-proven disseminated BCG infection after intravesical instillation for bladder cancer. *BMJ Case Rep* 2022; **15** [PMID: 35321917 DOI: 10.1136/bcr-2021-248681]

20 **Lupon E**, Martin-Blondel G, Pollon T, Berthier C, Lellouch AG, Mansat P. BCGitis of the wrist after intravesical BCG therapy: A case report. *Hand Surg Rehabil* 2020; **39**: 585-587 [PMID: 32659383 DOI: 10.1016/j.hansur.2020.05.011]

21 **Adami M**, Marsteller I, Mazzucchelli L, Cerny A, Bernasconi E, Bertoli R. Granulomatous hepatitis after intravesical bacillus Calmette-Guérin treatment. *Scand J Infect Dis* 2011; **43**: 55-57 [PMID: 20854217 DOI: 10.3109/00365548.2010.515609]

22 **De Luca L**, Crocetto F, Barone B, Creta M, Pesce S, Aveta A, Campanino MR, Imbimbo C, Longo N. Granulomatous prostatitis mimicking prostate cancer in a patient with psoriatic arthritis: a case report. *Future Sci OA* 2020; **6**: FSO591 [PMID: 32802396 DOI: 10.2144/fsoa-2020-0031]

23 **Crocetto F**, Barone B, De Luca L, Creta M. Granulomatous prostatitis: a challenging differential diagnosis to take into consideration. *Future Oncol* 2020; **16**: 805-806 [PMID: 32180450 DOI: 10.2217/fon-2020-0185]

24 **Garrido-Abad P**, Rodríguez-Cabello MÁ, González-Gordaliza C, Vera-Berón R, Platas-Sancho A. BCG instillations can

mimic prostate cancer on multiparametric MRI. *Int Braz J Urol* 2018; **44**: 835-837 [PMID: 29570255 DOI: 10.1590/S1677-5538.IBJU.2017.0621]

25 **Białek W**, Rudzki S, Iberszer P, Wronecki L. Granulomatous prostatitis after intravesical immunotherapy mimicking prostate cancer. *J Ultrason* 2016; **16**: 404-410 [PMID: 28138411 DOI: 10.15557/JoU.2016.0040]

26 **Logan JK**, Walton-Diaz A, Rais-Bahrami S, Merino MJ, Turkbey B, Choyke PL, Pinto PA. Changes observed in multiparametric prostate magnetic resonance imaging characteristics correlate with histopathological development of chronic granulomatous prostatitis after intravesical Bacillus Calmette-Guerin therapy. *J Comput Assist Tomogr* 2014; **38**: 274-276 [PMID: 24637671 DOI: 10.1097/RCT.0b013e3182aac58a]

27 **Dianat SS**, Matoso A, Carter BH, Macura KJ. Multiparametric MRI findings of granulomatous prostatitis after intravesical bacillus Calmette-Guérin therapy in a patient undergoing active surveillance. *Clin Genitourin Cancer* 2014; **12**: e215-e219 [PMID: 24999165 DOI: 10.1016/j.clgc.2014.03.015]

28 **Pérez-Jacoiste Asín MA**, Fernández-Ruiz M, López-Medrano F, Lumbreras C, Tejido Á, San Juan R, Arrebola-Pajares A, Lizasoain M, Prieto S, Aguado JM. Bacillus Calmette-Guérin (BCG) infection following intravesical BCG administration as adjunctive therapy for bladder cancer: incidence, risk factors, and outcome in a single-institution series and review of the literature. *Medicine (Baltimore)* 2014; **93**: 236-254 [PMID: 25398060 DOI: 10.1097/MD.0000000000000119]

29 **Coello Torà I**, de la Cruz Ruiz M, Carrillo García P, Carmelo Pieras Ayala E. Epidemiological study of granulomatous prostatitis in a tertiary hospital: Associated risk factors and relationship with prostate cancer. *Urologia* 2022; **89**: 257-260 [PMID: 33300453 DOI: 10.1177/0391560320979859]

30 **Caulier P**, Yombi JC, Dufaux M, Feyaerts A, Abi AA, Hainaut P. Prostate abscess following intravesical BCG therapy. *Acta Clin Belg* 2009; **64**: 436-437 [PMID: 19999393 DOI: 10.1179/acb.2009.072]

31 **Wang Z**, Han C, Xu Y, Yu X, Kang W, Xiang Y, Yuan Y, Li L, Wang M. The role of prostate-specific antigen and multiparametric magnetic resonance imaging in the diagnosis of granulomatous prostatitis induced by intravesical Bacillus Calmette-Guérin vaccine therapy in patients with nonmuscle invasive bladder cancer. *J Cancer Res Ther* 2021; **17**: 625-629 [PMID: 34269291 DOI: 10.4103/jcrt.JCRT_1684_20]

32 **Serretta V**, Gesolfo CS, Di Maida F, Caruana G, Rocchini L, Moschini M, Colombo R, Simonato A. The clinical value of PSA increase during intravesical adjuvant therapy for nonmuscle-invasive bladder cancer. *Urologia* 2016; **83**: 145-148 [PMID: 27516352 DOI: 10.5301/uro.5000189]

33 **Beltrami P**, Ruggera L, Cazzoletti L, Schiavone D, Zattoni F. Are prostate biopsies mandatory in patients with prostate-specific antigen increase during intravesical immuno- or chemotherapy for superficial bladder cancer? *Prostate* 2008; **68**: 1241-1247 [PMID: 18484098 DOI: 10.1002/pros.20790]

34 **Leibovici D**, Zisman A, Chen-Levyi Z, Cypele H, Siegel YI, Faitelovich S, Lindner A. Elevated prostate specific antigen serum levels after intravesical instillation of bacillus Calmette-Guerin. *J Urol* 2000; **164**: 1546-1549 [PMID: 11025701]

35 **Hong S**, Kim SC, Kwon T, Jeong IG, Kim CS, Ahn H, Hong JH. Is bladder tumor location associated with prostate cancer detection after intravesical bacillus Calmette-Guérin instillation? *PLoS One* 2014; **9**: e103791 [PMID: 25072158 DOI: 10.1371/journal.pone.0103791]

36 **Borofsky S**, George AK, Gaur S, Bernardo M, Greer MD, Mertan FV, Taffel M, Moreno V, Merino MJ, Wood BJ, Pinto PA, Choyke PL, Turkbey B. What Are We Missing? *Radiology* 2018; **286**: 186-195 [PMID: 29053402 DOI: 10.1148/radiol.2017152877]

37 **Le JD**, Tan N, Shkolyar E, Lu DY, Kwan L, Marks LS, Huang J, Margolis DJ, Raman SS, Reiter RE. Multifocality and prostate cancer detection by multiparametric magnetic resonance imaging: correlation with whole-mount histopathology. *Eur Urol* 2015; **67**: 569-576 [PMID: 25257029 DOI: 10.1016/j.eururo.2014.08.079]

38 **Bratan F**, Niaf E, Melodelima C, Chesnais AL, Souchon R, Mège-Lechevallier F, Colombel M, Rouvière O. Influence of imaging and histological factors on prostate cancer detection and localisation on multiparametric MRI: a prospective study. *Eur Radiol* 2013; **23**: 2019-2029 [PMID: 23494494 DOI: 10.1007/s00330-013-2795-0]

39 **Gottlieb J**, Princenthal R, Cohen MI. Multi-parametric MRI findings of granulomatous prostatitis developing after intravesical bacillus calmette-guérin therapy. *Abdom Radiol (NY)* 2017; **42**: 1963-1967 [PMID: 28224172 DOI: 10.1007/s00261-017-1081-z]

40 **Lee S**, Oh YT, Kim HM, Jung DC, Hong H. Imaging Patterns of Bacillus Calmette-Guérin-Related Granulomatous Prostatitis Based on Multiparametric MRI. *Korean J Radiol* 2022; **23**: 60-67 [PMID: 34983094 DOI: 10.3348/kjr.2020.1369]

41 **Suzuki T**, Takeuchi M, Naiki T, Kawai N, Kohri K, Hara M, Shibamoto Y. MRI findings of granulomatous prostatitis developing after intravesical Bacillus Calmette-Guérin therapy. *Clin Radiol* 2013; **68**: 595-599 [PMID: 23384503 DOI: 10.1016/j.crad.2012.12.005]

42 **Matsushima M**, Kikuchi E, Akita H, Miyajima A, Oya M, Jinzaki M. Natural course of asymptomatic abnormal prostate findings incidentally detected by CT after intravesical BCG therapy. *Int J Clin Oncol* 2017; **22**: 554-562 [PMID: 28185020 DOI: 10.1007/s10147-017-1096-z]

43 **Wilkinson C**, Chowdhury F, Scarsbrook A, Smith J. BCG-induced granulomatous prostatitis--an incidental finding on FDG PET-CT. *Clin Imaging* 2012; **36**: 413-415 [PMID: 22726988 DOI: 10.1016/j.clinimag.2011.09.004]

44 **Quon JS**, Moosavi B, Khanna M, Flood TA, Lim CS, Schieda N. False positive and false negative diagnoses of prostate cancer at multi-parametric prostate MRI in active surveillance. *Insights Imaging* 2015; **6**: 449-463 [PMID: 26002487 DOI: 10.1007/s13244-015-0411-3]

45 **Ponticiello A**, Perna F, Maione S, Stradolini M, Testa G, Terrazzano G, Ruggiero G, Malerba M, Sanduzzi A. Analysis of local T lymphocyte subsets upon stimulation with intravesical BCG: a model to study tuberculosis immunity. *Respir Med* 2004; **98**: 509-514 [PMID: 15191035 DOI: 10.1016/j.rmed.2003.12.003]

46 **Miyashita H**, Troncoso P, Babaian RJ. BCG-induced granulomatous prostatitis: a comparative ultrasound and pathologic study. *Urology* 1992; **39**: 364-367 [PMID: 1557848 DOI: 10.1016/0090-4295(92)90214-h]

47 **Butel R**, Ball R. The distribution of BCG prostatitis: A clue for pathogenetic processes? *Prostate* 2018; **78**: 1134-1139 [PMID: 29987889 DOI: 10.1002/pros.23688]

48 **Lamm DL**, van der Meijden PM, Morales A, Brosman SA, Catalona WJ, Herr HW, Soloway MS, Steg A, Debruyne FM.

Incidence and treatment of complications of bacillus Calmette-Guerin intravesical therapy in superficial bladder cancer. *J Urol* 1992; **147**: 596-600 [PMID: 1538436 DOI: 10.1016/s0022-5347(17)37316-0]

49 **Balasar M**, Doğan M, Kandemir A, Taskapu HH, Cicekci F, Toy H, Gurbuz R. Investigation of granulomatous prostatitis incidence following intravesical BCG therapy. *Int J Clin Exp Med* 2014; **7**: 1554-1557 [PMID: 25035779]

50 **Bevers RF**, Kurth KH, Schamhart DH. Role of urothelial cells in BCG immunotherapy for superficial bladder cancer. *Br J Cancer* 2004; **91**: 607-612 [PMID: 15266312 DOI: 10.1038/sj.bjc.6602026]

51 **Kim TJ**, Yu YD, Hwang SI, Lee HJ, Hong SK, Lee SE, Oh JJ. Analysis of risk factors for post-bacillus Calmette-Guerin-induced prostatitis in patients with non-muscle invasive bladder cancer. *Sci Rep* 2020; **10**: 9763 [PMID: 32555265 DOI: 10.1038/s41598-020-66952-4]

52 **Ye HY**, Xu QQ, Huang XB, Ma K, Wang XF. [Tuberculous prostatic abscess following intravesical bacillus Calmette-Guerin immunotherapy: a case report]. *Beijing Da Xue Xue Bao Yi Xue Ban* 2015; **47**: 1039-1041 [PMID: 26679674]

53 **Doo SW**, Kim JH, Yang WJ, Kim SI, Lee DW, Hong SS, Song YS. A case of tuberculous prostatitis with abscess. *World J Mens Health* 2012; **30**: 138-140 [PMID: 23596601 DOI: 10.5534/wjmh.2012.30.2.138]

54 **Aust TR**, Massey JA. Tubercular prostatic abscess as a complication of intravesical bacillus Calmette-Guérin immunotherapy. *Int J Urol* 2005; **12**: 920-921 [PMID: 16323989 DOI: 10.1111/j.1442-2042.2005.01183.x]

55 **Okusa H**, Irie A, Chin I, Baba S, Mitomi H, Shitara T. [Cases of bacillus Calmette-Guerin-induced granulomatous prostatitis and prostatic stromal invasion of the bladder carcinoma in situ, showing similar clinical findings]. *Hinyokika Kiyo* 2003; **49**: 555-557 [PMID: 14598697]

World Journal of Clinical Cases

Submit a Manuscript: https://www.f6publishing.com

World J Clin Cases 2023 March 26; 11(9): 2060-2066

DOI: 10.12998/wjcc.v11.i9.2060

ISSN 2307-8960 (online)

CASE REPORT

Unusual capitate fracture with dorsal shearing pattern and concomitant carpometacarpal dislocation with a 6-year follow-up: A case report

Chien-Cheng Lai, Hsu-Wei Fang, Chih-Hung Chang, Jwo-Luen Pao, Chun-Chien Chang, Yeong-Jang Chen

Specialty type: Orthopedics

Provenance and peer review: Unsolicited article; Externally peer reviewed.

Peer-review model: Single blind

Peer-review report's scientific quality classification

Grade A (Excellent): 0
Grade B (Very good): 0
Grade C (Good): C, C
Grade D (Fair): 0
Grade E (Poor): 0

P-Reviewer: Cebula M, Poland; Yuan HJ, China

Received: December 2, 2022
Peer-review started: December 2, 2022
First decision: February 2, 2023
Revised: February 10, 2023
Accepted: February 27, 2023
Article in press: February 27, 2023
Published online: March 26, 2023

Chien-Cheng Lai, Chih-Hung Chang, Jwo-Luen Pao, Chun-Chien Chang, Department of Orthopedic Surgery, Far Eastern Memorial Hospital, New Taipei City 220, Taiwan

Chien-Cheng Lai, Hsu-Wei Fang, Department of Chemical Engineering and Biotechnology, National Taipei University of Technology, Taipei 106, Taiwan

Chih-Hung Chang, Graduate School of Biotechnology and Bioengineering, Yuan Ze University, Taoyuan 320, Taiwan

Yeong-Jang Chen, Department of Orthopedics, Fu Jen Catholic University Hospital, Fu Jen Catholic University, New Taipei City 243, Taiwan

Corresponding author: Yeong-Jang Chen, MD, Surgeon, Department of Orthopedics, Fu Jen Catholic University Hospital, Fu Jen Catholic University, No. 69 Guizi Road, Taishan District, New Taipei City 243, Taiwan. yjchen71@gmail.com

Abstract

BACKGROUND

Isolated capitate fractures are rare carpal fractures. Following high-energy injuries, capitate fractures are usually associated with other carpal fractures or ligament injuries. The management of capitate fractures depends on the fracture pattern. Here, we report an unusual capitate fracture with a dorsal shearing pattern and concomitant carpometacarpal dislocation, with a 6-year follow-up. To the best of our knowledge, this fracture pattern and surgical management have not been previously reported.

CASE SUMMARY

A 28-year-old man presented with left-hand volar tenderness and decreased grip strength that persisted for one month after a traffic accident. Radiography showed a distal capitate fracture with carpometacarpal joint incongruence. Computed tomography (CT) revealed a distal capitate fracture with carpometacarpal joint dislocation. The distal fragment was rotated by 90° in the sagittal plane, and an oblique shearing fracture pattern was noted. Open reduction and internal fixation (ORIF) with a locking plate were performed using the dorsal approach. The imaging studies performed 3 mo and 6 years following surgery revealed a healed fracture, and the Disabilities of the Arm, Shoulder, and Hand and visual analog scale scores were significantly improved.

CONCLUSION
CT can detect capitate fractures with dorsal shearing pattern and concomitant carpometacarpal dislocation. ORIF using a locking plate are possible.

Key Words: Isolated capitate fracture; Carpometacarpal dislocation; Dorsal intercarpal ligament; Case report

Core Tip: Isolated capitate fractures with distal fragment rotated by 90° in the sagittal plane, dorsal shearing pattern and concomitant carpometacarpal dislocation have not been previously reported. Open reduction and internal fixation with a locking plate using the dorsal approach are possible. Long term radiological and clinical outcomes, including the Disabilities of the Arm, Shoulder, and Hand and visual analog scale scores were improved significantly.

Citation: Lai CC, Fang HW, Chang CH, Pao JL, Chang CC, Chen YJ. Unusual capitate fracture with dorsal shearing pattern and concomitant carpometacarpal dislocation with a 6-year follow-up: A case report. *World J Clin Cases* 2023; 11(9): 2060-2066
URL: https://www.wjgnet.com/2307-8960/full/v11/i9/2060.htm
DOI: https://dx.doi.org/10.12998/wjcc.v11.i9.2060

INTRODUCTION

Capitate fractures are rare and usually associated with other carpal bone fractures or ligament injuries. The reported incidence of these fractures is 0.42-4.9% of all adult carpal fractures[1-3]. The most frequent injury mechanism is a fall on an outstretched hand. With a greater energy injury mechanism, more neighboring structures may be injured. Greater arc perilunate fracture-dislocation is typically a high-energy injury with several bone fractures, including the scaphoid, capitate, and triquetrum. Scaphocapitate syndrome is a rare, greater arc fracture in which the proximal capitate fragment rotates 90°-180° in the sagittal plane[4,5]. The treatment of capitate fractures depends on the fracture pattern and associated injuries. Short-arm cast immobilization is indicated for isolated non-displaced capitate fractures. Displaced capitate fractures associated with injuries to neighboring structures, including carpal fractures and ligament tears, require surgical treatment[5,6]. Isolated capitate fractures have rarely been reported; when they have, fracture types have also been reported[5]. Most of these studies were small case series[3,5]. In this study, we report a case of capitate fracture with dorsal shearing fracture-dislocation of the distal pole that was treated using plate fixation. To our knowledge, this fracture pattern and surgical management have not been previously reported.

CASE PRESENTATION

Chief complaints

A 28-year-old man presented with left-hand pain that persisted for one month after he was hit by a car while riding a motorcycle.

History of present illness

Medical records were obtained and retrospectively examined after obtaining approval from the institutional review board of our hospital. Multiple injuries were found, including a brain concussion, spleen laceration, and left pelvic and femoral shaft fractures. The patient was taken to another hospital, where he received treatment. One month after discharge, he visited our clinic because of pain in his left hand.

History of past illness

There was no history of past illness.

Personal and family history

There was no personal and family history.

Physical examination

During the physical examination, left carpal volar tenderness with decreased grip strength was noted.

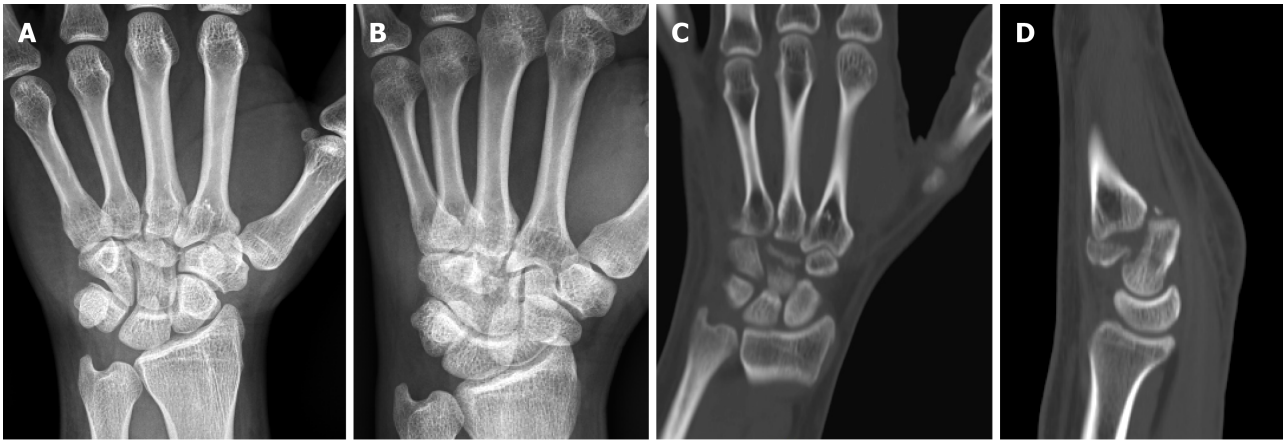

DOI: 10.12998/wjcc.v11.i9.2060

Figure 1 A fracture of the distal capitate with carpometacarpal joint dislocation is seen. A and B: Radiography; C and D: Computed tomography of the left hand.

Laboratory examinations

Blood test results were within normal limit.

Imaging examinations

Radiography of the left hand showed a distal capitate fracture with carpometacarpal joint incongruence (Figure 1A and B). Computed tomography of the left hand revealed a distal capitate fracture with carpometacarpal joint dislocation (Figure 1C and D).

FINAL DIAGNOSIS

The patient was diagnosed with capitate fracture with dorsal shearing pattern and concomitant carpometacarpal dislocation of the left hand.

TREATMENT

The patient underwent surgical treatment after serial examinations. Under general anesthesia, he was positioned supine with an arm table. Through a dorsal approach, a longitudinal skin incision was made over the 3rd carpometacarpal joint, followed by blunt dissection. The extensor tendon was identified and protected. The dorsal intercarpal ligament, distal fragment of the capitate fracture, and ruptured capsule were identified. After removing fibrotic tissue, the distal fragment of the capitate fracture was rotated by 90° in the sagittal plane, and an oblique shearing fracture pattern was observed. After reduction and repair of the capsule, we fixed the fracture using Strut Plate 1.3 (DePuy Synthes, Paoli, PA, United States), a mini-locking plate. The wound was closed in layer.

OUTCOME AND FOLLOW-UP

The patient was discharged three days after the operation. His hand was immobilized with a short-arm splint for 2 wk. Finger active range of motion rehabilitation were allowed immediately after operation. Wrist active range of motion and forearm rotation were allowed 2 wk postoperatively. Full weight-bearing was allowed 4 wk postoperatively, and he returned to his electronic technician job. The 3-month postoperative radiographs demonstrated appropriate plate and screw placement with no fracture site collapse (Figure 2A and B). His grip strength increased, and the left carpal volar tenderness resolved. The flexion/extension of the left wrist was comparable to that of the dominant right wrist (Figure 2C and D). Radiography and computed tomography performed 6 years later revealed a healed fracture with no avascular necrosis of the capitate (Figure 3). Figure 4 shows clinical photos of the left wrist six years postoperatively. The flexion/extension of the left wrist and forearm rotation are comparable to that of the dominant right wrist. Clinical outcomes were evaluated using the Disabilities of the Arm, Shoulder and Hand (DASH) and visual analog scale (VAS) scores at 3 mo and 6 years postoperatively. The DASH scores decreased from 45.0 to 18.3, while the VAS scores decreased from 3 to 0 at three

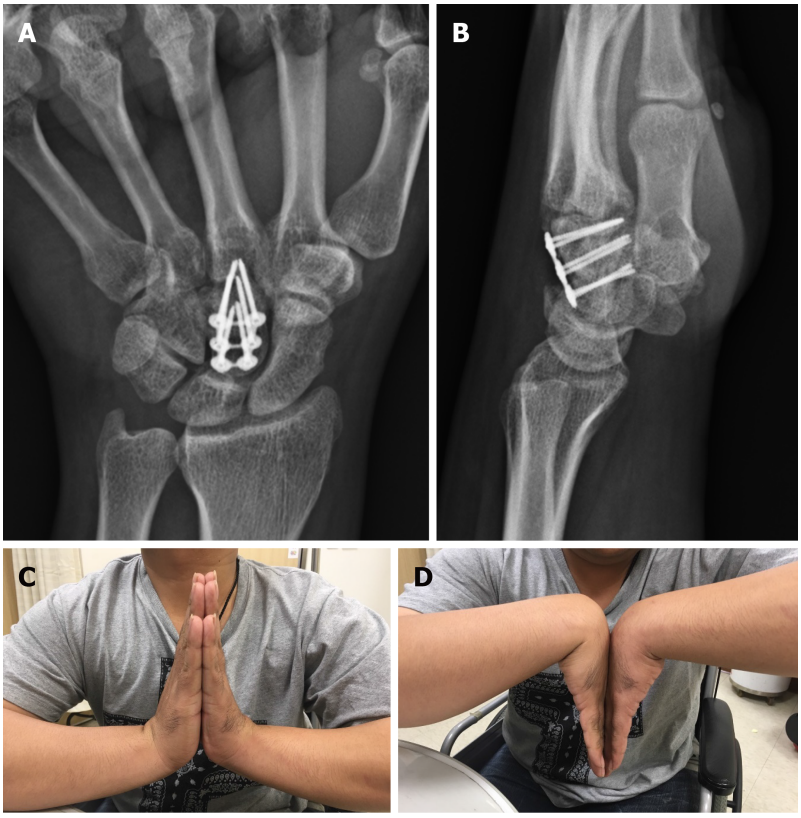

DOI: 10.12998/wjcc.v11.i9.2060

Figure 2 The flexion/extension of the left wrist is comparable to that of the dominant right wrist. A and B: Radiography; C and D: Clinical photos of the left wrist three months postoperatively. Appropriate plate and screw placement with no fracture site collapse is observed.

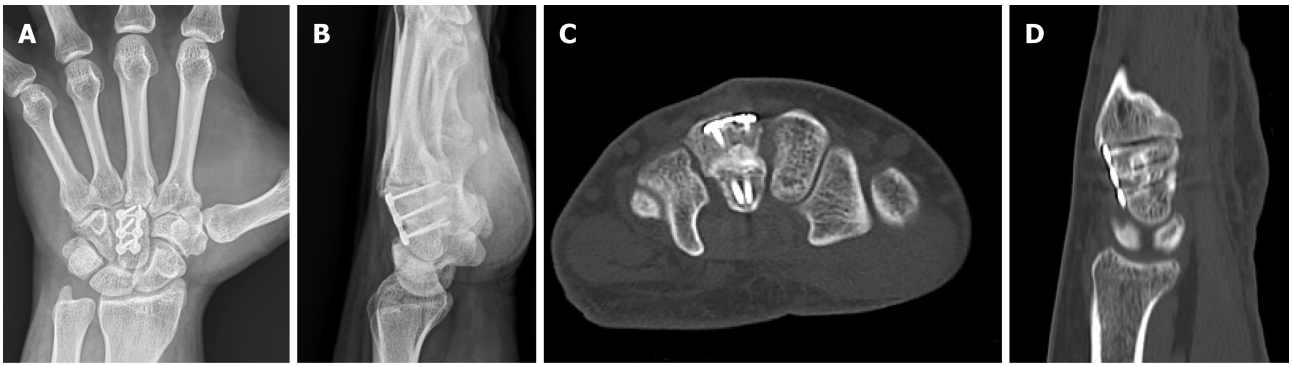

DOI: 10.12998/wjcc.v11.i9.2060

Figure 3 A healed fracture with no avascular necrosis of the capitate is seen. A and B: Radiography; C and D: Computed tomography of the left hand six years postoperatively.

months and six years postoperatively, respectively. No complications were noted in this patient.

DISCUSSION

Four common capitate fracture patterns have been described: Transverse pole, transverse body, verticofrontal, and parasagittal[6]. Moran *et al*[5] reported the largest retrospective case series, which included 53 patients classified into three groups: capitate body (including stellate comminuted, oblique high and low, and transverse high and low), avulsion tip (including dorsal and volar tip avulsions), and shear depression (including coronal shear and dorsal depression) fractures. In our study, the patient presented with a dorsal shearing fracture of the distal pole with concomitant carpometacarpal dislocation and fracture fragment rotated by 90° in the sagittal plane. To our knowledge, this is the first such reported case. The common mechanism of injury is direct axial loading on the third metacarpal

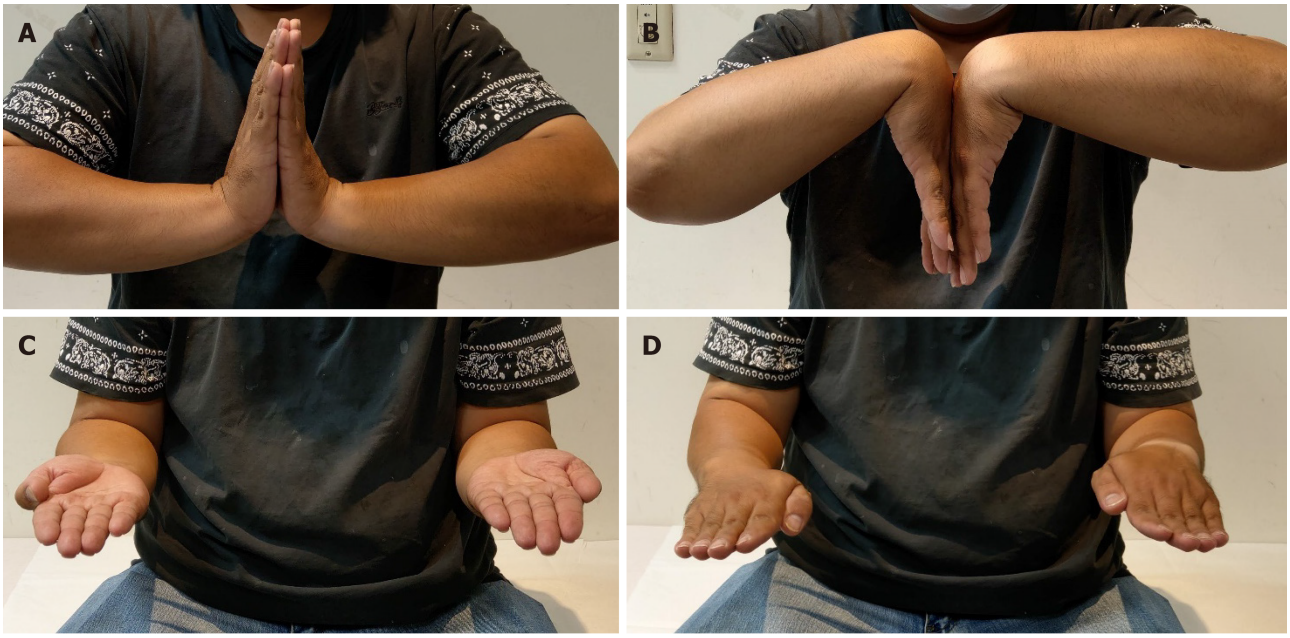

DOI: 10.12998/wjcc.v11.i9.2060

Figure 4 Clinical photos of the left wrist six years postoperatively. A and B: The flexion/extension of left wrist; C and D: Forearm rotation are comparable to that of the dominant right wrist.

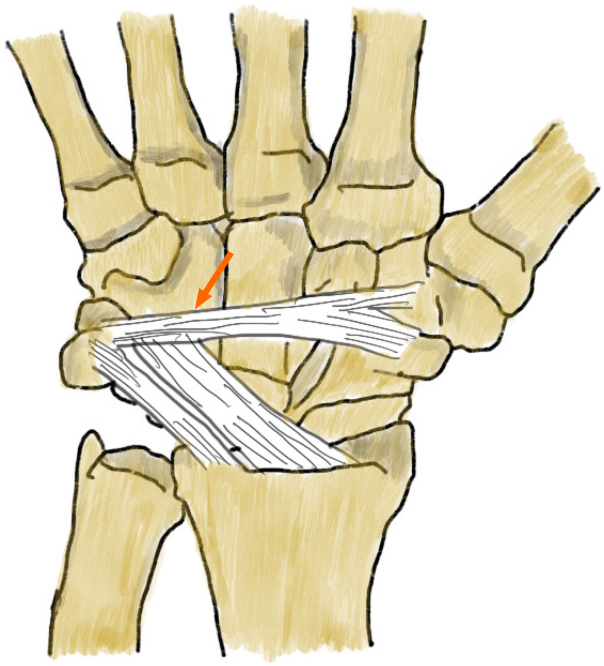

DOI: 10.12998/wjcc.v11.i9.2060

Figure 5 The proposed mechanism of injury. The fragment is rotated by 90° because the dorsal intercarpal ligament blocks the proximal part of the fragment and due to direct axial loading on the third metacarpal base with an extremely outstretched hand.

base with an outstretched hand. On the dorsal aspect, the dorsal intercarpal (DIC) and dorsal radiocarpal ligaments provide stability to the carpal bones, including the scaphoid and lunate[7]. In our study, the distal fragment of the capitate fracture was rotated by 90° in the sagittal plane with carpometacarpal dislocation. The possible mechanisms of injury leading to a 90° rotated fragment were blocking of the proximal part of the fragment by the DIC ligament and direct axial loading on the third metacarpal base with an extremely outstretched hand (Figure 5). Michael *et al*[8] reported the *in vivo* kinematics of the carpals during extreme wrist flexion and extension. In extreme extension, the capitate extends more than the scaphoid and lunate. The pressure between the dorsal aspect of the capitate and the DIC ligament also increases. As axial loading increases on the third metacarpal base, fracture-

dislocation may occur.

The management of capitate fractures should be determined by the fracture location and concomitant injuries. The treatment options include surgical and non-surgical treatments. Open reduction and internal fixation with Kirschner wires or headless cannulated compression screws in displaced fractures and fracture dislocations have been reported[2,5,9,10]. For rigid fixation, stability and early rehabilitation, we used a locking plate to fix the unique fracture pattern, and the fracture was healed at the final follow-up. The most common complication after a capitate fracture is nonunion[3,5,6], with a reported nonunion rate of 19.6%[11]. Other complications have also been reported, including nonunion followed by avascular necrosis[12] and post-traumatic degenerative arthrosis of the mid-carpal joint[5]. In our case, no complications occurred. For diagnosis, physical examinations and radiographic images of the hand were important. If follow-up CT of the hand was available, the fracture pattern of capitate could have been precisely assessed and the surgical plan could be adequately prepared. To avoid nonunion complications, open reduction with rigid internal fixation with a locking plate could be an appropriate approach.

CONCLUSION

An unusual capitate fracture with a dorsal shearing fracture and concomitant carpometacarpal dislocation can be identified using computed tomography. Open reduction and internal fixation using locking plates are possible.

ACKNOWLEDGEMENTS

The authors thank the staff involved in the study at the Far Eastern Memorial Hospital, National Taipei University of Technology and Fu Jen Catholic University Hospital.

FOOTNOTES

Author contributions: Lai CC contributed to data acquisition, measurements, and analysis and was involved in the conception and design of the study; Fang HW, Chang CH, Pao JL, Chang CC, and Chen YJ performed data acquisition, measurements, and analysis and were involved in the conception and design of the study; Chen YJ performed the surgery; all authors reviewed the draft manuscript and approved the final version.

Informed consent statement: All study participants or their legal guardian provided informed written consent about personal and medical data collection prior to study enrolment.

Conflict-of-interest statement: All the authors report no relevant conflicts of interest for this article.

CARE Checklist (2016) statement: The authors have read the CARE Checklist (2016), and the manuscript was prepared and revised according to the CARE Checklist (2016).

Country/Territory of origin: Taiwan

ORCID number: Chien-Cheng Lai 0000-0001-8638-548X; Hsu-Wei Fang 0000-0001-8931-8434; Chih-Hung Chang 0000-0002-6992-7176; Jwo-Luen Pao 0000-0002-2000-5146; Chun-Chien Chang 0000-0002-8253-2531; Yeong-Jang Chen 0000-0001-7729-9539.

S-Editor: Xing YX
L-Editor: A
P-Editor: Xing YX

REFERENCES

1 **Adler JB**, Shaftan GW. Fractures of the capitate. *J Bone Joint Surg Am* 1962; **44-A**: 1537-1547 [PMID: 14040732 DOI: 10.2106/00004623-196244080-00003]

2 **Freeland AE**, Pesut TA. Oblique capitate fracture of the wrist. *Orthopedics* 2004; **27**: 287-290 [PMID: 15058451 DOI: 10.3928/0147-7447-20040301-13]

3 **Rand JA**, Linscheid RL, Dobyns JH. Capitate fractures: a long-term follow-up. *Clin Orthop Relat Res* 1982; 209-216 [PMID: 7075062 DOI: 10.1097/00003086-198205000-00032]

4 **Monahan PR**, Galasko CS. The scapho-capitate fracture syndrome. A mechanism of injury. *J Bone Joint Surg Br* 1972; **54**: 122-124 [PMID: 5011738]

5 **Kadar A**, Morsy M, Sur YJ, Akdag O, Moran SL. Capitate Fractures: A Review of 53 Patients. *J Hand Surg Am* 2016; **41**: e359-e366 [PMID: 27524693 DOI: 10.1016/j.jhsa.2016.07.099]

6 **Suh N**, Ek ET, Wolfe SW. Carpal fractures. *J Hand Surg Am* 2014; **39**: 785-91; quiz 791 [PMID: 24679911 DOI: 10.1016/j.jhsa.2013.10.030]

7 **Mitsuyasu H**, Patterson RM, Shah MA, Buford WL, Iwamoto Y, Viegas SF. The role of the dorsal intercarpal ligament in dynamic and static scapholunate instability. *J Hand Surg Am* 2004; **29**: 279-288 [PMID: 15043902 DOI: 10.1016/j.jhsa.2003.11.004]

8 **Rainbow MJ**, Kamal RN, Leventhal E, Akelman E, Moore DC, Wolfe SW, Crisco JJ. In vivo kinematics of the scaphoid, lunate, capitate, and third metacarpal in extreme wrist flexion and extension. *J Hand Surg Am* 2013; **38**: 278-288 [PMID: 23266007 DOI: 10.1016/j.jhsa.2012.10.035]

9 **Sabat D**, Arora S, Dhal A. Isolated capitate fracture with dorsal dislocation of proximal pole: a case report. *Hand (N Y)* 2011; **6**: 333-336 [PMID: 22942861 DOI: 10.1007/s11552-011-9337-5]

10 **Yoshihara M**, Sakai A, Toba N, Okimoto N, Shimokobe T, Nakamura T. Nonunion of the isolated capitate waist fracture. *J Orthop Sci* 2002; **7**: 578-580 [PMID: 12355134 DOI: 10.1007/s007760200103]

11 **Rico AA**, Holguin PH, Martin JG. Pseudarthrosis of the capitate. *J Hand Surg Br* 1999; **24**: 382-384 [PMID: 10433464 DOI: 10.1054/jhsb.1998.0056]

12 **Vander Grend R**, Dell PC, Glowczewskie F, Leslie B, Ruby LK. Intraosseous blood supply of the capitate and its correlation with aseptic necrosis. *J Hand Surg Am* 1984; **9**: 677-683 [PMID: 6386955 DOI: 10.1016/s0363-5023(84)80012-x]

World Journal of Clinical Cases

Submit a Manuscript: https://www.f6publishing.com

World J Clin Cases 2023 March 26; 11(9): 2067-2073

DOI: 10.12998/wjcc.v11.i9.2067

ISSN 2307-8960 (online)

CASE REPORT

Live births from *in vitro* fertilization-embryo transfer following the administration of gonadotropin-releasing hormone agonist without gonadotropins: Two case reports

Mai Li, Ping Su, Li-Ming Zhou

Specialty type: Reproductive biology

Provenance and peer review: Unsolicited article; Externally peer reviewed.

Peer-review model: Single blind

Peer-review report's scientific quality classification

Grade A (Excellent): 0
Grade B (Very good): B
Grade C (Good): 0
Grade D (Fair): D, D
Grade E (Poor): 0

P-Reviewer: Mokhtar MN, Malaysia; Shah RA, India; Zhai J, China

Received: December 13, 2022
Peer-review started: December 13, 2022
First decision: January 20, 2023
Revised: March 1, 2023
Article in press: March 1, 2023
Published online: March 26, 2023

Mai Li, Li-Ming Zhou, Reproductive Center, Ningbo Women and Children's Hospital, Ningbo 315000, Zhejiang Province, China

Ping Su, Reproductive Center, Institution of Reproductive Health, Tongji Medical College, Wuhan 430030, Hubei Province, China

Corresponding author: Li-Ming Zhou, BMed, Chief Physician, Reproductive Center, Ningbo Women and Children's Hospital, No. 339 Liuting Street, Ningbo 315000, Zhejiang Province, China. zhou.li.ming@163.com

Abstract

BACKGROUND

The prevalence of female infertility between the ages of 25 and 44 is 3.5% to 16.7% in developed countries and 6.9% to 9.3% in developing countries. This means that infertility affects one in six couples and is recognized by the World Health Organization as the fifth most serious global disability. The International Committee for Monitoring Assisted Reproductive Technology reported that the global total of babies born as a result of assisted reproductive technology procedures and other advanced fertility treatments is more than 8 million. Advancements in controlled ovarian hyperstimulation procedures led to crucial accomplishments in human fertility treatments. The European Society for Human Reproduction and Embryology guideline on ovarian stimulation gave us valuable evidence-based recommendations to optimize ovarian stimulation in assisted reproductive technology. Conventional ovarian stimulation protocols for *in vitro* fertilization (IVF)–embryo transfer are based upon the administration of gonadotropins combined with gonadotropin-releasing hormone (GnRH) analogues, either GnRH agonists (GnRHa) or antagonists. The development of ovarian cysts requires the combination of GnRHa and gonadotropins for controlled ovarian hyperstimulation. However, in rare cases patients may develop an ovarian hyper response after administration of GnRHa alone.

CASE SUMMARY

Here, two case studies were conducted. In the first case, a 33-year-old female diagnosed with polycystic ovary syndrome presented for her first IVF cycle at our reproductive center. Fourteen days after triptorelin acetate was administrated (day 18 of her menstrual cycle), bilateral ovaries presented polycystic manifest-

ations. The patient was given 5000 IU of human chorionic gonadotropin. Twenty-two oocytes were obtained, and eight embryos formed. Two blastospheres were transferred in the frozen-thawed embryo transfer cycle, and the patient was impregnated. In the second case, a 37-year-old woman presented to the reproductive center for her first donor IVF cycle. Fourteen days after GnRHa administration, the transvaginal ultrasound revealed six follicles measuring 17-26 mm in the bilateral ovaries. The patient was given 10000 IU of human chorionic gonadotropin. Three oocytes were obtained, and three embryos formed. Two high-grade embryos were transferred in the frozen-thawed embryo transfer cycle, and the patient was impregnated.

CONCLUSION

These two special cases provide valuable knowledge through our experience. We hypothesize that oocyte retrieval can be an alternative to cycle cancellation in these conditions. Considering the high progesterone level in most cases of this situation, we advocate freezing embryos after oocyte retrieval rather than fresh embryo transfer.

Key Words: Gonadotropin-releasing hormone agonist; Ovarian hyperstimulation; *In vitro* fertilization; Live birth; Infertility; Frozen-thawed embryo transfer; Human chorionic gonadotropin; Case report

Core Tip: Gonadotropin-releasing hormone agonist (GnRHa) is administered in the 'long protocol' regimen for pituitary downregulation *in vitro* fertilization-embryo transfer. The development of ovarian cysts requires gonadotropin administration after pituitary downregulation in the long protocol. However, our cases presented an extremely special condition that a very small group of patients can develop called ovarian hyperstimulation receiving GnRHa alone. It is extremely rare that both patients had a successful egg retrieval during their first *in vitro* fertilization cycle and were impregnated. These cases provide some experience for clinical judgment and a new insight into the possible mechanisms of GnRHa action without gonadotropins.

Citation: Li M, Su P, Zhou LM. Live births from *in vitro* fertilization-embryo transfer following the administration of gonadotropin-releasing hormone agonist without gonadotropins: Two case reports. *World J Clin Cases* 2023; 11(9): 2067-2073

URL: https://www.wjgnet.com/2307-8960/full/v11/i9/2067.htm

DOI: https://dx.doi.org/10.12998/wjcc.v11.i9.2067

INTRODUCTION

Gonadotropin-releasing hormone agonist (GnRHa) has been widely administered since the 1980s in the "long protocol" regimen for pituitary downregulation[1-5]. It manifests pulsatile secretion in the physiological state and has a self-priming effect. If it is given persistently, the pituitary will be inhibited. Follicle-stimulating hormone (FSH), luteinizing hormone (LH), and estrogen levels decrease in a response similar to menopause, and this occurrence is called "pituitary downregulation." After 6-8 wk, the effects of inhibition recover. The use of GnRHa in the long protocol effectively inhibits the preovulatory LH surge[6], which reportedly occurs in 20%-25% of *in vitro* fertilization (IVF) cycles[7]. Thus, GnRHa can significantly reduce the preovulatory rate to 2%[8].

Generally, the development of ovarian cysts requires the administration of gonadotropins (Gn) after pituitary downregulation in the long protocol. However, several case reports have presented an extremely special condition where a patient developed ovarian hyperstimulation after receiving GnRHa alone[9-12]. Only a small number of these cases underwent oocyte aspiration from the follicles in the first cycle of IVF and had a successful pregnancy; our two cases were similar. However, our cases were extremely rare because the eggs from both patients were retrieved during their first IVF cycle. The patients both had successful pregnancies and delivered healthy babies. The results provided knowledge based upon clinical experience that will inform clinical judgment and impart new insight into the possible mechanisms of GnRHa action without Gn.

CASE PRESENTATION

Chief complaints

Case 1: A 33-year-old female in our reproductive center was first referred to IVF because of polycystic ovary syndrome (PCOS).

Case 2: A 37-year-old female presented to the reproductive center for her first donor IVF cycle.

History of present illness

Case 1: The patient had a 3-year history of secondary infertility. Her menstrual cycles were irregular, and she was diagnosed with PCOS.

Case 2: The patient had an 8-year history of primary infertility. Her husband suffered from severe hepatic disease, diabetes, and hypertension and was unable to discontinue the drugs affecting the reproductive system. The patient's menstrual cycles were irregular.

History of past illness

Case 1: The patient underwent many cycles of ovulation induction with different ovulation-stimulating drugs but without conception.

Case 2: The patient underwent three ovulation induction cycles with donor intrauterine insemination without conception.

Personal and family history

The patient's family in both cases had no related diseases.

Physical examination

Case 1: The patient's body mass index was 18.4 kg/m^2. No abnormalities were found.

Case 2: The patient's body mass index was 21.9 kg/m^2. No abnormalities were found.

Laboratory examinations

Case 1: The patient's husband's seminal sample analysis finding was within the normal limits. The patient's basic hormonal profile was as follows: FSH of 8.17 mIU/mL (normal range: 4.00-15.00 mIU/mL); LH of 5.12 mIU/mL (normal range: 4.00-30.00 mIU/mL); estradiol of 90.00 pg/mL (normal range: 15.16-127.81 pg/mL); progesterone of 0.67 ng/mL (normal range: 0-1.00 ng/mL); and testosterone of 40.88 ng/mL (normal range: 6.00-86.00 ng/mL).

Case 2: The seminal sample was from a donor. The patient's basic hormonal profile was as follows: FSH of 6.72 mIU/mL (normal range: 3.85-8.78 mIU/mL); LH of 4.04 mIU/mL (normal range: 2.12-10.89 mIU/mL); estradiol of 33.00 pg/mL (normal range: 95.00-433.00 pg/mL); and progesterone of 0.620 ng/mL (normal range: 0.057-0.893 ng/mL).

Imaging examinations

Case 1: The ultrasound showed polycystic manifestations.

Case 2: The ultrasound showed that her antral follicle count was 12.

FINAL DIAGNOSIS

Case 1: Secondary infertility and PCOS.

Case 2: Primary infertility.

TREATMENT

Case 1: On day 18 of the patient's menstrual cycle, daily treatment was started with 0.1 mg triptorelin acetate (Decapeptyl; Ferring, Kiel, Germany). Fourteen days later, the patient complained of mild abdominal distension. Her bilateral ovaries were surprisingly enlarged under ultrasonography and contained approximately 15 follicles with a diameter of 18-22 mm and endometrial thickness of 10 mm. The laboratory investigations showed estradiol levels of 5110.00 pg/mL and progesterone levels of 4.47 ng/mL. The patient received 5000 IU of human chorionic gonadotropin (HCG; Livzon, Guangzhou, China). Oocyte retrieval was performed 36 h later, and 22 oocytes were obtained. Twenty oocytes were

fertilized, and eight high-quality embryos were formed. All embryos were frozen because of the elevated progesterone. Two blastospheres were transferred in the subsequent frozen-thawed embryo transfer cycle (Tables 1 and 2).

Case 2: The patient was given 0.1 mg of triptorelin acetate (Decapeptyl; Ferring) daily from the mid-luteal phase (day 20 of her menstrual cycle) for 14 d. The progesterone level increased to 7.13 ng/mL. Fourteen days after GnRHa administration, the transvaginal ultrasound revealed six follicles measuring 17-26 mm in the bilateral ovaries. The endometrial thickness was 8 mm. Laboratory investigations revealed an estradiol level of 2664.00 pg/mL, FSH of 2.29 U/L, LH of 1.38 U/L, and progesterone of 3.36 ng/mL. The patient did not feel abnormal. She decided to continue the IVF treatment after communicating with her attending doctor. Then, she was given 10000 IU HCG (Livzon), and oocyte retrieval was performed 36 h later. A total of three oocytes were retrieved and fertilized by IVF, which underwent subsequent cleavage. The three embryos were frozen because of the high progesterone levels. Two months later, the patient underwent a frozen-thawed embryo transfer cycle with estradiol valerate tablets (Progynova; Schering, Berlin, Germany). After the endometrial thickness exceeded 8 mm and serum estradiol concentration reached 268.00 pg/mL, two high-grade embryos were transferred (Tables 3 and 4).

OUTCOME AND FOLLOW-UP

Case 1: The patient was impregnated. Her b-HCG concentration was 8897 mIU/mL 14 d after embryo transfer. Two gestational sacs and fetal pulses were detected on ultrasound 14 d later. She gave birth to two healthy babies weighing 1950 g and 3100 g at 37 wk of gestational age.

Case 2: The patient's b-HCG concentration was 473.3 mIU/mL 14 d after embryo transfer. A single gestational sac and fetal pulse were detected upon ultrasound at 7 wk. She gave birth to a full-term baby at 39 wk of gestational age.

DISCUSSION

The conventional long protocol of ovarian stimulation for IVF-embryo transfer is based upon the administration of exogenous Gn combined with GnRHa. The aim of using GnRHa is to prevent the premature rise of LH due to positive feedback by the high serum concentration of estradiol[13-15]. The use of GnRHa is associated with an increased incidence of functional ovarian cysts; this may be the effect of the "flare-up" phenomenon of GnRHa. GnRHa can stimulate the pituitary gland and cause a temporary increase in FSH, LH, and other sex hormones secreted by the ovaries[9]. This may cause the formation of sporadic cysts (generally one or two). The cysts can be aspirated or ignored if the serum hormones are normal.

However, a few reports have observed that ovarian hyperstimulation occurred following the use of GnRHa alone in the long protocol[9-12]. These reports documented evidence of hyperstimulation and extremely high estradiol levels after the administration of GnRHa. Park *et al*[16] reported a case of depot preparation (3.75 mg) of tryptorelin without Gns induced ovarian multifollicular enlargement with a high estradiol level and was followed by HCG administration and oocyte retrieval. Then, three embryos were transferred to the recipient, but none resulted in pregnancy. For instance, Parinaud *et al*[17] demonstrated that GnRHa-related cysts could be used to retrieve oocytes after HCG administration. Subsequently, oocyte retrieval has been reported instead of cycle cancellation, and several cases of high-quality embryo transfers and pregnancies were confirmed[11,18].

Ovarian hyperstimulation following the use of GnRHa without Gn is extremely rare. The pathogenesis of this phenomenon remains controversial. Some reports have suggested that the incidence is higher in older patients in which GnRHa was started in the follicular phase instead of the mid-luteal phase[19]. Nevertheless, this phenomenon can also happen in younger patients[20].

Some researchers proposed that GnRHa may result in a transient "flare-up effect" on the pituitary, and this surge triggers the development of primordial follicles. GnRHa are typically administered during the mid-luteal phase in the conventional long protocol, which occurs approximately 1 wk after ovulation. At this phase, the endogenous Gn levels are lowest, and the "flare-up" is least likely to stimulate a new wave of follicular development. We hypothesized that some patient subgroups begin follicular recruitment earlier than normal. Instead of inhibiting follicular development, they stimulate waves of follicular development, which leads to a hyperstimulation state.

Furthermore, it appears that some follicles may become highly sensitive to short-term stimulation of Gn caused by GnRHa. However, this hypothesis cannot explain why these "cysts" continue growing without exogenous Gn stimulation for a prolonged period. An increase in serum FSH and LH concentrations within the first 48 h of GnRHa administration was demonstrated. A transient increase in estradiol levels is also observed. However, continuous administration of GnRHa for 4 d results in

Table 1 Protocol timeline for Case 1

Date	Protocol
June 9, 2015	Triptorelin acetate 0.1 mg/d for 14 d
June 23, 2015	HCG 5000 IU im
June 25, 2015	Oocyte retrieval
June 28, 2015	D3 embryos frozen
June 30, 2015	D5 embryos frozen
August 31, 2015	Two blastospheres were transferred

HCG: Human chorionic gonadotropin.

Table 2 Hormone concentrations before and after treatment for Case 1

	Hormone concentrations before treatment	Hormone concentrations after treatment
FSH in mIU/mL	8.17	8.68
LH in mIU/mL	5.15	5.17
E2 in pg/mL	90.00	5110.00
Progesterone in ng/mL	0.67	4.47

E2: Estradiol; FSH: Follicle-stimulating hormone; LH: Luteinizing hormone.

Table 3 Protocol timeline for Case 2

Date	Protocol
March 28, 2015	Triptorelin acetate 0.1 mg/d for 14 d
March 12, 2015	HCG 10000 IU im
March 14, 2015	Oocyte retrieval
March 17, 2015	D3 embryos frozen
June 14, 2015	Two D3 embryos were transferred

HCG: Human chorionic gonadotropin.

Table 4 Hormone concentrations before and after treatment for Case 2

	Hormone concentrations before treatment	Hormone concentrations after treatment
FSH in mIU/mL	6.72	2.29
LH in mIU/mL	4.04	1.38
E2 in pg/mL	33.00	2664.00
Progesterone in ng/mL	0.62	3.36

E2: Estradiol; FSH: Follicle-stimulating hormone; LH: Luteinizing hormone.

decreased serum estradiol levels. Nevertheless, estradiol production by these "cysts" continues, and their growth persists. It may be possible that these cysts exert the "flare-up effect" at a later time and can stimulate ovarian hyperstimulation from the initial Gn concentration. It may also result from the increased sensitivity of ovarian follicles to circulating Gn.

Another possibility is that pituitary desensitization takes longer than 14 d in some women following the long protocol. Therefore, the circulating sex hormone concentrations may not have decreased to

"hypophysectomized" levels. We have observed the presence of "functional cysts" and continuously increased levels of FSH, LH, or estradiol in some patients during GnRHa administration. It is likely that the circulating Gn levels do not decrease. Instead, circulating Gn levels increase and generate self-feedback, which results in ovarian hyperstimulation.

It has also been hypothesized that GnRHa may directly affect the ovaries and steroidogenesis. This theory is based on the observations of GnRHa receptors on the ovary and GnRHa-induced steroidogenesis in cultured human granulosa cells[17]. However, there is no definitive evidence of direct action of GnRHa on the ovary.

The procedure presented in our report suggests that ovarian hyperstimulation following the administration of GnRHa without Gn may tend to occur in patients with PCOS. A previous study analyzed the nucleotide mutations of the *LH* and *LHR* genes in PCOS patients and found that *LHβ* TC and CC genotypes were closely related to the risk of PCOS, indicating that variants of these genes may affect the metabolic pathways of PCOS[21]. These variant genotypes likely cause abnormal responses to GnRHa. Both patients began downregulation in the mid-luteal phase without receiving an oral contraceptive pill pretreatment. GnRHa administration during the luteal phase may have the advantage of yielding more follicles because LH-stimulated androgen production and circulating androgen levels are more effectively suppressed throughout folliculogenesis[22].

Most previous reports are of cases that resulted in no pregnancies. Researchers have hypothesized that the aberrant rise in serum estradiol after GnRHa administration may cause imperfect pituitary suppression, with subsequent effects on oocyte and embryo quality[23]. However, there are reports of live births following administration of GnRHa without Gn, like in our cases. Therefore, it is possible that these patients can achieve a positive outcome after optimal management. Instead of cycle cancellation, oocyte retrieval can be an acceptable choice for these patients. Our two cases successfully underwent oocyte retrieval, and high-quality embryos were obtained after administration of HCG at the proper time. It was appropriate to undertake embryo cryopreservation, considering the presence of high progesterone and impaired endometrial receptivity.

CONCLUSION

Ovarian hyperstimulation following the administration of GnRHa without Gn can occur, though the mechanism is still unclear. This report may provide new insights into the possible mechanisms of GnRHa and indicated that oocyte retrieval can be an alternative to cycle cancellation in the appropriate conditions. The optimal and standard management of this condition is still unclear because of the paucity of data. Considering the high progesterone level in most cases of this situation, we advocate freezing embryos after oocyte retrieval rather than fresh embryo transfer.

FOOTNOTES

Author contributions: Li M contributed significantly to case collections and analysis and wrote the manuscript; Zhou LM contributed to the conception of the study; Su P contributed to manuscript preparation.

Informed consent statement: Informed written consent was obtained from the patients.

Conflict-of-interest statement: The authors declare having no conflicts of interest.

CARE Checklist (2016) statement: The authors have read the CARE Checklist (2016), and the manuscript was prepared and revised according to the CARE Checklist (2016).

Country/Territory of origin: China

ORCID number: Mai Li 0000-0003-1861-4628; Li-Ming Zhou 0000-0002-6990-3510.

S-Editor: Liu JH
L-Editor: Filipodia
P-Editor: Liu JH

REFERENCES

1 **Farquhar CM**, Bhattacharya S, Repping S, Mastenbroek S, Kamath MS, Marjoribanks J, Boivin J. Female subfertility. *Nat Rev Dis Primers* 2019; **5**: 7 [PMID: 30679436 DOI: 10.1038/s41572-018-0058-8]

2 **Mascarenhas MN**, Flaxman SR, Boerma T, Vanderpoel S, Stevens GA. National, regional, and global trends in infertility prevalence since 1990: a systematic analysis of 277 health surveys. *PLoS Med* 2012; **9**: e1001356 [PMID: 23271957 DOI: 10.1371/journal.pmed.1001356]

3 European Society of Human Reproduction and Embryology. [DOI: 10.1093/oxfordjournals.humrep.a136692]

4 **Niederberger C**, Pellicer A, Cohen J, Gardner DK, Palermo GD, O'Neill CL, Chow S, Rosenwaks Z, Cobo A, Swain JE, Schoolcraft WB, Frydman R, Bishop LA, Aharon D, Gordon C, New E, Decherney A, Tan SL, Paulson RJ, Goldfarb JM, Brännström M, Donnez J, Silber S, Dolmans MM, Simpson JL, Handyside AH, Munné S, Eguizabal C, Montserrat N, Izpisua Belmonte JC, Trounson A, Simon C, Tulandi T, Giudice LC, Norman RJ, Hsueh AJ, Sun Y, Laufer N, Kochman R, Eldar-Geva T, Lunenfeld B, Ezcurra D, D'Hooghe T, Fauser BCJM, Tarlatzis BC, Meldrum DR, Casper RF, Fatemi HM, Devroey P, Galliano D, Wikland M, Sigman M, Schoor RA, Goldstein M, Lipshultz LI, Schlegel PN, Hussein A, Oates RD, Brannigan RE, Ross HE, Pennings G, Klock SC, Brown S, Van Steirteghem A, Rebar RW, LaBarbera AR. Forty years of IVF. *Fertil Steril* 2018; **110**: 185-324.e5 [PMID: 30053940 DOI: 10.1016/j.fertnstert.2018.06.005]

5 **Ovarian Stimulation TEGGO**, Bosch E, Broer S, Griesinger G, Grynberg M, Humaidan P, Kolibianakis E, Kunicki M, La Marca A, Lainas G, Le Clef N, Massin N, Mastenbroek S, Polyzos N, Sunkara SK, Timeva T, Töyli M, Urbancsek J, Vermeulen N, Broekmans F. ESHRE guideline: ovarian stimulation for IVF/ICSI(†). *Hum Reprod Open* 2020; **2020**: hoaa009 [PMID: 32395637 DOI: 10.1093/hropen/hoaa009]

6 **Balasch J**, Vidal E, Peñarrubia J, Casamitjana R, Carmona F, Creus M, Fábregues F, Vanrell JA. Suppression of LH during ovarian stimulation: analysing threshold values and effects on ovarian response and the outcome of assisted reproduction in down-regulated women stimulated with recombinant FSH. *Hum Reprod* 2001; **16**: 1636-1643 [PMID: 11473955 DOI: 10.1093/humrep/16.8.1636]

7 **Weissman A**, Barash A, Shapiro H, Casper RF. Ovarian hyperstimulation following the sole administration of agonistic analogues of gonadotropin releasing hormone. *Hum Reprod* 1998; **13**: 3421-3424 [PMID: 9886527 DOI: 10.1093/humrep/13.12.3421]

8 **Allahbadia**, GNMR. Ovarian Stimulation Protocols. Springer: New Delhi 2016; 121–134 [DOI: 10.1007/978-81-322-1121-1_10]

9 **Yeh J**, Barbieri RL, Ravnikar VA. Ovarian hyperstimulation associated with the sole use of leuprolide for ovarian suppression. *J In Vitro Fert Embryo Transf* 1989; **6**: 261-263 [PMID: 2515236 DOI: 10.1007/BF01132875]

10 **Brett S**, Yong PY, Thong KJ. Ovarian hyperstimulation after the sole use of a gonadotropin-releasing hormone agonist (Nafarelin) as a complication of in vitro fertilisation treatment. *J Assist Reprod Genet* 2001; **18**: 353-356 [PMID: 11495415 DOI: 10.1023/a:1016680504614]

11 **Azem F**, Almog B, Ben-Yosef D, Kapustiansky R, Wagman I, Amit A. First live birth following IVF-embryo transfer and use of GnRHa alone for ovarian stimulation. *Reprod Biomed Online* 2009; **19**: 162-164 [PMID: 19712549 DOI: 10.1016/s1472-6483(10)60067-3]

12 **Chen C**, Geng L, Hou Z, Liu D, Meng F, Ma W, Xia X. Ovarian Hyperresponse Following the Sole Administration of GnRH Agonist. *Comb Chem High Throughput Screen* 2022; **25**: 1082-1085 [PMID: 33653244 DOI: 10.2174/1386207324666210302095049]

13 **Kadoura S**, Alhalabi M, Nattouf AH. Conventional GnRH antagonist protocols versus long GnRH agonist protocol in IVF/ICSI cycles of polycystic ovary syndrome women: a systematic review and meta-analysis. *Sci Rep* 2022; **12**: 4456 [PMID: 35292717 DOI: 10.1038/s41598-022-08400-z]

14 **Manna C**, Rahman A, Sbracia M, Pappalardo S, Mohamed EI, Linder R, Nardo LG. Serum luteinizing hormone, follicle-stimulating hormone and oestradiol pattern in women undergoing pituitary suppression with different gonadotropin-releasing hormone analogue protocols for assisted reproduction. *Gynecol Endocrinol* 2005; **20**: 188-194 [PMID: 16019360 DOI: 10.1080/09513590400027141]

15 **Umemmuo MU**, Efetie ER, Agboghoroma CO, Momoh JA, Ikechebelu JI. Comparison of clinical efficacy of long- versus short-acting gonadotropin-releasing hormone agonists for pituitary down regulation in In vitro fertilisation cycles. *Niger Postgrad Med J* 2020; **27**: 171-176 [PMID: 32687115 DOI: 10.4103/npmj.npmj_65_20]

16 **Park HT**, Bae HS, Kim T, Kim SH. Ovarian hyper-response to administration of an GnRH-agonist without gonadotropins. *J Korean Med Sci* 2011; **26**: 1394-1396 [PMID: 22022197 DOI: 10.3346/jkms.2011.26.10.1394]

17 **Parinaud J**, Cohen K, Oustry P, Perineau M, Monroziès X, Rème JM. Influence of ovarian cysts on the results of in vitro fertilization. *Fertil Steril* 1992; **58**: 1174-1177 [PMID: 1459269 DOI: 10.1016/s0015-0282(16)55565-4]

18 **Almagor M**, Hovav Y. The development of an oocyte-containing follicle during gonadotropin-releasing hormone agonist administration. *Hum Reprod* 2001; **16**: 1698-1699 [PMID: 11473966 DOI: 10.1093/humrep/16.8.1698]

19 **Keltz MD**, Jones EE, Duleba AJ, Polcz T, Kennedy K, Olive DL. Baseline cyst formation after luteal phase gonadotropin-releasing hormone agonist administration is linked to poor in vitro fertilization outcome. *Fertil Steril* 1995; **64**: 568-572 [PMID: 7641912 DOI: 10.1016/s0015-0282(16)57794-2]

20 **Naifer R**, Ajina M, Merdassi G, Bibi M, Ibala S, Saad A. Ovarian hyperstimulation induced by a GnRH agonist. About one case. *Gynecol Obstet Fertil* 2005; **33**: 994-997 [PMID: 16330236 DOI: 10.1016/j.gyobfe.2005.06.023]

21 **Deswal R**, Nanda S, Dang AS. Association of Luteinizing hormone and LH receptor gene polymorphism with susceptibility of Polycystic ovary syndrome. *Syst Biol Reprod Med* 2019; **65**: 400-408 [PMID: 30958034 DOI: 10.1080/19396368.2019.1595217]

22 **Speroff L**, Fritz MA. Clinical gynecologic endocrinology and infertility. 7th ed. Philadelphia, PA: Lippincott Williams & Wilkins. 2005; 1175–1274 [DOI: 10.1016/s0015-0282(00)00647-6]

23 **Penzias AS**, Lee G, Seifer DB, Shamma FN, DeCherney AH, Reindollar RH, Jones EE. Aberrant estradiol flare despite gonadotropin-releasing hormone-agonist-induced suppression is associated with impaired implantation. *Fertil Steril* 1994; **61**: 558-560 [PMID: 8137986 DOI: 10.1016/s0015-0282(16)56595-9]

World Journal of Clinical Cases

Submit a Manuscript: https://www.f6publishing.com

World J Clin Cases 2023 March 26; 11(9): 2074-2083

DOI: 10.12998/wjcc.v11.i9.2074

ISSN 2307-8960 (online)

CASE REPORT

Spontaneous conus infarction with "snake-eye appearance" on magnetic resonance imaging: A case report and literature review

Qiao-Yu Zhang, Lin-Ying Xu, Ming-Li Wang, Hua Cao, Xiao-Fei Ji

Specialty type: Neurosciences

Provenance and peer review: Unsolicited article; Externally peer reviewed.

Peer-review model: Single blind

Peer-review report's scientific quality classification

Grade A (Excellent): 0
Grade B (Very good): B
Grade C (Good): C
Grade D (Fair): D
Grade E (Poor): 0

P-Reviewer: Arboix A, Spain, Spain; Ji X, China

Received: December 16, 2022
Peer-review started: December 16, 2022
First decision: January 12, 2023
Revised: January 27, 2023
Accepted: March 3, 2023
Article in press: March 3, 2023
Published online: March 26, 2023

Qiao-Yu Zhang, Lin-Ying Xu, Ming-Li Wang, Hua Cao, Xiao-Fei Ji, Department of Neurology, The First Affiliated Hospital of Dalian Medical University, Dalian 116011, Liaoning Province, China

Qiao-Yu Zhang, Department of Neurology, Nanchuan People's Hospital Affiliated to Chongqing Medical University, Chongqing 408400, China

Corresponding author: Xiao-Fei Ji, MD, PhD, Chief Physician, Department of Neurology, The First Affiliated Hospital of Dalian Medical University, No. 222 Zhongshan Road, Dalian 116011, Liaoning Province, China. jixiaofei1979@163.com

Abstract

BACKGROUND

Infarction of the conus medullaris is a rare form of spinal cord infarction. The first symptom is usually acute non-characteristic lumbar pain, followed by lower limb pain, saddle numbness, fecal incontinence, and sexual dysfunction. Spontaneous conus infarction with "snake-eye appearance" on magnetic resonance imaging has rarely been reported.

CASE SUMMARY

We report a 79-year-old male patient with spontaneous conus infarction who had acute lower extremity pain and dysuria as the first symptoms. He did not have any recent history of aortic surgery and trauma. Magnetic resonance imaging revealed a rare "snake-eye appearance." In addition, we reviewed the literature on 23 similar cases and summarized the clinical features and magnetic resonance manifestations of common diseases related to the "snake-eye sign" to explore the etiology, imaging findings, and prognosis of spontaneous conus infarction.

CONCLUSION

We conclude that acute onset of conus medullaris syndrome combined with "snake-eye appearance" should be strongly suspected as conus medullaris infarction caused by anterior spinal artery ischemia. This special imaging manifestation is helpful in the early diagnosis and treatment of conus infarction.

Key Words: Spinal cord disease; Infarction; Paralysis; Dysuria; Magnetic resonance imaging; Case report

Core Tip: Infarction of the conus medullaris is a rare form of spinal cord infarction, and there is no specific examination method in clinic. On the other hand, the "Snake-Eye Appearance" on the diffusion-weighted imaging sequence of magnetic resonance imaging highly suggests spinal cord infarction, although few cases of conus infarction have been reported. This special imaging manifestation is helpful in the early diagnosis and treatment of conus infarction.

Citation: Zhang QY, Xu LY, Wang ML, Cao H, Ji XF. Spontaneous conus infarction with "snake-eye appearance" on magnetic resonance imaging: A case report and literature review. *World J Clin Cases* 2023; 11(9): 2074-2083
URL: https://www.wjgnet.com/2307-8960/full/v11/i9/2074.htm
DOI: https://dx.doi.org/10.12998/wjcc.v11.i9.2074

INTRODUCTION

Spinal cord infarctions account for approximately 1.2% of all ischemic strokes[1], and less than 10% of acute non-traumatic myelopathies[2]. The most common infarct sites are the cervical and thoracic segments[3]. The common clinical manifestations of spinal cord infarction are motor and sensory disorders with impaired autonomic nerve function, and the specific manifestations are related to the affected sites[4]. Combined with the observation of the clinical manifestations, magnetic resonance imaging (MRI) and cerebrospinal fluid examination are helpful in distinguishing this condition from optic neuromyelitis pedigree diseases, acute disseminated encephalomyelitis, spinal cord tumors, multiple sclerosis, intervertebral disc herniation, and other spinal cord diseases. However, the lack of specific MRI features in conus medullaris infarction increases the difficulty of early diagnosis and recognition. In this paper, we report a case of spontaneous conus medullaris infarction. Simultaneously providing an analysis of the literature, we focus on the special imaging manifestations and etiological mechanisms of this condition to improve clinicians' understanding of this disease.

CASE PRESENTATION

Chief complaints

A 71-year-old Chinese man with a complaint of sudden onset of pain in both lower extremities and urination disorders for 2 d.

History of present illness

The patient experienced continuous pain on the back of both lower limbs when standing up from the sofa before 2 d, accompanied by muscle spasm, increased pain while sitting, urinary incontinence, and difficulty defecating, but no erectile dysfunction.

History of past illness

The patient had a history of hypertension for 5 years and diabetes for 2 years. In the last year, the patient regular oral administration of Amlodipine besylate tablets was 5 mg qd, and the blood pressure was stable at 17-20/9-11 kPa; Metformin 0.5 g tid and the glycosylated hemoglobin was 6.8%.

Personal and family history

The patient has been smoking for 43 years, about 10 cigarettes a day. The patient denies any family history of disease.

Physical examination

After 48 h of onset, neurological examination showed normal muscle strength and muscle tension in both lower limbs. The bilateral knee reflex was symmetrical, with no hyperactivity and weakness, the bilateral Achilles tendon reflex disappeared, the saddle area sense was normal, anal reflex was weakened, the urinary retention was moderate, and lack of the bilateral Babinski sign.

Laboratory examinations

No obvious abnormalities were found in the test results of perfect nail work, serum immunology, tumor markers, or coagulation images.

Imaging examinations

On the 4th day of onset, lumbar MRI revealed a high signal on the L1 horizontal axial T2-weighted image

with a "snake-eye appearance", and conus infarction was thus considered. On the 5th day of onset, lumbar MRI showed a high signal on L1 horizontal sagittal diffusion-weighted imaging (DWI) (Figure 1).

FURTHER DIAGNOSTIC WORK-UP

Spinal angiography and aortic angiography (CTA) improved, but no definite vascular stenosis or malformation was identified. On the 7th day of onset, the measurement of nerve conduction velocity revealed that the F-wave latency of the left tibial nerve was prolonged.

LITERATURE REVIEW

We used the key terms "conus medullaris infarction," "conus medullaris syndrome," "spinal cord ischemia," "spinal cord infarction," "snake-eye appearance" and "owl-eye appearance" to search the literature on PubMed. We thus identified and summarized 23 cases of conus medullaris infarction from January 1971 to January 2021 (Table 1)[5-21]. The male to female ratio was 1.3:1. The median age at onset was 63 years. Eleven cases (47.8%) were complicated by cardiovascular risk factors, 7 (30.4%) were related to aortic disease, and 3 (13.0%) were secondary to postural changes, similar to the present case. Other causes included dural arteriovenous fistulas, spinal cord venous thrombosis, fibrocartilage embolism, and so on; 9 cases (39.1%) showed a high signal on axial T2-weighted imaging, of which 2 cases showed the typical "snake-eye appearance" high signal on sagittal T2-weighted imaging in the T10 to L1 vertebral segments, 3 cases (13.0%) showed limited DWI, 5 cases (21.7%) involved the vertebral body/muscle/ligament at the same time, and 16 cases (69.6%) showed a partial recovery of neurological deficit, with sequelae of varying degrees, while 5 cases (21.7%) had no improvement, and the overall prognosis was poor.

FINAL DIAGNOSIS

Combined with the patient's medical history, spontaneous spinal cord infarction was confirmed.

TREATMENT

The patient was admitted to the hospital and administered clopidogrel to facilitate antiplatelet aggregation and atorvastatin calcium tablets to reduce blood lipid levels.

OUTCOME AND FOLLOW-UP

After 10 d of treatment, the pain in both lower extremities was relieved, and the symptoms of urinary retention were relieved. After discharge, the patient continued to take clopidogrel and atorvastatin calcium tablets orally. After 3 mo of telephone follow-up, the patient complained of left lower limb pain and prolonged urination time.

DISCUSSION

Conus medullaris infarction is rare, and its incidence is unclear. A study on the clinical and magnetic resonance imaging manifestations and short-term prognosis of patients with spinal cord infarction showed that only 12.5% had isolated conus medullaris infarction[22]. The blood supply to the conus medullaris is very rich and mainly supplied by the anterior spinal artery, posterior spinal artery, and nerve root medullary artery. The anterior spinal artery supplies the first two-thirds of the conus medullaris, and the posterior spinal artery supplies the last one-third. These form a coronary artery ring at the level of the conus medullaris, which then branches from the artery ring into the conus medullaris. In addition, the thick nerve root medullary artery (Adamkiewicz artery) from the intercostal or lumbar artery from T9 to T12 and the desproges gotteron artery originating from the iliolumbar artery are also involved in the blood supply to the spinal conus[6,23-25]. At present, the diagnosis of conus medullaris infarction is mainly based on clinical manifestations and MRI findings. Lumbar puncture cerebrospinal fluid examination is helpful in distinguishing between inflammatory and demyelinating diseases. In

Table 1 Overview of reported cases of conus infarction

Ref.	Age/gender	Risk factors	Pathogeny/mechanism	Prognosis	MRI findings			
					T2WI l high signal (Axial)	T2WI high signal (Sagittal)	DWI high signal	Involve centrum/muscle/ligament
Herrick *et al* [5]	84/M	NA	Aortic dissection aneurysm	Partial improvement, died of rupture of aortic dissection aneurysm on the 18th day of admission	NA	NA	NA	NA
	79/M	Heart failure	Aortic atherosclerosis	No improvement, died of acute myocardial infarction on the 25th day of admission	NA	NA	NA	NA
Anderson *et al* [6]	54/M	Coronary diseaseHeart failure	Aortic balloon pump implantation	Some improved strength in the legs before death 7 wk after the ictus	NA	NA	NA	NA
	75/M	Smoking	Repair operation of abdominal aortic aneurysm	Persistent urinary incontinence with some improvement in bowel function and in motor and sensory signs 16 mo after the ictus	NA	NA	NA	NA
	66/M	Smoking	Aortic atherosclerosis	Some functions recovered 2 mo after the ictus	NA	NA	NA	NA
	51/M	Smoking	NA	Persistent urinary incontinence with some functions recovered 28 mo after the ictus	NA	NA	NA	NA
	47/F	NA	NA	No improvement in 2 yr	NA	NA	NA	NA
Ohbu *et al*[7]	69/F	Hypertension	NA	NA	NA	NA	NA	NA
Andrews *et al* [8]	71/F	NA	NA	Walking independently, mild hypoesthesia, but persistent urinary incontinence 2 mo after the ictus	NA	NA	NA	NA
Mhiri *et al*[9]	28/M	NA	Dural arteriovenous fistula	No improvement	NA	NA	NA	NA
Sinha *et al*[10]	63/M	HypertensionCoronary disease	Coronary artery bypass grafting (CABG)	persistent urinary incontinence 5 yr after the ictus	NA	NA	NA	NA
Greiner-Perth *et al*[11]	66/M	NA	NA	No improvement in 8 mo	NA	T12-L1	NA	NA
Combarros *et al*[12]	69/F	Hypertension	NA	The bladder function returned to normal and can walk with a walker 2 mo after the ictus	NA	NA	NA	NA
Wildgruber *et al*[13]	44/F	NA	Spinal venous thrombosis	Motor function recovered partially and leaving hypoesthesia 6 mo after the ictus	Bilateral anterior horn of gray matter (Snake-eye appearance)	T12-L1	NA	NA
Wong *et al*[14]	79/F	Coronary disease	Aortic atherosclerosis	Partial neurologic recovery	Bilateral gray matter and central white matter	T12-L1	Yes	NA

Konno *et al* [15]	77/F	Hypertension	Spinal venous thrombosis	Symptoms improved rapidly	Diffuse	L1	NA	Yes
Diehn *et al*[16]	24/M	NA	Fibrocartilage embolism	No improvement	Bilateral anterior horn of gray matter	T10-L1	NA	Yes
Alanazy[17]	48/M	NA	Overstretch	Walking resumed on day 105	Diffuse	T11-L1	NA	NA
Hor *et al*[18]	51/F	NA	NA	NA	Bilateral gray matter and central white matter	T12	NA	NA
Kamimura *et al*[19]	70/F	NA	Spinal venous thrombosis	Sensory disturbance improved, leaving numbness in the sellar area and urinary incontinence	Bilateral posterior funiculus, right posterior horn, right lateral funiculus	T12	NA	Yes
Weng *et al*[20]	55/M	Hyperlipidemia	Sofa sedentary	Calf muscle atrophy, perianal hypoesthesia and neurogenic bladder 3 yr after ictus	Bilateral anterior horn of gray matter	T11-12	Yes	Yes
	34/F	NA	Toilet sedentary	Calf muscle atrophy, perianal hypoesthesia and neurogenic bladder 4 yr after ictus	NA	T12	Yes	NA
Breitling *et al* [21]	52/M	NA	NA	Motor function recovered partially, leaving bladder and rectum dysfunction	Bilateral anterior horn of gray matter (Snake-eye appearance)	L1	NA	Yes

DWI: Diffusion-weighted imaging; NA: Not available.

January 2019, Zalewski *et al*[26] proposed the diagnostic criteria for spontaneous spinal cord infarction, emphasizing that the high signal on a MRI intramedullary T2-weighted image is evidence of acute spinal cord infarction, while the DWI/apparent diffusion coefficient diffusion is limited, accompanied by corresponding pyramidal infarction, arterial dissection, or occlusion near the lesion. However, it is important to note that T2-weighted magnetic resonance imaging has a low sensitivity.

In a clinical study[27], only 45% of patients with acute spinal cord infarction showed a high signal on T2-weighted magnetic resonance imaging. The volume of the conus medullaris is smaller, the magnetic sensitivity artifact tendency of DWI is higher, and the detection sensitivity is much lower than those of acute cerebral infarction. Therefore, early neurological function evaluation is very important in identifying patients with negative MRI findings. The MRI results of this patient were consistent with the above standards. It is worth noting that the patient had an isolated "snake-eye appearance" high signal on axial T2-weighted MRI at the level of the spinal cord cone. This "snake-eye appearance" was first described in the results of delayed myelography in 7 patients with compressive cervical spondylotic myelopathy in 1986[28], and is also known as "owl-eye appearance". The main pathological changes which can result in this appearance are cystic necrosis of the central gray matter of the ventrolateral column of the spinal cord and loss of neurons in the anterior horn of the spinal cord[29]. It is usually related to lower motor neuron syndrome, such as Hirayama disease[30,31], spinal muscular atrophy syndrome[32], cervical spondylotic myelopathy[33], amyotrophic lateral sclerosis[34], and anterior spinal artery ischemia[35-37], Detailed identification is shown in Table 2[34,38-41]. There is a watershed area between the sulcus commissural artery and the coronary artery ring sent by the anterior spinal

Table 2 Identification of common diseases related to snake eye sign

Disease	Clinical features	Magnetic resonance performance	Neuroelectrophysiological manifestations
Conus medullaris infarction [38]	The main manifestations are sensory disturbance in the sellar region, bladder and rectal incontinence, bulbar anal reflex weakening or disappearing, erectile dysfunction, root neuralgia and lower limb motor neuron paralysis when combined with cauda equina damage	T12-L1 horizontal magnetic resonance T2WI and DWI high signal, T1W1 low signal	There are few reports about the neurophysiological characteristics of conus medullaris infarction. The reappearance of F wave after infarction may mark the improvement of clinical prognosis
Hirayama disease[39]	The self-limited disease, which is mainly characterized by unilateral muscle atrophy of the distal end of the upper limb, mainly affects the intrinsic muscles of the hand and forearm muscle groups. Typical clinical manifestations also include "cold paralysis", "finger extension tremor" and "muscle bundle tremor"	Asymmetric cervical spinal cord flattening, atrophy and intramedullary T2W1 high signal in cervical flexion position, disappearance of cervical physiological flexion, expansion and increase of epidural venous plexus, and anterior displacement of dural sac after over-extension and over-flexion position	The neurogenic damage of the affected muscle group mainly occurred in the C7-8 sarcomere and T1 sarcomere, while the C5-6 sarcomere (i.e. deltoid, biceps brachii and radial brachii) was not affected
Amyotrophiclateralsclerosis [34]	Malignant degenerative motor neuron disease characterized by multiple or localized progressive muscular atrophy and apraxia is characterized by limb spasms, tendon hyperreflexia, localized or multiple muscle weakness, muscular atrophy and fascicular tremor	T2WI, FLAIR and DWI can find symmetrical high signal in the pyramidal tract of the brain. In a few patients, SWI can see the deposition of hemosiderin along the motor cortex	The muscles innervated by different nerve segments of medulla oblongata, neck, chest and lumbosacral appear progressive denervation and chronic nerve regeneration
Cervical spondylotic myelopathy[40]	Based on cervical degeneration, the main manifestation is atrophy of the proximal or distal muscles of the upper limb, which usually occurs in one side, usually without sensory abnormalities	It is usually manifested as spinal cord thinning, intervertebral disc protrusion or prolapse. Due to long-term compression of the spinal cord, venous hyperemia and infarction can be caused, which can be secondary to cystic necrosis of the anterior horn of the spinal cord, forming T2WI snake-eye sign	Segmental neurogenic damage consistent with the distribution of the injured nerve root
Spinal muscular atrophy syndrome[41]	The most common autosomal recessive disease in childhood is progressive and symmetrical weakness and atrophy of limbs and trunk muscles	Anterior horn of spinal cord α-Degeneration and degeneration of motor neurons led to T2WI snake-eye sign	Typical neuronal damage, fiber fibrillation wave and positive sharp wave can be seen at rest, bundle fibrillation potential can be seen occasionally, and regular spontaneous motor unit activity potential is the characteristic manifestation of its EMG

DWI: Diffusion-weighted imaging; EMG: Electromyography; FLAIR: Fluid-attenuated inversion-recovery; SWI: Susceptibility weighted imaging; T2WI: T2-weighted imaging.

artery. The anterior horn cells of the spinal gray matter in this area are highly sensitive to hypoxia; when local or overall perfusion is insufficient, they are prone to degeneration and necrosis, forming a "snake-eye appearance" high signal limited to the anterior horn of spinal gray matter on the T2-weighted image of the magnetic resonance imaging axis[42,43]. When this "snake-eye appearance" appears during acute onset myelopathy, a vascular origin should be highly suspected. The most commonly used method is aortic CTA. Thoracic and abdominal CTA can help detect aortic atherosclerotic plaques, dissection, aneurysm, and mural thrombosis. If the CTA result is negative, spinal angiography is necessary to exclude dural arteriovenous fistula and spinal intramedullary arteriovenous malformation[4]. Wildgrube *et al*[13] previously reported a case of conus medullaris infarction with "snake-eye appearance", caused by spinal cord venous thrombosis. Thus, it is necessary to evaluate thrombophilic factors and improve spinal cord angiography to distinguish between venous and arterial conus medullaris infarction. The cell number and IgG index of cerebrospinal fluid in patients with spinal conus infarction are usually normal. There is no oligoclonal band, and the protein content in cerebrospinal fluid can be slightly increased in some patients[6-7,20,26]. A previous study[44] proposed two mechanisms of spinal cord infarction: (1) Infarction triggered by mechanical factors (bilateral anterior or posterior spinal cord artery infarction and unilateral infarction); and (2) infarction caused by long-term hypotension or arterial insufficiency (central spinal cord artery infarction and transverse spinal cord infarction). In this case, the patient was associated with cardiovascular risk factors, such as hypertension, diabetes, and smoking, but had no definite history of trauma before disease onset. However, upon presentation, he complained of suffering from bilateral lower extremity pain after completing mechanical action from the sofa, and urination disorder was observed. We speculated that

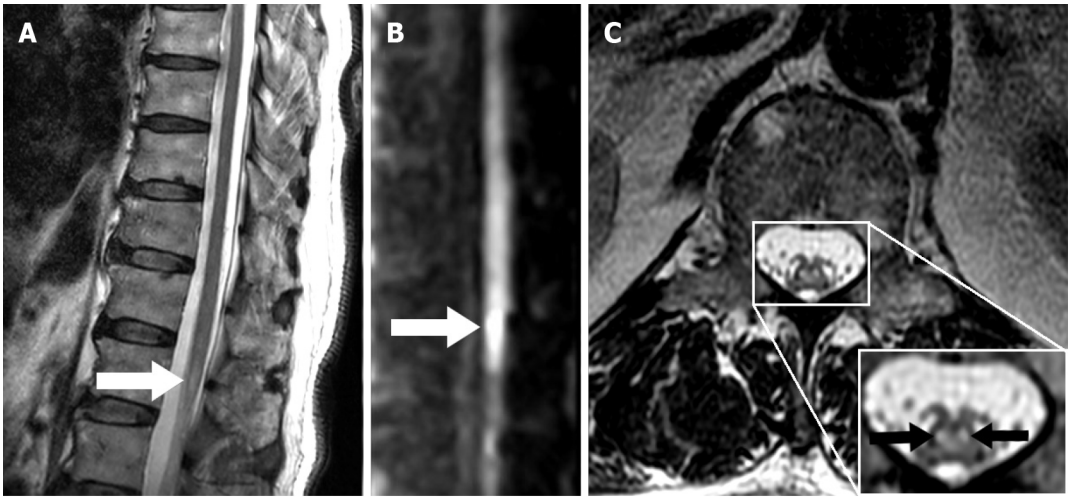

DOI: 10.12998/wjcc.v11.i9.2074

Figure 1 Conus medullaris magnetic resonance exam and "snake-eye appearance". A: The arrow shows conus infarction on T2 weighted magnetic resonance imaging (MRI) (sagittal position); B: The arrow shows conus infarction on diffusion-weighted imaging image (sagittal position); C: The arrows show "snake-eye appearance" on T2 weighted MRI (axial position).

the possible mechanism was based on atherosclerosis in the anterior spinal cord. Mechanical stress can lead to anterior spinal artery ischemia. At present, the treatment principles for spinal cord infarction mainly refer to the guidelines for acute ischemic stroke. Old age, severe initial neurological deficit, and long segment lesions are considered to be related to poor prognosis[22,27,45,46]. The prognostic value of the "snake-eye appearance" on magnetic resonance imaging in acute myelopathy is unclear, but may be related to the poor prognosis of chronic myelopathy[29,47,48].

Conus medullaris infarction is rare in the clinic and has a high misdiagnosis rate. Detailed medical history and physical examination were the basis of the diagnosis. Although the "snake-eye appearance" is not specific to spinal cord MRI, acute low back pain or bilateral lower limb pain is usually the first symptom, and its clinical manifestation is conus syndrome or cauda equina syndrome. When the axial T2-weighted image of MRI shows "snake-eye appearance", it is necessary to differentiate between spinal conus infarction caused by anterior spinal artery ischemia. Improving aortography, spinal angiography, and cerebrospinal fluid examination will help to clarify the etiology.

The limitations of this report are its short follow-up period and lack of imaging and neurophysiological evaluation results during the follow-up period. Although we have reviewed previously reported cases of conus medullaris infarction, authors may have different descriptions of clinical characteristics and results. More cases need to be analyzed in the future to improve clinicians' understanding of this disease.

CONCLUSION

We conclude that acute onset of conus medullaris syndrome combined with "snake-eye appearance" should be strongly suspected as conus medullaris infarction caused by anterior spinal artery ischemia. This special imaging manifestation is helpful in the early diagnosis and treatment of conus infarction.

ACKNOWLEDGEMENTS

We would like to thank Dr. Bo Sun and Dr. Dan Ren for providing high-resolution MRI and CTA images. Finally, we thank the patient for his participation.

FOOTNOTES

Author contributions: Zhang QY contributed to manuscript writing and editing, and data collection; Xu LY and Wang ML contributed to data analysis; Cao H and Ji XF contributed to conceptualization and supervision; all authors have read and approved the final manuscript.

Informed consent statement: Informed written consent was obtained from the patient for publication of this report

and any accompanying images.

Conflict-of-interest statement: All the authors declare that they have no conflict of interest to disclose.

CARE Checklist (2016) statement: The authors have read the CARE Checklist (2016), and the manuscript was prepared and revised according to the CARE Checklist (2016).

Country/Territory of origin: China

ORCID number: Qiao-Yu Zhang 0000-0002-4059-8161; Lin-Ying Xu 0000-0001-9237-9131; Ming-Li Wang 0000-0003-0902-8221; Hua Cao 0000-0001-9732-5773; Xiao-Fei Ji 0000-0002-6104-1952.

S-Editor: Liu JH
L-Editor: A
P-Editor: Liu JH

REFERENCES

1 **Sandson TA**, Friedman JH. Spinal cord infarction. Report of 8 cases and review of the literature. *Medicine (Baltimore)* 1989; **68**: 282-292 [PMID: 2677596]
2 **Rubin MN**, Rabinstein AA. Vascular diseases of the spinal cord. *Neurol Clin* 2013; **31**: 153-181 [PMID: 23186899 DOI: 10.1016/j.ncl.2012.09.004]
3 **Weidauer S**, Nichtweiß M, Hattingen E, Berkefeld J. Spinal cord ischemia: aetiology, clinical syndromes and imaging features. *Neuroradiology* 2015; **57**: 241-257 [PMID: 25398656 DOI: 10.1007/s00234-014-1464-6]
4 **Nasr DM**, Rabinstein A. Spinal Cord Infarcts: Risk Factors, Management, and Prognosis. *Curr Treat Options Neurol* 2017; **19**: 28 [PMID: 28688063 DOI: 10.1007/s11940-017-0464-3]
5 **Herrick MK**, Mills PE Jr. Infarction of spinal cord. Two cases of selective gray matter involvement secondary to asymptomatic aortic disease. *Arch Neurol* 1971; **24**: 228-241 [PMID: 5101615 DOI: 10.1001/archneur.1971.00480330056005]
6 **Anderson NE**, Willoughby EW. Infarction of the conus medullaris. *Ann Neurol* 1987; **21**: 470-474 [PMID: 3592640 DOI: 10.1002/ana.410210510]
7 **Ohbu S**, Ishimoto A, Honda M, Fukuda H, Hata Y, Tada S. Infarction of the conus medullaris. *Eur Neurol* 1990; **30**: 343-344 [PMID: 2289512 DOI: 10.1159/000117369]
8 **Andrews BT**, Kwei U, Greco C, Miller RG. Infarct of the conus medullaris simulating a spinal cord tumor: case report. *Surg Neurol* 1991; **35**: 139-142 [PMID: 1990482 DOI: 10.1016/0090-3019(91)90266-c]
9 **Mhiri C**, Miladi MI, Triki C, Kechaou MS. Sacral meningeal arteriovenous fistula supplied by branches of the hypogastric artery revealed by conus medullaris infarction. *Spinal Cord* 2000; **38**: 711-714 [PMID: 11114782 DOI: 10.1038/sj.sc.3101086]
10 **Sinha S**, Sirigiri SR, Kanakamedala SK, Singh MK, Sharma RM. Duloxetine for treatment of male sphincteric incontinence following partial conus medullaris infarction after coronary bypass surgery. *Cases J* 2009; **2**: 9094 [PMID: 20062731 DOI: 10.1186/1757-1626-2-9094]
11 **Greiner-Perth R**, Schenke H, Böhm H, Both R. Spinal cord tumour simulated by an infarction of the conus medullaris. *Acta Neurochir (Wien)* 1999; **141**: 661-662 [PMID: 10929733 DOI: 10.1007/s007010050357]
12 **Combarroso O**, Sánchez-Pernaute R, Orizaola P, Berciano J. Absence of F-waves as an early electrodiagnostic finding in infarction of the conus medullaris. *Muscle Nerve* 1995; **18**: 552-554 [PMID: 7739646 DOI: 10.1002/mus.880180514]
13 **Wildgruber D**, Kuntz R, Kermer P, Bartel J, Fetter M, Dichgans J. Elsberg syndrome due to infarction of the conus medullaris associated with a prothrombin mutation. *J Neurol* 1999; **246**: 507-508 [PMID: 10431782 DOI: 10.1007/s004150050394]
14 **Wong JJ**, Dufton J, Mior SA. Spontaneous conus medullaris infarction in a 79 year-old female with cardiovascular risk factors: a case report. *J Can Chiropr Assoc* 2012; **56**: 58-65 [PMID: 22457542]
15 **Konno T**, Suwabe T, Kasahara S, Umeda Y, Oyake M, Fujita N. [A case of conus medullaris infarction expanding to the vertebral bodies, major psoas and erector spinae muscles]. *Rinsho Shinkeigaku* 2015; **55**: 661-664 [PMID: 26165811 DOI: 10.5692/clinicalneurol.cn-000729]
16 **Diehn FE**, Hunt CH, Lehman VT, Schwartz KM, Eckel LJ, Black DF, Wood CP, Kotsenas AL, Wald JT, Hocker SE. Vertebral body infarct and ventral cauda equina enhancement: two confirmatory findings of acute spinal cord infarct. *J Neuroimaging* 2015; **25**: 133-135 [PMID: 24118402 DOI: 10.1111/jon.12058]
17 **Alanazy MH**. Conus medullaris stroke. Does F wave predict return of ambulation? *Neurosciences (Riyadh)* 2016; **21**: 260-263 [PMID: 27356660 DOI: 10.17712/nsj.2016.3.20150554]
18 **Hor H**, Nader H, Tarnutzer AA. Absent F-waves in conus medullaris stroke mimicking Guillain-Barré syndrome. *BMJ Case Rep* 2018; **11** [PMID: 30567145 DOI: 10.1136/bcr-2018-227726]

19 **Kamimura T**, Nezu T, Aoki S, Ueno H, Hosomi N, Maruyama H. Conus Medullaris Infarction Involving the Paraspinal Muscles and Nerve Roots. *J Stroke Cerebrovasc Dis* 2020; **29**: 104983 [PMID: 32689651 DOI: 10.1016/j.jstrokecerebrovasdis.2020.104983]

20 **Weng YC**, Chin SC, Wu YY, Kuo HC. Clinical, neuroimaging, and nerve conduction characteristics of spontaneous Conus Medullaris infarction. *BMC Neurol* 2019; **19**: 328 [PMID: 31847829 DOI: 10.1186/s12883-019-1566-1]

21 **Breitling B**, Schmeel FC, Radbruch A, Kaut O. Sudden paraparesis due to spinal cord ischemia with initial contrast enhancement of the cauda equina and time-delayed owl-eyes sign on follow-up MR imaging: a case report. *Neurol Res Pract* 2021; **3**: 13 [PMID: 33789775 DOI: 10.1186/s42466-021-00112-5]

22 **Masson C**, Pruvo JP, Meder JF, Cordonnier C, Touzé E, De La Sayette V, Giroud M, Mas JL, Leys D; Study Group on Spinal Cord Infarction of the French Neurovascular Society. Spinal cord infarction: clinical and magnetic resonance imaging findings and short term outcome. *J Neurol Neurosurg Psychiatry* 2004; **75**: 1431-1435 [PMID: 15377691 DOI: 10.1136/jnnp.2003.031724]

23 **Yoshioka K**, Niinuma H, Ehara S, Nakajima T, Nakamura M, Kawazoe K. MR angiography and CT angiography of the artery of Adamkiewicz: state of the art. *Radiographics* 2006; **26** Suppl 1: S63-S73 [PMID: 17050520 DOI: 10.1148/rg.26si065506]

24 **Martirosyan NL**, Kalani MY, Lemole GM Jr, Spetzler RF, Preul MC, Theodore N. Microsurgical anatomy of the arterial basket of the conus medullaris. *J Neurosurg Spine* 2015; **22**: 672-676 [PMID: 25746117 DOI: 10.3171/2014.10.SPINE131081]

25 **Montalbano MJ**, Loukas M, Oskouian RJ, Tubbs RS. Innervation of the blood vessels of the spinal cord: a comprehensive review. *Neurosurg Rev* 2018; **41**: 733-735 [PMID: 27709410 DOI: 10.1007/s10143-016-0788-6]

26 **Zalewski NL**, Rabinstein AA, Krecke KN, Brown RD Jr, Wijdicks EFM, Weinshenker BG, Kaufmann TJ, Morris JM, Aksamit AJ, Bartleson JD, Lanzino G, Blessing MM, Flanagan EP. Characteristics of Spontaneous Spinal Cord Infarction and Proposed Diagnostic Criteria. *JAMA Neurol* 2019; **76**: 56-63 [PMID: 30264146 DOI: 10.1001/jamaneurol.2018.2734]

27 **Nedeltchev K**, Loher TJ, Stepper F, Arnold M, Schroth G, Mattle HP, Sturzenegger M. Long-term outcome of acute spinal cord ischemia syndrome. *Stroke* 2004; **35**: 560-565 [PMID: 14726546 DOI: 10.1161/01.STR.0000111598.78198.EC]

28 **Jinkins JR**, Bashir R, Al-Mefty O, Al-Kawi MZ, Fox JL. Cystic necrosis of the spinal cord in compressive cervical myelopathy: demonstration by iopamidol CT-myelography. *AJR Am J Roentgenol* 1986; **147**: 767-775 [PMID: 3489379 DOI: 10.2214/ajr.147.4.767]

29 **Mizuno J**, Nakagawa H, Inoue T, Hashizume Y. Clinicopathological study of "snake-eye appearance" in compressive myelopathy of the cervical spinal cord. *J Neurosurg* 2003; **99**: 162-168 [PMID: 12956458 DOI: 10.3171/spi.2003.99.2.0162]

30 **Sarawagi R**, Narayanan S, Lakshmanan PM, Chakkalakkoombil SV. Hirayama disease: imaging profile of three cases emphasizing the role of flexion MRI. *J Clin Diagn Res* 2014; **8**: RD03-RD04 [PMID: 25300741 DOI: 10.7860/JCDR/2014/8433.4716]

31 **Xu H**, Shao M, Zhang F, Nie C, Wang H, Zhu W, Xia X, Ma X, Lu F, Jiang J. Snake-Eyes Appearance on MRI Occurs during the Late Stage of Hirayama Disease and Indicates Poor Prognosis. *Biomed Res Int* 2019; **2019**: 9830243 [PMID: 30756087 DOI: 10.1155/2019/9830243]

32 **Hsu CF**, Chen CY, Yuh YS, Chen YH, Hsu YT, Zimmerman RA. MR findings of Werdnig-Hoffmann disease in two infants. *AJNR Am J Neuroradiol* 1998; **19**: 550-552 [PMID: 9541317]

33 **Zhang Z**, Wang H. Is the "snake-eye" MRI sign correlated to anterior spinal artery occlusion on CT angiography in cervical spondylotic myelopathy and amyotrophy? *Eur Spine J* 2014; **23**: 1541-1547 [PMID: 24823850 DOI: 10.1007/s00586-014-3348-1]

34 **Verma A**. Clinical Manifestation and Management of Amyotrophic Lateral Sclerosis. In: Amyotrophic Lateral Sclerosis [Internet]. Brisbane (AU): Exon Publications; 2021-Jul-25 [PMID: 34473441]

35 **Bekci T**, Yucel S, Aslan K, Gunbey HP, Incesu L. "Snake eye" appearance on a teenage girl with spontaneous spinal ischemia. *Spine J* 2015; **15**: e45 [PMID: 26070288 DOI: 10.1016/j.spinee.2015.06.002]

36 **Alves JN**, Machado C, Taveira M, Soares-Fernandes J, Ferreira C, Pinho J. Teaching NeuroImages: Restricted diffusion "snake eyes appearance" in acute spinal cord ischemia. *Neurology* 2016; **86**: e204-e205 [PMID: 27164724 DOI: 10.1212/WNL.0000000000002661]

37 **Martínez Tébar MJ**, Baeza Román A, Mejia Olmos GJ. «Snake eye» and «pencil-like» signs together with diaphragmatic paralysis in a patient with anterior spinal cord ischemia. *Med Intensiva (Engl Ed)* 2019; **43**: 452 [PMID: 30545722 DOI: 10.1016/j.medin.2018.11.002]

38 **Tan YJ**, Manohararaj N. Isolated Infarctions of the Conus Medullaris: Clinical Features and Outcomes. *J Stroke Cerebrovasc Dis* 2021; **30**: 106055 [PMID: 34433121 DOI: 10.1016/j.jstrokecerebrovasdis.2021.106055]

39 **Iacono S**, Di Stefano V, Gagliardo A, Cannella R, Virzì V, Pagano S, Lupica A, Romano M, Brighina F. Hirayama disease: Nosological classification and neuroimaging clues for diagnosis. *J Neuroimaging* 2022; **32**: 596-603 [PMID: 35394668 DOI: 10.1111/jon.12995]

40 **Zhang J**, Liu MS, Cui LY, Li BH, DU H. [A clinical, electromyographic, and magnetic resonance imaging study of cervical spondylotic myelopathy: analysis of 96 cases]. *Zhonghua Yi Xue Za Zhi* 2009; **89**: 328-330 [PMID: 19563711 DOI: 10.3760/cma.j.issn.0376-2491.2009.05.011]

41 **Mercuri E**, Finkel RS, Muntoni F, Wirth B, Montes J, Main M, Mazzone ES, Vitale M, Snyder B, Quijano-Roy S, Bertini E, Davis RH, Meyer OH, Simonds AK, Schroth MK, Graham RJ, Kirschner J, Iannaccone ST, Crawford TO, Woods S, Qian Y, Sejersen T; SMA Care Group. Diagnosis and management of spinal muscular atrophy: Part 1: Recommendations for diagnosis, rehabilitation, orthopedic and nutritional care. *Neuromuscul Disord* 2018; **28**: 103-115 [PMID: 29290580 DOI: 10.1016/j.nmd.2017.11.005]

42 **Pullicino P**. Bilateral distal upper limb amyotrophy and watershed infarcts from vertebral dissection. *Stroke* 1994; **25**: 1870-1872 [PMID: 8073471 DOI: 10.1161/01.str.25.9.1870]

43 **Gelfan S**, Tarlov IM. Differential vulnerability of spinal cord structures to anoxia. *J Neurophysiol* 1955; **18**: 170-188 [PMID: 14354454 DOI: 10.1152/jn.1955.18.2.170]

44 **Novy J**, Carruzzo A, Maeder P, Bogousslavsky J. Spinal cord ischemia: clinical and imaging patterns, pathogenesis, and outcomes in 27 patients. *Arch Neurol* 2006; **63**: 1113-1120 [PMID: 16908737 DOI: 10.1001/archneur.63.8.1113]

45 **Salvador de la Barrera S**, Barca-Buyo A, Montoto-Marqués A, Ferreiro-Velasco ME, Cidoncha-Dans M, Rodriguez-Sotillo A. Spinal cord infarction: prognosis and recovery in a series of 36 patients. *Spinal Cord* 2001; **39**: 520-525 [PMID: 11641795 DOI: 10.1038/sj.sc.3101201]

46 **Hsu JL**, Cheng MY, Liao MF, Hsu HC, Weng YC, Chang KH, Chang HS, Kuo HC, Huang CC, Lyu RK, Lin KJ, Ro LS. The etiologies and prognosis associated with spinal cord infarction. *Ann Clin Transl Neurol* 2019; **6**: 1456-1464 [PMID: 31402616 DOI: 10.1002/acn3.50840]

47 **Fontanella MM**, Zanin L, Bergomi R, Fazio M, Zattra CM, Agosti E, Saraceno G, Schembari S, De Maria L, Quartini L, Leggio U, Filosto M, Gasparotti R, Locatelli D. Snake-Eye Myelopathy and Surgical Prognosis: Case Series and Systematic Literature Review. *J Clin Med* 2020; **9** [PMID: 32664657 DOI: 10.3390/jcm9072197]

48 **Funaba M**, Imajo Y, Suzuki H, Nishida N, Nagao Y, Sakamoto T, Fujimoto K, Sakai T. Impact of various MRI signal intensity changes on radiological parameters, the neurological status, and surgical outcomes in degenerative cervical myelopathy. *Clin Neurol Neurosurg* 2021; **207**: 106802 [PMID: 34273664 DOI: 10.1016/j.clineuro.2021.106802]

World Journal of Clinical Cases

Submit a Manuscript: https://www.f6publishing.com

World J Clin Cases 2023 March 26; 11(9): 2084-2090

DOI: 10.12998/wjcc.v11.i9.2084

ISSN 2307-8960 (online)

CASE REPORT

Transseptal approach for catheter ablation of left-sided accessory pathways in children with Marfan syndrome: A case report

Zi-Yan Dong, Wei Shao, Yue Yuan, Li Lin, Xia Yu, Lang Cui, Zhen Zhen, Lu Gao

Specialty type: Cardiac and cardiovascular systems

Provenance and peer review: Unsolicited article; Externally peer reviewed.

Peer-review model: Single blind

Peer-review report's scientific quality classification

Grade A (Excellent): 0
Grade B (Very good): B, B
Grade C (Good): 0
Grade D (Fair): 0
Grade E (Poor): 0

P-Reviewer: Atanasova EG, Bulgaria; Gupta P, United States

Received: December 28, 2022
Peer-review started: December 28, 2022
First decision: February 8, 2023
Revised: February 20, 2023
Accepted: March 3, 2023
Article in press: March 3, 2023
Published online: March 26, 2023

Zi-Yan Dong, Wei Shao, Yue Yuan, Li Lin, Xia Yu, Lang Cui, Zhen Zhen, Department of Cardiology, Beijing Children's Hospital, Capital Medical University, Beijing 100045, China

Lu Gao, National Center for Children's Health, Beijing Children's Hospital, Capital Medical University, Beijing 100045, China

Corresponding author: Lu Gao, MD, Chief Physician, National Center for Children's Health, Beijing Children's Hospital, Capital Medical University, No. 56 South Lish Road, Beijing 100045, China. gaoluga33400122@163.com

Abstract

BACKGROUND

Left-sided accessory pathways (APs) can be accessed with either a transaortic (TA) or transseptal approach (TS). For children with Marfan syndrome (MFS) who have aortic disease, the use of TA can aggravate the disease, making TS the best choice for these patients.

CASE SUMMARY

A 10-year-old girl was hospitalized because of intermittent heart palpitations and chest tightness. She was diagnosed with MFS, supraventricular tachycardia, Wolff-Parkinson-White syndrome, and left-sided AP was detected by cardiac electrophysiological. Catheter ablation was successfully performed *via* TS under the guidance of the Ensite system. During the follow-up, no recurrence or complications occurred.

CONCLUSION

The TS for catheter ablation of left-sided APs can be considered in children with MFS. Adequate evaluation and selection of the appropriate puncture site are particularly important.

Key Words: Transseptal approach; Left-sided accessory pathway; Catheter ablation; Pediatric; Marfan syndrome; Case report

Core Tip: Left-sided accessory pathways (APs) can be accessed with either a transseptal (TS) or transaortic approach (TA). For children with Marfan syndrome (MFS) who have aortic disease, however, the use of TA can aggravate the disease. We report a case of successful catheter ablation of the left-sided accessory pathway by TS in one such child. The TS approach for catheter ablation of left-sided APs appears to be a safe and effective therapeutic option applicable in older children with MFS, though it requires a certain level of training and experience to perform.

Citation: Dong ZY, Shao W, Yuan Y, Lin L, Yu X, Cui L, Zhen Z, Gao L. Transseptal approach for catheter ablation of left-sided accessory pathways in children with Marfan syndrome: A case report. *World J Clin Cases* 2023; 11(9): 2084-2090
URL: https://www.wjgnet.com/2307-8960/full/v11/i9/2084.htm
DOI: https://dx.doi.org/10.12998/wjcc.v11.i9.2084

INTRODUCTION

Catheter ablation is the main method for eradicating supraventricular tachycardia (SVT) in children, and left-sided accessory pathways (APs) can be accessed by using a transaortic approach (TA) or a transseptal approach (TS). Reports show that children with Marfan syndrome (MFS) have a higher risk of developing SVT than healthy children[1] and that they also often have aortic lesions. When left-sided APs are accessed in these children, TA for catheter ablation may result in aggravated aortic disease. Hence, TS may be a better method. However, due to the combination of mitral valve disease, the difficulty of catheter ablation in MFS, and the small amount of experience most providers have with atrial septal puncture in children, there are currently no relevant reports on this technique. We therefore report a case of successful ablation of the left-sided AP by TS in a child with MFS and review the current literature, providing new ideas for the treatment of MFS.

CASE PRESENTATION

Chief complaints

A 10-year-old girl was admitted to Beijing Children's Hospital in May, 2021 for a 4-year history of intermittent heart palpitations and chest tightness.

History of present illness

Symptoms started 4 years before the child was admitted to the hospital. She presented with intermittent episodes of heart palpitations and chest tightness with pallor. Each episode lasted from 15 min to 3 h, with a frequency of about twice a year. Paroxysmal SVT was diagnosed at a local hospital, and could be converted to sinus rhythm after application of propafenone. Four months before admission to Beijing Children's Hospital, her palpitations increased in frequency and had occurred 4 times in the last month. Antiarrhythmic drugs were needed to convert.

History of past illness

Pectus excavatum was found at birth. In April, 2014, Nuss pectus excavatum correction was performed, and congenital short esophagus and congenital diaphragmatic hernia were diagnosed. In April 2016, the corrective plate was removed.

Personal and family history

The child was born full-term to nonconsanguineous, healthy parents by normal vaginal delivery after an uneventful pregnancy.

Physical examination

The weight of the patient was 27.5 kg, and her height was 153 cm. A surgical scar of about 6 cm was observed under her right armpit, and she was noted to have dysmorphic features including long and thin extremities with hyperflexible joints, prior pectus excavatum, and scoliosis. Both wrist sign and thumb sign were positive. Marfan syndrome was suspected and additional tests were carried out.

Laboratory examinations

No abnormalities were found in routine blood or urine analyses.

Imaging examinations

Chest X-ray revealed a right diaphragmatic hernia and scoliosis. Echocardiography showed mild mitral and tricuspid prolapse and regurgitation, and the aortic sinus and ascending aorta were widened. Cardiac computed tomography (CT) scan and reconstruction demonstrated severe aortic root dilatation, with left-right diameters of 3.56 cm (z-score of +6.41), anteroposterior diameters of 3.32 cm (z-score of +5.33), and perforating septum thickness of approximately 13.9 mm (Figure 1). Ophthalmic examination revealed high myopia in both eyes and mild opacification of the posterior lens capsule in the right eye. Finally, genetic testing revealed a heterozygous mutation in the FBN1 gene, c.5841delC (p.C1947). Because she had an aortic root Z-score ≥ 2, a pathogenic FBN1 gene mutation, and a systemic score of 7, MFS was diagnosed according to the 2010 revised Ghent Criteria[2] (Table 1).

Further diagnostic work-up

During hospitalization, the child still suffered from palpitation attacks. Electrocardiogram (ECG) during an episode revealed SVT with a heart rate of 214/min. After a few minutes, the episode terminated spontaneously. The ECG showed sinus rhythm with a ventricular pre-excitation pattern. Paroxysmal SVT and Wolff-Parkinson-White syndrome type A were subsequently diagnosed.

After general anesthesia, cardiac electrophysiological examination was performed under the guidance of Ensite NavX mapping system (Figure 2). Electrode catheters were placed in the coronary sinus (CS) and the right ventricle. Atrioventricular nodal jump phenomenon was not found during atrial program stimulation. Stable narrow QRS tachycardia could be induced by stimulation at 270 ms, with a ventricular rate of 200 bpm and an A/V ratio of 1. The A wave of the CS catheter was eccentrically distributed, and was the most advanced at 1-2 electrodes. Atrioventricular reentrant tachycardia (AVRT) with AP located on the left side was diagnosed.

FINAL DIAGNOSIS

Based on the child's medical history, her final diagnosis was MFS, SVT, Wolff-Parkinson-White syndrome, and left-sided AP.

TREATMENT

Considering that the child had aortic sinus disease, there was a greater risk of retrograde delivery of ablation catheter through the aorta, so we delivered the ablation catheter to the left side of the heart by transseptal puncture performed under X-ray fluoroscopy. The introducer sheath and dilator, followed with the guide wire, were introduced into right femoral vein and placed to the superior vena cava. After that, we pushed the transseptal needle (Brockenbrough BRK, 71 cm, St. Jude Medical/Abbott) to about 1 cm from the end of the dilator. The needle and sheath were rotated clockwise until the tip pointed toward 4 o'clock, and then were slowly retracted. After two "jumps" the tip of the sheath fell into the fossa ovalis. We then adjusted the direction of the introducer sheath tip in the right anterior oblique view, advanced the puncture needle, and injected contrast agent to confirm that the needle tip was in the left atrium. In the left anterior oblique view, the outer sheath had been guided to the left atrium.

The ablation catheter (Safire, 7-F, 115 cm, St. Jude Medical/Abbott) was then advanced into the left atrium along with the sheath, and the target was subsequently mapped. A satisfactory target was marked on the atrial side at a location of 3:30 (o'clock) of the mitral annulus. During sinus rhythm, the ablation was performed at 52°C and 30 W. After 2 s of discharge, the body surface pre-excitation pattern disappeared, and the V-A wave separated. Under ventricular pacing, the V-A wave of the ablation catheter separated, and the reverse A wave of the CS catheter changed to a centripetal distribution. Consolidation discharges were performed at the target for a total of 120 s, and repeated cardiac electrophysiological examination and intravenous isoproterenol failed to induce AVRT or other arrhythmias during the 48-h observation period after ablation. Ventricular pre-excitation was not restored, and echocardiography showed no aggravation of valve injury.

OUTCOME AND FOLLOW-UP

Regular follow-up was performed at 1, 3, 6, and 12 mo, during which ECG, echocardiography, and dynamic ECG were re-examined. No complication or recurrence of SVT were detected at any of these follow-ups.

Table 1 Marfan syndrome score of the child

	Wrist and thumb sign	Pectus excavatum	Myopia > 3 diopters	Scoliosis	Mitral valve prolapse
Score	3	1	1	1	1

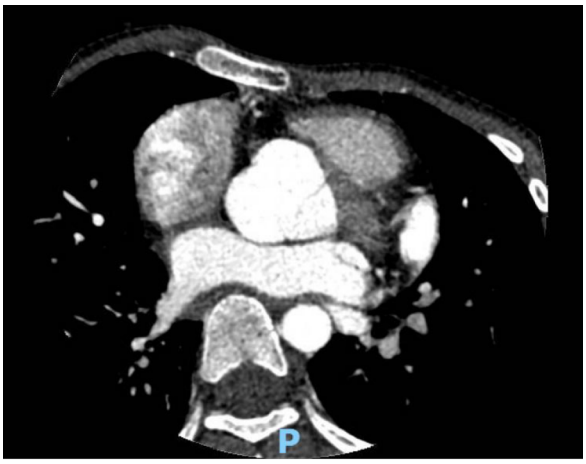

DOI: 10.12998/wjcc.v11.i9.2084

Figure 1 Cardiac computed tomography scan and reconstruction showed severe aortic root dilatation resulting in a narrow septum.

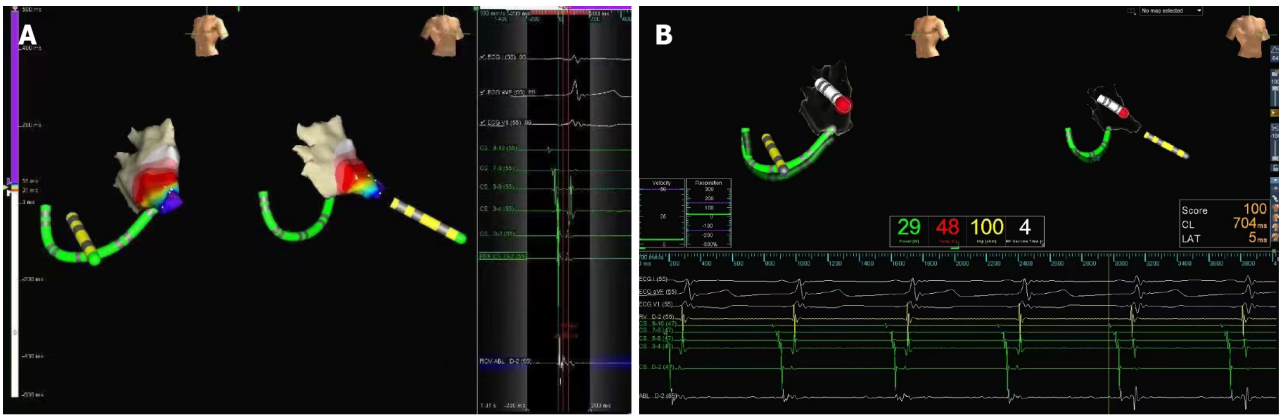

DOI: 10.12998/wjcc.v11.i9.2084

Figure 2 Cardiac electrophysiological examination and catheter ablation were performed guided by an Ensite NavX system. A: A satisfactory target was marked on the atrial side at 3:30 (o'clock) on the mitral annulus; B: The body surface pre-excitation pattern disappeared.

DISCUSSION

MFS is an autosomal dominant disorder of the connective tissue that usually occurs due to mutations in the FBN1 gene and has an incidence of 1.5–17.2 per 100000[3]. About 50% of MFS patients have aortic dilatation in early childhood that gradually progresses. Aortic root disease, which was initially considered to be the main cause of complications and death in patients with MFS, became the target of most treatments and clinical studies. However, the German Marfan Organization believes that some manifestations of MFS may seriously threaten the health of patients, including SVT, ventricular tachycardia, and repolarization abnormalities[4]. Wafa *et al*[5] showed that the burden of inpatient arrhythmia in MFS is higher than the general non-Marfan population and that SVTs were significant predictors of higher adjusted health care–associated cost. In addition, early aortic repair is recommended by the Ghent guidelines[2], and surgical treatment should also be considered in patients with aortic aneurysm or valvular insufficiency. Postoperative scarring both increases the incidence of arrhythmias and poses difficulties for catheter ablation, however. Demolder *et al*[6] demonstrated that heart failure and arrhythmia have become the primary causes of death for patients with MFS after aortic surgery. Therefore, eradicating arrhythmias in patients with MFS in childhood who have not undergone intracardiac surgery has the potential to save lives. Furthermore, with modern the improvements in aortic repair, the treatment of arrhythmias in children with MFS should be the focus of future research.

The TS is preferred for catheter ablation to avoid aggravated aortic injury when there is a left-sided AP. The TS does not enter the left side of the heart through the aorta, which effectively avoids the risks of aortic valve injury and ascending aortic aneurysm rupture, among others. Moreover, for children with APs located in the left posterior lateral or left posterior septum, the operation of the ablation catheter is more flexible by a TS[7]. In adults, a TS is associated with a higher success rate and lower recurrence and complication rates, and the safety and feasibility of this method have also been demonstrated by recent studies. Yoshida, Rami, and Koca showed that TS for ablation was safe and effective even in children weighing less than 30 kg[8-10]. However, considering of the need for special training and the risk of serious potential complications (cardiac tamponade and pericardial effusion), TS is still not recommended by most cardiovascular pediatricians at present[11].

Our center at Beijing Children's Hospital is a national children's medical center, and our staff are experienced in ablating left-sided AP in children using a TS. The child in this report was the only one with left-sided AP who had confirmed MFS, however. She had mitral and tricuspid regurgitation, pectus excavatum, previous history of thoracic surgery, and may also have had a potential delay in vascular healing and repair that presents in most patients with MFS. These factors not only increase the risk of arrhythmia but also pose difficult challenges for atrial septal puncture and radiofrequency ablation[12,13].

The complications of atrial septal puncture include pericardial effusion and cardiac tamponade, as well as others. Cardiac ultrasound, cardiac CT scan and reconstruction must be performed to understand fully the shape and degree of aortic dilatation and cardiac chamber size. Although the child had mitral and tricuspid regurgitation, fortunately the atrial size was normal and had little change at the puncture site. However, her noncoronary sinus, located in the anterosuperior aspect of the interatrial septum, was significantly dilated and pushed against the septum, resulting in a narrow septum. In a case like this the needle tip should therefore be slightly oriented away from the aortic root during puncture (moved backward and downward compared to normal children) to avoid perforating the aorta. In addition, the child weighed < 30 kg, leading to a small heart size. To reduce the risk of penetrating the heart chamber we increased the curvature of the puncture needle.

For safety, a small amount of radiation is required during the puncture. Transseptal puncture under fluoroscopy provides real-time images of surrounding organs (trachea and spine) and CS electrodes, which is helpful in locating the puncture site. However, zero-radiation transseptal puncture can be achieved with the assistance of other imaging tools, such as transthoracic echocardiography, transesophageal echocardiography, or intracardiac echocardiography, but these methods have rarely been used in children[14].

Children are more sensitive to radiation, which may increase their risk of developing hematologic or intracranial tumors[15]. Thus, our subsequent ablation procedure was guided by 3D mapping to minimize the radiation dose while ensuring safety and efficacy. Radiofrequency ablation complications can include valve injury, atrioventricular block, cardiac tamponade, and thromboembolism. Furthermore, valve disease associated with MFS can increase the risk of thromboembolism. Because of the patient's tricuspid regurgitation, to avoid aggravation of injury, gentle operation low movement amplitude of the ablation catheter at the valve site were necessary. Additionally, in the presences of mitral regurgitation, careful mapping should be performed to determine the ablation site in order to reduce the potential damage of repeated discharges to the valve. For the patient in this case report, echocardiography was performed after catheter ablation and showed that valve damages were not aggravated.

Since the operation, there has been no recurrence of SVT, and no complication have been found during the 1-year follow-up period. The child has gone to school and lived a normal life. For children with aortic diseases such as MFS, who cannot undergo catheter ablation by TA, a TS can be attempted in experienced medical centers. However, infantile MFS is more severe than classical MFS[16]. Severe mitral valve disease and small heart size make ablation much more difficult, and atrial enlargement also causes changes in the puncture site, increasing the risk of accidental atrial or aortic penetration. Weight < 15 kg and age < 4/5 years have also been used as criteria for high risk of catheter ablation in previous studies and guidelines[17]. The weight of this child was large enough so that our conclusions are not applicable to infantile MFS; subsequent studies are needed for using a TS in infantile MFS patients specifically.

CONCLUSION

In conclusion, it is necessary to perform catheter ablation for MFS patients in order to eliminate SVT in childhood before intracardiac surgery. TS for catheter ablation of left-sided APs, appears to be safe, effective and applicable in older children with MFS, can certainly be attempted in experienced medical centers. Increasing the curvature of the puncture needle and moving the tip posteriorly and inferiorly may be safer for children weighing < 30 kg who have significantly dilated aorta. Gentle manipulation is needed to avoid damaging the valve during ablation.

FOOTNOTES

Author contributions: Dong ZY and Shao W designed the study; Dong ZY wrote the original manuscript; Shao W, Yuan Y, Yu X, Cui L, Zhen Z, Gao L reviewed and revised the manuscript; All authors have read and approve the final manuscript.

Informed consent statement: Informed written consent was obtained from the patient for publication of this report and any accompanying images.

Conflict-of-interest statement: All the authors declare that they have no conflict of interest to disclose.

CARE Checklist (2016) statement: The authors have read the CARE Checklist (2016), and the manuscript was prepared and revised according to the CARE Checklist (2016).

Country/Territory of origin: China

ORCID number: Lu Gao 0000-0002-6780-2660.

S-Editor: Liu JH
L-Editor: A
P-Editor: Liu JH

REFERENCES

1 **Andersen NH**, Groth KA, Berglund A, Hove H, Gravholt CH, Stochholm K. Non-aortic cardiovascular disease in Marfan syndrome: a nationwide epidemiological study. *Clin Res Cardiol* 2021; **110**: 1106-1115 [PMID: 33885997 DOI: 10.1007/s00392-021-01858-3]
2 **Loeys BL**, Dietz HC, Braverman AC, Callewaert BL, De Backer J, Devereux RB, Hilhorst-Hofstee Y, Jondeau G, Faivre L, Milewicz DM, Pyeritz RE, Sponseller PD, Wordsworth P, De Paepe AM. The revised Ghent nosology for the Marfan syndrome. *J Med Genet* 2010; **47**: 476-485 [PMID: 20591885 DOI: 10.1136/jmg.2009.072785]
3 **von Kodolitsch Y**, De Backer J, Schüler H, Bannas P, Behzadi C, Bernhardt AM, Hillebrand M, Fuisting B, Sheikhzadeh S, Rybczynski M, Kölbel T, Püschel K, Blankenberg S, Robinson PN. Perspectives on the revised Ghent criteria for the diagnosis of Marfan syndrome. *Appl Clin Genet* 2015; **8**: 137-155 [PMID: 26124674 DOI: 10.2147/TACG.S60472]
4 **von Kodolitsch Y**, Demolder A, Girdauskas E, Kaemmerer H, Kornhuber K, Muino Mosquera L, Morris S, Neptune E, Pyeritz R, Rand-Hendriksen S, Rahman A, Riise N, Robert L, Staufenbiel I, Szöcs K, Vanem TT, Linke SJ, Vogler M, Yetman A, De Backer J. Features of Marfan syndrome not listed in the Ghent nosology - the dark side of the disease. *Expert Rev Cardiovasc Ther* 2019; **17**: 883-915 [PMID: 31829751 DOI: 10.1080/14779072.2019.1704625]
5 **Wafa SEI**, Chahal CAA, Sawatari H, Khanji MY, Khan H, Asatryan B, Ahmed R, Deshpande S, Providencia R, Deshmukh A, Owens AT, Somers VK, Padmanabhan D, Connolly H. Frequency of Arrhythmias and Postural Orthostatic Tachycardia Syndrome in Patients With Marfan Syndrome: A Nationwide Inpatient Study. *J Am Heart Assoc* 2022; **11**: e024939 [PMID: 36000435 DOI: 10.1161/JAHA.121.024939]
6 **Demolder A**, von Kodolitsch Y, Muiño-Mosquera L, De Backer J. Myocardial Function, Heart Failure and Arrhythmia in Marfan Syndrome: A Systematic Literature Review. *Diagnostics (Basel)* 2020; **10** [PMID: 32992882 DOI: 10.3390/diagnostics10100751]
7 **Yu X**, Dong Z, Gao L, Lin L, Cui L, Shao W, Yu W, Zhen Z, Yuan Y. Transseptal Approach Versus Transaortic Approach for Catheter Ablation of Left-Sided Accessory Pathways in Children. *Front Pediatr* 2022; **10**: 888029 [PMID: 35783318 DOI: 10.3389/fped.2022.888029]
8 **Yoshida S**, Suzuki T, Yoshida Y, Watanabe S, Nakamura K, Sasaki T, Kawasaki Y, Ehara E, Murakami Y, Kato T, Nakamura Y. Feasibility and safety of transseptal puncture procedures for radiofrequency catheter ablation in small children weighing below 30 kg: single-centre experience. *Europace* 2016; **18**: 1581-1586 [PMID: 26705553 DOI: 10.1093/europace/euv383]
9 **Fogelman R**, Birk E, Dagan T, Fogelman M, Einbinder T, Bruckheimer E, Swissa M. Catheter ablation of left-sided accessory pathways in small children. *J Arrhythm* 2019; **35**: 742-747 [PMID: 31624515 DOI: 10.1002/joa3.12219]
10 **Koca S**, Akdeniz C, Tuzcu V. Transseptal Puncture for Catheter Ablation in Children. *Pediatr Cardiol* 2019; **40**: 799-804 [PMID: 30729261 DOI: 10.1007/s00246-019-02069-4]
11 **Ayabakan C**, Şahin M, Çeliker A. Radiofrequency catheter ablation of left-sided accessory pathways *via* retrograde aortic approach in children. *J Arrhythm* 2016; **32**: 176-180 [PMID: 27354861 DOI: 10.1016/j.joa.2015.12.007]
12 **Goumans MJ**, Ten Dijke P. TGF-β Signaling in Control of Cardiovascular Function. *Cold Spring Harb Perspect Biol* 2018; **10** [PMID: 28348036 DOI: 10.1101/cshperspect.a022210]
13 **Lazea C**, Bucerzan S, Crisan M, Al-Khzouz C, Miclea D, Şufană C, Cismaru G, Grigorescu-Sido P. Cardiovascular

manifestations in Marfan syndrome. *Med Pharm Rep* 2021; **94**: S25-S27 [PMID: 34527904 DOI: 10.15386/mpr-2223]

14 **Sharma SP**, Nalamasu R, Gopinathannair R, Vasamreddy C, Lakkireddy D. Transseptal Puncture: Devices, Techniques, and Considerations for Specific Interventions. *Curr Cardiol Rep* 2019; **21**: 52 [PMID: 31065869 DOI: 10.1007/s11886-019-1136-6]

15 **von Graffenried T**, Rizzi M, Russo M, Nydegger A, Kayemba-Kay's S. Atypical hematological manifestation of celiac disease: A case report of aplastic anemia in a 2-year-old child and review of the literature. *Pediatr Investig* 2021; **5**: 159-162 [PMID: 34179715 DOI: 10.1002/ped4.12267]

16 **Ardhanari M**, Barbouth D, Swaminathan S. Early-Onset Marfan Syndrome: A Case Series. *J Pediatr Genet* 2019; **8**: 86-90 [PMID: 31061752 DOI: 10.1055/s-0038-1675338]

17 **Brugada J**, Blom N, Sarquella-Brugada G, Blomstrom-Lundqvist C, Deanfield J, Janousek J, Abrams D, Bauersfeld U, Brugada R, Drago F, de Groot N, Happonen JM, Hebe J, Yen Ho S, Marijon E, Paul T, Pfammatter JP, Rosenthal E; European Heart Rhythm Association; Association for European Paediatric and Congenital Cardiology. Pharmacological and non-pharmacological therapy for arrhythmias in the pediatric population: EHRA and AEPC-Arrhythmia Working Group joint consensus statement. *Europace* 2013; **15**: 1337-1382 [PMID: 23851511 DOI: 10.1093/europace/eut082]

World Journal of Clinical Cases

Submit a Manuscript: https://www.f6publishing.com

World J Clin Cases 2023 March 26; 11(9): 2091-2097

DOI: 10.12998/wjcc.v11.i9.2091

ISSN 2307-8960 (online)

CASE REPORT

Occipital artery bypass importance in unsuitable superficial temporal artery: Two case reports

Jong-Hwan Hong, Sung-Chan Jung, Han-Seung Ryu, Tae-Sun Kim, Sung-Pil Joo

Specialty type: Surgery

Provenance and peer review: Unsolicited article; Externally peer-reviewed.

Peer-review model: Single-blind

Peer-review report's scientific quality classification

Grade A (Excellent): 0
Grade B (Very good): B
Grade C (Good): C
Grade D (Fair): 0
Grade E (Poor): 0

P-Reviewer: Showkat HI, India; Tan JK, Malaysia

Received: December 24, 2022
Peer-review started: December 24, 2022
First decision: January 30, 2023
Revised: January 31, 2023
Accepted: February 27, 2023
Article in press: February 27, 2023
Published online: March 26, 2023

Jong-Hwan Hong, Sung-Chan Jung, Han-Seung Ryu, Tae-Sun Kim, Sung-Pil Joo, Department of Neurosurgery, Chonnam National University Hospital and Medical School, Gwangju 61469, South Korea

Corresponding author: Sung-Pil Joo, MD, PhD, Professor, Department of Neurosurgery, Chonnam National University Hospital and Medical School, Jebong-ro 42, Gwangju 61469, South Korea. nsjsp@chonnam.ac.kr

Abstract

BACKGROUND

Superficial temporal artery-middle cerebral artery (STA-MCA) bypass helps treat cerebral ischemia. However, the STA is not available for bypass in some conditions. Therefore, with some technical tips, the authors introduced a bypass technique using the occipital artery (OA).

CASE SUMMARY

Two female patients complained of hemiparesis. Brain magnetic resonance imaging (MRI) indicated contralateral infarction from the MCA steno-occlusion. On Diamox single photon emission computed tomography or perfusion MRI, the contralateral front parietotemporal reserve was diminished. On transfemoral cerebral angiography, the STA was thin with a weak flow; however, the OA was prominent. Direct OA-MCA end-to-side extracranial-intracranial bypass surgery was implemented instead of STA because the caliber was too narrow. The postoperative course was uneventful in both cases, with well-maintained bypass patency and neurological stability during follow-up.

CONCLUSION

OA might be an acceptable alternative for MCA cerebral ischemic cases with an unsuitable STA.

Key Words: Bypass; Occipital artery; Superficial temporal artery; Cerebral ischemia; Case report

Core Tip: In cases of cerebral ischemic disease or progressive ischemia where the Superficial temporal artery is unsuitable in the middle cerebral artery territory, occipital artery might be an acceptable donor artery for a less invasive EC-IC bypass surgery.

Citation: Hong JH, Jung SC, Ryu HS, Kim TS, Joo SP. Occipital artery bypass importance in unsuitable superficial temporal artery: Two case reports. *World J Clin Cases* 2023; 11(9): 2091-2097
URL: https://www.wjgnet.com/2307-8960/full/v11/i9/2091.htm
DOI: https://dx.doi.org/10.12998/wjcc.v11.i9.2091

INTRODUCTION

Superficial temporal artery-middle cerebral artery (STA-MCA) bypass helps treat cerebral ischemia, complex cerebral aneurysms, and tumors[1,2]. If the STA is inaccessible after preceding bypass operations, injuries, or atrophy, graft bypass can be attempted through the radial artery, great saphenous vein, or occipital artery (OA). However, the graft would anastomose two sites, increasing bypass occlusion and surgical wound complication risks. In this study, the authors introduced a technique to relieve ischemia *via* direct bypassing of the OA to the MCA.

CASE PRESENTATION

Chief complaints

Case 1: The patient complained of motor weakness in the right extremities and intermittent headaches.

Case 2: The patient complained of motor weakness in the left extremities.

Present illness history

Case 1: In August 2019, a 55-year-old female patient visited this institution's neurology department, reporting intermittent weakness in the right extremities and headaches.

Case 2: In August 2021, a 68-year-old male patient visited this institution's emergency room for left extremities weakness.

Past illness history

Case 1: There was no significant past illness.

Case 2: There was no previous complaint of left-side motor weakness.

Personal and family history

Case 1: There was no significant past or family history.

Case 2: He had right-sided hemiparesis due to the sequelae of traumatic brain injury 15 years ago.

Physical examination

Case 1: There was no significant motor weakness at the outpatient clinic.

Case 2: The left motor grade was IV/IV in the manual muscle test.

Laboratory examinations

There were no significant laboratory test findings in both cases.

Imaging examinations

Case 1: Magnetic resonance imaging (MRI) showed left frontal infarction from the left MCA stenosis (Figure 1A). A follow-up brain MRI on July 2021 indicated that the left MCA stenotic lesion had progressed to occlusion (Figure 1A). Therefore, the patient was referred to this department for surgery. Upon acetazolamide-loading single-photon-emission computed tomography (Diamox SPECT), the left front parietotemporal reserve was diminished (Figure 1C). In addition, the transfemoral cerebral angiography (TFCA) revealed a thin left STA with a weak flow but a prominent OA (Figure 1B).

Case 2: An MRI showed a right MCA territory infarction due to right MCA occlusion. After three months of conservative treatment, a follow-up perfusion MRI exhibited worsening cerebral perfusion

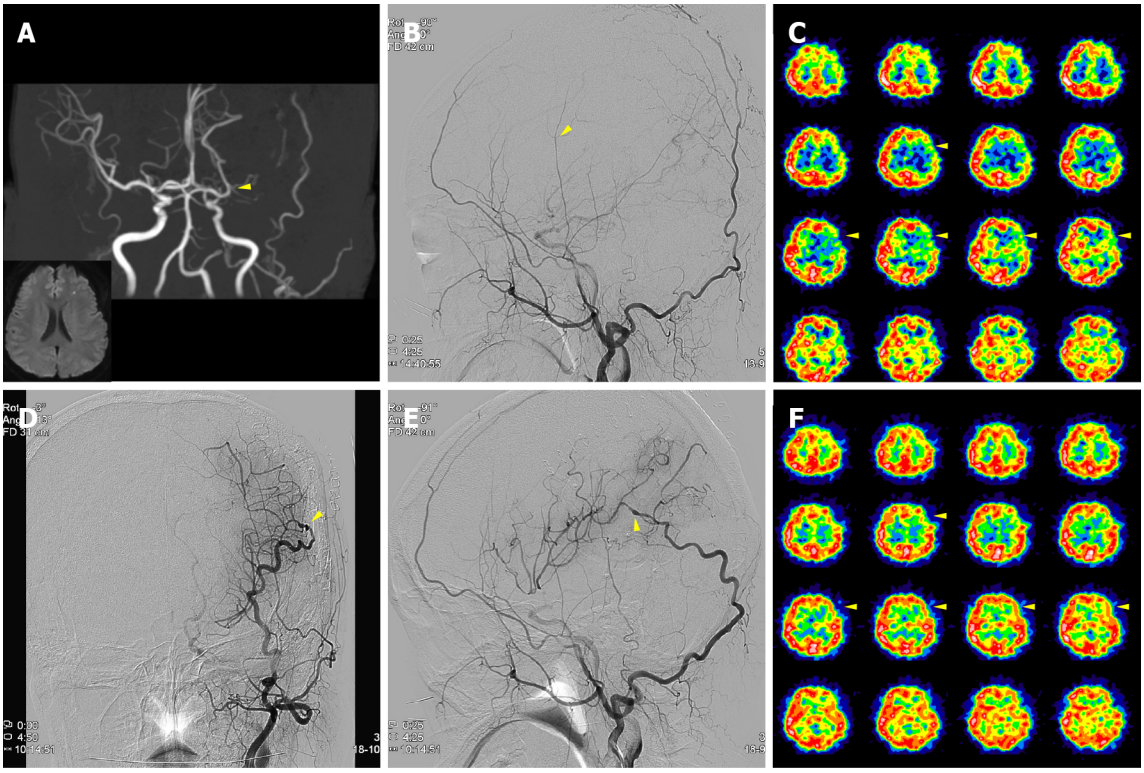

DOI: 10.12998/wjcc.v11.i9.2091

Figure 1 Case 1 perioperative imaging. A: Initial magnetic resonance imaging indicated a small left frontal infarction from the left middle cerebral artery (MCA) stenosis (yellow arrow); B: On the transfemoral cerebral angiography (TFCA), the left superficial temporal artery was thin with weak flow (yellow arrow); however, the occipital artery (OA) was prominent (black arrows); C-F: After the OA-MCA bypass, blood flow at the surgical site was intact on postoperative TFCA (D and E; yellow arrow), with a perfusion defect improvement on postoperative Diamox SPECT compared with the preoperative scan (C and F; yellow arrows).

throughout the MCA territory (Figure 2C). On TFCA, the right STA was noticeably thin with a weak flow, yet the OA was prominent (Figure 2A and B).

FINAL DIAGNOSIS

The authors diagnosed the patients with symptomatic steno-occlusive MCA infarction by combining imaging and clinical findings.

TREATMENT

Thus, OA-MCA bypass surgery was decided in both cases. The OA and MCA were end-to-side anastomosed.

OUTCOME AND FOLLOW-UP

Case 1

After bypass, blood flow at the surgical site was intact (Figure 1D and E), with perfusion defect improvement on the postoperative Diamox SPECT (Figure 1F). The patient was discharged without symptoms in a weak and has not experienced any follow-up care complications one year after surgery.

Case 2

After bypass, blood flow at the surgical site was intact (Figure 2D and E), with perfusion defect improvement on the postoperative perfusion MRI (Figure 2F). The patient was discharged without any symptom aggravations in a weak and has not experienced any follow-up care complications one year after surgery.

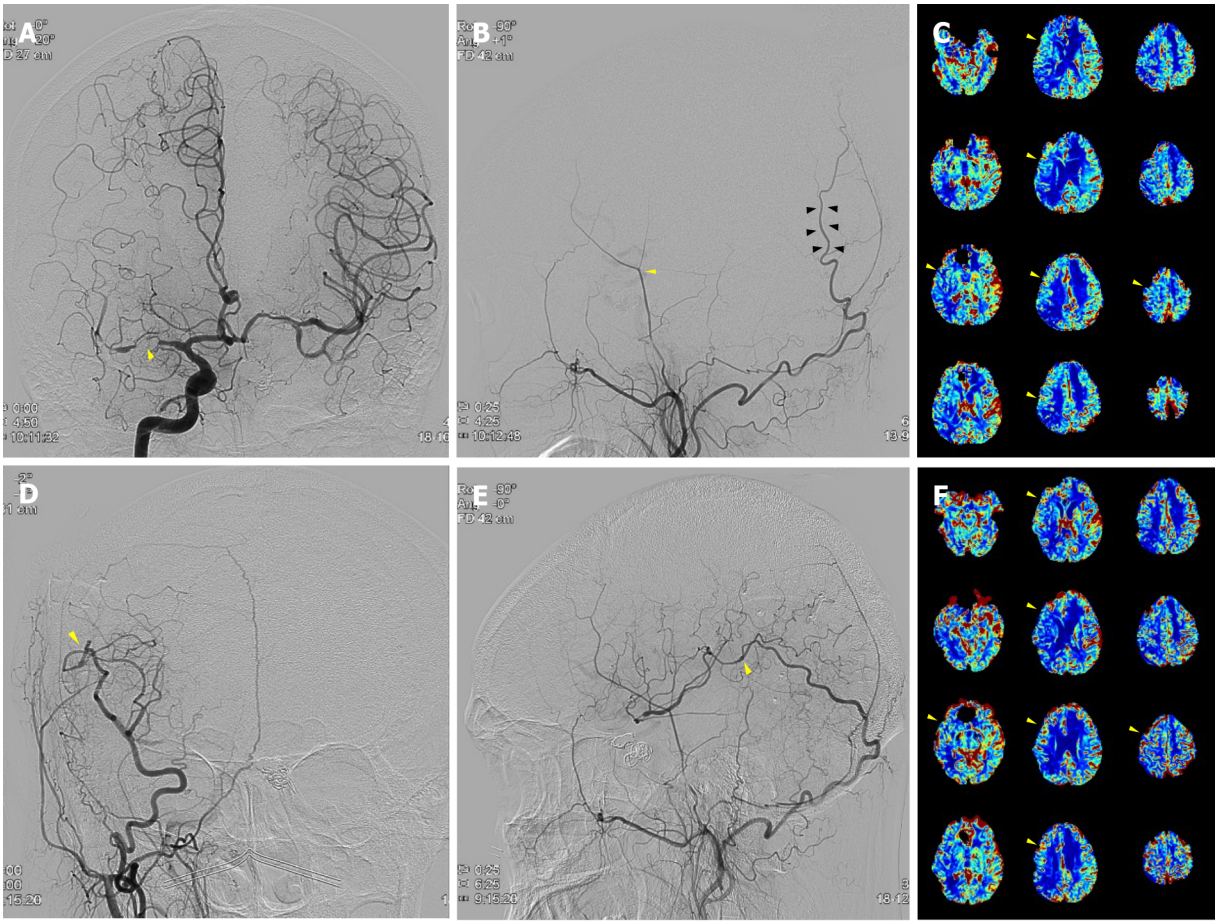

DOI: 10.12998/wjcc.v11.i9.2091

Figure 2 Case 2 perioperative imaging. A: Initial transfemoral cerebral angiography (TFCA) indicated right middle cerebral artery (MCA) occlusion (yellow arrow); b: The right superficial temporal artery was thin with weak flow (yellow arrow); however, the occipital artery (OA) was prominent (black arrows); C-F: After the OA-MCA bypass, blood flow at the surgical site was intact on postoperative TFCA (D and E; yellow arrows), with a perfusion defect improvement on postoperative perfusion magnetic resonance imaging compared with the preoperative scan (C and F; yellow arrows).

DISCUSSION

The cerebrovascular steno-occlusive disease can cause acute cerebral infarction or transient ischemic accident (TIA) symptoms. An unstable TIA can originate from decreased cerebral perfusion; therefore, immediate and adequate blood supply is the most crucial consideration in bypass surgery. STA-MCA bypass is a relatively simple and efficient surgical modality, especially for cerebrovascular occlusive diseases with a high patency rate during a short period. However, the STA is inaccessible for bypass in cases of previous operations, injuries, or atrophy. In this condition, interposition graft surgery is considered. The graft technique is more complex and requires additional anastomosis, increasing operation difficulty and requiring more time. However, there are disadvantages to this technique, such as donor site complications and size discrepancy-related graft failure. Moreover, there is a hyperperfusion syndrome risk if the donor artery is large[3].

Direct OA bypass can be an alternative to the interposition graft with the advantage of arterial graft use. In cases 1 and 2 presented here, the OA was selected as an alternative because the STA was too thin. Direct OA-MCA bypass for ischemic stroke has rarely been reported in literature[4-7]. OA is a frequently used donor artery for trapping and bypassing aneurysm surgeries arising from posterior circulation. Meanwhile, bypass from the OA to the MCA is not commonly performed because of its technical difficulties. The OA is more onerous to harvest than the STA because it passes through several tortuous layers[8].

Successful OA-MCA bypass techniques

In the three-quarter position, the retrosigmoid area was at the top, and the vertex was slightly raised to reduce venous pressure (Figure 3A). After marking the OA path, as confirmed through angiography and fingertip palpation, a microscopy-guided incision was made on the OA course (Figure 3A). The artery was located, and the soft tissue was bluntly dissected. Small OA branches were identified and cut after meticulous cauterization. The proximal part was secured through dissection to where the OA

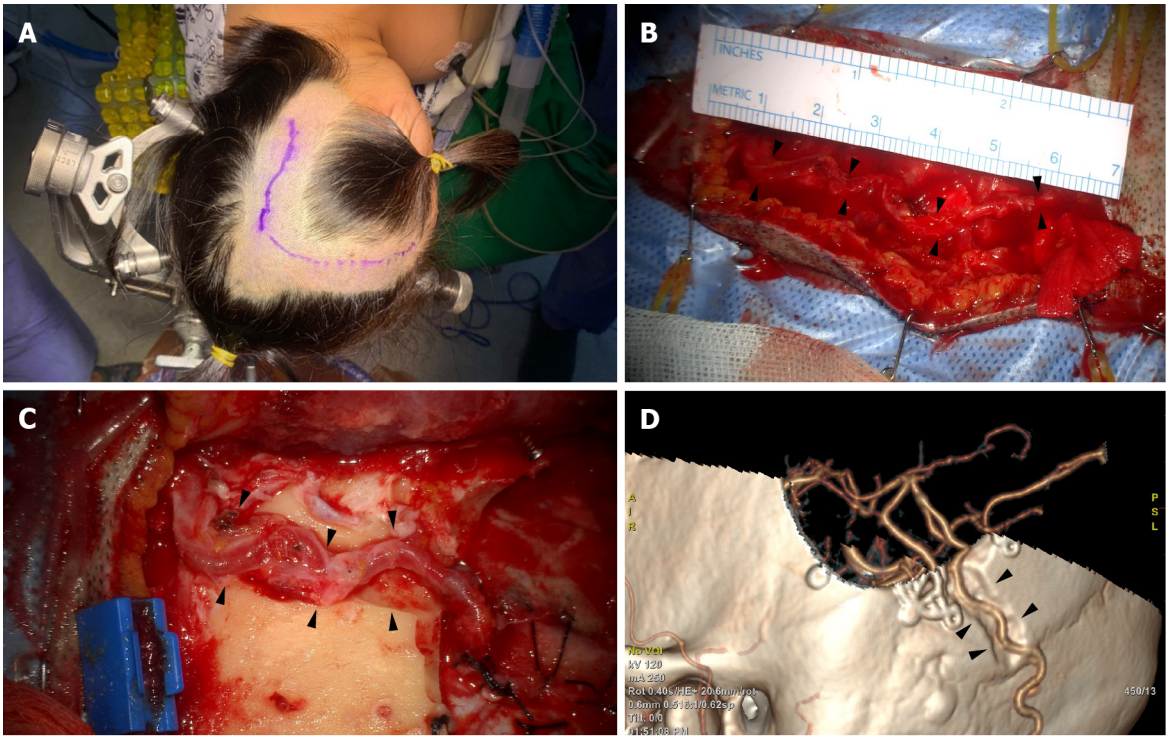

DOI: 10.12998/wjcc.v11.i9.2091

Figure 3 Occipital artery-middle cerebral artery bypass surgical position and incision. A: In the three-quarter position, the retrosigmoid area was at the top, and the vertex was slightly raised. The occipital artery (OA) course was confirmed through angiography with fingertip palpating. An incision was created consecutively at the craniotomy site for the recipient artery; B: The OA's main artery had a very tortuous course (black arrows); therefore, the soft tissue was dissected along the bend to secure the stretched curve's full length to the recipient site, at least 7 cm; C and D: To prevent donor artery compression in the supine position, a route between the craniotomy site and OA's proximal part was cut to create a sough (black arrows).

penetrated the splenius capitis muscle. The large branch in the main artery's subgaleal portion was likely to be used for a second anastomosis and could be cleaned of the donor artery to ensure its preservation to the greatest extent[9]. The splenius capitis muscle was incised along the OA. Free space was secured by dissecting and retracting the muscle, creating a vascular groove. The descending branch that supplies blood flow to the suboccipital muscle was preserved as much as possible; however, if OA's full length was not long enough, it was selectively cut after ligation. A length sufficient for MCA bypass is approximately 7 cm above the proximal stump, which is just below the superior nuchal line (Figure 3B). However, this varies depending on OA functionality and condition.

The posterior Sylvian fissure area should be exposed to access the donor artery for MCA bypass[5]. The incision was extended according to the recipient's target craniotomy location. To achieve an MCA bypass, the skull was exposed enough to incise the skin by anteriorly turning it vertically along the superior temporal line. If the OA was bent superomedially, a separate incision was conducted in the temporal region for craniotomy of the recipient artery. Following this, the OA can be passed through the subcutaneous tunnel for an OA-MCA bypass[5]. To prevent donor artery compression in the supine position, a route between the craniotomy site and the OA's proximal part was cut to create a sough (Figure 3C and D). Particular caution was exercised on the secured OA when making the furrow. Small fabrics were not typically placed around the drill. An end-to-side anastomosis was performed with nylon 10-0 in the recipient artery, such as the angular artery. As the OA had a tortuous path, the surgeon did not point the anastomotic end in a direction that twisted the blood vessel. The recipient artery was a peripheral artery and thinner than the M4 used for STA-MCA bypass. Therefore, the arteriotomy must be slightly longer than the STA-MCA bypass to match the anastomosis length accurately. With these points in mind, the authors successfully performed a less invasive bypass surgery.

A particular postoperative wound necrosis risk is possible due to insufficient collateral superficial blood circulation if an ipsilateral bypass surgery has been performed previously[10]. In patients who have undergone the indirect bypass alone, additional surgery might worsen the overlying scalp's blood circulation, resulting in ischemia in the existing bypass area. Therefore, accurate confirmation is necessary for the donor artery course based on preoperative imaging tests, including angiography, and to minimize collateral blood vessel damage during skin incision and dissection.

The recipient artery choice is controversial. Bypassing at the best location is vital for improving the patient's symptoms; however, it might be preferred to select a nearby artery considering the OA's available length. Hirano *et al*. have proposed two incision methods to approach the recipient artery

regarding the OA's travel direction and distance to the recipient artery: an extension of the OA incision and an additional incision, respectively[5]. The recipient artery was accessed through a single incision in the cases presented here. When an OA of sufficient length is harvested, bypass surgery can be performed less invasively without additional incision. This is also advantageous from a cosmetic point of view.

CONCLUSION

In cases where the STA is unsuitable in cerebral ischemic disease or progressive ischemia of the MCA territory, OA may be an acceptable donor artery for less invasive extracranial-intracranial bypass surgery.

FOOTNOTES

Author contributions: Joo SP performed the operation and evaluated patients; Hong JH wrote the manuscript (first author); Joo SP and Kim TS provided writing assistance; Ryu HS and Jung SC evaluated and reviewed the chart.

Supported by a grant from Chonnam National University Hospital Biomedical Research Institute, No. BCRI22053.

Informed consent statement: Informed written consent was obtained from the patient for publication of this report and any accompanying images.

Conflict-of-interest statement: The authors declare that they have no potential or actual conflicts of interest regarding this article.

CARE Checklist (2016) statement: The authors have read the CARE Checklist (2016), and the manuscript was prepared and revised following the CARE Checklist (2016).

Country/Territory of origin: South Korea

ORCID number: Jong-Hwan Hong 0000-0002-7864-1145; Sung-Pil Joo 0000-0002-4983-0174.

S-Editor: Yan JP
L-Editor: A
P-Editor: Yan JP

REFERENCES

1 **Hanakita S**, Lenck S, Labidi M, Watanabe K, Bresson D, Froelich S. The Occipital Artery as an Alternative Donor for Low-Flow Bypass to Anterior Circulation After Internal Carotid Artery Occlusion Failure prior to Exenteration for an Atypical Cavernous Sinus Meningioma. *World Neurosurg* 2018; **109**: 10-17 [PMID: 28887285 DOI: 10.1016/j.wneu.2017.08.181]
2 **Yasargil MG**, Yonekawa Y. Results of microsurgical extra-intracranial arterial bypass in the treatment of cerebral ischemia. *Neurosurgery* 1977; **1**: 22-24 [PMID: 615948 DOI: 10.1227/00006123-197707000-00005]
3 **Stiver SI**, Ogilvy CS. Acute hyperperfusion syndrome complicating EC-IC bypass. *J Neurol Neurosurg Psychiatry* 2002; **73**: 88-89 [PMID: 12082061 DOI: 10.1136/jnnp.73.1.88]
4 **Kimura T**, Morita A. Occipital Artery to Middle Cerebral Artery Bypass: Operative Nuances. *World Neurosurg* 2017; **108**: 201-205 [PMID: 28870823 DOI: 10.1016/j.wneu.2017.08.126]
5 **Hirano T**, Mikami T, Suzuki H, Hirano T, Kimura Y, Komatsu K, Akiyama Y, Wanibuchi M, Mikuni N. Occipital Artery to Middle Cerebral Artery Bypass in Cases of Unavailable Superficial Temporal Artery. *World Neurosurg* 2018; **112**: 101-108 [PMID: 29371165 DOI: 10.1016/j.wneu.2018.01.103]
6 **Zenonos GA**, Morcos JJ. Occipital to Angular Artery Bypass for Post-irradiation Ischemia: 3-Dimensional Operative Video. *Oper Neurosurg (Hagerstown)* 2020; **18**: E78 [PMID: 31173139 DOI: 10.1093/ons/opz125]
7 **Chung Y**, Lee SH, Ryu J, Kim J, Chung SB, Choi SK. Tailored Double-Barrel Bypass Surgery Using an Occipital Artery Graft for Unstable Intracranial Vascular Occlusive Disease. *World Neurosurg* 2017; **101**: 813.e5-813.e9 [PMID: 28323188 DOI: 10.1016/j.wneu.2017.03.043]

8 **Alvernia JE**, Fraser K, Lanzino G. The occipital artery: a microanatomical study. *Neurosurgery* 2006; **58**: ONS114-22; discussion ONS114 [PMID: 16543868 DOI: 10.1227/01.NEU.0000193519.00443.34]
9 **Funaki T**, Takahashi JC, Takagi Y, Yoshida K, Araki Y, Kikuchi T, Kataoka H, Iihara K, Miyamoto S. Impact of posterior cerebral artery involvement on long-term clinical and social outcome of pediatric moyamoya disease. *J Neurosurg Pediatr* 2013; **12**: 626-632 [PMID: 24138143 DOI: 10.3171/2013.9.PEDS13111]
10 **Takanari K**, Araki Y, Okamoto S, Sato H, Yagi S, Toriyama K, Yokoyama K, Murotani K, Matsui S, Wakabayashi T, Kamei Y. Operative wound-related complications after cranial revascularization surgeries. *J Neurosurg* 2015; **123**: 1145-1150 [PMID: 26140494 DOI: 10.3171/2014.12.JNS132602]

World Journal of Clinical Cases

Submit a Manuscript: https://www.f6publishing.com

World J Clin Cases 2023 March 26; 11(9): 2098-2103

DOI: 10.12998/wjcc.v11.i9.2098

ISSN 2307-8960 (online)

CASE REPORT

Anesthetic management of a patient with preoperative R-on-T phenomenon undergoing laparoscopic-assisted sigmoid colon resection: A case report

Xiao-Xi Li, Yun-Feng Yao, Hong-Yu Tan

Specialty type: Anesthesiology

Provenance and peer review: Unsolicited article; Externally peer reviewed.

Peer-review model: Single blind

Peer-review report's scientific quality classification

Grade A (Excellent): 0
Grade B (Very good): B, B
Grade C (Good): 0
Grade D (Fair): 0
Grade E (Poor): 0

P-Reviewer: Kvolik S, Croatia; Yamada T, United States

Received: December 26, 2022
Peer-review started: December 26, 2022
First decision: January 12, 2023
Revised: January 18, 2023
Accepted: February 21, 2023
Article in press: February 21, 2023
Published online: March 26, 2023

Xiao-Xi Li, Hong-Yu Tan, Department of Anesthesiology, Peking University Cancer Hospital & Institute, Beijing 100142, China

Yun-Feng Yao, Department of Unit III & Ostomy Service, Gastrointestinal Cancer Center, Peking University Cancer Hospital & Institute, Beijing 100142, China

Corresponding author: Hong-Yu Tan, MD, PhD, Chief Doctor, Professor, Department of Anesthesiology, Peking University Cancer Hospital & Institute, No. 52 Fucheng Street, Haidian District, Beijing 100142, China. maggitan@yeah.net

Abstract

BACKGROUND

The R-on-T phenomenon is a malignant arrhythmia associated with potentially catastrophic consequences. It may initiate ventricular tachycardia or ventricular fibrillation, which can result in syncope or sudden cardiac death. This manifestation poses a great challenge for anesthesiologists. However, it is rarely encountered in the perioperative setting.

CASE SUMMARY

We herein present a case in which the R-on-T phenomenon was incidentally revealed by 24-h Holter monitoring in a patient diagnosed with sigmoid colon cancer. Careful evaluation and treatment with mexiletine were carried out preoperatively under consultation with a cardiovascular specialist, and surgery was uneventfully performed under general anesthesia after thorough preparation.

CONCLUSION

Physicians should be vigilant about this infrequent but potentially fatal arrhythmia. Our experience suggests that the anesthetic process can be greatly optimized with careful preparation.

Key Words: R-on-T phenomenon; Premature ventricular contraction; Sigmoid colon cancer; Sigmoid colon resection; General anesthesia; Case report

Core Tip: The R-on-T phenomenon is associated with an increased risk of fatal arrhythmia. It may initiate ventricular tachycardia and ventricular fibrillation, and its appearance seem to be associated with a poor prognosis. However, this phenomenon is rarely encountered in the preoperative inpatient setting. The anesthetic management of patients with this particular manifestation poses a great challenge. We herein describe a patient who was scheduled for laparoscopic-assisted sigmoid colon resection when the R-on-T phenomenon was incidentally discovered. Our experience suggests that the anesthetic process can be greatly optimized by detailed preoperative assessment and preparation with interdisciplinary cooperation.

Citation: Li XX, Yao YF, Tan HY. Anesthetic management of a patient with preoperative R-on-T phenomenon undergoing laparoscopic-assisted sigmoid colon resection: A case report. *World J Clin Cases* 2023; 11(9): 2098-2103
URL: https://www.wjgnet.com/2307-8960/full/v11/i9/2098.htm
DOI: https://dx.doi.org/10.12998/wjcc.v11.i9.2098

INTRODUCTION

The R-on-T phenomenon was first reported by Smirk[1], who described it as R waves interrupting T waves. The R-on-T phenomenon may initiate ventricular tachycardia (VT), torsade de pointes, and ventricular fibrillation (VF)[2-5]. This phenomenon is associated with an increased risk of fatal arrhythmia. The anesthetic management of patients with this particular manifestation poses a great challenge. However, the R-on-T phenomenon is seldom encountered in the preoperative inpatient setting. We found no report describing the anesthetic management of patients with a preoperative electrocardiographic (ECG) manifestation of R-on-T, and there is an extreme lack of experience to which clinicians can refer.

We herein present a case of successful anesthetic management in a patient who was incidentally found to have the R-on-T phenomenon before undergoing laparoscopic-assisted sigmoid colon resection. We also discussed the cause of the appearance of the R-on-T phenomenon and the main issue requiring special precaution during perioperative anesthetic management.

CASE PRESENTATION

Chief complaints

A 69-year-old man was diagnosed with a sigmoid colon mass during a physical examination.

History of present illness

The patient had undergone a colonoscopy 20 d previously, and a sigmoid colon mass was discovered. The diagnosis of sigmoid colon cancer was considered based on pathological biopsy findings. The patient was admitted to our hospital for sigmoid colon resection.

History of past illness

The patient had been previously diagnosed with a congenital ventricular septal defect, and he had a history of fundus hemorrhage 3 years previously. He had been undergoing treatment with Chinese patent medicine containing *Panax notoginseng saponins* as well as *Aescuven forte* until 1 mo before presentation to our hospital. He had no history of other systemic diseases such as hypertension, diabetes mellitus, or coronary heart disease.

Personal and family history

The patient had a 50-year smoking history. He had undergone an open appendectomy 5 years previously. His brother was diagnosed with colon cancer.

Physical examination

Physical examination revealed no obvious abnormalities except for an old appendiceal incision scar.

Laboratory examinations

Preoperative laboratory results, including a full blood cell count, blood biochemistry (including electrolytes), and coagulation tests, were unremarkable except for a slightly elevated fibrinogen concentration of 456.3 mg/dL and uric acid concentration of 455 μmol/L.

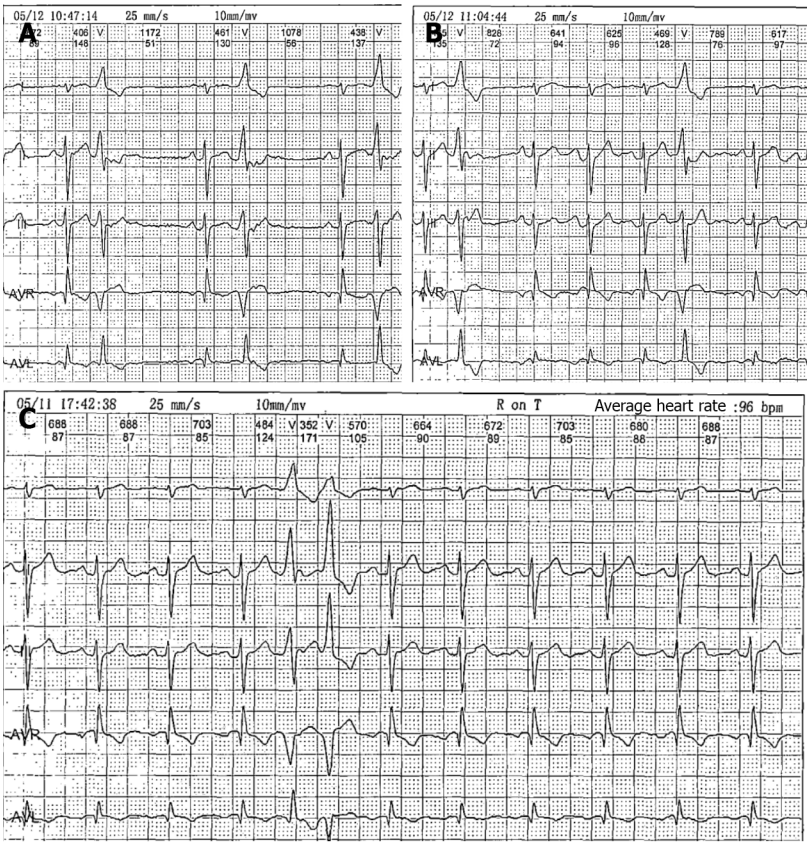

DOI: 10.12998/wjcc.v11.i9.2098

Figure 1 Twenty-four-hour Holter monitoring taken 3 d before surgery showing premature ventricular contractions and the R-on-T phenomenon. A and B: Premature ventricular contractions; C: The R-on-T phenomenon.

Imaging examinations

Chest X-ray findings and abdominal computed tomography (CT) findings were unremarkable. A transthoracic echocardiogram showed minor regurgitation of the aortic, mitral, and tricuspid valves; reduced left ventricular diastolic function; and an ejection fraction of 62%. Notably, 24-h Holter monitoring performed 2 d earlier revealed occasional atrial premature beats and frequent premature ventricular contractions (PVCs). The PVCs consisted of 7.5% of the total daily beats (8803 per day), partially occurred in pairs, and occasionally occurred in bigeminy and trigeminy; Twenty-five R-on-T phenomena were revealed (Figure 1).

MULTIDISCIPLINARY EXPERT CONSULTATION

During pre-anesthetic assessment the day before surgery, the patient denied any history of palpitations, dizziness, syncope, or any symptoms of angina. He stated that his ventricular septal defect was minimal and required no medication or surgical treatment and that his physical activity was not limited. His relatives provided the results of coronary artery CT and exercise myocardial perfusion imaging that had been performed 18 mo previously. The coronary artery CT showed a minimal periventricular septal defect with no hemodynamic effects as well as calcification of the left anterior descending artery, circumflex branch artery, and right coronary artery; the images were negative for arterial stenosis. The exercise myocardial perfusion imaging revealed no definite evidence of myocardial ischemia.

FINAL DIAGNOSIS

The final diagnoses were sigmoid colon cancer, congenital ventricular septal defect, and arrhythmia.

TREATMENT

Surgical procedure

The patient was scheduled for laparoscopic-assisted sigmoid colon resection under general anesthesia. Myocardial enzyme and electrolyte measurements and continuous ECG monitoring were advised for further evaluation by the anesthesiologist, and a cardiovascular specialist was invited for consultation. All laboratory results were normal. The cardiovascular specialist suggested the administration of mexiletine at 150 mg three times daily and continuous infusion of lidocaine during surgery, and he advised that a defibrillator should be prepared in advance. The surgery was scheduled 1 day after the consultation, and a total of 450 mg of mexiletine was administered preoperatively. The patient underwent continuous bedside ECG monitoring. His heart rate (HR) remained between 67 and 81 bpm. There was a slight trend of slowing of the HR compared with his previous 24-h Holter monitoring (average HR, 84 bpm). There was no sign of QT prolongation. PVCs occurred during observation. However, the patient reported no discomfort.

Management of general anesthesia

Standard monitoring on the day of the operation included measurement of the patient's arterial blood pressure (ABP), ECG, SpO_2, bispectral index, and arterial blood gas analysis. Monitoring of cardiac function by a FloTrac system (Edwards Lifesciences, Irvine, CA, United States) was also performed. The patient was in stable condition with a HR of 72 bpm, ABP of 155/80 mmHg, and SpO_2 of 99% on room air. The ECG monitoring revealed that the number of PVCs had markedly decreased (approximately two PVCs within 10 min), and no R-on-T phenomenon was observed. The results of the arterial blood gas analysis were within normal range (pH, 7.43; potassium, 4.2 mmol/L; calcium, 1.19 mmol/L; glucose, 5.5 mmol/L). Defibrillation electrode slices were placed on the patient, and rescue medications were prepared. He was premedicated with 5 mg of dexamethasone. After preoxygenation, anesthesia was induced with 20 μg of sufentanil, 40 mg of lidocaine, 20 mg of etomidate, 80 mg of propofol, and 20 mg of cisatracurium. Esmolol (20 mg) was administered at the time of intubation to inhibit the stress response of endotracheal intubation. The patient was intubated successfully with the GlideScope video laryngoscope (Verathon, Bothell, WA, United States). Anesthesia was maintained with propofol, remifentanil, and sevoflurane. Muscle relaxation was achieved with intermittent administration of cisatracurium. Lidocaine was continuously administered at a speed of 40 mg/h throughout the surgery. During surgery, 6 mg of ephedrine was administered once to correct hypotension when the ABP had fallen to 100/60 mmHg. The patient's ABP was maintained at 100-168/60-82 mmHg, and his HR remained between 55 and 88 bpm. An arterial blood gas analysis performed 1 h after the beginning of surgery showed a pH of 7.33, partial pressure of carbon dioxide of 48 mmHg, and all electrolyte levels within the reference ranges. The ventilator parameters were adjusted according to these results to maintain normal acid base balance and electrolyte levels. His cardiac output and stroke volume variation as monitored by the FloTrac system were within normal limits during surgery. Fluid therapy was directed according to his HR, ABP, cardiac output, and stroke volume variation. Infusion heating and a forced air warmer were used to maintain his body temperature. Occasional PVCs occurred, but the patient was otherwise stable. The amount of bleeding during surgery was 50 mL.

OUTCOME AND FOLLOW-UP

The patient's surgery and remaining hospital stay were uneventful. He was discharged home in a stable state on postoperative day 6.

DISCUSSION

The appearance of the R-on-T phenomenon is associated with an increased risk of syncope and sudden cardiac death. The literature shows that the R-on-T phenomenon can be triggered by myocardial damage, reperfusion injury after revascularization, electrolyte imbalance (especially hypokalemia), or hypothermia[1]. In rare cases, the administration of antibiotics can also cause the R-on-T phenomenon [6]. Among all causes, cardiac ischemia and cardiac infarction are most common. A detailed preoperative anesthetic assessment with emphasis on the cardiovascular system is important. Previous cardiac assessment and examinations are helpful for comparison with current data. In the present case, the definitive cause of the R-on-T phenomenon was unclear. Although the patient had a congenital ventricular septal defect, the defect was minimal and had no hemodynamic effects. He had no history of coronary heart disease and no evidence of cardiac ischemia. He was not taking any medication presently and had no electrolyte imbalances. Therefore, we considered the possibility that his arrhythmia was idiopathic.

PVCs, especially with the R-on-T phenomenon, can initiate VT or VF[7-9]. The PVCs that precede VF are considered to trigger the VF episodes in arrhythmic storm. VF recurrence can be avoided by suppressing these PVCs using drugs, pacing, or ablation. The risk of the R-on-T phenomenon can be eliminated or greatly diminished by treatment with antiarrhythmic drugs[1,10,11]. In the present study, the patient was medically treated with the class Ib antiarrhythmic agent mexiletine, and he appeared to respond well to mexiletine based on the fact that the number of PVCs was significantly reduced and the R-on-T phenomenon disappeared on his arrival to the operating room. The literature shows that the application of cardiac resynchronization therapy and catheter ablation can also be an effective remedy when drug therapy is unsatisfactory[9,10,12,13].

The patient had a favorable prognosis in the present case; this was attributed to a detailed preoperative assessment and preparation with interdisciplinary cooperation among the surgery, anesthesiology, and cardiovascular departments. Full preparation including elaborate monitoring, rescue medications, and a readily available defibrillator prepared in advance are crucial to decrease patient risk. We placed defibrillation electrode slices on the patient before anesthetic induction in case of VT or VF. Continuous lidocaine infusion can be used for both prophylaxis and treatment of ventricular arrhythmia. All factors that can deteriorate the arrhythmia, including hemodynamic instability, fluid and electrolyte imbalances (meticulous electrolyte control is important especially during laparoscopic surgeries), and hypothermia, should be avoided. Induction drugs that are less likely to cause hypotension, such as etomidate, are preferred. Avoidance of fluid and electrolyte imbalances is essential. Goal-directed fluid therapy is instructive. Insulation measures, including the use of infusion heating and forced air warmers, should also be applied to prevent hypothermia.

CONCLUSION

The R-on-T phenomenon is rarely encountered in the perioperative setting. Physicians should be vigilant about this infrequent but potentially fatal arrhythmia. The perioperative anesthetic management of patients with this manifestation can be challenging. However, our experience suggests that the anesthetic process can be greatly optimized with careful evaluation, multidisciplinary consultation, and thorough preparation.

FOOTNOTES

Author contributions: Li XX conceived the study and wrote the manuscript; Yao YF participated in the diagnosis and treatment of the patient; Tan HY supervised the study; all authors have read and approved the final manuscript.

Informed consent statement: Informed written consent was obtained from the patient for publication of this report and any accompanying images.

Conflict-of-interest statement: The authors declare that they have no conflict of interest to disclose.

CARE Checklist (2016) statement: The authors have read the CARE Checklist (2016), and the manuscript was prepared and revised according to the CARE Checklist (2016).

Country/Territory of origin: China

ORCID number: Hong-Yu Tan 0000-0002-8721-5068.

S-Editor: Yan JP
L-Editor: A
P-Editor: Yan JP

REFERENCES

1 **Smirk FH**. R waves interrupting T waves. *Br Heart J* 1949; **11**: 23-36 [PMID: 18113467 DOI: 10.1136/hrt.11.1.23]
2 **Schulman PM**, Merkel MJ, Rozner MA. Accidental, unintentional reprogramming of a temporary external pacemaker leading to R-on-T and cardiac arrest. *J Cardiothorac Vasc Anesth* 2013; **27**: 944-948 [PMID: 22959843 DOI:

10.1053/j.jvca.2012.07.013]
3 **Ergul Y**, Kafali HC, Uysal F. Accelerated idioventricular rhythm resulting in torsades de pointes and cardiac arrest in a child: successfully cryoablated in left'coronary cusp. *Cardiol Young* 2020; **30**: 418-421 [PMID: 31858927 DOI: 10.1017/S1047951119002993]
4 **Cho J**, Afolabi B. Ventricular fibrillation associated with Graves' disease and amiodarone induced thyrotoxicosis. *Cardiovasc Endocrinol Metab* 2019; **8**: 119-124 [PMID: 31942554 DOI: 10.1097/XCE.0000000000000184]
5 **Marume K**, Ishibashi K, Noda T, Ohta-Ogo K, Yasuda S, Kusano K. Short coupled Torsade de pointes with myocardial injury: A possible sequela of myocarditis. *J Cardiol Cases* 2019; **19**: 62-65 [PMID: 31193697 DOI: 10.1016/j.jccase.2018.10.004]
6 **Anyfantakis D**, Makrakis G. R on T Phenomenon and Long QTc Syndrome due to Moxifloxacin in a Healthy Female. *P R Health Sci J* 2019; **38**: 196-197 [PMID: 31536636]
7 **Oksuz F**, Sensoy B, Sahan E, Sen F, Baser K, Cetin H, Unal S, Ozeke O, Topaloglu S, Aras D. The classical "R-on-T" phenomenon. *Indian Heart J* 2015; **67**: 392-394 [PMID: 26304578 DOI: 10.1016/j.ihj.2015.02.030]
8 **Nakamori Y**, Maeda T, Ohnishi Y. Reiterative ventricular fibrillation caused by R-on-T during temporary epicardial pacing: a case report. *JA Clin Rep* 2016; **2**: 3 [PMID: 29497660 DOI: 10.1186/s40981-016-0029-6]
9 **Lasocka Z**, Dąbrowska-Kugacka A, Lewicka E, Liżewska-Springer A, Królak T. Successful Catheter Ablation of the "R on T" Ventricular Fibrillation. *Int J Environ Res Public Health* 2021; **18** [PMID: 34574512 DOI: 10.3390/ijerph18189587]
10 **Vyas A**, Lokhandwala Y. Coronary sinus as a site for stable temporary atrial pacing to tide over premature ventricular complex-triggered recurrent ventricular fibrillation in a patient with severe left ventricular dysfunction after coronary bypass surgery. *Indian Heart J* 2018; **70** Suppl 3: S483-S485 [PMID: 30595312 DOI: 10.1016/j.ihj.2018.07.012]
11 **Sánchez Muñoz JJ**, García-Alberola A, Martínez-Sánchez J, Peñafiel-Verdú P, Caro-Martínez C, Manzano-Fernández S, Valdés Chávarri M. Premature ventricular complexes as a trigger for ventricular fibrillation. *Rev Esp Cardiol* 2010; **63**: 798-801 [PMID: 20609313 DOI: 10.1016/s1885-5857(10)70164-x]
12 **Jeon DS**, Park JS. Rapid and Potent Antiarrhythmic Effect of Cardiac Resynchronization Therapy in a Patient with Advanced Dilated Cardiomyopathy and a Large Ventricular Arrhythmia Burden. *Korean Circ J* 2017; **47**: 523-527 [PMID: 28765745 DOI: 10.4070/kcj.2016.0361]
13 **Katis G**, Wiles B, Saba MM. Short-coupled ventricular ectopics leading to cardiac arrest in a young woman. *Egypt Heart J* 2022; **74**: 32 [PMID: 35467248 DOI: 10.1186/s43044-022-00272-y]

World Journal of Clinical Cases

Submit a Manuscript: https://www.f6publishing.com

World J Clin Cases 2023 March 26; 11(9): 2104-2109

DOI: 10.12998/wjcc.v11.i9.2104

ISSN 2307-8960 (online)

CASE REPORT

Pembrolizumab combined with axitinib in the treatment of skin metastasis of renal clear cell carcinoma to nasal ala: A case report

Shuai Dong, Yang-Chun Xu, Yuan-Chen Zhang, Jian-Xin Xia, Yan Mou

Specialty type: Dermatology

Provenance and peer review: Unsolicited article; Externally peer reviewed.

Peer-review model: Single blind

Peer-review report's scientific quality classification

Grade A (Excellent): 0
Grade B (Very good): 0
Grade C (Good): C, C
Grade D (Fair): 0
Grade E (Poor): 0

P-Reviewer: Bal'afif F, Indonesia; Sedaghattalab M, Iran

Received: January 4, 2023
First decision: January 20, 2023
Revised: January 28, 2023
Accepted: February 27, 2023
Article in press: February 27, 2023
Published online: March 26, 2023

Shuai Dong, Yang-Chun Xu, Yuan-Chen Zhang, Jian-Xin Xia, Yan Mou, Department of Dermatology, The Second Hospital of Jilin University, Changchun 130041, Jilin Province, China

Corresponding author: Yan Mou, Doctor, MD, PhD, Associate Professor, Senior Consultant Dermatologist, Department of Dermatology, The Second Hospital of Jilin University, No. 218 Ziqiang Street, Changchun 130041, Jilin Province, China. muyan_20031017@jlu.edu.cn

Abstract

BACKGROUND

Renal clear cell carcinoma (RCC) is a malignant tumor of the genitourinary system with a predilection for males. The most common metastatic sites are the lung, liver, lymph nodes, contralateral kidney or adrenal gland, however, skin metastasis has only been seen in 1.0%-3.3% of cases. The most common site of skin metastasis is the scalp, and metastasis to the nasal ala region is rare.

CASE SUMMARY

A 55-year-old man with clear cell carcinoma of the left kidney was treated with pembrolizumab and axitinib for half a year after surgery and was found to have a red mass on his right nasal ala for 3 mo. The skin lesion of the patient grew rapidly to the size of 2.0 cm × 2.0 cm × 1.2 cm after discontinuation of targeted drug therapy due to the coronavirus disease 2019 epidemic. The patient was finally diagnosed with skin metastasis of RCC in our hospital. The patient refused to undergo surgical resection and the tumor shrank rapidly after resuming target therapy for 2 wk.

CONCLUSION

It is rare for an RCC to metastasize to the skin of the nasal ala region. The tumor size change of this patient before and after treatment with targeted drugs shows the effectiveness of combination therapy for skin metastasis.

Key Words: Skin metastasis; Renal clear cell carcinoma; Pembrolizumab; Axitinib; Case report

Core Tip: The skin metastasis of renal cell carcinoma can be diagnosed by pathological biopsy and immunohistochemical staining. The patient's history, laboratory examination and imaging examination can assist in the diagnosis. The occurrence of skin metastasis often indicates a poor prognosis, and surgical treatment may improve the prognosis. Our patient refused surgery and returned to targeted drug therapy, resulting in significant improvement in skin lesions.

Citation: Dong S, Xu YC, Zhang YC, Xia JX, Mou Y. Pembrolizumab combined with axitinib in the treatment of skin metastasis of renal clear cell carcinoma to nasal ala: A case report. *World J Clin Cases* 2023; 11(9): 2104-2109
URL: https://www.wjgnet.com/2307-8960/full/v11/i9/2104.htm
DOI: https://dx.doi.org/10.12998/wjcc.v11.i9.2104

INTRODUCTION

It is rare for renal clear cell carcinoma (RCC) to metastasize to the facial region, but dermatologists should be alert to the presence of a facial mass in patients with a history of RCC. Here, we report the diagnosis of this patient in detail and provide our experience for the diagnosis of this kind of disease. In addition, this patient also demonstrated the efficacy of pembrolizumab and axitinib for skin metastasis from renal cancer.

CASE PRESENTATION

Chief complaints

The patient presented to our department due to the tumor on his right nasal ala for three months.

History of present illness

The patient reported that a tumor of 0.3 cm × 0.3 cm × 0.2 cm appeared on his right nasal ala with no significant inducement in January 2022. He felt no pain or itching. There was a small amount of bloody exudation on the surface of the tumor. The diagnosis of granuloma was assigned to the patient and the tumor was treated with CO_2 laser physiotherapy at a local hospital. In March 2022, the tumor recurred and grew up to 2.0 cm × 2.0 cm × 1.2 cm, so the patient presented to our hospital. Since the onset of the tumor, the patient presented no fever, no nausea, no vomiting and no significant loss of body weight.

History of past illness

In January 2017, a tumor was identified in the left kidney of the patient by physical examination. The patient underwent a robot-assisted partial nephrectomy at a local hospital. Postoperative pathological examination showed left RCC. No adjuvant therapy was performed. In July 2021, the patient underwent a left renal radical resection in the local hospital. Postoperative pathological examination revealed left RCC. The tumor volume was 3.5 cm × 3 cm × 2.5 cm. Invasion of renal sinus adipose tissue at the maximum diameter of 0.7 cm was observed, vascular cancer infiltration was seen and fat necrosis nodules with fibrosis and calcification occurred in the surrounding renal tissue, pTNM: T3a (2017 AJCC 8th). August 2021, the positron emission tomography/computed tomography (CT) results displayed left renal cell carcinoma after surgery, the surgical area showed high metabolism, and metastasis was suspected. It was found that metastasis occurred to the left humerus, 1st and 12th thoracic vertebrae. In September 2021, posterior thoracic tumor resection and decompression plus radiofrequency ablation, internal fixation plus nerve root exploration were performed in another hospital. Postoperative pathological results showed broken bone and tumor cell infiltration in fibrous soft tissue, cell nest distribution and some empty cytoplasm, which was consistent with renal cell carcinoma metastasis. Pembrolizumab and axitinib were administered regularly after the operation, however, the treatment was discontinued due to the coronavirus disease 2019 epidemic between March and April 2022.

Personal and family history

The patient has had a history of hypertension for 5 years and smoked for over 30 years. No member of his family has a similar disease.

Physical examination upon admission

The general condition of the patient was fair, the left kidney was deficient. Physical examination showed bilateral renal tenderness and tapping pain negative, thoracic surgery, spinal tenderness and tapping pain negative. Limbs and lung examination showed no obvious abnormalities.

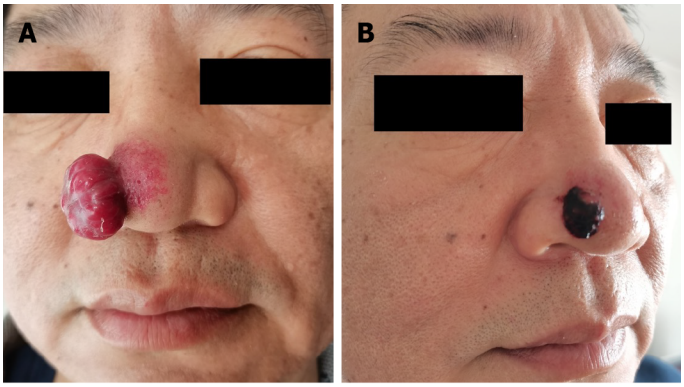

DOI: 10.12998/wjcc.v11.i9.2104

Figure 1 Clinical photograph of the lesion at the initial visit and after resumption of target therapy. A: A 2.0 cm × 2.0 cm × 1.2 cm red mass was seen on the right alar of the nose, with soft texture and clear boundary. A small amount of bloody exudate was seen on the surface. The skin vessels around the mass were hyperplastic and dilated; B: Two weeks after the resumption of combined treatment, the mass was reduced to 0.8 cm × 0.8 cm × 0.5 cm, covered with blood scabs, and the hyperplasia and dilation of skin vessels around the mass decreased.

A tumor of 2.0 cm × 2.0 cm × 1.2 cm was seen on the right nasal ala, there was a small amount of bloody exudation on the surface, and no tenderness (Figure 1A). There was no bleeding in the nasal cavity. The superficial lymph nodes of the whole body were not enlarged.

Imaging examinations

Lung CT showed nodular high-density shadows in each lobe of both lungs, with a size of about 0.2-1.1 cm, and some edges are lobulated, which indicated lung metastasis. Magnetic resonance results showed once surgery and signal changes at the 1st and 2nd thoracic vertebrae and their partial attachment area. Based on the disease history of the patient, tumor metastasis to the vertebrae was suspected. There were 2 suspected tumors in the left head of the humerus and shaft of the humerus. No obvious abnormality was found in the blood routine, coagulation routine, liver and kidney function, thyroid function, myocardial enzyme and electrocardiogram.

Laboratory examinations

There were significant changes in the epidermis, and the tumor cells gathered to form a mass in the dermis, some tumor cells formed a lumen structure. There were a lot of clear cells and abundant blood vessels (Figure 2).

Tumor immune pathology detection: S100-, HMB45-, CK7-, AR-, CK5/6-, CAIX-, Vimentin+, EMA weak+, CD10+, PAX8 weak+, PAX2 weak+ and Ki67 30%+ (Figure 3).

FINAL DIAGNOSIS

Skin metastasis of RCC.

TREATMENT

The proposal for surgical resection of the tumors on the nasal ala was rejected by the patient and the patient also refused to have his suspected bone metastasis or lung metastasis biopsied and treated. The patient resumed his treatment with pembrolizumab and axitinib for 2 wk, and the tumor on his nasal ala shrank to 0.8 cm × 0.8 cm × 0.5 cm (Figure 1B).

OUTCOME AND FOLLOW-UP

200 mg pembrolizumab was administered to the patient through intravenous infusion once every 3 wk combined with axitinib 5 mg twice a day orally. After 8 wk of treatment, the skin lesion was 0.6 cm × 0.6 cm × 0.4 cm. Upon subsequent follow-up, his lesion remained 0.6 cm × 0.6 cm × 0.4 cm and there were no new lesions. Unfortunately, he died of multiple organ failure in December 2022.

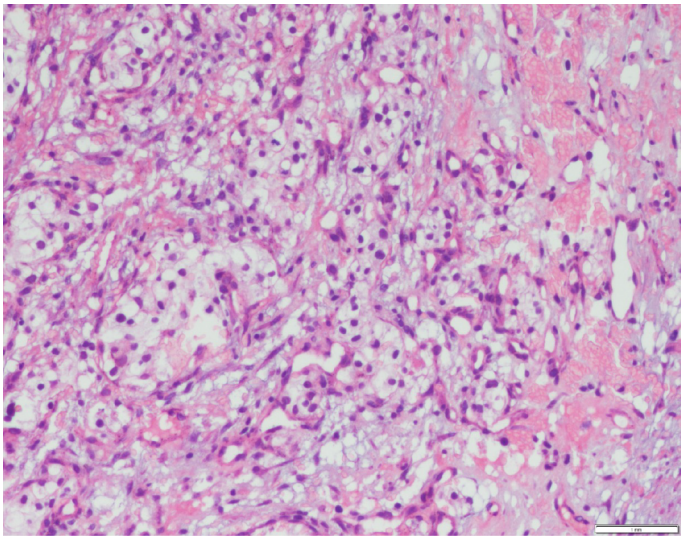

DOI: 10.12998/wjcc.v11.i9.2104

Figure 2 The histopathology of the mass (hematoxylin & eosin staining). Lumplike infiltration of tumor cells was observed in the dermis, some of which formed lumenlike structures with a large number of clear cells and abundant blood vessels.

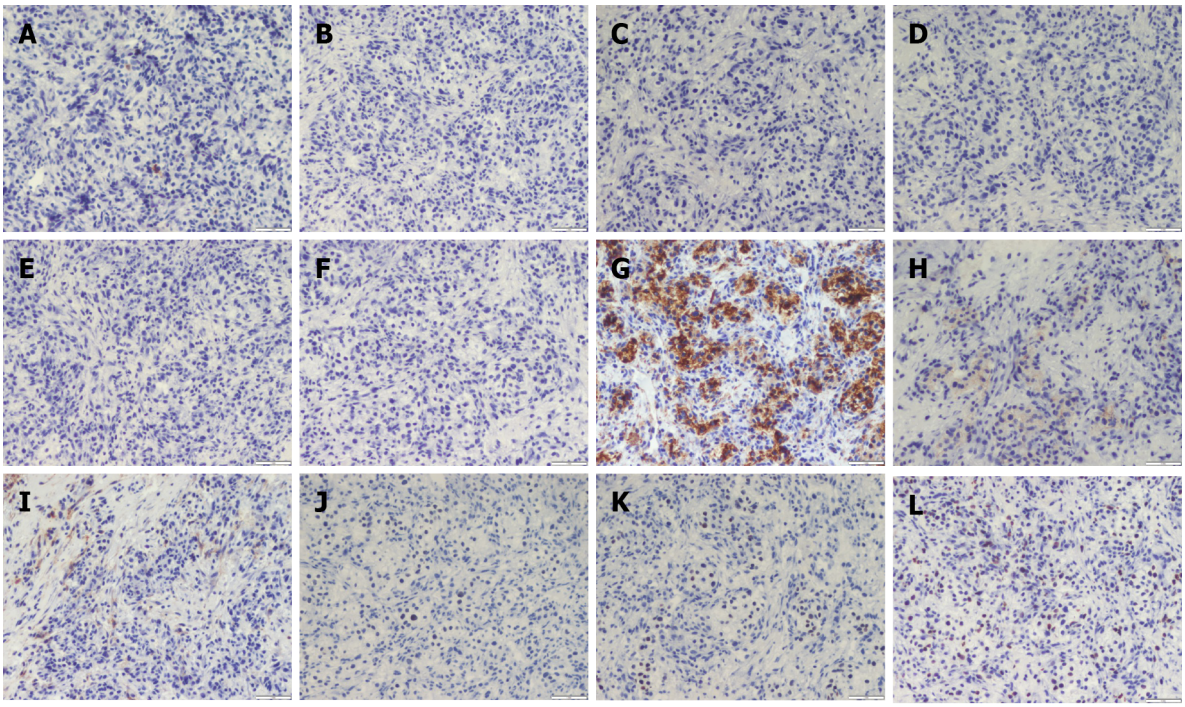

DOI: 10.12998/wjcc.v11.i9.2104

Figure 3 Immunopathology of the mass. A: S100(-); B: HMB45(-); C: CK7(-); D: AR(-); E: CK5/6(-); F: CAIX(-); G: Vimentin(+); H: EMA(+); I: CD10(+); J: PAX8(+); K: PAX2(+); L: Ki67(+).

DISCUSSION

RCC is a kind of malignant tumor of the genitourinary system, which usually occurs in males. The most common metastatic sites are the lung, liver, lymph node, contralateral kidney or adrenal gland. Skin metastasis is rare, only in 1.0%-3.3% of RCC cases[1]. Skin metastasis from renal carcinoma mostly occurs in the scalp, rarely in the nasal ala[2]. Balawender *et al*[3] reported cases of cutaneous metastasis of renal cell carcinoma from 2000 to 2019, with only two cases of nasal cutaneous metastasis.

A cutaneous metastatic lesion from renal cell carcinoma is often present as painless nodules, plaques or pulsatile masses of normal to purplish-red skin and grow rapidly[4]. Vascular-rich metastases are hard to distinguish from hemangiomas, pyogenic granulomas or Kaposi's sarcoma[5]. The histopathology of this case showed a mass-like infiltration of tumor cells in the dermis with clear

cytoplasm and nuclei in the center, which should be differentiated from sebaceous adenocarcinoma, melanoma and clear cell squamous cell carcinoma. PAX8 and PAX2 are nuclear transcription factors that are expressed in approximately 90% of renal cell tumors and can be used as markers for the diagnosis of distant metastatic tumors originating from the kidney; CD10 can be used as a marker for the recognition of tumors originating from the renal tubules and CD10 is positive in clear cell renal tumor; EMA and Vimentin are frequently expressed in clear cell renal cell carcinoma, which is uncommon in other clear cell tumors[6]. Immunohistochemical staining of this case showed that melanoma could be excluded because S100 and HMB45 were negative, sebaceous adenocarcinoma could be excluded because CK7 and AR were negative, clear cell squamous cell carcinoma could be excluded because CK5/6 and CAIX were negative[7]. Vimentin positive, EMA weakly positive, CD10 positive, PAX8 weakly positive, PAX2 weakly positive and Ki67 30% positive can be diagnosed as skin metastasis of RCC.

Metastatic RCC is insensitive to both radiotherapy and chemotherapy[8]. Surgical resection of isolated skin metastases has the potential to improve survival[9]. Axitinib is a class of oral small-molecule tyrosine kinase inhibitors that inhibit receptors such as VEGR and PDGFR-B, thereby inhibiting tumor angiogenesis and preventing tumor growth and metastasis[10]. Pembrolizumab, a humanized monoclonal antibody that binds to the PD-1 receptor, blocking the interaction of PD-1 with PD-L1 and PD-L2, relieving the suppression of the immune response mediated by the PD-1 pathway, enhances the body's immune system for the killing of tumor cells. Pembrolizumab and axitinib are used as first-line therapy for advanced renal cancer, the skin lesion of this patient developed rapidly after discontinuation of this regimen, and the tumor shrank significantly after treatment was resumed, which demonstrated the effectiveness of this treatment for skin metastases.

CONCLUSION

It is very rare for RCC to metastasize to the skin of the nasal ala region. It is easily misdiagnosed as hemangioma, pyogenic granuloma or Kaposi's sarcoma. Learning the detailed medical history and histopathology examination can help to avoid misdiagnosis. RCC patients with skin metastases often have a poor prognosis, and surgical removal of the metastases can be an option to improve the prognosis, but further systemic examination and comprehensive treatment are necessary. In this patient, pembrolizumab in combination with axitinib significantly reduced the size of the lesion, demonstrating the efficacy of the targeted drug for skin metastases.

ACKNOWLEDGEMENTS

We thank the patients and their families for their support.

FOOTNOTES

Author contributions: Dong S collected the data, did the literature searching and contributed to the manuscript drafting; Xu YC, Zhang YC and Xia JX did the follow-up and contributed to the manuscript drafting; Mou Y was the patient's doctor, and revised and reviewed the manuscript; all authors gave final approval for the version to be submitted.

Supported by the National Natural Science Foundation of China, No. 81803160.

Informed consent statement: Informed consent was obtained from the patient for the publication of this report and any accompanying images.

Conflict-of-interest statement: The authors declare that they have no conflict of interest.

CARE Checklist (2016) statement: The authors have read the CARE Checklist, and the manuscript was prepared and revised according to the CARE Checklist (2016).

Country/Territory of origin: China

ORCID number: Shuai Dong 0000-0002-7728-4537; Yang-Chun Xu 0000-0003-2236-8562; Yuan-Chen Zhang 0000-0002-7131-503X; Jian-Xin Xia 0000-0002-0067-2910; Yan Mou 0000-0002-9152-6301.

S-Editor: Yan JP
L-Editor: A
P-Editor: Yan JP

REFERENCES

1 **Singh P**, Somani K. Latent distant metastasis of renal cell carcinoma to skin: A case report. *Clin Case Rep* 2020; **8**: 1138-1141 [PMID: 32695344 DOI: 10.1002/ccr3.2844]
2 **Vilaça M**, Braga F, Mesquita A. Cutaneous Metastases and Long-Term Survival of a Patient With Clear Cell Renal Carcinoma. *Cureus* 2022; **14**: e23598 [PMID: 35494987 DOI: 10.7759/cureus.23598]
3 **Balawender K**, Przybyła R, Orkisz S, Wawrzyniak A, Boroñ D, Grabarek BO. Cutaneous metastasis as the first sign of renal cell carcinoma - crossroad between literature analysis and own observations. *Postepy Dermatol Alergol* 2022; **39**: 553-558 [PMID: 35950122 DOI: 10.5114/ada.2021.108275]
4 **Altinkaya A**, Yazar S, Karadag EC, Er O. Large solitary scalp metastasis of renal cell carcinoma: A case report. *Niger J Clin Pract* 2021; **24**: 629-631 [PMID: 33851688 DOI: 10.4103/njcp.njcp_584_19]
5 **Kramer DE**, Kerolus MG, Tan LA, Patel S, Reddy V, Chen M. Embolization of an Exophytic Posterior Neck Mass Secondary to a Cutaneous Renal Cell Carcinoma Metastasis. *Neurointervention* 2020; **15**: 162-166 [PMID: 32772032 DOI: 10.5469/neuroint.2020.00206]
6 **Ozcan A**, de la Roza G, Ro JY, Shen SS, Truong LD. PAX2 and PAX8 expression in primary and metastatic renal tumors: a comprehensive comparison. *Arch Pathol Lab Med* 2012; **136**: 1541-1551 [PMID: 23194047 DOI: 10.5858/arpa.2012-0072-OA]
7 **Khoury ZH**, Bugshan A, Lubek JE, Papadimitriou JC, Basile JR, Younis RH. Glycogen-Rich Clear Cell Squamous Cell Carcinoma Originating in the Oral Cavity. *Head Neck Pathol* 2017; **11**: 552-560 [PMID: 28342060 DOI: 10.1007/s12105-017-0812-3]
8 **Paula TAd**, Silva PSLd, Berriel LGS. Carcinoma de células renais com metástase cutânea: relato de caso. *Jornal Brasileiro de Nefrologia* 2010; **32**: 213-215 [DOI: 10.1590/s0101-28002010000200010]
9 **Leve PP**, Felício J, Carneiro R, Zagalo C. Recurrent renal cell carcinoma presenting as a cutaneous metastasis: A case report and review of the literature. *Urol Ann* 2021; **13**: 174-176 [PMID: 34194146 DOI: 10.4103/UA.UA_2_20]
10 **Keating GM**. Axitinib: a review in advanced renal cell carcinoma. *Drugs* 2015; **75**: 1903-1913 [PMID: 26487541 DOI: 10.1007/s40265-015-0483-x]

World Journal of Clinical Cases

Submit a Manuscript: https://www.f6publishing.com

World J Clin Cases 2023 March 26; 11(9): 2110-2115

DOI: 10.12998/wjcc.v11.i9.2110

ISSN 2307-8960 (online)

CASE REPORT

Successful treatment of a rare subcutaneous emphysema after a blow-out fracture surgery using needle aspiration: A case report

Ha-Jong Nam, Syeo-Young Wee

Specialty type: Surgery

Provenance and peer review: Unsolicited article; Externally peer reviewed.

Peer-review model: Single blind

Peer-review report's scientific quality classification

Grade A (Excellent): 0
Grade B (Very good): B, B
Grade C (Good): C
Grade D (Fair): 0
Grade E (Poor): 0

P-Reviewer: Fan L, China; Jian X, China; Sultana N, Bangladesh

Received: January 13, 2023
Peer-review started: January 13, 2023
First decision: January 30, 2023
Revised: February 1, 2023
Accepted: February 27, 2023
Article in press: February 27, 2023
Published online: March 26, 2023

Ha-Jong Nam, Syeo-Young Wee, Department of Plastic and Reconstructive Surgery, Soonchunhyang University Gumi Hospital, Gumi-si 39371, Gyeonsangbuk-do, South Korea

Corresponding author: Syeo-Young Wee, MD, PhD, Doctor, Professor, Department of Plastic and Reconstructive Surgery, Soonchunhyang University Gumi Hospital, 1 Gongdan-ro 179, Gumi-si 39371, Gyeonsangbuk-do, South Korea. 94061@schmc.ac.kr

Abstract

BACKGROUND

Many cases of emphysema associated with blow-out fractures occur before surgery due to trauma. However, emphysema can occur even after surgery, and most of such cases are managed conservatively and allowed to resolve. Swelling in the periorbital area due to emphysema that occurs after surgery can make early recovery difficult.

CASE SUMMARY

Herein, we describe a case of postoperative subcutaneous emphysema that was treated using a simple needle aspiration method. A 48-year-old male patient visited the hospital with a blow-out fracture of the left medial orbital wall and nasal bone fracture. One day postoperatively, swelling and crepitus in the left periorbital area were observed, and follow-up computed tomography showed emphysema in the left periorbital subcutaneous area. Needle aspiration using an 18-gauge needle and syringe was used to relieve the emphysema. The symptoms of sudden swelling improved immediately, and no recurrence was observed.

CONCLUSION

We conclude that needle aspiration is a useful method that could help in relieving symptom, resolving discomfort, and enabling early return to daily life in patients with postoperative subcutaneous emphysema.

Key Words: Blow out fracture; Subcutaneous emphysemas; Mechanical aspiration; Case report

Core Tip: A cases of postoperative subcutaneous emphysema is relatively rare. Though orbital emphysema is usually self-limited, we report a case report of postoperative subcutaneous emphysema that treated with a simple method using immediate needle aspiration to relieve discomfort and enable recovery to daily life.

Citation: Nam HJ, Wee SY. Successful treatment of a rare subcutaneous emphysema after a blow-out fracture surgery using needle aspiration: A case report. *World J Clin Cases* 2023; 11(9): 2110-2115
URL: https://www.wjgnet.com/2307-8960/full/v11/i9/2110.htm
DOI: https://dx.doi.org/10.12998/wjcc.v11.i9.2110

INTRODUCTION

The orbit is highly exposed to physical facial injuries because of its anatomical location and the lack of protective tissues. Isolated orbital fractures account for in 4%-16% of all facial fractures, and orbital fracture combined with any other type of fracture occurs in 30%-55% of zygomatic complex fractures and naso-orbital-ethmoid fractures[1,2].

Orbital emphysema, which is the abnormal presence of air within the orbit, is a typical finding in blow-out fractures owing to its communication with the paranasal sinus[3]. In the setting of trauma, the presence of orbital emphysema significantly increases the likelihood of an orbital fracture, with up to 75% of patients having medial orbital wall fractures with some degree of orbital emphysema[4]. Orbital emphysema can also occur after surgery as a complication that causes postoperative discomfort and delays recovery to daily life. In previous literature, case reports and treatment of preoperative emphysema have been reported; however, there is a tendency to rely on conservative treatment for subcutaneous emphysema that occur postoperatively because the symptoms in such cases are often not severe. However, this may be time-consuming and cause discomfort to the patient until spontaneous resolution is achieved.

Herein, we describe a case of postoperative subcutaneous emphysema that was treated with a simple method using immediate needle aspiration to relieve discomfort and enable recovery to daily life.

CASE PRESENTATION

Chief complaints

A 48-year-old male patient visited the hospital after experiencing direct trauma to the nose and periorbital area 9 d prior.

History of present illness

He had mild swelling and tenderness in nose and periorbital area due to the direct trauma. The day after hospitalization, orbital wall reconstruction using a bioresorbable polycaprolactone mesh implant (Osteomesh, Osteopore International, Singapore) and closed reduction of the nasal bone were performed. One day after the operation, the patient complained of difficulty in opening his left eye, and severe swelling in the left periorbital area was observed.

History of past illness

He had no remarkable medical history or chronic illness.

Personal and family history

There was no significant personal or family history.

Physical examination

At the time of admission, periorbital swelling was not significant (Figure 1). Extraocular movement was normal, and the patient did not complain of other visual symptoms including blurred vision or diplopia. One day after the operation, crepitus was observed during skin palpations.

Laboratory examinations

The blood results were within normal limit; a white blood cell count of 7.2 × 10^3/mL; a red blood cell count of 4.3 × 10^6/mL; a platelet count of 192 × 10^3/mL; a hemoglobin count of 12.9 g/dL; a blood urea nitrogen value of 11 mg/dL; serum creatinine value of 0.63 mg/dL; potassium, 3.3 mmol/L; sodium, 141 mmol/L; albumin, 35 g/L; total bilirubin of 3 μmol/L; alanine aminotransferase, 17 IU/L; aspartate aminotransferase, 15 IU/L; and alkaline phosphatase, 65 IU/L.

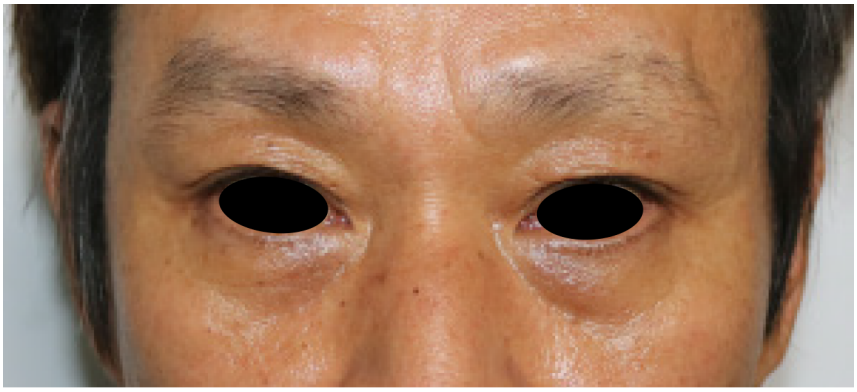

DOI: 10.12998/wjcc.v11.i9.2110

Figure 1 A facial photograph taken at the moment of admission. The swelling around the periorbital area was not significant.

Imaging examinations

The size of the blow-out fracture was 25 mm × 20 mm accompanied by a nasal bone fracture on computed tomography that was performed after visiting the hospital.

Further diagnostic work-up

Postoperatively, follow-up computed tomography was done and revealed emphysema in the form of scattered air bubbles in the left periorbital subcutaneous area (Figure 2).

FINAL DIAGNOSIS

The patient was diagnosed as postoperative subcutaneous emphysema.

TREATMENT

Negative pressure was applied using the needle and syringe pull-back method at three points above the eyelid crease with an 18-gauge needle, and approximately 2 mL of air was removed at each point (Figure 3). The symptoms of sudden swelling immediately improved (Figure 4). Simple foam dressing and mild compression after aspiration were performed.

OUTCOME AND FOLLOW-UP

No symptoms, such as bleeding or hematoma, were observed in the upper eyelid. On the fourth day postoperatively, there was no recurrence of swelling, the patient was discharged, and could immediately returned to his daily activities (Figure 5). During outpatient follow-up, recurrence of emphysema was not observed.

DISCUSSION

Orbital emphysema is commonly observed in orbital fractures[5]. A large retrospective study spanning 10 years concluded that clinically apparent orbital emphysema had a specificity of 99.6% and a positive predictive value of 98.4% for orbital fracture[6]. In cases of orbital emphysema related to orbital fractures, there is often a history of post-traumatic sneezing, coughing or nose blowing precipitating orbital emphysema[7-11]. An acute incident resulting in increased intranasal pressure, such as sneezing or nose blowing, usually promote the episode[12].

The clinical presentation of orbital emphysema varies, depending on its severity. Patients often experience tenderness, pain or pressure sensation and may complain of changes in visual acuity or field. Signs of orbital emphysema include periorbital subcutaneous crepitus, proptosis, decreased vision, relative afferent pupillary defect, and subconjunctival emphysema[5]. Given the tendency of air to localize superiorly, a crescent-shaped area of radiolucency in the superior aspect of the orbit demonstrated on a radiograph termed the "black eyebrow sign" is highly suggestive of orbital emphysema[13,14].

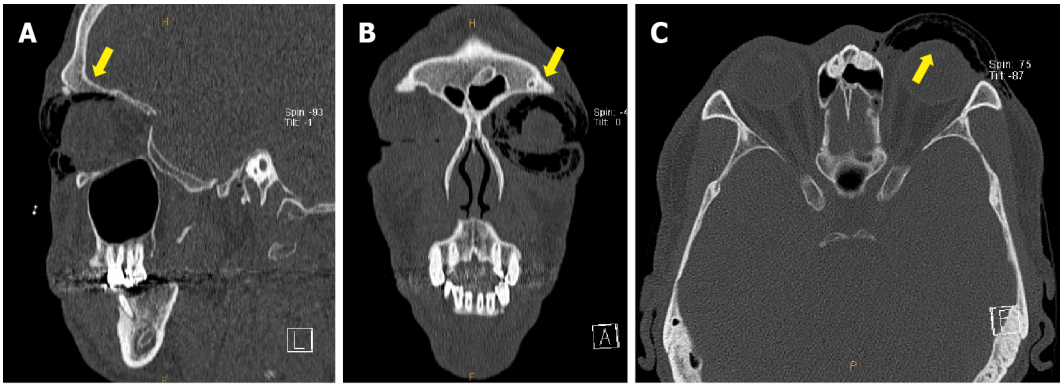

DOI: 10.12998/wjcc.v11.i9.2110

Figure 2 A Follow up computed tomography scan 2 d postoperatively. The emphysema is seen in the form of scattered air bubbles in the left periorbital subcutaneous area (yellow arrow), indicating the "black eyebrow sign'. A: Sagittal view; B: Coronal view; C: Axial view.

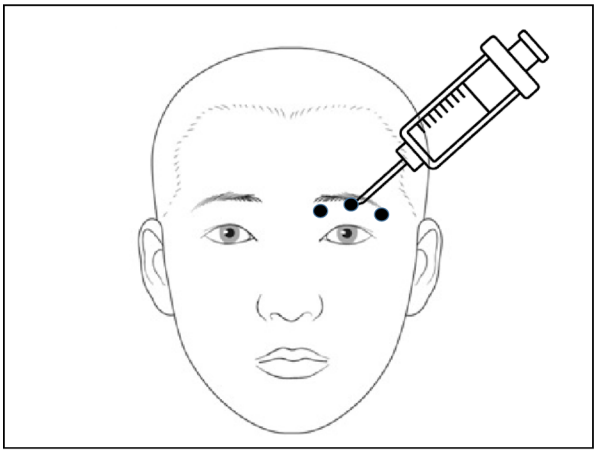

DOI: 10.12998/wjcc.v11.i9.2110

Figure 3 A schematic drawing of needle injection point (black circles). Above the upper eyelid, the needle was inserted at points where air was most palpable and negative pressure was applied using the pull-back method.

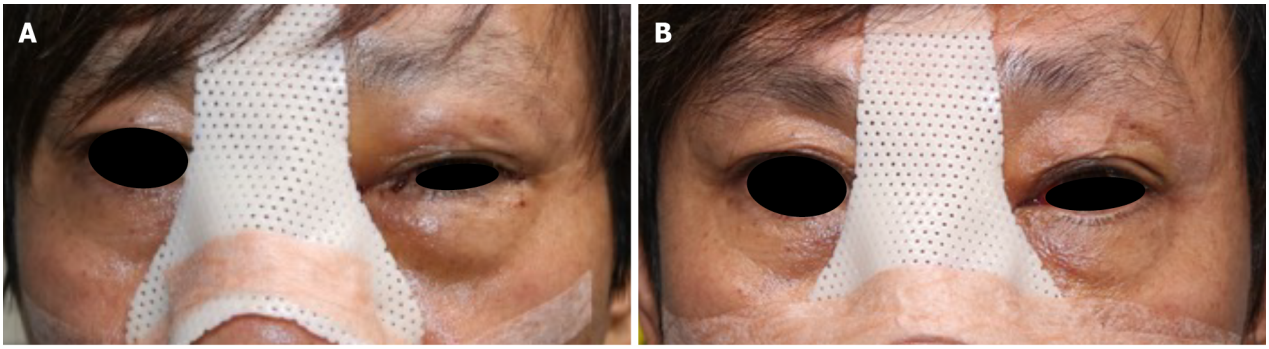

DOI: 10.12998/wjcc.v11.i9.2110

Figure 4 A facial photograph taken after the procedure. A: One day postoperatively, swelling in the left periorbital area was observed; B: The swelling improved immediately after needle aspiration decompression.

Most cases of orbital emphysema are self-limited and typically resolve within 7-10 d[15-18]. Moon *et al*[7] reviewed 348 orbits with isolated medial wall fractures and concluded that the majority of these patients recovered spontaneously without the need for surgical intervention. Patients who underwent needle aspiration and decompression tended to have a moderately decreased visual acuity. Those who underwent orbital decompression were more likely to have additional signs of optic nerve compression, indicated by the presence of a relative afferent pupillary defect and more severe impairment in visual acuity[10,19].

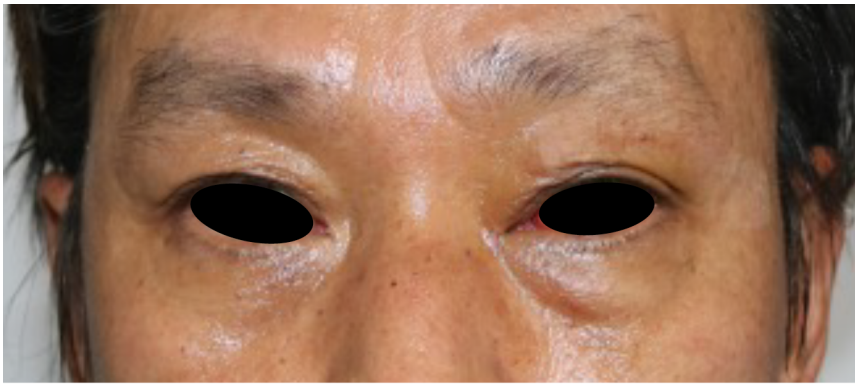

DOI: 10.12998/wjcc.v11.i9.2110

Figure 5 A facial photograph 4 d postoperatively. No recurrence of swelling was observed.

In our case, a sudden increase in swelling was observed, and follow-up computed tomography revealed a black eyebrow sign. As shown in the literature, orbital emphysema is often caused by trauma or soft tissue injury. However, in this case, it occurred postoperatively after reconstruction of the orbital blow-out fracture, and it is different from reports in the literature of cases, as this case was caused by an increase in intranasal pressure during sneezing. The patient experienced spontaneous sneezing, which prompted him to blow his nose the night prior to the onset of symptoms. The patient also had a nasal bone fracture, suggesting that an increase in intranasal pressure caused air to enter the surrounding subcutaneous tissue. In this case, the method of needle aspiration was used. Although it is highly likely that the emphysema would have resolved gradually, this method allowed immediate and dramatic resolution, enabling quick recovery to daily life. In addition, it has the advantage of being more comfortable and less burdensome to the patient than removal through surgical intervention.

The limitation of the method used in this case is that it was not possible to target the exact air collection area, and the procedure was performed based on palpation. In addition, resolution of emphysema after the procedure was not confirmed by follow-up imaging. As a point for improvement, we suggest that if additional diagnostic devices, such as handheld sonography are used during the procedure, needle aspiration would be a useful treatment option for orbital emphysema. Moreover, because our study represents only a single case, further investigations are required to validate our method as a viable treatment option for postoperative subcutaneous emphysema.

CONCLUSION

Orbital emphysema is a rare complication that can occur after blow-out surgery. Although orbital emphysema is often self-limiting, needle aspiration is a useful treatment method that could relieve symptoms, resolve discomfort, and enable early return to daily life in patients with postoperative subcutaneous emphysema.

FOOTNOTES

Author contributions: Nam HJ contributed to manuscript writing and visualization and data collection; Wee SY contributed to conceptualization and methodology and project administration and manuscript review and editing, and supervision; all authors have read and approved the final manuscript.

Supported by Soonchunhyang research fund, No. 2023-0024.

Informed consent statement: Informed written consent was obtained from the patient for publication of this report and any accompanying images.

Conflict-of-interest statement: The authors declare that they have no conflict of interest to disclose.

CARE Checklist (2016) statement: The authors have read the CARE Checklist (2016), and the manuscript was prepared and revised according to the CARE Checklist (2016).

Country/Territory of origin: South Korea

ORCID number: Ha-Jong Nam 0000-0002-2494-0991; Syeo-Young Wee 0000-0002-1787-9715.

S-Editor: Yan JP
L-Editor: A
P-Editor: Yan JP

REFERENCES

1 **Nakamura T**, Gross CW. Facial fractures. Analysis of five years of experience. *Arch Otolaryngol* 1973; **97**: 288-290 [PMID: 4696044 DOI: 10.1001/archotol.1973.00780010296016]
2 **Khojastepour L**, Moannaei M, Eftekharian HR, Khaghaninejad MS, Mahjoori-Ghasrodashti M, Tavanafar S. Prevalence and severity of orbital blowout fractures. *Br J Oral Maxillofac Surg* 2020; **58**: e93-e97 [PMID: 32680725 DOI: 10.1016/j.bjoms.2020.07.001]
3 **Sarbajna T**, Valencia MRP, Kakizaki H, Takahashi Y. Orbital Blowout Fracture and Orbital Emphysema caused by Nose Blowing. *J Craniofac Surg* 2020; **31**: e82-e84 [PMID: 31634313 DOI: 10.1097/SCS.0000000000005941]
4 **Shinohara H**, Shirota Y, Fujita K. Implication of differences in the incidence of orbital emphysema in ethmoidal and maxillary sinus fractures. *Ann Plast Surg* 2004; **53**: 565-569 [PMID: 15602254 DOI: 10.1097/01.sap.0000134538.44898.1f]
5 **Rubinstein TJ**, Sires BS. Re: "Orbital Emphysema: A Case Report and Comprehensive Review of the Literature". *Ophthalmic Plast Reconstr Surg* 2019; **35**: 300 [PMID: 31793923 DOI: 10.1097/IOP.0000000000001348]
6 **Büttner M**, Schlittler FL, Michel C, Exadaktylos AK, Iizuka T. Is a black eye a useful sign of facial fractures in patients with minor head injuries? *Br J Oral Maxillofac Surg* 2014; **52**: 518-522 [PMID: 24793410 DOI: 10.1016/j.bjoms.2014.03.018]
7 **Moon H**, Kim Y, Wi JM, Chi M. Morphological characteristics and clinical manifestations of orbital emphysema caused by isolated medial orbital wall fractures. *Eye (Lond)* 2016; **30**: 582-587 [PMID: 26795415 DOI: 10.1038/eye.2015.285]
8 **Tomasetti P**, Jacbosen C, Gander T, Zemann W. Emergency decompression of tension retrobulbar emphysema secondary to orbital floor fracture. *J Surg Case Rep* 2013; **2013** [PMID: 24964422 DOI: 10.1093/jscr/rjt011]
9 **Ababneh OH**. Orbital, subconjunctival, and subcutaneous emphysema after an orbital floor fracture. *Clin Ophthalmol* 2013; **7**: 1077-1079 [PMID: 23766631 DOI: 10.2147/OPTH.S44649]
10 **Jordan DR**, White GL Jr, Anderson RL, Thiese SM. Orbital emphysema: a potentially blinding complication following orbital fractures. *Ann Emerg Med* 1988; **17**: 853-855 [PMID: 3394993 DOI: 10.1016/s0196-0644(88)80571-7]
11 **Gauguet JM**, Lindquist PA, Shaffer K. Orbital Emphysema Following Ocular Trauma and Sneezing. *Radiol Case Rep* 2008; **3**: 124 [PMID: 27303505 DOI: 10.2484/rcr.v3i1.124]
12 **Gonzalez F**, Cal V, Elhendi W. Orbital emphysema after sneezing. *Ophthalmic Plast Reconstr Surg* 2005; **21**: 309-311 [PMID: 16052149 DOI: 10.1097/01.iop.0000170415.93858.6f]
13 **Feyaerts F**, Hermans R. The black eyebrow sign in orbital blowout fracture. *JBR-BTR* 2009; **92**: 251-252 [PMID: 19999329]
14 **Sawicki WK**, Hunter G. Eyebrow sign in facial trauma. *Emerg Med J* 2011; **28**: 962 [PMID: 21285280 DOI: 10.1136/emj.2010.110403]
15 **Ozdemir O**. Orbital Emphysema Occurring During Weight Lifting. *Semin Ophthalmol* 2015; **30**: 426-428 [PMID: 24475915 DOI: 10.3109/08820538.2013.874469]
16 **Chiu WC**, Lih M, Huang TY, Ku WC, Wang W. Spontaneous orbital subcutaneous emphysema after sneezing. *Am J Emerg Med* 2008; **26**: 381.e1-381.e2 [PMID: 18358968 DOI: 10.1016/j.ajem.2007.05.021]
17 **Tseng WS**, Lee HC, Kang BH. Periorbital emphysema after a wet chamber dive. *Diving Hyperb Med* 2017; **47**: 198-200 [PMID: 28868601 DOI: 10.28920/dhm47.3.198-200]
18 **van Issum C**, Courvoisier DS, Scolozzi P. Posttraumatic orbital emphysema: incidence, topographic classification and possible pathophysiologic mechanisms. A retrospective study of 137 patients. *Oral Surg Oral Med Oral Pathol Oral Radiol* 2013; **115**: 737-742 [PMID: 23332507 DOI: 10.1016/j.oooo.2012.10.021]
19 **Chaudhry IA**, Al-Amri A, Shamsi FA, Al-Rashed W. Visual recovery after evacuation of orbital emphysema. *Orbit* 2007; **26**: 283-285 [PMID: 18097969 DOI: 10.1080/01676830600987391]

World Journal of Clinical Cases

Submit a Manuscript: https://www.f6publishing.com

World J Clin Cases 2023 March 26; 11(9): 2116-2118

DOI: 10.12998/wjcc.v11.i9.2116

ISSN 2307-8960 (online)

LETTER TO THE EDITOR

Are biopsies during endoscopic ultrasonography necessary for a suspected esophageal leiomyoma? Is laparoscopy always feasible?

Hazem Beji, Mohamed Fadhel Chtourou, Slim Zribi, Yassine Kallel, Mahdi Bouassida, Hassen Touinsi

Specialty type: Medicine, research and experimental

Provenance and peer review: Invited article; Externally peer reviewed.

Peer-review model: Single blind

Peer-review report's scientific quality classification

Grade A (Excellent): 0
Grade B (Very good): 0
Grade C (Good): C, C
Grade D (Fair): 0
Grade E (Poor): 0

P-Reviewer: Sato H, Japan; Yalçınkaya İ, Turkey

Received: December 12, 2022
Peer-review started: December 12, 2022
First decision: January 17, 2023
Revised: January 18, 2023
Accepted: March 3, 2023
Article in press: March 3, 2023
Published online: March 26, 2023

Hazem Beji, Mohamed Fadhel Chtourou, Slim Zribi, Yassine Kallel, Mahdi Bouassida, Hassen Touinsi, Department of General Surgery Hospital Mohamed Taher Maamouri Nabeul, University of Tunis El Manar-Faculty of Medicine of Tunis, Nabeul 8000, Tunisia

Corresponding author: Hazem Beji, MD, Surgeon, Department of General Surgery Hospital Mohamed Taher Maamouri Nabeul, University of Tunis El Manar-Faculty of Medicine of Tunis, 1007 Street Jabbari Tunis Tunisia, Nabeul 8000, Tunisia. hazembj@gmail.com

Abstract

The present letter to the editor is related to the work entitled "Large leiomyoma of lower esophagus diagnosed by endoscopic ultrasonography-fine needle aspiration: A case report." Although endoscopic ultrasonography seems necessary in a suspected leiomyoma of the esophagus, the performance of biopsies *via* fine needle aspiration is controversial as it increases the risk of complications such as bleeding, infection, and intraoperative perforations. Laparoscopy is the best treatment strategy for small tumors. Laparotomy with tumor enucleation or esophageal resection can be considered in large leiomyomas.

Key Words: Esophageal Leiomyoma; Endoscopic ultrasonography; Biopsy; Surgical resection

Core Tip: Endoscopic ultrasonography seems necessary in a suspected leiomyoma of the esophagus. However, the performance of biopsies *via* fine needle aspiration is controversial. It increases the risk of complications such as bleeding, infection, and intraoperative perforations. Moreover, there is a possibility of an inconclusive biopsy due to inadequate material. Laparoscopy is the best treatment option for small tumors. Laparotomy with tumor enucleation or esophageal resection can be considered in large leiomyomas.

Citation: Beji H, Chtourou MF, Zribi S, Kallel Y, Bouassida M, Touinsi H. Are biopsies during endoscopic ultrasonography necessary for a suspected esophageal leiomyoma? Is laparoscopy always feasible? *World J Clin Cases* 2023; 11(9): 2116-2118
URL: https://www.wjgnet.com/2307-8960/full/v11/i9/2116.htm
DOI: https://dx.doi.org/10.12998/wjcc.v11.i9.2116

TO THE EDITOR

We read with interest a case report by Rao *et al*[1], who presented a patient having leiomyoma of the lower esophagus, successfully treated with laparoscopic local resection.

We agree with the authors on the importance of performing endoscopic ultrasonography (EUS) for large esophageal leiomyomas to rule malignancies. EUS is highly specific to leiomyoma with a diagnostic accuracy of 94.7%[2]. Esophageal leiomyoma presents on EUS as a homogenous, hypoechoic lesion with obvious margins, encircled by an hyperechoic area, and is easily distinguishable from an esophageal cyst, lipoma, or hemangioma[2,3]. However, performing biopsies *via* fine needle aspiration is controversial and presents many risks. It is associated with many complications such as intraoperative perforations, bleeding, and infection[3]. Moreover, an inconclusive biopsy is possible due to inadequate material[4]. Therefore, malignancy can only be ruled out after surgical resection[5-7].

The authors opted for laparoscopic local resection of the tumor. It is the treatment of choice, especially in small tumors < 5 cm[8]. However, a trans-Hiatal approach *via* laparotomy could have been discussed as a therapeutic option knowing that the tumor was large (8 cm × 6 cm × 3.5 cm), originated from the cardia, and entered the abdominal cavity next to the diaphragm and liver.

An esophageal resection can also be considered for big tumors situated at the gastroesophageal junction due to technical problems, poor wound healing in the defect of the esophageal muscle, and dysfunction of the lower esophageal sphincter following enucleation[9,10].

Submucosal tunneling endoscopic resection represents another therapeutic option. However this technique presents technical difficulties for tumors > 35 mm due to the reduced space of the submucosal tunnel[11].

FOOTNOTES

Author contributions: Beji H and Chtourou MF designed the study; Zribi S and Kallel Y performed the research; Chtourou MF analyzed the data; Beji H wrote the letter; Bouassida M and Touinsi H revised the letter.

Conflict-of-interest statement: All the authors report no relevant conflicts of interest for this article.

Country/Territory of origin: Tunisia

ORCID number: Hazem Beji 0000-0002-2376-5351; Mahdi Bouassida 0000-0002-4624-1905.

S-Editor: Li L
L-Editor: Filipodia
P-Editor: Li L

REFERENCES

1 **Rao M**, Meng QQ, Gao PJ. Large leiomyoma of lower esophagus diagnosed by endoscopic ultrasonography-fine needle aspiration: A case report. *World J Clin Cases* 2020; **8**: 5809-5815 [PMID: 33344578 DOI: 10.12998/wjcc.v8.i22.5809]
2 **Xu GQ**, Zhang BL, Li YM, Chen LH, Ji F, Chen WX, Cai SP. Diagnostic value of endoscopic ultrasonography for gastrointestinal leiomyoma. *World J Gastroenterol* 2003; **9**: 2088-2091 [PMID: 12970912 DOI: 10.3748/wjg.v9.i9.2088]
3 **Punpale A**, Rangole A, Bhambhani N, Karimundackal G, Desai N, de Souza A, Pramesh CS, Jambhekar N, Mistry RC. Leiomyoma of esophagus. *Ann Thorac Cardiovasc Surg* 2007; **13**: 78-81 [PMID: 17505413]
4 **Sun X**, Wang J, Yang G. Surgical treatment of esophageal leiomyoma larger than 5 cm in diameter: A case report and review of the literature. *J Thorac Dis* 2012; **4**: 323-326 [PMID: 22754674 DOI: 10.3978/j.issn.2072-1439.2011.11.02]

5 **Ramos D**, Priego P, Coll M, Cornejo Mde L, Galindo J, Rodríguez-Velasco G, García-Moreno F, Carda P, Lobo E. Comparative study between open and minimally invasive approach in the surgical management of esophageal leiomyoma. *Rev Esp Enferm Dig* 2016; **108**: 8-14 [PMID: 26765229 DOI: 10.17235/reed.2015.3845/2015]

6 **Mujawar P**, Pawar T, Chavan RN. Video Assisted Thoracoscopic Surgical Enucleation of a Giant Esophageal Leiomyoma Presenting with Persistent Cough. *Case Rep Surg* 2016; **2016**: 7453259 [PMID: 26977331 DOI: 10.1155/2016/7453259]

7 **Aurea P**, Grazia M, Petrella F, Bazzocchi R. Giant leiomyoma of the esophagus. *Eur J Cardiothorac Surg* 2002; **22**: 1008-1010 [PMID: 12467830 DOI: 10.1016/s1010-7940(02)00569-9]

8 **Kent M**, d'Amato T, Nordman C, Schuchert M, Landreneau R, Alvelo-Rivera M, Luketich J. Minimally invasive resection of benign esophageal tumors. *J Thorac Cardiovasc Surg* 2007; **134**: 176-181 [PMID: 17599505 DOI: 10.1016/j.jtcvs.2006.10.082]

9 **Beji H**, Bouassida M, Kallel Y, Tormane MA, Mighri MM, Touinsi H. Leiomyoma of the esophagus: A case report and review of the literature. *Int J Surg Case Rep* 2022; **94**: 107078 [PMID: 35439728 DOI: 10.1016/j.ijscr.2022.107078]

10 **O'Hanlon DM**, Clarke E, Lennon J, Gorey TF. Leiomyoma of the esophagus. *Am J Surg* 2002; **184**: 168-169 [PMID: 12169363 DOI: 10.1016/s0002-9610(02)00905-4]

11 **Tan Y**, Lv L, Duan T, Zhou J, Peng D, Tang Y, Liu D. Comparison between submucosal tunneling endoscopic resection and video-assisted thoracoscopic surgery for large esophageal leiomyoma originating from the muscularis propria layer. *Surg Endosc* 2016; **30**: 3121-3127 [PMID: 26487221 DOI: 10.1007/s00464-015-4567-1]

World Journal of Clinical Cases

Submit a Manuscript: https://www.f6publishing.com

World J Clin Cases 2023 March 26; 11(9): 2119-2122

DOI: 10.12998/wjcc.v11.i9.2119

ISSN 2307-8960 (online)

LETTER TO THE EDITOR

Vaginal microbes confounders and implications on women's health

Wassan Nori, Ban H-Hameed

Specialty type: Medicine, research and experimental

Provenance and peer review: Unsolicited article; Externally peer reviewed.

Peer-review model: Single blind

Peer-review report's scientific quality classification

Grade A (Excellent): 0
Grade B (Very good): B, B
Grade C (Good): C
Grade D (Fair): 0
Grade E (Poor): 0

P-Reviewer: García-Mena J, Mexico; Hegazy AA, Egypt

Received: December 20, 2022
Peer-review started: December 20, 2022
First decision: January 30, 2023
Revised: January 30, 2023
Accepted: March 1, 2023
Article in press: March 1, 2023
Published online: March 26, 2023

Wassan Nori, Ban H-Hameed, Department of Obstetrics and Gynecology, Mustansiriyah University, Baghdad 10052, Al Saydyah, Iraq

Corresponding author: Wassan Nori, PhD, Academic Editor, Academic Research, Senior Researcher, Department of Obstetrics and Gynecology, Mustansiriyah University, Al Amin, Street No. 38, Baghdad 10052, Al Saydyah, Iraq. dr.wassan76@uomustansiriyah.edu.iq

Abstract

The vagina has diverse vaginal microbes (Vm). A disturbance in the delicate balance maintained in Vm is linked to women's obstetrical and reproductive tract problems. Vaginal microbes play an essential role in protecting the health of the female reproductive tract by alleviating gynecological infection. However, Vm profiling has many confounders that need to be addressed during sampling, including age, race, pregnancy, medical illness, and smoking. Vm profiling improves reproduction odds, may serve as a marker for genital malignancies and have a therapeutic application in menopausal women and women with cervical cancers.

Key Words: Vaginal microbes; Lactobacillus; Infertility; Probiotics; Cancer; Menapuse

Core Tip: The vaginal ecosystem has a key role in women's health. Vaginal microbes (Vm) affect the obstetrical performance of pregnant women and, in turn, can be affected by age, gestational age, race, and time of sampling. For infertile women, Vm composition can affect fertilization odds, the success of assisted reproduction technique, and even may predict the chances of live birth. The therapeutic aspect of Vm was introduced to enhance vaginal protection against infection, alleviate menopausal symptoms, and, finally, in genital malignancies. Vm was used as a signature marker in predicting and preventing ovarian and cervical malignancies, respectively.

Citation: Nori W, H-Hameed B. Vaginal microbes confounders and implications on women's health. *World J Clin Cases* 2023; 11(9): 2119-2122
URL: https://www.wjgnet.com/2307-8960/full/v11/i9/2119.htm
DOI: https://dx.doi.org/10.12998/wjcc.v11.i9.2119

TO THE EDITOR

We read with interest Liao *et al*'s study[1] published in *World J Clin Cases* that discusses the influence of vaginal microbes (Vm) on pregnant women's health and how the integrity of the vaginal ecosystem is maintained by a delicate balance of vaginal sanitation and group B streptococcus status[1].

Studying the Vm has many implications for obstetrical and gynecological diseases in women. Earlier work has examined confounders that can affect Vm, which was not discussed in Liao *et al's* study[1], including; women's age, race, pregnancy and gestational age at sampling, smoking, and sexual activity [2-4].

A recent meta-analysis described the effect of race and age on the unique ecosystem of Vm. The study confirmed that Chinese females hosted a distinct Vm from other ethnicities. In good agreement, Dunlop *et al* discussed different Vm in a group of African American women *vs* non-African American study population they examined[5,6].

Certain behaviors and customs can influence human races. Male circumcision, which is performed in some societies, is believed to minimize Human papillomavirus (HPV) transmission, a significant factor in the development of cervical cancer. Furthermore, in other communities, females may have several male partners, which may enhance the transmission of sexually transmitted diseases, including HPV[7, 8].

Other studies addressed the difference between Vm in the pregnant *vs* non-pregnant population due to different hormonal influences[5].

Even for pregnant women, the sampling timing affects the observed Vm seen, as Laghi *et al's* study[9] suggested. Moreover, they discussed the effect of females' age, diet, smoking, and sex on modifying the Vm composition[9,10].

Diseases caused by vaginal infections inversely impact obstetrical performance, like preterm labor and abortion. Furthermore, the implication of Vm on fertility outcomes and women's health in menopause was explored, given the increasing number of women entering menopause. An emphasis was made on Vm's benefit in the management of menopausal symptoms, reducing the risk of osteoporosis, regulating the nervous system, and lipid profiling for menopausal women[11-13].

Polycystic ovarian syndrome is a common cause of female infertility; research showed reduced Lactobacillus in the vagina and cervix of affected women. Consequently, fertilization rates were reduced due to oocyte damage by colonizing microbes in the oocyte's follicular fluid[14,15]. For infertile couples seeking assisted reproductive technique(ART), an alteration in Vm and male seminal fluid microbes were linked to unsuccessful ART outcome; in fact, Lactobacillus presence in the women's lower and upper genital tract favors positive outcomes[16-18].

Additionally, Vm profiling was used to predict successful *in-vitro* fertilization with or without intracytoplasmic sperm injection cycle and showed a predictive accuracy of 94%. Lactobacillus dominance was key in predicting pregnancy success and odds of live birth (odds ratio 0.66, 95% confidence interval 0.50–0.88)[19,20].

It is well known that genital infection causes a change of Vm predominant; interestingly, a correlation was found between the alteration of Vm and the development of epithelial ovarian cancer, a malignancy that is usually present in late or advanced stages. It was proposed that Vm could serve as a useful biomarker for earlier diagnosis and prevention of ovarian and cervical cancers[21-23].

Detection and clustering of Vm were based on culture-dependent methods[9,21]. However, due to their limitations, detection of Vm was shifted to culture-independent methods in the last few years, for example, Sanger sequencing of the 16S rRNA of bacterial colonies and Illumina-based amplicon sequencing of the V6 region of the 16S rRNA gene[10,21].

A therapeutic avenue of Vm was also suggested; a probiotic is a preparation containing viable microbial agents to improve health. Treatment with probiotics to relieve genitourinary sequelae in postmenopausal women (PMW) is a promising option *via* restoring Lactobacillus abundance in the vagina. Recent evidence shows that oral and direct administration of probiotics in the vagina is an adjuvant therapy to estrogen withdrawal in PMW[13,24].

Probiotics were also used for their anticancer activities in cervical cancer *via* activating the maturation of natural killer cells and promoting cellular and humoral immunity. Additionally, probiotics were added to reduce the side effects of radiation therapy for cervical malignancies[25].

The Corona Virus Infectious Disease(COVID)-19 pandemic has had a detrimental effect on fetal-maternal outcomes[26]. Celik *et al*[27] discovered a considerable change in Vm in affected cases. In fact, the more severe the maternal illness, the more Vm is altered. As a result, the researchers hypothesized that COVID-19 fosters an undesirable vaginal microenvironment. These findings point to the potential use of microbiome-associated indicators as a risk assessment tool for preterm birth in COVID-19 pregnant women. In addition, a therapeutic avenue can be created *via* the modification of Vm in affected cases[27].

In conclusion, Vm have confounders that need to be adjusted before sampling; moreover, Vm has implication for women's obstetrical and fertility potential. Vm can protect against infection development, be a signature biomarker for predicting ovarian cancer, and have promising therapeutic applications for PMW and patients with cervical cancer.

ACKNOWLEDGEMENTS

To our beloved university, Mustansiriyah, for continuous support.

FOOTNOTES

Author contributions: Nori W designed the research and reviewed data, wrote and revised the letter; H-Hameed B reviewed the scientific content; both authors have read and agreed on the final version of the manuscript.

Conflict-of-interest statement: All the authors report no relevant conflicts of interest for this article.

Country/Territory of origin: Iraq

ORCID number: Wassan Nori 0000-0002-8749-2444; Ban H-Hameed 0000-0001-8451-652X.

S-Editor: Li L
L-Editor: A
P-Editor: Li L

REFERENCES

1 **Liao Q**, Zhang XF, Mi X, Jin F, Sun HM, Wang QX. Influence of group B streptococcus and vaginal cleanliness on the vaginal microbiome of pregnant women. *World J Clin Cases* 2022; **10**: 12578-12586 [PMID: 36579104 DOI: 10.12998/wjcc.v10.i34.12578]
2 **Elovitz MA**, Gajer P, Riis V, Brown AG, Humphrys MS, Holm JB, Ravel J. Cervicovaginal microbiota and local immune response modulate the risk of spontaneous preterm delivery. *Nat Commun* 2019; **10**: 1305 [PMID: 30899005 DOI: 10.1038/s41467-019-09285-9]
3 **Romero R**, Hassan SS, Gajer P, Tarca AL, Fadrosh DW, Nikita L, Galuppi M, Lamont RF, Chaemsaithong P, Miranda J, Chaiworapongsa T, Ravel J. Correction: The composition and stability of the vaginal microbiota of normal pregnant women is different from that of non-pregnant women. *Microbiome* 2014; **2**: 10 [PMID: 24735933 DOI: 10.1186/2049-2618-2-10]
4 **Romero R**, Hassan SS, Gajer P, Tarca AL, Fadrosh DW, Bieda J, Chaemsaithong P, Miranda J, Chaiworapongsa T, Ravel J. The vaginal microbiota of pregnant women who subsequently have spontaneous preterm labor and delivery and those with a normal delivery at term. *Microbiome* 2014; **2**: 18 [PMID: 24987521 DOI: 10.1186/2049-2618-2-18]
5 **Hotkani ZG**, Ghaedmohammadi S, Mozdoori N. Meta-analysis of race and age influence on the vaginal microbiome in pregnant and nonpregnant healthy women. *Future Microbiol* 2022; **17**: 1147-1159 [PMID: 35950983 DOI: 10.2217/fmb-2021-0209]
6 **Dunlop AL**, Satten GA, Hu YJ, Knight AK, Hill CC, Wright ML, Smith AK, Read TD, Pearce BD, Corwin EJ. Vaginal Microbiome Composition in Early Pregnancy and Risk of Spontaneous Preterm and Early Term Birth Among African American Women. *Front Cell Infect Microbiol* 2021; **11**: 641005 [PMID: 33996627 DOI: 10.3389/fcimb.2021.641005]
7 **Hegazy AA**, Al-Rukban MO. Male circumcision: review and authors perspective. *The Health* 2012; **3**: 24-30
8 Hegazy DAA. Mode of Hepatitis C Transmission through Sexual Intercourse: Author Perspective. *AANAT* 2016; **2** [DOI: 10.21276/aanat.2016.2.2.1]
9 **Laghi L**, Zagonari S, Patuelli G, Zhu C, Foschi C, Morselli S, Pedna MF, Sambri V, Marangoni A. Vaginal metabolic profiles during pregnancy: Changes between first and second trimester. *PLoS One* 2021; **16**: e0249925 [PMID: 33831087 DOI: 10.1371/journal.pone.0249925]
10 **Song SD**, Acharya KD, Zhu JE, Deveney CM, Walther-Antonio MRS, Tetel MJ, Chia N. Daily Vaginal Microbiota Fluctuations Associated with Natural Hormonal Cycle, Contraceptives, Diet, and Exercise. *mSphere* 2020; **5** [PMID: 32641429 DOI: 10.1128/mSphere.00593-20]
11 **Kroon SJ**, Ravel J, Huston WM. Cervicovaginal microbiota, women's health, and reproductive outcomes. *Fertil Steril* 2018; **110**: 327-336 [PMID: 30098679 DOI: 10.1016/j.fertnstert.2018.06.036]
12 **Nori W**, Shallal F, Zghair MAG. Aspirin effect on Mid luteal Phase Doppler Indices in Patients with Recurrent Pregnancy Loss. *Int J Pharm Res* 2020; **12**: 2929-2934 [DOI: 10.31838/ijpr/2020.12.03.413]
13 **Chen Q**, Wang H, Wang G, Zhao J, Chen H, Lu X, Chen W. Lactic Acid Bacteria: A Promising Tool for Menopausal Health Management in Women. *Nutrients* 2022; **14** [PMID: 36364729 DOI: 10.3390/nu14214466]
14 **Tu Y**, Zheng G, Ding G, Wu Y, Xi J, Ge Y, Gu H, Wang Y, Sheng J, Liu X, Jin L, Huang H. Comparative Analysis of Lower Genital Tract Microbiome Between PCOS and Healthy Women. *Front Physiol* 2020; **11**: 1108 [PMID: 33013474 DOI: 10.3389/fphys.2020.01108]
15 **Ali AI**, Nori W. Correlation of Serum Visfatin Level in Non-obese Women with Polycystic Ovary Syndrome and Matched Control. *Reprod Sci* 2022; **29**: 3285-3293 [PMID: 35687303 DOI: 10.1007/s43032-022-00986-z]

16 **Bracewell-Milnes T**, Saso S, Nikolaou D, Norman-Taylor J, Johnson M, Thum MY. Investigating the effect of an abnormal cervico-vaginal and endometrial microbiome on assisted reproductive technologies: A systematic review. *Am J Reprod Immunol* 2018; **80**: e13037 [PMID: 30133062 DOI: 10.1111/aji.13037]

17 **Chen S**, Xue X, Zhang Y, Zhang H, Huang X, Chen X, Deng G, Luo S, Gao J. Vaginal Atopobium is Associated with Spontaneous Abortion in the First Trimester: a Prospective Cohort Study in China. *Microbiol Spectr* 2022; **10**: e0203921 [PMID: 35311570 DOI: 10.1128/spectrum.02039-21]

18 **Tsonis O**, Gkrozou F, Paschopoulos M. Microbiome affecting reproductive outcome in ARTs. *J Gynecol Obstet Hum Reprod* 2021; **50**: 102036 [PMID: 33307241 DOI: 10.1016/j.jogoh.2020.102036]

19 **Koedooder R**, Singer M, Schoenmakers S, Savelkoul PHM, Morré SA, de Jonge JD, Poort L, Cuypers WJSS, Beckers NGM, Broekmans FJM, Cohlen BJ, den Hartog JE, Fleischer K, Lambalk CB, Smeenk JMJS, Budding AE, Laven JSE. The vaginal microbiome as a predictor for outcome of in vitro fertilization with or without intracytoplasmic sperm injection: a prospective study. *Hum Reprod* 2019; **34**: 1042-1054 [PMID: 31119299 DOI: 10.1093/humrep/dez065]

20 **Zeng H**, He D, Hu L, Abdullah RK, Zhang L, Jiang B, Xie H, Liu N. Non-Lactobacillus dominance of the vagina is associated with reduced live birth rate following IVF/ICSI: a propensity score-matched cohort study. *Arch Gynecol Obstet* 2022; **305**: 519-528 [PMID: 34370072 DOI: 10.1007/s00404-021-06171-y]

21 **Punzón-Jiménez P**, Labarta E. The impact of the female genital tract microbiome in women health and reproduction: a review. *J Assist Reprod Genet* 2021; **38**: 2519-2541 [PMID: 34110573 DOI: 10.1007/s10815-021-02247-5]

22 **Banerjee S**, Tian T, Wei Z, Shih N, Feldman MD, Alwine JC, Coukos G, Robertson ES. The ovarian cancer oncobiome. *Oncotarget* 2017; **8**: 36225-36245 [PMID: 28410234 DOI: 10.18632/oncotarget.16717]

23 **Nejman D**, Livyatan I, Fuks G, Gavert N, Zwang Y, Geller LT, Rotter-Maskowitz A, Weiser R, Mallel G, Gigi E, Meltser A, Douglas GM, Kamer I, Gopalakrishnan V, Dadosh T, Levin-Zaidman S, Avnet S, Atlan T, Cooper ZA, Arora R, Cogdill AP, Khan MAW, Ologun G, Bussi Y, Weinberger A, Lotan-Pompan M, Golani O, Perry G, Rokah M, Bahar-Shany K, Rozeman EA, Blank CU, Ronai A, Shaoul R, Amit A, Dorfman T, Kremer R, Cohen ZR, Harnof S, Siegal T, Yehuda-Shnaidman E, Gal-Yam EN, Shapira H, Baldini N, Langille MGI, Ben-Nun A, Kaufman B, Nissan A, Golan T, Dadiani M, Levanon K, Bar J, Yust-Katz S, Barshack I, Peeper DS, Raz DJ, Segal E, Wargo JA, Sandbank J, Shental N, Straussman R. The human tumor microbiome is composed of tumor type-specific intracellular bacteria. *Science* 2020; **368**: 973-980 [PMID: 32467386 DOI: 10.1126/science.aay9189]

24 **Petrova MI**, Lievens E, Malik S, Imholz N, Lebeer S. Lactobacillus species as biomarkers and agents that can promote various aspects of vaginal health. *Front Physiol* 2015; **6**: 81 [PMID: 25859220 DOI: 10.3389/fphys.2015.00081]

25 **Negi D**, Singh A, Joshi N, Mishra N. Cisplatin and Probiotic Biomass Loaded Pessaries for the Management of Cervical Cancer. *Anticancer Agents Med Chem* 2020; **20**: 589-598 [PMID: 31823703 DOI: 10.2174/1871520619666191211110640]

26 **Farhan FS**, Nori W, Al Kadir ITA, Hameed BH. Can Fetal Heart Lie? *J Obstet Gynaecol India* 2022; **72**: 479-484 [PMID: 35634476 DOI: 10.1007/s13224-022-01663-6]

27 **Celik E**, Ozcan G, Vatansever C, Paerhati E, Kuşkucu MA, Dogan O, Cekic SG, Ergonul O, Gürsoy A, Keskin Ö, Can F. Alterations in vaginal microbiota among pregnant women with COVID-19. *J Med Virol* 2023; **95**: e28132 [PMID: 36068653 DOI: 10.1002/jmv.28132]

Published by **Baishideng Publishing Group Inc**
7041 Koll Center Parkway, Suite 160, Pleasanton, CA 94566, USA
Telephone: +1-925-3991568
E-mail: bpgoffice@wjgnet.com
Help Desk: https://www.f6publishing.com/helpdesk
https://www.wjgnet.com